BioMed Research International

Novel Drugs Development for Cardio-/Cerebrovascular Diseases

Guest Editors: Joen-Rong Sheu, Philip Aloysius Thomas, and Juei-Tang Cheng

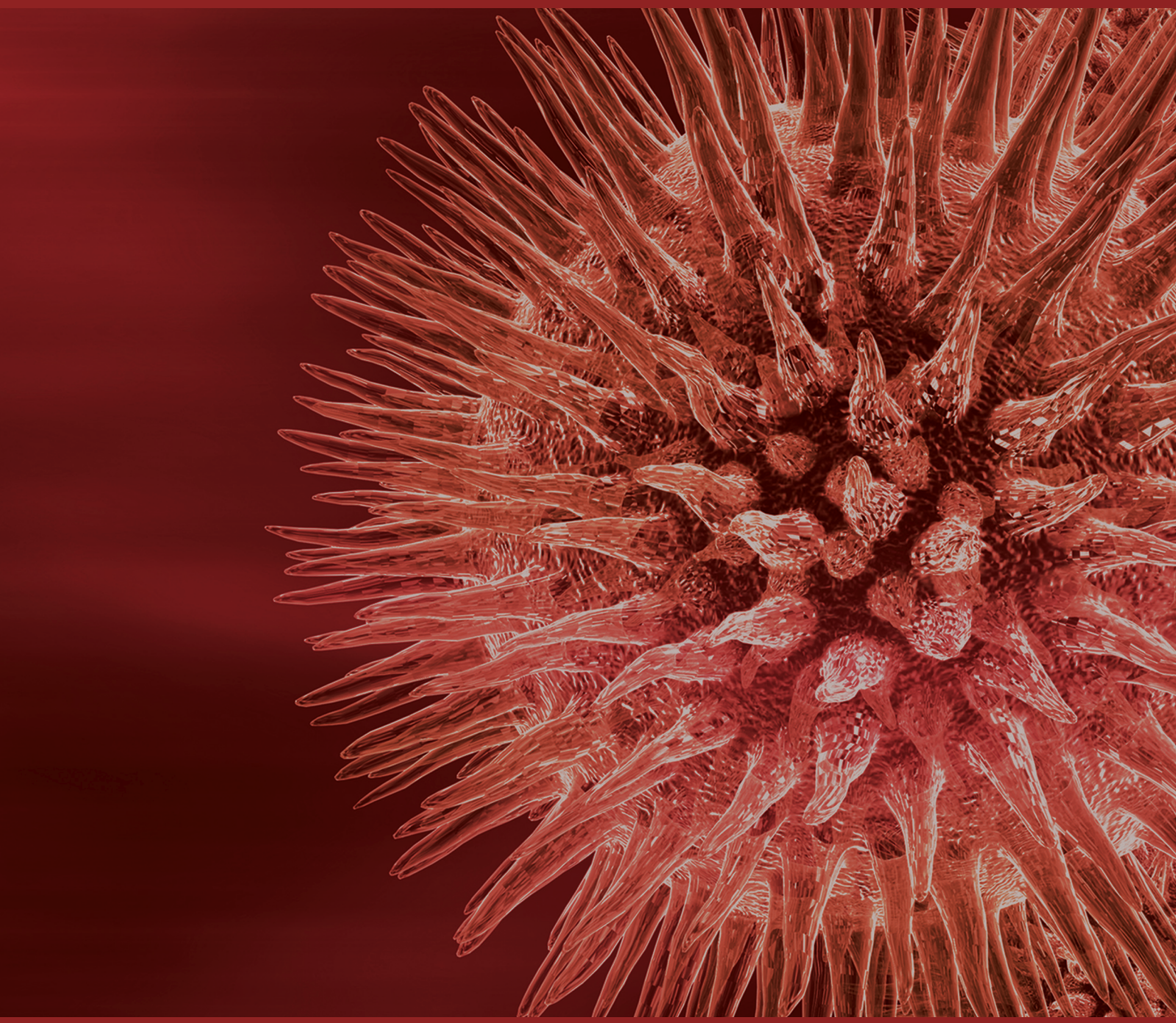

Novel Drugs Development for Cardio-/Cerebrovascular Diseases

BioMed Research International

Novel Drugs Development for Cardio-/Cerebrovascular Diseases

Guest Editors: Joen-Rong Sheu, Philip Aloysius Thomas, and Juei-Tang Cheng

Contents

Hindawi Publishing Corporation
BioMed Research International
Volume 2014, Article ID 467936, 2 pages
http://dx.doi.org/10.1155/2014/467936

Editorial

Novel Drugs Development for Cardio-/Cerebrovascular Diseases

Joen-Rong Sheu,[1] Philip Aloysius Thomas,[2] and Juei-Tang Cheng[3]

[1] *Graduate Institute of Medical Sciences, College of Medicine, Taipei Medical University, Taipei 110, Taiwan*
[2] *Department of Microbiology, Institute of Ophthalmology, Joseph Eye Hospital, Tiruchirappalli, Tamil Nadu 620 001, India*
[3] *Department of Medical Research, Chi-Mei Medical Center, Yung Kang City, Tainan 101, Taiwan*

Correspondence should be addressed to Joen-Rong Sheu; sheujr@tmu.edu.tw

Received 31 May 2014; Accepted 31 May 2014; Published 17 June 2014

Cardiovascular and cerebrovascular diseases are the leading causes of death worldwide. According to the current epidemiological data, it is expected that, till 2020, coronary artery disease and cerebral hemorrhage are still the first and second causes of death of human beings, even though the order of the death causes due to human diseases would be changed significantly. Despite various advances in the understanding of the diseases, pharmacological treatment by conventional medicine has not obtained satisfactory results. However, recent studies suggest that natural products and traditional herbal medicine are a potential candidate for the preventative treatment of the disorders. Therefore, we have invited the researchers to contribute few research/review papers to provide solid evidence that supports the application of bioactives/traditional herbal medicine (THM) in prevention and treatment of cardiovascular and cerebrovascular diseases.

The first paper of this special issue investigates the role of peroxisome proliferator-activated receptors (PPARδ) in ginseng-induced modification of cardiac contractility. It was suggested that ginseng could enhance cardiac contractility through increased PPARδ expression in cardiac cells. The second paper investigates the role of musclin, a novel skeletal muscle-derived factor found in the signal sequence trap of mouse skeletal muscle cDNAs, using animal model of hypertension and characterizes its direct effect on vascular contraction. This paper provides the evidence that supports the fact that musclin is involved in hypertension and, thus, it is appropriate to consider as a novel target for treatment of hypertension, and another paper in this issue suggests that allantoin, as imidazoline I-1 receptors (I-1R) agonist, has the potential to develop as a new therapeutic agent for hypertension.

Amarogentin prevents platelet activation through the inhibition of PLCγ2-PKC cascade and MAPK pathway. This hypothesis is well presented in this special issue and findings suggest that amarogentin may offer therapeutic potential for preventing or treating thromboembolic disorders. Many clinical reports have suggested that the ascorbyl free radical ($Asc^{\bullet}$) can be treated as a noninvasive, reliable, real-time marker of oxidative stress, but its generation mechanisms in human blood have rarely been discussed. A paper in this issue studied upstream substances, enzyme inhibitors, and free radical scavengers to delineate the mechanisms of $Asc^{\bullet}$ formation in human platelet-rich plasma (PRP). This paper shows a well-defined protocol that adopts the hypothesis that $Asc^{\bullet}$ formation is associated with the inhibitors of NADPH oxidase (NOX), cyclooxygenase (COX), lipoxygenase (LOX), cytochrome P450 (CYP450), mitochondria complex III, nitric oxide synthase (NOS), and mitochondria in human PRP. Another subsequent paper shows that the cardioprotective effect of hypertonic saline is associated with inhibitory effect on macrophage migration inhibitory factor in sepsis; the authors of this paper suggest that hypertonic saline improves endotoxemia-induced myocardial contractility and prevents circulatory failure, contributing to the improvement of intracellular calcium handling process.

Another interesting paper in this special issue presents a pig model of myocardial ischemia/reperfusion (MIR) injury to investigate the maximum rate of change of left ventricular pressure, left ventricular end-diastolic pressure, and left intraventricular pressure. The role of δ-opioid receptor activation

using D-Ala2, D-Leu5-enkephalin (DADLE) in both early (D1) and late (D2) phases of cardioprotection is identified in this paper and shows that DADLE after the ischemia has no benefit but combined treatment with anisodamine, a naturally occurring atropine-like compound, seems to have a marked postischemic cardioprotection. Therefore, this paper recommends that anisodamine is helpful in combination with DADLE for postischemic cardioprotection. Rutaecarpine (RUT), a major bioactive ingredient isolated from the Chinese herb *Evodia rutaecarpa*, possesses a wide spectrum of biological activities, including anti-inflammation and prevention of cardiovascular diseases. A derivative of this compound, bromo-dimethoxyrutaecarpine (Br-RUT), has been taken for a study in this special issue to evaluate its cardioprotective role. This paper establishes that Br-RUT has very low cytotoxicity in RAW 264.7 macrophages but retains its activities against inflammation and vasodilation via enhanced expression of transient receptor potential vanilloid type 1 and activated endothelial nitric oxide synthase (NOS) that could be beneficial for cardiovascular disease therapeutics.

We anticipate that readers will find that this special issue reports the important contests, prospects, and existing advances that are presently being oppressed in cardiovascular research with the potential to encourage the application of novel drug development for elevating the attention and treatment of patients with cardiovascular disease.

Joen-Rong Sheu
Philip Aloysius Thomas
Juei-Tang Cheng

Hindawi Publishing Corporation
BioMed Research International
Volume 2014, Article ID 182657, 8 pages
http://dx.doi.org/10.1155/2014/182657

Research Article

Research of Electrosurgical Ablation with Antiadhesive Functionalization on Thermal and Histopathological Effects of Brain Tissues In Vivo

Wen-Tien Hsiao,[1] Chun-Ming Kung,[2,3,4] Jan-Show Chu,[5] Keng-Liang Ou,[4,6,7,8] and Pei-Wen Peng[9]

[1] *School of Dentistry, Taipei Medical University, Taipei 110, Taiwan*
[2] *Department of Dentistry, Cathay General Hospital, Taipei 106, Taiwan*
[3] *Department of Dentistry, Cathay General Hospital, Sijhih, Taipei 221, Taiwan*
[4] *Research Center for Biomedical Devices and Prototyping Production, Taipei Medical University, Taipei 110, Taiwan*
[5] *Department of Pathology, School of Medicine, Taipei Medical University, Taipei 110, Taiwan*
[6] *Graduate Institute of Biomedical Materials and Tissue Engineering, Taipei Medical University, No. 250, Wu-Hsing Street, Taipei 110, Taiwan*
[7] *Department of Dentistry, Taipei Medical University, Shuang Ho Hospital, Taipei 235, Taiwan*
[8] *Research Center for Biomedical Implants and Microsurgery Devices, Taipei Medical University, Taipei 110, Taiwan*
[9] *School of Dental Technology, Taipei Medical University, No. 250, Wu-Hsing Street, Taipei 110, Taiwan*

Correspondence should be addressed to Keng-Liang Ou; klou@tmu.edu.tw and Pei-Wen Peng; apon@tmu.edu.tw

Received 27 February 2014; Revised 23 April 2014; Accepted 23 April 2014; Published 22 May 2014

Academic Editor: Joen-Rong Sheu

Thermal injury and tissue sticking are two major concerns in the electrosurgery. In the present study, the effect of lateral thermal injury caused by different electrosurgical electrodes on wound healing was investigated. An electrosurgical unit equipped with untreated (SS) and titanium oxide layer-coated (TiO_2-coated) stainless steel needle-type electrodes was used to create lesions on the rat brain tissue. TiO_2 layers were produced by radiofrequency plasma and magnetron sputtering in the form of amorphous (TO-SS-1), anatase (TO-SS-2), and rutile (TO-SS-3) phase. Animals were sacrificed for evaluations at 0, 2, 7, and 28 days postoperatively. TO-SS-3 electrodes generated lower levels of sticking tissue, and the thermographs showed that the recorded highest temperature in brain tissue from the TO-SS-3 electrode was significantly lower than in the SS electrode. The total injury area of brain tissue caused by TO-SS-1 and TO-SS-3 electrodes was significantly lower than that caused by SS electrodes at each time point. The results of the present study reveal that the plating of electrodes with a TiO_2 film with rutile phases is an efficient method for improving the performance of electrosurgical units and should benefit wound healing.

1. Introduction

Electrosurgery has been widely accepted by physicians to aid in the removal of tumors since its original application by Bovie and Cushing in the 1920s. The basic components of a monopolar electrosurgery consist of the high-intensity radiofrequency (RF) generator, the active electrode, the dispersive pad, and the patient. RF alternating current flows through tissue from an active electrode to a dispersive pad, resulting in tissue cutting, coagulation, and ablation [1].

RF tissue ablation makes thermal lesions and tissue coagulation around the tip of an active needle electrode. Although needle ablation has been widely applied to cardiology, urology, neurosurgery, and otolaryngology, there are still rare but occasionally serious complications that accompany the procedure [2]. The heat can destroy the targeted tumor in a range of 65–75°C, and the temperatures above 75°C cause significant adjacent structures destruction [3]. Nontarget thermal damage to vital structures and tissue destruction adjacent to targeted lesions are the common complications

from the needle ablation due to a rapid local temperature rise from the high current density. Carbonized charred tissue sticking to the electrode causes an abrupt drop in current density and eventually ceasing the operation [4]. Meanwhile, the sufficient lesion depth and diameter are difficult to obtain. To address these concerns, the RF ablation has incorporated different strategies to minimize the lateral spread of thermal energy and carbonized charred tissues, such as the automatic thermal monitoring system [5], the image-guide system [6], and the percutaneous saline-enhanced and impedance-controlled system [7]. Recently, a relative simple method, the surface modification of the electrode, has been introduced to prevent lateral thermal damage and increase the precision of the lesion depth and diameter. Çeviker et al. [8] introduced the Teflon- (tetrafluoroethylene, PTFE-) coated electrode substrate to reduce the level of tissue sticking and charring. Simmons et al. [9] compared the gold- and platinum-coated electrodes on myocardial lesion size and suggested that deeper lesions should be able to be made when RF energy is delivered to a gold rather than platinum tip electrode. However, the optimal approach is still under development and an alternative coating material, titanium dioxide (TiO_2), has attempted to overcome the clinical drawbacks in the present study.

TiO_2 was used in a wide range of technological applications due to its high refractive index, excellent transmittance, and photocatalytic property [10, 11]. Recently, TiO_2 has been reported to be good biocompatible and blood compatible. The TiO_2 group is composed of three types of crustal structures, and especially the rutile and anatase phases have evolved as the model system in the surface coatings for biomedical materials [12]. Rutile and anatase phases have similar band-gap energies and they can be changed from insulator to a semiconductor by means of altering processing parameters [13].

The present study was directed toward quantification and comparison of the lesion position and thermal distribution produced by the monopolar RF energy application with different coatings. Specifically, the present study evaluated the effect of the various coatings of monopolar on the short-term histologic properties of brain tissue in an in vivo rat model.

2. Materials and Methods

2.1. TiO_2 Thin Film Deposition and Property Evaluations. A deposition process that combined radiofrequency plasma and magnetron sputtering system equipped with one pure Ti target (99.99% purity) was utilized to deposit the TiO_2 film on commercial electrode (needle-type austenite AISI 304 stainless steel denoted as a SS electrode). All of the substrates were cleaned in an ultrasonic bath with a sequence of acetone and ethanol for 15 min followed by air drying before being loaded into the chamber. Subsequently, the chamber was evacuated at vacuum pressure 2.0×10^{-6} torr for 15 min and then the substrates were presputtered by Ar^+ cleaning for 10 min to remove the native adsorbed contaminants and impurities under a radiofrequency power 225 W with chamber running pressure 8.0×10^{-3} torr. After cleaning process, a mixture of O_2/Ar with a fixed flow ratio (40/60) was introduced through mass flow controller to keep a working pressure of 8.0×10^{-3} torr. Then, the substrate holder was heated and kept at 300°C during the following deposition. The untreated Ti was treated at a negative bias voltage of 200 V and the varying powers for 30 min, creating a controlled TiO_2 layer. For ease of identification, the SS electrodes coated with TiO_2 layer at the amorphous, anatase, and rutile phases were labeled as TO-SS-1, TO-SS-2, and TO-SS-3 electrodes, respectively.

Raman spectra were recorded using the Horiba HR800 (Protrustech Co., Ltd., Taipei, Taiwan) with a 633 nm laser to detect the TiO_2 phases. Topographical analyses were conducted using an atomic force microscope (AFM, DPN 5000, NanoInk, Skokie, IL, USA). The silicon nitride probe was scanned over a $1\,\mu m \times 1\,\mu m$ area in the tapping mode. The contact angles of the specimens were assessed by dropping 0.4 mL of distilled water on specimens and measured using a video-based goniometer (EA-01, Jeteazy Co., Ltd., Hsinchu, Taiwan). The specimens were tested 6 times to obtain average contact angle values.

2.2. In Vivo Study

2.2.1. Animal Models. RF-induced thermal lesion experiments were conducted in normal rat brain model. The animal procedures were approved and conducted by the Institutional Animal Care and Use Committee at Taipei Medical University (number LAC-99-0037). A total of 48 male Sprague-Dawley rats (weighing 276–300 g, BioLASCO Taiwan Co., Ltd., Taipei, Taiwan) were purchased and housed in cages for 14 days prior to experimentation. Food and water were available ad libitum. The animals were randomly allocated into 3 different experimental groups of 16 animals each.

2.2.2. Surgical Procedures. Aseptic precautions were utilized in all surgical procedures. The animals were positioned in a stereotactic frame under pentobarbital anaesthesia (40 mg/kg IP). Bilateral cranial burr holes (1 mm) were drilled on the right and the left, at the coronal suture 4.0 mm lateral to the midline. Lesions were performed bilaterally using an ERBE ICC 300 RF generator (Elektromedizin GmbH, Tübingen, Germany). A monopolar current at 20 W power setting was used and the duration of each penetration was 3 s. Three TiO_2-coated electrodes (TO-SS-1, TO-SS-2, and TO-SS-3) were evaluated and the regular SS electrode without any coatings was used as the control (SS). The TiO_2-coated electrode was applied to one side and the SS electrode to the other. Performance of each electrode group was determined based on thermometry, tissue sticking, and histological examination.

2.2.3. Real-Time Thermometry and Quantification of Tissue Sticking. Real-time thermometry data was recorded from the initiation to completion of each lesion using a thermal-imaging infrared camera with the thermal analysis simulation software (Advanced Thermo TVS-500EX, NEC Avio Technologies, Tokyo, Japan). The weight of each electrode was

Table 1: Surface roughness, contact angle, and water drop profiles for SS and TiO_2-coated electrodes.

Description	TiO_2 phase	Roughness (nm)	Contact angle (degree)	Water drop profiles
SS	Untreated	5.73 ± 0.31	70.3 ± 1.4	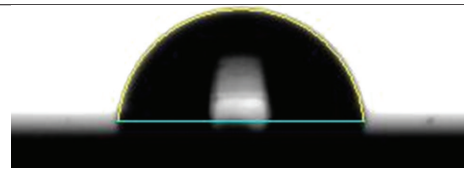
TO-SS-1	Amorphous	2.41 ± 0.37	89.3 ± 3.1	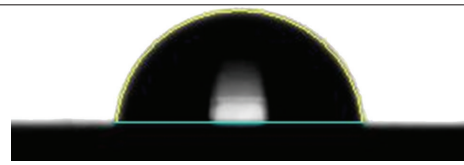
TO-SS-2	Anatase	2.52 ± 0.21	91.9 ± 2.2	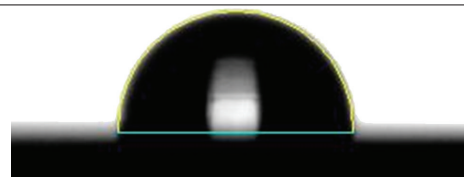
TO-SS-3	Rutile	3.44 ± 0.27	92.8 ± 2.4	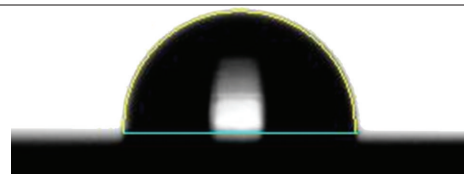

measured before and after the operation. The degree of tissue sticking was calculated as the weight of sample after operation minus the weight of sample before operation.

2.2.4. Injury Area and Histological Examination. Rats in each group were sacrificed after 0, 2, 7, and 28 days' recovery period ($n = 4$). Perfusion was done with 0.9% saline and then paraformaldehyde. Brains were taken and fixed in 10% buffered formalin and the samples covering lesions were cut from the brain specimens. They were treated in a graded alcohol series and embedded in paraffin. Continuous tissue sections (3 μm) for all brain samples were taken for hematoxylin and eosin (H&E, 3008-1&3204-2, Muto, Japan). Stained samples were observed under a light microscope (BX51, Olympus, Japan). The total injury area in lesions for each group was quantified by the image software (SPOT basic software, SPOT imaging solutions, MI, USA).

2.3. Statistical Analysis. Statistical analyses were performed using the commercially available software program, SPSS 14.0 (Statistical Package for the Social Sciences, SPSS Inc., Chicago, IL, USA). For each experiment, data from 6 replicates were expressed as mean ± standard deviation (SD) per variable, which were repeated to ensure validity. Analysis of variance (ANOVA) for comparison between groups was first performed and then Student-Newman-Keuls test was used in every other group. The statistical significance level was set at $P < 0.05$.

3. Result and Discussions

Raman spectra of TiO_2-coated electrodes are shown in Figure 1. No peaks were observed in the Raman spectra of the TO-SS-1 electrode. For the TO-SS-2 electrode, the Raman lines at 151, 409, 515, and 633 cm^{-1} were assigned as the E_g, B_{1g}, A_{1g} or B_{1g}, and E_g modes of the anatase phase, respectively, indicating that an anatase phase was formed in the SS electrode [14]. For the TO-SS-3 electrode, a band at 142.3 cm^{-1} was related to the long-range ordered structure of the crystalline rutile phase [15]. The 245.2 cm^{-1} mode is frequently observed in nanophase TiO_2, whereas the mode at 442.2 is associated with the E_g phase of the rutile phase, and 609.5 cm^{-1} is associated with the A_{1g} modes of the rutile phase [16].

Figure 2 shows the surface morphologies of the SS and TiO_2-coated electrodes using an AFM, which were acquired in a scanned range of $5 \times 5\ \mu m^2$. The SS electrode exhibited relatively planar surfaces with parallel polishing traces, as shown in Figure 2(a). The TiO_2-coated electrodes exhibited similar topographies as shown in Figures 2(b) to 2(d), which exhibited the formation of a more uniform and denser TiO_2 layer nanostructure with round grains. Table 1 lists the average surface roughness values. There was no difference between groups.

The contact angle of distilled water on SS and TiO_2-coated surfaces was examined, with results shown in Table 1. The SS surfaces had the lowest value (70.3 ± 1.4), whereas TO-SS-1 surfaces exhibited comparative hydrophobicity, with

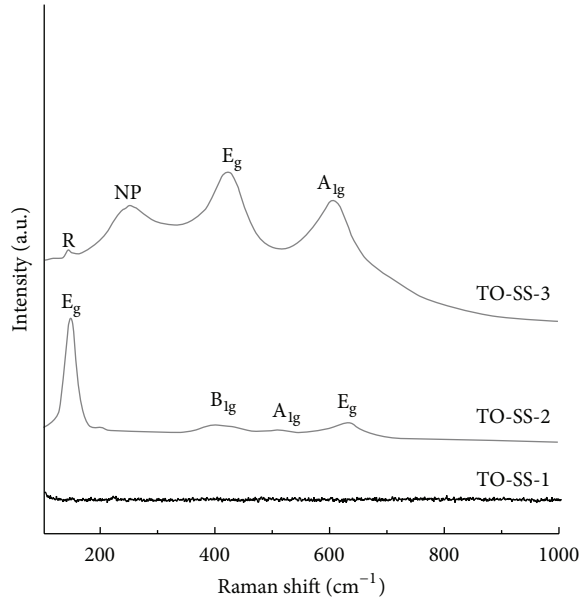

FIGURE 1: Raman spectrum of SS and TiO_2-coated electrodes.

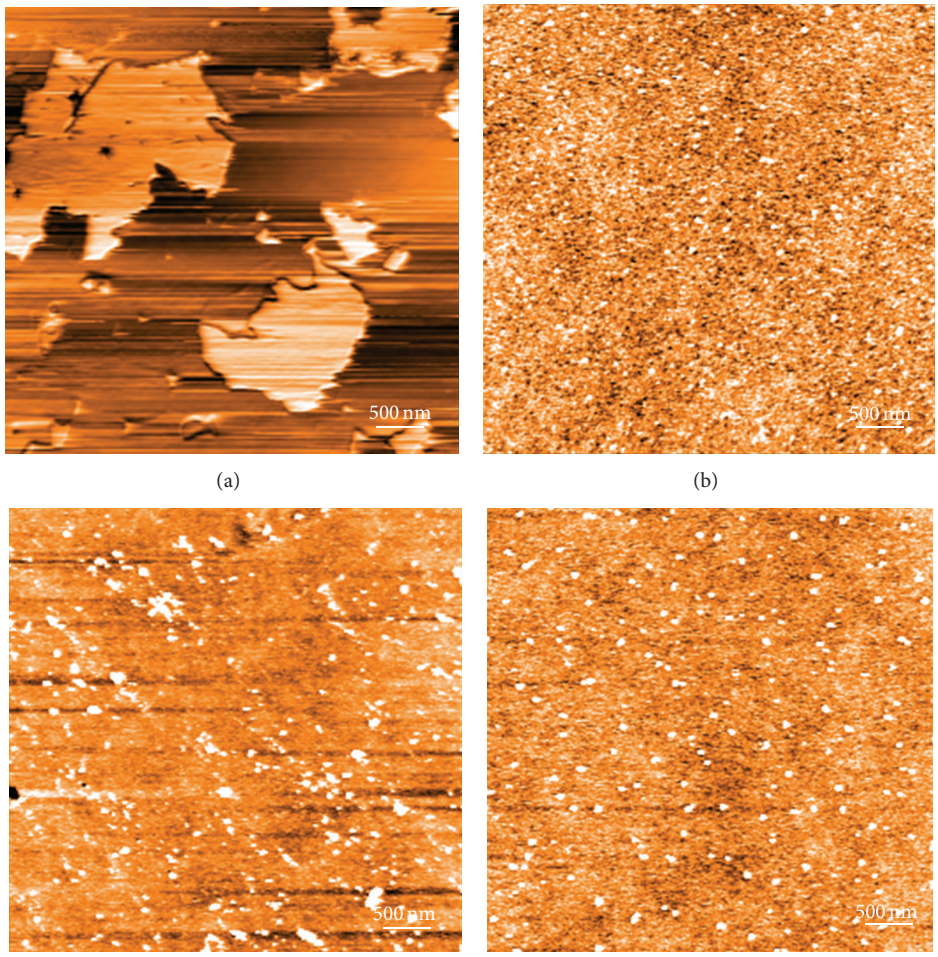

FIGURE 2: AFM tapping mode images (scan area 5 μm × 5 μm) of (a) SS, (b) TO-SS-1, (c) TO-SS-2, and (d) TO-SS-3 electrodes ((a, c) are 2D mode and (b, d) are 3D mode).

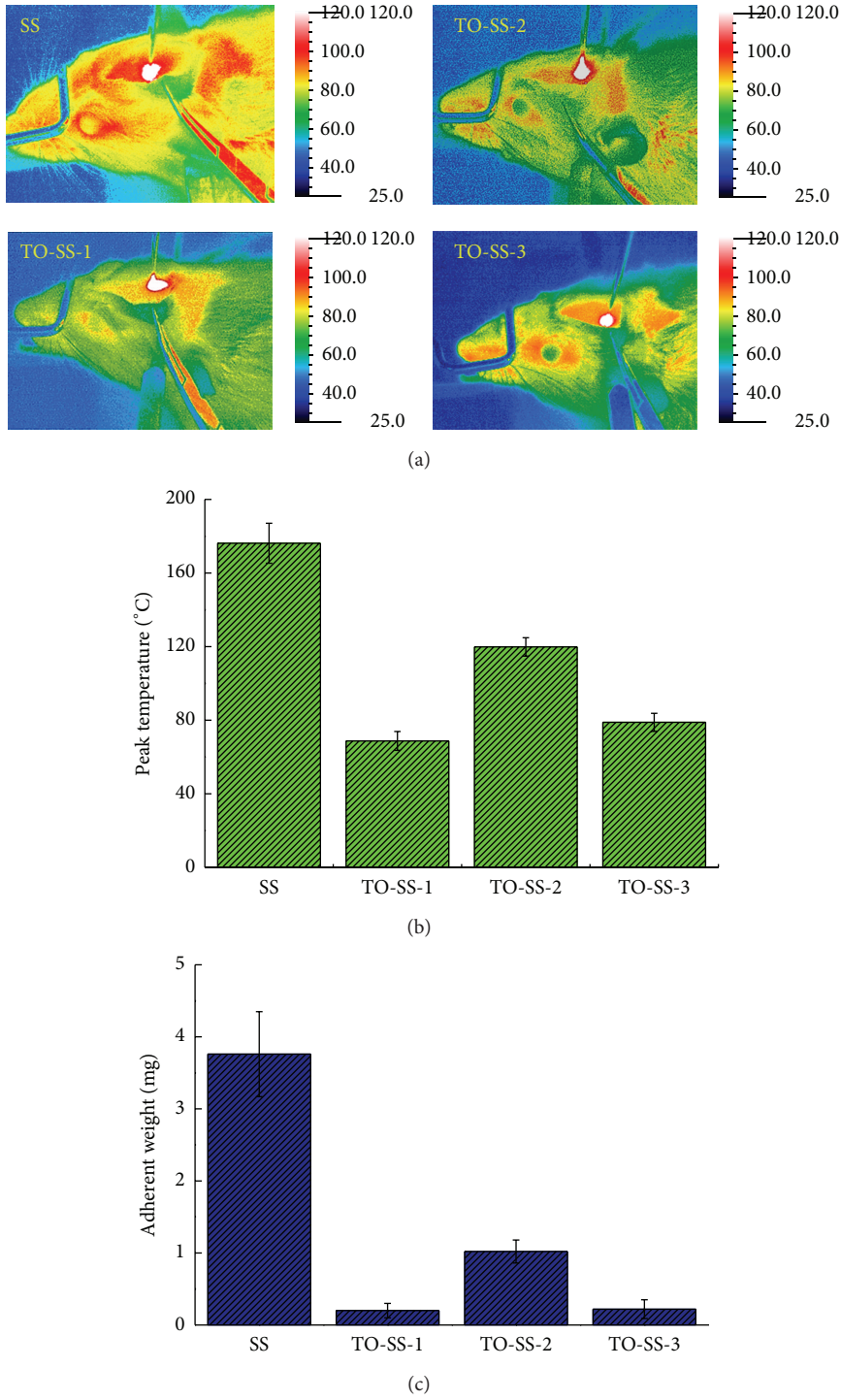

FIGURE 3: Comparisons of (a) thermographs, (b) the peak temperature, and (c) adherent weight for SS and TiO_2-coated electrodes.

a value of 92.8 ± 2.4. One-way ANOVA revealed a significant difference between the SS and TiO_2-coated electrodes ($P < 0.05$). However, no significant difference between the TiO_2-coated electrodes was observed ($P > 0.05$).

The temperature distributions in ex vivo rat brain tissue around the SS and TiO_2-coated electrodes measured using an infrared thermal imaging camera are shown in Figure 3(a). A similar temperature distribution was found in experiments carried out with each needle type. Carbonization and tissue sticking occurred at the needle tips of each electrode, where the maximum temperatures were found in a concentric ring 3–5 mm. The highest temperature recorded while applying a SS sample was 176.18 ± 10.87°C. The highest temperatures recorded for TO-SS-1, TO-SS-2, and TO-SS-3 electrodes were

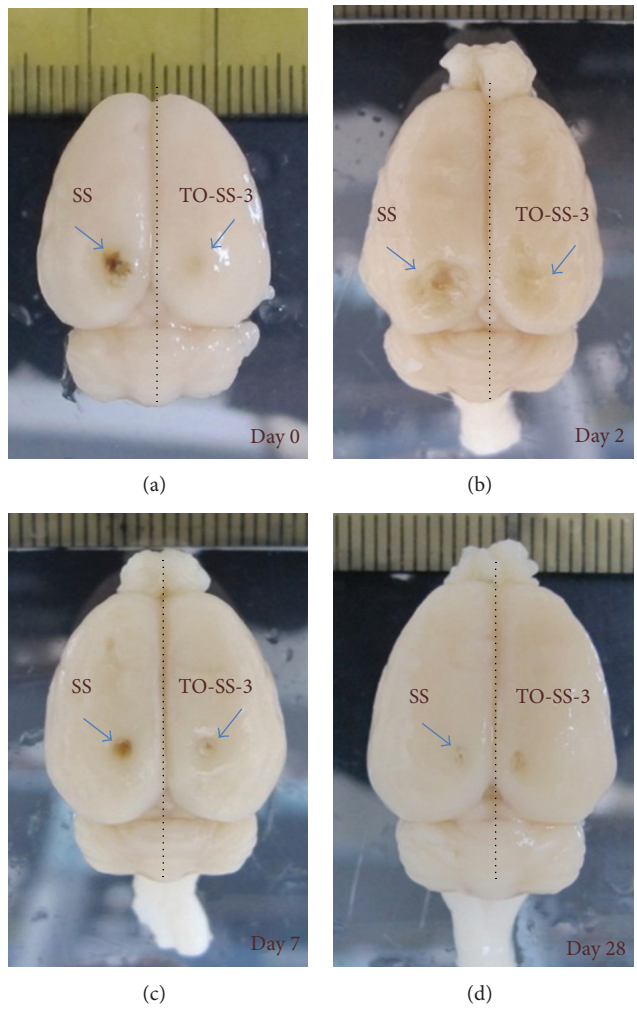

Figure 4: Gross observations showed the injury site created by SS (left) and TO-SS-3 (right) electrodes at (a) day 0, (b) day 2, (c) day 7, and (d) day 28.

68.73 ± 5.12°C, 119.85 ± 5.01°C, and 78.83 ± 4.92°C, respectively, which were significantly lower than that in the SS group ($P < 0.01$) (Figure 3(b)). Electrodes were weighed before and after the operation for each group in order to measure the amount of tissue sticking to the needle tip (Figure 3(c)). The SS electrode needle tip showed a significantly higher amount of adhering tissue than the TiO_2-coated electrode ($P < 0.05$). Among the TiO_2-coated electrodes, the TO-SS-2 electrode exhibited the lowest amount of tissue adherent.

Pictures shown in Figure 4 reveal the difference in the total lesion areas caused by SS and TO-SS-3 electrodes. The injury created by the SS electrode was larger than that of the TO-SS-3 electrode as shown in Figure 4(a). The borders of the lesions sites for both electrodes were beginning to heal by the end of day 2, being both wider and shallower than immediately after the operation (Figure 4(b)). By day 7 the lesion areas were smaller for both the SS and TO-SS-3 electrodes, and few blood cells remained (Figure 4(c)). By the end of day 28, the lesion created by TO-SS-3 electrodes was healed, and the small lesion site created by SS electrodes still remained as shown in Figure 4(d).

Histological examination of specimens for all electrode types showed varying amounts of coagulation necrosis and bleeding, indicating heat damage to the tissue as shown in Figure 5. When TO-SS-3 and TO-SS-1 electrodes were used, no obvious bleeding was detected postoperatively in treated tissues. In contrast, hemorrhaging caused by SS and TO-SS-2 electrodes was evident. At day 2, hemorrhaging in SS groups was markedly higher than in the other groups, and infections and apoptosis were observed at the treated site. The thermal-injury areas caused by SS electrodes were larger than those by the TiO_2-treated electrodes, with the least tissue damage found when using the TO-SS-3 electrode. The thermal-injury areas tended to diminish for all groups at the end of day 7.

Commercially available electrosurgical electrodes are usually coated with Teflon to avoid tissue sticking. However, surgical smoke with an unfavorable flavor encouraged the advanced approaches. The objective of the present study was to establish an in vivo rat model to study the thermal effects on damage to brain tissue caused by electrosurgical ablation with TiO_2-coated needle-type electrodes.

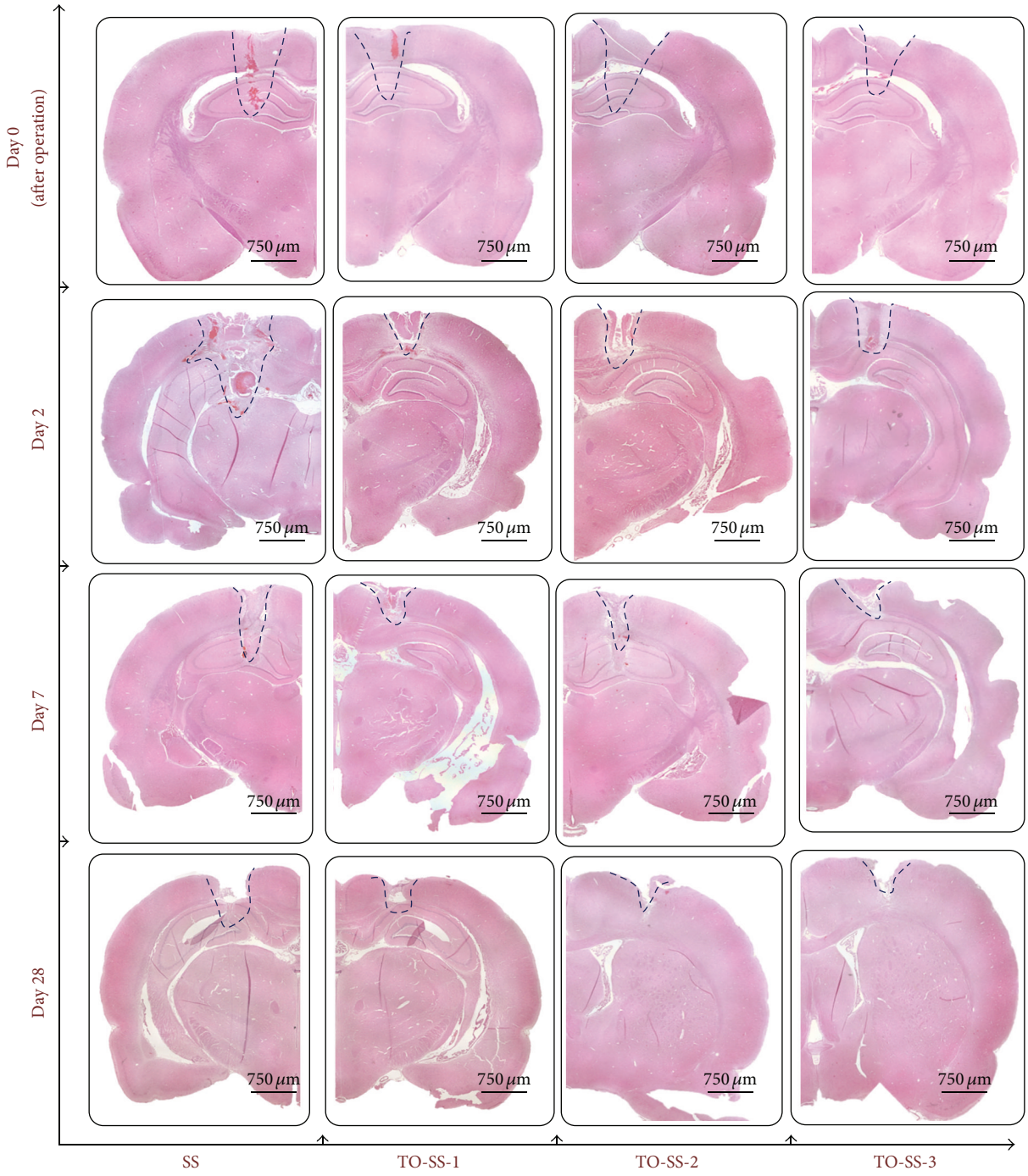

Figure 5: Histological observation of injury area caused by SS and TiO_2-coated electrodes at the end of day 0, day 2, day 7, and day 28.

It is well known that titanium possesses its excellent biocompatibility due to its very stable and corrosion resistant oxide layer [17, 18]. TiO_2 layers have been considered a promising coating for implants with proven biocompatibility and blood compatibility [13, 19]. Therefore, coatings of TiO_2 layers have been deposited on various devices via various technologies to increase clinical effectiveness. By means of radiofrequency plasma and magnetron sputtering, a layer of rutile, anatase, or amorphous phase TiO_2 layer was deposited on commercially available electrodes.

Tissue thermographs showed that temperatures recorded for TO-SS-3 electrodes were significantly lower than those for SS electrodes under the same RF power setting. This can be attributed to the high electric and thermal conductivity of rutile phase TiO_2 film [20]. Hence a TO-SS-3 electrode can deliver electrical energy to the target tissue more efficiently.

This can prevent overheating of the electrode substrate and reduce the incidence of thermal injury. Macroscopic observation and histological examination showed clearly that TO-SS-3 electrodes produce a smaller area of injury than commercial SS electrodes.

4. Conclusion

A TiO_2 film accompanied with hydrophobic surface can be formed and bonded on the needle-type electrode substrate via radiofrequency plasma and magnetron sputtering system. The enhanced thermal conductivity and surface hydrophobicity of TiO_2 coatings with rutile phase can improve the performance of electrosurgical electrodes, in terms of tissue sticking and thermal injury. TO-SS-3 electrodes had lower levels of sticking tissue with lower surgical temperatures during electrosurgery. The total injury area of rats brain tissue treated with TO-SS-3 electrodes was significantly smaller than those of rat brain tissues treated with SS electrodes at all time points. This study reveals that the plating of TiO_2 coatings on electrode substrates is a simple and effective means of improving the performance of electrosurgical units.

Conflict of Interests

The authors declare that there is no conflict of interests regarding the publication of this paper.

Authors' Contribution

Wen-Tien Hsiao and Chun Ming Kung contributed equally to this work.

Acknowledgment

This work was supported by a Grant from Taipei Medical University, under Grant no. TMU101-AE3-Y12.

References

[1] T. L. Smith and J. M. Smith, "Electrosurgery in otolaryngology-head and neck surgery: principles, advances, and complications," *The Laryngoscope*, vol. 111, no. 5, pp. 769–780, 2001.

[2] H. Rhim, G. D. Dodd III, K. N. Chintapalli et al., "Radiofrequency thermal ablation of abdominal tumors: lessons learned from complications," *Radiographics*, vol. 24, no. 1, pp. 41–52, 2004.

[3] P. Hecht, K. Hayashi, A. J. Cooley et al., "The thermal effect of monopolar radiofrequency energy on the properties of joint capsule: an in vivo histologic study using a sheep model," *The American Journal of Sports Medicine*, vol. 26, no. 6, pp. 808–814, 1998.

[4] T. Lorentzen, "A cooled needle electrode for radiofrequency tissue ablation: thermodynamic aspects of improved performance compared with conventional needle design," *Academic Radiology*, vol. 3, pp. 556–563, 1996.

[5] H. Calkins, E. Prystowsky, M. Carlson, L. S. Klein, J. P. Saul, and P. Gillette, "Temperature monitoring during radiofrequency catheter ablation procedures using closed loop control. Atakr Multicenter Investigators Group," *Circulation*, vol. 90, no. 3, pp. 1279–1286, 1994.

[6] S. Clasen and P. L. Pereira, "Magnetic resonance guidance for radiofrequency ablation of liver tumors," *Journal of Magnetic Resonance Imaging*, vol. 27, no. 2, pp. 421–433, 2008.

[7] J. Kettenbach, W. Köstler, E. Rücklinger et al., "Percutaneous saline-enhanced radiofrequency ablation of unresectable hepatic tumors: initial experience in 26 patients," *The American Journal of Roentgenology*, vol. 180, no. 6, pp. 1537–1545, 2003.

[8] N. Çeviker, S. Keskil, and K. Baykaner, "A new coated bipolar coagulator: technical note," *Acta Neurochirurgica*, vol. 140, no. 6, pp. 619–620, 1998.

[9] W. N. Simmons, S. Mackey, D. S. He, and F. I. Marcus, "Comparison of gold versus platinum electrodes on myocardial lesion size using radiofrequency energy," *Pacing and Clinical Electrophysiology*, vol. 19, pp. 398–402, 1996.

[10] J. C. Yu, W. Ho, J. Lin, H. Yip, and P. K. Wong, "Photocatalytic activity, antibacterial effect, and photoinduced hydrophilicity of TiO_2 films coated on a stainless steel substrate," *Environmental Science and Technology*, vol. 37, no. 10, pp. 2296–2301, 2003.

[11] U. Diebold, "Structure and properties of TiO_2 surfaces: a brief review," *Applied Physics A*, vol. 76, no. 5, pp. 681–687, 2003.

[12] Y. Liu and A. R. West, "Semiconductor-insulator transition in undoped rutile, TiO_2, ceramics," *Journal of the American Ceramic Society*, vol. 96, pp. 218–222, 2013.

[13] M. F. Maitz, M.-T. Pham, E. Wieser, and I. Tsyganov, "Blood compatibility of titanium oxides with various crystal structure and element doping," *Journal of Biomaterials Applications*, vol. 17, no. 4, pp. 303–319, 2003.

[14] W. F. Zhang, Y. L. He, M. S. Zhang, Z. Yin, and Q. Chen, "Raman scattering study on anatase TiO_2 nanocrystals," *Journal of Physics D*, vol. 33, no. 8, pp. 912–916, 2000.

[15] M. S. P. Francisco and V. R. Mastelaro, "Inhibition of the anatase-rutile phase transformation with addition of CeO2 to CuO-TiO_2 system: raman spectroscopy, X-ray diffraction, and textural studies," *Chemistry of Materials*, vol. 14, no. 6, pp. 2514–2518, 2002.

[16] J. Zhang, M. Li, Z. Feng, J. Chen, and C. Li, "UV raman spectroscopic study on TiO_2-I. phase transformation at the surface and in the bulk," *Journal of Physical Chemistry B*, vol. 110, no. 2, pp. 927–935, 2006.

[17] M. S. Wang, F. P. Lee, Y. D. Shen, C. H. Chen, K. L. Ou, and S. F. Ou, "Surface, biocompatible and hemocompatible properties of meta-amorphous titanium oxide film," *International Journal of Applied Ceramic Technology*, 2013.

[18] P. C.-H. Kuo, H.-H. Chou, Y.-H. Lin, P.-W. Peng, and K.-L. Ou, "Effects of surface functionalization on the nanostructure and biomechanical properties of binary titanium-niobium alloys," *Journal of the Electrochemical Society*, vol. 159, no. 5, pp. E103–E107, 2012.

[19] Z. Yang, J. Wang, R. Luo et al., "Improved hemocompatibility guided by pulsed plasma tailoring the surface amino functionalities of TiO_2 coating for covalent immobilization of heparin," *Plasma Processes and Polymers*, vol. 8, no. 9, pp. 850–858, 2011.

[20] H. Okubo, "Enhancement of electrical insulation performance in power equipment based on dielectric material properties," *IEEE Transactions on Dielectrics and Electrical Insulation*, vol. 19, pp. 733–754, 2012.

Hindawi Publishing Corporation
BioMed Research International
Volume 2014, Article ID 728019, 9 pages
http://dx.doi.org/10.1155/2014/728019

Research Article

Amarogentin, a Secoiridoid Glycoside, Abrogates Platelet Activation through PLCγ2-PKC and MAPK Pathways

Ting-Lin Yen,[1] Wan-Jung Lu,[1] Li-Ming Lien,[2,3] Philip Aloysius Thomas,[4] Tzu-Yin Lee,[1] Hou-Chang Chiu,[3,5] Joen-Rong Sheu,[1] and Kuan-Hung Lin[1,6]

[1] *Graduate Institute of Medical Sciences and Department of Pharmacology, College of Medicine, Taipei Medical University, 250 Wu-Hsing Street, Taipei 110, Taiwan*
[2] *School of Medicine, Taipei Medical University, 250 Wu-Hsing Street, Taipei 110, Taiwan*
[3] *Department of Neurology, Shin Kong Wu Ho-Su Memorial Hospital, 95 Wen-Chang Road, Taipei 111, Taiwan*
[4] *Department of Microbiology, Institute of Ophthalmology, Joseph Eye Hospital, 138 Melapudur, Tiruchirappalli, Tamil Nadu 620 001, India*
[5] *College of Medicine, Fu-Jen Catholic University, 510 Zhongzheng Road, New Taipei City 242, Taiwan*
[6] *Central Laboratory, Shin-Kong Wu Ho-Su Memorial Hospital, 95 Wen-Chang Road, Taipei 111, Taiwan*

Correspondence should be addressed to Joen-Rong Sheu; sheujr@tmu.edu.tw and Kuan-Hung Lin; d102092002@tmu.edu.tw

Received 25 January 2014; Accepted 9 April 2014; Published 29 April 2014

Academic Editor: Juei-Tang Cheng

Amarogentin, an active principle of *Gentiana lutea*, possess antitumorigenic, antidiabetic, and antioxidative properties. Activation of platelets is associated with intravascular thrombosis and cardiovascular diseases. The present study examined the effects of amarogentin on platelet activation. Amarogentin treatment (15~60 μM) inhibited platelet aggregation induced by collagen, but not thrombin, arachidonic acid, and U46619. Amarogentin inhibited collagen-induced phosphorylation of phospholipase C (PLC)γ2, protein kinase C (PKC), and mitogen-activated protein kinases (MAPKs). It also inhibits *in vivo* thrombus formation in mice. In addition, neither the guanylate cyclase inhibitor ODQ nor the adenylate cyclase inhibitor SQ22536 affected the amarogentin-mediated inhibition of platelet aggregation, which suggests that amarogentin does not regulate the levels of cyclic AMP and cyclic GMP. In conclusion, amarogentin prevents platelet activation through the inhibition of PLCγ2-PKC cascade and MAPK pathway. Our findings suggest that amarogentin may offer therapeutic potential for preventing or treating thromboembolic disorders.

1. Introduction

Gentiana lutea is a plant that belongs to the family Gentianaceae, which grows in the mountains of central and southern Europe and in western Asia [1]. It is commonly used to treat digestive diseases. The extract of this plant was reported to inhibit cell proliferation of vascular smooth muscle cells [2] and exhibit antioxidant and radioprotective activities [3, 4]. It contains some of the most bitter-tasting compounds known and is used as a scientific basis for the measurement of bitterness. The active principle amarogentin, which is isolated from the extract of *Gentiana lutea*, is a bitter-tasting secoiridoid glycoside that was found to activate the human bitter taste receptor hTAS2R50 [5]. Amarogentin has also been reported to possess antitumorigenic [6, 7] and antidiabetic activities [8].

It is well-known that blood platelets play important roles in haemostatic processes and wound repair. When blood vessels are damaged, blood platelets will form platelet plugs on the sites of vessel injury in order to prevent blood loss [9]. However, deregulation of platelet activity may cause a wide variety of cardiovascular diseases, such as intraluminal thrombosis and atherosclerosis. Therefore, the development of antiplatelet agents that can prevent heart attack and ischemic stroke is warranted.

Although previous studies have suggested that amarogentin effectively prevents vascular diseases, its effects on platelet activation and thrombosis remains unclear. Since

our preliminary study showed that amarogentin (15~60 μM) inhibits collagen-induced platelet aggregation in human platelets, we further systematically investigated the detailed mechanisms underlying the amarogentin-mediated inhibition of platelet activation.

2. Materials and Methods

2.1. Materials. Amarogentin (88.9%) was purchased from ChromaDex (Irvine, CA). Arachidonic acid (AA), collagen (type I), 9,11-dideoxy-11α,9α-epoxymethanoprostaglandin (U46619), luciferin-luciferase, thrombin, SQ22536, phorbol-12,13-dibutyrate (PDBu), and 1H-[1,2,4]qxadiazolo[4,3-a]quinoxalin-1-one (ODQ) were purchased from Sigma (St. Louis, MO). The anti-phospho-c-Jun N-terminal kinase (JNK) (Thr^{183}/Tyr^{185}) and anti-phospho-p38 mitogen-activated protein kinase (MAPK) monoclonal antibodies (mAbs), and the anti-phospho-p44/p42 extracellular signal-regulated kinase (ERK) (Thr^{202}/Tyr^{204}), anti-phospholipase Cγ2 (PLCγ2), and anti-phospho (Tyr^{759}) PLCγ2 polyclonal antibodies (pAbs) were purchased from Cell Signaling (Beverly, MA). The anti-phospho-p38 MAPK Ser^{182} mAb was purchased from Santa Cruz (Santa Cruz, CA). The anti-α-tubulin mAb was purchased from NeoMarkers (Fremont, CA). The anti-phospho-Akt (Ser^{473}) and anti-Akt mAbs were purchased from Biovision (Mountain View, CA). The horseradish peroxidase- (HRP-) conjugated donkey anti-rabbit immunoglobulin G (IgG), the Hybond-P polyvinylidene difluoride (PVDF) membrane, the sheep anti-mouse IgG, and the enhanced chemiluminescence western blotting detection reagent were purchased from Amersham (Buckinghamshire, UK). The amarogentin was dissolved in DMSO and stored at 4°C.

2.2. Platelet Aggregation and ATP Release. The methods described by Sheu et al. [10] and Lin et al. [11] were followed for the preparation of human platelet suspensions. Blood was collected from healthy human volunteers (informed consent) who did not take medication during the preceding 2 wk and was mixed with acid-citrate-dextrose solution (1 : 9). The blood samples were subjected to centrifugation at 120 g for 10 min, and platelet-rich plasma (PRP) was collected. PRP was supplemented with PGE_1 (0.5 μM) and heparin (6.4 IU/mL) and then incubated for 10 min at 37°C. After centrifugation at 500 g for 10 min, the platelet pellets were suspended in Tyrode's solution containing 3.5 mg/mL bovine serum albumin (BSA), pH 7.3 (NaCl 11.9 mM, KCl 2.7 mM, $MgCl_2$ 2.1 mM, NaH_2PO_4 0.4 mM, $NaHCO_3$ 11.9 mM, and glucose 11.1 mM). Then, PGE_1 (0.5 μM), apyrase (1.0 U/mL), and heparin (6.4 IU/mL) were added, and the mixture was incubated for 10 min at 37°C. The mixtures were centrifuged at 500 g for 10 min and subjected for the repeated washing procedure. Finally, the platelet pellets were resuspended by Tyrode's solution, and then calcium chloride was added to platelet suspensions in which the concentration of Ca^{2+} was 1 mM. This study wasapproved by the Institutional Review Board of Taipei Medical University and conformed to the directives of the Helsinki Declaration.

As previously described [10, 11], platelet aggregation was measured according to the turbidity of platelet suspensions and recorded by a Lumi-Aggregometer (Payton Associates, Scarborough, ON, Canada). Before the addition of agonists to induce platelet aggregation, the platelet suspensions (3.6×10^8cells/mL) were pretreated with various concentrations of amarogentin or an isovolumetric solvent control (0.5% DMSO) for 3 min. Light-transmission unit was used to present the extent of platelet aggregation. For the measurement of ATP release, a 20 μL of luciferin-luciferase mixture was added 1 min before adding amarogentin or agonists, and the relative amount of ATP release was compared to the solvent control.

2.3. Western Blotting. Western blotting assay was performed as described previously [11]. Briefly, after pretreatment of various concentrations of amarogentin, agonists were added to the washed platelets (1.2×10^9 cells/mL) for the indicated time to trigger platelet activation. The platelet pellets were collected after centrifugation and then immediately lysed in extraction buffer. Samples containing 80 μg of protein were subjected to sodium dodecyl sulfate polyacrylamide gel electrophoresis (SDS-PAGE, 10–12%) and electrotransferred onto the polyvinylidene difluoride (PVDF) membranes by Bio-Rad semidry transfer unit (Hercules, CA). Blots were blocked with 5% BSA in TBST (10 mM Tris-base, 100 mM NaCl, and 0.01% Tween 20) for 1 h and probed with the various primary antibodies (1 : 1000) for 2 h. The membranes were incubated with horseradish peroxidase- (HRP-) conjugated anti-mouse IgG or anti-rabbit IgG (1 : 3000) for 1 h. Immunoreactivity was detected by an enhanced chemiluminescence system. The quantitative data were obtained by scanning the reactive bands and quantifying the optical density using a computing densitometer and Bio-profil Biolight software, version V2000.01 (Vilber Lourmat, Marne-la-Vallée, France).

2.4. Fluorescein-Induced Thrombus Formation in the Microvessels of Mouse Mesentery. The protocols conformed to the Guide for the Care and Use of Laboratory Animals (NIH publication no. 85-23, 1996). The methods to measure thrombus formation was performed as described previously [11, 12]. In brief, an external jugular vein was cannulated with a PE-10 to intravenously administer the dye and drugs after mice were anesthetized. Venules (30–40 μm) were selected under a microscope. After administering 15 μg/kg sodium fluorescein, the selected venules were irradiated at wavelengths below 520 nm to produce a microthrombus, and the time required to occlude the microvessel as a result of thrombus formation (occlusion time) was recorded. In this study, 9 and 18 mg/kg amarogentin were administered to evaluate its antithrombotic effects.

2.5. Statistical Analysis. The results are presented as the mean ± SEM at least 3 independent experiments ($n = 3$). Each experiment performs with blood from different donors. For the *in vivo* study, Paired Student's t-test was used to evaluate the differences of the occlusion time in the same mouse. For the *in vitro* study, if appropriate, the one-way analysis of

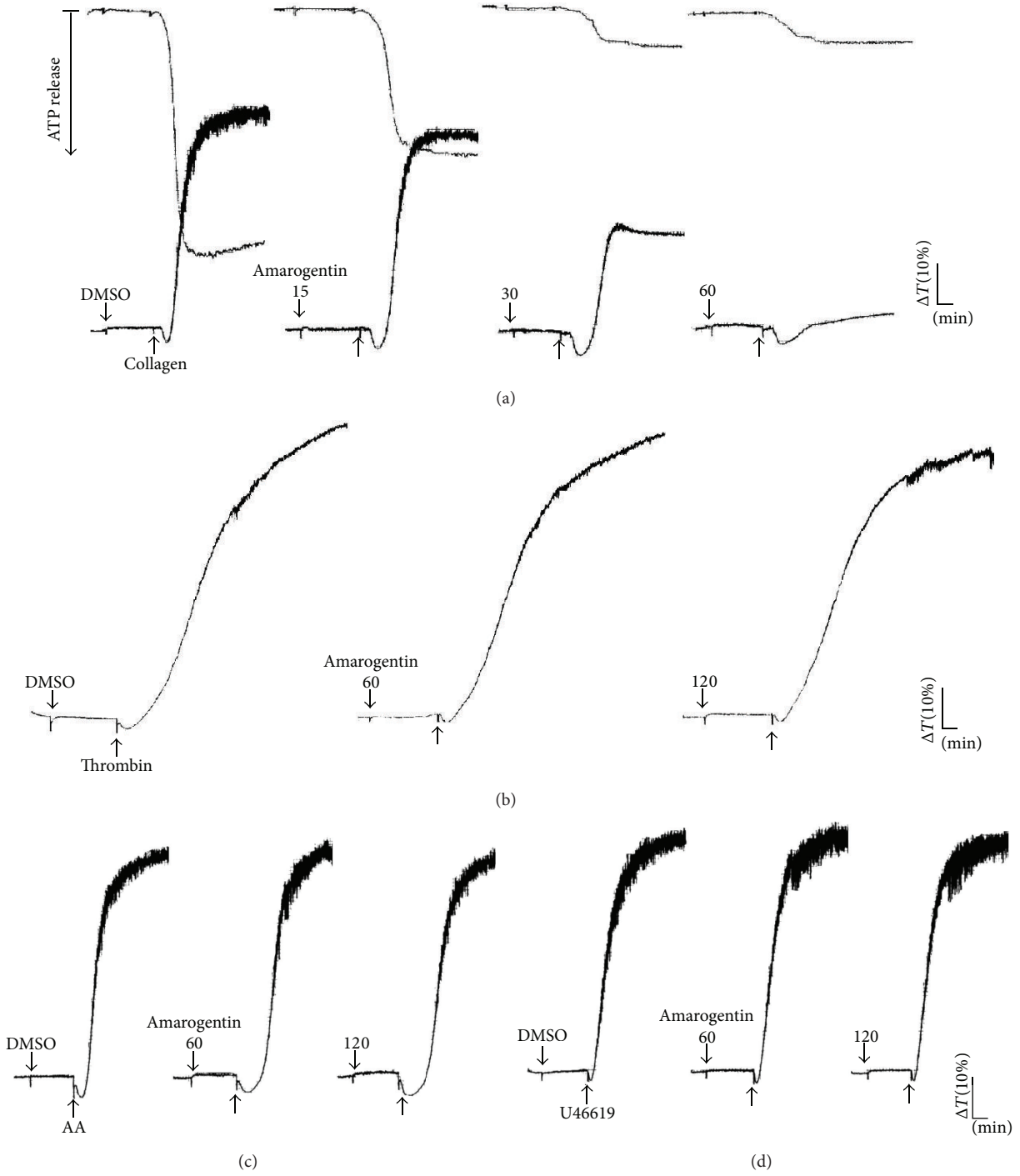

Figure 1: Amarogentin inhibits collagen-induced platelet aggregation and ATP release. Washed platelets (3.6×10^8 cells/mL) were incubated with solvent control (0.5% DMSO) or amarogentin (15 μM~120 μM) for 3 min in an aggregometer cuvette. Then, 1 μg/mL collagen (a), 0.01 IU/mL thrombin (b), 60 μM arachidonic acid (AA) (c), or 1 μM U46619 (d) was added to induce platelet aggregation and ATP-release ((a), upper tracings) for 6 min. Profiles ((a)–(d)) are representative of 3 independent experiments.

variance (ANOVA) followed by the Student-Newman-Keuls test was used to determine the statistical differences among groups. $P < 0.05$ was considered statistically significant. Statistical analyses were performed using SAS, version 9.2 (SAS Inc., Cary, NC).

3. Results

3.1. Amarogentin Inhibits Platelet Aggregation and ATP Release. Amarogentin (15~60 μM) showed more potent activity in inhibiting platelet aggregation and ATP release induced

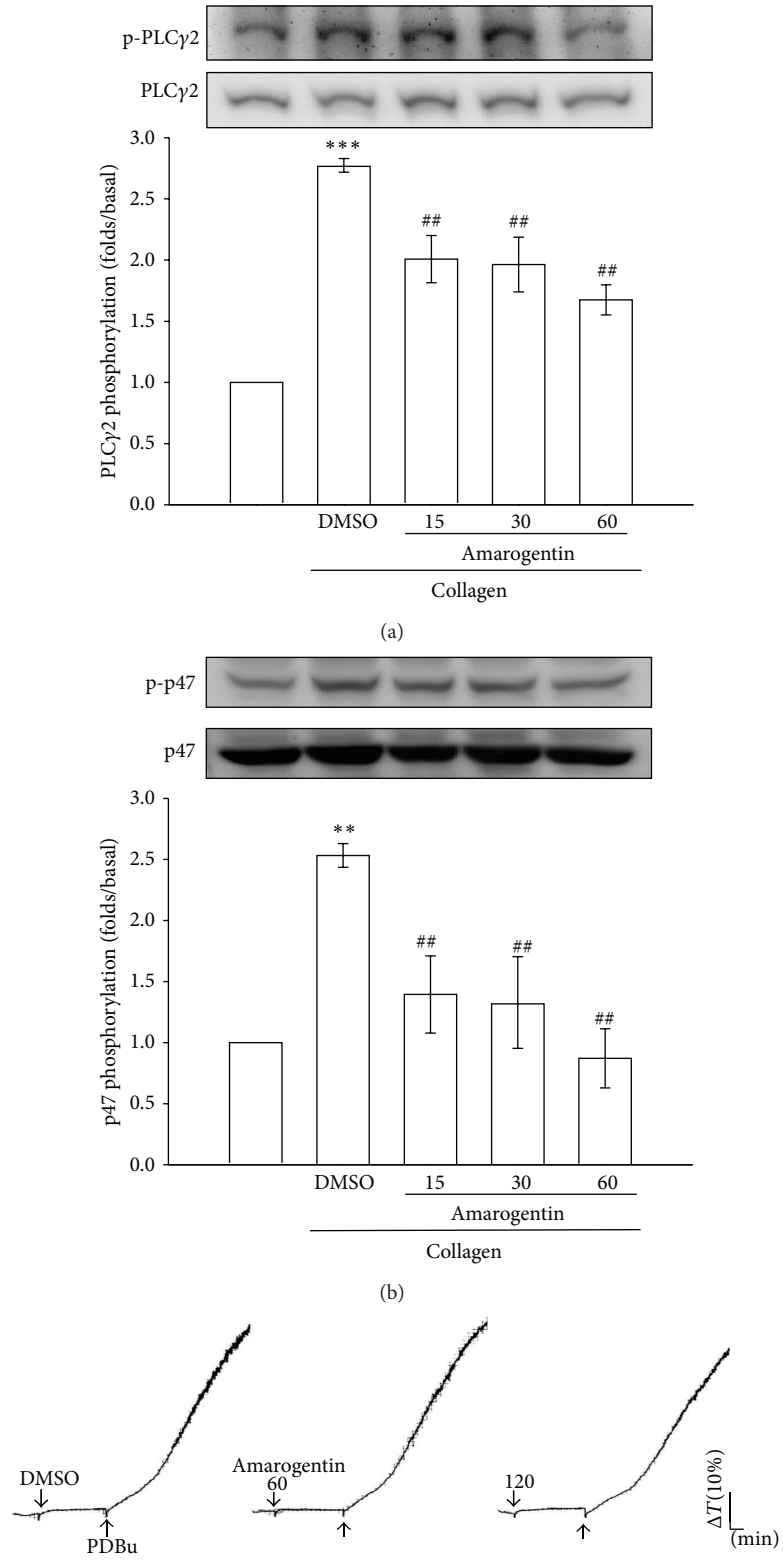

Figure 2: Effects of amarogentin on collagen-induced PLCγ2 and PKC activation. Washed platelets (1.2×10^9 cells/mL) were incubated with solvent control (0.5% DMSO) or amarogentin (15 μM~120 μM) for 3 min. Then, 1 μg/mL collagen was added to induce the phosphorylation of PLCγ2 (a) and p47 (b) for 5 min and 10 min, respectively. ((a) and (b)) The subcellular extracts were analyzed for PLCγ2 (a) and p47 (b) by western blotting. (c) Washed platelets (3.6×10^8 cells/mL) were incubated with solvent control (0.5% DMSO) or amarogentin (15 μM~120 μM) for 3 min and then treated with 150 nM PDBu to induce platelet aggregation. Data ((a) and (b)) are presented as the mean ± SEM ($n = 3$). $^{**}P < 0.01$ and $^{***}P < 0.001$, compared with the solvent control group (resting); $^{\#\#}P < 0.01$, compared with the positive control group (collagen only). Profiles (c) are representative of 3 independent experiments.

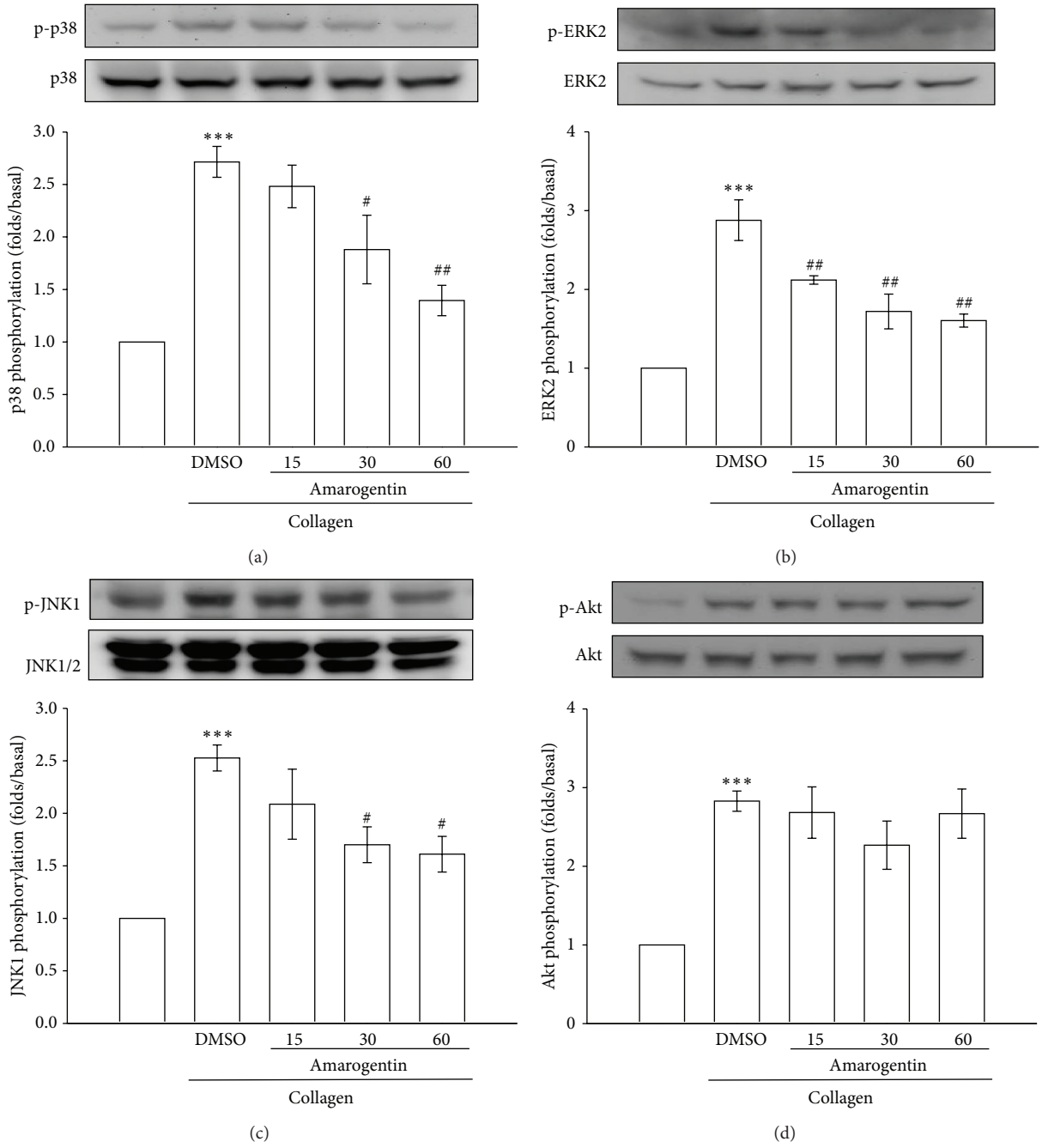

Figure 3: Effects of amarogentin on the phosphorylation of MAPK and Akt induced by collagen in human platelets. Washed platelets (1.2×10^9 cells/mL) were incubated with solvent control (0.5% DMSO) or amarogentin (15 μM~60 μM) and then treated with 1 μg/mL collagen to induce platelet activation. The subcellular extracts were analyzed for the phosphorylation of p38 (a), ERK2 (b), JNK1 (c), and Akt (d) by western blotting. Data are presented as the mean ± SEM ($n = 3$). $^{***}P < 0.001$, compared with the solvent control group (resting); $^{\#}P < 0.05$ and $^{\#\#}P < 0.01$, compared with the positive control group (collagen only).

by collagen (1 μg/mL) (Figure 1(a)). However, amarogentin (120 μM) did not affect platelet aggregation triggered by 0.01 IU/mL thrombin, 60 μM AA, or 1 μM U46619 (Figures 1(b)–1(d)). The half maximal inhibitory concentration (IC_{50}) of amarogentin for platelet aggregation induced by collagen was approximately 30 μM. Moreover, the solvent control (0.5% DMSO) did not affect platelet activity (data not shown). The agonist collagen was used to investigate the antiplatelet mechanisms of amarogentin.

3.2. Effects of Amarogentin on the Phosphorylation of PLCγ2 and p47. The PLC enzyme hydrolyzes phosphatidylinositol 4,5-bisphosphate (PIP_2) to generate diacylglycerol (DAG) and inositol 1,4,5-trisphosphate (IP_3). Subsequently, DAG

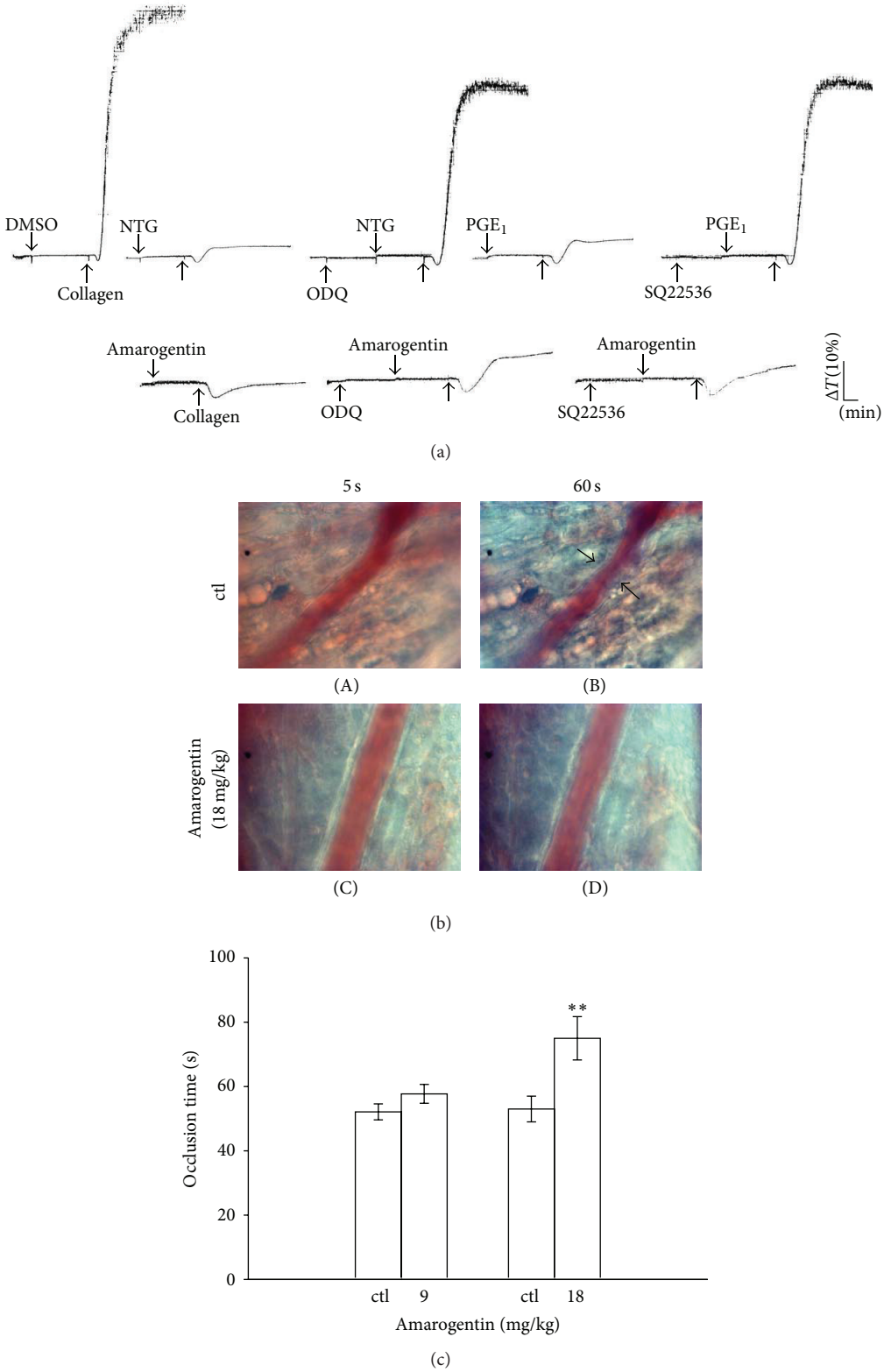

Figure 4: Effects of amarogentin on cyclic nucleotides in human platelets and on thrombus formation in mice. (a) Washed platelets (3.6×10^8 cells/mL) were preincubated with 10 μM nitroglycerin (NTG), 0.5 nM prostaglandin E_1 (PGE_1), or 60 μM amarogentin with or without 10 μM ODQ or 100 μM SQ22536, followed by treatment with 1 μg/mL collagen to induce platelet aggregation. ((b) and (c)) Mice were administered 0.5% DMSO (solvent control; ctl) and amarogentin (9- or 18 mg/kg). Then, mesenteric venules were selected and irradiated to induce microthrombus formation. The data in the bar graphs are presented as the mean ± SEM of the occlusion time which is seconds ($n = 5$). $^{**}P < 0.01$ compared with the individual solvent control group (ctl).

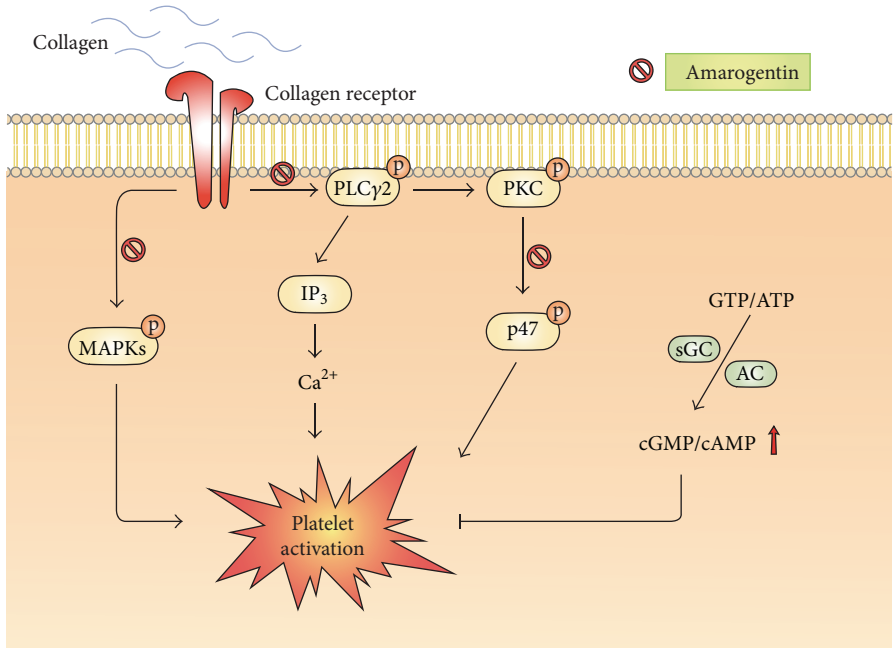

FIGURE 5: Hypothesis regarding the inhibitory signaling of amarogentin in platelet activation. Amarogentin may inhibit both the PLCγ2-PKC-p47 cascades and MAPK signaling pathway, ultimately inhibiting platelet activation. DAG: diacylglycerol; IP_3: inositol 1,4,5-trisphosphate.

triggers PKC activation, thereby leading to protein phosphorylation and ATP release in agonist-stimulated platelets [13]. Then, PKC phosphorylates p47 protein (pleckstrin) [13]. While platelets were treated with amarogentin, it attenuated the phosphorylation of PLCγ2 and p47 triggered by collagen in a concentration (15~60 μM)-dependent manner (Figures 2(a) and 2(b)) but did not affect PDBu-induced platelet aggregation (Figure 2(c)).

3.3. Effects of Amarogentin on the Phosphorylation of MAPKs and Akt. Previous studieshave suggested that MAPKs and Akt are involved in platelet activation and thrombosis [14, 15]. Thus, we determined these signaling molecules in collagen-activated platelets to investigate the antiplatelet mechanisms of amarogentin. We found that amarogentin concentration dependently (30~60 μM) inhibited collagen-induced phosphorylation of p38, ERK2, and JNK1 (Figures 3(a)–3(c)) but did not affect the phosphorylation of Akt (Figure 3(d)). These findings suggest that amarogentin inhibits collagen-induced platelet activation via MAPKs, but not Akt.

3.4. Effects of Amarogentin on Cyclic Nucleotides in Human Platelets. As shown in Figure 4(a), both ODQ (10 μM) and SQ22536 (100 μM) significantly reversed the inhibition of platelet aggregation mediated by nitroglycerin (10 μM)- and PGE_1 (0.5 nM), respectively. However, these inhibitors do not reverse the amarogentin (60 μM)-mediated inhibition of collagen-induced platelet aggregation, which indicates that cyclic AMP (cAMP) and cyclic GMP (cGMP) are not involved in the antiplatelet effects of amarogentin.

3.5. Effects of Amarogentin on Thrombus Formation in Mice. For the *in vivo* study, fluorescein sodium (15 μg/kg) was intravenously administrated and irradiated to induce thrombus formation in the mesenteric microvessels of mice and the time of occlusion was found to be approximated at 60 s (Figure 4(b)). Treatment of mice with 18 mg/kg amarogentin prolonged the occlusion time (75.2 ± 6.7 s) of thrombus formation, compared with the solvent control (53.0 ± 4.0 s) (Figure 4(c)).

4. Discussion

We investigated the effect of amarogentin, an active principle of *Gentiana lutea*, on platelet activation *in vitro* and thrombus formation in a mouse model. In the present study, we demonstrated for the first time that amarogentin inhibits platelet activation *in vitro* via inhibiting PLCγ2-PKC/MAPK cascade and *in vivo* through reversing thethrombus formation. Our results revealed that amarogentin concentration dependently inhibited collagen-induced platelet activation. Moreover, amarogentin did not affect the responses stimulated by AA, U46619, and thrombin in human platelets. These findings indicate that amarogentin mainly inhibits collagen-induced platelet activation.

GPVI, a member of the immunoglobulin superfamily, is required for collagen-induced platelet activation [9]. When

platelets are exposed to collagen, a signaling complex, including LAT, SLP-76, and Gads, activates PLCγ2, leading to PKC activation and Ca^{2+} release [9]. In the present study, we found that amarogentin could inhibit the phosphorylation of PLCγ2 and PKC. However, amarogentin did not affect the PKC activator PDBu-stimulated platelet aggregation, indicating that amarogentin may act on the upstream of PKC.

It is well established that MAPKs, including ERKs, JNKs, and p38, have been identified in platelets [16], where they are activated by collagen and thrombin, and are involved in thrombosis [14]. The ERK and p38 play important roles in stimulating the secretion of granules and facilitating clot retraction [17]. During platelet activation, the AA metabolism may offer a positive feedback amplifier to activate p38, followed by the stimulation of cytosolic phospholipase A_2, which promotes thromboxane A_2 formation [18]. In addition, JNK1 is reportedly involved in collagen-induced platelet aggregation and thrombus formation [19]. The time of thrombus formation was significantly prolonged in $JNK1^{-/-}$ arterioles in an *in vivo* model and platelet secretion was impaired in $JNK1^{-/-}$ platelets *in vitro* [20]. In this study, we demonstrated that the activation of MAPKs is inhibited by amarogentin, suggesting that amarogentin attenuated platelet activation and thrombus formation, at least in part, through MAPK cell-signaling pathway. In addition, several studies showed that PI3K/Akt plays an important role in regulating platelet aggregation and thrombus formation [15, 21, 22]. Thus, we also observed the influence of amarogentin on Akt and found that Akt was not associated with amarogentin-mediated inhibition of platelet activation.

cAMP and cGMP have been known to inhibit many aspects of platelet activation, including Ca^{2+} release, G-protein activation, granule release, and platelet adhesion and aggregation [23]. cAMP and cGMP strongly attenuate the elevation of cytosolic Ca^{2+} concentrations, at least in part, via phosphorylating IP_3 receptor, and are also reported to block p38 activation in platelets [23]. We found that SQ22536 and ODQ did not reverse the amarogentin-mediated inhibition of platelet aggregation. These results revealed that amarogentin did not regulate the level of cAMP and cGMP.

In conclusion, we demonstrated that amarogentin abrogates platelet activation probably via inhibiting the PLCγ2-PKC-p47 cascades and MAPK signaling pathway (Figure 5), finally reducing thrombus formation. Our findings suggest that amarogentin may provide therapeutic potential for preventing or treating thromboembolic disorders.

Conflict of Interests

The authors declare that they have no conflicts of interests.

Acknowledgments

This work was supported by Grants from the National Science Council of Taiwan (NSC101-2811-B-038-002, NSC102-2320-B-341-001-MY3, and NSC102-2811-B-038-026) and Shin Kong Wu Ho-Su Memorial Hospital (SKH-8302-102-NDR-04 and SKH-8302-103-NDR-05).

References

[1] A. Singh, "Phytochemicals of Gentianaceae: a review of pharmacological properties," *International Journal of Pharmaceutical Sciences and Nanotechnology*, vol. 1, no. 1, pp. 33–36, 2008.

[2] R. Kesavan, U. R. Potunuru, B. Nastasijevic, T. Avaneesh, G. Joksic, and M. Dixit, "Inhibition of vascular smooth muscle cell proliferation by *Gentiana lutea* root extracts," *PLoS ONE*, vol. 8, no. 4, Article ID e61393, 2013.

[3] B. Nastasijevic, T. Lazarevic-Pasti, S. Dimitrijevic-Brankovic et al., "Inhibition of myeloperoxidase and antioxidative activity of *Gentiana lutea* extracts," *Journal of Pharmaceutical and Biomedical Analysis*, vol. 66, pp. 191–196, 2012.

[4] N. Menkovic, Z. Juranic, T. Stanojkovic et al., "Radioprotective activity of *Gentiana lutea* extract and mangiferin," *Phytotherapy Research*, vol. 24, no. 11, pp. 1693–1696, 2010.

[5] M. Behrens, A. Brockhoff, C. Batram, C. Kuhn, G. Appendino, and W. Meyerhof, "The human bitter taste receptor hTAS2R50 is activated by the two natural bitter terpenoids andrographolide and amarogentin," *Journal of Agricultural and Food Chemistry*, vol. 57, no. 21, pp. 9860–9866, 2009.

[6] D. Pal, S. Sur, S. Mandal et al., "Prevention of liver carcinogenesis by amarogentin through modulation of G1/S cell cycle check point and induction of apoptosis," *Carcinogenesis*, vol. 33, no. 12, pp. 2424–2431, 2012.

[7] P. Saha, S. Mandal, A. Das, and S. Das, "Amarogentin can reduce hyperproliferation by downregulation of Cox-II and upregulation of apoptosis in mouse skin carcinogenesis model," *Cancer Letters*, vol. 244, no. 2, pp. 252–259, 2006.

[8] S. Phoboo, M. D. S. Pinto, A. C. L. Barbosa et al., "Phenolic-linked biochemical rationale for the anti-diabetic properties of Swertia chirayita (Roxb. ex Flem.) Karst," *Phytotherapy Research*, vol. 27, no. 2, pp. 227–235, 2013.

[9] Z. Li, M. K. Delaney, K. A. O'Brien, and X. Du, "Signaling during platelet adhesion and activation," *Arteriosclerosis, Thrombosis, and Vascular Biology*, vol. 30, no. 12, pp. 2341–2349, 2010.

[10] J.-R. Sheu, C.-R. Lee, C.-H. Lin et al., "Mechanisms involved in the antiplatelet activity of Staphylococcus aureus lipoteichoic acid in human platelets," *Thrombosis and Haemostasis*, vol. 83, no. 5, pp. 777–784, 2000.

[11] K. H. Lin, J. R. Kuo, W. J. Lu et al., "Hinokitiol inhibits platelet activation ex vivo and thrombus formation in vivo," *Biochemical Pharmacology*, vol. 85, no. 10, pp. 1478–1485, 2013.

[12] G. Hsiao, K. H. Lin, Y. Chang et al., "Protective mechanisms of inosine in platelet activation and cerebral ischemic damage," *Arteriosclerosis, Thrombosis, and Vascular Biology*, vol. 25, no. 9, pp. 1998–2004, 2005.

[13] W. D. Singer, H. A. Brown, and P. C. Sternweis, "Regulation of eukaryotic phosphatidylinositol-specific phospholipase C and phospholipase D," *Annual Review of Biochemistry*, vol. 66, pp. 475–509, 1997.

[14] F. Adam, A. Kauskot, J.-P. Rosa, and M. Bryckaert, "Mitogen-activated protein kinases in hemostasis and thrombosis," *Journal of Thrombosis and Haemostasis*, vol. 6, no. 12, pp. 2007–2016, 2008.

[15] D. Woulfe, H. Jiang, A. Morgans, R. Monks, M. Birnbaum, and L. F. Brass, "Defects in secretion, aggregation, and thrombus formation in platelets from mice lacking Akt2," *Journal of Clinical Investigation*, vol. 113, no. 3, pp. 441–450, 2004.

[16] F. Bugaud, F. Nadal-Wollbold, S. Lévy-Toledano, J.-P. Rosa, and M. Bryckaert, "Regulation of c-Jun-NH2 terminal kinase and

extracellular-signal regulated kinase in human platelets," *Blood*, vol. 94, no. 11, pp. 3800–3805, 1999.

[17] P. Flevaris, Z. Li, G. Zhang, Y. Zheng, J. Liu, and X. Du, "Two distinct roles of mitogen-activated protein kinases in platelets and a novel Rac1-MAPK-dependent integrin outside-in retractile signaling pathway," *Blood*, vol. 113, no. 4, pp. 893–901, 2009.

[18] L. Coulon, C. Calzada, P. Moulin, E. Véricel, and M. Lagarde, "Activation of p38 mitogen-activated protein kinase/cytosolic phospholipase A2 cascade in hydroperoxide-stressed platelets," *Free Radical Biology and Medicine*, vol. 35, no. 6, pp. 616–625, 2003.

[19] A. Kauskot, F. Adam, A. Mazharian et al., "Involvement of the mitogen-activated protein kinase c-Jun NH 2-terminal kinase 1 in thrombus formation," *Journal of Biological Chemistry*, vol. 282, no. 44, pp. 31990–31999, 2007.

[20] F. Adam, A. Kauskot, P. Nurden et al., "Platelet JNK1 is involved in secretion and thrombus formation," *Blood*, vol. 115, no. 20, pp. 4083–4092, 2010.

[21] J. M. E. M. Cosemans, I. C. A. Munnix, R. Wetzker, R. Heller, S. P. Jackson, and J. W. M. Heemskerk, "Continuous signaling via PI3K isoforms β and γ is required for platelet ADP receptor function in dynamic thrombus stabilization," *Blood*, vol. 108, no. 9, pp. 3045–3052, 2006.

[22] J. Chen, S. De, D. S. Damron, W. S. Chen, N. Hay, and T. V. Byzova, "Impaired platelet responses to thrombin and collagen in AKT-1-deficient mice," *Blood*, vol. 104, no. 6, pp. 1703–1710, 2004.

[23] A. Smolenski, "Novel roles of cAMP/cGMP-dependent signaling in platelets," *Journal of Thrombosis and Haemostasis*, vol. 10, no. 2, pp. 167–176, 2012.

Hindawi Publishing Corporation
BioMed Research International
Volume 2014, Article ID 217865, 11 pages
http://dx.doi.org/10.1155/2014/217865

Research Article

Activity Exerted by a Testosterone Derivative on Myocardial Injury Using an Ischemia/Reperfusion Model

Figueroa-Valverde Lauro,[1] Díaz-Cedillo Francisco,[2] García-Cervera Elodia,[1] Pool-Gómez Eduardo,[1] López-Ramos Maria,[1] Rosas-Nexticapa Marcela,[3] Hau-Heredia Lenin,[1] Sarabia-Alcocer Betty,[4] and Velázquez-Sarabia Betty Monica[4]

[1] *Laboratory of Pharmaco-Chemistry, Faculty of Chemical Biological Sciences, University Autonomous of Campeche, Avenida Agustín Melgar s/n, Colonia Buenavista, 24039 San Francisco de Campeche, CAM, Mexico*
[2] *Escuela Nacional de Ciencias Biológicas del Instituto Politéecnico Nacional, Prolongación de Carpio y Plan de Ayala s/n, Col. Santo Tomas, 11340 Mexico City, DF, Mexico*
[3] *Facultad de Nutrición, Médicos y Odontologos s/n, Unidad del Bosque, 91010 Xalapa, VER, Mexico*
[4] *Faculty of Medicine, University Autonomous of Campeche, Avenida Patricio Trueba de Regil s/n, Col Lindavista, 24090 San Francisco de Campeche, CAM, Mexico*

Correspondence should be addressed to Figueroa-Valverde Lauro; lauro_1999@yahoo.com

Received 19 January 2014; Revised 4 March 2014; Accepted 5 March 2014; Published 16 April 2014

Academic Editor: Joen-Rong Sheu

Some reports indicate that several steroid derivatives have activity at cardiovascular level; nevertheless, there is scarce information about the activity exerted by the testosterone derivatives on cardiac injury caused by ischemia/reperfusion (I/R). Analyzing these data, in this study, a new testosterone derivative was synthetized with the objective of evaluating its effect on myocardial injury using an ischemia/reperfusion model. In addition, perfusion pressure and coronary resistance were evaluated in isolated rat hearts using the Langendorff technique. Additionally, molecular mechanism involved in the activity exerted by the testosterone derivative on perfusion pressure and coronary resistance was evaluated by measuring left ventricular pressure in the absence or presence of the following compounds: flutamide, prazosin, metoprolol, nifedipine, indomethacin, and PINANE TXA_2. The results showed that the testosterone derivative significantly increases ($P = 0.05$) the perfusion pressure and coronary resistance in isolated heart. Other data indicate that the testosterone derivative increases left ventricular pressure in a dose-dependent manner (0.001–100 nM); however, this phenomenon was significantly inhibited ($P = 0.06$) by indomethacin and PINANE-TXA_2 ($P = 0.05$) at a dose of 1 nM. In conclusion, these data suggest that testosterone derivative induces changes in the left ventricular pressure levels through thromboxane receptor activation.

1. Introduction

Several reports indicate that myocardial infarction is a major cause of death and disability worldwide [1, 2]; this cardiovascular disease is due to cell death of cardiac myocytes caused by prolonged myocardial ischemia. Acute myocardial infarction can produce alterations in the topography of both the infarcted and noninfarcted regions of the ventricle [3]. There are some reports which show that the most effective method of limiting necrosis is restoration of blood flow; however, the effects of reperfusion itself may also be associated with tissue injury [4]. A study [5] showed that ischemic preconditioning (PC) upregulates the expression and activity of COX-2 in the heart and that this increase in COX-2 activity mediates the protective effects of the late phase of PC against both myocardial stunning and myocardial infarction. Another study [6] indicates that activation of COX-2 produces cardioprotection via synthesis or release of prostanoids such as PGI_2 and PGE_2 which induce a cardiac protective effect against ischemia-reperfusion injury in experimental animals [7–9]. It is important to mention that there are studies which suggest that the release of these prostanoids may be the result of the effect induced by some steroids on the COX-2 activity; this phenomenon results in

a decrease in the ischemia-reperfusion injury [10–13]. For example, there is a study which shows that 17β-estradiol reduced injury by ischemia/reperfusion via activation of PGI_2 in an animal model [14]. However, another data showed that administration of other types of steroid (testosterone) is associated with a reduced susceptibility to myocardial ischemia and this phenomenon results in the regulation of intracellular calcium levels on ischemia/reperfusion injury [15]. In addition, another study shows that testosterone exerted activation of STAT3 (signal transducers and activators of transcription 3) and SOCS3 (suppressor of cytokine signaling 3) after ischemia/reperfusion injury [16]. Another report indicates that testosterone indirectly regulates the activation of Akt (protein kinase) during cardiac ischemia/reperfusion [17]. However, other reports suggest that endogenous testosterone may have a negative effect on the heart subjected to acute ischemia/reperfusion via androgen receptor [18, 19]. Furthermore, a study [20] demonstrated that administration of a derivative of testosterone (nandrolone) increases ischemia/reperfusion by changes in the concentrations of both AMP (adenosine monophosphate) and TNFα (tumor necrosis factor alpha). Another data indicate that another type of testosterone derivative (dehydroepiandrosterone) regulates gene expression of both VEGF (vascular endothelial growth factor) and interleukins (IL-1 and IL-6) on ischaemia/reperfusion injury [21]. All these experimental results indicate that testosterone and its derivatives exert effects on ischemia/reperfusion injury; however, the cellular site and actual molecular mechanisms of testosterone and its derivatives are very confusing; therefore, data are needed for characterizing the activity induced by this steroid and its derivative on ischemia-reperfusion injury. To provide this information, the present study was designed to investigate the effects of testosterone and its derivative in an ischemia/reperfusion injury model. In addition, the activity of testosterone and its derivative on perfusion pressure and coronary resistance were evaluated in isolated rat hearts using the Langendorff technique. In order to evaluate the molecular mechanism involved in the activity induced by the testosterone derivative on left ventricular pressure the following compounds were used as pharmacological tools: flutamide (androgenic receptor antagonist) [22], prazosin (α_1 adrenoreceptor antagonist) [23], metoprolol (selective β_1 receptor blocker) [24], nifedipine (antagonist of calcium-channel) [25], indomethacin (a nonselective inhibitor of cyclooxygenase) [26], and PINANE TXA_2 (thromboxane receptor antagonist) [27].

2. Material and Methods

2.1. Chemical Synthesis. The compounds evaluated in this study were purchased from Sigma-Aldrich Co., Ltd. The melting point for the testosterone derivative was determined with an Electrothermal (900 model). Infrared spectra (IR) were recorded using KBr pellets on a Perkin Elmer Lambda 40 spectrometer. ^1H and ^{13}C NMR (nuclear magnetic resonance) spectra were recorded on a Varian VXR-300/5 FT NMR spectrometer at 300 and 75.4 MHz (megahertz) in $CDCl_3$ (deuterated chloform) using TMS (tetramethylsilane) as internal standard. EIMS (electron impact mass spectroscopy) spectra were obtained with a Finnigan Trace Gas Chromatography Polaris Q Spectrometer. Elementary analysis data were acquired from a Perkin Elmer Ser. II CHNS/0 2400 elemental analyzer.

*2.1.1. Synthesis of 1-[4-(2-Amino-ethylimino)-4-(4-fluoro-cyclohexyl)-butyl]-4-(4-chloro-phenyl)-piperidin-4-ol (Compound **3**).* A solution of haloperidol (100 mg, 0.26 mmol), ethylenediamine (80 μL, 1.19 mmol), and boric acid (40 mg, 0.65 mmol) in 10 mL of methanol was stirred for 72 h at room temperature. The reaction mixture was evaporated to dryness under reduced pressure; the residue washed 4 times with water. Then the precipitate was separated and dried at room temperature.

*2.1.2. Synthesis of 4-(4-Chloro-phenyl)-1-{4-(4-fluoro-phenyl)-4-[2-(17-hydroxy-10,13-dimethyl-1,2,6,7,8,9,10,11,12,13,14,15,16,17-tetradecahydro-cyclopenta[a]phenanthren-3-ylideneamino)-ethylimino]-butyl}-piperidin-4-ol (Compound **5**).* A solution of compound **3** (100 mg, 0.24 mmol), testosterone (70 mg, 0.24 mmol), and boric acid (40 mg, 0.65 mmol) in 10 mL of methanol was stirred for 72 h at room temperature. The reaction mixture was evaporated to dryness under reduced pressure; the residue washed 3 times with water. Then the precipitate was separated and dried at room temperature.

2.2. Biological Method. All experimental procedures and protocols used in this investigation were reviewed and approved by the Animal care and use Committee of University Autonomous of Campeche (no. PI-420/12) and were in accordance with the Guide for the Care and Use of Laboratory Animals [28]. Male Wistar rats ($n = 105$), weighing 200–250 g, were obtained from University Autonomous of Campeche.

2.3. Reagents. All drugs were dissolved in methanol and different dilutions were obtained using Krebs-Henseleit solution ($\leq$0.01%, v/v).

2.4. Experimental Design. Briefly, the male rat (200–250 g) was anesthetized by injecting them with pentobarbital at a dose rate of 50 mg/Kg body weight. Then the chest was opened, and a loose ligature passed through the ascending aorta. The heart was then rapidly removed and immersed in ice cold physiologic saline solution. The heart was trimmed of noncardiac tissue and retrograde perfused via a non-circulating perfusion system at a constant flow rate. The perfusion medium was the Krebs-Henseleit solution (pH = 7.4, 37°C) composed of (mmol) 117.8, NaCl; 6, KCl; 1.75, $CaCl_2$; 1.2, $NaHPO_4$; 1.2, $MgSO_4$; 24.2, $NaHCO_3$; 5, glucose; 7 and 5, sodium pyruvate. The solution was actively bubbled with a mixture of O_2/CO_2 (95 : 5/5%). The coronary flow was adjusted with a variable speed peristaltic pump. An initial perfusion rate of 15 mL/min for 5 min was followed by a 15 min equilibration period at a perfusion rate of

10 mL/min. All experimental measurements were done after this equilibration period.

2.5. Perfusion Pressure. Evaluation of measurements of perfusion pressure changes induced by drugs administration in this study was assessed using a pressure transducer connected to the chamber where the hearts were mounted and the results entered into a computerized data capture system (Biopac).

2.6. Inotropic Activity. Contractile function was assessed by measuring left ventricular developed pressure (LV/dP), using a saline-filled latex balloon (0.01 mm, diameter) inserted into the left ventricle via the left atrium. The latex balloon was bound to cannula which was linked to pressure transducer that was connected with the MP100 data acquisition system.

2.6.1. First Stage

Activity Induced by Testosterone and Its Derivative Using an Ischemia/Reperfusion Model. After 15 minutes of equilibration time, the hearts were subjected to ischemia for 30 minutes by turning off the perfusion system [29]. After this period, the system was restarted and the hearts were reperfused by 30 minutes with Krebs-Henseleit solution. The hearts were randomly divided into 3 major treatment groups with $n = 9$.

Group I. Hearts were subjected to ischemia/reperfusion but received vehicle only (Krebs-Henseleit solution).

Group II. Hearts were subjected to ischemia/reperfusion and treated with testosterone at a dose of 0.001 nM before ischemia period (for 10 minutes) and during the entire period of reperfusion.

Group III. Hearts were subjected to ischemia/reperfusion and treated with the testosterone derivative at a dose of 0.001 nM before ischemia period (for 10 minutes) and during the entire period of reperfusion.

It is noteworthy that, at the end of each experiment, the perfusion pump was stopped and 0.5 mL of fluorescein solution (0.10%) was injected slowly through a sidearm port connected to the aortic cannula. The dye was passed through the heart for 10 sec to ensure its uniform tissue distribution. The presence of fluorescein was used to demarcate the tissue that was not subjected to regional ischemia, as opposed to the risk region. The heart was removed from the perfusion apparatus and cut into two transverse sections at right angles to the vertical axis. The right ventricle, apex, and atrial tissue were discarded. The areas of the normal left ventricle nonrisk region, area at risk, and infarct region were determined using the technique reported by both and coworkers [29]. Total area at risk was expressed as the percentage of the left ventricle.

2.6.2. Second Stage

Effect Induced by Testosterone and Its Derivative on Perfusion Pressure. Changes in perfusion pressure as a consequence of increases in time (3 to 18 min) in the absence (control) or presence of testosterone and its derivative at a concentration of 0.001 nM were determined. The effects were obtained in isolated hearts perfused at a constant flow rate of 10 mL/min.

Evaluation of Effects Exerted by the Testosterone and Its Derivative on Coronary Resistance. The coronary resistance in the absence (control) or presence of testosterone and its derivative at a concentration of 0.001 nM was evaluated. It is noteworthy that Coronary resistance was calculated as the ratio of perfusión pressure at coronary flow assayed (10 mL/min).

2.6.3. Third Stage

Effects Induced by Testosterone and Its Derivative on Left Ventricular Pressure through Androgen Receptors. Intracoronary boluses (50 μL) of testosterone and its derivative (0.001 to 100 nM) were administered and the corresponding effect on the left ventricular pressure was determined. The dose-response curve (control) was repeated in the presence of flutamide at a concentration of 1 nM (duration of preincubation with flutamide was by a 10 min equilibration period).

Effects Induced by the Testosterone Derivative on Left Ventricular Pressure through β_1-Adrenergic Receptor. Intracoronary boluses (50 μL) of the testosterone derivative (0.001 to 100 nM) were administered and the corresponding effect on the left ventricular pressure was determined. The dose-response curve (control) was repeated in the presence of metoprolol at a concentration of 1 nM (duration of preincubation with metoprolol was by a 10 min equilibration period).

Effects Exerted by the Testosterone Derivative on Left Ventricular Pressure through α_1-Adrenergic Receptor. Intracoronary boluses (50 μL) of the testosterone derivative (0.001 to 100 nM) were administered and the corresponding effect on the left ventricular pressure was determined. The dose-response curve (control) was repeated in the presence of prazosin at a concentration of 1 nM (duration of preincubation with prazosin was by a 10 min equilibration period).

Effects of the Testosterone Derivative on Left Ventricular Pressure through the Calcium Channel. Intracoronary boluses (50 μL) of the testosterone derivative [0.001 to 100 nM] were administered and the corresponding effect on the left ventricular pressure was evaluated. The dose-response curve (control) was repeated in the presence of nifedipine at a concentration of 1 nM (duration of the preincubation with nifedipine was for a period of 10 min).

Effect Exerted by the Testosterone Derivative on Left Ventricular Pressure in the Presence of Indomethacin. The boluses (50 μL) of the testosterone derivative [0.001 to 100 nM] were administered and the corresponding effect on the left ventricular pressure was evaluated. The bolus injection administered was done in the point of cannulation. The dose-response curve (control) was repeated in the presence of indomethacin at a concentration of 1 nM (duration of the preincubation with indomethacin was for a period of 10 min).

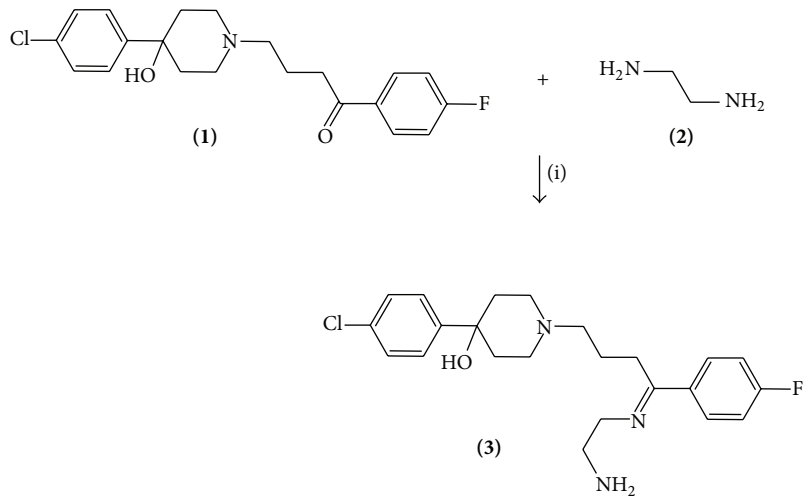

Figure 1: Synthesis of 1-[4-(2-amino-ethylimino)-4-(4-fluoro-cyclohexyl)-butyl]-4-(4-chloro-phenyl)-piperidin-4-ol (**3**). Reaction of haloperidol with ethylenediamine using boric acid as catalyst (i) to form the compound **3**.

Effects of the Testosterone Derivative on Left Ventricular Pressure through the TXA_2 Receptor Activation. Intracoronary boluses (50 μL) of the testosterone derivative [0.001 to 100 nM] were administered and the corresponding effect on the left ventricular pressure was evaluated. The dose-response curve (control) was repeated in the presence of PINANE TXA_2 at a concentration of 1 nM (duration of the preincubation with PINANE TXA_2 was for a period of 10 min).

2.6.4. Fourth Stage

Activity Induced by Indomethacin and PINANE TXA_2 in Presence y Absence of the Testosterone Derivative Using an Ischemia/Reperfusion Model. After 15 minutes of equilibration time, the hearts were subjected to ischemia for 30 minutes by turning off the perfusion system [29]. After this period, the system was restarted and the hearts were reperfused by 30 minutes with Krebs-Henseleit solution. The hearts were randomly divided into 3 major treatment groups with $n = 6$.

Group I. Hearts were subjected to ischemia/reperfusion but received vehicle only (Krebs-Henseleit solution).

Group II. Hearts were subjected to ischemia/reperfusion and treated with the testosterone derivative at a dose of 0.001 nM before ischemia period (for 10 minutes) and during the entire period of reperfusion.

Group III. Hearts were subjected to ischemia/reperfusion and treated with testosterone derivative at a dose of 0.001 nM before ischemia period (for 10 minutes) and during the entire period of reperfusion. The dose-response curve (control) was repeated in the presence of indomethacin at a concentration of 1 nM.

Group IV. Hearts were subjected to ischemia/reperfusion and treated with testosterone derivative at a dose of 0.001 nM before ischemia period (for 10 minutes) and during the entire period of reperfusion. The dose-response curve (control) was repeated in the presence of PINANE TXA_2 at a concentration of 1 nM.

Group V. Hearts were subjected to ischemia/reperfusion and treated with the indomethacin at a dose of 0.001 nM before ischemia period (for 10 minutes) and during the entire period of reperfusion.

Group VI. Hearts were subjected to ischemia/reperfusion and treated with the PINANE TXA_2 at a dose of 0.001 nM before ischemia period (for 10 minutes) and during the entire period of reperfusion.

The areas of the normal left ventricle nonrisk region, area at risk, and infarct region were determined using the technique reported by both and coworkers [29]. Total area at risk was expressed as the percentage of the left ventricle.

2.7. Statistical Analysis. The obtained values are expressed as average ± SE. The data obtained were put under analysis of variance (ANOVA) with the Bonferroni correction factor using the SPSS 12.0 program [30]. The differences were considered significant when P was equal or smaller than 0.05.

3. Results

The yielding of compound **3** (Figure 1) was of 85% with melting point of 78–80°C. In addition, the spectroscopic analyses showed signals for IR (V_{max}, cm^{-1}) at 3412, 3382, and 3330. The chemical shifts of the spectroscopic analyses of ^1H NMR and ^{13}C NMR for compound **3** are showed in Tables 1 and 2. Finally, the results of mass spectroscopy (MS) (70 eV) are shown, m/z 417.10 [M^+, 10]. Additionally, the elementary analysis data for compound **3** ($C_{23}H_{29}ClFN_3O$) was calculated (C, 66.10; H, 6.99; Cl, 8.48; F, 4.55; N, 10.05; O, 3.83) and found (C, 66.08; H, 6.97).

Furthermore, other results (Figure 2) showed a yielding of 64% and a melting point of 170–172°C, for the testosterone

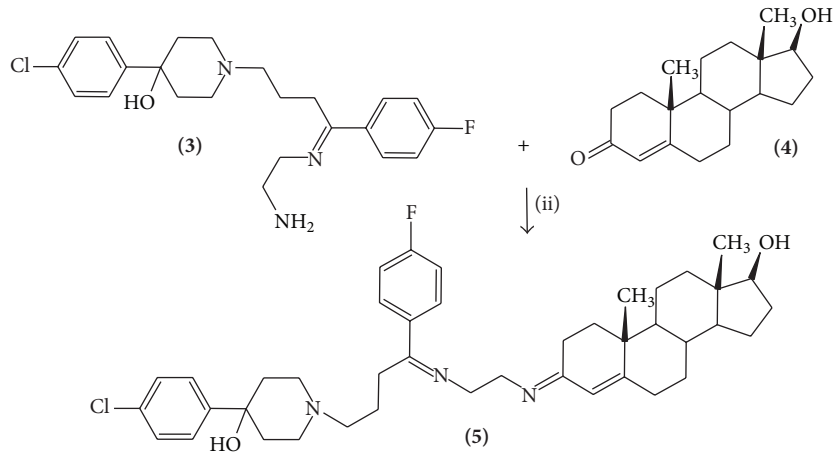

Figure 2: Synthesis of 4-(4-chloro-phenyl)-1-{4-(4-fluoro-phenyl)-4-[2-(17-hydroxy-10,13-dimethyl-1,2,6,7,8,9,10,11,12,13,14,15,16,17-tetradecahydro-cyclopenta[a]phenan thren-3-ylideneamino)-ethylimino]-butyl}-piperidin-4-ol (**5**). Reaction of 1-[4-(2-amino-ethylimino)-4-(4-fluoro-cyclohexyl)-butyl]-4-(chloro-phenyl)-piperidin-4-ol (**3**) with testosterone (**2**) to form the compound **3**. (ii) = boric acid.

Table 1: ^{1}H NMR (300 MHz, $CDCl_3$) data for the haloperidol derivative (compound **3**).

1.52–1.69 (m, 4H), 1.71 (t, 2H, J = 6.9 Hz), 2.31 (t, 2H, J = 6.9 Hz), 2.50 (t, 2H, J = 6.9 Hz), 2.753.03 (m, 4H), 3.08 (t, 2H,J = 6.5 Hz,), 3.51 (t, 2H, J = 6.5 Hz), 4.63 (s, 3H), 7.06–8.10 (m, 8H) ppm.

Table 2: ^{13}C NMR (300 MHz, $CDCl_3$) data for the haloperidol derivative (compound **3**).

26.15, 28.47, 38.40, 41.02, 47.04, 53.63, 54.09, 70.12, 115.08, 126.80, 128.64, 129.15, 134.40, 136.17, 145.22, 162.11, 163.30 ppm.

Table 3: ^{1}H NMR (300 MHz, $CDCl_3$) data for the testosterone derivative (compound **5**).

0.80 (s, 3H), 0.96–1.02 (m, 3H), 1.05 (s, 3H), 1.08–1.48 (m, 6H), 1.54 (m, 2H), 1.58–1.62 (m, 3H), 1.64 (m, 2H), 1.69 (m, 1H), 1.74 (t, 2H, J = 6.54), 1.86–2.38 (m, 7H), 2.42 (t, 2H, J = 6.54), 2.54 (t, 2H, J = 6.54), 2.78–3.00 (m, 4H), 3.60 (m, 1H), 3.70 (t, 2H, J = 6.54), 3.80 (t, 2H, J = 6.54), 4.74 (broad, 2H), 5.86 (m, 1H), 6.90–8.10 (m, 8H) ppm.

Table 4: ^{13}C NMR (300 MHz, $CDCl_3$) data for the testosterone derivative (compound **5**).

11.10, 17.70, 21.08, 23.32, 26.78, 28.72, 30.26, 30.38, 31.10, 31.28, 31.70, 35.20, 35.34, 36.66, 38.30, 42.80, 47.04, 50.20, 50.56, 51.70, 52.40, 54.22, 70.00, 80.78, 115.08, 115.38, 126.80, 128.60, 129.15, 136.17, 136.72, 145.18, 157.40, 162.12, 163.84, 165.82 ppm.

derivative (compound **5**). Additionally, the spectroscopic analyses showed signals for IR (V_{max}, cm^{-1}) at 3410, 3,338, and 2912. The chemical shifts of the spectroscopic analyses of ^{1}H NMR and ^{13}C NMR for the testosterone derivative are showed in Tables 3 and 4. Finally, the results of mass spectroscopy (MS) (70 eV) are shown, m/z 687.32 [M^{+},12]. Additionally, the elementary analysis data for compound **5** ($C_{42}H_{55}ClFN_3O_2$) was calculated (C, 73.28; H, 8.05; Cl, 5.15; F, 2.76; N, 6.10; O, 4.65) and found (C, 73.26; H, 8.04).

3.1. Biological Evaluation

3.1.1. First Stage

Activity Induced the Testosterone Derivative Using an Ischemia/Reperfusion Model. The results (Figure 3) showed that the testosterone derivative significantly reduced (P = 0.06) infarct size (expressed as a percentage of the area at risk) compared with both testosterone and vehicle-treated hearts.

3.1.2. Second Stage. In this study, the activity induced by the testosterone and its derivative on perfusion pressure and coronary resistance in the isolated rat heart was evaluated. The results obtained (Figure 4) from changes in perfusion pressure as a consequence of increases in the time (3–18 min) showed that the testosterone derivative at a dose of 0.001 nM significantly increases the perfusion pressure (**P** = 0.05) in comparison with the control conditions and testosterone [0.001 nM]. Other result (Figure 5) showed that coronary resistance, calculated as the ratio of perfusion pressure at coronary flow assayed (10 mL/min), was significantly higher (**P** = 0.05) in the presence of steroid derivative [0.001 nM] than in control conditions and testosterone [0.001 nM].

3.1.3. Third Stage. Figure 6 showed that the testosterone and its derivative induce an increase on left ventricular pressure in a dose-dependent manner [0.001 to 100 nM]; however, only the effect exerted by testosterone was significantly inhibited by flutamide at a dose of 1 nM (**P** = 0.06).

On the other hand, other experiments showed that the testosterone derivative increased left ventricular pressure in a dose-dependent manner [0.001 to 100 nM] and this effect was not inhibited in presence of prazosin or metoprolol (Figure 7)

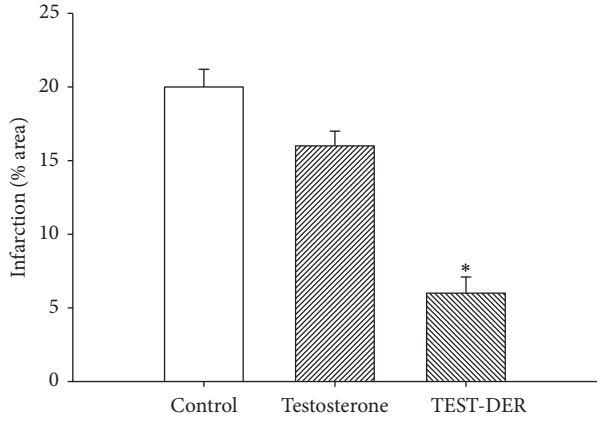

Figure 3: Effect exerted by the testosterone and its derivative (TEST-DER) on cardiac ischemia/reperfusion. The results showed that the testosterone derivative significantly reduced infarct size expressed as a percentage of the area at risk compared with testosterone and the vehicle-treated hearts (**P** = 0.06). Each bar represents the mean ± SE of 9 experiments.

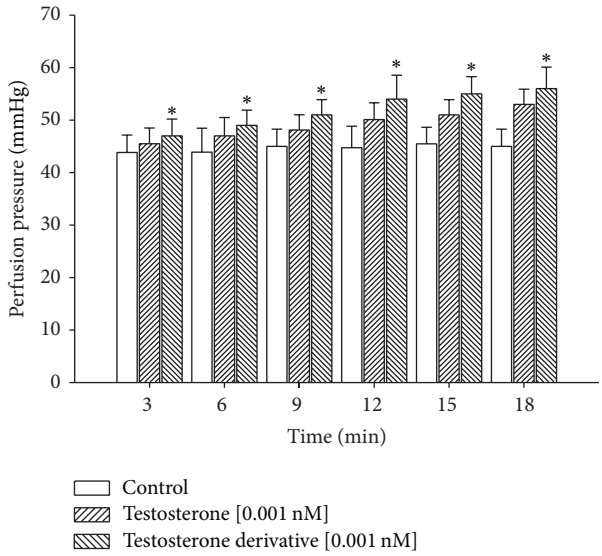

Figure 4: Effect induced by the testosterone and its derivative on perfusion pressure. The results showed that the testosterone derivative significantly increases perfusion pressure (**P** = 0.05) through time in comparison with the control conditions and testosterone. Each bar represents the mean ± SE of 9 experiments.

at a concentration of 1 nM. Additionally, other results indicate that effect induced by the testosterone derivative on left ventricular pressure (Figure 8) in presence of nifedipine at a concentration of 1 nM was not blocked. Finally, other results (Figure 9) indicate that activity exerted by the testosterone derivative [0.001 to 100 nM] on left ventricular of testosterone was significantly blocked in presence of indomethacin (**P** = 0.05) and PINAME TXA_2 (**P** = 0.05) at a dose of 1 nM.

3.1.4. Fourth Stage. The results (Figure 10) showed that the testosterone derivative significantly reduced (P = 0.06)

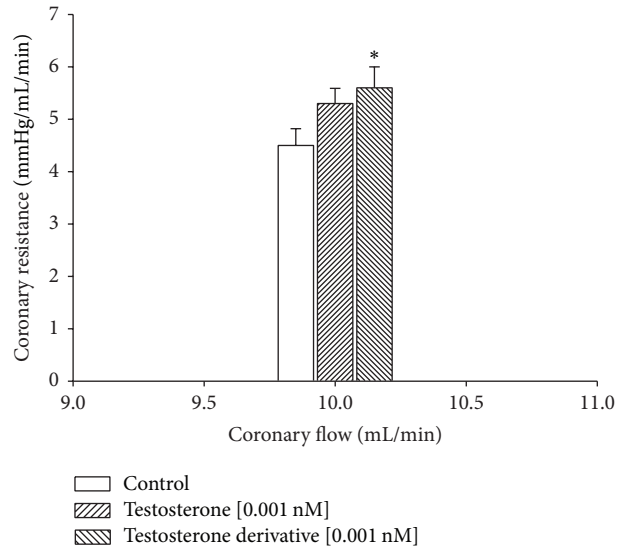

Figure 5: Activity exerted by the testosterone derivative and its derivative on coronary resistance. The results show that coronary resistance was higher (**P** = 0.05) in the presence of the testosterone derivative in comparison with the control conditions and testosterone. Each bar represents the mean ± SE of 9 experiments.

infarct size (expressed as a percentage of the area at risk) compared with vehicle-treated hearts. However, this effect was partially blocked by indomethacin and PINANE TXA_2. Other data indicate that Indomethacin significantly decreased infarct size (P = 0.05) in comparison with testosterone derivative, PINANE TXA_2, and vehicle-treated hearts.

4. Discussion

4.1. Chemical Synthesis. There are many procedures for preparation of several androgen derivatives; nevertheless, despite its wide scope, have some drawbacks; for example, several agents used have limited stability and their preparation requires special conditions [31, 32]. Analyzing these data, we report a straightforward route for synthesis of an androgen derivative using some strategies. The first stage was achieved by the synthesis of 1-[4-(2-amino-ethylimino)-4-(4-fluoro-cyclohexyl)-butyl]-4-(4-chloro-phenyl)-piperidin-4-ol (**3**) which has an imine group (Schiff base) involved in their chemical structure (Figure 1). It is noteworthy that there are several procedures for the synthesis of imine groups which are described in the literature [33, 34]. However, in this study, the synthesis of compound **3** was developed by the reaction of haloperidol with ethylenediamine using boric acid as catalyst to form **3**. The structure of compound **3** was confirmed using IR and NMR spectroscopy (Tables 1 and 2). The IR spectra contained characteristic vibrations at 3412 for hydroxyl group; at 3382 for amino group; at 3330 for imino groups, and 2910 piperidine ring. The ^{1}H NMR spectrum of **3** shows signals at 1.52–1.69 ppm for piperidine ring; at 1.71–2.50 ppm for methylene groups bound to both imino and piperidine groups; at 2.75–3.03 ppm for piperidine

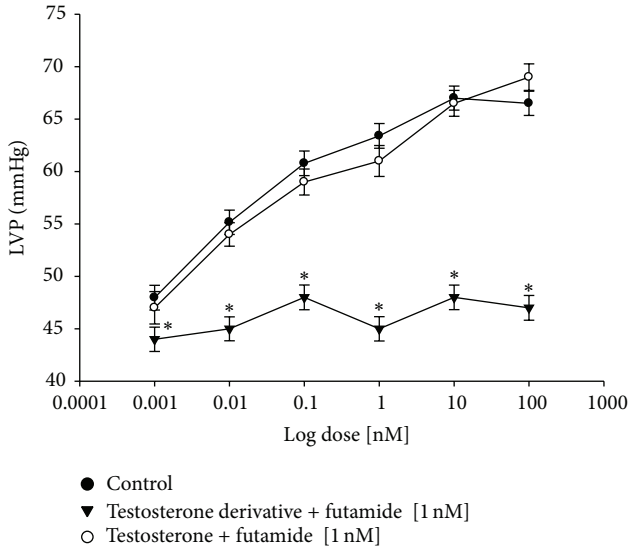

Figure 6: Effects induced by the testosterone and its derivative on LVP through androgen receptor. Intracoronary boluses (50 μL) of the testosterone and its derivative [0.001 to 100 nM] were administered and the corresponding effect on the LVP was determined. The dose-response curve (control) was repeated in the presence of flutamide (duration of preincubation with flutamide was by a 10 min equilibration period). The results showed that only the activity exerted of testosterone on LVP was significantly inhibited (**P** = 0.06). Each bar represents the mean ± SE of 9 experiments. LVP: left ventricular pressure.

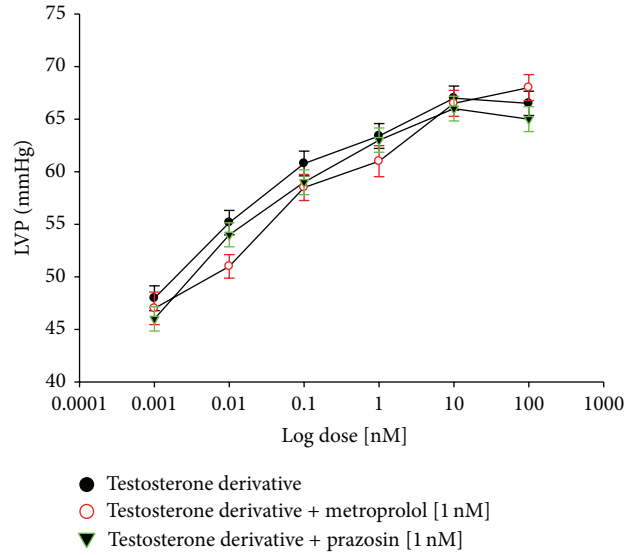

Figure 7: Activity exerted by the testosterone derivative on LVP through of adrenergic receptors. Testosterone derivative [0.001 to 100 nM] was administered (intracoronary boluses, 50 μL) and the corresponding effect on the LVP was evaluated in the absence and presence of prazosin or metoprolol. The results showed that activity induced by the testosterone derivative on LVP was not inhibited in the presence of prazosin or metoprolol. Each bar represents the mean ± SE of 9 experiments. LVP: left ventricular pressure.

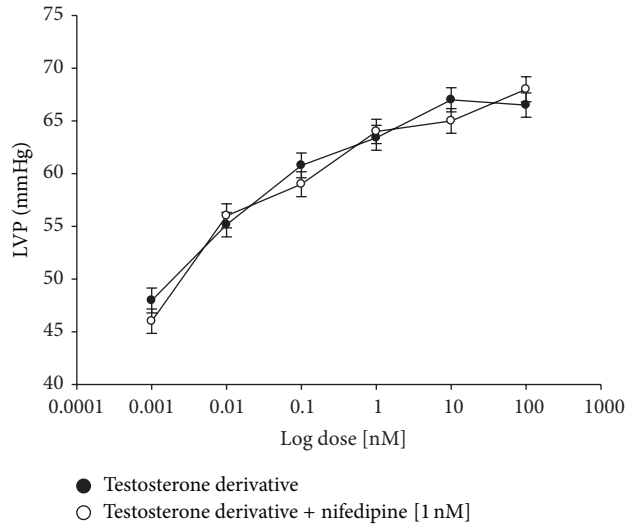

Figure 8: Effects induced by the testosterone derivative on LVP through calcium channel activation. Intracoronary boluses (50 μL) of the testosterone derivative [0.001 to 100 nM] were administered and the corresponding effect on the LVP was determined in the absence and presence of nifedipine. The results showed that the testosterone derivative increases the LVP in a dose-dependent manner and this effect was not inhibited in the presence of nifedipine. Each bar represents the mean ± SE of 9 experiments. LVP: left ventricular pressure.

ring; at 3.08–3.51 ppm for methylene groups bound to both imino and amino groups; at 4.63 ppm for both hydroxyl and amino groups; at 7.06–8.10 ppm for both phenyl groups. The ^{13}C NMR spectra showed chemical shifts at 26.15, 28.47, and 53.63 ppm for methylene groups bound to both imino and piperidine groups; at 38.40, 47.04, and 70.12 ppm for piperidine ring; at 41.02 and 54.09 ppm for methylene groups bound to both amino and imino groups; at 115.08–145.22 and 163.30 ppm for both phenyl groups; at 162.11 ppm for imino group. Finally, the presence of testosterone derivative was further confirmed from mass spectrum which showed a molecular ion at m/z 417.12.

The second stage was achieved by the synthesis of the testosterone derivative by the reaction of compound **3** with testosterone using boric acid as catalyst to form a new imino group involved in the chemical structure of the steroid derivative. The structure of the testosterone derivative was confirmed using IR and NMR spectroscopy (Tables 3 and 4). The IR spectra contained characteristic vibrations at 3410 for hydroxyl group; at 3338 for both imino groups and 2912 piperidine ring. The ^{1}H NMR spectrum of the testosterone derivative shows signals at 0.80 and 1.05 ppm for methyl groups bound to steroid nucleus; at 0.96–1.02, 1.08–1.48, 1.58–1.62, 1.69, 1.86–2.38, 3.60, and 5.86 ppm for steroid nucleus; at 1.54, 1.64 and 2.78–3.00 ppm for piperidine ring; at 1.74 and 2.42–2.54 ppm for methylene groups bound to both piperidine ring and imine groups; at 3.70 and 3.80 3.99 ppm for methylene groups bound to both imino groups. Finally, two signals at 4.74 ppm for both hydroxyl groups and at 6.90–8.10 ppm for phenyl groups were found.

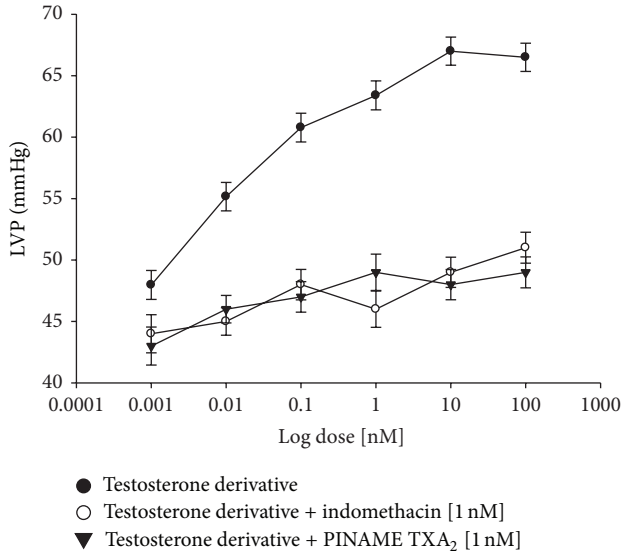

Figure 9: Effects induced by the testosterone derivative on LVP through prostaglandins synthesis and thromboxane receptor. Intracoronary boluses (50 μL) of the testosterone derivative [0.001 to 100 nM] were administered and the corresponding effect on the LVP was determined in the absence and presence of indomethacin and PINANE TXA_2. The results showed that the testosterone derivative increases the LVP in a dose-dependent manner and this effect was significantly inhibited in the presence of indomethacin ($P = 0.05$) and PINANE TXA_2 ($P = 0.05$). Each bar represents the mean ± SE of 9 experiments. LVP: left ventricular pressure.

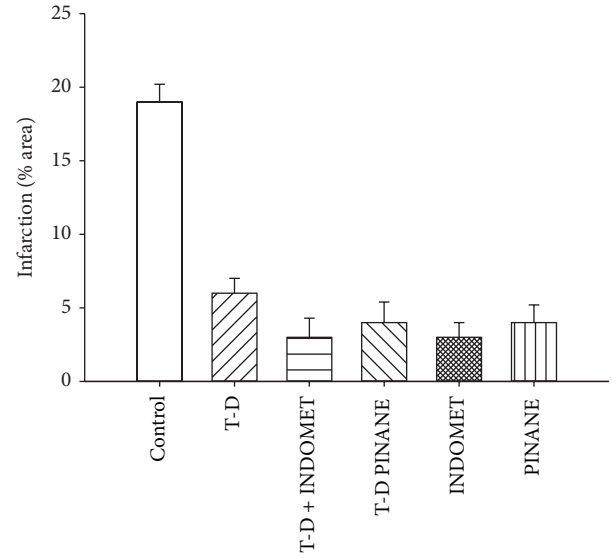

Figure 10: Effect exerted by indomethacin (INDOMET) and PINANE TXA2 (PINANE) in presence and absence of testosterone derivative (T-D) on cardiac ischemia/reperfusion.The results showed that T-D significantly reduced infarct size expressed as a percentage of the area at risk compared with testosterone and the vehicle-treated hearts (**P** = 0.06). However, this effect was partially blocked by INDOMET and PINANE. Other data indicate that INDOMET significantly decreased infarct size ($P = 0.05$) in comparison with PINANE. Each bar represents the mean ± SE of 6 experiments.

On the other hand, the ^{13}C NMR spectra showed chemical shifts at 11.10 and 17.70 ppm for both methyl groups bound to steroid nucleus; at 21.08–23.32, 30.26–30.66, 42.80, 50.20–50.56, 80.78, 115.38, and 157.40 ppm for steroid nucleus; at 26.78–28.72 and 54.22 ppm for methylene groups bound to both piperidine and imino groups; at 38.30, 47.04, and 70.00 ppm for piperidine ring; at 51.70–52.40 ppm for methylene groups bound to both imino groups; at 115.06, 126.80, 136.72, and 163.84 ppm for phenyl group bound to imino group; at 128.60–136.17 and 145.18 ppm for phenyl group bound to piperidine ring; at 162.12 and 165.82 ppm for both imino groups. Finally, the presence of testosterone derivative was further confirmed from mass spectrum which showed a molecular ion at m/z 687.36.

4.2. Biological Evaluation. In this study, the activity of the testosterone derivative on myocardial injury using an ischaemia/reperfusion model was evaluated. The results showed that the testosterone derivative significantly reduced infarct size (expressed as a percentage of the area at risk) compared with both testosterone and vehicle-treated hearts. This effect can be conditioned by changes in the chemical structure of testosterone which may consequently bring activation of some biological structures (e.g., ionic channels or specific receptors) involved in the endothelium of coronary artery [35] or by the influence exerted by the testosterone derivative on blood pressure which consequently bring reduction in the infarct size and decrease the myocardial injury after ischemia/reperfusion similar to other reports for other types of steroids [36]. To assess these hypotheses, the effect induced by the testosterone and its derivative on blood vessel capacity and coronary resistance, translated as changes in perfusion pressure, was evaluated in an isolated rat heart model. The experimental results showed that the testosterone derivative significantly increases the perfusion pressure over time (3–18 min) compared with testosterone and the control conditions. These data suggest that activity induced by the testosterone derivative on perfusion pressure could modify vascular tone and coronary resistance of heart. Therefore, in this study, the activity exerted by testosterone and its derivative on coronary resistance was evaluated. The results indicate that coronary resistance was increased in presence of the steroid derivative. These data suggest that the testosterone derivative exerts effects on vascular tone through the generation or activation of vasoactive substances such as intracellular calcium. This phenomenon is similar to the activity exerted by other compounds such as the carbamazepine-alkyne derivative [37].

In order to characterize the molecular mechanism of this phenomenon and analyze the reports of some investigations which indicate that testosterone induces its effect on blood pressure via activation of the androgen receptor [38], we used flutamide (androgen-receptor blocker) to determine if the effects of testosterone and its derivative on perfusion pressure were via the androgen receptor. Our results showed that only the effect of testosterone was significantly inhibited

in presence of flutamide; however, the testosterone derivative was not inhibited by the androgen-receptor blocker, suggesting that the molecular mechanism for the testosterone derivative is not via the androgenic receptor. In search of molecular mechanism involved in the activity of the testosterone derivative and analyzing a study which indicates that some androgens such as dehydroisoandrosterone 3-sulfate stimulate catecholamines production and this phenomenon may induce a positive inotropic effect [39, 40] which has an important role in the development or maintenance of elevated blood pressure [41]. For this reason, in this study, the effect exerted by the testosterone derivative on left ventricular pressure was evaluated in the absence or presence of prazosin or metoprolol. The experimental results showed that the effect induced by the testosterone derivative was not inhibited in the presence of these compounds. These data indicated that the molecular mechanism involved in the activity of testosterone derivative is not via adrenergic system.

Analyzing the results obtained and other reports which indicate that some steroid derivatives can induce changes on blood pressure by increasing calcium levels [42]; in this study, we also considered validating the effect induced by the testosterone derivative on left ventricular pressure via the calcium channels activation using as pharmacological tool to nifedipine. The results showed that the effect induced by the testosterone derivative was not inhibited in the presence of nifedipine. These results indicate that activity of the testosterone derivative was not through calcium channels activation.

On the other hand, in the search of the molecular mechanism involved in effect induced by the testosterone derivative on left ventricular pressure and analyzing previous reports, which indicate that some steroids exert its effect on left ventricular pressure via prostaglandins synthesis [43]. In this sense, other alternative experiments were conducted to evaluate the possibility that the activities exerted by the testosterone derivative on left ventricular pressure involve stimulation and secretion of prostaglandins using as pharmacological tool indomethacin. The results showed that effect induced by the testosterone derivative on left ventricular pressure was blocked by indomethacin. These results indicate that the molecular mechanism involved in the effect exerted by the testosterone derivative was via prostaglandins. To assess whether the activity exercised by the derivative of testosterone on left ventricular pressure involves the activation or release of a specific prostaglandin such as thromboxane A_2 as (TXA_2) which is a substance that induces a vasoconstriction effect in heart [44]. In addition, it is important to mention that TXA_2 has been found into the coronary circulation in patients with ischemic heart disease [45]. Therefore, in this study, other experiments were conducted using thromboxane receptor antagonist (PINANE TXA_2) as pharmacological tool. The results indicate that effect exerted by the testosterone derivative was significantly inhibited by PINANE TXA2; these experimental data suggest that activity of the testosterone derivative on left ventricular pressure could be through receptor thromboxane A2 activation which consequently brings decrease in the ischemia/reperfusion injury. To assess this hypothesis, several experiments were conducted to evaluate the activity of indomethacin and PINANE TXA_2 on ischemia/reperfusion injury in the presence or absence of the testosterone derivative. The results showed that effect exerted by steroid derivative on ischemia/reperfusion injury was inhibited partiality with indomethacin and PINANE TXA_2. Additionally, other data showed that beneficial effects on ischemia/reperfusion injury induced by indomethacin and PINANE TXA_2 were higher in comparison with testosterone derivative. All these data indicate that; (1) indomethacin blocked the activity of COX and this phenomenon consequently bring inhibition of synthesis or release to two prostaglandins such as PGI2 (prostaciclin) and TXA2 (tromboxane A_2) which exert effects on ischemia/reperfusion injury such as happening in other types of studies [7–9, 14]; (2) the testosterone derivative decreases the ischemia/reperfusion injury through thromboxane receptor activation; (3) the steroid derivative could induce an imbalance in the relation of PGI_2/TXA_2 which may consequently bring changes in the metabolism of myocardium and induce a decrease of the ischemia/reperfusion injury.

5. Conclusions

The testosterone derivative is a particularly interesting drug, because the activity induced for this compound on ischemia/reperfusion injury involves a molecular mechanism different in comparison with other drugs. This phenomenon may constitute a novel therapy for ischemia/reperfusion injury.

Conflict of Interests

The authors declare that this paper does not have any conflict of interests (political, personal, religious, ideological, academic, intellectual, commercial, or otherwise) regarding the publication of the paper.

References

[1] S. Yusuf, S. Hawken, and S. Ounpuu, "Effect of potentially modifiable risk factors associated with myocardial infarction in 52 countries (the INTERHEART study): case-control study," *The Lancet*, vol. 366, no. 9497, pp. 1640–1649, 2005.

[2] K. Thygesen, J. S. Alpert, and H. D. White, "Universal definition of myocardial infarction," *Journal of the American College of Cardiology*, vol. 50, no. 22, pp. 2173–2195, 2007.

[3] M. A. Pfeffer, "Left ventricular remodeling after acute myocardial infarction," *Annual Review of Medicine*, vol. 46, pp. 455–466, 1995.

[4] P. Zhai, T. E. Eurell, R. Cotthaus, E. H. Jeffery, J. M. Bahr, and D. R. Gross, "Effect of estrogen on global myocardial ischemia-reperfusion injury in female rats," *The American Journal of Physiology—Heart and Circulatory Physiology*, vol. 279, no. 6, pp. H2766–H2775, 2000.

[5] H. Yadav, M. Singhg, P. Sharma, D. Mittal, T. Behl, and A. Pal, "Possible role of cyclooxygenase-2 in remote aortic preconditioning induced cardioprotection in rat heart," *Pharmacologia*, vol. 3, no. 1, pp. 1–8, 2012.

[6] K. Shinmura, R. Bolli, S. Liu et al., "Aldose reductase is an obligatory mediator of the late phase of ischemic preconditioning," *Circulation Research*, vol. 91, no. 3, pp. 240–246, 2002.

[7] L. Calabresi, G. Rossoni, M. Gomaraschi, F. Sisto, F. Berti, and G. Franceschini, "High-density lipoproteins protect isolated rat hearts from ischemia-reperfusion injury by reducing cardiac tumor necrosis factor-α content and enhancing prostaglandin release," *Circulation Research*, vol. 92, no. 3, pp. 330–337, 2003.

[8] M. G. W. Camitta, S. A. Gabel, P. Chulada et al., "Cyclooxygenase-1 and -2 knockout mice demonstrate increased cardiac ischemia/reperfusion injury but are protected by acute preconditioning," *Circulation*, vol. 104, no. 20, pp. 2453–2458, 2001.

[9] R. Bolli, K. Shinmura, X. Tang et al., "Discovery of a new function of cyclooxygenase (COX)-2: COX-2 is a cardioprotective protein that alleviates ischemia/reperfusion injury and mediates the late phase of preconditioning," *Cardiovascular Research*, vol. 55, no. 3, pp. 506–519, 2002.

[10] L. Khalaj, H. Peirovi, F. Khodagholi, A. Abdi, L. Dargahi, and A. Ahmadiani, "Acute 17β-estradiol pretreatment protects against abdominal aortic occlusion induced spinal cord ischemic-reperfusion injury," *Neurochemical Research*, vol. 36, no. 2, pp. 268–280.

[11] X. Song, G. Li, J. Vaage, and G. Valen, "Effects of sex, gonadectomy, and oestrogen substitution on ischaemic preconditioning and ischaemia-reperfusion injury in mice," *Acta Physiologica Scandinavica*, vol. 177, no. 4, pp. 459–466, 2003.

[12] M. A. Cavasin, S. S. Sankey, A. Yu, S. Menon, and X. Yang, "Estrogen and testosterone have opposing effects on chronic cardiac remodeling and function in mice with myocardial infarction," *The American Journal of Physiology—Heart and Circulatory Physiology*, vol. 284, no. 5, pp. H1560–H1569, 2003.

[13] J. W. Horton, D. J. White, and D. L. Maass, "Gender-related differences in myocardial inflammatory and contractile responses to major burn trauma," *The American Journal of Physiology—Heart and Circulatory Physiology*, vol. 286, no. 1, pp. H202–H213, 2004.

[14] E. A. Booth, R. R. Flint, K. L. Lucas, A. K. Knittel, and B. R. Lucchesi, "Estrogen protects the heart from ischemia-reperfusion injury via COX-2-derived PGI2," *Journal of Cardiovascular Pharmacology*, vol. 52, no. 3, pp. 228–235, 2008.

[15] F. Callies, H. Strömer, R. H. G. Schwinger et al., "Administration of testosterone is associated with a reduced susceptibility to myocardial ischemia," *Endocrinology*, vol. 144, no. 10, pp. 4478–4483, 2003.

[16] M. Wang, Y. Wang, A. Abarbanell et al., "Both endogenous and exogenous testosterone decrease myocardial STAT3 activation and SOCS3 expression after acute ischemia and reperfusion," *Surgery*, vol. 146, no. 2, pp. 138–144, 2009.

[17] C. Huang, H. Gu, W. Zhang, J. L. Herrmann, and M. Wang, "Testosterone-down-regulated akt pathway during cardiac ischemia/reperfusion: a mechanism involving BAD, Bcl-2 and FOXO3a," *Journal of Surgical Research*, vol. 164, no. 1, pp. e1–e11, 2010.

[18] D. E. Remmers, W. G. Cioffi, K. I. Bland, P. Wang, M. K. Angele, and I. H. Chaudry, "Testosterone: the crucial hormone responsible for depressing myocardial function in males after trauma-hemorrhage," *Annals of Surgery*, vol. 227, no. 6, pp. 790–799, 1998.

[19] D. E. Remmers, P. Wang, W. G. Cioffi, K. I. Bland, and I. H. Chaudry, "Testosterone receptor blockade after trauma-hemorrhage improves cardiac and hepatic functions in males," *The American Journal of Physiology—Heart and Circulatory Physiology*, vol. 273, no. 6, pp. H2919–H2925, 1997.

[20] E. F. du Toit, E. Rossouw, J. van Rooyen, and A. Lochner, "Proposed mechanisms for the anabolic steroid-induced increase in myocardial susceptibility to ischaemia/reperfusion injury," *Cardiovascular Journal of South Africa*, vol. 16, no. 1, pp. 21–28, 2005.

[21] A. Vannay, A. Fekete, R. Langer et al., "Dehydroepiandrosterone pretreatment alters the ischaemia/reperfusion-induced VEGF, IL-1 and IL-6 gene expression in acute renal failure," *Kidney and Blood Pressure Research*, vol. 32, no. 3, pp. 175–184, 2009.

[22] J. Simard, I. Luthy, J. Guay, A. Bélanger, and F. Labrie, "Characteristics of interaction of the antiandrogen flutamide with the androgen receptor in various target tissues," *Molecular and Cellular Endocrinology*, vol. 44, no. 3, pp. 261–270, 1986.

[23] R. M. Graham, H. F. Oates, L. M. Stoker, and G. S. Stokes, "Alpha blocking action of the antihypertensive agent, prazosin," *Journal of Pharmacology and Experimental Therapeutics*, vol. 201, no. 3, pp. 747–752, 1977.

[24] C. Bengtsson, G. Johnsson, and C. G. Regardh, "Plasma levels and effects of metoprolol on blood pressure and heart rate in hypertensive patients after an acute dose and between two doses during long term treatment," *Clinical Pharmacology and Therapeutics*, vol. 17, no. 4, pp. 400–408, 1975.

[25] P. D. Henry, "Comparative pharmacology of calcium antagonists: nifedipine, verapamil and diltiazem," *The American Journal of Cardiology*, vol. 46, no. 6, pp. 1047–1058, 1980.

[26] T. L. Owen, I. C. Ehrhart, W. J. Weidner, J. B. Scott, and F. J. Haddy, "Effects of indomethacin on local blood flow regulation in canine heart and kidney," *Proceedings of the Society for Experimental Biology and Medicine*, vol. 149, no. 4, pp. 871–876, 1975.

[27] S. E. Burke, A. M. Lefer, K. C. Nicolaou, G. M. Smith, and J. B. Smith, "Responsiveness of platelets and coronary arteries from different species to synthetic thromboxane and prostaglandin endoperoxide analogues," *The British Journal of Pharmacology*, vol. 78, no. 2, pp. 287–292, 1983.

[28] K. Bayne, "Revised guide for the care and use of laboratory animals available. American physiological society," *The Physiologist*, vol. 39, no. 4, pp. 199–211, 1996.

[29] E. A. Booth, N. R. Obeid, and B. R. Lucchesi, "Activation of estrogen receptor-α protects the in vivo rabbit heart from ischemia-reperfusion injury," *The American Journal of Physiology—Heart and Circulatory Physiology*, vol. 289, no. 5, pp. H2039–H2047, 2005.

[30] C. Hocht, L. Opezzo, S. Gorzalczany, G. Bramuglia, and C. Tiara, "Una aproximación cinética y dinámica de metildopa en ratas con coartación aórtica mediante microdiálisis," *Revista Argentina de Cardiologia*, vol. 67, pp. 769–773, 1999.

[31] M. E. Herr and F. W. Heyl, "'Enamine' derivatives of steroidal carbonyl compounds. III. The synthesis of C11-oxygenated testosterones," *Journal of the American Chemical Society*, vol. 75, no. 23, pp. 5927–5930, 1953.

[32] D. E. Stevenson, J. N. Wright, and M. Akhtar, "Synthesis of 19-functionalised derivatives of 16α-hydroxy-testosterone: mechanistic studies on oestriol biosynthesis," *Journal of the Chemical Society—Chemical Communications*, vol. 16, pp. 1078–1080, 1985.

[33] A. K. Shirayev, I. K. Moiseev, and S. S. Karpeev, "Synthesis and cis/trans isomerism of N-alkyl-1,3-oxathiolane-2-imines," *Arkivoc*, vol. 2005, no. 4, pp. 199–207, 2005.

[34] D. J. Uppiah, M. G. Bhowon, and S. J. Laulloo, "Solventless synthesis of imines derived from diphenyldisulphide diamine or p-Vanillin," *E-Journal of Chemistry*, vol. 6, no. 1, pp. S195–S200, 2009.

[35] D. Bouïs, G. A. P. Hospers, C. Meijer, G. Molema, and N. H. Mulder, "Endothelium in vitro: a review of human vascular endothelial cell lines for blood vessel-related research," *Angiogenesis*, vol. 4, no. 2, pp. 91–102, 2001.

[36] S. Beer, M. Reincke, M. Kral et al., "Susceptibility to cardiac ischemia/reperfusion injury is modulated by chronic estrogen status," *Journal of Cardiovascular Pharmacology*, vol. 40, no. 3, pp. 420–428, 2002.

[37] L. Figueroa-Valverde, F. Díaz-Cedillo, M. López-Ramos, E. García-Cervera, and K. Quijano-Ascencio, "Inotropic activity induced by carbamazepine-alkyne derivative in an isolated heart model and perfused to constant flow," *Biomedica*, vol. 31, no. 2, pp. 232–241, 2011.

[38] L. Figueroa-Valverde, H. Luna, C. Castillo-Henkel, O. Muñoz-Garcia, T. Morato-Cartagena, and G. Ceballos-Reyes, "Synthesis and evaluation of the cardiovascular effects of two, membrane impermeant, macromolecular complexes of dextran-testosterone," *Steroids*, vol. 67, no. 7, pp. 611–619, 2002.

[39] S. J. Hutchison, A. E. M. Browne, E. Ko et al., "Dehydroepiandrosterone sulfate induces acute vasodilation of porcine coronary arteries in vitro and in vivo," *Journal of Cardiovascular Pharmacology*, vol. 46, no. 3, pp. 325–332, 2005.

[40] J. Tan, Y. Sharief, K. G. Hamil et al., "Dehydroepiandrosterone activates mutant androgen receptors expressed in the androgen-dependent human prostate cancer xenograft CWR22 and LNCaP cells," *Molecular Endocrinology*, vol. 11, no. 4, pp. 450–459, 1997.

[41] J. J. Lilley, J. Golden, and R. A. Stone, "Adrenergic regulation of blood pressure in chronic renal failure," *Journal of Clinical Investigation*, vol. 57, no. 5, pp. 1190–1200, 1976.

[42] L. Figueroa-Valverde, F. Díaz-Cedillo, E. García-Cervera et al., "Positive inotropic activity induced by a dehydroisoandrosterone derivative in isolated rat heart model," *Archives of Pharmacal Research*, vol. 36, no. 10, pp. 1270–1278, 2013.

[43] C. Seillan, C. Ody, F. Russo-Marie, and D. Duval, "Differential of sex steroids of prostaglandin secretion by male and female cultured piglet endothelial cells," *Prostaglandins*, vol. 26, no. 1, pp. 3–12, 1983.

[44] Y. Yokoyama, H. Xu, N. Kresge et al., "Role of thromboxane A2 in early BDL-induced portal hypertension," *The American Journal of Physiology—Gastrointestinal and Liver Physiology*, vol. 284, no. 3, pp. G453–G460, 2003.

[45] P. D. Hirsh, L. D. Hillis, W. B. Campbell, B. G. Firth, and J. T. Willerson, "Release of prostaglandins and thromboxane into the coronary circulation in patients with ischemic heart disease," *The New England Journal of Medicine*, vol. 304, no. 12, pp. 685–691, 1981.

Hindawi Publishing Corporation
BioMed Research International
Volume 2014, Article ID 615363, 7 pages
http://dx.doi.org/10.1155/2014/615363

Research Article

Effect of *Toona microcarpa* Harms Leaf Extract on the Coagulation System

Hao Chen,[1,2] Min Jin,[1,2] Yi-Fen Wang,[3] Yong-Qing Wang,[2] Ling Meng,[2] Rong Li,[3] Jia-Ping Wang,[3] Li Gao,[3] Yi Kong,[1] and Ji-Fu Wei[2]

[1] *School of Life Science & Technology, China Pharmaceutical University, Nanjing 210009, China*
[2] *Research Division of Clinical Pharmacology, The First Affiliated Hospital, Nanjing Medical University, Nanjing 210029, China*
[3] *State Key Laboratory of Phytochemistry and Plant Resources in West China, Kunming Institute of Botany, Chinese Academy of Sciences, Lanhei Road, Heilongtan, Kunming 650201, China*

Correspondence should be addressed to Yi Kong; yikong668@163.com and Ji-Fu Wei; weijifu@hotmail.com

Received 30 December 2013; Revised 11 March 2014; Accepted 12 March 2014; Published 10 April 2014

Academic Editor: Joen-Rong Sheu

Toona microcarpa Harms is a tonic, antiperiodic, antirheumatic, and antithrombotic agent in China and India and an astringent and tonic for treating diarrhea, dysentery, and other intestinal infections in Indonesia. In this study, we prepared ethyl-acetate extract from the air-dried leaves of *Toona microcarpa* Harms and investigated the anticoagulant activities *in vitro* by performing activated partial thromboplastin time (APTT), prothrombin time (PT), and thrombin time (TT) assays. Antiplatelet aggregation activity of the extract was examined using adenosine diphosphate (ADP), collagen, and thrombin as agonists, and the inhibitions of factor Xa and thrombin were also investigated. Bleeding and clotting times in mice were used to determine its anticoagulant activities *in vivo*. It is found that *Toona microcarpa* Harms leaf extract (TMHE) prolonged APTT, PT, and TT clotting times in a dose-dependent manner and significantly inhibited platelet aggregation induced by thrombin, but not ADP or collagen. Clotting time and bleeding time assays showed that TMHE significantly prolonged clotting and bleeding times *in vivo*. In addition, at the concentration of 1 mg/mL, TMHE inhibited human thrombin activity by 73.98 ± 2.78%. This is the first report to demonstrate that THME exhibits potent anticoagulant effects, possibly via inhibition of thrombin activity.

1. Introduction

Many traditional Chinese herbal medicines have been used for thousands of years in clinical practice because of their proven efficacy, wide indications, high safety profile, and low toxicity [1]. *Toona microcarpa* Harms, a tree reaching 10 m, is a perennial hardwood of the family *Meliaceae* that is found in India, Bhutan, Laos, Malaysia, Myanmar, Papua New Guinea, Thailand, Sikkim, Indochina, and southern China. This species yields excellent timber and has long been used as a traditional Chinese medicine (TCM) for treating various conditions as its leaves, seeds, and root bark have medicinal effects. Specifically, the bark is used as a powerful astringent and purgative, and the leaf extract has antithrombotic effect and antibiotic activity against *Staphylococcus*, with leaf tip concoctions applied to swellings. *Toona microcarpa* Harms is considered a tonic, antiperiodic, antirheumatic, and antithrombotic agent in China and India and is used as an astringent and tonic for treating diarrhea, dysentery, and other intestinal infections in Indonesia [2]. However, there are few reports about the antithrombotic activities of *Toona microcarpa* Harms and the mechanism is unknown.

Thrombosis is a major cause of morbidity and mortality and is closely related to activated platelet adhesion, aggregation, secretion functions, and activation of intrinsic and extrinsic coagulation systems, which cause blood coagulation and fibrin formation [3]. In TCM, thrombotic disorders are described as blood stasis syndrome. *Toona microcarpa* Harms has some effects on activating blood circulation to dissipate blood stasis; however, the mechanism underlying its effect has been poorly studied. In this study, we prepared ethylacetate extract from the air-dried leaves of *Toona microcarpa* Harms and investigated its antithrombotic activity and underlying mechanism.

2. Materials and Methods

2.1. Preparation of Toona microcarpa Harms Leaf Extract (TMHE). The aerial parts of *Toona microcarpa* Harms were collected in February 2013 from the Jinghong region of Yunnan Province, China. The plant was identified by Dr. Rong Li, and a voucher specimen (KIB 13-02-08) was deposited in the State Key Laboratory of Phytochemistry and Plant Resources in west China, Kunming Institute of Botany, Chinese Academy of Sciences. Air-dried and powdered leaves of *Toona microcarpa* Harms (1 kg) were extracted with 90% ethanol (5000 mL × 2) at room temperature and concentrated *in vacuo* to yield crude extract. The dry extract was resuspended in distilled water (1000 mL) and extracted twice with petroleum (30–60°C) to remove pigments and lipids, followed by two more extractions with ethylacetate using liquid-liquid partitioning. After removing the solvent using a rotary vacuum evaporator, the ethylacetate fraction was used to determine its bioactivity. TMHE was dissolved in dimethylsulfoxyde to obtain stock solutions of 50 mg/mL. Working solutions were obtained by dilution with distilled water.

2.2. Activated Partial Thromboplastin Time (APTT), Prothrombin Time (PT), and Thrombin Time (TT) Assays In Vitro. Male imprinting control region (ICR) mice (28–32 g) were supplied by the animal center of Nanjing Medical University. All animal experiments were approved by the Animal Care and Use Committee of The First Affiliated Hospital of Nanjing Medical University. Blood was drawn from the eyeball of ICR mice and separately centrifuged at 3000 rpm for 15 min to obtain platelet poor plasma (PPP). For *in vitro* APTT assays, 50 μL normal citrated PPP was incubated with 50 μL TMHE (0.5, 1, 2, 3, or 4 mg/mL) and 50 μL APTT reagent for 3 min at 37°C. APTT clotting time was immediately recorded after the addition of 100 μL calcium chloride (20 mM). For *in vitro* PT assays, 50 μL normal citrated PPP was incubated with 50 μL (0.5, 1, 2, 3, or 4 mg/mL) TMHE for 3 min at 37°C. Clotting time was immediately recorded after the addition of 100 μL PT reagent [4]. For *in vitro* TT assay, 100 μL normal citrated PPP was incubated with 100 μL (0.5, 1, 2, 3, or 4 mg/mL) TMHE for 2 min at 37°C. Clotting time was immediately recorded after the addition of 100 μL TT reagent [5]. All coagulation assays were performed in triplicate. Heparin (1 mg/mL) and argatroban (TIPR Pharmaceutical Responsible Co., Ltd., 0.05 mg/mL) were used as positive controls, and the extract solvents were used as negative controls.

2.3. Platelet Aggregation Test. Male New Zealand rabbits (4-5 kg) were supplied by the animal center of Nanjing Medical University. All animal experiments were approved by the Animal Care and Use Committee of The First Affiliated Hospital of Nanjing Medical University. After application of the local anesthetic lidocaine, blood was drawn from the carotid artery of male New Zealand rabbits and directly collected into vials containing sodium citrate (1 : 9 v/v) mixture. The blood samples were centrifuged at 1000 rpm for 10 min at room temperature to prepare platelet rich plasma (PRP), and the residue was centrifuged at 3000 rpm for 15 min at room temperature to obtain PPP [6]. Briefly, 270 μL PRP and 30 μL TMHE were incubated at 37°C in an aggregometer. After a 3 min preincubation, 30 μL of agonists (ADP, collagen, or thrombin, the final concentrations are 5 μM, 2 μL/mL, and 1 NIH/mL) was added to initiate aggregation, which was monitored for 6 min. The extract solvents were used as negative controls; aspirin (1 mg/mL) and argatroban (0.005 mg/mL) were used as positive controls. The inhibition rate was calculated as follows: inhibition rate = (Av – At)/Av × 100%; Av is the platelet aggregation percent of negative control and At is the platelet aggregation percent of the TMHE group, respectively.

2.4. Thrombin Inhibition Assay. TMHE (20 μL) (0.1, 0.2, 0.3, 0.5, 0.8, or 1 mg/mL) and 20 μL human thrombin (5 NIH/mL) (Hyphen-BioMed, France) in 20 μL Tris-HCl buffer (0.05 M, pH 7.5) were incubated for 15 min in a 96-well plate. The reaction was initiated by adding 20 μL thrombin chromogenic substrate CS-01(38) (2.5 mg/mL), and the absorbance at 405 nm was recorded every 0.5 min for 5 min. The background absorbance was measured just before adding the substrate. In A-t curve, the curve slope was considered the reaction rate (v). The enzyme inhibition percentage (I) was determined as follows: $I = (V_0 - V_i)/V_0 \times 100\%$. V_0 is the rate of extract solvents, and V_i is the rate of TMHE. Extract solvents were used as negative controls, whereas argatroban (TIPR Pharmaceutical Responsible Co., Ltd., 5 μg/mL) was used as a positive control. The results were expressed as mean ± SD for three independent experiments.

2.5. Factor Xa Inhibition Assay. The same protocol as described for thrombin was followed using 20 μL human factor Xa (2.5 μg/mL) (Hyphen-BioMed) in 20 μL PBS buffer (1/15 M, pH 8.34) and 20 μL CS-11(22) substrate (2.5 mg/mL). Rivaroxaban (Bayer, 0.5 μg/mL) was used as a positive control. The results were expressed as mean ± SD for three independent experiments.

2.6. APTT and PT Assays Ex Vivo. ICR mice (18–22 g) were divided into five treatment groups (both sexes, six per group) and orally administered extract solvents (control), low dose TMHE (20 mg/kg body weight), medium dose TMHE (40 mg/kg body weight), high dose TMHE (80 mg/kg body weight), and dabigatran etexilate (Boehringer Ingelheim, 20 mg/kg body weight). Blood was collected intracardially at 120 min after dosing [5]. The APTT and PT assays were performed as described in Section 2.2, except that test samples were not added to the blood samples.

2.7. Clotting Time Assay In Vivo. Whole blood clotting time in mice was measured by the capillary glass tube method [7]. ICR mice (18–22 g) were divided into five groups (both sexes, six per group) and orally administered extract solvents (control), low dose TMHE (20 mg/kg body weight), medium dose TMHE (40 mg/kg body weight), high dose TMHE (80 mg/kg body weight), and dabigatran etexilate (20 mg/kg body weight). Each group was administered drug for four

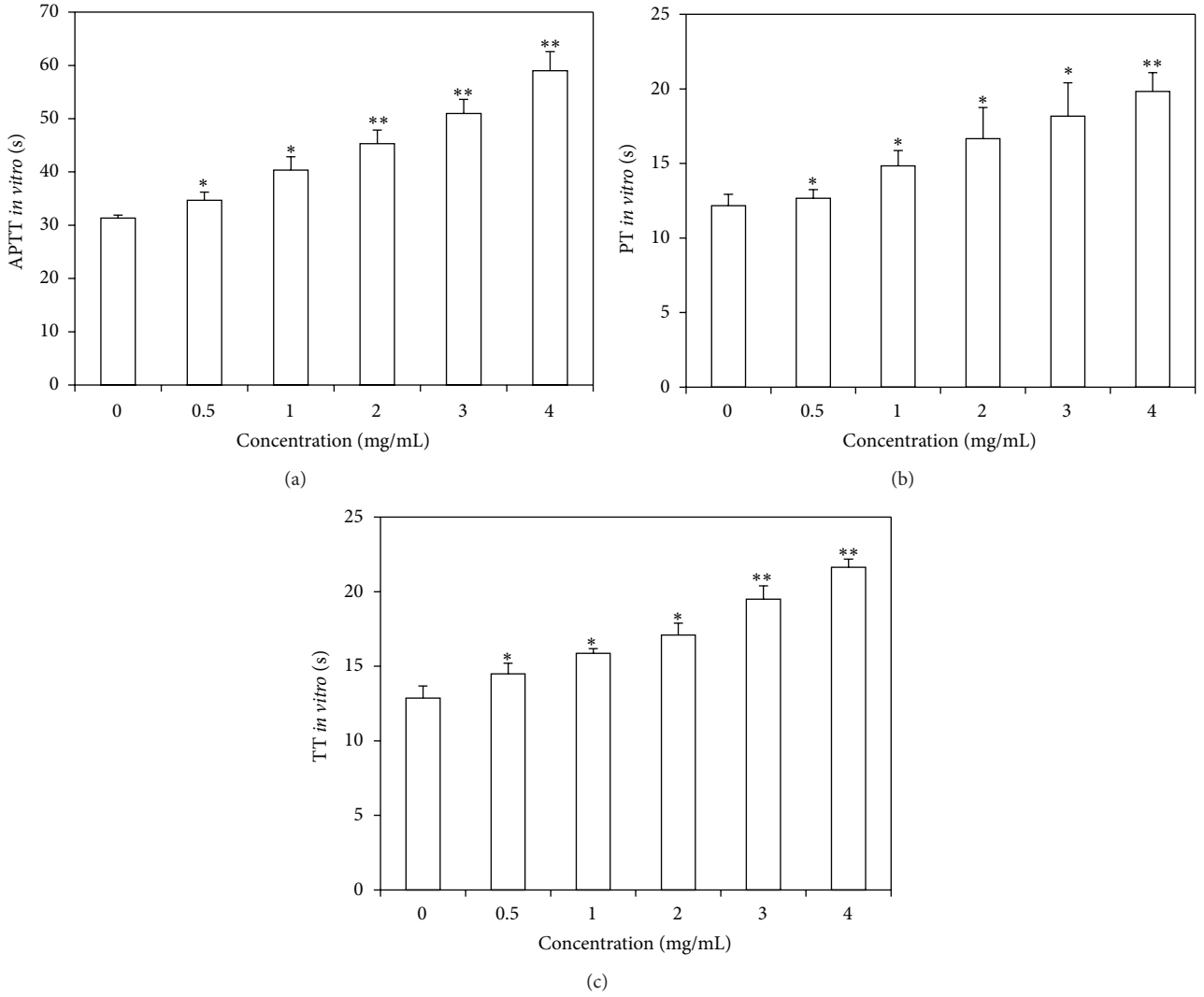

Figure 1: Anticoagulant assays *in vitro*. (a) TMHE prolonged the APTT clotting time in a dose-dependent manner. (b) TMHE prolonged PT clotting time in a dose-dependent manner. (c) TMHE prolonged PT clotting time in a dose-dependent manner. $^{**}P < 0.01$, $^{*}P < 0.05$, compared with extract solvent.

consecutive days. Ninety minutes after the last administration, blood samples were collected via the retroorbital plexus with a glass capillary tube and kept on a slide to allow clotting. The blood was stirred with a dry needle every 30 s until the needle wire provoked a fibrous protein, which was defined as clotting time [3].

2.8. Bleeding Time Assay In Vivo. ICR mice (18–22 g) were divided into five groups (both sexes, six per group) and orally administered extract solvents (control), low dose TMHE (20 mg/kg body weight), medium dose TMHE (40 mg/kg body weight), high dose TMHE (80 mg/kg body weight), and dabigatran etexilate (20 mg/kg body weight). Each group was administered drug for four consecutive days. Ninety minutes after the last administration, the mice tails were marked with a tag approximately 5 mm long and then cut at the mark. Then, the tip of the tail was immersed in saline at 37°C, and the time from cutting the tip of the tail to stopping the bleeding was recorded; this interval was defined as bleeding time [8].

2.9. Acute Toxicity. The acute toxicity of TMHE was evaluated in mice according to the description of Wang et al. [9]. Six ICR mice (18–22 g) of both sexes were orally administered with TMHE (2 g/kg body weight) by gavage. Four hours after administration, the mice were observed for toxic symptoms continuously. Finally, the number of survivors was noted after 24 h and these animals were then maintained for further 13 days with observations made daily.

3. Results

3.1. APTT, PT, and TT Assays In Vitro. For *in vitro* coagulation assays, TMHE prolonged APTT, TT, and PT clotting times in a dose-dependent manner (Figure 1). It prolonged APTT clotting time from 34.67 ± 1.53 to 59 ± 3.61 s

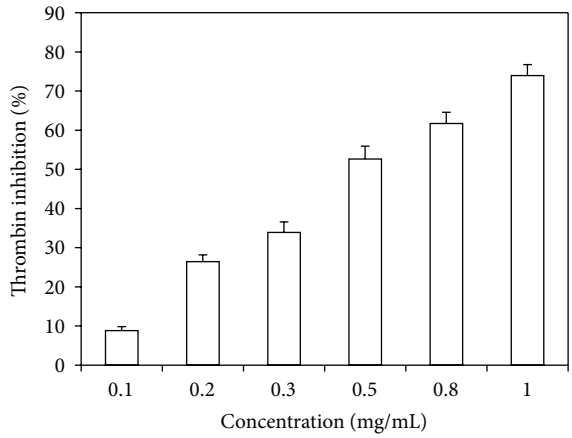

Figure 2: Thrombin inhibition of TMHE. TMHE inhibited the activity of thrombin in a dose-dependent manner.

(Figure 1(a)), PT clotting time from 12.67 ± 0.76 to 19.83 ± 1.26 s (Figure 1(b)), and TT clotting time from 14.5 ± 0.7 to 21.63 ± 0.55 s (Figure 1(c)) at the concentration of 4 mg/mL. Heparin prolonged APTT and PT clotting times more than 120 s and 60 s, respectively, at a concentration of 1 mg/mL. Argatroban prolonged TT clotting times more than 120 s at a concentration of 0.05 mg/mL.

3.2. In Vitro Antiplatelet Aggregation Assay. The potential antiplatelet aggregation activity of TMHE was investigated using antiplatelet aggregation assays using ADP or collagen or thrombin as agonists. TMHE at a concentration up to 8 mg/mL did not significantly inhibit platelet aggregation induced by the two platelet agonists. However, TMHE inhibited the thrombin stimulated platelet aggregation activity by 31.41 ± 7.84% at the concentration of 1 mg/mL. Argatroban inhibited the thrombin stimulated platelet aggregation activity by 78.21 ± 3.29% at the concentration of 0.005 mg/mL.

3.3. Thrombin and Factor Xa Inhibition Assays. As shown in Figure 2, TMHE inhibited the activity of human thrombin in a dose-dependent manner. Specifically, it inhibited human thrombin activity by 73.98 ± 2.78% at a concentration of 1 mg/mL, whereas at a concentration of 5 μg/mL argatroban inhibited thrombin activity by 36.32 ± 2.24%. However, TMHE did not inhibit the activity of human factor Xa.

3.4. APTT and PT Assays Ex Vivo. For *ex vivo* coagulation assays, mice were treated with 20, 40, or 80 mg/kg body weight TMHE. An increase in APTT clotting time was observed with medium and high doses of TMHE 90 min after oral administration (Figure 3(a)). However, no significant changes were observed in PT clotting time (Figure 3(b)).

3.5. Clotting and Bleeding Times In Vivo. Compared to the control group, medium and high doses of TMHE significantly prolonged the clotting time, indicating that TMHE has anticoagulant effects (Figure 3(c)). Moreover, the dabigatran etexilate treated group had longer bleeding times than the TMHE treatment groups (Figure 3(d)).

3.6. Acute Oral Toxicity. No death was recorded in the 14 days observation period in the mice given 2 g/kg of TMHE orally. All of animals did not show any changes in the general appearance during the observation period.

4. Discussion

Toona microcarpa Harms has traditionally been used as an herbal medicine in Chinese culture for activating blood circulation to remove stasis. In this study, we used bleeding and clotting times in mouse models to investigate the *in vivo* hematological effect of TMHE. The results showed that TMHE significantly prolonged bleeding and clotting times in a dose-dependent manner, indicating that TMHE has potent antihemostatic effects. Hemostasis is divided into two consecutive stages: platelet aggregation and coagulation cascade. Therefore, both platelet and coagulation factors play roles in blood hemostasis. An increase in bleeding and clotting times suggests a defect or inhibition of either platelet aggregation or blood coagulation pathways. Firstly, we evaluated the potential antiplatelet activity of TMHE using ADP, collagen, and thrombin as agonists. The results showed that TMHE can inhibit platelet aggregation induced by thrombin, but not by ADP and collagen.

Secondly, the anticoagulant activities of TMHE were measured by APTT, PT, and TT. APTT is used to evaluate the coagulation factors such as VIII, IX, XI, XII, and prekallikrein in intrinsic coagulation pathway while PT is used to evaluate the coagulation factors V, VII, and X in extrinsic coagulation pathway [10]. TT reflects the blood coagulation status that transforms fibrinogen into fibrin, which is directly induced by the addition of thrombin. The test only detects disturbances in the final stages of coagulation, especially dysfibrinogenemia or the presence of thrombin inhibitors [11]. In our study, the results of APTT, PT, and TT assays *in vitro* showed that TMHE significantly prolonged APTT, PT, and TT clotting times in a dose-dependent manner; the *ex vivo* coagulation assays results showed that an increase in APTT clotting time was observed with medium and high doses of TMHE while no significant changes were observed in PT clotting time. These results indicated that TMHE may mainly exhibit anticoagulant activity correlating with the intrinsic coagulation process.

Thirdly, to further investigate the anticoagulant activity or mechanism of TMHE, coagulation factors (thrombin and FXa) inhibition tests were used. Thrombin and FXa are two highly validated targets that function at key steps in the coagulation cascade [12]. Many clinically used anticoagulant drugs are thrombin inhibitors (e.g., argatroban) or FXa inhibitors (e.g., rivaroxaban). Thrombin plays a central role in maintaining the integrity of hemostasis, interacts with most zymogens and their cofactors, and plays multiple procoagulant and anticoagulant roles in blood coagulation [13]. FXa, in combination with its cofactor Va, converts prothrombin to thrombin, resulting in initial fibrin formation. It sits at the

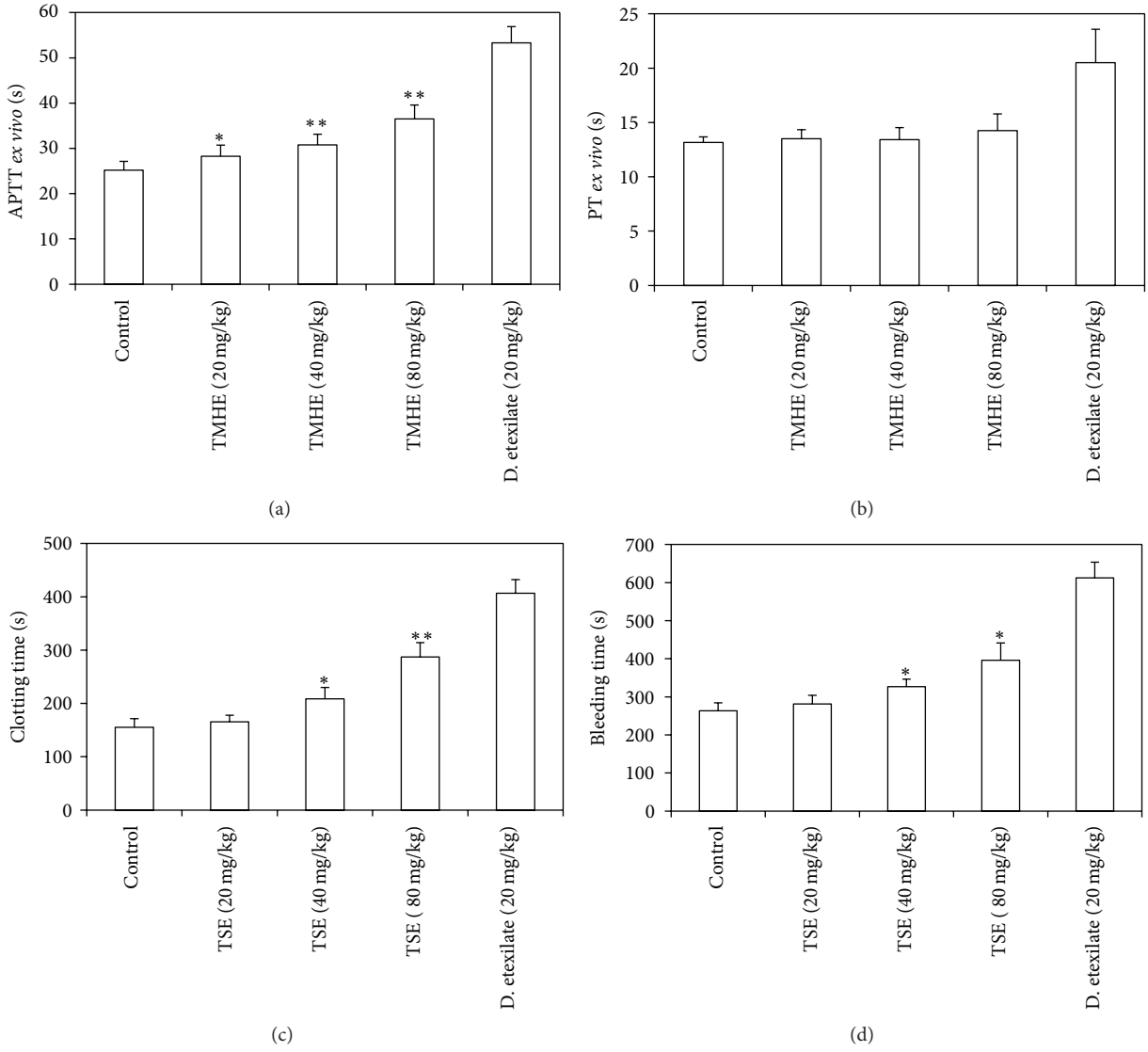

Figure 3: Anticoagulant assays *in vivo*. (a) APTT clotting time increased at medium and high doses of TMHE. (b) There were no significant changes in PT clot time. (c) Effect of TMHE on clotting time. (d) Effect of TMHE on bleeding time. $^{**}P < 0.01$, $^{*}P < 0.05$, compared with control group.

junction of the extrinsic and the intrinsic pathways and plays a critical role in controlling the hemostatic network [4]. In this study, we found that TMHE inhibited thrombin activity in a dose-dependent manner but had no significant effect on FXa activity. Thrombin appears as the major target of the TMHE.

In summary, TMHE prolonged APTT, PT, and TT clotting times, inhibited the thrombin but not ADP or collagen stimulated platelet aggregation, and prolonged the whole bleeding and clotting time, possibly *via* inhibition of thrombin. These results will be helpful to understand the antithrombotic mechanism of *Toona microcarpa* Harms.

Many TCMs have been demonstrated to have anticoagulant activity. Danggui (*Radix angelicae Sinensis*), Honghua (*Flos carthami*), and Danshen (*Salvia miltiorrhiza Bunge*) are examples of TCM herbs that are used to activate blood circulation to remove blood stasis [14]. In addition, Taoren (*Persicae semen*) and Honghua (*Flos carthami*) used in pair named as Taoren-Honghua herb pair have also been used for many years to promote blood circulation to dissipate blood stasis [15]. In some studies, herbs extracts were found to have anticoagulant activities; for example, Xin et al. found that 95% ethanol extract of dragon's blood inhibits platelet aggregation and prolongs anticoagulation activities [16]. Zeng et al. found that the methanol extract of *Geum japonicum* at a concentration of 2 mg/mL has significant anticoagulant activity in the extrinsic coagulation pathway [17]. Han et al. found that 70% ethanol fraction from an aqueous extract of *Rubus chingii* leaves is the most antithrombotic fraction *in vitro* and *in vivo*, and flavonoids make an important contribution [18]. Wang et al. found that the *Erigeron breviscapus* extract has anticoagulant activity [19]. However, these studies mostly focused on their anticoagulant or antiplatelet activities, without implying the role of coagulation factors or platelet. Few studies further

studied the effects of herb on the coagulation factors or platelet. Ku et al. found that persicarin and isorhamnetin which are isolated from *Oenanthe javanica* inhibit not only the activities of thrombin and FXa but also the generations of thrombin and FXa in human umbilical vein endothelial cells [20]. Robert et al. found that the leaf extracts especially the aqueous extract of *Croton zambesicus* Müell. Arg exhibited both the thrombin and FXa inhibition but no antiplatelet activity [21]. In this study, we also investigated TMHE's effect on coagulation factors or platelet and found that TMHE could inhibit the thrombin activity, but no effects on FXa or platelet.

In conclusion, this is the first report to demonstrate that TMHE has anticoagulant activity, most likely via its ability to inhibit thrombin activity. *Toona microcarpa* Harms may be a thrombin inhibitor that can function as an anticoagulant therapeutic. However, the anticoagulant activity of TMHE is weaker compared with positive control drugs such as heparin, argatroban, and dabigatran etexilate. It may be due to that TMHE is merely raw product which is extracted from the air-dried leaves of *Toona microcarpa* Harms by ethylacetate. We will perform further separation and purification for the active components.

Conflict of Interests

The authors declare that there is no conflict of interests regarding the publication of this paper.

Authors' Contribution

Hao Chen, Min Jin, and Yi-Fen Wang contributed to this paper equally.

Acknowledgments

This study was sponsored by Chinese National Natural Science Foundation (31340073, 81273274, and 81273375), Jiangsu Province's Key Provincial Talents Program (RC201170), National Major Scientific and Technological Special Project for "Significant New Drugs Development" (2011ZX09302-003-02), Jiangsu Province Major Scientific and Technological Special Project (BM2011017), and a project funded by the Priority Academic Program Development of Jiangsu Higher Education Institutions.

References

[1] A.-P. Lu, H.-W. Jia, C. Xiao, and Q.-P. Lu, "Theory of traditional chinese medicine and therapeutic method of diseases," *World Journal of Gastroenterology*, vol. 10, no. 13, pp. 1854–1856, 2004.

[2] H. Peng and J. M. Edmonds, "Toona," in *Flora of China*, Z. Y. Wu and P. H. Raven, Eds., vol. 11, pp. 112–115, Science Press, Beijing & Missouri Botanical Garden Press, St. Louis, Miss, USA, 2008.

[3] G. Gong, Y. Qin, and W. Huang, "Anti-thrombosis effect of diosgenin extract from *Dioscorea zingiberensis* C.H. Wright *in vitro* and *in vivo*," *Phytomedicine*, vol. 18, no. 6, pp. 458–463, 2011.

[4] Y. Kong, Y. Shao, H. Chen et al., "A novel factor Xa-inhibiting peptide from centipedes venom," *International Journal of Peptide Research and Therapeutics*, vol. 19, pp. 303–311, 2013.

[5] Y. Li and N. Wang, "Antithrombotic effects of Danggui, Honghua and potential drug interaction with clopidogrel," *Journal of Ethnopharmacology*, vol. 128, no. 3, pp. 623–628, 2010.

[6] Y. Kong, J.-L. Huo, W. Xu, J. Xiong, Y.-M. Li, and W.-T. Wu, "A novel anti-platelet aggregation tripeptide from *Agkistrodon acutus* venom: isolation and characterization," *Toxicon*, vol. 54, no. 2, pp. 103–109, 2009.

[7] X. Li, G. Han, S. Zhang et al., "Effects of veratrum nigrum var. ussuriense alkaloids on platelet aggregation and time of coagulation and bleeding," *Chinese Traditional and Herbal Drugs*, vol. 11, pp. 1269–1272, 2004.

[8] M. Kogushi, T. Matsuoka, T. Kawata et al., "The novel and orally active thrombin receptor antagonist E5555 (Atopaxar) inhibits arterial thrombosis without affecting bleeding time in guinea pigs," *European Journal of Pharmacology*, vol. 657, no. 1–3, pp. 131–137, 2011.

[9] J. P. Wang, H. X. Xu, Y. X. Wu et al., "Ent-16β,17-dihydroxy-kauran-19-oic acid, a kaurane diterpene acid from *Siegesbeckia pubescens*, presents antiplatelet and antithrombotic effects in rats," *Phytomedicine*, vol. 18, no. 10, pp. 873–878, 2011.

[10] A. P. S. Azevedo, J. C. Farias, G. C. Costa et al., "Anti-thrombotic effect of chronic oral treatment with *Orbignya phalerata* Mart," *Journal of Ethnopharmacology*, vol. 111, no. 1, pp. 155–159, 2007.

[11] E. Koch and A. Biber, "Treatment of rats with the *Pelargonium sidoides* extract EPs 7630 has no effect on blood coagulation parameters or on the pharmacokinetics of warfarin," *Phytomedicine*, vol. 14, no. 1, pp. 40–45, 2007.

[12] H. Nar, "The role of structural information in the discovery of direct thrombin and factor Xa inhibitors," *Trends in Pharmacological Sciences*, vol. 33, no. 5, pp. 279–288, 2012.

[13] T. E. Adams and J. A. Huntington, "Thrombin-cofactor interactions: Structural insights into regulatory mechanisms," *Arteriosclerosis, Thrombosis, and Vascular Biology*, vol. 26, no. 8, pp. 1738–1745, 2006.

[14] T. O. Cheng, "Cardiovascular effects of Danshen," *International Journal of Cardiology*, vol. 121, no. 1, pp. 9–22, 2007.

[15] L. Liu, J.-A. Duan, Y. Tang et al., "Taoren-Honghua herb pair and its main components promoting blood circulation through influencing on hemorheology, plasma coagulation and platelet aggregation," *Journal of Ethnopharmacology*, vol. 139, no. 2, pp. 381–387, 2012.

[16] N. Xin, Y.-J. Li, Y. Li et al., "Dragon's Blood extract has antithrombotic properties, affecting platelet aggregation functions and anticoagulation activities," *Journal of Ethnopharmacology*, vol. 135, no. 2, pp. 510–514, 2011.

[17] F. Q. Zeng, H. X. Xu, K. Y. Sim et al., "The anticoagulant effects of *Geum japonicum* extract and its constituents," *Phytotherapy Research*, vol. 12, pp. 146–148, 1998.

[18] N. Han, Y. Gu, C. Ye, Y. Cao, Z. Liu, and J. Yin, "Antithrombotic activity of fractions and components obtained from raspberry leaves (Rubus chingii)," *Food Chemistry*, vol. 132, no. 1, pp. 181–185, 2012.

[19] Y. Wang, X. Yang, H. Liu, and X. Tang, "Study on effects of Erigeron breviscapus extract on anticoagulation," *Journal of Chinese Medicinal Materials*, vol. 26, no. 9, pp. 656–658, 2003.

[20] S. K. Ku, T. H. Kim, and J. S. Bae, "Anticoagulant activities of persicarin and isorhamnetin," *Vascular Pharmacology*, vol. 58, pp. 272–279, 2013.

[21] S. Robert, C. Baccelli, P. Devel, J.-M. Dogné, and J. Quetin-Leclercq, "Effects of leaf extracts from *Croton zambesicus* Müell. Arg. on hemostasis," *Journal of Ethnopharmacology*, vol. 128, no. 3, pp. 641–648, 2010.

Hindawi Publishing Corporation
BioMed Research International
Volume 2014, Article ID 182846, 7 pages
http://dx.doi.org/10.1155/2014/182846

Research Article

Characterization of Imidazoline Receptors in Blood Vessels for the Development of Antihypertensive Agents

Mei-Fen Chen,[1,2] Jo-Ting Tsai,[3] Li-Jen Chen,[4] Tung-Pi Wu,[5] Jia-Jang Yang,[2] Li-Te Yin,[2] Yu-lin Yang,[2] Tai-An Chiang,[2] Han-Lin Lu,[6] and Ming-Chang Wu[1]

[1] *Department of Food Science, National Pingtung University of Science and Technology, Neipu, Pingtung 91201, Taiwan*
[2] *College of Medicine and Life Science, Chung Hwa University of Medical Technology, Rende District, Tainan City 71703, Taiwan*
[3] *Department of Radiation Oncology, Taipei Medical University-Shuang Ho Hospital, and College of Medicine, Taipei Medical University, Taipei City 10361, Taiwan*
[4] *Institute of Basic Medical Sciences, College of Medicine, National Cheng Kung University, Tainan City 70101, Taiwan*
[5] *Department of Obs/Gyn, Tainan Sin-Lau Hospital, The Presbyterian Church in Taiwan, Tainan City 70142, Taiwan*
[6] *Department of Chinese Medicine, Tainan Sin-Lau Hospital, The Presbyterian Church in Taiwan, Tainan City 70142, Taiwan*

Correspondence should be addressed to Han-Lin Lu; a0935265113@gmail.com and Ming-Chang Wu; mcwu@mail.npust.edu.tw

Received 16 February 2014; Accepted 9 March 2014; Published 3 April 2014

Academic Editor: Juei-Tang Cheng

It has been indicated that activation of peripheral imidazoline I_2-receptor (I-2R) may reduce the blood pressure in spontaneously hypertensive rats (SHRs). Also, guanidinium derivatives show the ability to activate imidazoline receptors. Thus, it is of special interest to characterize the I-2R using guanidinium derivatives in blood vessels for development of antihypertensive agent(s). Six guanidinium derivatives including agmatine, amiloride, aminoguanidine, allantoin, canavanine, and metformin were applied in this study. Western blot analysis was used for detecting the expression of imidazoline receptor in tissues of Wistar rats. The isometric tension of aortic rings isolated from male rats was also estimated. The expression of imidazoline receptor on rat aorta was identified. However, guanidinium derivatives for detection of aortic relaxation were not observed except agmatine and amiloride which induced a marked relaxation in isolated aortic rings precontracted with phenylephrine or KCl. Both relaxations induced by agmatine and amiloride were attenuated by glibenclamide at concentration enough to block ATP-sensitive potassium (K_{ATP}) channels. Meanwhile, only agmatine-induced relaxation was abolished by BU224, a selective antagonist of imidazoline I_2-receptors. Taken together, we suggest that agmatine can induce vascular relaxation through activation of peripheral imidazoline I_2-receptor to open K_{ATP} channels. Thus, agmatine-like compound has the potential to develop as a new therapeutic agent for hypertension in the future.

1. Introduction

Hypertension is known as the main risk parameters in patients with cardiovascular diseases, such as myocardial infarction and stroke. Many agents used in clinics are mentioned to produce side effects. Thus, development of the better agent to handle hypertension is urgent [1].

Imidazoline receptors are introduced to play a role in cardiovascular regulation [2, 3]. In recent, 3 subtypes of imidazoline receptors have been proposed; activation of I-1 receptors regulates the blood pressure through central nervous system [4], whereas I-3 receptors participate in insulin release [5] and activation of I-2 receptors (I-2R) increases glucose uptake into muscle cells [6, 7]. The clinical used antihypertensive agent rilmenidine may reduce blood pressure via an activation of imidazoline I_1-receptors in brain to lower sympathetic tone [8, 9]. But, application of rilmenidine in hypertension is usually to produce some side effects such as mental depression, insomnia, and drowsiness. Thus, development of new agent for management of hypertension is essential. Recently, an activation of peripheral imidazoline I_2-receptor (I-2R) was documented to produce antihypertensive actions in spontaneous hypertensive rats (SHRs) [10]. Thus, peripheral I-2R seems a potential target in development of

antihypertensive drugs without side effects of sympathetic inhibition.

It has been documented that compounds with guanidine-like structures may bind to imidazoline receptors [11]. Thus, it is of special interest to investigate the effect of guanidinium derivatives on peripheral I-2R for vasodilatation. Then, this may help the development of new agent(s) for hypertension in the future.

2. Material and Methods

2.1. Animals. The male Wistar rats, weighing from 250 to 300 g, were obtained from the Animal Center of National Cheng Kung University Medical College. Animals were housed individually in plastic cages under standard laboratory conditions. We kept them under a 12 h light/dark cycle and had free access to food and water. All experiments were performed under anesthesia with 2% isoflurane to minimize the animals' suffering. The animal experiments were approved and conducted in accordance with local institutional guidelines for the care and use of laboratory animals, and the experiments conformed to the Guide for the Care and Use of Laboratory Animals as well as the guidelines of the Animal Welfare Act.

2.2. Preparation of Isolated Aortic Rings. Isolation of aortas was performed as described previously [10] from Wistar rats. After sacrifice under anesthesia with pentobarbital (50 mg/kg), the thoracic aortas were removed to put in the oxygenated Krebs' buffer (95% O_2, 5% CO_2). Aortas were cut into ring segments about 3 mm without fat and connective tissue. Then, as described previously [10], they were mounted in the organ baths containing 10 mL oxygenated Krebs' buffer (95% O_2, 5% CO_2) at 37°C.

Similar to previous report [10], each ring was connected to strain gauges (FT03; Grass Instrument, Quincy, MA, USA) to measure the isometric tension through chart software (MLS023, Powerlab; AD Instruments, Bella Vista, NSW, Australia). Samples were mounted to stabilize for 2 h. Each ring was then stretched gradually for optimal resting tension at 1 g.

2.3. Vasodilatation Caused by Guanidinium Derivatives. After the stabilization of resting tone, a solution of either phenylephrine (Sigma-Aldrich, St. Louis, MO, USA) or KCl prepared in distilled water was added to the bathing buffer to induce a marked raise in vascular tone followed by a stable vasoconstriction (tonic contraction). The final concentration in the organ bath of both phenylephrine and KCl was 1 μmol/L and 50 mmol/L, similar to previous report [10]. Rings of the treated group were exposed to agmatine, amiloride, metformin, allantoin, canavanine, and aminoguanidine (10 μM) for recording the alterations in tonic contraction (vasodilatation). Relaxation is expressed as the decreased percentage in maximal tonic contraction.

2.4. Effects of Blockers on Guanidinium Derivatives-Induced Vasodilatation. Aortic rings were exposed to BU224 (Research Biochemical, Wayland, MA, USA), a selective antagonist of imidazoline I_2-receptors, for 15 min prior to the addition of guanidinium derivatives into the organ bath. Glibenclamide (Tocris Cookson, Bristol, UK), as blocker specific for K_{ATP} channels, was administered in the same manner. The changes of vasodilatation after treatment with inhibitor were compared to vehicle-treated groups.

2.5. Western Blotting Analysis. Western blotting analysis was performed as the previous method [10] and we extracted protein from tissue homogenates using ice-cold radioimmunoprecipitation assay (RIPA) buffer supplemented with phosphatase and protease inhibitors (50 mmol/L sodium vanadate, 0.5 mM phenylmethylsulphonyl fluoride, 2 mg/mL aprotinin, and 0.5 mg/mL leupeptin). Concentrations of protein were determined with a Bio-Rad protein assay (Bio-Rad Laboratories, Inc., Hercules, CA, USA). Total proteins (30 μg) and were separated by SDS/polyacrylamide gel electrophoresis (10% acrylamide gel) using a Bio-Rad Mini-Protein II system. The protein was transferred to expanded polyvinylidene difluoride membranes (Pierce, Rockford, IL, USA) with a Bio-Rad Trans-Blot system. After transfer, the membranes were washed with PBS and blocked for 1 h at room temperature with 5% (w/v) skimmed milk powder in PBS. The manufacturer's instructions were followed for the primary antibody reactions. Following blocking, the blots were developed using antibodies for imidazoline receptors (IR) (Abcam, Cambridge, UK). The blots were subsequently hybridized using horseradish peroxidase-conjugated goat anti-goat IgG (Jackson ImmunoResearch Laboratories, Inc., PA, USA) and developed using the Western Lightning Chemiluminescence Reagent PLUS (PerkinElmer Life Sciences Inc., Boston, MA, USA). Densities of the obtained immunosblots at 37 KDa for imidazoline receptors (IR) and 43 KDa for actin were quantified using Gel-Pro analyser software 4.0 (Media Cybernetics, Silver Spring, MD, USA).

2.6. Statistical Analysis. Results were expressed as mean ± SE of each group. Statistical analysis was carried out using Student's t-test analysis. Statistical significance was set as $P < 0.05$.

3. Results

3.1. Identification of Imidazoline Receptor Expression in Tissues Using Western Blotting Analysis. The anti-NISCH (imidazoline) antibody positively reacted with the tissue lysate prepared from heart, aorta, pancreas, skeletal muscle, kidney, prostate, and urinary bladder using western blotting analysis (Figure 1). The expression of imidazoline receptor in aorta can thus be identified.

3.2. Effects of Guanidinium Derivatives on Vascular Tone. Six guanidinium derivatives of agmatine, amiloride, metformin, allantoin, canavanine, and aminoguanidine were tested in current study. Aortic ring strips are markedly contracted by the application of phenylephrine (1 μmol/L) or KCl (50 mmol/L) as described previously [12]. Similar

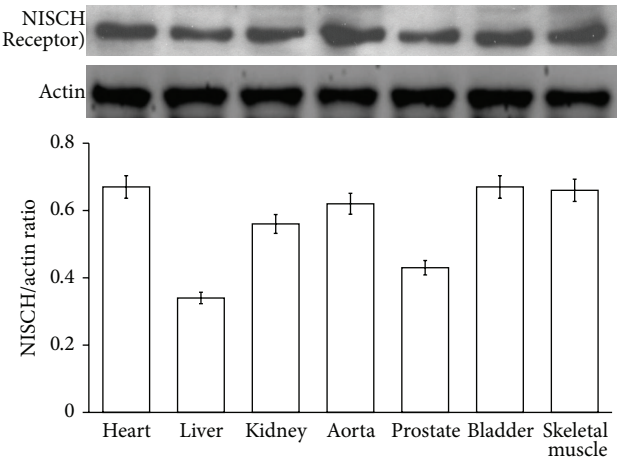

Figure 1: Detection of the expressions of imidazoline receptors in tissue homogenates by western blot analysis. The anti-NISCH (imidazoline receptors) antibody positively reacted with tissue lysate of heart, liver, aorta, skeletal muscle (SM), kidney, prostate, and bladder by western blot analysis. All values are presented as mean ± SEM ($n = 8$).

to the previous report [13], most guanidinium derivatives did not modify the vascular tone of aortic rings at the pharmacological concentration (10 μmol/L) but agmatine and amiloride significantly relaxed the tonic contraction of rats' aortic rings induced by phenylephrine. Similarly, KCl-induced tonic vasoconstriction was relaxed by agmatine and amiloride (Figure 2).

3.3. Effects of Imidazoline Receptor Antagonism on Agmatine or Amiloride-Induced Vasodilatation. Agmatine or amiloride at concentration of 10 μmol/L attenuated the tonic contraction of aortic rings induced by phenylephrine similar to that observed in KCl-induced tonic vasoconstriction. BU224 (0.01–1 μmol/L) produced a concentration-dependent inhibition of agmatine-induced relaxation in phenylephrine- or KCl-precontracted aortic rings (Figure 3(a)). However, BU224 did not modify the vascular relaxing action of amiloride (Figure 3(b)).

3.4. The Role of ATP-Sensitive K^+ (K_{ATP}) Channels in Agmatine- or Amiloride-Induced Vasodilatation. Glibenclamide (0.1–10 nmol/L) produced a concentration-dependent inhibition of agmatine-induced vasodilatation in phenylephrine- or KCl-precontracted aortic rings (Figure 4(a)). Similar inhibitions were also observed in amiloride-induced vasodilatation (Figure 4(b)). However, as shown in these figures, glibenclamide at 10 nmol/L abolished amiloride-induced vasodilatation totally but not agmatine-induced vasodilatation.

3.5. Enhanced Vasodilatation in Aortic Rings by Cotreatment with Agmatine and Amiloride. At the maximal concentration (10 μmol/L), agmatine or amiloride relaxed the tonic contraction of aortic rings induced by phenylephrine in a way similar to that in KCl-induced tonic vasoconstriction. The vasodilatation in aortic ring was enhanced by cotreatment with agmatine and amiloride (Figure 5).

4. Discussion

In the present study, we identified the expression of imidazoline receptor in aortic tissues isolated from rats. This is consistent with a previous report [10]. Then, we investigated the vasodilatation of guanidinium derivatives using agmatine, amiloride, metformin, allantoin, canavanine, and aminoguanidine. But only two agents, agmatine and amiloride, were effective for further characterizations. BU224, the well-known antagonist of imidazoline I_2-receptors, showed no effect on amiloride-induced vascular relaxation at the dose effective to block agmatine-induced relaxation. Both agmatine- and amiloride-induced relaxations were attenuated by glibenclamide at concentration sufficient to block ATP-sensitive potassium (K_{ATP}) channels. However, glibenclamide with the concentration effective to abolish amiloride-induced vasodilatation failed to block agmatine-induced vasodilatation totally (Figure 4). Also, enhanced vasodilatation was observed in aortic ring receiving the cotreatment with agmatine and amiloride at maximal concentration. Thus, agmatine-induced vascular relaxation seems not through the same mechanism as amiloride, while agmatine is known as the ligand of imidazoline receptors.

The imidazoline receptors are known to involve in cardiovascular regulations [14, 15]. Vascular tone is introduced as the main parameter in blood pressure regulations [16]. Actually, blood pressure is regulated by complicated factors; changes of blood pressure are widely used as the total peripheral resistance which is primarily a function of the resistance terminal arterioles [17]. Compounds with guanidine-like structures are known to bind with imidazoline receptors [11]. In this study, we employed six guanidinium derivatives including agmatine, amiloride, metformin, allantoin, canavanine, and aminoguanidine to screen the effects on vascular tone under the pharmacological dosage of 10 μM. The results show that only agmatine and amiloride significantly relaxed the phenylephrine- or KCl-induced tonic contraction of aortic rings isolated from rats to consist with the previous reports [10, 18].

It has been mentioned that metformin can inhibit phenylephrine-mediated aortic contraction at the dosage of 2 mM [19]. It seems different with our results. Actually, the dosage used at 2 mM seems too high and the result is mostly considered as nonspecific action. Moreover, allantoin failed to produce vasodilatation in isolated aortic ring. This finding is further supporting our previous report showing that antihypertensive effect of allantoin is mainly through an activation of imidazoline receptor in central nervous system [20]. However, before now, no report mentioned the vasodilatation of canavanine or aminoguanidine. It is possible that the guanidine derivatives including canavanine and aminoguanidine may induce vasodilatation at the dose higher than that used in current study and this view needs more investigation in the future.

In an attempt to know the role of imidazoline I-2 receptor (I2-R) in agmatine- or amiloride-induced vasodilatations,

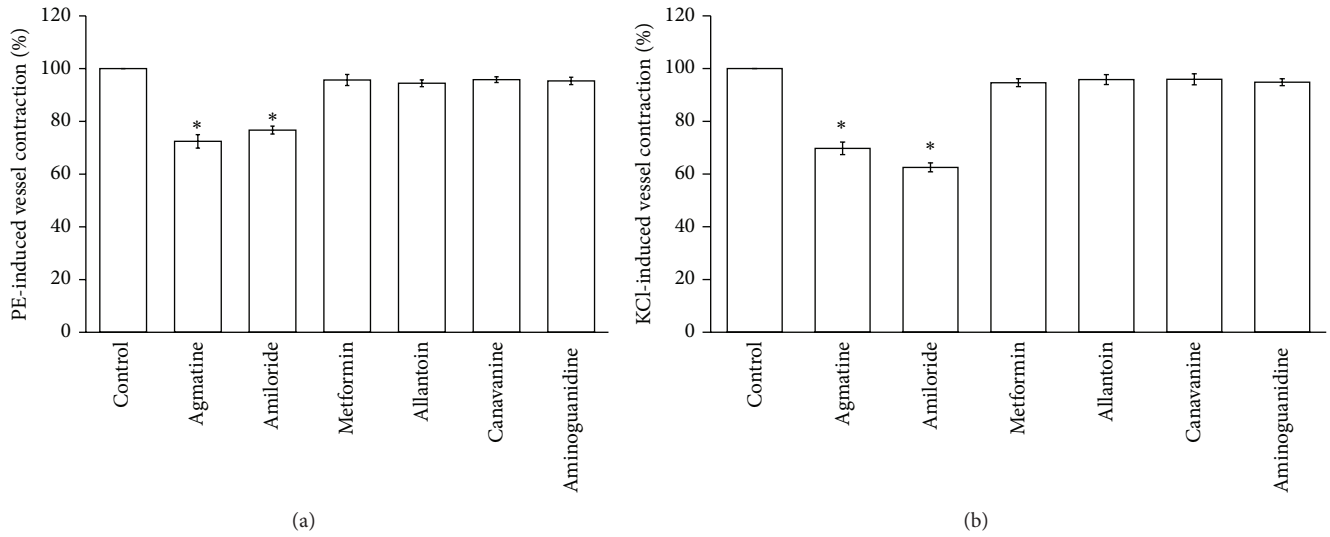

Figure 2: Screening of guanidinium derivatives for vasodilatation. Guanidinium derivatives (10 μmol/L), agmatine, amiloride, metformin, allantoin, canavanine, and aminoguanidine induced relaxation in isolated aortic rings precontracted with 1 μmol/L phenylephrine (a) or 50 mmol/L KCl (b). Data represent the mean ± SEM of eight animals in each column. All values are presented as mean ± SEM ($n = 8$). $^{*}P < 0.05$ as compared to the precontracted value.

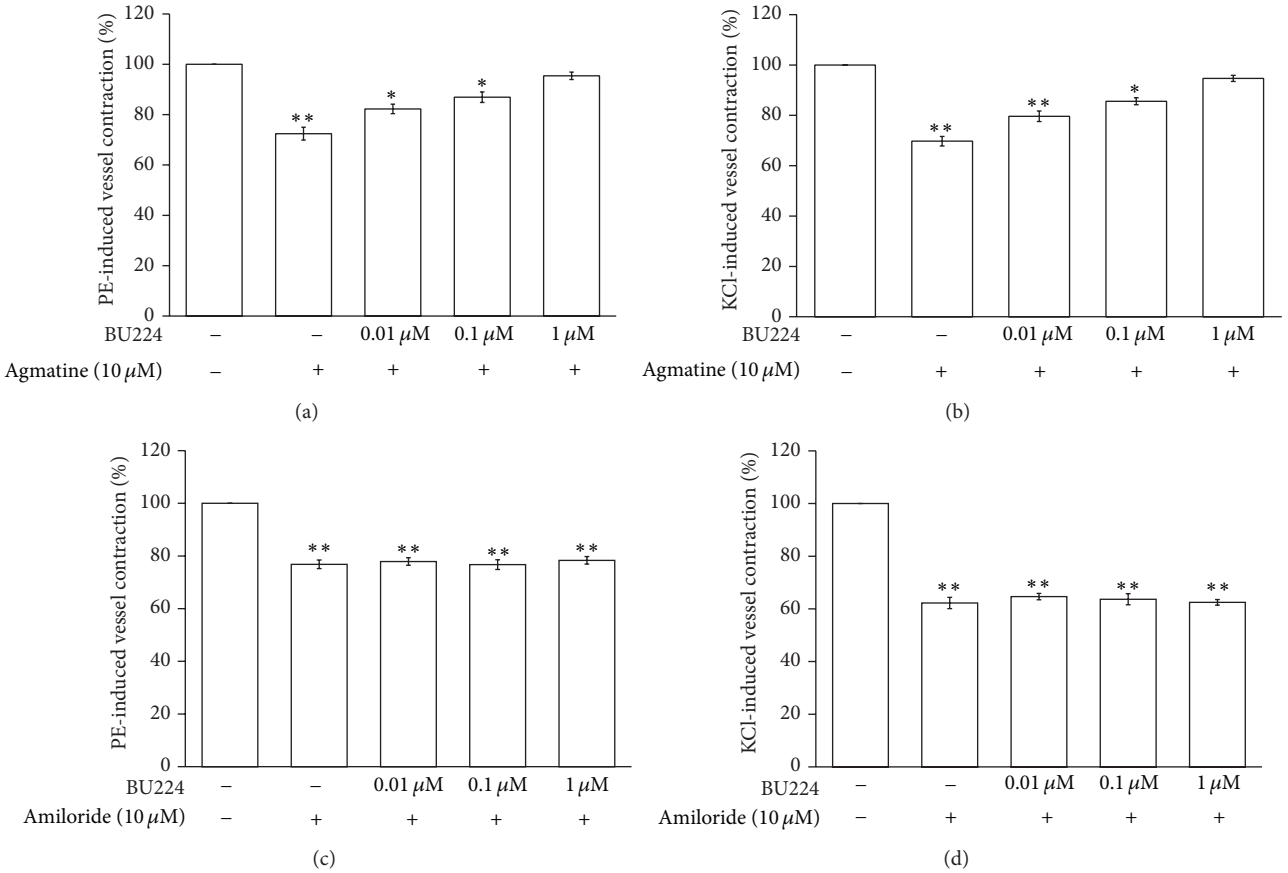

Figure 3: Effects of imidazoline receptor blockade on agmatine- or amiloride-induced vasodilatation. Effect of BU224 on concentration-dependent inhibition of agmatine- and amiloride- (10 μmol/L) induced relaxation in isolated aortic rings precontracted with 1 μmol/L phenylephrine ((a) and (b)) or 50 mmol/L KCl ((c) and (d)). All values are presented as mean ± SEM ($n = 8$). $^{*}P < 0.05$ and $^{**}P < 0.01$ as compared to agmatine-treated group.

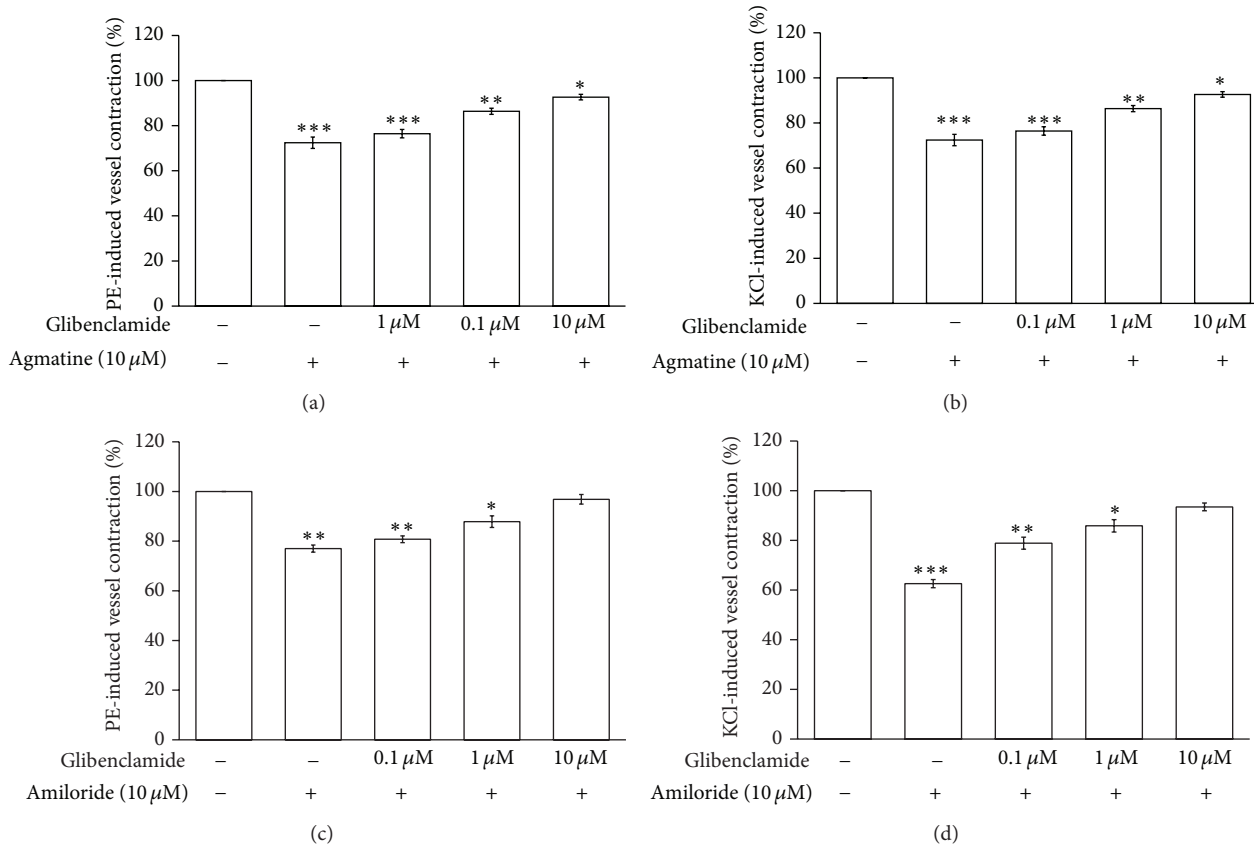

Figure 4: Effects of K_{ATP} blockade on agmatine- or amiloride-induced vasodilatation. Inhibitory effect of glibenclamide on the agmatine- or amiloride- (10 μmol/L) induced relaxation in isolated aortic rings precontracted with 1 μmol/L phenylephrine ((a) and (b)) or 50 mmol/L KCl (c and d). All values are presented as mean ± SEM ($n = 8$). $^{*}P < 0.05$, $^{**}P < 0.01$, and $^{***}P < 0.001$ as compared to the precontracted value.

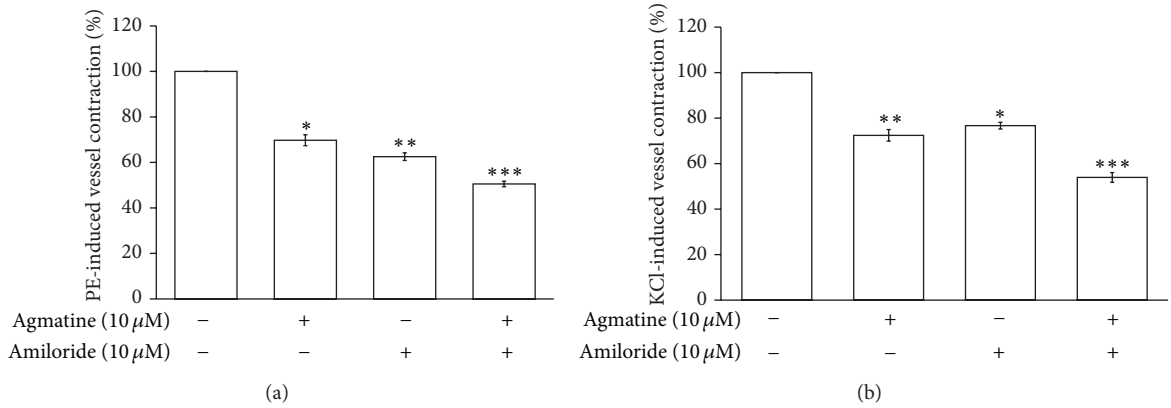

Figure 5: Vasodilatation in isolated aortic ring after cotreatment with agmatine and amiloride. Vasodilatation was enhanced by cotreatment with agmatine (10 μmol/L) and amiloride (10 μmol/L) in isolated aortic rings precontracted with 1 μmol/L phenylephrine (a) or 50 mmol/L KCl (b). All values are shown as mean ± SEM ($n = 8$). $^{**}P < 0.01$ and $^{***}P < 0.001$ as compared to the precontracted value.

imidazoline I-2R specific antagonist named BU224 was applied. Actually, the relaxation of agmatine was markedly reduced by pretreatment with BU224 at a concentration sufficient to block imidazoline I-2Rs. Thus, a direct effect of agmatine on I-2Rs can be identified. However, BU224 failed to modify the amiloride-induced vascular relaxation. The vessel dilatation of amiloride seems not to be through the activation of I-2Rs.

Due to a guanidino structure, amiloride binds to imidazoline $I_{2A}R$ through a high affinity for blockade of $I_{2A}R$ at

0.1 μM and inhibition of I_{2BR} at a higher concentration of 2 μM [21]. Thus, amiloride is widely used to distinguish the subtype of imidazoline I-2Rs. Previous study has also indicated that amiloride can induce vascular relaxation through an activation of Na^+-H^+ exchanger and consequently affect the K_{ATP} channel activity [22, 23]. In this study, BU224 failed to modify the 10 μM amiloride-induced vascular relaxation. It is possible that vasodilatation induced by amiloride at the concentration of 10 μM is mainly through the activation of K_{ATP} channels.

Potassium channels are mentioned as important in vascular relaxation [24]. ATP-sensitive potassium (K_{ATP}) channels are known to have four inwardly rectifying K^+ channel subunits and four regulatory sulfonylurea receptors [25]. Many contractions-induced endogenous substances are related to inhibition of K_{ATP} channels [25, 26]. Activation of K_{ATP} channels may produce hyperpolarization to relax vascular tone consequently. K_{ATP} channels dysfunction in aortic cells has been introduce to the impaired vasodilatation and/or hypertension observed in deoxycorticosterone acetate (DOCA) salt hypertensive rats [27]. In the present study, the relaxation induced by agmatine or amiloride in rat aortic rings was abolished by pretreatment with glibenclamide at a concentration sufficient to block K_{ATP} channels, as described previously [10, 23, 28, 29]. Thus, there is no doubt that K_{ATP} channels are involved in the aortic relaxation induced by agmatine or amiloride. However, agmatine-induced aortic relaxation seems not so simple although K_{ATP} channel is responsible for vasodilatation in PE- or KCl-induced contractions.

Agmatine has been introduced as an endogenous ligand of imidazoline receptors [30]. Activation of imidazoline I-2R by agmatine has also been mentioned in adrenal gland [31]. In this study, we demonstrated that BU224 at the dose enough to block imidazoline I-2Rs inhibited agmatine-induced vasodilatation. Thus, we suggest that agmatine has the ability to activate imidazoline I-2R on peripheral arterioles. As additional evidence, vasodilatation induced by agmatine at maximal dose was enhanced by cotreatment with amiloride. It means that amiloride has the ability to produce vasodilatation regardless of the total activation of imidazoline receptors. Amiloride seems not effective on imidazoline receptors only. Another mechanism for action of amiloride shall be investigated in the future.

5. Conclusion

According to the obtained data, we suggest that agmatine may act as peripheral antihypertensive agent through activation of imidazoline I-2 receptor for vasodilatation mainly through open of K_{ATP} channel. Thus, agmatine-like compound but not based on guanidinium structure has the potential to develop as a new antihypertensive agent in the future.

Conflict of Interests

The authors declare that there is no conflict of interests regarding the publication of this paper.

Authors' Contribution

Mei-Fen Chen and Jo-Ting Tsai contributed equally to this work.

Acknowledgments

The authors thank Mr. K.F. Liu for technical assistance and Professor King-Pong Lin for kind support and direction in this study. The present study was supported mainly by the Grants of National Sciences Council (NSC 102-2911-I-002-303 and NSC 103-2911-I-002-303).

References

[1] D. L. Cohen and R. R. Townsend, "Update on pathophysiology and treatment of hypertension in the elderly," *Current Hypertension Reports*, vol. 13, no. 5, pp. 330–337, 2011.

[2] S. Regunathan, C. Youngson, W. Raasch, H. Wang, and D. J. Reis, "Imidazoline receptors and agmatine in blood vessels: a novel system inhibiting vascular smooth muscle proliferation," *The Journal of Pharmacology and Experimental Therapeutics*, vol. 276, no. 3, pp. 1272–1282, 1996.

[3] J. Yang, W.-Z. Wang, F.-M. Shen, and D.-F. Su, "Cardiovascular effects of agmatine within the rostral ventrolateral medulla are similar to those of clonidine in anesthetized rats," *Experimental Brain Research*, vol. 160, no. 4, pp. 467–472, 2005.

[4] P. Ernsberger, M. E. Graves, L. M. Graff et al., "I_1-imidazoline receptors. Definition, characterization, distribution, and transmembrane signaling," *Annals of the New York Academy of Sciences*, vol. 763, pp. 22–42, 1995.

[5] N. G. Morgan, S. L. Chan, M. Mourtada, L. K. Monks, and C. A. Ramsden, "Imidazolines and pancreatic hormone secretion," *Annals of the New York Academy of Sciences*, vol. 881, pp. 217–228, 1999.

[6] T.-N. Lui, C.-W. Tsao, S.-Y. Huang, C.-H. Chang, and J.-T. Cheng, "Activation of imidazoline I_{2B} receptors is linked with AMP kinase pathway to increase glucose uptake in cultured C_2C_{12} cells," *Neuroscience Letters*, vol. 474, no. 3, pp. 144–147, 2010.

[7] C.-H. Chang, H.-T. Wu, K.-C. Cheng, H.-J. Lin, and J.-T. Cheng, "Increase of β-endorphin secretion by agmatine is induced by activation of imidazoline I_{2A} receptors in adrenal gland of rats," *Neuroscience Letters*, vol. 468, no. 3, pp. 297–299, 2010.

[8] P. A. van Zwieten and S. L. Peters, "Central I_1-imidazoline receptors as targets of centrally acting antihypertensive drugs. Clinical pharmacology of moxonidine and rilmenidine," *Annals of the New York Academy of Sciences*, vol. 881, pp. 420–429, 1999.

[9] M. Esler, "High blood pressure management: potential benefits of I_1 agents," *Journal of Hypertension*, vol. 16, no. 3, pp. S19–S24, 1998.

[10] G.-Y. Mar, M.-T. Chou, H.-H. Chung, N.-H. Chiu, M.-F. Chen, and J.-T. Cheng, "Changes of imidazoline receptors in spontaneously hypertensive rats," *International Journal of Experimental Pathology*, vol. 94, no. 1, pp. 17–24, 2013.

[11] C. Dardonville and I. Rozas, "Imidazoline binding sites and their ligands: an overview of the different chemical structures," *Medicinal Research Reviews*, vol. 24, no. 5, pp. 639–661, 2004.

[12] F. L. Wynne, J. A. Payne, A. E. Cain, J. F. Reckelhoff, and R. A. Khalil, "Age-related reduction in estrogen receptor-mediated mechanisms of vascular relaxation in female spontaneously

hypertensive rats," *Hypertension*, vol. 43, no. 2, pp. 405–412, 2004.

[13] W. Raasch, U. Schäfer, F. Qadri, and P. Dominiak, "Agmatine, an endogenous ligand at imidazoline binding sites, does not antagonize the clonidine-mediated blood pressure reaction," *British Journal of Pharmacology*, vol. 135, no. 3, pp. 663–672, 2002.

[14] F. Messerli, "Moxonidine: a new and versatile antihypertensive," *Journal of Cardiovascular Pharmacology*, vol. 35, no. 4, pp. S53–S56, 2000.

[15] E. B. Monroy-Ordoñez, C. M. Villalón, L. E. Cobos-Puc, J. A. Márquez-Conde, A. Sánchez-López, and D. Centurión, "Evidence that some imidazoline derivatives inhibit peripherally the vasopressor sympathetic outflow in pithed rats," *Autonomic Neuroscience: Basic & Clinical*, vol. 143, no. 1, pp. 40–45, 2008.

[16] R. A. Khalil, "Modulators of the vascular endothelin receptor in blood pressure regulation and hypertension," *Current Molecular Pharmacology*, vol. 4, no. 3, pp. 176–186, 2011.

[17] G. V. Guinea, J. M. Atienza, F. J. Rojo et al., "Factors influencing the mechanical behaviour of healthy human descending thoracic aorta," *Physiological Measurement*, vol. 31, no. 12, pp. 1553–1565, 2010.

[18] T. M. Cocks, P. J. Little, J. A. Angus, and E. J. Cragoe Jr., "Amiloride analogues cause endothelium-dependent relaxation in the canine coronary artery in vitro: possible role of Na^+/Ca^{2+} exchange," *British Journal of Pharmacology*, vol. 95, no. 1, pp. 67–76, 1988.

[19] J. Y. Sung and H. C. Choi, "Metformin-induced AMP-activated protein kinase activation regulates phenylephrine-mediated contraction of rat aorta," *Biochemical and Biophysical Research Communications*, vol. 421, no. 3, pp. 599–604, 2012.

[20] M.-F. Chen, J.-T. Tsai, L.-J. Chen et al., "Antihypertensive action of allantoin in animals," *BioMed Research International*, vol. 2014, Article ID 690135, 6 pages, 2014.

[21] S. Diamant, T. Eldar-Geva, and D. Atlas, "Imidazoline binding sites in human placenta: evidence for heterogeneity and a search for physiological function," *British Journal of Pharmacology*, vol. 106, no. 1, pp. 101–108, 1992.

[22] T. Miura, Y. Liu, M. Goto et al., "Mitochondrial ATP-sensitive K^+ channels play a role in cardioprotection by Na^+–H^+ exchange inhibition against ischemia/reperfusion injury," *Journal of the American College of Cardiology*, vol. 37, no. 3, pp. 957–963, 2001.

[23] W. I. Rosenblum, E. P. Wei, and H. A. Kontos, "Vasodilation of brain surface arterioles by blockade of Na–H^+ antiport and its inhibition by inhibitors of KATP channel openers," *Brain Research*, vol. 1005, no. 1-2, pp. 77–83, 2004.

[24] E. A. Ko, J. Han, I. D. Jung, and W. S. Park, "Physiological roles of K^+ channels in vascular smooth muscle cells," *Journal of Smooth Muscle Research*, vol. 44, no. 2, pp. 65–81, 2008.

[25] J. E. Brayden, "Functional roles of KATP channels in vascular smooth muscle," *Clinical and Experimental Pharmacology and Physiology*, vol. 29, no. 4, pp. 312–316, 2002.

[26] N. Nakhostine and D. Lamontagne, "Adenosine contributes to hypoxia-induced vasodilation through ATP- sensitive K^+ channel activation," *American Journal of Physiology: Heart and Circulatory Physiology*, vol. 265, no. 4, pp. H1289–H1293, 1993.

[27] M. Ghosh, S. T. Hanna, R. Wang, and J. R. McNeill, "Altered vascular reactivity and KATP channel currents in vascular smooth muscle cells from deoxycorticosterone acetate (DOCA)-salt hypertensive rats," *Journal of Cardiovascular Pharmacology*, vol. 44, no. 5, pp. 525–531, 2004.

[28] C.-C. Tsai, T.-Y. Lai, W.-C. Huang, I.-M. Liu, and J.-T. Cheng, "Inhibitory effects of potassium channel blockers on tetramethylpyrazine-induced relaxation of rat aortic strip in vitro," *Life Sciences*, vol. 71, no. 11, pp. 1321–1330, 2002.

[29] K.-L. Wong, P. Chan, H.-Y. Yang et al., "Isosteviol acts on potassium channels to relax isolated aortic strips of Wistar rat," *Life Sciences*, vol. 74, no. 19, pp. 2379–2387, 2004.

[30] W. Raasch, U. Schäfer, J. Chun, and P. Dominiak, "Biological significance of agmatine, an endogenous ligand at imidazoline binding sites," *British Journal of Pharmacology*, vol. 133, no. 6, pp. 755–780, 2001.

[31] S.-L. Hwang, I.-M. Liu, T.-F. Tzeng, and J.-T. Cheng, "Activation of imidazoline receptors in adrenal gland to lower plasma glucose in streptozotocin-induced diabetic rats," *Diabetologia*, vol. 48, no. 4, pp. 767–775, 2005.

Hindawi Publishing Corporation
BioMed Research International
Volume 2014, Article ID 586501, 8 pages
http://dx.doi.org/10.1155/2014/586501

Research Article

Cerebrovascular and Neuroprotective Effects of Adamantane Derivative

Ruben S. Mirzoyan,[1] Tamara S. Gan'shina,[1] Denis V. Maslennikov,[1] Georgy I. Kovalev,[1] Ivan A. Zimin,[1] Boris M. Pyatin,[1] Nina I. Avdyunina,[1] Anna M. Kukhtarova,[1] Nelly G. Khostikyan,[2] Vahe S. Meliksetyan,[2] Cristina B. Alikhanyan,[2] and Narine R. Mirzoyan[2]

[1] *Zakusov Institute of Pharmacology RAMS, 8 Baltiyskaya Street, Moscow 125315, Russia*
[2] *Yerevan State Medical University after Mkhitar Heratsi, 2 Koryun Street, 0025 Yerevan, Armenia*

Correspondence should be addressed to Ruben S. Mirzoyan; cerebropharm@mail.ru

Received 15 January 2014; Revised 12 February 2014; Accepted 13 February 2014; Published 20 March 2014

Academic Editor: Joen-Rong Sheu

Objectives. The influence of 5-hydroxyadamantane-2-on was studied on the rats' brain blood flow and on morphological state of brain tissue under the condition of brain ischemia. The interaction of the substance with NMDA receptors was also studied. *Methods*. Study has been implemented using the methods of local blood flow registration by laser flowmeter, [^{3}H]-MK-801binding, and morphological examination of the brain tissue. We used the models of global transient ischemia of the brain, occlusion of middle cerebral artery, and hypergravity ischemia of the brain. *Results*. Unlike memantine, antagonist of glutamatergic receptors, the 5-hydroxyadamantane-2-on does not block NMDA receptors but enhances the cerebral blood flow of rats with brain ischemia. This effect is eliminated by bicuculline. Under conditions of permanent occlusion of middle cerebral artery, 5-hydroxyadamantane-2-on has recovered compensatory regeneration in neural cells, axons, and glial cells, and the number of microcirculatory vessels was increased. 5-Hydroxyadamantane-2-on was increasing the survival rate of animals with hypergravity ischemia. *Conclusions*. 5-Hydroxyadamantane-2-on, an adamantane derivative, which is not NMDA receptors antagonist, demonstrates significant cerebrovascular and neuroprotective activity in conditions of brain ischemia. Presumably, the GABA-ergic system of brain vessels is involved in mechanisms of cerebrovascular and neuroprotective activity of 5-hydroxyadamantane-2-on.

1. Introduction

The brain ischemia is accompanied by a cascade of pathophysiological and biochemical processes caused by oxygen and energy deficiency as well as functional changes like failure of balance between excitatory and inhibitory processes in CNS, which leads to irreversible damage of the neural tissue. The decrease in the rate of aerobic glycolysis brings, to intracellular acidosis, decrease in work efficiency of the sodium-potassium pump, changes in ionic gradients, enhanced discharge of excitatory amino acid glutamate, high concentrations of which cause increased flow of calcium ions into the cell, and activation of enzyme systems. Under these conditions the process of oxidative phosphorylation fails and toxins and free radicals, including NO, are produced; lipid peroxidation is activated and oxidative stress develops. All this results in damage of cytoplasmic organelles' membrane proteins and molecules of DNA and RNA, while expression of immediate early genes triggers the mechanism of cell death through necrosis or apoptosis [1–4].

It should be noted that GABA system is of high interest in conditions of brain ischemia, as GABA-ergic mechanisms play important role in terms of removing the imbalance between excitatory and inhibitory systems in CNS. It was demonstrated that concentration of GABA increases in early stages of ischemia and the high concentration of agonist usually leads to decreased sensitivity of receptors through negative feedback mechanism [5, 6]. There are also literature data stating that compounds, enhancing GABA-ergic transmission, have neuroprotective activity. These are agonists

and modulators of $GABA_A$ receptors, inhibitors of GABA transaminase, and GABA reuptake inhibitors [6]. GABA system, along with participation in inhibitory processes, plays important role in regulation of cerebral vascular tone. It is known that brain vessels contain GABA, as well as enzymes synthesizing and metabolizing GABA [7–9]. In pial vessels a high affinity of binding with $GABA_A$ receptors was observed at muscimol, a $GABA_A$ receptor agonist [10]. Earlier we showed that substances with GABA-ergic mechanism of action cause selective improvement of cerebral blood flow in conditions of ischemic damage of the brain [11–15].

Our attention was attracted by adamantane derivatives, which are able to block NMDA receptors and are widely used in neurological practice. Amantadine and memantine are used in the treatment of neurodegenerative diseases. Memantine in experiments prevents the development of neurotoxicity provoked by activation of NMDA receptors. It also blocks N-cholinoreceptors. Memantine improves cognitive functions in patients with mild to moderate vascular insufficiency [16, 17]. An adamantane derivative, 5-hydroxyadamantane-2-on, has ability to improve the blood supply of lower extremities in patients with chronic occlusive (obliterative) arterial disease of lower extremities [18].

In compliance with this, the aim of the current study was the comparative investigation of effects of 5-hydroxyadamantane-2-on and memantine on cerebral blood flow of intact rats and rats exposed to global transient brain ischemia. The study aimed also to investigate neuroprotective activity of 5-hydroxyadamantane-2-on in conditions of local permanent brain ischemia caused by occlusion of middle cerebral artery, with evaluation of morphological state of brain tissue. The survival rate of rats with hypergravity ischemia also was the objective of the study. There are some materials included in current study that analyze the mechanism of cerebrovascular and neuroprotective activity of studied substance.

2. Materials and Methods

Experiments of studying the brain blood flow were conducted on 76 narcotized (urethane 1.2 g/kg, i/p) nonlinear male rats weighting 180–400 g. Experiments of middle cerebral artery occlusion were conducted on 28 nonlinear male rats weighting 250–300 g, narcotized with chloral hydrate (400 mg/kg, i/p). 50 wakeful rats were involved in experiments with hypergravity ischemia and brains of 6 male Wistar rats (200–250 g) were used in experiments of radioligand binding.

The state of cerebral blood circulation in animals was estimated by the method of laser Doppler flowmetry. To register the local cerebral blood flow in parietal lobe of the brain cortex, BIOPAC MP100 system (USA) with laser Doppler flow module LDF100C was used; LD channel was calibrated in TPU (tissue perfusion unit) because this unit has better (~1) proportion to mL/min/100 grams of tissue than BPU (default unit for LDF100C). The 08 mm diameter needle-shaped detector of flowmeter was placed on the parietal lobe of the brain cortex of rats using micromanipulator and balancing arm. Changes of arterial pressure were registered simultaneously through a polyethylene catheter, preliminary inserted into the femoral artery. Based on data of detectors of blood flow and pressure, vascular resistance was estimated in real time. The recording of characteristics of blood flow, arterial pressure, and vascular resistance was conducted on polygraph "BIOPAC" (USA), connected with a personal computer. Investigating substances were administered through the polyethylene catheter into the femoral vein of animals.

The global transient ischemia in rats was achieved by 10-minute occlusion of both common carotid arteries with simultaneous decrease of arterial pressure down to 40–50 mm Hg, using method of bloodletting and following reperfusion.

The local permanent ischemia was obtained by the method of Tamura et al. [19], modified by Topchian et al. [20].

The morphological state of brain tissue was assessed on 6th and 12th days after occlusion of middle cerebral artery. These intervals were chosen based on existing literature data, according to which the most profound structural changes in the brain after occlusion of middle cerebral artery in rats are seen on 6th and 12th days [20, 21]. Animals were decapitated on 6th or 12th day after operation. The brain was extracted and fixed in 10% neutral solution of formaldehyde during the preparation for morphological examination and then sagittal incision was done including tissue supplied by middle cerebral artery. Furthermore, the tissue was fixed in a paraffin block. This block was sliced step by step into tissue specimens and was stained with universal histological dye, hematoxylin/eosin.

The first two series of morphological examination were done on two control groups of animals which underwent an occlusion of middle cerebral artery and were decapitated after 6 and 12 days, respectively.

In the following series of experiments animals were involved with occlusion of middle cerebral artery and treated with 5-hydroxyadamantane-2-on (100 mg/kg, i/p, once daily) 30 minutes after the occlusion and the following 6 and 12 days, respectively.

To study the survival rate of animals in conditions of hypergravity loading [22] wakeful rats were placed into special containers of centrifuge in craniocaudal orientation relatively to the vector of acceleration. In case of craniocaudal vector of acceleration (9 g during 12 minutes) the movement of blood occurs towards caudal orientation: as a result, the perfusion pressure falls dramatically down to the zero in all vessels of the head and brain ischemia develops.

2.1. Binding to NMDA Receptors. Binding to NMDA receptor subtype was studied using the method [23] with modifications. Tritium-labeled MK-801 (dizocilpine) with a specific activity of 210 Ci/mol was used [24]. The rat's hippocampal tissue was homogenized in a Potter homogenizer (Teflon glass) in 10 volumes of 5 mM HEPES/4.5 mM Tris buffer (pH 7.6) containing 0.32 M sucrose (buffer-1). The homogenate was diluted with 50 volumes of buffer-2 (5 mM HEPES/4.5 mM Tris buffer, pH 7.6) and centrifuged for 10 min at 1000 g. The supernatant was taken and again centrifuged for 20 min at 25000 g. The pellet was homogenized in 50 volumes of buffer-2 and centrifuged for 20 min at 8000 g. The supernatant and its soft unstable upper coat were taken and centrifuged for 20 min at 25000 g. The resulting

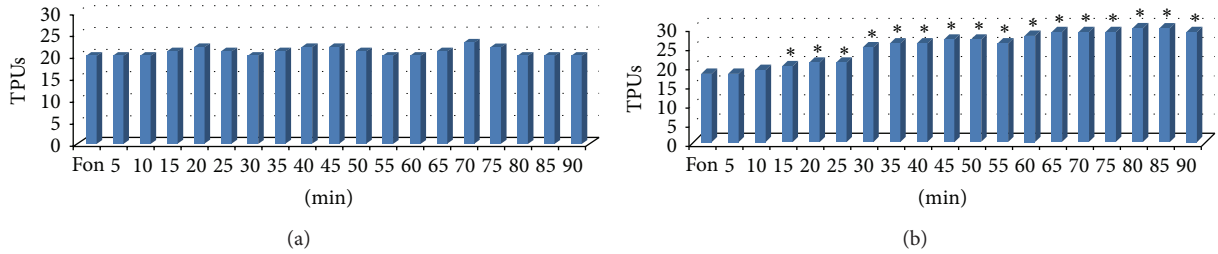

Figure 1: The influence of 5-hydroxyadamantane-2-on (100 mg/kg, IV) on CBF of intact rats (a) and animals with global transient brain ischemia (b).

precipitate was suspended in buffer-3 (5 mM HEPES/4.5 mM Tris buffer containing 1 mM NaEDTA, pH 7.6), and the suspension was centrifuged again. This washing procedure was repeated four times, with EDTA being excluded in the last wash. The final precipitate was resuspended in 5 volumes of buffer-2 and then stored in liquid nitrogen. The reaction mixture (final volume 0.5 mL) contained 200 μl of buffer-2, 50 μl of labeled ligand (50 nM solution), and 250 μl of protein suspension. The nonspecific binding was determined at the presence of 50 μl of unlabeled ligand. The reaction mixture was incubated at room temperature (20°C) for 2 h. After the incubation, the samples were filtered through GF/B filters (Whatman) which were presoaked in 0.3% polyethylenimine for 2 h at 4°C. Each test tube was washed 1 time with cold buffer-2, and the filters were then washed three times with the same buffer volume. The filters were dried on air and transferred to the scintillation vials. The radioactivity was determined on a Wallac 1411 scintillation counter with a counting efficiency of approximately 45%.

3. Statistical Analyses

The statistical analysis of data was carried out using the software Statistica 8.0 (Statistica Inc., USA). The normal distribution was defined by Shapiro-Wilk test. Generally, normal distribution was lacking; thus for the following analysis nonparametrical method of Wilcoxon signed-rank test was used. Survival data of animals in conditions of circulatory ischemia was calculated by Fisher criterion. *GraphPad Prism 5* software was used in experiments of radioligand binding. Results were considered statistically significant, when $P < 0.05$.

4. Results

4.1. The Influence of Adamantane Derivatives, 5-Hydroxyadamantane-2-on and Memantine, on Local Blood Flow of Brain Cortex in Intact Rats and Those with Global Transient Ischemia. Experiments on intact rats revealed that 5-hydroxyadamantane-2-on with intravenous administration of dose 100 mg/kg does not cause significant changes in blood flow of rats' brain cortex (Figure 1(a)). The adamantane derivative causes decrease of blood pressure in intact rats from 30 to 90 minutes by average of 11–14%.

In 10 minutes after intravenous administration of memantine (5 mg/kg) to intact narcotized rats, the decrease of local cerebral blood flow by 15% in average was registered. Further decrease of blood flow was observed, which reached 53% by the end of experiment. Memantine virtually did not affect the level of arterial blood pressure.

On the next series of experiments the influence of adamantane derivatives was studied on the brain blood flow after global transient ischemia. It was shown that 5-hydroxyadamantane-2-on (100 mg/kg, IV) causes slowly developing increase of local cerebral blood flow, which reaches its peak after 60 minutes (76.5%). This improvement of cerebral blood flow over the initial level lasts till the end of experiment (90 minutes and more) (Figures 1(b) and 2(b)). In these conditions, adamantane derivative lowers arterial pressure in rats by 11% in average.

Memantine (5 mg/kg) decreased (though in a less degree) local cerebral blood flow in the brain cortex of experimental animals as well as of intact rats. In the same experiment with memantine, arterial blood pressure failed statistically significantly by 14% in average.

Thus, the conducted experiments established that cerebrovascular effect of 5-hydroxyadamantane-2-on, unlike memantine, develops in conditions of ischemic brain damage and is absent in intact animals. It should be noted that increase of blood flow is a result of the influence of the substance on brain vascular tone. The results of rated resistance prove this, as adamantane derivatives along with increase in brain blood flow cause decrease in arterial pressure.

4.2. The Investigation of Neurochemical Mechanisms of Action of 5-Hydroxyadamantane-2-on. It is known that amino derivatives of adamantane (amantadine, memantine) possess their protective effects via noncompetitive antagonism with glutamate for NMDA receptors. However, there is no evidence of such mechanism for hydroxy derivatives, particularly 5-hydroxyadamantane-2-on. Thus, we observed the influence of this substance on binding of ligand of receptor's channel site, [^{3}H]-MK-801 (dizocilpine), with hippocampal membranes of rat. This effect was compared with that of memantine (Figure 6).

Results suggest that memantine actively competes with labeled dizocilpine in size of IC_{50} = 1.14 μM (95% confidence intervals: 0.82–1.57 μM, *GraphPad Prism 5*), while 5-hydroxyadamantane-2-on has no effect through the all range of concentrations.

In further studies we observed the influence of 5-hydroxyadamantane-2-on on local brain blood flow while

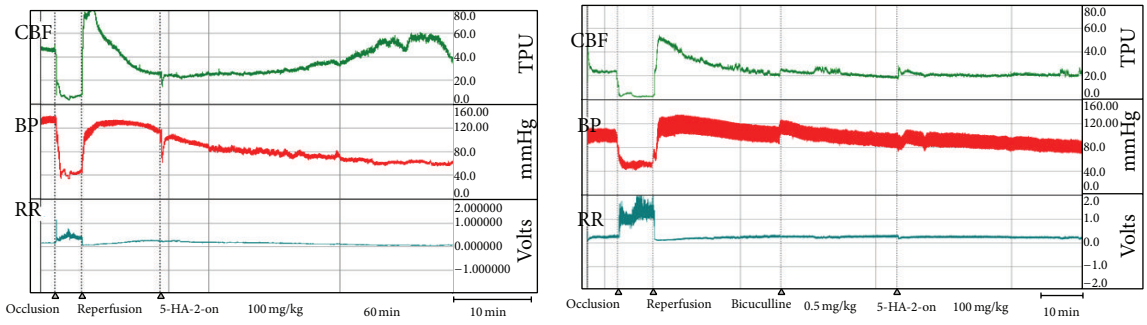

(a) (b)

Figure 2: The influence of 5-hydroxyadamantane-2-on (100 mg/kg, IV) (5HA-2-on) on local cerebral blood (CBF), blood pressure (BP), and rated resistance (RR) of rats after global transient ischemia of the brain (a) and with action of bicuculline (b).

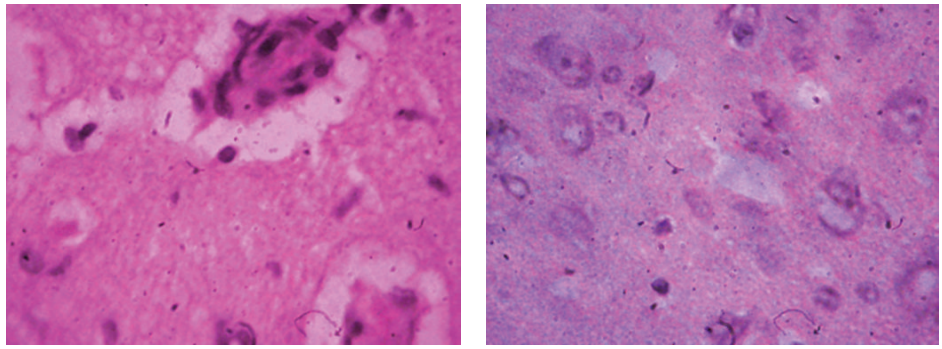

(a) (b)

Figure 3: Morphological picture of brain tissue of rats with occlusion of middle cerebral artery. (a) An expressed perivascular and pericellular edema of the brain, stasis in arterioles, and foci of empty neural and glial cells (staining hematoxylin/eosin ×400). (b) Against the background of necrobiosis, anuclear shadow cells of neurons as well as dystrophic neural and glial cells are seen (staining hematoxylin/eosin ×400).

blocking with bicuculline, a $GABA_A$ receptor blocker. This was reasonable, as substances with GABA-ergic mechanism of action reveal vasodilating activity in ischemic conditions. Bicuculline was administered by dose 0.5 mg/kg after ischemic damage of the brain, and then adamantane derivative was administered after 30 minutes. It was found out that, while blocking of GABA-receptors with bicuculline, 5-hydroxyadamantane-2-on does not increase the local brain blood flow (Figure 2(b)). These results indicate the participation of GABA-ergic mechanisms of cerebrovascular effects of 5-hydroxyadamantane-2-on in brain ischemia.

4.3. The Influence of 5-Hydroxyadamantane-2-on on Morphological State of Brain Tissue after the Occlusion of Middle Cerebral Artery. To study the neuroprotective activity of 5-hydroxyadamantane-2-on, its influence was observed on morphological injury of brain tissue provoked by occlusion of middle cerebral artery.

The morphological examination of specimens of control group (with occlusion of middle cerebral artery and without treatment) revealed an expressed perivascular and pericellular edema of brain tissue. In edematous brain tissue there are visible cells with dystrophy of neuronal cytoplasm and nucleus, zones of karyorrhexis, karyopyknosis, and karyolysis of neural and glial cells. Capillars and arterioles in state of stasis and microthrombosis are seen along with empty microcirculatory vessels. These arterioles are surrounded by emptied neural and glial cells (Figure 3(a)). There are zones of necrobiosis through all layers of cortical cells with wash-out, lysis of neural and large glial cells' nucleoplasm. Anuclear, necrotizing shadow cells as well as areas of dystrophic neurosecretory cells of paraventricular and supraoptic nuclei are detectible against the background of necrobiosis of cortical pyramidal cells (Figure 3(b)). Borders of all cortical layers are cleared. Several hypertrophic neurons with hyperchromic nuclei are seen between or near the profound ischemic foci. This indicates the intracellular regeneration of individual intact neural and glial cells. There are also proliferation zones of oligodendrocytes and astrocytes. Similar changes are registered also in neurosecretory cells located in the basin of middle cerebral artery. Punctuate and linear hemorrhages, meningeal edema, stasis in vessels of pia, and dura mater are seen in intercellular substance. Zones of hemosiderosis are also visible.

These obtained results correspond to the literature data of previous studies that showed up bilateral disturbances of brain blood flow, hypoxic damage of cortical neurocytes, and conduction pathways synaptic terminals

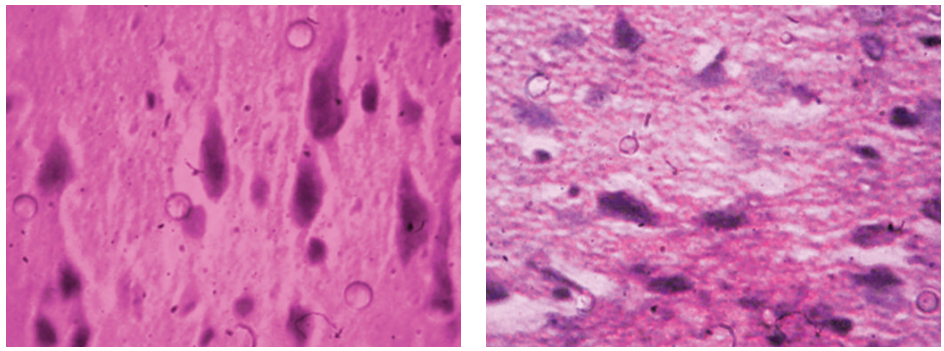

(a) (b)

Figure 4: Morphological picture of brain tissue of rats with occlusion of middle cerebral artery after treatment with 5-hydroxyadamantane-2-on. (a) Hypertrophic pyramidal cells with preserved neuritis (staining hematoxylin/eosin ×400); (b) along with hypertrophic cells, those without axons and with wrinkled cytoplasm and nucleus are seen (staining hematoxylin/eosin ×400).

in analogous periods after occlusion of middle cerebral artery.

In the next two series the influence of 5-hydroxiadamantane-2-on (100 mg/kg, i/p) was studied on morphological state of brain tissue of rats with occlusion of middle cerebral artery after 6 (3rd group) and 12 (4th group) days of treatment.

The morphological changes of brain tissue were examined on sagittal incisions of brain. This made it possible to detect tissue changes in regions of both left and right middle cerebral arteries and to provide comparative morphological picture of occluded (left) and not occluded (right) hemispheres.

Some neurons and groups of neurons are seen in the state of necrobiosis on serial tissue specimens of the 3rd group of animals, in the left hemisphere. Small foci of empty neural and glial cells and dystrophic changes of pyramidal cells of brain cortex are also seen. Pericellular and perivascular edema is marked slightly, vessels of microcirculatory bed are hyperemic as well as foci of extravasates, and old small hemorrhages with hemosiderin pigment are seen. Foci of glial cells', oligodendrocytes', and astrocytes' proliferation are also found.

Processes of dystrophy and individual cells in conditions of necrosis and necrobiosis are seen in neurosecretory cells of paraventricular and supraoptic nuclei. Against the background of above-described changes large hypertrophic neurosecretory cells are detected in paraventricular and supraoptic nuclei with the presence of multiple neurosecretory granules.

Similar changes and compensatory-regenerative processes are observed in all pyramidal cells of the cortex (Figure 4(a)). Axons of above-mentioned hypertrophic neurons are preserved through all length.

There are cells without neurites in the basin of middle cerebral artery, on the left side, with wrinkled cytoplasm and nucleus (Figure 4(b)). In ependymal cells of brain ventricles proliferation is observed, while in sinusoidal vessels hyperemia is observed. In response to harmful, polycystic changes there is a focal lymphoid-macrophagal reaction in individual preserved zones of necrosis and edema (Figure 5). There are also microvessels with obliterating white thrombotic bodies.

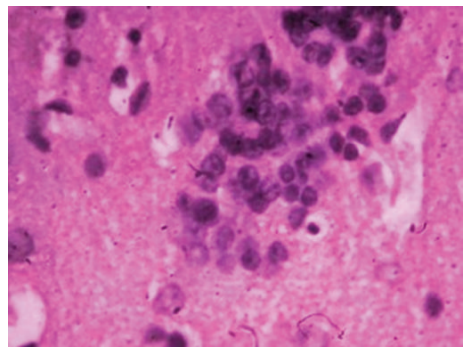

Figure 5: Morphological picture of brain tissue of rats with occlusion of middle cerebral artery after treatment with 5-hydroxyadamantane-2-on. Lymphoid-macrophagal reaction is observed in zones of necrosis and marked edema in response to impaired polycystic changes of brain tissue (staining hematoxylin/eosin ×400).

In the 4th group of animals the treatment with 5-hydroxiadamantane-2-on was conducted in the course of 12 days after occlusion of middle cerebral artery and the observed morphological changes had more reparative-regenerative and proliferative character. In general, the disposition of layers of cortical cells is preserved. There is a slight pericellular and perivascular edema of meninges and brain tissue along with hyperemia of microcirculatory vessels. Small foci of shadow neural and glial cells are visible. In the basin of left middle cerebral artery there are generally wide zones of pyramidal neurosecretory and glial cells of normal size, with precise borders between cytoplasm and nucleus and with available nucleolus. Granules of neurosecretory substance are observed in neurosecretory cells. There are ischemic zones in certain parts of third ventricle, where contours of neurons, glial cells, neuritis, and neuropile are vague. Hypertrophic neurocytes with hyperchromic nuclei are observed near these zones as well as functionally active neurosecretory cells with multiple secretory granules.

The morphological picture of the right hemisphere in basin of right middle cerebral artery was also examined on the same tissue specimens and a following comparison

Table 1: The influence of 5-hydroxyadamantane-2-on (5-HA-2-on) on survival rate of animals in conditions of hypergravity loading.

	Control		5-HA-2-on 50 mg/kg		5-HA-2-on 100 mg/kg		5-HA-2-on 150 mg/kg		5-HA-2-on 200 mg/kg	
	N	%	*N*	%	*N*	%	*N*	%	*N*	%
Number of survived animals	2	20	2	20	8*	80	6	60	6	60
Number of dead animals	8	80	8	80	2	20	4	40	4	40

* $P \leq 0.05$.

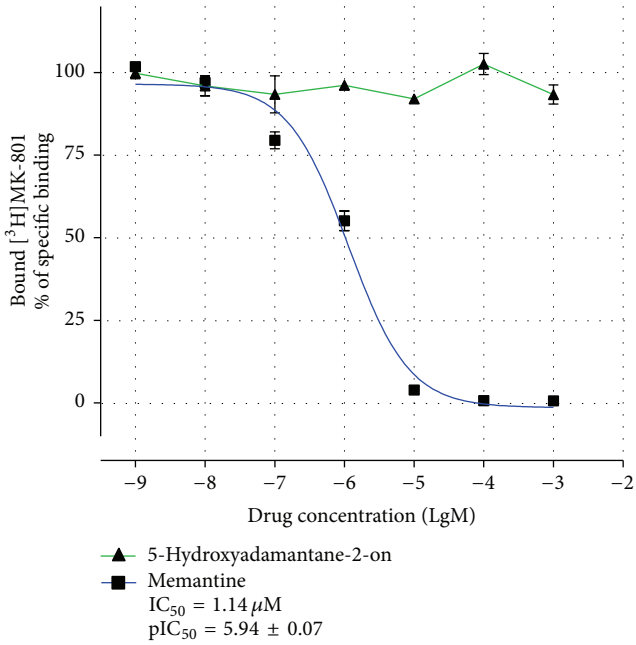

Figure 6: The influence of memantine and 5-hydroxyadamantane-2-on on specific binding of [^{3}H]-MK-801 with rat hippocampal membranes (pIC_{50} = m ± S.E.).

characteristic of morphological picture was made (the picture of secondary control on the same animals). There are insignificant perivascular and pericellular edema, hyperemia of microcirculatory bed in all series of the experiment (in control groups and groups treated with 5-hydroxyadamantane-2-on for 6 and 12 days), on the right hemisphere. There are compensatory-regenerative processes, that is, intracellular regeneration of organelles, hypertrophy of pyramidal cells and large glial cells, and increase in number of microcirculatory vessels. These processes are more significant on the 12th day after occlusion. Typically, in conditions of damage of one part of the brain, other parts of brain or another hemisphere (right—in this case) compensate and repair morphofunctional balance of the CNS.

4.4. The Influence of 5-Hydroxyadamantane-2-on on Survival Rate of Animals in Conditions of Hypergravity Loading. Antiischemic properties of adamantane derivative were observed on trials with wakeful rats in conditions of hypergravity loading. 5-Hydroxyadamantane-2-on was studied in doses 50–100–150–200 mg/kg injected intraperitoneally. Experiments revealed that the mortality rate from hypergravity overload is 80% in control group, while survival rate is 20%. After administration of adamantane derivative by the dose 100 mg/kg, survival rate rises up to 80% (Table 1). In doses 150–200 mg/kg survival rate was 60%. In these cases the data are not statistically significant. It can be concluded that adamantane derivative in doses 100 mg/kg reveals antiischemic effects in conditions of hypergravity ischemia like its effects in global permanent ischemia.

5. Conclusions

This paper introduces new data about cerebrovascular and neuroprotective activities of adamantane derivative, 5-hydroxyadamantane-2-on. Comparative study of cerebrovascular activity was done between two adamantane derivatives: 5-hydroxyadamantane-2-on and memantine, antagonist of glutamate receptors. There was revealed a substantial difference between their effects on blood flow of ischemic brain. 5-Hydroxyadamantane-2-on enhances blood flow and decreases vascular tone of rats with global permanent brain ischemia and has no such cerebrovascular effects on brains of intact rats, while memantine decreases blood flow in both intact and ischemic brains.

Further experiments studied the influence of 5-hydroxyadamantane-2-on on NMDA receptors taking into consideration that many adamantane derivatives, memantine particularly, are able to block NMDA receptors. It was found out that unlike memantine and many other amino derivatives of adamantane, 5-hydroxyadamantane-2-on does not interact with this site of NMDA receptors. Moreover, both of these compounds did not compete with [^{3}H]-7OH-DPAT for the binding site of dopamine receptors as well as with [^{3}H]-8OH-DPAT and [^{3}H]-ketanserin for the binding site of 5-HT1A- and 5-HT2A receptors, respectively.

The investigation of neuroprotective activity of 5-hydroxyadamantane-2-on in conditions of permanent occlusion of middle cerebral artery in rats was the other objective of this study. The compound was administered (100 mg/kg) 30 minutes after occlusion, once daily during 6 and 12 days. Experiments have shown that 5-hydroxyadamantane-2-on promotes the recovery of compensatory regeneration processes in neural cells, axons, glial cells. It also increases the quantity of vessels of microcirculatory bed. Results obtained indicate the neuroprotective effects of compound that was confirmed by results from experiments with hypergravity ischemia in rats, where survival rate of animals was increased

by treatment with the same dose of 5-hydroxyadamantane-2-on.

One of neuroprotective mechanisms demonstrated for 5-hydroxyadamantane-2-on was its capacity to enhance the blood flow of ischemic brain, which was not manifested in the background of action of specific $GABA_A$-receptor antagonist bicuculline. This proves the participation of GABA-ergic mechanisms in regulation of brain vessels' tone to realize cerebrovascular effects of studied compound.

As a conclusion, it should be noted that 5-hydroxyadamantane-2-on, an adamantane derivative, which is not a NMDA receptor antagonist, has significant cerebrovascular and neuroprotective activity in conditions of global and local brain ischemia which is manifested by enhancement of blood flow of ischemic brain, prevention of structural disturbances, and increase in survival rate of animals with global ischemia provoked by hypergravity loading. It can be supposed that GABA-ergic system of brain vasculature has a great value in cerebrovascular and neuroprotective activities of 5-hydroxyadamantane-2-on. Our results conform to the literature data as well as to the results of our own preview studies, according to which compounds enhancing GABA-ergic conduction, agonists and modulators of $GABA_A$ receptors, inhibitors of GABA transaminase, GABA reuptake inhibitors, possess neuroprotective activity [6, 11–15].

Conflict of Interests

The authors declare that there is no conflict of interests regarding the publication of this paper.

References

[1] E. H. Lo, T. Dalkara, and M. A. Moskowitz, "Mechanisms, challenges and opportunities in stroke," *Nature Reviews Neuroscience*, vol. 4, no. 5, pp. 399–415, 2003.

[2] E. H. Lo, M. A. Moskowitz, and T. P. Jacobs, "Exciting, radical, suicidal: how brain cells die after stroke," *Stroke*, vol. 36, no. 2, pp. 189–192, 2005.

[3] J. Lok, P. Gupta, S. Guo et al., "Cell-cell signaling in the neurovascular unit," *Neurochemical Research*, vol. 32, no. 12, pp. 2032–2045, 2007.

[4] B. R. S. Broughton, D. C. Reutens, and C. G. Sobey, "Apoptotic mechanisms after cerebral ischemia," *Stroke*, vol. 40, no. 5, pp. e331–e339, 2009.

[5] F. Galeffi, S. Sinnar, and R. D. Schwartz-Bloom, "Diazepam promotes ATP recovery and prevents cytochrome c release in hippocampal slices after in vitro ischemia," *Journal of Neurochemistry*, vol. 75, no. 3, pp. 1242–1249, 2000.

[6] R. D. Schwartz-Bloom and R. Sah, "γ-aminobutyric acid A neurotransmission and cerebral ischemia," *Journal of Neurochemistry*, vol. 77, no. 2, pp. 353–371, 2001.

[7] S. A. Mirzoian and V. P. Akopian, "Effect of gamma-aminobutyric acid on cerebral circulation and oxygen tension in the brain," *Farmakologiya i Toksikologiya*, vol. 30, no. 5, pp. 572–574, 1967 (Russian).

[8] S. A. Mirzoian, B. A. Kazarian, and V. P. Akopian, "Presence of gamma-aminobutyric acid in the cerebral and large vessels of man and animals," *Doklady Akademii Nauk SSSR*, vol. 186, no. 1, pp. 231–232, 1969 (Russian).

[9] S. A. Mirzoian, R. G. Boroian, and E. S. Sekoian, "The effect of gamma-aminobutyric acid on reflex reactions of the cerebral vessels and systemic arterial pressure," *Farmakologiia i Toksikologiia*, vol. 36, no. 5, pp. 520–521, 1973 (Russian).

[10] D. N. Krause, E. Wong, P. Degener, and E. Roberts, "GABA receptors in bovine cerebral blood vessels: binding studies with [^{3}H]muscimol," *Brain Research*, vol. 185, no. 1, pp. 51–57, 1980.

[11] R. S. Mirzoian, "Neuroprotective and cerebrovascular effects of GABA mimetics," *Eksperimental'naia i Klinicheskaia Farmakologiia*, vol. 66, no. 2, pp. 53–56, 2003 (Russian).

[12] I. V. Silkina, T. S. Gan'shina, S. B. Seredenin, and R. S. Mirzoyan, "Gabaergic mechanism of cerebrovascular and neuroprotective effects of afobazole and picamilon," *Eksperimental'naya i Klinicheskaya Farmakologiya*, vol. 68, no. 1, pp. 20–24, 2005.

[13] I. N. Kurdyumov, T. S. Gan'shina, N. R. Mirzoyan et al., "Cerebrovascular and antiaggregative effects of GABA—docosahexaenoyldopamine conjugate," *Eksperimental'naya i Klinicheskaya Farmakologiya*, vol. 71, no. 4, pp. 26–29, 2008.

[14] A. V. Gnezdilova, T. S. Gan'shina, and R. S. Mirzoyan, "Gabaergic mechanism of cerebrovascular effect of mexidol," *Eksperimental'naya i Klinicheskaya Farmakologiya*, vol. 73, no. 10, pp. 11–13, 2010 (Russian).

[15] D. V. Maslennikov, T. S. Gan'shina, O. N. Oleĭnikova, I. N. Kurdiumov, and R. S. Mirzoian, "GABAergic mechanism of the cerebrovascular effect of melatonin," *Eksperimental'naya i Klinicheskaya Farmakologiya*, vol. 75, no. 4, pp. 13–16, 2012.

[16] C. G. Parsons and K. Gilling, "Memantine as an example of a fast, voltage-dependent, open channel N-methyl-D-aspartate receptor blocker," *Methods in Molecular Biology*, vol. 403, pp. 15–36, 2007.

[17] L. V. Kalia, S. K. Kalia, and M. W. Salter, "NMDA receptors in clinical neurology: excitatory times ahead," *The Lancet Neurology*, vol. 7, no. 8, pp. 742–755, 2008.

[18] I. E. Kovalev, V. M. Koshkin, N. V. Shipulina, and E. I. Rumyantseva, "An adamantanone derivative that is an original modulator of redox processes in the cytochrome P-450 system can serve as an effective remedy against obliterating angiopathy of lower extremities," *Doklady Biochemistry and Biophysics*, vol. 391, no. 1–6, pp. 201–203, 2003.

[19] A. Tamura, D. I. Graham, J. McCulloch, and G. M. Teasdale, "Focal cerebral ischaemia in the rat: I. Description of technique and early neuropathological consequences following middle cerebral artery occlusion," *Journal of Cerebral Blood Flow and Metabolism*, vol. 1, no. 1, pp. 53–60, 1981.

[20] A. V. Topchian, R. S. Mirzoian, and M. G. Balasanian, "Local cerebral ischemia in rats induced by ligation of the middle cerebral artery," *Eksperimental'naia i Klinicheskaia Farmakologiia*, vol. 59, no. 5, pp. 62–64, 1996.

[21] R. S. Mirzoian, A. V. Topchian, A. S. Kanaian, and M. G. Balasanian, "The effect of nimodipine on a local ischemic brain lesion," *Vestnik Rossiiskoi Akademii Meditsinskikh Nauk*, no. 11, pp. 46–51, 1998.

[22] M. D. Gaevyĭ, L. M. Adzhienko, L. M. Makarova, and A. A. Abdulsalam, "Brain ischemia induced by gravitational overload," *Eksperimental'naia i Klinicheskaia Farmakologiia*, vol. 63, no. 3, pp. 63–64, 2000.

[23] G. Nowak, R. Trullas, R. T. Layer, P. Skolnick, and I. A. Paul, "Adaptive changes in the N-methyl-D-aspartate receptor complex after chronic treatment with imipramine and 1-aminocyclopropanecarboxylic acid," *Journal of Pharmacology and Experimental Therapeutics*, vol. 265, no. 3, pp. 1380–1386, 1993.

[24] I. A. Zolotarev, I. I. Firstova, D. A. Abaimov et al., "Ligands of glutamate and dopamine receptors evenly labeled with hydrogen isotopes," *Bioorganicheskaia Khimiia*, vol. 35, no. 3, pp. 323–333, 2009.

Hindawi Publishing Corporation
BioMed Research International
Volume 2014, Article ID 484161, 8 pages
http://dx.doi.org/10.1155/2014/484161

Research Article

Merit of Ginseng in the Treatment of Heart Failure in Type 1-Like Diabetic Rats

Cheng-Chia Tsai,[1,2] Paul Chan,[3] Li-Jen Chen,[4] Chen Kuei Chang,[5] Zhongmin Liu,[6] and Jia-Wei Lin[5]

[1] *Department of Neurosurgery, Mackay Memorial Hospital, Taipei 104, Taiwan*
[2] *Graduate Institute of Injury Prevention and Control, Taipei Medical University, Taipei 110, Taiwan*
[3] *Department of Cardiology, College of Medicine, Wan Fang Hospital, Taipei Medical University, Taipei 116, Taiwan*
[4] *Institute of Basic Medical Sciences, College of Medicine, National Cheng Kung University, Tainan 701, Taiwan*
[5] *Department of Neurosurgery, College of Medicine, Shuang Ho Hospital, Taipei Medical University, Taipei 110, Taiwan*
[6] *Department of Cardiothoracic Surgery, Shanghai East Hospital, Tongji University, Shanghai, China*

Correspondence should be addressed to Zhongmin Liu; zhongmin_liu@sina.com.cn and Jia-Wei Lin; ns246@tmu.edu.tw

Received 16 January 2014; Accepted 6 February 2014; Published 17 March 2014

Academic Editor: Juei-Tang Cheng

The present study investigated the merit of ginseng in the improvement of heart failure in diabetic rats and the role of peroxisome proliferator-activated receptors δ (PPARδ). We used streptozotocin-induced diabetic rat (STZ-rat) to screen the effects of ginseng on cardiac performance and PPARδ expression. Changes of body weight, water intake, and food intake were compared in three groups of age-matched rats; the normal control (Wistar rats) received vehicle, STZ-rats received vehicle and ginseng-treated STZ-rats. We also determined cardiac performances in addition to blood glucose level in these animals. The protein levels of PPARδ in hearts were identified using Western blotting analysis. In STZ-rats, cardiac performances were decreased but the food intake, water intake, and blood glucose were higher than the vehicle-treated control. After a 7-day treatment of ginseng in STZ-rats, cardiac output was markedly enhanced without changes in diabetic parameters. This treatment with ginseng also increased the PPARδ expression in hearts of STZ-rats. The related signal of cardiac contractility, troponin I phosphorylation, was also raised. Ginseng-induced increasing of cardiac output was reversed by the cotreatment with PPARδ antagonist GSK0660. Thus, we suggest that ginseng could improve heart failure through the increased PPARδ expression in STZ-rats.

1. Introduction

Diabetes ranks among the main risk factors in the development of chronic heart failure (CHF) [1, 2]. Many patients with CHF and hyperglycemic symptoms have accompanying abnormalities including obesity, dyslipidemia, and hypertension that also lead to structural and functional disorders of heart in cardiac dysfunction and CHF [3–6].

Ginseng varieties have been garnering increasing interest recently for their effects on the cardiovascular system [7]. It has been demonstrated that ginseng could prevent cardiac hypertrophy and heart failure through a mechanism likely involving the prevention of calcineurin activation [8] and the latter representing a key factor for myocardial hypertrophy and remodeling [9, 10].

Peroxisome proliferator-activated receptors (PPARs) are introduced as the ligand-activated transcriptional factors to regulate the expression of genes [11]. It has been classified into three subtypes: PPARα, PPARγ, and PPARδ to modulate the gene expressions for various bioactivities [11]. PPARα is expressed in tissues with a high oxidative capacity, such as liver and heart, while PPARγ is observed in limited tissues, primarily the adipose tissue [11, 12]. PPARδ is known to increase lipid catabolism in both adipose and muscles [11], while PPARδ-dependent cardiac function is also identified [13–15]. Deletion of cardiac PPARδ is mentioned to result in

decreased contraction and lowered cardiac output, showing an incidence of cardiac failure [13].

A marked decrease of PPARδ expression in the hearts of streptozotocin-induced hyperglycemic rats (STZ-rats) [16] has been shown. It has also been indicated that impaired relaxation is the prominent cardiac abnormality due to the depressed troponin function in the hearts of STZ-rats [17, 18]. Thus, cardiomyopathy in STZ-rats is mainly associated with the reduced PPARδ expression in hearts [16].

It has been documented that cardiac agents, such as digoxin and dobutamine, can restore the cardiac contractility in diabetic rats [19–21]. Also, cardiac agent improved cardiac contraction in STZ-rats is mainly related to the increased expression of cardiac PPARδ [16]. Thus, in the present study, we employed STZ-rats to investigate the merits of ginseng in the restoration of cardiac performance in diabetic rats showing heart failure.

2. Material and Methods

2.1. Materials. GSK0660 (a specific PPARδ antagonist) was purchased from Santa Cruz Biotechnology, Inc. (Santa Cruz, CA, USA). Antibodies specific to PPARδ, cardiac troponin I (TnI), and phospho-troponin I (p-TnI) (Ser 23/24) were all the products of Cell Signaling Technology (Beverly, MA, USA).

2.2. Animals. We purchased the male Wistar rats, weighing from 250 to 280 g, from the Animal Center of National Cheng Kung University Medical College. All experiments were performed under the anesthesia with 2% isoflurane and all efforts were made to minimize suffering. The animal experiments were performed in accordance with the Guide for the Care and Use of Laboratory Animals as well as the guidelines of the Animal Welfare Act.

2.3. Animals and Experimental Protocol. Diabetes was induced by an intravenous injection of 60 mg/kg streptozotocin (STZ) [1]. Animals were considered to be useful as the plasma glucose concentration is up to 20 mmol/L or greater in addition to polyuria and other hyperglycemic features. The concentration of plasma glucose was measured by the glucose oxidase method (Quik-Lab, Ames, Miles, Inc., Elkhart, IN, USA). All studies were carried out 10 weeks after induction of diabetes in rats showing cardiomyopathy as described previously [2]. The STZ-rats received ginseng powder (150 mg/kg/day, orally) for 7 days. Another group of STZ-rats received same volume of vehicle; saline (0.9% sodium chloride, orally) was used for comparison, while the age-matched normal rats received same treatment with vehicle were taken as normal control. Then, they were anesthetized for cannulation in the right femoral artery with polyethylene catheters (PE-50). Mean arterial pressure (MAP) and heart rate (HR) were then measured in a polygraph (MP35, BIOPAC, Goleta, Calif) as described in our previous report [22]. Basically, all rats were kept under artificial ventilation while the cardiac output (CO) was calculated from the aortic blood flow, and the stroke volume (SV) was expressed as CO divided by HR according to our previous method [22]. After the experiment, hearts were isolated to rinse with ice-cold phosphate-buffered saline (PBS) and weighed.

2.4. Treatment of Antagonist. We used GSK0660 (1 mg/kg) as specific antagonist of PPARδ as described previously [23]. GSK0660 from Tocris bioscience (Bristol, UK) dissolved in vehicle (Dimethyl sulfoxide, DMSO, 0.1%) was prepared to the desired dose in each assay. STZ-rats received ginseng powder (150 mg/kg/day, orally) for 7 days were injected with antagonist at one hour before the application of ginseng daily. Then, animals were anesthetized for determination of cardiac performance as described above.

2.5. Characterization of Hemodynamic dP/dt. We used hemodynamic dP/dt to measure the cardiac contractility as described in our previous report [24]. Basically, the pacing electrode of LV (IX-214; iWorx Systems, Inc., Dover, NH, USA) was placed in the anterior wall through the superior vena cava. After femoral artery and venous insertion using the Seldinger technique [25], pressure transducer was wired into the heart to monitor the RV, aortic, mean blood, and LV pressures. Pressure catheters and pacing leads were connected to the machine devise (iWorx Systems, Inc., Dover, NH, USA) to monitor the heart rate and to calculate hemodynamic signals. Body temperature was kept at 37.5°C in whole experiment.

2.6. Western Blotting Analysis. We used the ice-cold radioimmunoprecipitation assay (RIPA) buffer to extract the protein from tissue homogenates or cell lysates as described in our previous method [16]. The protein level was characterized using Biorad protein assay (Biorad Laboratories, Inc., Hercules, CA, USA). After separation of proteins (30 μg) by SDS/polyacrylamide gel electrophoresis (10% acrylamide gel) through a Biorad Miniprotein II system, it was transferred to the expanded polyvinylidene difluoride membranes (Pierce, Rockford, IL, USA) with a Biorad Trans-Blot system. Then, the membranes were washed and blocked for 1 h at room temperature with 5% (w/v) skimmed milk powder according to our previous method [16]. The primary antibody reactions were performed following the manufacturer's instructions. The blots were incubated with goat polyclonal antibody (1 : 1000) to bind actin that served as the internal control. After removal of primary antibody, the washed blots were incubated with the appropriate peroxidase-conjugated secondary antibody for 2 h at room temperature. The blots were then developed using an ECL-Western blotting system (Amersham International, Buckinghamshire, UK). Each immunoblot, including PPARδ (50 kDa), cardiac troponin I (28 kDa), or phospho-troponin I (28 kDa), was then quantified by a laser densitometer.

2.7. Statistical Analysis. Results were expressed as mean ± SE of each group. Statistical analysis was carried out using ANOVA analysis and Newman-Keuls post hoc analysis. Statistical significance was set as $P < 0.05$.

Table 1: Characteristics of normal rats, diabetic rats, and ginseng-treated diabetic rats.

Parameters	Normal rats	Diabetic rats	Ginseng-treated diabetic rats
Food intake (g/day)	23.8 ± 3.6	42.5 ± 8.3**	43.6 ± 4.7**
Water intake (g/day)	41.5 ± 6.9	176.3 ± 11.9**	178.2 ± 11.3**
Plasma glucose (mmol/L)	5.8 ± 0.7	30.4 ± 3.8***	31.2 ± 2.8***
Body weight (g)	386.8 ± 13.5	247.6 ± 11.2**	253.4 ± 14.6**
Systolic blood pressure (mmHg)	117.3 ± 3.6	84.5 ± 8.2**	109.8 ± 4.7##
Diastolic blood pressure (mmHg)	81.7 ± 5.4	51.9 ± 7.2**	78.7 ± 7.6##
Heart rate (beats/min)	374.7 ± 23.2	303.4 ± 18.6*	297.3 ± 14.5#
Cardiac output (mL/min)	24.7 ± 0.5	12.4 ± 0.8*	19.2 ± 0.7##

Values were obtained from normal rats, vehicle-treated diabetic rats and ginseng-treated diabetic rats. All values were presented as mean ± SEM ($n = 6$ per group). The ginseng-treated group received the ginseng (150 mg/kg/day, orally for 7 days). $^{*}P < 0.05$, $^{**}P < 0.01$, and $^{***}P < 0.001$ as compared with normal rats. $^{\#}P < 0.05$ and $^{\#\#}P < 0.01$ as compared with vehicle-treated diabetic rats.

3. Results

3.1. Effects of Ginseng on Cardiac Abnormalities in Diabetic Rats. Streptozotocin (STZ) induced the characteristic symptoms of diabetes including hyperglycemia, hypoinsulinemia, and decreased body weight gain along with increased food and water intake when compared with age-matched normal rats (Table 1). The systolic pressure, diastolic pressure, and cardiac output in STZ-rats were markedly lower than those in normal rats (Table 1). The reduced systolic pressure and diastolic pressure in STZ-rats were recovered by ginseng after repeated treatments for 7 days (Table 1). The cardiac output in STZ-diabetic rats was also markedly enhanced by ginseng (Table 1). However, the ginseng-treated STZ-rats did not modify the blood glucose (Table 1). Also, ginseng did not influence the mean ratio of heart and body weight in STZ-rats as compared to the age-matched vehicle-treated STZ-rats (Table 1).

3.2. Effect of Ginseng on PPARδ in the Heart of Diabetic Rats. The level of PPARδ protein was significantly reduced in the heart of diabetic rats as compared with the normal rats (Figure 1). However, a marked increase in the expression of PPARδ was observed in the heart from ginseng-treated STZ-rats (Figure 1).

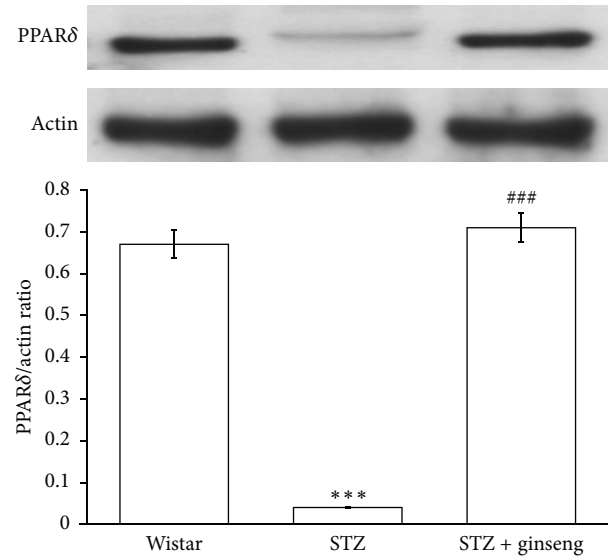

Figure 1: PPARδ expressions in the heart isolated from vehicle-treated diabetic rats, ginseng-treated diabetic rats, or Wistar rats. Changes in PPARδ expressions were investigated in age-matched Wistar rats (Control rats), vehicle-treated diabetic rats, and ginseng-treated diabetic rats. The expression of PPARδ was measured using Western blotting analysis. All values are expressed as mean ± SEM ($n = 8$ per group). $^{***}P < 0.001$ as compared with Wistar rats. $^{\#\#\#}P < 0.001$ as compared with vehicle-treated diabetic rats.

3.3. Level of TnI Phosphorylation Was Restored by Ginseng in Diabetic Rats. Change in TnI phosphorylation has been introduced to produce a profound effect on cardiac contractility and pumping [26] because phosphorylation of TnI increased cross-bridge cycling rate and enhanced the contraction power [26, 27]. The present study showed that the reduced level of TnI phosphorylation in the hearts of STZ-rats was markedly recovered by ginseng treatment (Figure 2).

3.4. The Recovery of Cardiac Output by Ginseng in Diabetic Rats Was Diminished by Blockade of PPARδ Using GSK0660. Phosphorylation of cTnI is known to induce a marked increase in myofilament Ca^{2+} sensitivity and the force of cardiac contraction [28]. Thus, we investigated the cardiac output in STZ rats. The volume of cardiac output was markedly raised in ginseng treated-STZ group. But, as shown in Figure 3, this action of ginseng was inhibited by PPARδ antagonist named GSK0660 at an effective dose mentioned in previous report [23].

3.5. The Recovery of Cardiac Contractility by Ginseng in Diabetic Rats Was Diminished by Blockade of PPARδ Using GSK0660. The dP/dt_{max} was also restored by ginseng after the repeated treatment for 7 days in STZ-rats, as compared with the vehicle-treated STZ-rats. However, as shown in Figure 4(a), this response disappeared in STZ-rats receiving coadministration of GSK0660 at the effective dose described in previous report [29]. Treatment of ginseng did not modify

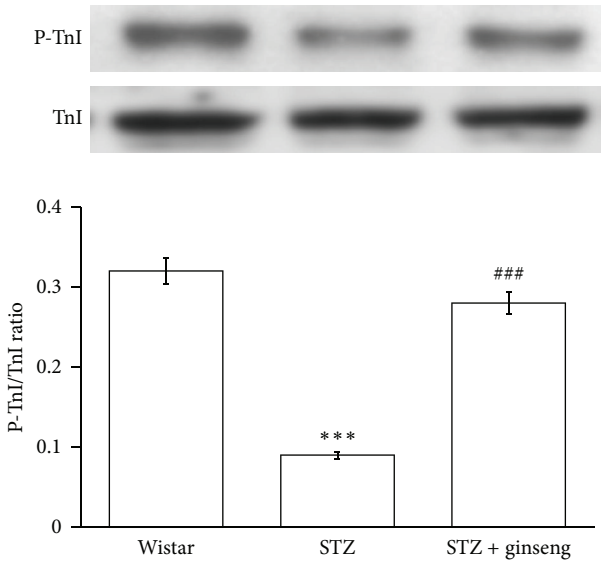

Figure 2: Troponin I phosphorylation in the heart isolated from vehicle-treated diabetic rats, ginseng-treated diabetic rats, or Wistar rats. Changes in Troponin I phosphorylation were investigated in age-matched Wistar rats (Control rats), vehicle-treated diabetic rats, and ginseng-treated diabetic rats. Troponin I phosphorylation was measured using Western blotting analysis. All values are expressed as mean ± SEM ($n = 8$ per group). $^{***}P < 0.001$ as compared with Wistar rats. $^{###}P < 0.001$ as compared with vehicle-treated diabetic rats.

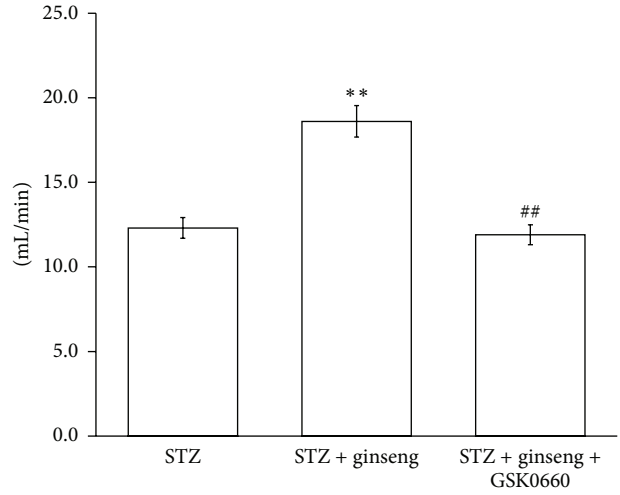

Figure 3: Changes of cardiac output in vehicle-treated diabetic rats (STZ), ginseng-treated diabetic rats (Ginseng-treated STZ) and ginseng-treated diabetic rats received GSK0660 (Ginseng-treated STZ + GSK0660). All values were presented as mean ± SEM ($n = 8$ per group). The ginseng-treated group was obtained from diabetic rats received the treatment of ginseng (150 mg/kg/day, orally for 7 days). $^{**}P < 0.01$ as compared with vehicle-treated diabetic rats (STZ rats). The ginseng-treatment plus GSK0660 group (Ginseng-treated STZ + GSK0660) was obtained from diabetic rats received the treatment of ginseng and injected with GSK0660 (1 mg/kg) at one hour before the treatment of ginseng daily. $^{##}P < 0.01$ as compared with the ginseng-treated diabetic rats.

the heart rate but produced a slight increase in blood pressure that was also blocked by GSK0660 (Figures 4(b) and 4(c)).

4. Discussion

The present study found that administration of ginseng caused a marked recovery of cardiac output in addition to the lowered cardiac PPARδ expression and troponin I phosphorylation in type 1-like diabetic rats. As shown in Table 1, the reduced cardiac output in diabetic rats was also markedly reversed by this repeated treatment of ginseng (150 mg/kg, orally) for 7 days that showed the most effective period. In anesthetized STZ-rats, cardiac contraction (dP/dt_{max}) was also significantly restored by ginseng and this change was blocked by GSK0660. However, ginseng did not modify the heart beating at this dosing. Thus, to the best of our knowledge, this is the first study to show that ginseng could restore heart failure through an activation of PPARδ in type 1-like diabetic rats.

Multiple actions of ginseng are related to the treated concentrations. It has been indicated that oral administration of ginseng (12 mg/kg a daily for a 2 weeks) showed neuronal protective effect on rat with Parkinson's disease [30]. Also, rat treated with ginseng (250 or 500 mg/kg) inhibited the myocardial infarction after acute myocardial ischemia reperfusion injury [31] and isoproterenol-induced cardiac injury in rats [32]. Moreover, it was mentioned that ginseng (400 mg/kg) may enhance cardiac performance through an increase in the expression of PPARδ and without altering the heart rate in normal rats [33]. In the present study, the cardiac performance in diabetic rats was also improved by repeated oral intake of ginseng at 150 mg/kg/day for one week and this used dose is markedly lower than used in previous reports for cardiac diseases [7, 8, 32, 34]. Also, this dose is equal to human oral dose about 1452 mg/kg by using the U.S. FDA HED (human equivalent dose) equation for calculation [35–37].

It has been indicated that type 1-like diabetes in STZ-induced animal is characterized by bradycardia and hypotension [38]. In conscious rats, the cardiomyopathy in this kind of animal model for heart failure was expressed by low indices of contractility and relaxation [39]. Actually, we observed the decreased cardiac dp/dt and cardiac output in STZ-induced diabetic rats similar to previous reports [22, 40].

In vivo and *in vitro* investigations have revealed a number of significant actions of ginsenosides and ginseng extracts in cardioprotection, such as reducing myocardial ischemia-reperfusion induced damage via NO pathway in rats and mice [41], slowing down deterioration of cardiac contractions, preventing the development of arrhythmias [42], and relaxing the muscles of the aorta [43]. Also, it has been documented that ginseng increases cardiac lipid metabolism by enhancement of PPARδ expression and this action of ginseng can be blocked by the specific antagonist GSK0660 [44]. In this study, we found that ginseng could increase PPARδ expression and TnI phosphorylation in the heart of diabetic rats.

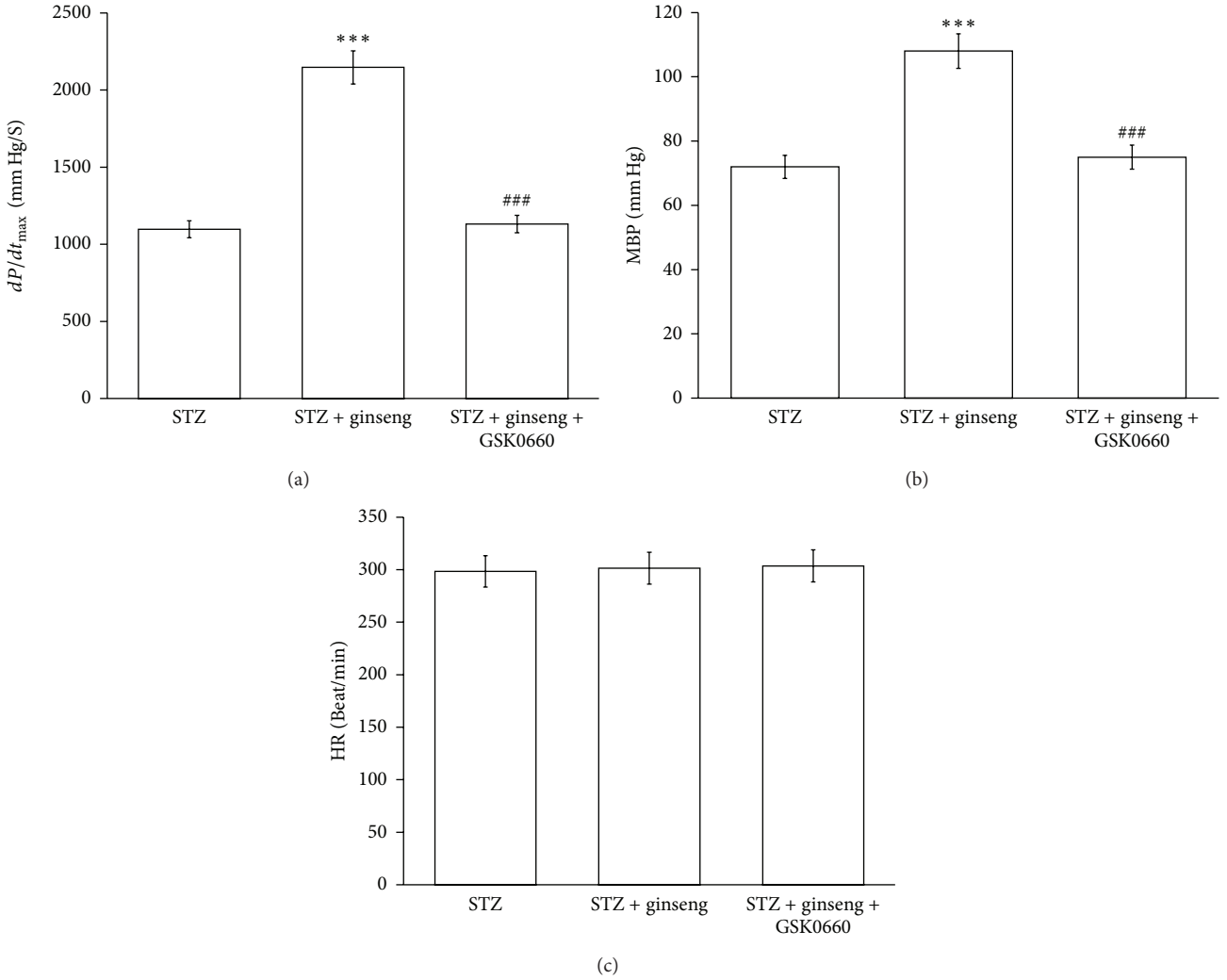

Figure 4: Effects of ginseng on cardiac performance in anesthetized rats. The effects of coadministration of ginseng and/or GSK0660 were investigated in the anesthetized STZ-rats. The changes in hemodynamic dP/dt (a), mean blood pressure (MBP) (b), and heart rate (HR) (c) were recorded continuously throughout the whole experiment. All values are presented as mean ± SEM ($n = 8$). $^{***}P < 0.001$ as compared to normal rats. $^{###}P < 0.001$ as compared with the ginseng-treated diabetic rats.

It has been established that PPARδ plays an important role in the regulation of cardiac performance [17–19]. In this study, we demonstrated that ginseng increases cardiac contractility without affecting heart rate in STZ-rats. Also, this cardiac tonic action of ginseng was reversed by blockade of PPARδ using antagonist. Furthermore, activation of PPARδ using ginseng may enhance the hemodynamic dP/dt_{max} in the STZ-rats. Both actions of ginseng were inhibited by GSK0660 at a dose sufficient to block PPARδ [39, 40]. The restoration of cardiac contractility in STZ-rats by ginseng through an activation of PPARδ is then characterized.

The decreased level of TnI phosphorylation was reversed by ginseng in STZ-diabetic rats. Previous study showed an increase of TnI phosphorylation in rats after induction of diabetes for 8 weeks [45]. However, the reduced phosphorylation of TnI was observed in the failing heart of human studies [46]. In the present study, the reduction of TnI phosphorylation may indicate severe contractile defects in the heart of rats after induction of diabetes for 12 weeks or more. Furthermore, the lower TnI phosphorylation was also raised in the heart of STZ-diabetic rats by ginseng. Previous study indicated many phosphorylation sites on cardiac troponin I (cTnI) in physiological and pathophysiological cardiac function [47]. Studies of proteomic analysis on human heart samples taken from end-stage heart failure and rat heart samples demonstrate that Ser23/Ser24 are the major and perhaps the only sites likely to be relevant to control cardiac function [48]. Previous studies have demonstrated that TnI phosphorylation most likely acts through an enhanced off rate during Ca^{2+} exchange with TnC, leading to acceleration of relaxation and an increase in cardiac output [45, 46, 49–51]. It is suggested that the influence of ginseng on increased phosphorylation of TnI

may be mediated through increasing Ca^{2+} concentrations. However, this view needs more investigations to support in the future.

The inotropic action of ginseng showed cardiac output and cardiac dp/dt was reversed by blockade of PPARδ using chemical antagonist named GSK0660 as described previously [23]. In the present study, the increased cardiac output or cardiac dp/dt by ginseng was inhibited in diabetic rats receiving combined treatment with antagonist of PPARδ. Thus, we conclude that activation of PPARδ is involved in the ginseng-induced increase of cardiac contractility known as inotropic action. However, the effects of GSK0660 on changes of downstream signals and cardiac TnI phosphorylation or others shall be investigated in the future.

A change in heart rate is the most serious side effect of cardiac agents [41, 42]. In the present study, we showed that ginseng generated cardiac tonic action in animals without impacting the heart rate. Thus, ginseng can be used as cardiac agent without side effect of arrhythmia.

In cardiac agents, the PPARδ agonist (GW0742) enhanced cardiac contractility was higher than that in the dobutamine treated samples. The increase in cardiac output caused by GW0742 was also higher than dobutamine in animals. Also, there is a slight elevation of mean blood pressure with no change of heart rate in rats treated with GW0742. This result is different to the action of dobutamine [24]. Also, the effects of ginseng on STZ rats are similar to the actions of digoxin in STZ rats and both agents restored the expression of PPARδ and the cardiac contractility in STZ rats [22]. However, ginseng shows no side effect on heart rate unlike digoxin or other clinical used agents. Thus, application of ginseng to enhance cardiac performance through the activation of PPARδ may be a good therapeutic strategy.

5. Conclusion

According to these findings, we suggest that the expression of PPARδ restored by ginseng results in cardiac troponin phosphorylation in STZ-rats. Subsequently, the cardiac performance is reversed. Taken together, ginseng restored cardiac contractility through an increase in PPARδ expression at the dose that did not modify the heart beating in STZ-rats. Thus, ginseng could be developed as a good cardiac agent without the side effect on heart rate in treatment of diabetic heart failure.

Conflict of Interests

The authors have not disclosed any conflict of interests.

Authors' Contribution

Cheng-Chia Tsai and Paul Chan equally contributed to the work.

Acknowledgments

The authors thank Yang-Lian Yan and Yi-Zhi Chen for their assistance in our experiments. The present study was supported in part by Grant (TMU102-AE2-1013) from Taipei Medical University, Taipei, Taiwan.

References

[1] W. B. Kannel, M. Hjortland, and W. P. Castelli, "Role of diabetes in congestive heart failure: the Framingham study," *American Journal of Cardiology*, vol. 34, no. 1, pp. 29–34, 1974.

[2] W. B. Kannel and D. L. McGee, "Diabetes and cardiovascular disease. The Framingham study," *Journal of the American Medical Association*, vol. 241, no. 19, pp. 2035–2038, 1979.

[3] K. Malmberg and L. Ryden, "Myocardial infarction in patients with diabetes mellitus," *European Heart Journal*, vol. 9, no. 3, pp. 259–264, 1988.

[4] J. Herlitz, K. Malmberg, B. W. Karlson, L. Ryden, and A. Hjalmarson, "Mortality and morbidity during a five-year follow-up of diabetics with myocardial infarction," *Acta Medica Scandinavica*, vol. 224, no. 1, pp. 31–38, 1988.

[5] I. G. Poornima, P. Parikh, and R. P. Shannon, "Diabetic cardiomyopathy: the search for a unifying hypothesis," *Circulation Research*, vol. 98, no. 5, pp. 596–605, 2006.

[6] D. An and B. Rodrigues, "Role of changes in cardiac metabolism in development of diabetic cardiomyopathy," *American Journal of Physiology*, vol. 291, no. 4, pp. H1489–H1506, 2006.

[7] M. Karmazyn, M. Moey, and X. T. Gan, "Therapeutic potential of ginseng in the management of cardiovascular disorders," *Drugs*, vol. 71, no. 15, pp. 1989–2008, 2011.

[8] J. Guo, X. T. Gan, J. V. Haist et al., "Ginseng inhibits cardiomyocyte hypertrophy and heart failure via nhe-1 inhibition and attenuation of calcineurin activation," *Circulation*, vol. 4, no. 1, pp. 79–88, 2011.

[9] N. Frey and E. N. Olson, "Cardiac hypertrophy: the good, the bad, and the ugly," *Annual Review of Physiology*, vol. 65, pp. 45–79, 2003.

[10] J. M. Berry, V. Le, D. Rotter et al., "Reversibility of adverse, calcineurin-dependent cardiac remodeling," *Circulation Research*, vol. 109, no. 4, pp. 407–417, 2011.

[11] Q. Yang and Y. Li, "Roles of PPARs on regulating myocardial energy and lipid homeostasis," *Journal of Molecular Medicine*, vol. 85, no. 7, pp. 697–706, 2007.

[12] I. Issemann and S. Green, "Activation of a member of the steroid hormone receptor superfamily by peroxisome proliferators," *Nature*, vol. 347, no. 6294, pp. 645–650, 1990.

[13] L. Cheng, G. Ding, Q. Qin et al., "Cardiomyocyte-restricted peroxisome proliferator-activated receptor-δ deletion perturbs myocardial fatty acid oxidation and leads to cardiomyopathy," *Nature Medicine*, vol. 10, no. 11, pp. 1245–1250, 2004.

[14] L. Cheng, G. Ding, Q. Qin et al., "Peroxisome proliferator-activated receptor δ activates fatty acid oxidation in cultured neonatal and adult cardiomyocytes," *Biochemical and Biophysical Research Communications*, vol. 313, no. 2, pp. 277–286, 2004.

[15] G. D. Barish, V. A. Narkar, and R. M. Evans, "PPARδ: a dagger in the heart of the metabolic syndrome," *Journal of Clinical Investigation*, vol. 116, no. 3, pp. 590–597, 2006.

[16] B.-C. Yu, C.-K. Chang, H.-Y. Ou, K.-C. Cheng, and J.-T. Cheng, "Decrease of peroxisome proliferator-activated receptor delta expression in cardiomyopathy of streptozotocin-induced

diabetic rats," *Cardiovascular Research*, vol. 80, no. 1, pp. 78–87, 2008.

[17] F. S. Fein, L. B. Kornstein, and J. E. Strobeck, "Altered myocardial mechanics in diabetic rats," *Circulation Research*, vol. 47, no. 6, pp. 922–933, 1980.

[18] F. S. Fein, J. E. Strobeck, and A. Malhotra, "Reversibility of diabetic cardiomyopathy with insulin in rats," *Circulation Research*, vol. 49, no. 6, pp. 1251–1261, 1981.

[19] M. T. Chou, S. H. Lo, K. C. Cheng, Y. X. Li, L. J. Chen, and J. T. Cheng, "Activation of β-adrenoceptors by dobutamine may induce a higher expression of peroxisome proliferator-activated receptors δ (PPARδ) in neonatal rat cardiomyocytes," *The Scientific World Journal*, vol. 2012, Article ID 248320, 8 pages, 2012.

[20] Z.-C. Chen, B.-C. Yu, L.-J. Chen, K.-C. Cheng, H. J. Lin, and J.-T. Cheng, "Characterization of the mechanisms of the increase in PPARδ expression induced by digoxin in the heart using the H9c2 cell line," *British Journal of Pharmacology*, vol. 163, no. 2, pp. 390–398, 2011.

[21] J. Zhao, W. D. Cai, Y. X. Gan et al., "A comparison of HIV infection and related risk factors between money boys and noncommercial men who have sex with men in Shenzhen, China," *Sexually Transmitted Diseases*, vol. 39, no. 12, pp. 942–948, 2012.

[22] S. C. Fan, B. C. Yu, Z. C. Chen, L. J. Chen, H. H. Chung, and J. T. Cheng, "The decreased expression of Peroxisome Proliferator-Activated Receptors (PPAR) is reversed by digoxin in the heart of diabetic rats," *Hormone and Metabolic Research*, vol. 42, no. 9, pp. 637–642, 2010.

[23] B. G. Shearer, D. J. Steger, J. M. Way et al., "Identification and characterization of a selective peroxisome proliferator-activated receptor β/δ (NR1C2) antagonist," *Molecular Endocrinology*, vol. 22, no. 2, pp. 523–529, 2008.

[24] Z. C. Chen, K. S. Lee, L. J. Chen, L. Y. Wang, H. S. Niu, and J. T. Cheng, "Cardiac peroxisome proliferator-activated receptor δ (PPARδ) as a new target for increased contractility without altering heart rate," *PLoS ONE*, vol. 8, no. 5, Article ID e64229, 2013.

[25] S. I. Seldinger, "Catheter replacement of the needle in percutaneous arteriography: a new technique," *Acta Radiologica*, vol. 49, no. 434, pp. 47–52, 2008.

[26] J. Layland, R. J. Solaro, and A. M. Shah, "Regulation of cardiac contractile function by troponin I phosphorylation," *Cardiovascular Research*, vol. 66, no. 1, pp. 12–21, 2005.

[27] J. M. Metzger and M. V. Westfall, "Covalent and noncovalent modification of thin filament action: the essential role of troponin in cardiac muscle regulation," *Circulation Research*, vol. 94, no. 2, pp. 146–158, 2004.

[28] T. Kobayashi, L. Jin, and P. P. de Tombe, "Cardiac thin filament regulation," *Pflugers Archiv*, vol. 457, no. 1, pp. 37–46, 2008.

[29] I. Paterniti, E. Esposito, E. Mazzon et al., "Evidence for the role of peroxisome proliferator-activated receptor-β/δ in the development of spinal cord injury," *Journal of Pharmacology and Experimental Therapeutics*, vol. 333, no. 2, pp. 465–477, 2010.

[30] J. Y. Wang, J. Y. Yang, F. Wang et al., "Neuroprotective effect of pseudoginsenoside-F11 on a rat model of Parkinson's disease induced by 6-hydroxydopamine," *Evidence-Based Complementary and Alternative Medicine*, vol. 2013, Article ID 152798, 9 pages, 2013.

[31] L. Pei, H. Shaozhen, D. Gengting, C. Tingbo, L. Liang, and Z. Hua, "Effectiveness of Panax ginseng on acute myocardial ischemia reperfusion injury was abolished by flutamide via endogenous testosterone-mediated akt pathway," *Evidence-Based Complementary and Alternative Medicine*, vol. 2013, Article ID 817826, 9 pages, 2013.

[32] K. H. Lim, D. Ko, and J. H. Kim, "Cardioprotective potential of Korean Red Ginseng extract on isoproterenol-induced cardiac injury in rats," *Journal of Ginseng Research*, vol. 37, no. 3, pp. 273–282, 2013.

[33] J. W. Lin, Y. G. Cherng, L. J. Chen, H. S. Niu, C. K. Chang, and C. S. Niu, "Ginseng is useful to enhance cardiac contractility in animals," *BioMed Research International*, vol. 2014, Article ID 723084, 9 pages, 2014.

[34] H.-X. Li, S.-Y. Han, X. Ma et al., "The saponin of red ginseng protects the cardiac myocytes against ischemic injury in vitro and in vivo," *Phytomedicine*, vol. 19, no. 6, pp. 477–483, 2012.

[35] I. Cavero, "10th annual meeting of the Safety Pharmacology Society: an overview," *Expert Opinion on Drug Safety*, vol. 10, no. 2, pp. 319–333, 2011.

[36] W. C. Buhles, "Compassionate use: a story of ethics and science in the development of a new drug," *Perspectives in Biology and Medicine*, vol. 54, no. 3, pp. 304–315, 2011.

[37] T. Keida, N. Hayashi, and M. Kawashima, "Application of the Food and Drug Administration (FDA) bioequivalent guidance of topical dermatological corticosteroid in yellow-skinned Japanese population: validation study using a chromameter," *Journal of Dermatology*, vol. 33, no. 10, pp. 684–691, 2006.

[38] B. D. Schaan, P. Dall'Ago, C. Y. Maeda et al., "Relationship between cardiovascular dysfunction and hyperglycemia in streptozotocin-induced diabetes in rats," *Brazilian Journal of Medical and Biological Research*, vol. 37, no. 12, pp. 1895–1902, 2004.

[39] G. R. Borges, M. de Oliveira, H. C. Salgado, and R. Fazan Jr., "Myocardial performance in conscious streptozotocin diabetic rats," *Cardiovascular Diabetology*, vol. 5, article 26, 2006.

[40] Y. Z. Cheng, L. J. Chen, W. J. Lee, M. F. Chen, H. J. Lin, and J. T. Cheng, "Increase of myocardial performance by Rhodiola-ethanol extract in diabetic rats," *Journal of Ethnopharmacology*, vol. 144, no. 2, pp. 234–239, 2012.

[41] H. Zhou, S. Z. Hou, P. Luo et al., "Ginseng protects rodent hearts from acute myocardial ischemia-reperfusion injury through GR/ER-activated RISK pathway in an endothelial NOS-dependent mechanism," *Journal of Ethnopharmacology*, vol. 135, no. 2, pp. 287–298, 2011.

[42] G. I. Scott, P. B. Colligan, B. H. Ren, and J. Ren, "Ginsenosides Rb1 and Re decrease cardiac contraction in adult rat ventricular myocytes: role of nitric oxide," *British Journal of Pharmacology*, vol. 134, no. 6, pp. 1159–1165, 2001.

[43] S. Y. Kang, V. B. Schini-Kerth, and N. D. Kim, "Ginsenosides of the protopanaxatriol group cause endothelium-dependent relaxation in the rat aorta," *Life Sciences*, vol. 56, no. 19, pp. 1577–1586, 1995.

[44] S. C. Kuo, P. M. Ku, L. J. Chen, H. S. Niu, and J. T. Cheng, "Activation of receptors δ (PPARδ) by agonist (GW0742) may enhance lipid metabolism in heart both in vivo and in vitro," *Hormone and Metabolic Research*, vol. 45, no. 12, pp. 880–886, 2013.

[45] X. Liu, N. Takeda, and N. S. Dhalla, "Troponin I phosphorylation in heart homogenate from diabetic rat," *Biochimica et Biophysica Acta*, vol. 1316, no. 2, pp. 78–84, 1996.

[46] A. E. Messer, A. M. Jacques, and S. B. Marston, "Troponin phosphorylation and regulatory function in human heart muscle: dephosphorylation of Ser23/24 on troponin I could account

for the contractile defect in end-stage heart failure," *Journal of Molecular and Cellular Cardiology*, vol. 42, no. 1, pp. 247–259, 2007.

[47] S. Ayaz-Guner, J. Zhang, L. Li, J. W. Walker, and Y. Ge, "In vivo phosphorylation site mapping in mouse cardiac troponin I by high resolution top-down electron capture dissociation mass spectrometry: Ser22/23 are the only sites basally phosphorylated," *Biochemistry*, vol. 48, no. 34, pp. 8161–8170, 2009.

[48] G. A. MacGowan, C. Evans, T. C.-C. Hu et al., "Troponin I protein kinase C phosphorylation sites and ventricular function," *Cardiovascular Research*, vol. 63, no. 2, pp. 245–255, 2004.

[49] C. A. Tate, M. F. Hyek, and G. E. Taffet, "The role of calcium in the energetics of contracting skeletal muscle," *Sports Medicine*, vol. 12, no. 3, pp. 208–217, 1991.

[50] L. Li, J. Desantiago, G. Chu, E. G. Kranias, and D. M. Bers, "Phosphorylation of phospholamban and troponin I in β-adrenergic-induced acceleration of cardiac relaxation," *American Journal of Physiology*, vol. 278, no. 3, pp. H769–H779, 2000.

[51] Y. Pi, K. R. Kemnitz, D. Zhang, E. G. Kranias, and J. W. Walker, "Phosphorylation of troponin I controls cardiac twitch dynamics: evidence from phosphorylation site mutants expressed on a troponin I-null background in mice," *Circulation Research*, vol. 90, no. 6, pp. 649–656, 2002.

Hindawi Publishing Corporation
BioMed Research International
Volume 2014, Article ID 690135, 6 pages
http://dx.doi.org/10.1155/2014/690135

Research Article

Antihypertensive Action of Allantoin in Animals

Mei-Fen Chen,[1,2] Jo-Ting Tsai,[3] Li-Jen Chen,[4] Tung-Pi Wu,[5] Jia-Jang Yang,[2] Li-Te Yin,[2] Yu-lin Yang,[2] Tai-An Chiang,[2] Han-Lin Lu,[6] and Ming-Chang Wu[1]

[1] *Department of Food Science, National Pingtung University of Science and Technology, Neipu, Pingtung City 91201, Taiwan*
[2] *College of Medicine and Life Science, Chung Hwa University of Medical Technology, Rende District, Tainan City 71703, Taiwan*
[3] *Department of Radiation Oncology, Taipei Medical University-Shuang Ho Hospital, and College of Medicine, Taipei Medical University, Taipei City 10361, Taiwan*
[4] *Institute of Basic Medical Sciences, College of Medicine, National Cheng Kung University, Tainan City 70101, Taiwan*
[5] *Department of Obs/Gyn, Tainan SinLau Hospital, The Presbyterian Church in Taiwan, Tainan City 70142, Taiwan*
[6] *Department of Chinese Medicine, Tainan SinLau Hospital, The Presbyterian Church in Taiwan, Tainan City 70142, Taiwan*

Correspondence should be addressed to Han-Lin Lu; a0935265113@gmail.com and Ming-Chang Wu; mcwu@mail.npust.edu.tw

Received 17 January 2014; Accepted 10 February 2014; Published 12 March 2014

Academic Editor: Juei-Tang Cheng

The agonists of imidazoline I-1 receptors (I-1R) are widely used to lower blood pressure. It has been indicated that guanidinium derivatives show an ability to activate imidazoline receptors. Also, allantoin has a chemical stricture similar to guanidinium derivatives. Thus, it is of special interest to characterize the effect of allantoin on I-1R. In conscious male spontaneous hypertensive rats (SHRs), mean blood pressure (MBP) was recorded using the tail-cuff method. Furthermore, the hemodynamic analyses in catheterized rats were applied to measure the actions of allantoin in vivo. Allantoin decreased blood pressures in SHRs at 30 minutes, as the most effective time. Also, this antihypertensive action was shown in a dose-dependent manner from SHRs treated with allantoin. Moreover, in anesthetized rats, allantoin inhibited cardiac contractility and heart rate as showing in hemodynamic dP/dt max significantly. Also, the peripheral blood flow was markedly increased by allantoin. Both actions were diminished by efaroxan at the dose sufficient to block I-1R. Thus, we suggest that allantoin, as I-1R agonist, has the potential to develop as a new therapeutic agent for hypertension in the future.

1. Introduction

Neurotransmitters after binding to specific receptors are known to involve in the regulation of cardiovascular functions, especially the arterial blood pressure. In this regulation, noradrenaline, acetylcholine, serotonin, angiotensin II, and g-amino-butyric acid are widely introduced as the central regulators of blood pressure [1]. Potentially, most of neurotransmitters and/or receptors in brain could be considered as the targets in development of centrally acting antihypertensive agents [2].

Allantoin is known rich contained in in yam (*Dioscorea spp.*) as the principle active compound [3]. Yam is an important plant that is widely used in drug industry, while *Dioscorea rhizome* contained ureides including allantoin for the prevention of inflammation and ulcers [4]. Actually, the herbs from Dioscoreaceae are introduced to be merit in the improvement of diabetic disorders [5]. In Chinese traditional medicine, Shan-Yaw (*Dioscorea opposita*) is effective to improve insulin resistance [6] and it has also been characterized in animals [7], while allantoin is mentioned to be contained in this herb [8].

The presence of imidazoline receptors in brain seems to be related to the central regulation of blood pressure [9]. It has been dissociated the centrally mediated effects of clonidine (an imidazoline compound) on blood pressure from those of catecholamines [9]. Accordingly, the detailed radioligand binding studies largely confirmed the presence of imidazoline receptors [10]. After the characterization of agmatine as the endogenous ligand of this receptor, 3 subtypes of imidazoline receptors have been proposed; activation of I-1 receptors

regulates blood pressure [11], whereas I-3 receptors participate in insulin release [12] and activation of I-2 receptors (I-2R) increases glucose uptake into muscle cells [13, 14]. Moreover, it has been documented that compounds with guanidine-like structures may bind to imidazoline receptors [15], while metformin has been identified to this group [16]. Because allantoin also belongs to guanidinium derivative, it is of special interest to understand the effect of allantoin on I-1R. Thus, we speculated that allantoin may have central antihypertensive activity through activation of I-1R. Then, in the present study, we investigated the antihypertensive action of allantoin in relation to I-1R in both normal rats and spontaneous hypertensive rats (SHRs).

2. Material and Methods

2.1. Animals. Twelve-week-old male Wistar rats and spontaneously hypertensive rats (SHR), weighing from 250 to 300 g, were obtained from the Animal Center of National Cheng Kung University Medical College. The rats were housed individually in plastic cages under standard laboratory conditions. They were kept under a 12 h light/dark cycle and had free access to food and water. All experiments were performed under anesthesia with 2% isoflurane, and all efforts were made to minimize the animals' suffering. The animal experiments were approved and conducted in accordance with local institutional guidelines for the care and use of laboratory animals, and the experiments conformed to the Guide for the Care and Use of Laboratory Animals as well as the guidelines of the Animal Welfare Act.

2.2. Drug Administration. Animals were randomly assigned into four groups: (I) the control group ($n = 8$) treated with the vehicle, saline (0.9% sodium chloride, i.v.); (II) the allantoin group ($n = 8$) treated by intravenous injection of allantoin at 0.5 mg/kg as described previously [17, 18]; (III) the allantoin + efaroxan group ($n = 8$) treated with allantoin at the most effective dose (0.5 mg/kg, i.v.) according to previous report [17, 18] and efaroxan at effective dose (1.5 mg/kg, i.v.) [17] 30 minutes before injection of allantoin; and (IV) the allantoin treated SHRs group ($n = 8$) treated by intravenous injection of allantoin at various dose for desired time. Because allantoin has been documented to be easily degraded in intestinal tract [19] for resulting in a marked loss of activity after oral administration [20, 21], we administered it using intravenous injection in the present study.

2.3. Determination of Mean Blood Pressure. After treatment of allantoin, the rats were placed into a holder for the determination of the mean blood pressure (MBP) using a noninvasive tail-cuff monitor (MK2000; Muromachi Kikai, Tokyo, Japan). The values for each animal were determined in triplicate.

2.4. Determination of Blood Flow. Then, the rats were anesthetized and cannulated in the right femoral artery with polyethylene catheters (PE-50). Mean arterial pressure (MAP) and heart rate (HR) were recorded using a polygraph (MP35, BIOPAC, Goleta, Calif.). The rat's trachea was intubated for artificial ventilation (Small Animal Ventilator Model 683, Harvard Apparatus, Holliston, Mass.) at 50 breaths/min with a tidal volume of 8 mL/kg and a positive end expiratory pressure of 5 cm H_2O. After incision into the rat's chest at the third intercostal space to expose the heart, a small section (1 cm long) of the ascending aorta was freed from the connective tissue. A Transonic Flowprobe (2.5PSB923, Transonic System Inc., Ithaca, N.Y.) was implanted around the root of the ascending aorta and connected to a Transonic transit-time blood flowmeter (T403, Transonic System Inc.). The MAP, HR, and blood flow were record for further analysis.

2.5. Catheterization for Hemodynamic dP/dt Measurement. Temporary pacing leads were used for the short-term study and were placed in the right atrium and RV apex. A venogram image in 2 different angulations (left anterior oblique 30° and anteroposterior) was obtained to determine the anatomy of the coronary sinus venous system. An LV pacing electrode (IX-214; iWorx Systems, Inc., Dover, NH, USA) was placed either in the free wall region via the lateral or posterior vein or in the anterior region via the great cardiac vein. After femoral artery and venous puncture using the Seldinger technique [22], pressure transducer catheters were inserted into the heart to provide the RV, aortic, mean blood, and LV pressures. Pressure catheters and pacing leads were connected to an external pacing computer (iWorx Systems, Inc., Dover, NH, USA) to monitor the heart rate and to acquire hemodynamic signals. Body temperature of the rats was also maintained at 37.5°C throughout whole procedure.

2.6. Statistical Analysis. Results were expressed as mean ± SE of each group. Statistical analysis was carried out using ANOVA analysis and the Newman-Keuls post hoc analysis. Statistical significance was set as $P < 0.05$.

3. Results

3.1. Effects of Allantoin on the Blood Pressure in Conscious SHRs. We investigated the most effective time point of allantoin using the intravenous injection of allantoin into SHRs for 0–120 minutes at the dose of 0.5 mg/kg according to previous study [17]. The most effective time point of 30 min was then obtained and used for further study (Figure 1(a)). Intravenous injection of allantoin from 0.1 to 0.5 mg/kg decreased MBP in conscious SHRs in a dose-dependent manner (Figure 1(b)). Then, the time point of 30 min and the dose of 0.5 mg/kg were used for further experiments.

3.2. The Reduction of MAP and HR by Allantoin in Rats Was Diminished by Blockade of I-1R Using Efaroxan. In order to clarify that allantoin may produce antihypertensive effect through central I-1R, we measured the MAP and HR in normal rats. The MAP and HR were markedly decreased after injection of allantoin (Figure 2). However, as shown in Figure 2, this action was extinguished by I-1R specific

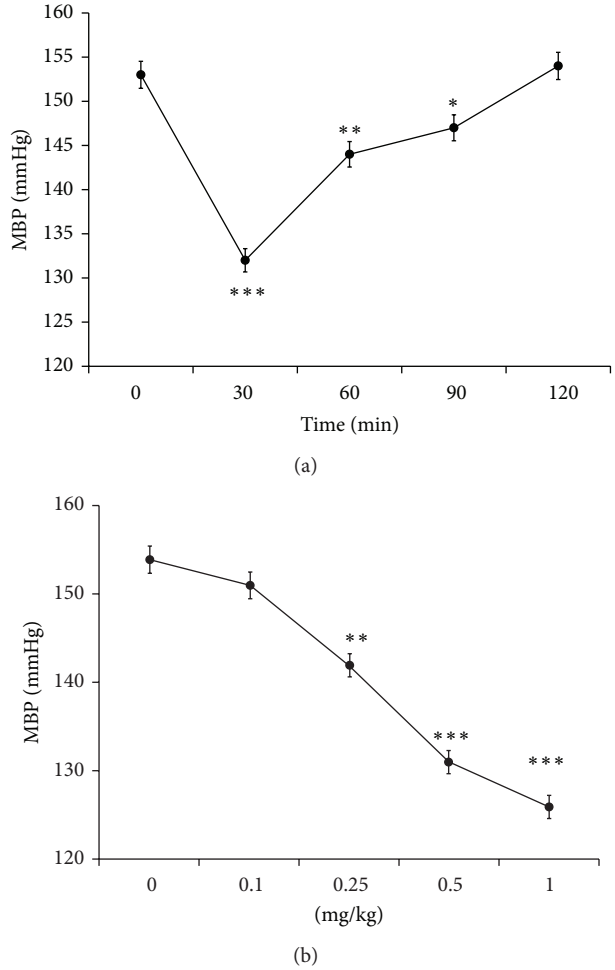

Figure 1: Antihypertensive action of allantoin in spontaneous hypertensive rats (SHRs). Time course (a) and dose-dependent (b) decrease of mean blood pressure (MBP) induced by allantoin in conscious spontaneously hypertensive rats (SHRs). Data represent the mean ± SEM of eight animals ($n = 8$). $^{*}P < 0.05$, $^{**}P < 0.01$, and $^{***}P < 0.001$ compared with control (at zero).

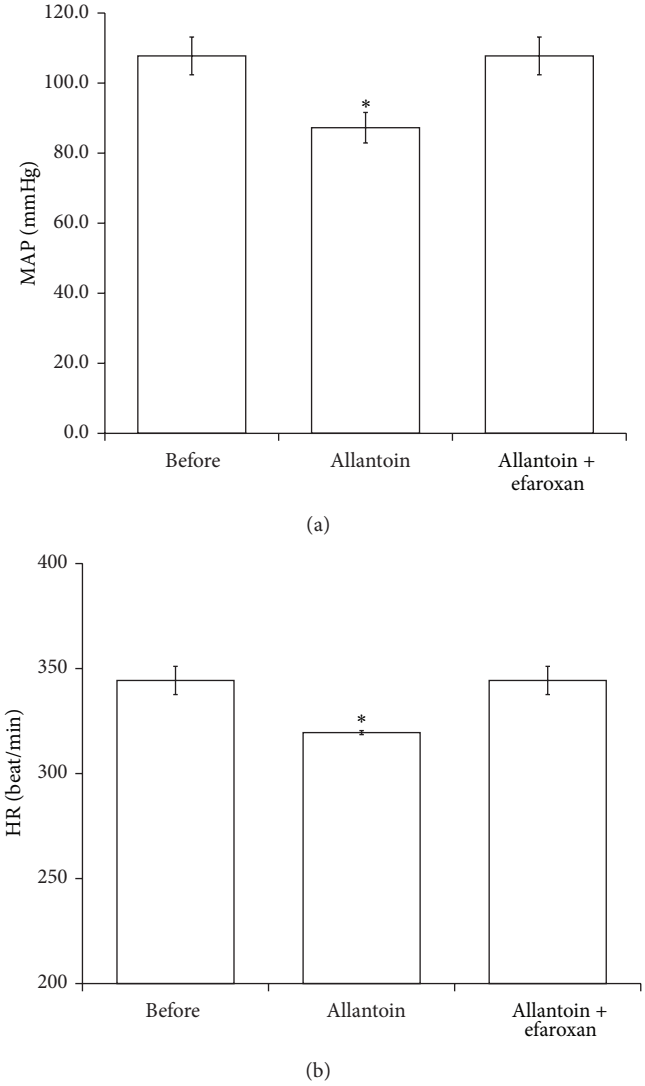

Figure 2: Effects of allantoin on mean arterial pressure (MAP) and heart rate (HR) in rats. The representative picture shows the change in MAP and HR caused by allantoin in anesthetized rats. HR and MAP were recorded in anesthetized rats treated with allantoin or cotreatment with efaroxan. The changes in MAP (a) and HR (b) were recorded at 30 min after injection of allantoin. All values are presented as mean ± SEM ($n = 8$). $^{*}P < 0.05$ as compared to the data in before.

antagonist named efaroxan at the effective dose as showed in previous report [17].

3.3. Effect of Allantoin on Cardiac Performance in the Anesthetized Rats. The dP/dt was significantly reduced by allantoin (0.5 mg/kg, i.v.) after treatment for 30 min in the anesthetized rats, compared with the vehicle-treated control. However, as shown in Figure 3, this effect disappeared by coadministration of efaroxan at effective dose (1.5 mg/kg, i.v.) [17].

3.4. Effect of Allantoin on Peripheral Blood Flow in the Anesthetized Rats. The peripheral blood flow was markedly increased by allantoin (0.5 mg/kg, i.v.) after treatment for 30 min in the anesthetized rats, compared with the vehicle-treated control. However, as shown in Figure 4, this effect was also deleted by coadministration of efaroxan at effective dose (1.5 mg/kg, i.v.) [17]. This result reflects the decrease of total peripheral resistance of arterioles by allantoin via an activation of I-1R.

4. Discussion

In the present study, we found that allantoin induced a dose-dependent reduction of MBP in SHRs at 30 minutes later, the most effective time point. In anesthetized rats, the heart rate, mean arterial pressure, and cardiac contraction (dP/dt) were also significantly reduced by allantoin in a way blocked by efaroxan. Moreover, the peripheral blood flow was markedly increased by allantoin in these anesthetized rats. Thus, to the

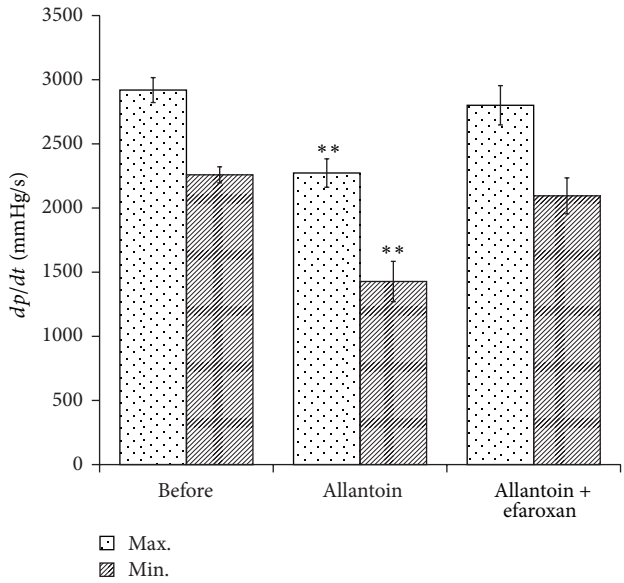

Figure 3: Effects of allantoin on cardiac performance in anesthetized rats. The effects of coadministration of allantoin and/or efaroxan were investigated in the anesthetized rats. The changes in hemodynamic dP/dt were recorded at 30 min after injection of allantoin. All values are presented as mean ± SEM ($n = 8$). $^{**}P < 0.01$ as compared to the data in before.

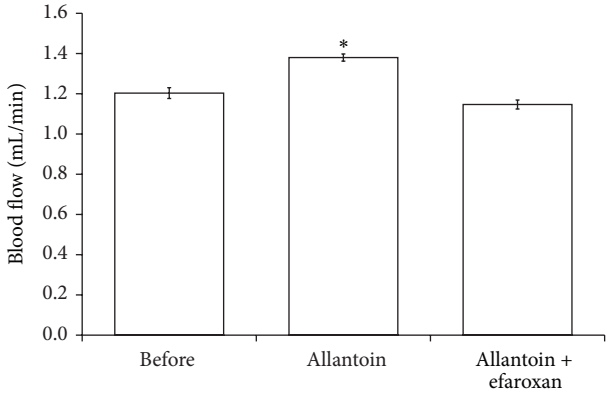

Figure 4: Effects of allantoin on peripheral blood flow in anesthetized rats. The effects of allantoin or cotreatment with efaroxan were investigated in the anesthetized rats. The changes in peripheral blood flow were recorded at 30 min after injection of allantoin. All values are presented as mean ± SEM ($n = 8$). $^{*}P < 0.05$ as compared to the data in before.

best of our knowledge, this is the first study to indicate that allantoin shows the central antihypertensive action in rats. Moreover, it seems likely that an activation of I-1R is required for this action of allantoin.

Imidazoline I1-receptors (I1-IRs) are known to be expressed in the rostral ventrolateral medulla (RVLM) of nucleus tract solitary (NTS) that seems essential for the sympathoinhibitory action of clonidine-, rilmenidine-, and moxonidine-like antihypertensive agents [23, 24]. These agents were introduced to reduce blood pressure mainly through an activation of specific receptors in RVLM [23, 24]. It has been documented that I1- IR agonist(s) may provide more useful therapy of hypertension than clonidine due to the low incidence of the side effect(s) including sedation [25].

Imidazoline receptors (I-Rs) have been introduced to play a role in the regulation of cardiovascular function [26]. The antihypertensive agent rilmenidine lowered the blood pressure via an activation of central I1-IR leading to the peripheral sympathoinhibition [27]. Antihypertensive drugs through lowering of central sympathetic nervous system (SNS) activity may contribute to reducing the heart rate, cardiac contractility, and vascular tone leading to a marked decrease of blood pressure [28, 29]. In the present study, intravenous injection of allantoin relieves the blood pressure through the decrease of cardiac output and peripheral resistance. These results suggested that the effects of allantoin is mainly through its' action in the brain. Also, heart rate, mean arterial pressure, and cardiac contractility (dP/dt) were significantly reduced in anesthetized rats by allantoin in a way blocked by efaroxan. The antihypertensive action of allantoin through an activation of I1-IR in brain can thus be elucidated.

It is generally recognized that both human and experimental hypertension are mainly characterized by the higher intravascular pressure due to constriction of vascular smooth muscle cells (VSMCs) in arteries, and this behavior, known as myogenic tone, is a key element of hypertension [30, 31]. Vascular tone is an important factor in the regulation of blood pressure [32]. Although blood pressure is regulated by multiple factors, it is generally agreed that the level of blood pressure, and particularly in hypertension, is determined in large part by total peripheral resistance that is primarily a main function of the resistance of terminal arterioles [33]. Then, we detected the peripheral arterial flow to reflect the total peripheral resistance. The peripheral blood flow was markedly increased by allantoin in anesthetized rats. Moreover, this action of allantoin was deleted by coadministration of efaroxan at the dose sufficient to block I1-IR. Then, decrease of total peripheral resistance by allantoin via activation of I1-IR can be identified. The central antihypertensive effect of allantoin can thus be confirmed.

Allantoin is nature-identical, safe, and nontoxic [34]. The present study characterizes that allantoin aids in the regulation of blood pressure in animals. Allantoin is easily degraded in the intestinal tract [19] and lost the activity after oral administration [20, 21]. Antihypertensive agents are usually administrated to patients by oral intake. However, allantoin is not suitable to follow this way. Thus, modification of chemical structure to help allantoin from degradation may develop the application of allantoin in the future.

Allantoin has been mentioned to improve lipid metabolism in high fat diet- (HFD-) fed mice [35] by decreasing energy intake and epididymal white adipose tissue (eWAT) accumulation [17]. Also, allantoin may improve glucose utilization in STZ-diabetic rats [18]. In the current study, we found that allantoin produced antihypertension at the dose the same as that for antihyperglycemic action and others. Thus, allantoin seems suitable to develop as an agent for metabolic syndrome in the future.

5. Conclusion

According to the obtained data, we suggest that allantoin may act as central antihypertensive agent through activation of imidazoline I-1 receptor for decrease of mean arterial pressure, heart rate, and cardiac contractility. Also, increase of the peripheral blood flow by allantoin shows the lowering of total peripheral resistance in rats. Thus, allantoin has the potential to develop as a new central antihypertensive agent in the future.

Conflict of Interests

The authors declare that they have no conflict of interests.

Authors' Contribution

Mei-Fen Chen and Jo-Ting Tsai contributed equally to this work.

Acknowledgments

The authors thank Professor King-Pong Lin for his kind support and direction in this study.

References

[1] P. A. van Zwieten and J. P. Chalmers, "Different types of centrally acting antihypertensives and their targets in the central nervous system," *Cardiovascular Drugs and Therapy*, vol. 8, no. 6, pp. 787–799, 1994.

[2] J. Chalmers and P. Pilowsky, "Brainstem and bulbospinal neurotransmitter systems in the control of blood pressure," *Journal of Hypertension*, vol. 9, no. 8, pp. 675–694, 1991.

[3] K. Sagara, M. Ojima, K. Suto, and T. Yoshida, "Quantitative determination of allantoin in Dioscorea rhizome and an oriental pharmaceutical preparation, Hachimi-Gan, by high-performance liquid chromatography," *Planta Medica*, vol. 55, no. 1, p. 93, 1989.

[4] A. V. Shestopalov, T. P. Shkurat, Z. I. Mikashinovich et al., "Biological functions of allantoin," *Izvestiya Akademii Nauk*, no. 5, pp. 541–545, 2006.

[5] K. Sato, M. Iemitsu, K. Aizawa, and R. Ajisaka, "DHEA improves impaired activation of Akt and PKC ζ/λ-GLUT4 pathway in skeletal muscle and improves hyperglycaemia in streptozotocin-induced diabetes rats," *Acta Physiologica*, vol. 197, no. 3, pp. 217–225, 2009.

[6] X. Gao, B. Li, H. Jiang, F. Liu, D. Xu, and Z. Liu, "Dioscorea opposita reverses dexamethasone induced insulin resistance," *Fitoterapia*, vol. 78, no. 1, pp. 12–15, 2007.

[7] J.-H. Hsu, Y.-C. Wu, I.-M. Liu, and J.-T. Cheng, "Dioscorea as the principal herb of Die-Huang-Wan, a widely used herbal mixture in China, for improvement of insulin resistance in fructose-rich chow-fed rats," *Journal of Ethnopharmacology*, vol. 112, no. 3, pp. 577–584, 2007.

[8] W. Shujun, L. Hongyan, G. Wenyuan, C. Haixia, Y. Jiugao, and X. Peigen, "Characterization of new starches separated from different Chinese yam (Dioscorea opposita Thunb.) cultivars," *Food Chemistry*, vol. 99, no. 1, pp. 30–37, 2006.

[9] P. Bousquet, J. Feldman, and J. Schwartz, "Central cardiovascular effects of alpha adrenergic drugs: differences between catecholamines and imidazolines," *Journal of Pharmacology and Experimental Therapeutics*, vol. 230, no. 1, pp. 232–236, 1984.

[10] P. A. Van Zwieten, "Central imidazoline I_1 receptors as targets of centrally acting antihypertensives: moxonidine and rilmenidine," *Journal of Hypertension*, vol. 15, no. 2, pp. 117–125, 1997.

[11] P. Ernsberger, M. E. Graves, L. M. Graff et al., "I_1-imidazoline receptors—definition, characterization, distribution, and transmembrane signaling," *Annals of the New York Academy of Sciences*, vol. 763, pp. 22–42, 1995.

[12] N. G. Morgan, S. L. F. Chan, M. Mourtada, L. K. Monks, and C. A. Ramsden, "Imidazolines and pancreatic hormone secretion," *Annals of the New York Academy of Sciences*, vol. 881, pp. 217–228, 1999.

[13] T.-N. Lui, C.-W. Tsao, S.-Y. Huang, C.-H. Chang, and J.-T. Cheng, "Activation of imidazoline I_{2B} receptors is linked with AMP kinase pathway to increase glucose uptake in cultured C_2C_{12} cells," *Neuroscience Letters*, vol. 474, no. 3, pp. 144–147, 2010.

[14] C.-H. Chang, H.-T. Wu, K.-C. Cheng, H.-J. Lin, and J.-T. Cheng, "Increase of β-endorphin secretion by agmatine is induced by activation of imidazoline I_{2A} receptors in adrenal gland of rats," *Neuroscience Letters*, vol. 468, no. 3, pp. 297–299, 2010.

[15] C. Dardonville and I. Rozas, "Imidazoline binding sites and their ligands: an overview of the different chemical structures," *Medicinal Research Reviews*, vol. 24, no. 5, pp. 639–661, 2004.

[16] J.-P. Lee, W. Chen, H.-T. Wu, K.-C. Lin, and J.-T. Cheng, "Metformin can activate imidazoline I-2 receptors to lower plasma glucose in type 1-like diabetic rats," *Hormone and Metabolic Research*, vol. 43, no. 1, pp. 26–30, 2011.

[17] H. H. Chung, K. S. Lee, and J. T. Cheng, "Decrease of obesity by allantoin via imidazoline I_1-receptor activation in high fat diet-fed mice," *Evidence-Based Complementary and Alternative Medicine*, vol. 2013, Article ID 589309, 7 pages, 2013.

[18] C.-S. Niu, W. Chen, H.-T. Wu et al., "Decrease of plasma glucose by allantoin, an active principle of yam (Dioscorea spp.), in streptozotocin-induced diabetic rats," *Journal of Agricultural and Food Chemistry*, vol. 58, no. 22, pp. 12031–12035, 2010.

[19] L. P. Kahn and J. V. Nolan, "Kinetics of allantoin metabolism in sheep," *British Journal of Nutrition*, vol. 84, no. 5, pp. 629–634, 2000.

[20] N. Pak, G. Donoso, and M. A. Tagle, "Allantoin excretion in the rat," *British Journal of Nutrition*, vol. 30, no. 1, pp. 107–112, 1973.

[21] T. Koguchi, H. Nakajima, M. Wada et al., "Dietary fiber suppresses elevations of uric acid and allantoin in serum and urine induced by dietary RNA and increases its excretion to feces in rats," *Journal of Nutritional Science and Vitaminology*, vol. 48, no. 3, pp. 184–193, 2002.

[22] S. I. Seldinger, "Catheter replacement of the needle in percutaneous arteriography: a new technique," *Acta Radiologica*, vol. 49, no. 434, pp. 47–52, 2008.

[23] P. Ernsberger, R. Giuliano, R. N. Willette, and D. J. Reis, "Role of imidazole receptors in the vasodepressor response to clonidine analogs in the rostral ventrolateral medulla," *Journal of Pharmacology and Experimental Therapeutics*, vol. 253, no. 1, pp. 408–418, 1990.

[24] Y. Hikasa, K. Masuda, Y. Asakura et al., "Identification and characterization of platelet alpha2-adrenoceptors and imidazoline receptors in rats, rabbits, cats, dogs, cattle, and horses," *European Journal of Pharmacology*, vol. 720, pp. 363–375, 2013.

[25] K. Nikolic and D. Agbaba, "Imidazoline antihypertensive drugs: selective I_1-imidazoline receptors activation," *Cardiovascular Therapeutics*, vol. 30, pp. 209–216, 2012.

[26] J. Yang, W.-Z. Wang, F.-M. Shen, and D.-F. Su, "Cardiovascular effects of agmatine within the rostral ventrolateral medulla are similar to those of clonidine in anesthetized rats," *Experimental Brain Research*, vol. 160, no. 4, pp. 467–472, 2005.

[27] P. A. van Zwieten and S. L. M. Peters, "Central I_1-imidazoline receptors as targets of centrally acting antihypertensive drugs. Clinical pharmacology of moxonidine and rilmenidine," *Annals of the New York Academy of Sciences*, vol. 881, pp. 420–429, 1999.

[28] W. S. Colucci, "The effects of norepinephrine on myocardial biology: implications for the therapy of heart failure," *Clinical Cardiology*, vol. 21, no. 12, pp. I20–I24, 1998.

[29] B. G. Jacob, W. O. Richter, and P. Schwandt, "Effect of three antihypertensive drug groups on lipid metabolism. Effects of alpha receptor blockers, central sympatholytic drugs and vasodilators," *Fortschritte der Medizin*, vol. 111, no. 8, pp. 126–129, 1993.

[30] M. A. Hill, G. A. Meininger, M. J. Davis, and I. Laher, "Therapeutic potential of pharmacologically targeting arteriolar myogenic tone," *Trends in Pharmacological Sciences*, vol. 30, no. 7, pp. 363–374, 2009.

[31] D. Yamazaki, Y. Tabara, S. Kita et al., "TRIC-A channels in vascular smooth muscle contribute to blood pressure maintenance," *Cell Metabolism*, vol. 14, no. 2, pp. 231–241, 2011.

[32] R. A. Khalil, "Modulators of the vascular endothelin receptor in blood pressure regulation and hypertension," *Current Molecular Pharmacology*, vol. 4, no. 3, pp. 176–186, 2011.

[33] G. V. Guinea, J. M. Atienza, F. J. Rojo et al., "Factors influencing the mechanical behaviour of healthy human descending thoracic aorta," *Physiological Measurement*, vol. 31, no. 12, pp. 1553–1565, 2010.

[34] C. Thornfeldt, "Cosmeceuticals containing herbs: fact, fiction, and future," *Dermatologic Surgery*, vol. 31, no. 7, pp. 873–880, 2005.

[35] T. T. Yang, N. H. Chiu, H. H. Chung, C. T. Hsu, W. J. Lee, and J. T. Cheng, "Stimulatory effect of allantoin on imidazoline I_1 receptors in animal and cell line," *Hormone and Metabolic Research*, vol. 44, pp. 879–884, 2012.

Hindawi Publishing Corporation
BioMed Research International
Volume 2014, Article ID 354348, 7 pages
http://dx.doi.org/10.1155/2014/354348

Research Article

Characterization of Musclin as a New Target for Treatment of Hypertension

Jia-Wei Lin,[1] Cheng-Chia Tsai,[2] Li-Jen Chen,[3] Ho-Shan Niu,[4] Chen Kuei Chang,[1] and Chiang-Shan Niu[4]

[1] *Department of Neurosurgery, College of Medicine, Taipei Medical University and Shuang Ho Hospital, Taipei Medical University, Taipei City 10361, Taiwan*
[2] *Graduate Institute of Disease Prevention and Control, College of Medicine, Taipei Medical University and Shuang Ho Hospital, Taipei Medical University, Taipei City 10361, Taiwan*
[3] *Institute of Basic Medical Sciences, College of Medicine, National Cheng Kung University, Tainan City 70101, Taiwan*
[4] *Department of Nursing, Tzu Chi College of Technology, Hualien City 97005, Taiwan*

Correspondence should be addressed to Chiang-Shan Niu; ncs838@yahoo.com.tw

Received 11 January 2014; Accepted 1 February 2014; Published 9 March 2014

Academic Editor: Juei-Tang Cheng

Musclin is a novel skeletal muscle-derived factor found in the signal sequence trap of mouse skeletal muscle cDNAs. Recently, it has been demonstrated that musclin is involved in the pathogenesis of spontaneously hypertensive rats (SHRs). However, it is known as a genetic hypertension model. In the present study, we aim to investigate the role of musclin in another animal model of hypertension and characterize the direct effect of musclin on vascular contraction. The results show that expression of musclin was increased in arterial tissues isolated from DOCA-salt induced hypertensive rats or the normal rats received repeated vasoconstriction with phenylephrine. Additionally, direct incubation with phenylephrine did not modify the expression of musclin in the *in vitro* studies. Also, the direct effect of musclin on the increase of intracellular calcium was observed in a concentration-dependent manner. These results provide the evidence to support that musclin is involved in hypertension. Thus, musclin is suitable to be considered as a novel target for treatment of hypertension.

1. Introduction

Hypertension is a cardiovascular risk factor and a major healthcare problem [1]. So far, although it is well known that the vasculature, kidney, skeletal muscle, and central nervous system contribute to the development of hypertension, the mechanisms for the progression of higher blood pressure are still not completely clarified [1]. Basically, both human hypertension and experimental models of hypertension are mainly characterized by increased intravascular pressure that causes constriction of vascular smooth muscle cells (VSMCs) in resistant arteries, and this response, known as myogenic tone, is a key element for the maintenance of blood pressure [2, 3]. Moreover, this myogenic response, which has also been demonstrated to occur independently of neural control in isolated vessels, is considered to be an intrinsic function of the smooth muscle vessel wall [4].

Musclin is a novel muscle-derived secretory peptide found in the signal sequence trap of mouse skeletal muscle cDNAs. Musclin mRNA was almost exclusively expressed in the skeletal muscle of rodents and obesity models [5]. The function of musclin has been described as responsive to insulin *in vivo* and inducing insulin resistance *in vitro* [6, 7]. Furthermore, musclin is also known as a bone-active molecule that is highly expressed in cells of the osteoblast lineage of animals [5, 8].

Recently, a higher expression of musclin in arterial tissue has been observed in spontaneous hypertensive rats (SHRs) [9]. Then, authors claimed that musclin is involved in the pathogenesis of hypertension. However, SHR is known as a genetic disorder of hypertension. Experiments by using of different hypertensive animal model will be helpful to identify the role of musclin in the development of hypertension.

The main aim of this study is to investigate the expression of musclin in other hypertensive animal models and characterize the potential mechanism(s) for musclin induced hypertension.

2. Material and Methods

2.1. Animals. Eight-week-old male Wistar rats, weighing from 250 to 280 g, were obtained from the Animal Center of National Cheng Kung University Medical College. The rats were housed individually in plastic cages under standard laboratory conditions. They were kept under a 12 h light/dark cycle and had free access to food and water. All experiments were performed under anesthesia with 2% isoflurane, and all efforts were made to minimize the animals' suffering. The animal experiments were approved and conducted in accordance with local institutional guidelines for the Care and Use of Laboratory Animals in Chi-Mei Medical Center, and the experiments conformed to the Guide for the Care and Use of Laboratory Animals as well as the guidelines of the Animal Welfare Act.

2.2. Deoxycorticosterone Acetate and Sodium Chloride (DOCA-Salt) Induced Hypertensive Rats. According to previous reports [10–12], Wistar rats were anesthetized and underwent uninephrectomy (small flank incision, right side). One week after surgery, all rats started receiving the subcutaneous injections of DOCA (Sigma-Aldrich, Germany) (20 mg/kg during the first week, 12 mg/kg during the second and third weeks, and 6 mg/kg to the end of treatment) and the drinking water contained 1.0% NaCl and 0.2% KCl. The control rats (vehicle sham) received vehicle injections (1 : 1 mineral oil and propylene glycol) and normal tap water. Each rat was placed into a holder to determine the mean blood pressure (MBP) through a noninvasive tail-cuff monitor (MK2000; Muromachi Kikai, Tokyo, Japan) under conscious and values for each animal were estimated in triplicate. All rats were then sacrificed to isolate the aorta for assay of musclin expression through Western blotting analysis.

2.3. Phenylephrine (PE) Induced Hypertension. For challenge with hypertension, Wistar rats were injected intravenously (IV) with phenylephrine (10 μg/kg; Sigma Chemical) dissolved in 9% saline, 4 times daily, for 7 days as described previously [13, 14]. The age-matched rats were divided into three groups ($n = 8$): normal rats (Con), vehicle-treated normal rats (Veh), and PE induced hypertensive rats (PE). After a 7-day treatment, each rat was placed into a holder to determine the mean blood pressure (MBP) through a noninvasive tail-cuff monitor (MK2000; Muromachi Kikai, Tokyo, Japan) under conscious and values for each animal were estimated in triplicate. All rats were then sacrificed to isolate the aorta for assay of musclin expression using Western blotting analysis.

2.4. Cell Line and Culture Conditions. Rat cell line for vascular smooth muscle cells (A7r5 cells) (BCRC, Hsinchu, Taiwan) were cultured in RPMI-1640 medium (Gibco BRL, Paisley, Scotland) supplemented with 10% fetal calf serum (FCS) (Biologic Industries, Kibbutz Beit Haemek, Israel), penicillin (100 IU/mL), streptomycin (100 mg/mL) (Sigma, St. Louis, MO, USA), and amphotericin B (2.5 mg/mL, Gibco). The cells were trypsinized (trypsin used was purchased from Gibco) and subcultured once a week, and the medium was changed every 3-4 days. For the experiments, the cells were seeded on round (10 cm diameter) plastic dishes and cultured with PE under the doses of 0.1 μM and 1 μM for 24 hours. Samples were collected for detection of the expression of musclin by Western blotting analysis.

2.5. Measurement of Intracellular Calcium Concentrations. Musclin was purchased from Phoenix Pharmaceuticals Inc. (Burlingame, CA, USA). Changes in the intracellular calcium concentration were detected using the fluorescent probe fura-2 [15]. A7r5 cells were placed in buffered physiological saline solution (PSS) containing 140 mM NaCl, 5.9 mM KCl, 1.2 mM $CaCl_2$, 1.4 mM $MgCl_2$, 11.5 mM glucose, 1.8 mM Na_2HPO_4 , and 10 mM Hepes-Tris, next, 5 μM fura-2 was added to this solution, and then, the cells were incubated for 1 h in humidified atmosphere containing 5% CO_2 and 95% air at 37°C. The cells were washed and incubated for further 30 min in PSS. The A7r5 cells were then inserted into a thermostatic (37°C) cuvette containing 2 mL of PSS and various doses of musclin or inhibitor as indicated. The fluorescence was continuously recorded using a fluorescence spectrofluorimeter (Hitachi F-2000, Tokyo, Japan). The values of intracellular calcium ($[Ca^{2+}]^i$) were calculated from the ratio $R = F340/F380$ by the formula $[Ca^{2+}]^i = K_dB\ (R - R_{min})/(R_{max} - R)$, where K_d is 225 nM, F is the fluorescence measured at 340 nm and 380 nm, and B is the ratio of fluorescence of the free dye to that of the Ca^{2+}-bound dye measured at 380 nm. R_{max} and R_{min} were determined in separate experiments by using musclin to equilibrate $[Ca^{2+}]^i$ with ambient $[Ca^{2+}]$ (R_{max}) and adding 0.1 mM $MnCl_2$ and 1 mM EGTA (R_{min}). Background autofluorescence was measured in unloaded cells and was subtracted from all measurements.

2.6. Western Blotting Analysis. Protein was extracted from tissue homogenates and cell lysates using ice-cold radioimmunoprecipitation assay (RIPA) buffer supplemented with phosphatase and protease inhibitors (50 mmol/L sodium vanadate, 0.5 mM phenylmethylsulphonyl fluoride, 2 mg/mL aprotinin, and 0.5 mg/mL leupeptin). Protein concentrations were determined with a Bio-Rad protein assay (Bio-Rad Laboratories, Inc., Hercules, CA, USA). Total proteins (30 μg) were separated by SDS/polyacrylamide gel electrophoresis (10% acrylamide gel) using a Bio-Rad Mini-Protein II system. The protein was transferred to the expanded polyvinylidene difluoride membranes (Pierce, Rockford, IL, USA) with a Bio-Rad Trans-Blot system. After transfer, the membranes were washed with PBS and blocked for 1 h at room temperature with 5% (w/v) skimmed milk powder in PBS. The manufacturer's instructions were followed for the primary antibody reactions. Blots were incubated overnight at 4°C with an immunoglobulin-G polyclonal rabbit anti-mouse antibody

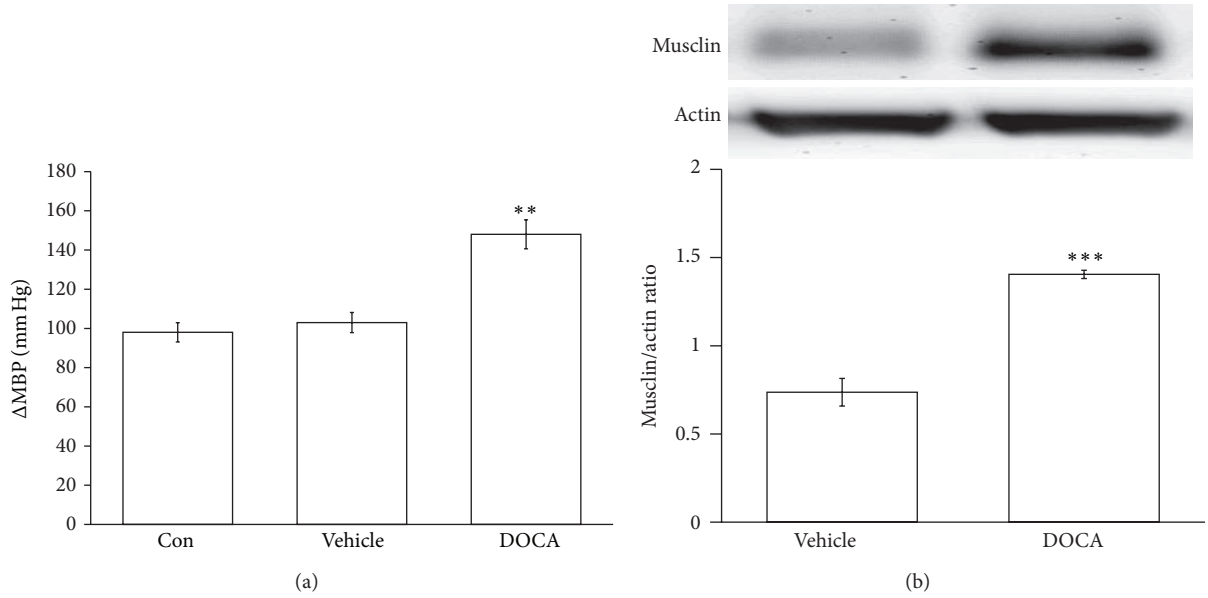

Figure 1: Effect of DOCA-salt induced hypertension on the mean blood pressure and the expression of musclin protein. Wistar rats underwent uninephrectomy and received subcutaneous injections of DOCA salt and drinking water supplemented with 1.0% NaCl and 0.2% KCl (DOCA group). The vehicle-sham rats (vehicle) received vehicle injections (1 : 1 mineral oil and propylene glycol) and normal tap water. The mean blood pressure (MBP) was recorded using a noninvasive tail-cuff monitor (a) while the expression of musclin protein (11 kDa) was determined using Western blotting analysis (b). The quantification of the results is indicated as the means with the SE ($n = 8$ per group) in each column shown in the lower panel. $^{**}P < 0.01$ and $^{***}P < 0.001$ compared with vehicle-sham group.

(Affinity BioReagents, Inc., Golden, CO, USA) (1 : 500) in 5% (w/v) skimmed milk powder dissolved in PBS/Tween 20 (0.5% by volume) to bind the target protein such as musclin. The blots were incubated with goat polyclonal antibody (1 : 1000) to bind the actin which served as the internal control. After the removal of the primary antibody, the blots were extensively washed with PBS/Tween 20 and then incubated for 2 h at room temperature with the appropriate peroxidase-conjugated secondary antibody diluted in 5% (w/v) skimmed milk powder and dissolved in PBS/Tween 20. The blots were developed by autoradiography using an ECL-Western blotting system (Amersham International, Buckinghamshire, UK). The immunoblots of musclin (11 kDa) were quantified with a laser densitometer.

2.7. Preparation of Isolated Arterial Strips. The isolated arterial strips from Wistar rats were used. Each rat was sacrificed by decapitation under anesthesia. After the arterial strips had been carefully freed from fat and connective tissue, the spirally cut strips were then mounted in organ baths filled with 10 mL oxygenated Krebs' buffer (95% O_2, 5% CO_2) at 37°C containing (in mmol/L) NaCl 135; KCl 5; $CaCl_2$ 2.5; $MgSO_4$ 1.3; KH_2PO_4 1.2; $NaHCO_3$ 20; and d-glucose 10 (pH 7.4). The calcium-free buffer was prepared in the same manner while $CaCl_2$ was not included. To exclude a possible role of the endothelium in musclin induced vasoconstriction, the tests were conducted in endothelium-denuded preparations. The endothelium was removed by gently rubbing it against the teeth of a pair of forceps. Successful removal of the endothelium was confirmed by histological identification and failure of 1 μmol/L acetylcholine to relax the rings that had been precontracted with potassium chloride as described previously [16].

Each preparation was connected to strain gauges (FT03; Grass Instrument, Quincy, MA, USA). Isometric tension was recorded using chart software (MLS023, Powerlab; ADInstruments, Bella Vista, NSW, Australia). Strips were mounted and allowed to stabilize for 2 h. Each preparation was then gradually stretched to achieve an optimal resting tension of 1 g. After the tension had stabilized, the arterial strips were exposed to musclin at various concentrations (0.01–10 nmol/L), with a wait time of 15–20 min between all musclin doses. Then, the increase in tonic contraction (vasoconstriction) was evaluated. Once the sample stabilized, oxygenated Krebs buffer was replaced, and then potassium chloride (50 mmol/L) (Sigma-Aldrich, St. Louis, MO, USA) was added as a positive control.

2.8. Statistical Analysis. Results were expressed as mean ± SE of each group. Statistical analysis was carried out using ANOVA analysis and Newman-Keuls post hoc analysis. Statistical significance was set as $P < 0.05$.

3. Results

3.1. Increase of Musclin Expression in Deoxycorticosterone Acetate and Sodium Chloride (DOCA-Salt) Induced Hypertensive Rats. We examined the expression of musclin in the aorta of DOCA-salt induced hypertensive rats. The mean blood pressure (MBP) in these animals was significantly elevated

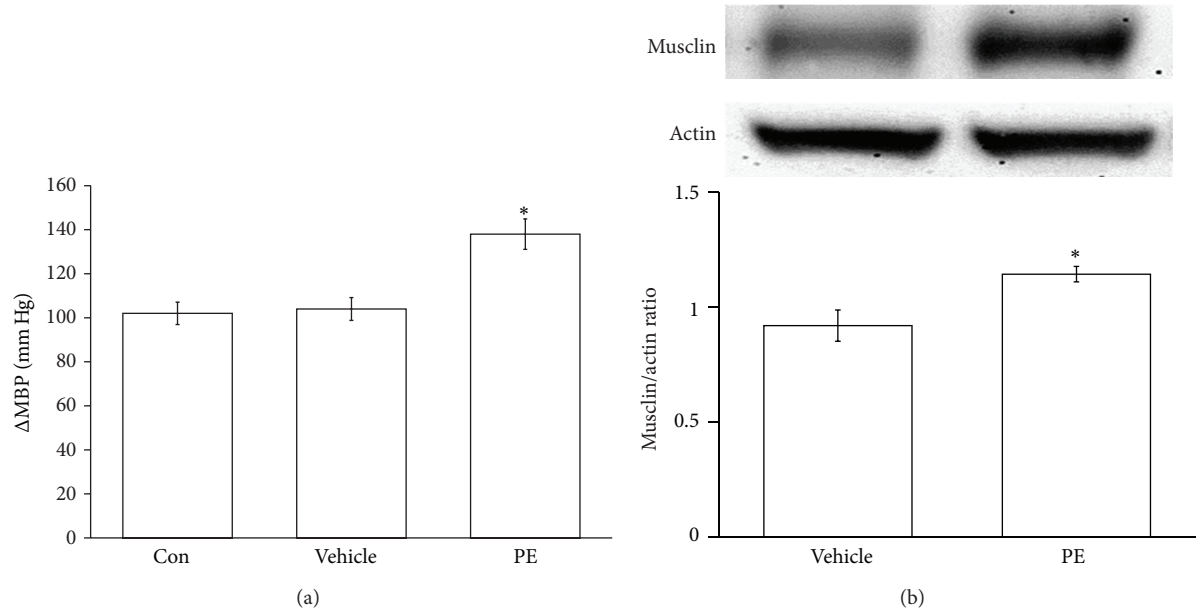

Figure 2: Effect of challenge with vasoconstrictor on the mean blood pressure and the expression of musclin protein. Wistar rats were injected intravenously (IV) with a vasoconstrictor named phenylephrine (PE; 10 μg/kg) dissolved in 9% saline, the used vehicle, 4 times daily for one week. The mean blood pressure (MBP) was recorded using a noninvasive tail-cuff monitor (a), while the expression of musclin protein (11 kDa) was determined using Western blotting analysis (b). The quantification of the results is indicated as the means with the SE ($n = 8$ per group) in each column shown in the lower panel. $^*P < 0.05$ compared to vehicle-treated group.

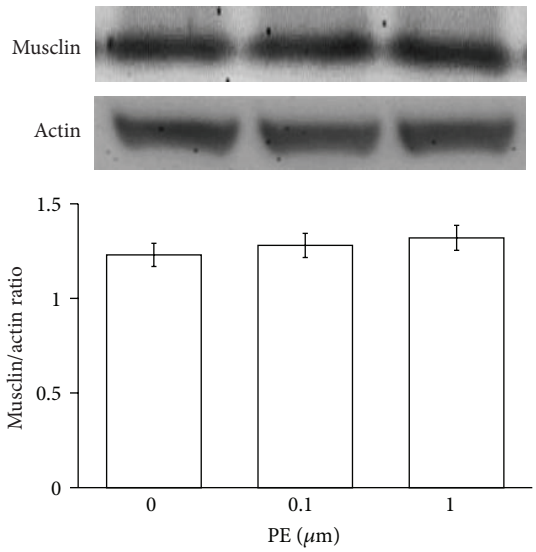

Figure 3: Effects of phenylephrine (PE) on the expression of musclin in A7r5 cells. Cells treated with PE for 24 hours were then harvested to measure the protein level of musclin expression using Western blotting analysis. All values are presented as mean ± SEM ($n = 8$). No difference was observed between all groups.

(Figure 1(a)) as compared to the vehicle-sham group. Also, the expression of musclin in aorta was markedly raised in DOCA-salt induced hypertensive rats (Figure 1(b)).

3.2. Increase of Musclin Expression by Phenylephrine Induced Hypertension. We examined the expression of musclin in the rat aorta of normotensive rats after repeated treatment with phenylephrine (PE) (four times a day) for one week. The mean blood pressure (MBP) after treatment with PE was significantly higher (Figure 2(a)) than the vehicle-treated group. PE also increased the expression of musclin protein in aorta isolated from treated animals (Figure 2(b)).

3.3. Effect of Phenylephrine on Musclin Expression in Rat Cell Line of Vascular Smooth Muscle Cells (A7r5 Cells). To identify the direct effect of PE on the expression of musclin, A7r5 cells were treated with PE. There is no difference in the expression of musclin in PE treated A7r5 cells (Figure 3).

3.4. Effect of Musclin on Arterial Strips Isolated from Rats. Vasoconstriction was induced in a dose-dependent manner by musclin (0.01–10 nmol/L) in the arterial strips isolated from normal rats. However, the response to musclin in arterial strips was markedly reduced in calcium-free buffer as compared with that in calcium-rich buffer (Figure 4(a)). The action of musclin disappeared by washing the strips with normal buffer, and the response could be reproduced by the retreatment with musclin.

3.5. Changes of Intracellular Calcium Influx by Musclin in A7r5 Cells. The fluorescent probe, fura2-AM, was used to detect the changes in intracellular calcium level in A7r5 cells. Musclin (0.01–10 nmol/L) showed the significant increase

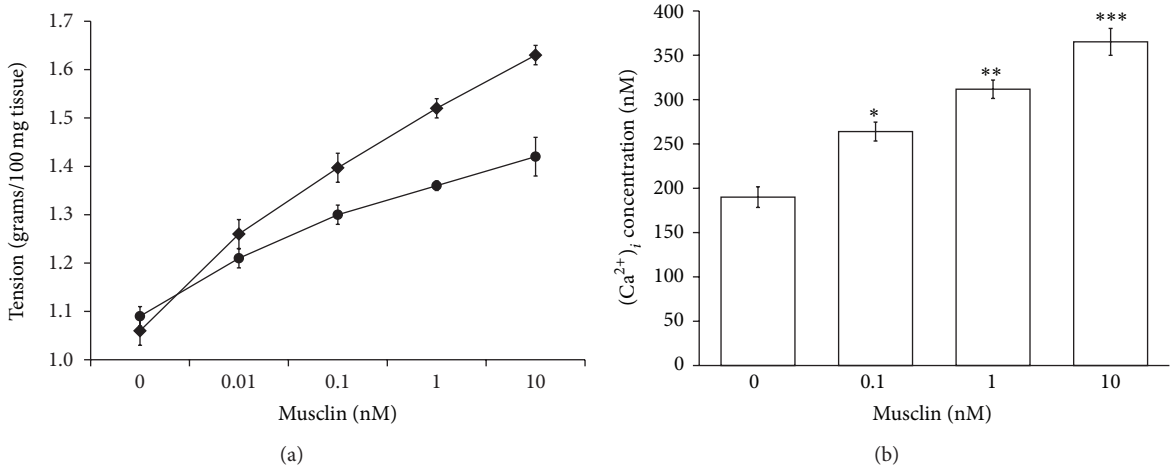

Figure 4: Effects of musclin on contraction of arterial strip and intracellular calcium in A7r5 cells. Vasoconstriction was induced in a concentration-dependent manner by musclin (0.01–10 nmol/L) in the arterial strips isolated from normal Wistar rats. The closed square showed the results in calcium-rich buffer while the closed circle showed the results in calcium-free buffer (a). Changes in intracellular calcium were detected with fura-2 by using a fluorescence spectrofluorometer. The cells were placed in buffered physiological saline solution with 5 μM of fura-2-AM and incubated for 1 h. After recording the baseline value, musclin was added into the cuvette to detect the free intracellular calcium (b). All values are presented as mean ± SEM ($n = 8$). $^{*}P < 0.05$, $^{**}P < 0.01$, and $^{***}P < 0.001$ compared with the control group (musclin 0 nM).

of intracellular calcium level in a concentration-dependent manner (Figure 4(b)).

4. Discussion

In the present study, we found that expression of musclin is raised in arterial tissues isolated from DOCA-salt induced hypertensive rats. Also, similar increase of arterial musclin expression was observed in normal rats after repeated vasoconstriction challenge using phenylephrine. However, phenylephrine treated vascular smooth muscle cells (A7r5 cells) did not modify the expression of musclin. The direct effect of phenylephrine can thus be ruled out, and changes in the expression of musclin seem related mainly to the vasoconstriction. Furthermore, musclin induced a sustained vasoconstriction in the arterial strips isolated from normal rats in a concentration-dependent manner. The response was reduced when arterial strips were immersed in calcium-free buffer. Sustained increase of calcium influx by musclin was also characterized in A7r5 cells. Thus, to the best of our knowledge, this is the first study to show the higher expression of musclin in response to vasoconstriction that generally occurred in hypertension.

The administration of a synthetic mineralocorticoid derivative, DOCA, in combination with salt loading in the diet to young adult Wistar rats following surgical removal of one kidney induces hypertension with characteristic of human volume-overload induced hypertension [17–19]. DOCA-salt rats mimic most of the changes in human hypertension and vascular dysfunction [20]. In this study, we observed the higher expression of musclin in the arterial tissue of DOCA-salt induced hypertensive rats using Western blots. Thus, a higher expression of musclin is not only in the genetic animal model of SHRs but also in DOCA-salt induced hypertensive rats.

The phenylephrine (PE) induced vasoconstriction is widely used as an experimental model of hypertension [21, 22]. In this study, we found a higher expression of musclin in arterial tissue isolated from the PE treated rats using Western blots. However, an activation of α_1-adrenoceptors by PE may influence the expression of genes and structure proteins [23]. Thus, we treated A7r5 cells with PE to investigate the direct effect of PE on the expression of musclin. However, PE did not modify the expression of musclin in cultured vascular cells. The higher expression of musclin in aorta seems related to vasoconstriction that generally occurred in hypertension.

Thus, an increase of aortic tone by hypertension may enhance the expression of musclin. Then, the raised expression of musclin could lead the hypertension to be more serious. For understanding the direct effect of musclin on aortic tone, the spirally cut aortic strips from normotensive rats were used. We gave up the use of aortic strips from SHRs that showed the pathologic state of vascular tone. Musclin induced sustained vasoconstriction was markedly reduced when arterial strips were immersed in calcium-free buffer. It has been indicated that vasoconstrictors may cause intracellular calcium release from intracellular calcium pool to develop the tension of arterial smooth muscle [24, 25]. Thus, the vasoconstriction induced by musclin seems not dependent on calcium influx only. Release of calcium from intracellular pool is also involved in the vasoconstriction of musclin.

Calcium ions are essential for muscle contraction while calcium influx is the major pathway to increase intracellular calcium. [26–29]. Modulation of myofilament properties by alterations in the calcium concentration has profound effects

on smooth muscle contractility [28]. In the present study, we demonstrated the vasoconstriction of musclin through calcium influx and an increase of intracellular calcium by musclin in A7r5 cells. Thus, musclin may increase vascular tone through enhancement of intracellular calcium that is important in the development of arterial hypertension.

The vasoconstriction induced by musclin appeared to be calcium dependent. However, intracellular signals for the action of musclin are still unclear. It has been suggested that musclin may activate its specific receptors and NPR-C receptors in cardiovascular tissues and cells [9]. Also, it has been established that ANP interacts with NPR-C in aorta to activate calcium-loaded calmodulin and others for vasoconstriction [30]. Thus, the potential mechanisms of musclin induced vasoconstriction could be elucidated in a calcium-dependent manner. But the real signals need more investigations in the future.

5. Conclusion

In the present study, we observed a higher expression of musclin in aorta during hypertension. Also, musclin contributed to the development of hypertension through increase of intracellular calcium in vascular smooth muscle. Thus, we suggest that musclin could be considered as a new target in the development of agent(s) for treatment of hypertension.

Conflict of Interests

The authors declare that there is no conflict of interests regarding the publication of this paper.

Acknowledgments

The authors thank Yang-Lian Yan and Yi-Zhi Chen for helpful assistance in the experiments. The present study was donated in part by a Grant from Taipei Medical University (TMU102-AE2-1013).

References

[1] S. MacMahon, "Blood pressure and the risk of cardiovascular disease," *The New England Journal of Medicine*, vol. 342, no. 1, pp. 50–52, 2000.

[2] M. A. Hill, G. A. Meininger, M. J. Davis, and I. Laher, "Therapeutic potential of pharmacologically targeting arteriolar myogenic tone," *Trends in Pharmacological Sciences*, vol. 30, no. 7, pp. 363–374, 2009.

[3] D. Yamazaki, Y. Tabara, S. Kita et al., "TRIC-A channels in vascular smooth muscle contribute to blood pressure maintenance," *Cell Metabolism*, vol. 14, no. 2, pp. 231–241, 2011.

[4] K. Sonoyama, A. Greenstein, A. Price, K. Khavandi, and T. Heagerty, "Vascular remodeling: implications for small artery function and target organ damage," *Therapeutic Advances in Cardiovascular Disease*, vol. 1, no. 2, pp. 129–137, 2007.

[5] H. Nishizawa, M. Matsuda, Y. Yamada et al., "Musclin, a novel skeletal muscle-derived secretory factor," *Journal of Biological Chemistry*, vol. 279, no. 19, pp. 19391–19395, 2004.

[6] W. J. Chen, Y. B. Sui, and X. H. Yin, "Musclin and insulin resistance," *Sheng Li Ke Xue Jin Zhan*, vol. 43, pp. 45–47, 2012.

[7] Y. Liu, X. Huo, X. F. Pang, Z. H. Zong, X. Meng, and G. L. Liu, "Musclin inhibits insulin activation of Akt/protein kinase B in rat skeletal muscle," *Journal of International Medical Research*, vol. 36, no. 3, pp. 496–504, 2008.

[8] A. Yasui, H. Nishizawa, Y. Okuno et al., "Foxo1 represses expression of musclin, a skeletal muscle-derived secretory factor," *Biochemical and Biophysical Research Communications*, vol. 364, no. 2, pp. 358–365, 2007.

[9] Y. X. Li, K. C. Cheng, A. Asakawa et al., "Role of musclin in the pathogenesis of hypertension in rat," *PLoS ONE*, vol. 8, no. 8, Article ID e72004, 2013.

[10] S. F. Rodrigues and D. N. Granger, "Cerebral microvascular inflammation in DOCA salt-induced hypertension: role of angiotensin II and mitochondrial superoxide," *Journal of Cerebral Blood Flow and Metabolism*, vol. 32, no. 2, pp. 368–375, 2012.

[11] J. Bhatia, F. Tabassum, A. K. Sharma et al., "Emblica officinalis exerts antihypertensive effect in a rat model of DOCA-salt-induced hypertension: role of (p) eNOS, NO and Oxidative Stress," *Cardiovascular Toxicology*, vol. 11, no. 3, pp. 272–279, 2011.

[12] B. Seifi, M. Kadkhodaee, S. M. Karimian, M. Zahmatkesh, J. Xu, and M. Soleimani, "Evaluation of renal oxidative stress in the development of doca-salt induced hypertension and its renal damage," *Clinical and Experimental Hypertension*, vol. 32, no. 2, pp. 90–97, 2010.

[13] W. E. Hoffman, G. Edelman, R. Ripper, and H. M. Koenig, "Sodium nitroprusside compared with isoflurane-induced hypotension: the effects on brain oxygenation and arteriovenous shunting," *Anesthesia and Analgesia*, vol. 93, no. 1, pp. 166–170, 2001.

[14] B. T. Kang, R. F. Leoni, D. E. Kim, and A. C. Silva, "Phenylephrine-induced hypertension during transient middle cerebral artery occlusion alleviates ischemic brain injury in spontaneously hypertensive rats," *Brain Research*, vol. 1477, pp. 83–91, 2012.

[15] P.-Y. Lee, W. Chen, I.-M. Liu, and J.-T. Cheng, "Vasodilatation induced by sinomenine lowers blood pressure in spontaneously hypertensive rats," *Clinical and Experimental Pharmacology and Physiology*, vol. 34, no. 10, pp. 979–984, 2007.

[16] Z.-C. Chen, J.-P. Shieh, H.-H. Chung, C.-H. Hung, H. J. Lin, and J.-T. Cheng, "Activation of peripheral opioid μ-receptors in blood vessel may lower blood pressure in spontaneously hypertensive rats," *Pharmacology*, vol. 87, no. 5-6, pp. 257–264, 2011.

[17] H. Selye, C. E. Hall, and E. M. Rowley, "Malignant hypertension produced by treatment with desoxycorticosterone acetate and sodium chloride," *Canadian Medical Association Journal*, vol. 49, pp. 88–92, 1943.

[18] C. G. Brilla and K. T. Weber, "Mineralocorticoid excess, dietary sodium, and myocardial fibrosis," *Journal of Laboratory and Clinical Medicine*, vol. 120, no. 6, pp. 893–901, 1992.

[19] L. Brown, B. Duce, G. Miric, and C. Sernia, "Reversal of cardiac fibrosis in deoxycorticosterone acetate-salt hypertensive rats by inhibition of the renin-angiotensin system," *Journal of the American Society of Nephrology*, vol. 10, supplement 11, pp. S143–S148, 1999.

[20] D. Loch, A. Hoey, and L. Brown, "Attenuation of cardiovascular remodeling in DOCA-salt rats by the vasopeptidase inhibitor, omapatrilat," *Clinical and Experimental Hypertension*, vol. 28, no. 5, pp. 475–488, 2006.

[21] R. M. McMurphy, M. R. Stoll, and R. McCubrey, "Accuracy of an oscillometric blood pressure monitor during phenylephrine-induced hypertension in dogs," *American Journal of Veterinary Research*, vol. 67, no. 9, pp. 1541–1545, 2006.

[22] D. Bia Santana, J. C. Grignola, R. L. Armentano, and F. F. Ginés, "Improved pulmonary artery buffering function during phenylephrine-induced pulmonary hypertension," *Molecular and Cellular Biochemistry*, vol. 246, no. 1-2, pp. 19–24, 2003.

[23] Y. Wang, R. Hou, P. Li et al., "Gene expression profiles in response to the activation of adrenoceptors in A7R5 aortic smooth muscle cells," *Clinical and Experimental Pharmacology and Physiology*, vol. 31, no. 9, pp. 602–607, 2004.

[24] A. V. Somlyo, M. Bond, A. P. Somlyo, and A. Scarpa, "Inositol trisphosphate-induced calcium release and contraction in vascular smooth muscle," *Proceedings of the National Academy of Sciences of the United States of America*, vol. 82, no. 15, pp. 5231–5235, 1985.

[25] K. Sato, H. Ozaki, and H. Karaki, "Changes in cytosolic calcium level in vascular smooth muscle strip measured simultaneously with contraction using fluorescent calcium indicator fura 2," *Journal of Pharmacology and Experimental Therapeutics*, vol. 246, no. 1, pp. 294–300, 1988.

[26] I. Ohtsuki and S. Morimoto, "Troponin: regulatory function and disorders," *Biochemical and Biophysical Research Communications*, vol. 369, no. 1, pp. 62–73, 2008.

[27] J. M. Metzger and M. V. Westfall, "Covalent and noncovalent modification of thin filament action: the essential role of troponin in cardiac muscle regulation," *Circulation Research*, vol. 94, no. 2, pp. 146–158, 2004.

[28] J. Layland, R. J. Solaro, and A. M. Shah, "Regulation of cardiac contractile function by troponin I phosphorylation," *Cardiovascular Research*, vol. 66, no. 1, pp. 12–21, 2005.

[29] M. D. Bootman and M. J. Berridge, "The elemental principles of calcium signaling," *Cell*, vol. 83, no. 5, pp. 675–678, 1995.

[30] S. D. Rybalkin, C. Yan, K. E. Bornfeldt, and J. A. Beavo, "Cyclic GMP phosphodiesterases and regulation of smooth muscle function," *Circulation Research*, vol. 93, no. 4, pp. 280–291, 2003.

Hindawi Publishing Corporation
BioMed Research International
Volume 2014, Article ID 403703, 10 pages
http://dx.doi.org/10.1155/2014/403703

Research Article

Brazilin Ameliorates High Glucose-Induced Vascular Inflammation via Inhibiting ROS and CAMs Production in Human Umbilical Vein Endothelial Cells

Thanasekaran Jayakumar,[1] Chao-Chien Chang,[1,2] Shoei-Loong Lin,[3] Yung-Kai Huang,[4] Chien-Ming Hu,[5] Antoinet Ramola Elizebeth,[6] Shih-Chang Lin,[7,8,9] and Cheuk-sing Choy[10,11]

[1] *Department of Pharmacology, College of Medicine, Taipei Medical University, Taipei, Taiwan*
[2] *Department of Cardiology, Cathay General Hospital, Taipei, Taiwan*
[3] *Department of Surgery, Taipei Hospital, Ministry of Health and Welfare, New Taipei City, Taiwan*
[4] *School of Oral Hygiene, College of Oral Medicine, Taipei Medical University, Taipei, Taiwan*
[5] *Taipei Medical University, Taiwan*
[6] *Department of Biotechnology, Periyar Maniammai University, Thanjavur, Tamil Nadu, India*
[7] *Division of Allergy and Immunology, Department of Internal Medicine, Cathay General Hospital, No. 280, Section 4, Jen-Ai Road, Taipei, Taiwan*
[8] *The Laboratory of Allergy and Immunology, Cathay Medical Research Institute, New Taipei City, Taiwan*
[9] *Department of Medicine, School of Medicine, Fu Jen Catholic University, New Taipei City, Taiwan*
[10] *Emergency Department, Taipei Hospital, Ministry of Health and Welfare, No. 127, Su-Yuan Road, Hsin-Chuang, New Taipei City, Taiwan*
[11] *Department of General Medicine, School of Medicine, College of Medicine, Taipei Medical University, Taipei, Taiwan*

Correspondence should be addressed to Shih-Chang Lin; sclin@cgh.org.tw and Cheuk-sing Choy; prof.choy@gmail.com

Received 16 October 2013; Revised 4 December 2013; Accepted 5 December 2013; Published 2 March 2014

Academic Editor: Joen-Rong Sheu

Vascular inflammatory process has been suggested to play a key role in the initiation and progression of atherosclerosis, a major complication of diabetes mellitus. Recent studies have shown that brazilin exhibits antihepatotoxic, antiplatelet, cancer preventive, or anti-inflammatory properties. Thus, we investigated whether brazilin suppresses vascular inflammatory process induced by high glucose (HG) in cultured human umbilical vein endothelial cells (HUVEC). HG induced nitrite production, lipid peroxidation, and intracellular reactive oxygen species formation in HUVEC cells, which was reversed by brazilin. Western blot analysis revealed that brazilin markedly inhibited HG-induced phosphorylation of endothelial nitric oxide synthase. Besides, we investigated the effects of brazilin on the MAPK signal transduction pathway because MAPK families are associated with vascular inflammation under stress. Brazilin blocked HG-induced phosphorylation of extracellular signal-regulated kinase and transcription factor NF-κB. Furthermore, brazilin concentration-dependently attenuated cell adhesion molecules (ICAM-1 and VCAM-1) expression induced by various concentrations of HG in HUVEC. Taken together, the present data suggested that brazilin could suppress high glucose-induced vascular inflammatory process, which may be closely related with the inhibition of oxidative stress, CAMs expression, and NF-κB activation in HUVEC. Our findings may highlight a new therapeutic intervention for the prevention of vascular diseases.

1. Introduction

Endothelial dysfunction is considered the primary cause in the pathogenesis of vascular disease in diabetes mellitus [1]. Diabetes is a metabolic disorder characterized by hyperglycemia and glucose intolerance due to lessened effectiveness of insulin action, insulin deficiency, or both. An increase of cardiovascular diseases due in part to hyperglycemia

is associated with diabetes, which can induce endothelial dysfunction [2]. Alterations in endothelial function lead the development of insulin resistance [3]. The most likely cause of endothelial damage induced by hyperglycemia is the overproduction of reactive oxygen species (ROS) in mitochondria [4]. In aortic endothelial cells, hyperglycemia induces increases of mitochondrial superoxide production and prevents activity and expression of endothelial nitric oxide synthase (eNOS) [5]. ROS can modify endothelial function by a variety of mechanisms, such as peroxidation of membrane lipids, activation of NF-κB, and decrease of the availability of nitric oxide (NO) [6]. Vascular disorders through overexpression of adhesion molecules are thought to play a role in the pathogenesis of atherosclerosis. Activation of NF-κB induces adhesion molecules, such as VCAM-1 and ICAM-1, and, subsequently, induces an increase in the migration and adhesion of monocytic cells to endothelial cells, which are very important events during the inflammatory process.

Oxidative stress, due to the high glucose concentration, plays a vital role in the progress of diabetic impediments [7]. Previous studies have shown that high glucose activates nuclear factor-κB (NF-κB), one of the transcription factors for proinflammatory genes. NF-κB is present in the cytoplasm as an inactive form bound to its inhibitor molecule, inhibitory factor of NF-κB-α (IκB-α). Translocation of NF-κB from the cytoplasm to the nucleus is preceded by the phosphorylation, ubiquitination, and proteolytic degradation of IκB-α [8]. It is assumed that high glucose-induced CAMs expression may depend on activation of NF-κB. Under oxidative stress, endothelial cells generate ROS, such as superoxides and peroxynitrite, leading to low-density lipo protein (LDL) oxidation. The formation of ROS together with inflammatory factors including chemokines, cytokines, and adhesion molecules has been shown to be increased in atherosclerotic lesions [9]. Inflammatory responses, including inflammatory gene transcription, appear to involve free radicals or oxidative stresses, and thus free radical scavengers can suppress inflammatory gene expression. However, the effect of brazilin on high glucose-induced oxidative stress was not cleared in vascular endothelial cells.

Sappan Lignum, the heart wood of *Caesalpinia sappan* L., (*C. sappan* L) is used traditionally for large number of ailments and reported to have a wide variety of medicinal properties. The anti-inflammatory, antiproliferative, and antioxidant activities of *C. sappan* have been well documented [10, 11]. Brazilin [7,11b-dihydrobenz[b]indeno[1,2-d]pyran-3,6a,9,10(6H)-tetrol], the major component of *C. sappan* L. [12], is a natural red pigment, largely used for histological staining. Brazilin is also a promising chemopreventive agent as it is generally nontoxic and interferes with the process of carcinogenesis. Several synthetic types' brazilin analogues have demonstrated cancer-preventive properties towards a number of human cancer cell lines including HT29, A549, HL60, and K562 in MTT assays [13]. Brazilin induced vasorelaxation is reported to be inhibited by NG-nitro-Larginine methyl ester (L-NAME) and it is suggested that the mechanism by which brazilin caused vasodilation might be endothelial dependent [14]. This study was designed to investigate the effect and molecular mechanisms of brazilin on high-glucose stimulated human endothelial cells and the subsequent expression of CAMs in these cells. Our findings indicate a novel molecular mechanism underlying the therapeutic effects of brazilin for the prevention of vascular diseases.

2. Materials and Methods

2.1. Materials. Brazilin (Figure 1(a)) was purchased from ICN Pharmaceuticals (Irvine, CA, USA). Cell culture reagents including M-199 medium, L-glutamine, penicillin, streptomycin, and fetal bovine serum were obtained from Gibco BRL (Grand Island, NY, USA). Antimouse and antirabbit immunoglobulin G-conjugated horseradish peroxidase (HRP) were purchased from Amersham Biosciences (Sunnyvale, CA, USA) and/or Jackson-Immuno Research (West Grove, PA, USA). A rabbit polyclonal antibody specific for NF-kB was purchased from Santa Cruz Biotechnology (Santa Cruz, CA, USA). The antiphospho-p42/p44 ERK (Thr202/Tyr204) was from Cell Signaling (Beverly, MA, USA). The hybond-P polyvinylidene difluoride (PVDF) membrane and enhanced chemiluminescence (ECL) western blotting detection reagent and analysis system were obtained from Amersham (Buckinghamshire, UK). All other chemicals used in this study were of reagent grade.

2.2. Human Umbilical Vein Endothelial Cells (HUVECs) Isolation and Culture. Human umbilical cords were obtained from the Hospital of National Taiwan University, and human umbilical vein endothelial cells were isolated by enzymatic digestion as described previously [15]. After 15-min incubation with 0.1% collagenase at 37 ± 0.5°C, umbilical cord vein segments were perfused with 30 mL of medium 199 containing 10 U/mL penicillin and 100 μg/mL streptomycin for the collection of cells. After centrifugation for 8 min at 900 ×g, the cell pellet was resuspended in previous medium supplemented with 20% heat-inactivated fetal bovine serum, 30 μg/mL endothelial cell growth supplement, and 90 μg/mL heparin. Confluent primary cells were detached by trypsin-EDTA (0.05% : 0.02%, v/v), and passages between three and five were used in the experiments. Cultures had typical cobblestone morphology and stained uniformly for human von Willebrand factor (vWF) [16] as assessed by indirect immunofluorescence.

2.3. Cell Viability Assay. The viability of HUVECs upon treatment of glucose, brazilin alone, and both combined together was measured by a colorimetric MTT assay. Briefly, HUVECs (2×10^5 cells/well) were seeded on 24-well plates and cultured in DMEM containing 10% FBS for 24 h. HUVECs were treated with glucose at concentrations of (5–150 μM), brazilin (10–100 μM) alone, and pretreated with brazilin (10–100 μM) in glucose (25 and 50 mM) induced cells or an isovolumetric solvent control (0.1% DMSO) for 24 or 48 h. The cell number was measured using a colorimetric assay based on the ability of mitochondria in viable cells to reduce MTT as previously

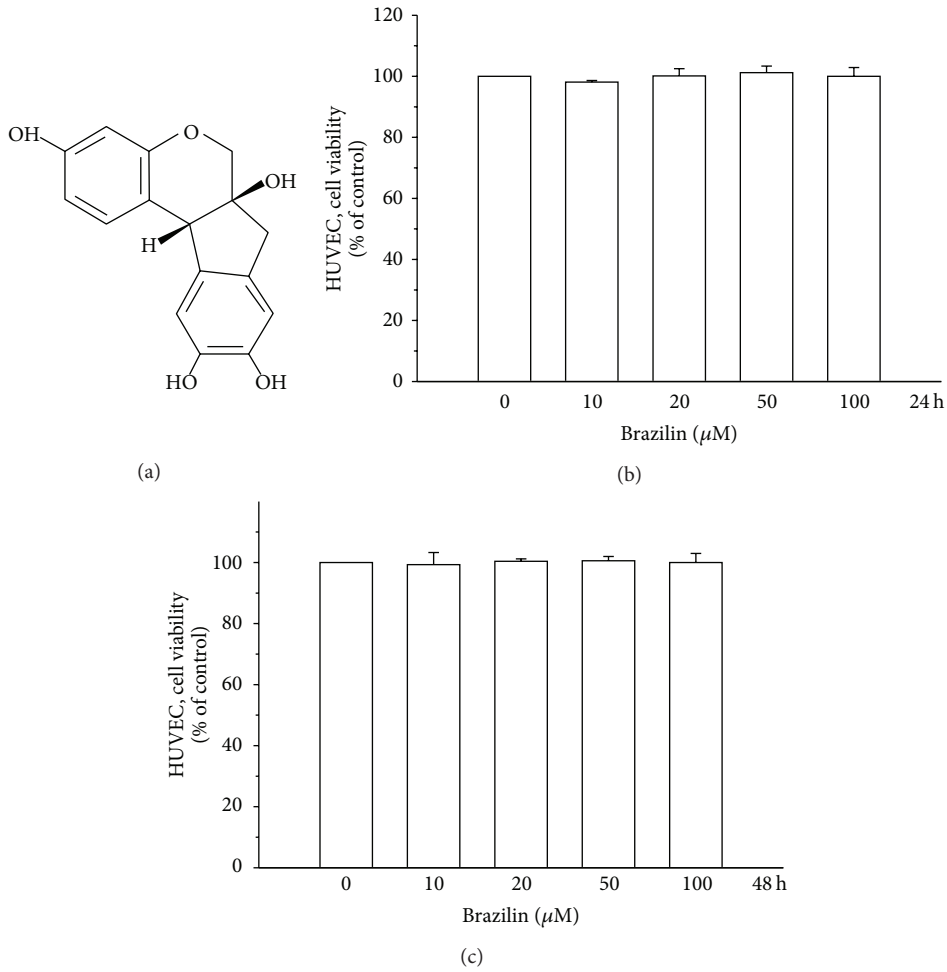

Figure 1: Effects of brazilin on the cell viability of human umbilical vein endothelial cells (HUVEC): (a) the structure of brazilin; (b) the viability of HUVECs during treatment with various concentrations (0–100 μM) of brazilin for 24 h; (c) the viability of HUVECs during treatment with various concentrations (0–100 μM) of brazilin for 48 h.

described [17]. The cell number index was calculated as the absorbance of treated cells/control cells × 100%.

2.4. Determination of Nitrite Production. Human umbilical vein endothelial cells cultured in 12-well plates were washed twice with Hanks balanced salt solution (HBSS) and then incubated at 37 ± 0.5°C in the same buffer for 30 min with various concentrations of brazilin. Acetylcholine (30 μM) was used as a positive control. Supernatants were collected and then injected into a nitrogen purge chamber containing vanadium (III) chloride in hydrochloric acid at 91 ± 0.5°C. All NO metabolites can be liberated as gaseous NO and reacted with ozone to form activated nitrogen dioxide that is luminescent in red and infrared spectra. The chemiluminescence was detected using a nitric oxide analyzer (NOA280, Sievers Instruments, Boulder, CO, USA) [18]. For calibration, the area under the curve was converted to nanomolar NO using a $NaNO_3$ standard curve, and the final data were expressed as pmol/mg protein.

2.5. Lipid Peroxidation Assay. Lipid peroxidation was assayed by the thiobarbituric acid (TBA) reaction. The cells were homogenized in ice-cold 1.15% KCl. The samples were used to measure the malondialdehyde (MDA) formed in a peroxidizing lipid system. The amount of thiobarbituric acid reactive substance (TBARS) was determined using a standard curve of 1,1,3,3-tetramethoxypropane.

2.6. Measurement of Intracellular ROS. Starved HUVECs (2×10^5 cells/well) were loaded with DCF-DA (20 μM) for 20 min. After treatment with brazilin (100 μM) or a solvent control for 20 min, cells were stimulated with glucose (5.5–75 mM) for 10 min, washed with PBS, and then detached using trypsin. Levels of intracellular ROS were detected by flow cytometry (Beckman Coulter). All experiments were repeated at least four times to ensure reproducibility.

2.7. SDS-Polyacrylamide Gel Electrophoresis (PAGE) and Western Blot Analysis. Western blot analyses were performed as previously described [19]. Lysates from each sample were

mixed with 6 × sample buffer (0.35 M Tris, 10% w/v SDS, 30% v/v glycerol, 0.6 M DTT, and 0.012% w/v bromophenol blue, pH 6.8) and heated to 95°C for 5 min. Proteins were separated by electrophoresis and transferred onto polyvinylidene difluoride (PVDF) membranes for pERK1/2, p-eNOS, pNF-kB, VCAM-1, and ICAM-1. The membranes were blocked with 5% nonfat milk in TBS-0.1% Tween 20 and sequentially incubated with primary antibodies and HRP-conjugated secondary antibodies, followed by enhanced chemiluminescence (ECL) detection (Amersham Biosciences). Bioprofil Bio-1D light analytical software (Vilber Lourmat, Marue La Vallee, France) was used for the quantitative densitometric analysis. Data of specific protein levels are presented as relative multiples in relation to the control.

2.8. Statistical Analyses. The experimental results are expressed as the mean ± SEM and are accompanied by the number of observations. For analysis of the results, a one-way analysis of variance (ANOVA) test was performed using Sigma Stat v3.5 software. When group comparisons showed a significant difference, the Student Newman-Keuls test was used. A P value of <0.05 was considered to be statistically significant.

3. Results

3.1. Effect of Brazilin on HG-Induced HUVECs Cell Viability. Initially, the cytotoxicity of brazilin to HUVECs cells was measured by MTT assay. Cell viability was not significantly altered by brazilin at 10–100 μM for 24 and 48 h with cell viability remaining stable (Figures 1(b) and 1(c)). Interestingly, treatment of cells with glucose (5.5–150 μM) concentration dependently decreased cell viability, whereas cells simultaneously incubated with glucose (25 and 50 mM) and brazilin (0–100 μM) increased cell viability in a concentration-dependent manner (Figures 2(a), 2(b), 2(c), and 2(d)).

3.2. Brazilin Inhibits HG-Induced LPO, NO, and ROS in HUVECs. It is known that damage to cell membranes causes the decreasing of cell viability through peroxidation of membrane lipids. Therefore, we estimated the levels of MDA in the present study. As shown in Figure 3(a), malonedi aldehyde (MDA), a marker of lipid peroxidation, was markedly induced in HUVEC cells by treatment with glucose (5.5–75 mM). However, pretreatment with brazilin (100 μM) significantly reduced glucose-induced lipid peroxidation. Similarly, HUVEC cells treated with glucose (5.5–75 mM) significantly increased nitrite formation in a concentration-dependent manner; however, this increase was markedly suppressed by brazilin at 100 μM (Figure 3(b)). To determine the efficiency of brazilin in inhibiting glucose-induced ROS formation in HUVECs, a cell-permeative ROS-sensitive dye, DCFDA (nonfluorescent in a reduced state but fluorescent upon oxidation by ROS), was used. In this study, glucose (5.5–75 mM) induced ROS formation concentration-dependently as compared to resting (untreated) cells, whereas treatment with brazilin (100 μM) markedly inhibited this formation with the same concentration dependent manner (Figure 3(c)).

3.3. Effect of Brazilin on HG-Stimulated Phosphorylations of eNOS and ERK in HUVECs. To determine whether brazilin affects the activation of p-eNOS and pERK, we analyzed the phosphorylation levels of these proteins. First, HUVECs were pretreated with 50 and 100 μM brazilin for 30 min and then stimulated with 50 mM glucose for 1 h. As shown in Figures 4(a) and 4(b), pretreatment of brazilin concentration-dependently inhibits the HG-induced phosphorylations of p-eNOS and pERK in HUVEC cells.

3.4. Effect of Brazilin on HG-Induced NF-κB Activation. ROS has been shown to activate various transcription factors including NF-κB in cultured endothelial cells [20]. In this study, it is proposed that the increased ROS production in HG-induced HUVEC cells may partially cause the activation of NF-κB. Therefore, we measured whether high glucose induced NF-κB activation in HUVECs. Western blotting analysis for NF-κB revealed that there was an increased expression of NF-κB protein in HUVEC treated with high glucose (75 mM). In addition, pretreatment with brazilin (25 and 50 μM) markedly inhibited the high glucose-induced increase of NF-κB expression levels. However, 75 μM of brazilin pretreatment did not affect the NF-κB expression of HG-induced HUVEC (Figure 5(a)).

3.5. Effect of Brazilin on HG-Induced Endothelial Adhesion Molecules. To investigate whether glucose induces expression of VCAM-1 and ICAM-1 in HUVECs, we cultured HUVECs at normal glucose (5.5 mM) and high-glucose (50 mM) concentrations for 24 h. Immunoblot analysis showed that stimulation of HUVECs with high concentrations of glucose increased the production of VCAM-1 and ICAM-1 (Figure 5(b)). To further determine whether brazilin can inhibit the expression of endothelial adhesion molecules, we pretreated HUVECs with brazilin at the indicated concentrations (50 and 100 μM) and stimulated the cells with 50 mM glucose for 24 h. As shown in Figure 5(b), pretreatment of brazilin in HUVEC significantly inhibited the HG-induced effect on the ICAM-1 and VCAM-1 levels in a concentration manner.

4. Discussion

The present study was undertaken to shed more light on the mechanisms by which brazilin exerts its inhibitory effects on high glucose-induced human umbilical vein endothelial cells. For the first time, we have demonstrated that brazilin inhibited the high glucose-induced vascular inflammation via inhibition of ROS, eNOS, ERK, CAMs, and NF-κB in primary cultured HUVEC. These results indicate that brazilin might be used as a potential candidate for the prevention of hyperglycemia-associated vascular inflammatory processes of endothelial cells. Notably, brazilin showed no cytotoxicity at used concentrations of 0–100 μM in HUVECs for 24 and 48 h stimulations. In line with previous studies [21, 22],

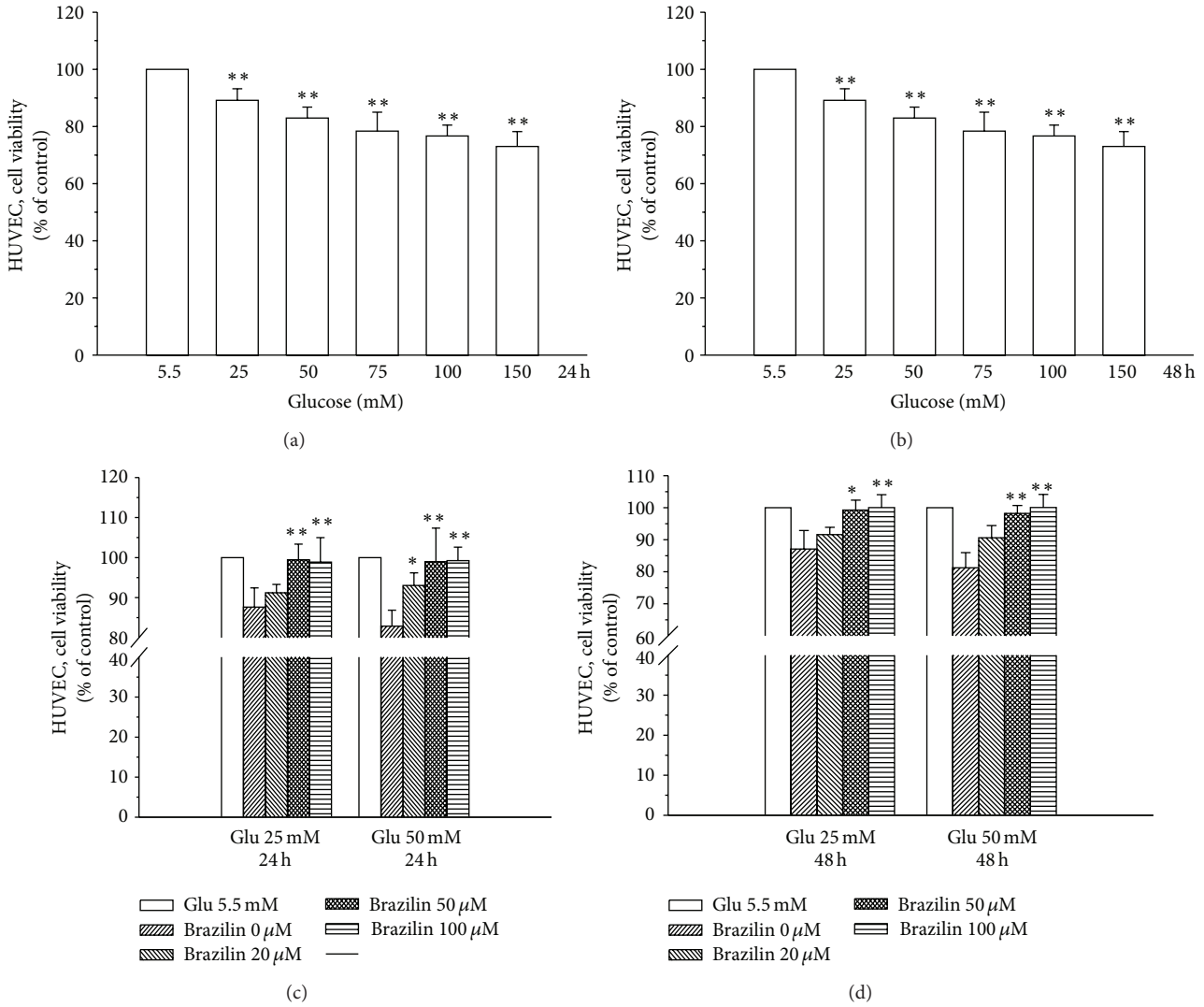

Figure 2: Effects of brazilin on glucose-induced cell viability of human umbilical vein endothelial cells (HUVEC): ((a) and (b)) the viability of HUVECs during treatment with various concentrations (25–150 mM) of glucose for 24 h and 48 h, respectively; ((c) and (d)) the viability of HUVECs during treatment with various concentrations (20–100 μM) of brazilin upon glucose (25 and 50 mM) stimulation for 24 and 48 h, respectively. Data are shown as the mean ± SEM of three independent experiments. $^{*}P < 0.05$ and $^{***}P < 0.001$, compared to the glucose treated group.

the results revealed that incubation of the HUVEC with high glucose (25–150 mM) for 24 and 48 h determined a consistent reduction of cell viability. These results confirmed the detrimental role of hyperglycemia in the HUVEC functionality. However, at the same time, the coincubation with brazilin significantly improved HUVEC viability.

Lipid peroxidation, a process induced by free radicals, leads to oxidative deterioration of polyunsaturated lipids. Under normal physiological conditions, only low levels of lipid peroxides occur in body tissues. The excessive generation of free radicals leads to peroxidative changes that ultimately result in enhanced lipid peroxidation [23]. The endproduct of stable aldehydes reacts with thiobarbituric acid (TBA) to form a thiobarbituric acid-malondialdehyde adduct [24]. In previous studies, it was found that the LPO level was increased in HUVECs when the cells were incubated with glycated protein and iron [25]. In the present study, HG treatment significantly increased lipid peroxidation in HUVECs concentration-dependent manner. Pretreatment of brazilin protected against HG-induced LPO probably because of its ability to inhibit ROS production.

This study further investigated whether brazilin affects oxidative stress via inhibiting ROS and NO production induced by glucose, as several lines of evidence indicated that high glucose induced ROS and NO production. The results revealed that brazilin significantly decreased the glucose-induced ROS and NO production (Figures 3(b) and 3(c)). Previous results of a study suggest that brazilin induces vasorelaxation by the increasing intracellular Ca^{2+} concentration in endothelial cells of blood vessels by activating

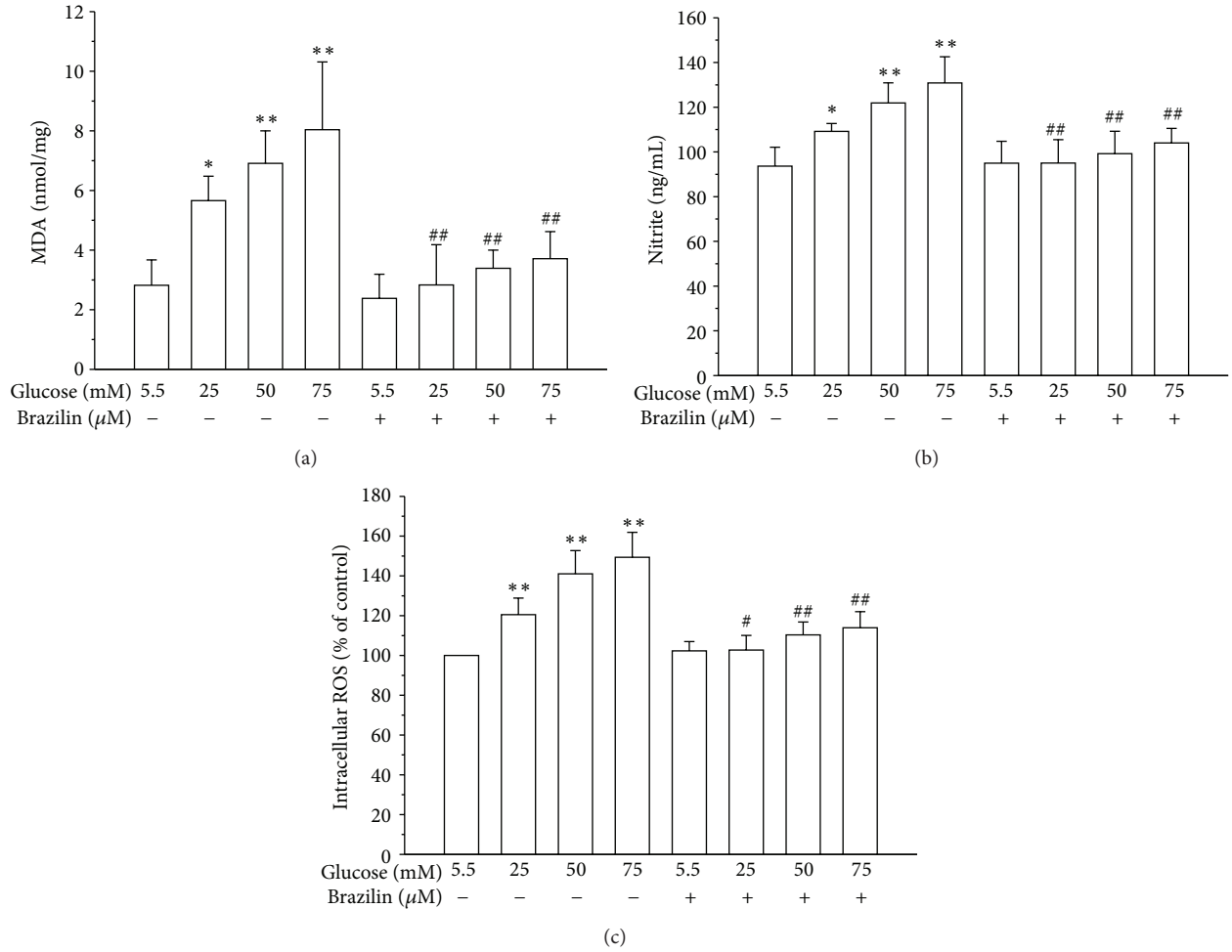

Figure 3: Effects of brazilin on glucose-induced LPO, NO, and ROS production in HUVECs: (a) lipid peroxidation was assayed by measuring the amount of TBARS formation (malondialdehyde, MDA); (b) the nitrite concentration in the culture medium was determined by Griess reagent. (c) ROS production was determined as described in Materials and Methods. Data are shown as the mean ± SEM of three independent experiments. $^{*}P < 0.05$ and $^{**}P < 0.01$, compared to the glucose treated group; $^{\#}P < 0.05$ and $^{\#\#}P < 0.01$, compared to the brazilin treated group.

Ca^{2+}-dependent NO synthesis [26]. NO production induced by glucose is reported to be associated with an increase in the expression of eNOS in HUVEC [27], indicating that eNOS is responsible for NO production. There are still arguments about the effect of high glucose on NO production in endothelial cells; a study showed that 30 mM of glucose induced the increase of NO and eNOS at 48 h in HUVEC [28]; however, another study showed that high glucose decreased NO concentration at 7 days in HUVEC cells [29]. In the present study, the results show that pretreatment with brazilin at concentration of 100 μM decreases NO in 25 mM glucose-induced HUVEC, whereas brazilin was not effective in 50 and 75 mM glucose-induced NO. These results may indicate that HUVEC is treated with brazilin as a protective mechanism, and at high glucose (hyperglycemia), it was not cope to reduce NO concentration may due to an enhancement of endothelial inflammation. Endothelial nitric oxide synthase (eNOS) is an important enzyme for the maintenance of cardiovascular function by producing NO. Nevertheless, eNOS can be detached, leading to generation of super-oxide instead of NO under certain pathological circumstances and oxidative stress conditions [30]. In this study, it shows that pretreatment of brazilin predominantly inhibited the phosphorylation of HG-induced endothelial nitric oxide synthase in HUVEC cells.

The production of ROS has been mechanistically associated with inflammatory responses [31, 32]. ROS production and inflammation are potential mediators of diabetes mellitus-associated vascular diseases. Recent study indicates that hyperglycemia activates the generation of free radicals and oxidative stress in various cell types [33]. ROS are considered to be important mediators of several biologic responses, including cell proliferation and extracellular matrix deposition. The formation of oxygen-derived radicals might lead to an activation of NF-κB and ROS-mediated NF-κB activation plays an important role in the pathogenesis of atherosclerosis. Role of ROS and NF-κB in the induction of apoptosis by high glucose has been demonstrated in primary

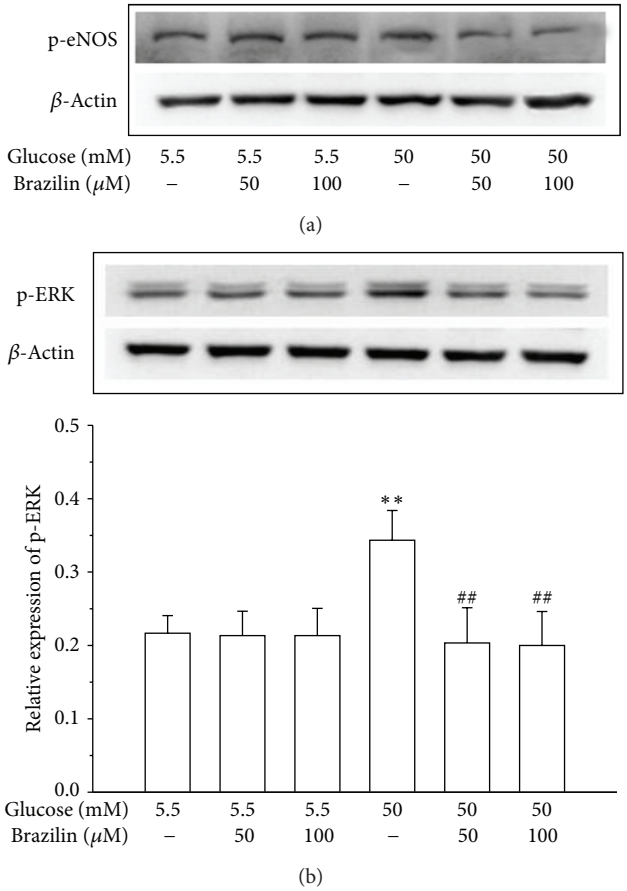

FIGURE 4: Effects of brazilin on glucose-induced expression of p-eNOS and pERK in HUVECs: HUVECs (2×10^5 cells/well) were pretreated with a solvent control (0.1% DMSO) or brazilin (50 and 100 μM) for 2 h and then treated with glucose (50 mM) for 30 min to detect the phosphorylation of (a) p-eNOS and (b) p-ERK1/2. The β-actin was used as an internal control.

cultured human endothelial cells [34]. In our results, high glucose-induced increment of the production of cellular ROS may suggest that high glucose-induced oxidative stress in HUVEC is important in determining the character of diabetic complication as well as vascular inflammation. In addition, pretreatment with brazilin significantly inhibited the high glucose-induced ROS formation, suggesting a role of protecting vascular inflammation via antioxidant activity.

An interesting finding of this study is that NF-κB might be a target of brazilin against HG-induced cell damage. NF-κB is an ubiquitous transcription factor that manages the expression of genes encoding cell adhesion molecules and some acute phase proteins in health and in various disease states [35]. Thus, advancement of modulatory approaches targeting this transcription factor may provide a novel therapeutic tool for the treatment of various diseases [36]. This transcription factor generally consists of two proteins, a p65 (RelA) subunit and a p50 subunit. In normal condition, NF-κB is bound to its inhibitor protein I-κB, which restricts NF-κB to the cytoplasm, whereas stimulation by cytokines or endotoxin results in the phosphorylation of inhibitor κB, the unbinding

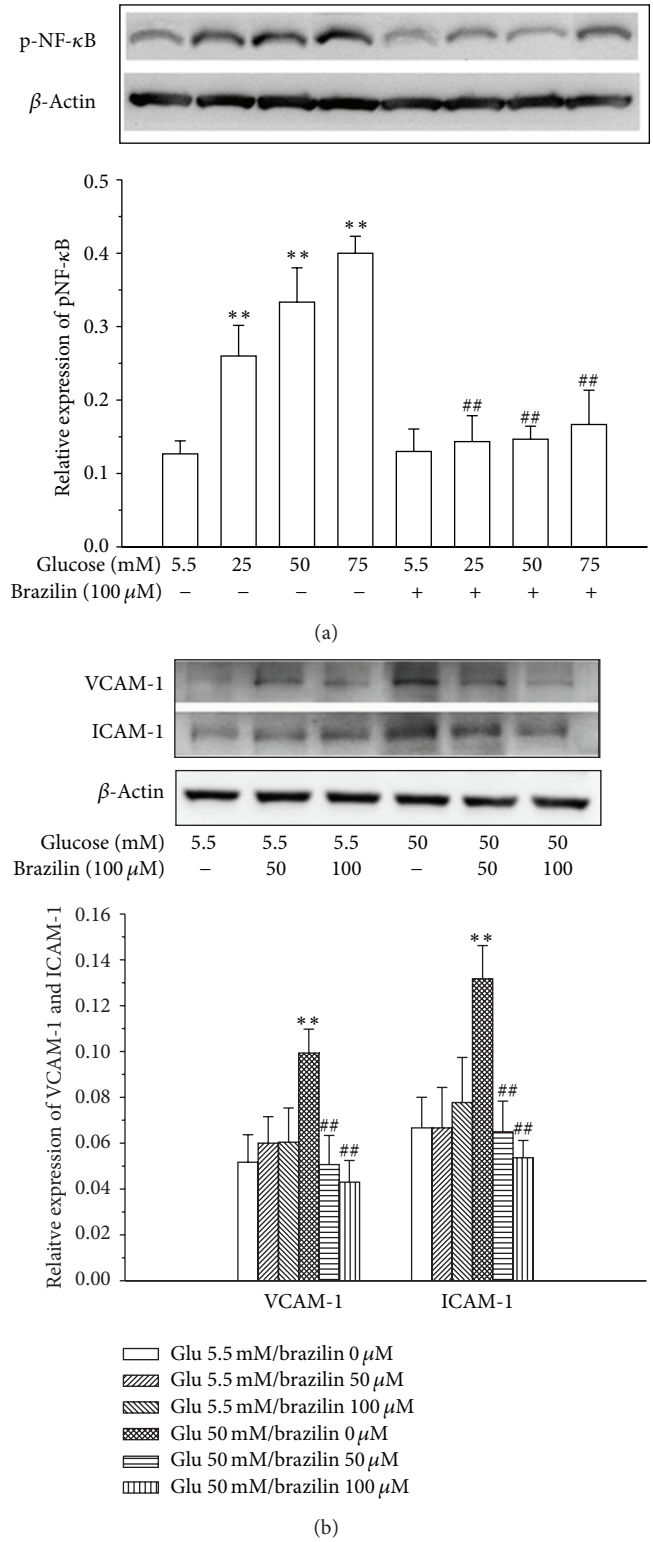

FIGURE 5: Effects of brazilin on glucose-induced expression of NF-κB and CAMs expression in HUVECs: HUVECs (2×10^5 cells/well) were pretreated with a solvent control (0.1% DMSO) or brazilin (50 and 100 μM) for 2 h and then treated with glucose (50 mM) for 30 min to detect the expression of (a) NF-κB and (b) VCAM-1 and ICAM-1. The β-actin was used as an internal control.

of NF-κB from inhibitor κB, and the activation of NF-κB, with its subsequent translocation into the nucleus [37]. This in turn induces the transcription of cell adhesion molecules, chemokines and macrophage migration inhibitory factor, matrix metalloproteinase-1 and 9, and many other genes that regulate transcription, apoptosis, and cell proliferation. Recent reports demonstrated that natural extracts inhibits cell adhesion molecules and monocytes adhesion to endothelial cells via the suppression of NF-κB activation under pathophysiological conditions, including high glucose or cytokines [38]. In the present study, we found that high glucose-induced NF-κB in HUVEC and pretreatment by brazilin blocked the high glucose-induced NF-κB expression in concentration-dependent manner. This result is supported by the previous study that medicinal plant extract such as rhubarb suppressed NF-κB p65 expression in vascular endothelial inflammation process [39]. The finding of this study demonstrated that high glucose-induced NF-κB activation inhibited by brazilin may indicate that brazilin has some inhibitory effect on the NF-κB pathways specific to the high glucose-induced adhesion molecules in HUVEC.

In human umbilical vein endothelial cells, high glucose could make a cellular damage leading to cell apoptosis probably via ERK activation. To make this hypothesis solid, we analysed ERK phosphorylation because the activation of ERK may participate in the defense signaling against oxidative damage in cells [40]. ERK is the signal cascade involved in the protection of oxidative damage and its activation is generally thought to mediate cell survival [41]. In this study, data from Western blot analysis indicate increases in expression of phosphorylated ERK (pERK) in high glucose-treated HUVEC cells, which were blocked by brazilin. Changes in expression of activated ERK closely reflect the cell damage; such results suggesting that high glucose-induced HUVEC cell damage is protected, at least partly, by inhibiting ERK activation.

This study also noticed that high glucose (50 mM) alone increased ICAM-1 and VCAM-1 expression when compared with nontreated control (5.5 mM) and pretreatment with brazilin (Figure 5(b)). These cell adhesion molecules primarily mediated the adhesion of monocytes specifically found in atherosclerosis lesions to the vascular endothelium. Some study showed that high glucose increased only ICAM-1 expression, but not other adhesion molecules [42], whereas other study showed high glucose-induced increased only VCAM-1 expression [43]. These results suggested that high glucose exhibited various effects on CAMs expression. Recently, various phytochemicals have been shown to inhibit the expression of adhesion molecules in endothelial cells. For instance, resveratrol reduced interleukin-6 (IL-6)-induced ICAM-1 expression by interfering with the Rac-mediated pathway through a decrease in the phosphorylation of signal transducer and activator of transcription 3 (STAT3) [44]. Epigallocatechin-3-O-gallate (EGCG) inhibits angiotensin II-induced adhesion molecule expression by inhibiting p38 MAPK and ERK1/2 phosphorylation [27]. Anthocyanins inhibited TNF-α-induced ICAM-1 and VCAM-1 expressions via the NF-κB-dependent pathway [45]. Phloretin inhibited the TNF-α-stimulated expression of adhesion molecules without activating NF-κB [46]. Grape-seed proanthocyanidin extract inhibited VCAM-1 expression in HUVECs via the NF-κB-independent pathway [47]. Quercetin downregulated ICAM-1 expression in human endothelial cell lines through inhibition of the activator protein-1 (AP-1) and c-Jun NH_2-terminal kinase (JNK) pathway [48]. Interestingly, we observed that pretreatment with brazilin suppressed HG-induced expression of ICAM-1 and VCAM-1 perhaps via inhibition of the ERK1/2 phosphorylation and NF-κB-dependent pathway. Thus, development of therapeutic drugs for diabetic vascular inflammation targeting CAMs expression may prove useful in the prevention of vascular inflammation.

In conclusion, the most important findings of this study demonstrate for the first time that brazilin was able to eliminate several inflammatory events induced by high concentrations of glucose in HUVEC. In this study, we observed that brazilin reduced CAMs expression in high glucose-induced HUVEC through NF-κB as well as ROS-dependent mechanisms. Therefore, this study suggested that brazilin could be very useful in the treatment of vascular inflammatory process and/or hyperglycemia via inhibition of oxidative stress and NF-κB activation in primary cultured HUVEC.

Conflict of Interests

The authors declare that there is no conflict of interests regarding the publication of this paper.

Authors' Contribution

Dr. Thanasekaran Jayakumar and Dr. Chao-Chien Chang contributed equally to this work.

Acknowledgments

This work was supported by the research grants from the Cathay General Hospital-Taipei Medical University (102CGH-TMU-01-2; CGH-MR-10216) and Taipei Hospital, Ministry of Health and Welfare (10104).

References

[1] R. de Caterina, "Endothelial dysfunctions: common denominators in vascular disease," *Current Opinion in Lipidology*, vol. 11, no. 1, pp. 9–23, 2000.

[2] R. J. Esper, R. A. Nordaby, J. O. Vilariño, A. Paragano, J. L. Cacharrón, and R. A. Machado, "Endothelial dysfunction: a comprehensive appraisal," *Cardiovascular Diabetology*, vol. 5, article 4, 2006.

[3] G. M. Reaven, "Pathophysiology of insulin resistance in human disease," *Physiological Reviews*, vol. 75, no. 3, pp. 473–486, 1995.

[4] I. A. M. van den Oever, H. G. Raterman, M. T. Nurmohamed, and S. Simsek, "Endothelial dysfunction, inflammation, and apoptosis in diabetes mellitus," *Mediators of Inflammation*, vol. 2010, Article ID 792393, 15 pages, 2010.

[5] S. Srinivasan, M. E. Hatley, D. T. Bolick et al., "Hyperglycaemia-induced superoxide production decreases eNOS expression via AP-1 activation in aortic endothelial cells," *Diabetologia*, vol. 47, no. 10, pp. 1727–1734, 2004.

[6] N. R. Madamanchi, A. Vendrov, and M. S. Runge, "Oxidative stress and vascular disease," *Arteriosclerosis, Thrombosis, and Vascular Biology*, vol. 25, no. 1, pp. 29–38, 2005.

[7] M. Brownlee, "Biochemistry and molecular cell biology of diabetic complications," *Nature*, vol. 414, no. 6865, pp. 813–820, 2001.

[8] B. L. Thurberg and T. Collins, "The nuclear factor-κB/inhibitor of kappa B autoregulatory system and atherosclerosis," *Current Opinion in Lipidology*, vol. 9, no. 5, pp. 387–396, 1998.

[9] D. Ham and S. C. Skoryna, "Cellular defense against oxidized low density lipoproteins and fibrillar amyloid beta in murine cells of monocyte origin with possible susceptibility to the oxidative stress induction," *Experimental Gerontology*, vol. 39, no. 2, pp. 225–231, 2004.

[10] J. Y. Ueda, Y. Tezka, A. H. Banskota et al., "Anti-proliferative activity of Vietnamese medicinal plants," *Biolological and Pharmaceutical Bulletin*, vol. 25, no. 6, pp. 753–760, 2002.

[11] S. Badami, S. Moorkoth, S. R. Rai, E. Kannan, and S. Bhojraj, "Antioxidant activity of *Caesalpinia sappan* heartwood," *Biological and Pharmaceutical Bulletin*, vol. 26, no. 11, pp. 1534–1537, 2003.

[12] H. Hikino, T. Taguchi, H. Fujimura, and Y. Hiramatsu, "Anti-inflammatory principles of *Caesalpinia sappan* wood and of Haematoxylon campechianum wood," *Planta Medica*, vol. 31, no. 3, pp. 214–220, 1977.

[13] C. Pan, X. Zeng, Y. Guan, X. Jiang, L. Li, and H. Zhang, "Design and synthesis of brazilin-like compounds," *Synlett*, no. 3, pp. 425–429, 2011.

[14] Y.-W. Xie, D.-S. Ming, H.-X. Xu, H. Dong, and P. P.-H. But, "Vasorelaxing effects of *Caesalpinia sappan* involvement of endogenous nitric oxide," *Life Sciences*, vol. 67, no. 15, pp. 1913–1918, 2000.

[15] P. Rosenkranz-Weiss, W. C. Sessa, S. Milstien, S. Kaufman, C. A. Watson, and J. S. Pober, "Regulation of nitric oxide synthesis by proinflammatory cytokines in human umbilical vein endothelial cells. Elevations in tetrahydrobiopterin levels enhance endothelial nitric oxide synthase specific activity," *The Journal of Clinical Investigation*, vol. 93, no. 5, pp. 2236–2243, 1994.

[16] N. Janel, A.-M. Dosne, B. Obert, D. Meyer, and D. Kerbiriou-Nabias, "Functional characterization of bovine von Willebrand factor gene promoter in bovine endothelial cells demonstrates species-specific properties," *Gene*, vol. 198, no. 2, pp. 127–134, 1997.

[17] C.-S. Choy, C.-M. Hu, W.-T. Chiu et al., "Suppression of lipopolysaccharide-induced of inducible nitric oxide synthase and cyclooxygenase-2 by Sanguis Draconis, a dragon's blood resin, in RAW 264.7 cells," *Journal of Ethnopharmacology*, vol. 115, no. 3, pp. 455–462, 2008.

[18] J. F. Ewing and D. R. Janero, "Specific S-nitrosothiol (thionitrite) quantification as solution nitrite after vanadium(III) reduction and ozone-chemiluminescent detection," *Free Radical Biology and Medicine*, vol. 25, no. 4-5, pp. 621–628, 1998.

[19] G. Hsiao, K. H. Lin, Y. Chang et al., "Protective mechanisms of inosine in platelet activation and cerebral ischemic damage," *Arteriosclerosis, Thrombosis, and Vascular Biology*, vol. 25, no. 9, pp. 1998–2004, 2005.

[20] S. Uemura, H. Matsushita, W. Li et al., "Diabetes mellitus enhances vascular matrix metalloproteinase activity: role of oxidative stress," *Circulation Research*, vol. 88, no. 12, pp. 1291–1298, 2001.

[21] S. Kuki, T. Imanishi, K. Kobayashi, Y. Matsuo, M. Obana, and T. Akasaka, "Hyperglycemia accelerated endothelial progenitor cell senescence via the activation of p38 mitogen-activated protein kinase," *Circulation Journal*, vol. 70, no. 8, pp. 1076–1081, 2006.

[22] Q. Yuan, J. Peng, S.-Y. Liu et al., "Inhibitory effect of resveratrol derivative BTM-0512 on high glucose-induced cell senescence involves dimethylaminohydrolase/asymmetric dimethylarginine pathway," *Clinical and Experimental Pharmacology and Physiology*, vol. 37, no. 5-6, pp. 630–635, 2010.

[23] L. E. Rikans and K. R. Hornbrook, "Lipid peroxidation, antioxidant protection and aging," *Biochimica et Biophysica Acta*, vol. 1362, no. 2-3, pp. 116–127, 1997.

[24] M. P. Barros, E. Pinto, P. Colepicolo, and M. Pedersén, "Astaxanthin and peridinin inhibit oxidative damage in Fe^{2+}-loaded liposomes: scavenging oxyradicals or changing membrane permeability?" *Biochemical and Biophysical Research Communications*, vol. 288, no. 1, pp. 225–232, 2001.

[25] G. C. Jagetia, T. K. Reddy, V. A. Venkatesha, and R. Kedlaya, "Influence of naringin on ferric iron induced oxidative damage in vitro," *Clinica Chimica Acta*, vol. 347, no. 1-2, pp. 189–197, 2004.

[26] C. M. Hu, J. J. Kang, C. C. Lee, C. H. Li, J. W. Liao, and Y. W. Cheng, "Induction of vasorelaxation through activation of nitric oxide synthase in endothelial cells by brazilin," *European Journal of Pharmacology*, vol. 468, no. 1, pp. 37–45, 2003.

[27] E. Huerta-García, J. L. Ventura-Gallegos, M. E. C. Victoriano, A. Montiél-Dávalos, G. Tinoco-Jaramillo, and R. López-Marure, "Dehydroepiandrosterone inhibits the activation and dysfunction of endothelial cells induced by high glucose concentration," *Steroids*, vol. 77, no. 3, pp. 233–240, 2012.

[28] N. Alvarado-Vásquez, E. Zapata, S. Alcázer-Leyva, F. Massó, and L. F. Montaño, "Reduced NO synthesis and eNOS mRNA expression in endothelial cells from newborns with a strong family history of type 2 diabetes," *Diabetes/Metabolism Research and Reviews*, vol. 23, no. 7, pp. 559–566, 2007.

[29] J. Liao, M. Lei, X. Chen, and F. Liu, "Effect of intermittent high glucose on synthesis of nitric oxide in human umbilical vein endothelial cells and its mechanism," *Zhong Nan Da Xue Xue Bao Yi Xue Ban*, vol. 35, no. 4, pp. 295–300, 2010.

[30] U. Förstermann, "Nitric oxide and oxidative stress in vascular disease," *Pflügers Archiv*, vol. 459, no. 6, pp. 923–939, 2010.

[31] T. Inoguchi, P. Li, F. Umeda et al., "High glucose level and free fatty acid stimulate reactive oxygen species production through protein kinase C-dependent activation of NAD(P)H oxidase in cultured vascular cells," *Diabetes*, vol. 49, no. 11, pp. 1939–1945, 2000.

[32] D. Jay, H. Hitomi, and K. K. Griendling, "Oxidative stress and diabetic cardiovascular complications," *Free Radical Biology and Medicine*, vol. 40, no. 2, pp. 183–192, 2006.

[33] M. L. Sheu, F. M. Ho, R. S. Yang et al., "High glucose induces human endothelial cell apoptosis through a phosphoinositide 3-kinase-regulated cyclooxygenase-2 pathway," *Arteriosclerosis, Thrombosis, and Vascular Biology*, vol. 25, no. 3, pp. 539–545, 2005.

[34] F. Chen, V. Castranova, X. Shi, and L. M. Demers, "New insights into the role of nuclear factor-κB, a ubiquitous transcription factor in the initiation of diseases," *Clinical Chemistry*, vol. 45, no. 1, pp. 7–17, 1999.

[35] S. Luqman and J. M. Pezzuto, "NFκB: a promising target for natural products in cancer chemoprevention," *Phytotherapy Research*, vol. 24, no. 7, pp. 949–963, 2010.

[36] P. Dandona, A. Chaudhuri, H. Ghanim, and P. Mohanty, "Proinflammatory effects of glucose and anti-inflammatory effect of insulin: relevance to cardiovascular disease," *The American Journal of Cardiology*, vol. 99, no. 4, pp. 15–26, 2007.

[37] E. Harokopakis, M. H. Albzreh, E. M. Haase, F. A. Scannapieco, and G. Hajishengallis, "Inhibition of proinflammatory activities of major periodontal pathogens by aqueous extracts from elder flower (*Sambucus nigra*)," *Journal of Periodontology*, vol. 77, no. 2, pp. 271–279, 2006.

[38] M. K. Moon, D. G. Kang, J. K. Lee, J. S. Kim, and H. S. Lee, "Vasodilatory and anti-inflammatory effects of the aqueous extract of rhubarb via a NO-cGMP pathway," *Life Sciences*, vol. 78, no. 14, pp. 1550–1557, 2006.

[39] H. Taki, A. Kashiwagi, Y. Tanaka, and K. Horiikc, "Expression of intercellular adhesion molecules 1 (ICAM-1) via an osmotic effect in human umbilical vein endothelial cells exposed to high glucose medium," *Life Sciences*, vol. 58, no. 20, pp. 1713–1721, 1996.

[40] A.-L. Glotin, A. Calipel, J.-Y. Brossas, A.-M. Faussat, J. Tréton, and F. Mascarelli, "Sustained versus transient ERK1/2 signaling underlies the anti- and proapoptotic effects of oxidative stress in human RPE cells," *Investigative Ophthalmology and Visual Science*, vol. 47, no. 10, pp. 4614–4623, 2006.

[41] X. Guillonneau, F. Régnier-Ricard, C. Dupuis, Y. Courtois, and F. Mascarelli, "Paracrine effects of phosphorylated and excreted FGF1 by retinal pigmented epithelial cells," *Growth Factors*, vol. 15, no. 2, pp. 95–112, 1998.

[42] F. Haubner, K. Lehle, D. Münzel, C. Schmid, D. E. Birnbaum, and J. G. Preuner, "Hyperglycemia increases the levels of vascular cellular adhesion molecule-1 and monocyte-chemoattractant-protein-1 in the diabetic endothelial cell," *Biochemical and Biophysical Research Communications*, vol. 360, no. 3, pp. 560–565, 2007.

[43] H. Schroeter, J. P. E. Spencer, C. Rice-Evans, and R. J. Williams, "Flavonoids protect neurons from oxidized low-density-lipoprotein-induced apoptosis involving c-Jun N-terminal kinase (JNK), c-Jun and caspase-3," *Biochemical Journal*, vol. 358, no. 3, pp. 547–557, 2001.

[44] Y. J. Chae, C. H. Kim, T. S. Ha, J. Hescheler, H. Y. Ahn, and A. Sachinidis, "Epigallocatechin-3-O-gallate inhibits the angiotensin II-induced adhesion molecule expression in human umbilical vein endothelial cell via inhibition of MAPK pathways," *Cellular Physiology and Biochemistry*, vol. 20, no. 6, pp. 859–866, 2007.

[45] H. J. Kim, I. Tsoy, J. M. Park, J. I. Chung, S. C. Shin, and K. C. Chang, "Anthocyanins from soybean seed coat inhibit the expression of TNF-α-induced genes associated with ischemia/reperfusion in endothelial cell by NF-κB-dependent pathway and reduce rat myocardial damages incurred by ischemia and reperfusion in vivo," *FEBS Letters*, vol. 580, no. 5, pp. 1391–1397, 2006.

[46] V. Stangl, M. Lorenz, A. Ludwig et al., "The flavonoid phloretin suppresses stimulated expression of endothelial adhesion molecules and reduces activation of human platelets," *The Journal of Nutrition*, vol. 135, no. 2, pp. 172–178, 2005.

[47] C. K. Sen and D. Bagchi, "Regulation of inducible adhesion molecule expression in human endothelial cells by grape seed proanthocyanidin extract," *Molecular and Cellular Biochemistry*, vol. 216, no. 1-2, pp. 1–7, 2001.

[48] H. Kobuchi, S. Roy, C. K. Sen, H. G. Nguyen, and L. Packer, "Quercetin inhibits inducible ICAM-1 expression in human endothelial cells through the JNK pathway," *The American Journal of Physiology—Cell Physiology*, vol. 277, no. 3, pp. C403–C411, 1999.

Hindawi Publishing Corporation
BioMed Research International
Volume 2014, Article ID 231012, 9 pages
http://dx.doi.org/10.1155/2014/231012

Research Article

Histone Deacetylase Inhibitor Impairs Plasminogen Activator Inhibitor-1 Expression via Inhibiting TNF-α-Activated MAPK/AP-1 Signaling Cascade

Wei-Lin Chen,[1] Joen-Rong Sheu,[1] Che-Jen Hsiao,[2] Shih-Hsin Hsiao,[3] Chi-Li Chung,[2,3] and George Hsiao[1]

[1] *Graduate Institute of Medical Sciences and Department of Pharmacology, College of Medicine, Taipei Medical University, 250 Wu-Hsing Street, Taipei 110-31, Taiwan*
[2] *School of Respiratory Therapy, College of Medicine, Taipei Medical University, Taipei 110-31, Taiwan*
[3] *Division of Pulmonary Medicine, Department of Internal Medicine, Taipei Medical University Hospital, Taipei 110-31, Taiwan*

Correspondence should be addressed to George Hsiao; geohsiao@tmu.edu.tw

Received 13 November 2013; Accepted 6 January 2014; Published 23 February 2014

Academic Editor: Philip Aloysius Thomas

Tumor necrosis factor-(TNF-)-α upregulates plasminogen activator inhibitor-(PAI-) 1 expression in pleural mesothelial cells (PMCs), contributing to fibrin deposition and pleural fibrosis. Histone deacetylases (HDACs) have been found implicated in fibrogenesis. However, the roles of TNF-α or HDAC in the regulation of PAI-1 expression have not been well investigated. We aimed to examine the effects and mechanisms of HDAC inhibition on TNF-α-induced PAI-1 expression in human PMCs. MeT-5A human PMCs were treated with TNF-α in the presence or absence of the *m*-carboxycinnamic acid bishydroxamide (CBHA), an HDAC class II inhibitor, and the HDAC activity, PAI-1 protein expression, mRNA, and activated signalings were analyzed. CBHA abrogated TNF-α-induced HDAC activity, PAI-1 protein and, mRNA expression in MeT-5A cells. Moreover, CBHA significantly enhanced mitogen-activated protein kinase phosphatase-(MKP-) 5/MKP-1 expression and inhibited p38/JNK activations, ATF2/c-Jun translocation, and PAI-1 promoter activity. Altogether, our data suggest that HDAC inhibition may abrogate TNF-α-activated MAPK/AP-1 signaling and PAI-1 expression in human PMCs. Given the antifibrotic effect through PAI-1 abrogation, CBHA may be utilized as a novel agent in the treatment of fibrotic diseases.

1. Introduction

Pleural fibrosis is a common sequel in a variety of inflammatory pleural effusions, such as empyema and tuberculous pleurisy [1]. In general, fibrin turnover in the pleural space is greatly affected by equilibrium between plasminogen activators (PAs) and plasminogen activator inhibitors (PAIs) [2]. The elevation of PAI-1 level in the pleural fluid decreases the fibrinolytic activity in the pleural space and leads to fibrin deposition and subsequent pleural fibrosis [3]. Tumor necrosis factor (TNF)-α, a potent inflammatory mediator involved in the pathogenesis of infectious pleural effusion [4], has been proved to stimulate the production of PAI-1 in human pleural mesothelial cells (PMCs) [5]. Previous studies demonstrated a positive correlation between the values of TNF-α and PAI-1 in tuberculous pleural effusion, and both proteins are significantly higher in the pleural fluids of those with residual pleural fibrosis [6, 7]. These findings suggest that TNF-α and PAI-1 are implicated in fibrogenesis of the pleural space. However, the underlying mechanism of TNF-α-induced PAI-1 expression in the pleural space is not clearly understood.

Histone acetyltransferase (HAT) and histone deacetylase (HDAC) regulate the acetylation of both histone and non-histone proteins and play critical roles in the modulation of gene expression in multiple cellular processes from signaling, transcription, and mRNA stability to protein degradation [8, 9]. Altered activities of HAT and HDAC in a given cell

may cause aberrant gene expression and lead to various pathological processes, such as cancer [10], inflammation [11], and fibrosis [12]. Recently, HDAC inhibitors have been found to correct aberrant protein acetylation and gene expression and are considered as promising therapeutic agents for malignancy [13] and cardiac fibrosis [14].

Moreover, our recent study demonstrated that m-carboxycinnamic acid bishydroxamide (CBHA), a hybrid-polar HDAC inhibitor, attenuates transforming growth factor (TGF)-β1-induced PAI-1 expression in human PMCs [15]. In addition, another HDAC inhibitor Trichostatin A (TSA) has been proved to block TGF-β1-induced fibroblast-myofibroblast differentiation through inhibition of phosphorylation of Akt and subsequent expression of α-SMA [16]. However, to our knowledge, the role of the proinflammatory cytokine, such as TNF-α, or HDAC in the regulation of PAI-1 expression in PMCs and the effect of HDAC inhibition on pleural fibrogenesis have not been well investigated. Therefore, in the present study, we used CBHA, a class II HDAC inhibitor, to explore the effects of HDAC inhibition on TNF-α-induced PAI-1 expression in human PMCs.

2. Materials and Methods

2.1. Reagents. Recombinant human TNF-α was purchased from Pepro Tech EC (London, UK). The PAI-1 reporter plasmid (p800Luc) that contains 800 bp of the proximal promoter sequences of human PAI-1 gene was a generous gift of Professor Daniel Rifkin (New York University) [15]. Except for PAI-1 (BD Biosciences, San Jose, CA), other antibodies were purchased from Cell Signaling Technology (Beverly, MA). Doxycycline and all of the other chemical reagents were purchased from Sigma-Aldrich (St. Louis, MO). CBHA, SB203580, SP600125, PD98059, LY294002, and parthenolide were obtained from Calbiochem (San Diego, CA).

2.2. Cell Line and Primary Culture of Human Pleural Mesothelial Cells. The Met-5A human pleural mesothelial cell line was obtained from American Type Culture Collection (ATCC, Manassas, VA). Cells culture was performed as described in our previous report [17]. Primary cultured human PMCs were harvested from the pleural fluids of patients with congestive heart failure. Ethics approval was obtained from the Institutional Review Board (IRB number: CRC-05-11-01) of Taipei Medical University, and the written informed consent was acquired. The human pleural fluids were centrifuged and cells were grown in medium 199 containing 10% FBS at 37°C in the humidified incubator of 5% CO_2. Mesothelial cells were used at passages three to six and were characterized by the cobblestone morphology, the presence of cytokeratin, and the absence of factor VIII [18].

2.3. Total Cellular HDAC Enzyme Activity Assay. Total HDAC enzyme activity was determined by using the HDAC fluorometric cellular activity assay (Enzo Life Sciences) according to the manufacturer's protocol. MeT-5A cells were treated with TNF-α for the indicated times or pretreated with CBHA for 15 min before stimulation with TNF-α for 2 h. The fluorescence intensity was measured on a fluorometric reader using excitation/emission wavelength of 360/460 nm. The results of cellular HDAC activity were presented as relative multiples as compared to the control.

2.4. Differential Protein Fractionation and Western Blot Analysis. The cellular lysates were performed as previously mentioned [17], and nuclear extracts were prepared using the NE-PER kit (Pierce, Rockford, IL). The proteins were separated in denaturing sodium dodecyl sulfate (SDS) polyacrylamide gels and electrophoretically transferred onto nitrocellulose membranes. Blotting membranes were incubated with specific primary and HRP-conjugated secondary antibodies. The quantitative densitometric analysis was performed as previously described [17].

2.5. Reverse Transcription-Polymerase Chain Reaction (RT-PCR). Total RNA was isolated from Met-5A cells using the TRIzol reagent (GIBCO) and RNA (1 μg) was used for cDNA synthesis (Super Script On-Step RT-PCR system, GIBCOTM). The cDNAs were amplified using the specific primers and the quantitative analyses were performed as previously described [17].

2.6. Transfection and Luciferase Activity Assay. MeT-5A cells were transfected with the PAI-1 reporter plasmid using the Lipofectamine 2000 transfection reagent (Invitrogen, Carlsbad, CA). After 24 h incubation with the transfection reagent in serum and antibiotic free medium, cells were treated with CBHA for 15 min and subsequently stimulated with TNF-α for another 24 h. PAI-1 luciferase activity was measured as described previously [15].

2.7. Statistical Analyses. Data analyses were performed with SigmaStat 3.5 (SYSTAT Software, San Jose, CA). Quantitative data are presented as means ± SEM. The statistical analysis was performed using one-way ANOVA. The Student-Newman-Keuls test was used if group comparisons showed a significance difference. $P < 0.05$ was considered statistically significant.

3. Results

3.1. Effect of CBHA on TNF-α-Induced HDAC Activity and PAI-1 Expression. To determine the functional relevance of CBHA, we assessed whether CBHA was able to inhibit the pan-HDAC activity in MeT-5A cells. As shown in Figure 1(a), TNF-α (10 ng/mL) stimulated significant increase by up to approximately 91 folds in cellular HDAC activity in MeT-5A cells at 2 h, compared with the resting condition. Pretreatment with CBHA (1 μM) strongly inhibited TNF-α-induced HDAC activity.

As shown in Figure 1(b), CBHA concentration (0.2, 0.5, 1, and 2 μM) dependently inhibited the TNF-α-stimulated production of PAI-1. Consistently, this inhibitory capacity of

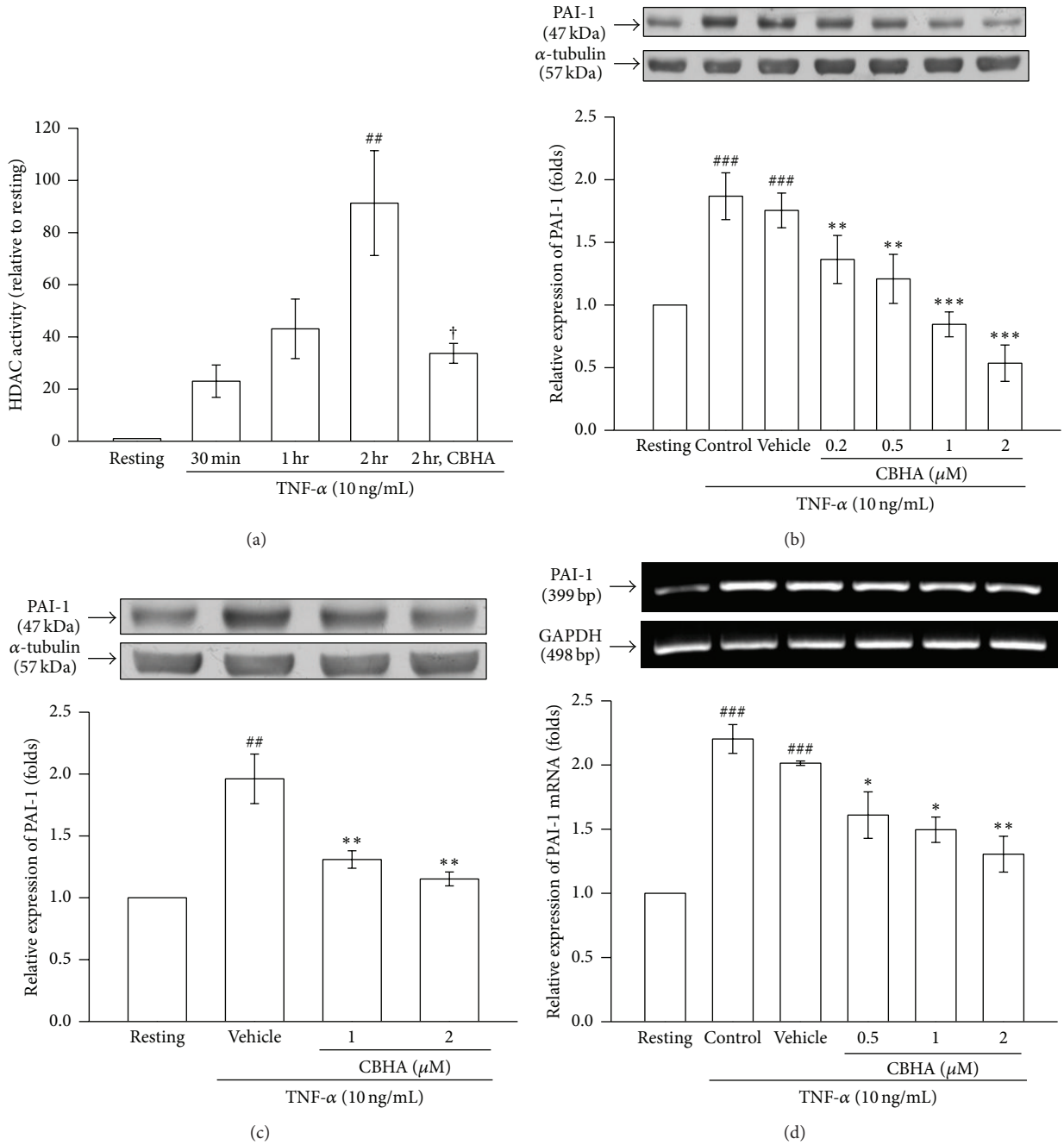

Figure 1: Effect of CBHA on HDAC activity and PAI-1 expression in human pleural mesothelial cells. (a) MeT-5A cells were treated with TNF-α (10 ng/mL) for the indicated times or pretreated with CBHA (1 μM) for 15 min before stimulation with TNF-α for 2 hours. Total HDAC enzyme activity was determined by using the HDAC fluorometric cellular activity assay. (b) MeT-5A cells and (c) primary cultured human pleural mesothelial cells were pretreated with CBHA, respectively, followed by stimulation with TNF-α (10 ng/mL) for 24 h. The levels of PAI-1 were assessed by Western blot. (d) MeT-5A cells were pretreated with CBHA (0.5–2 μM), followed by stimulation with TNF-α (10 ng/mL) for 6 h. PAI-1 mRNA concentrations were analyzed by semiquantitative reverse transcriptase PCR and normalized with glyceraldehyde 3-phosphate dehydrogenase (GAPDH) mRNA. Band intensity was quantified as described in Section 2. Data are shown as mean ± SEM of three independent experiments. $^{\#\#}P < 0.01$ and $^{\#\#\#}P < 0.001$ compared with the resting group; $^{*}P < 0.05$, $^{**}P < 0.01$, and $^{***}P < 0.001$ compared with the vehicle (DMSO) group; $^{\dagger}P < 0.05$ compared with the 2 hr TNF-α-treated group.

CBHA (1 and 2 μM) on PAI-1 expression was also verified in the purified human primary cultured PMCs (Figure 1(c)).

Moreover, TNF-α significantly increased expression of PAI-1 mRNA in MeT-5A cells as compared with the resting condition. Pretreatment with CBHA (0.5, 1, and 2 μM) significantly decreased TNF-α-induced PAI-1 mRNA expression (Figure 1(d)). These results indicated that CBHA markedly suppresses TNF-α-induced PAI-1 protein synthesis through inhibition of PAI-1 gene expression in MeT-5A cells.

3.2. Effect of Signaling Inhibitors and CBHA on TNF-α-Induced Activation and PAI-1 Expression. In order to verify the inhibitory mechanism of CBHA on TNF-α-induced PAI-1 expression in MeT-5A cells, we examined several TNF-α-dependent and -independent signaling pathways, including NF-κB, PI3K/AKT, or MAPKs, by using their specific pharmacologic inhibitors. As shown in Figure 2(a), PAI-1 expression induced by TNF-α was markedly attenuated by pretreatment with an IKK inhibitor (parthenolide), a p38 MAPK inhibitor (SB203580), and a JNK inhibitor (SP600125). Neither a MEK inhibitor (PD98059) nor a PI3K inhibitor (LY294002) affected TNF-α-stimulated PAI-1 protein production. Consistently, TNF-α significantly induced phosphorylation of both p38 and JNK (2/3) MAPK within 15 min and 30 min, compared with the resting condition (Figures 2(b) and 2(c), upper panel), respectively. Moreover, the elevation of p38 and JNK phosphorylation was strongly attenuated by CBHA in a concentration-dependent manner (Figures 2(b) and 2(c), lower panel). However, pretreatment with different concentrations of CBHA had no significant effect on TNF-α-activated IκBα phosphorylation and degradation (data not shown). These results suggested that CBHA suppressed TNF-α-induced PAI-1 expression via inhibiting p38/JNK phosphorylation, but not IκBα degredation in MeT-5A cells.

3.3. Effect of CBHA on TNF-α-Induced MKP Expression. MAPK phosphatase (MPK) is known to dephosphorylate and deactivate various members of the MAPK family, including p38 and JNK MAPK. To clarify the inhibitory mechanism of CBHA on activation of p38/JNK MAPK, we further examined the effect of CBHA on TNF-α-induced MKP-5 and MKP-1 expression. As shown in the time course studies in Figures 3(a) and 3(b) (upper panels), TNF-α increased MKP-5 and MKP-1 expression within 60 min, compared to the resting in MeT-5A cells. The inducing effect was significantly enhanced by pretreatment with CBHA (Figures 3(a) and 3(b), lower panel), especially MKP-5 enhancement, indicating that CBHA inhibits TNF-α-activated p38/JNK phosphorylation through increasing MKP-5/MKP-1 expression.

3.4. Effect of CBHA on TNF-α-Induced Activator Protein (AP)-1 Activation and PAI-1 Promoter Activity. We proposed that CBHA may consistently affect PAI-1 gene transcription via disruption of the activation and nuclear translocation of the downstream transcription factor AP-1. Therefore, the activation of AP-1 constituents including ATF2 and c-Jun in nuclear extracts was analyzed by Western blotting. As shown in Figures 4(a) and 4(b), TNF-α increased nuclear activation of ATF2 and c-Jun as compared with the resting condition. Pretreatment with CBHA attenuated TNF-α-induced phosphorylation of both ATF2 and c-Jun in nuclear extracts. These results indicated that CBHA may inhibit TNF-α-induced ATF2 and c-Jun nuclear activation and thereby impair AP-1 transcriptional activity and PAI-1 gene expression.

Next, to evaluate whether the inhibition of PAI-1 gene expression by CBHA occurred at the transcriptional level, we studied the effect of CBHA on TNF-α-induced PAI-1 promoter activity using p800luc reporter plasmid [19]. TNF-α significantly increased the luciferase activity compared with the resting condition. Pretreatment of cells with various concentrations of CBHA caused a significant inhibition of TNF-α-induced PAI-1 promoter activity (Figure 4(c)).

4. Discussion

In the present study, we investigated the potential mechanisms underlying the antifibrotic activity of HDAC inhibitor in human pleural mesothelial cells. Our study demonstrated that HDAC inhibition with CBHA may downregulate TNF-α-induced PAI-1 expression in human PMCs. CBHA may suppress TNF-α-stimulated cellular HDAC activity, increase MKP-5/MKP-1 expression, and thereby repress p38/JNK and ATF2/c-Jun activation and decrease PAI-1 promoter activity and gene expression. To our knowledge, this is the first study to show that TNF-α increases cellular HDAC activity and that HDAC inhibition abrogates TNF-α-activated cellular signalings, PAI-1 expression.

HDAC activation is an important mechanism in modulation of gene expression [20]. However, it has not been shown whether HDAC plays a role in TNF-α-induced PAI-1 expression in human PMCs. A previous report showed that pan-HDAC inhibitors amplified PAI-1 expression in LPS-stimulated mouse macrophages [21]. In contrast, our recent study revealed that the HDAC inhibitor CBHA attenuated TGF-β1-induced PAI-1 expression in human PMCs [15], suggesting that the role of HDAC in regulation of PAI-1 expression may be stimulant- or cell type-specific. On the other hand, in line with previous reports [2, 4], the present study demonstrated that TNF-α increased PAI-1 expression in human PMCs and that this upregulation effect was markedly attenuated by CBHA.

The molecular mechanisms by which signaling pathways are involved in the regulation of PAI-1 expression remain to be determined in TNF-α-stimulated human PMCs. TNF-α elicits inflammatory response via several signal transduction pathways, including NF-κB and MAPK pathways [22], and it is well known that the PAI-1 promoter contains binding sites for Smads, NF-κB, and AP-1 [19]. HDAC inhibitors have been shown to prevent renal interstitial fibrosis through inhibition of NF-κB activity [23]. Also, a previous study reported that HDAC4 silencing blocked TGF-β1-induced α-SMA expression in fibroblasts through impairing AKT phosphorylation [16]. Alternatively, our study showed that

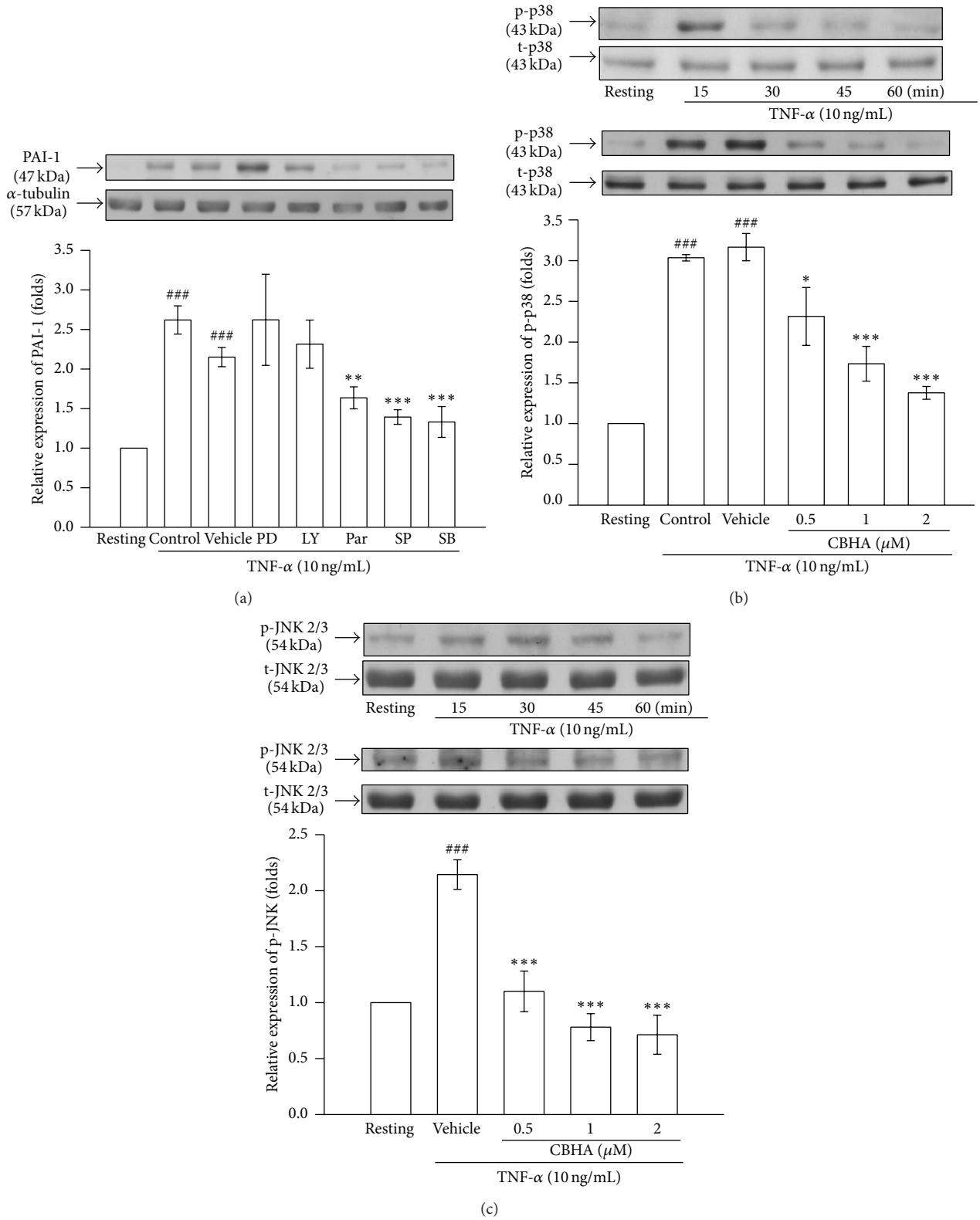

Figure 2: Effect of CBHA on TNF-α-activated signalings in MeT-5A cells. (a) Cells were pretreated with vehicle, PD98059 (PD, 20 μM), LY294002 (LY, 10 μM), Parthenolide (Par, 10 μM), SP600125 (SP, 10 μM), and SB203580 (SB, 20 μM), and then stimulated with TNF-α (10 ng/mL) for 24 h. PAI-1 protein expression was assessed by Western blot. (b) and (c) Cells were treated with TNF-α for the indicated times (upper panel) or pretreated with vehicle or CBHA (0.5–2 μM) for 15 min followed by TNF-α administration (lower panel). Phosphorylation of (b) p38 and (c) JNK MAPKs was analyzed by Western blotting with antibodies specific for either phosphorylated or total proteins.

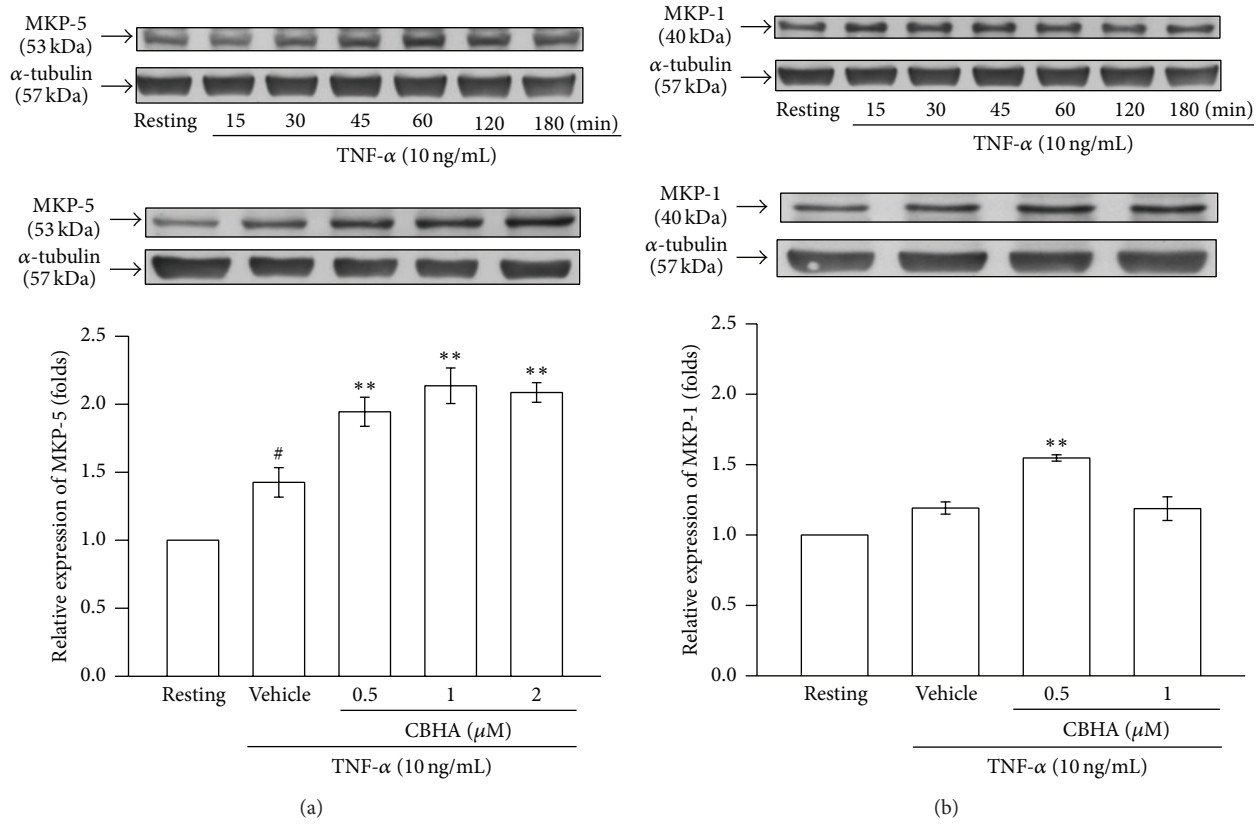

Figure 3: Effect of CBHA on TNF-α-induced MKP expression in MeT-5A cells. (a) and (b) Cells were treated with TNF-α for the indicated times (upper panel) or pretreated with CBHA (0.5–2 μM) for 15 min followed by TNF-α stimulation for 60 min and 15 min (lower panel), respectively. The expression of MKP-5/MKP-1 was analyzed by Western blotting. Relative multiples of densitometric data are expressed as mean ± SEM of three independent experiments. $^{\#}P < 0.05$ compared with the resting group; $^{**}P < 0.01$ and compared with vehicle group.

inhibition of HDAC activity with CBHA ablated TNF-α-stimulated phosphorylation of p38 and JNK MAPK, but not NF-κB activation (data not shown).

Additionally, the activity of the MAPK family is determined by a dynamic balance between phosphorylation and dephosphorylation. Among the numerous MAPK phosphatases, MKP-5 and MKP-1 are known to dephosphorylate and inactivate p38 and JNK MAPK [24]. Our data demonstrated that CBHA significantly increased MKP-5 and MKP-1 expression induced by TNF-α, suggesting that CBHA may inactivate MAPK signaling via enhancing MKP-5 and MKP-1 expression in human PMCs. Furthermore, as a transcription factor of MAPK signaling, AP-1 is composed of either homodimers or heterodimers between Fos, Jun, and ATF2 family members, which are activated by phosphorylated MAPKs and dimerize with each other to bind to AP-1 promoter site [25]. Correspondingly, the present study demonstrated that CBHA markedly repressed TNF-α-induced AP-1 transcriptional activity via disruption of ATF2/c-Jun transactivation into the nucleus and PAI-1 promoter activity. All these findings suggested that CBHA may abrogate TNF-α-induced PAI-1 expression in MeT-5A cells through induction of MKP-5/MKP-1 expression and repression of MAPK/AP-1 signal pathway (Figure 5). However, this study could not exclude other mechanisms such as epigenetic histone acetylation modulation and transcriptional and posttranscriptional regulation [15, 26], in the control of PAI-1 expression.

Collectively, CBHA attenuated PAI-1 expression via inhibition of TNF-α-activated signaling, indicating a potential antifibrotic effect of HDAC inhibitors. A recently published study demonstrated that MPT0E014, a novel HDAC inhibitor, decreased the expression of angiotensin II receptor and TGF-β1 in cardiac fibroblasts, inhibited their proliferation and migration, and reduced cardiac fibrosis in heart failure rats, which highly signified the direct antifibrotic activity through HDAC inhibition [14]. In parallel, our study disclosed the downregulation effect of CBHA on the profibrotic mediator PAI-1 in pleural mesothelial cells and verified the indirect action of HDAC inhibitors on pleural fibrosis. However, in contrast to the previous study [14], the current work did not explore the functional regulation of fibrogenesis by HDAC inhibition but focused on the modulation of TNF-α-mediated signaling by CBHA at multiple levels, which may revalidate the pluripotent effects of HDAC inhibitors [9]. Further *in vivo* studies are needed to examine the direct antifibrotic effect of CBHA.

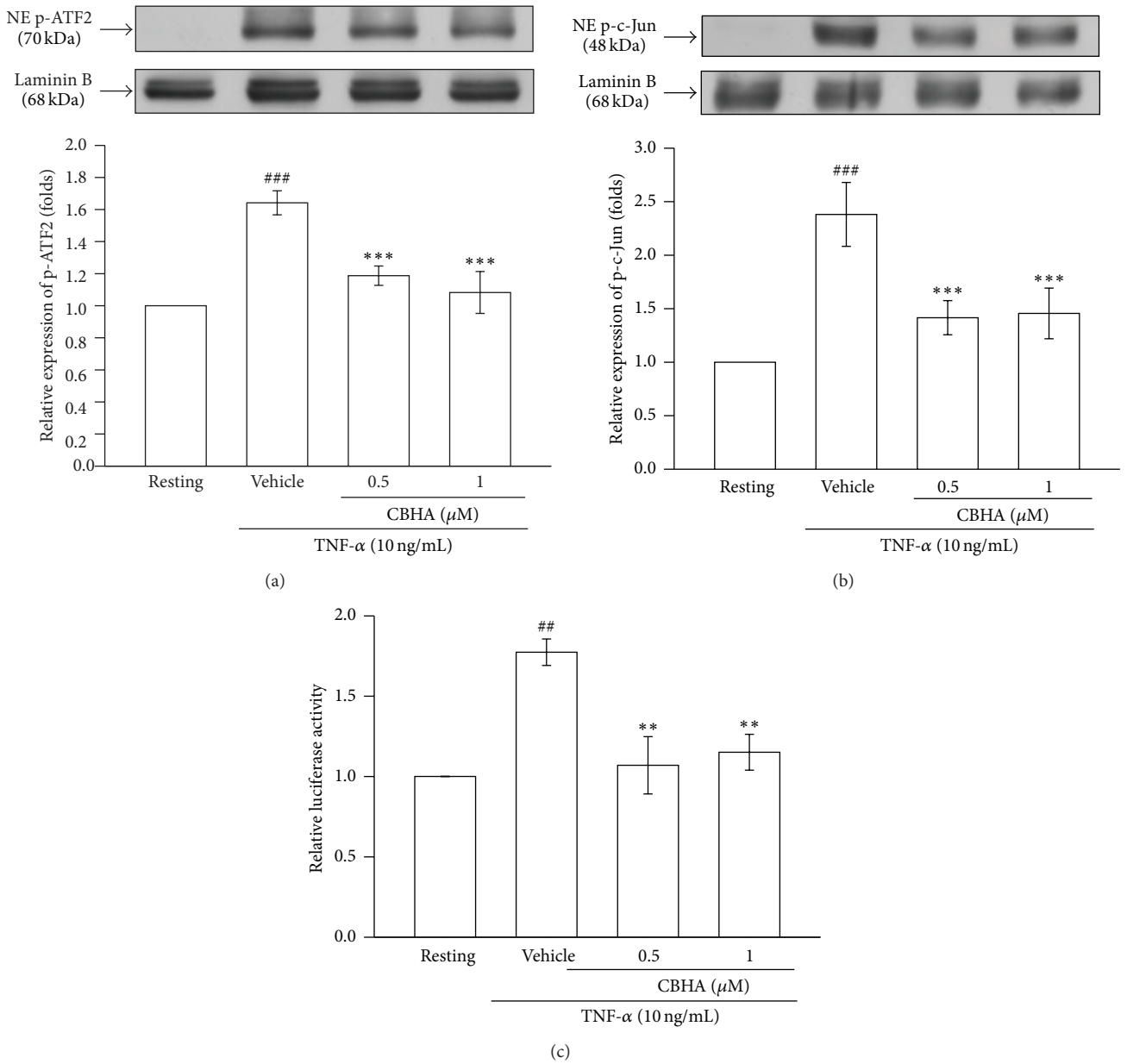

Figure 4: Effect of CBHA on TNF-α-induced activator protein (AP)-1 activity and PAI-1 promoter in MeT-5A cells. (a) and (b) Cells were pretreated with vehicle or CBHA (0.5–1 μM) for 15 min, followed by treatment with TNF-α (10 ng/mL) for 60 min. The nuclear amount of phosphorylated (a) ATF-2 and (b) c-Jun was detected by Western blot analysis of nuclear extracts (NE) with specific antibodies. (c) Cells were transfected with the specific PAI-1 reporter plasmid (p800Luc), together with internal plasmid (Renilla). Transfected cells were pretreated with vehicle or CBHA (0.5–2 μM) for 15 min and then stimulated with TNF-α (10 ng/mL) for 24 h. The luciferase activity of PAI-1 reporter gene was assessed. Data are representative of three to four experiments. $^{\#\#}P < 0.01$, $^{\#\#\#}P < 0.001$ compared with the resting group; $^{**}P < 0.01$, $^{***}P < 0.001$ compared with the vehicle group.

In conclusion, the present study demonstrated that inhibition of HDAC activity with CBHA may increase MKP-5/MKP-1 expression, abrogate TNF-α-activated MAPK/AP-1 signaling and thereby impair PAI-1 expression in human PMCs. Given the antifibrotic effect through PAI-1 abrogation, CBHA may be utilized as a novel agent in the treatment of fibrotic diseases.

Conflict of Interests

The authors declare no conflict of interests.

Authors' Contribution

Chi-Li Chung and George Hsiao contributed equally to this work.

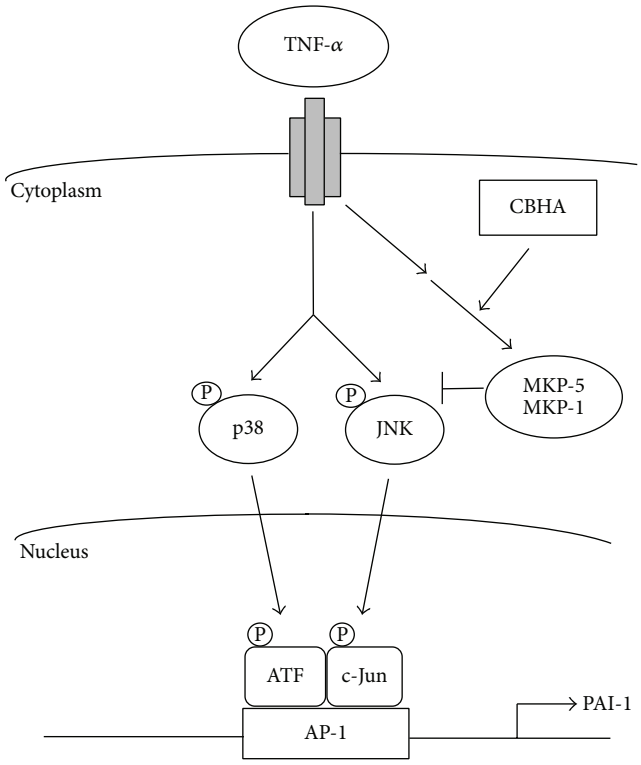

Figure 5: Schematic diagram shows that CBHA abrogates TNF-α-induced PAI-1 expression in human pleural mesothelial cells through enhancement of MKP-5/MKP-1 expression and repression of MAPK/AP-1 signal pathway (see test for further explanation). Single arrow, established signal pathway; double arrow, possible signal pathway. (P), phosphorylated.

Acknowledgments

This study was supported by the Grants from the National Science Council of Taiwan (NSC 101-2314-B-038-044-MY3 and NSC 99-2320-B-038-001-MY3) and Ministry of Economic Affairs of Taiwan (102-EC-17-A-20-S1-196).

References

[1] M. A. Jantz and V. B. Antony, "Pleural fibrosis," *Clinics in Chest Medicine*, vol. 27, no. 2, pp. 181–191, 2006.

[2] S. Idell, C. Zwieb, A. Kumar, K. B. Koenig, and A. R. Johnson, "Pathways of fibrin turnover of human pleural mesothelial cells in vitro," *The American Journal of Respiratory Cell and Molecular Biology*, vol. 7, no. 4, pp. 414–426, 1992.

[3] C.-L. Chung, C.-H. Chen, J.-R. Sheu, Y.-C. Chen, and S.-C. Chang, "Proinflammatory cytokines, transforming growth factor-β1, and fibrinolytic enzymes in loculated and free-flowing pleural exudates," *Chest*, vol. 128, no. 2, pp. 690–697, 2005.

[4] D. Orphanidou, M. Gaga, A. Rasidakis et al., "Tumour necrosis factor, interleukin-1 and adenosine deaminase in tuberculous pleural effusion," *Respiratory Medicine*, vol. 90, no. 2, pp. 95–98, 1996.

[5] S. A. Whawell, D. M. Scott-Coombes, M. N. Vipond, S. J. Tebbutt, and J. N. Thompson, "Tumour necrosis factor-mediated release of plasminogen activator inhibitor 1 by human peritoneal mesothelial cells," *British Journal of Surgery*, vol. 81, no. 2, pp. 214–216, 1994.

[6] C.-C. Hua, L.-C. Chang, Y.-C. Chen, and S.-C. Chang, "Proinflammatory cytokines and fibrinolytic enzymes in tuberculous and malignant pleural effusions," *Chest*, vol. 116, no. 5, pp. 1292–1296, 1999.

[7] F.-C. Lin, Y.-C. Chen, F.-J. Chen, and S.-C. Chang, "Cytokines and fibrinolytic enzymes in tuberculous and parapneumonic effusions," *Clinical Immunology*, vol. 116, no. 2, pp. 166–173, 2005.

[8] X.-J. Yang and E. Seto, "HATs and HDACs: from structure, function and regulation to novel strategies for therapy and prevention," *Oncogene*, vol. 26, no. 37, pp. 5310–5318, 2007.

[9] S. Spange, T. Wagner, T. Heinzel, and O. H. Krämer, "Acetylation of non-histone proteins modulates cellular signalling at multiple levels," *International Journal of Biochemistry and Cell Biology*, vol. 41, no. 1, pp. 185–198, 2009.

[10] S. Ropero and M. Esteller, "The role of histone deacetylases (HDACs) in human cancer," *Molecular Oncology*, vol. 1, no. 1, pp. 19–25, 2007.

[11] P. J. Barnes, I. M. Adcock, and K. Ito, "Histone acetylation and deacetylation: Importance in inflammatory lung diseases," *European Respiratory Journal*, vol. 25, no. 3, pp. 552–563, 2005.

[12] A. K. Ghosh, Y. Mori, E. Dowling, and J. Varga, "Trichostatin A blocks TGF-β-induced collagen gene expression in skin fibroblasts: involvement of Sp1," *Biochemical and Biophysical Research Communications*, vol. 354, no. 2, pp. 420–426, 2007.

[13] H. Duan, C. A. Heckman, and L. M. Boxer, "Histone deacetylase inhibitors down-regulate bcl-2 expression and induce apoptosis in t(14;18) lymphomas," *Molecular and Cellular Biology*, vol. 25, no. 5, pp. 1608–1619, 2005.

[14] Y. H. Kao, J. P. Liou, C. C. Chung et al., "Histone deacetylase inhibition improved cardiac functions with direct antifibrotic activity in heart failure," *International Journal of Cardiology*, vol. 168, no. 4, pp. 4178–4183, 2013.

[15] C.-L. Chung, J.-R. Sheu, W.-L. Chen et al., "Histone deacetylase inhibitor m-carboxycinnamic acid bis-hydroxamide attenuates plasminogen activator inhibitor-1 expression in human pleural mesothelial cells," *The American Journal of Respiratory Cell and Molecular Biology*, vol. 46, no. 4, pp. 437–445, 2012.

[16] W. Guo, B. Shan, R. C. Klingsberg, X. Qin, and J. A. Lasky, "Abrogation of TGF-β1-induced fibroblast-myofibroblast differentiation by histone deacetylase inhibition," *The American Journal of Physiology*, vol. 297, no. 5, pp. L864–L870, 2009.

[17] C.-L. Chung, J.-R. Sheu, H.-E. Liu et al., "Dynasore, a dynamin inhibitor, induces PAI-1 expression in MeT-5A human pleural mesothelial cells," *The American Journal of Respiratory Cell and Molecular Biology*, vol. 40, no. 6, pp. 692–700, 2009.

[18] N. Nasreen, K. A. Mohammed, K. K. Mubarak et al., "Pleural mesothelial cell transformation into myofibroblasts and haptotactic migration in response to TGF-β1 in vitro," *The American Journal of Physiology*, vol. 297, no. 1, pp. L115–L124, 2009.

[19] P. K. Vayalil, K. E. Iles, J. Choi, A.-K. Yi, E. M. Postlethwait, and R.-M. Liu, "Glutathione suppresses TGF-β-induced PAI-1 expression by inhibiting p38 and JNK MAPK and the binding of AP-1, SP-1, and Smad to the PAI-1 promoter," *The American Journal of Physiology*, vol. 293, no. 5, pp. L1281–L1292, 2007.

[20] M. Dokmanovic, C. Clarke, and P. A. Marks, "Histone deacetylase inhibitors: overview and perspectives," *Molecular Cancer Research*, vol. 5, no. 10, pp. 981–989, 2007.

[21] M. A. Halili, M. R. Andrews, L. I. Labzin et al., "Differential effects of selective HDAC inhibitors on macrophage inflammatory responses to the Toll-like receptor 4 agonist LPS," *Journal of Leukocyte Biology*, vol. 87, no. 6, pp. 1103–1114, 2010.

[22] V. Baud and M. Karin, "Signal transduction by tumor necrosis factor and its relatives," *Trends in Cell Biology*, vol. 11, no. 9, pp. 372–377, 2001.

[23] F. Kinugasa, T. Noto, H. Matsuoka et al., "Prevention of renal interstitial fibrosis via histone deacetylase inhibition in rats with unilateral ureteral obstruction," *Transplant Immunology*, vol. 23, no. 1-2, pp. 18–23, 2010.

[24] A. Theodosiou, A. Smith, C. Gillieron, S. Arkinstall, and A. Ashworth, "MKP5, a new member of the MAP kinase phosphatase family, which selectively dephosphorylates stress-activated kinases," *Oncogene*, vol. 18, no. 50, pp. 6981–6988, 1999.

[25] M. Karin and T. Hunter, "Transcriptional control by protein phosphorylation: signal transmission from the cell surface to the nucleus," *Current Biology*, vol. 5, no. 7, pp. 747–757, 1995.

[26] J. Backs, B. C. Worst, L. H. Lehmann et al., "Selective repression of MEF2 activity by PKA-dependent proteolysis of HDAC4," *The Journal of cell biology*, vol. 195, no. 3, pp. 403–415, 2011.

Hindawi Publishing Corporation
BioMed Research International
Volume 2014, Article ID 614506, 10 pages
http://dx.doi.org/10.1155/2014/614506

Research Article

Mechanisms of Ascorbyl Radical Formation in Human Platelet-Rich Plasma

Kou-Gi Shyu,[1,2] Chao-Chien Chang,[3,4] Yu-Chieh Yeh,[4] Joen-Rong Sheu,[4,5] and Duen-Suey Chou[5]

[1] *Division of Cardiology, Shin Kong Wu Ho-Su Memorial Hospital, 95 Wenchang Road, Shihlin Taipei 111, Taiwan*
[2] *Graduate Institute of Clinical Medicine, Taipei Medical University, 250 Wu-Hsing Street, Taipei 110, Taiwan*
[3] *Department of Cardiology, Cathay General Hospital, 280 Jen Ai Road, Section 4, Taipei 106, Taiwan*
[4] *Graduate Institute of Medical Sciences, Taipei Medical University, 250 Wu-Hsing Street, Taipei 110, Taiwan*
[5] *Department of Pharmacology, Taipei Medical University, 250 Wu-Hsing Street, Taipei 110, Taiwan*

Correspondence should be addressed to Joen-Rong Sheu; sheujr@tmu.edu.tw and Duen-Suey Chou; fird@tmu.edu.tw

Received 21 November 2013; Accepted 9 January 2014; Published 17 February 2014

Academic Editor: Philip Aloysius Thomas

Recently, many clinical reports have suggested that the ascorbyl free radical ($Asc^{\bullet}$) can be treated as a noninvasive, reliable, real-time marker of oxidative stress, but its generation mechanisms in human blood have rarely been discussed. In this study, we used upstream substances, enzyme inhibitors, and free radical scavengers to delineate the mechanisms of $Asc^{\bullet}$ formation in human platelet-rich plasma (PRP). Our results show that the doublet signal was detected in PRP samples by using electron spin resonance, and the hyperfine splitting of the doublet signal was $a^{H} = 1.88$ gauss and g-factor = 2.00627, which was determined to be the $Asc^{\bullet}$. We observed that the inhibitors of NADPH oxidase (NOX), cyclooxygenase (COX), lipoxygenase (LOX), cytochrome P450 (CYP450), mitochondria complex III, and nitric oxide synthase (NOS), but not xanthine oxidase, diminished the intensity of the $Asc^{\bullet}$ signal dose dependently. All enzyme inhibitors showed no obvious antioxidant activity during a Fenton reaction assay. In summary, the obtained data suggest that $Asc^{\bullet}$ formation is associated with NOX, COX, LOX, CYP450, eNOS, and mitochondria in human PRP.

1. Introduction

Interest in treating oxidative stress has grown in medicine over the past 2 decades. The oxidative status of a biosystem represents a relative level of oxidation in living organisms and is crucial for understanding numerous human physiological and pathophysiological processes [1]. Overproduction of ROS results in oxidative stress, a pathophysiological process that can damage cell structures and induce cancer, cardiovascular disease, atherosclerosis, hypertension, diabetes mellitus, neurodegenerative diseases, rheumatoid arthritis, and ageing. In contrast, ROS play a physiological role in protection against infectious organisms, in the function of several cellular signalling pathways, and the generation of a mitogenic response at low/moderate concentrations [1]. Oxidative status can be estimated using biochemical assays, such as the 2,2′-azino-bis(3-ethylbenzthiazoline-6-sulphonic acid) assay [2], and by measuring the activity of superoxide dismutating enzymes (Mn superoxide dismutase (SOD) and CuZnSOD), catalase (CAT), GSH peroxidase, and reductase [3–5], as well as the level of S-glutathionylation [6]. However, Spasojević suggested that these techniques be supplemented by electron spin resonance (ESR) spectroscopy to enable acquiring data on oxidative status that are more specific [7]. Certain endogenous paramagnetic molecules, such as the ascorbyl free radical ($Asc^{\bullet}$), tocopheryl radical, and melanin radical, are biomarkers of oxidative status that can be detected using ESR spectroscopy [7].

Ascorbic acid is an essential biological component that can be oxidized through a two-step oxidation process involving a free radical intermediate; this oxidation process may be performed by nearly all oxidizing species intrinsic to the

biological environment [7]. When using ESR spectroscopy, the concentration of the $Asc^{\bullet}$ can be measured using a lower limit of approximately 5 nM with a standard deviation of <1 nM [8]. The characteristics of the $Asc^{\bullet}$ are relatively stable and it has a long half-life, indicating that it is the most useful biomarker of oxidative status in living systems [7].

ESR spectroscopy was first applied in detecting the $Asc^{\bullet}$ in oxidative status research in 1993 [9]. Thus far, the $Asc^{\bullet}$ has been treated as a noninvasive, reliable, real-time biomarker of oxidative stress in various biological samples including plasma, serum, whole blood, cerebrospinal fluid, extracellular fluid, synovial fluid, seminal fluid, tumor, and heart tissue samples [7]; however, the generation mechanisms of the $Asc^{\bullet}$ in human blood have rarely been discussed.

Ascorbate (the reduced form of vitamin C) is an important radical scavenger and antioxidant in human plasma. $Asc^{\bullet}$ has been detected by ESR in various biological samples including plasma, serum, whole blood, cerebrospinal fluid, skin, extracellular fluid, synovial fluid, gastric mucosa, seminal fluid, tumors, heart tissue, and others [7]. We recently applied ESR spectroscopy in detecting the $Asc^{\bullet}$ to investigate the mechanisms of oxidative stress caused by lymphedema in mice [10]. In this study, we used upstream substances, enzyme inhibitors, and free radical scavengers to delineate the mechanisms of $Asc^{\bullet}$ formation in human platelet-rich plasma (PRP).

2. Materials and Methods

2.1. Materials. AA861, allopurinol, antimycin, arachidonic acid (AA), baicalein, CAT, clotrimazole, dimethyl sulfoxide (DMSO), diphenyleneiodonium (DPI), ethylenediaminetetraacetic acid, hemoglobin, indomethacin, NG-nitro-L-arginine methyl ester (L-NAME), quinacrine, and SOD were purchased from Sigma Chemical (St. Louis, MO, USA). L(+)-ascorbic acid was purchased from Wako Pure Chemical Industries (Osaka, Japan).

2.2. Human Blood Collection Procedure. This study was approved by the Institutional Review Board of Taipei Medical University and conformed to the principles outlined in the Helsinki Declaration. All human volunteers provided informed consent to participate.

2.3. Preparation of Human Blood Components. Whole blood was collected from healthy human volunteers who had taken no medicine during the preceding 2 wk and was mixed with acid/citrate/glucose. After centrifugation at 120 ×g for 10 min at room temperature, the supernatant (PRP) was supplemented with PGE_1 (0.5 μM) and heparin (6.4 IU/mL) and then incubated for 10 min at 30°C and centrifuged at 500 ×g for 10 min. The supernatant was platelet-poor plasma (PPP) and was used in subsequent experiments.

2.4. Isolation of Red Blood Cells. Whole blood was centrifuged at 650 ×g for 5 min. Plasma was removed carefully and the white buffy layer was completely removed through aspiration using a pipette with utmost care. The red blood cells (RBCs) were then washed three additional times with Tyrode's solution.

2.5. Measurement of the Ascorbyl Free Radical in Platelet-Rich Plasma Using Electron Paramagnetic Resonance Spectrometry. The ESR method involved using a Bruker EMX ESR spectrometer (Bruker Instruments Inc., Billerica, MA, USA) as described previously [11]. The PRP was prewarmed to 37°C for 2 min, and enzyme inhibitors or other reagents were then added. ESR spectra were recorded at room temperature by using a quartz flat cell designed for aqueous solutions. ESR spectrometry was conducted under the following conditions: 20 mW of power at 9.78 GHz, with a scan range of 100 G and a receiver gain of 5×10^4. The modulation amplitude, sweep time, and time constant are provided in the figure legends.

2.6. Fenton Reaction Model System with Electron Paramagnetic Resonance Detection of the Hydroxyl Radical. The hydroxyl radical generated in a standard Fenton reaction was trapped using DMPO according to the method previously described [12]. A Fenton reaction solution (50 μM $FeSO_4$ + 500 μM H_2O_2) was pretreated with a solvent control (0.6% DMSO) or reagent (10 μM). The ESR spectra were recorded after precisely 3 min.

2.7. Statistical Analysis. The experimental results are expressed as the mean ± SEM and are accompanied by the number (n) of observations. The data were assessed using an analysis of variance (ANOVA). When this analysis indicated significant differences among the group means, each group was compared using the Newman-Keuls method. A P value <0.05 was considered statistically significant.

3. Results

3.1. Electron Spin Resonance Investigations of Free Radicals Formed in Human Blood Components. Free radical signals were detected using ESR in human PPP, PRP, RBCs, and whole blood. A doublet signal radical was observed in PPP and PRP, but not in RBCs or whole blood (Figure 1(a)). PRP exhibited the strongest signal among the human blood components and was used in subsequent experiments. The hyperfine splitting and g-factor of this doublet signal were 1.88 G and 2.00627, respectively. In each instance, the signals exhibited doublet peaks and a line width of approximately 4 G. The radical species was identified to be ascorbyl based on the close similarity of the hyperfine coupling constants and g-factor of the observed signal to those of published data [13, 14]. No notable oxygen-derived free radicals were detected in this study, probably because of the presence of ascorbic acid and other antioxidants in human PRP.

3.2. Effect of Exogenous Ascorbic Acid on the g = 2.00627 Radical Formation in Human Platelet-Rich Plasma. To confirm that the g = 2.00627 radical was a typical $Asc^{\bullet}$, we added exogenous ascorbic acid to human PRP. The intensity

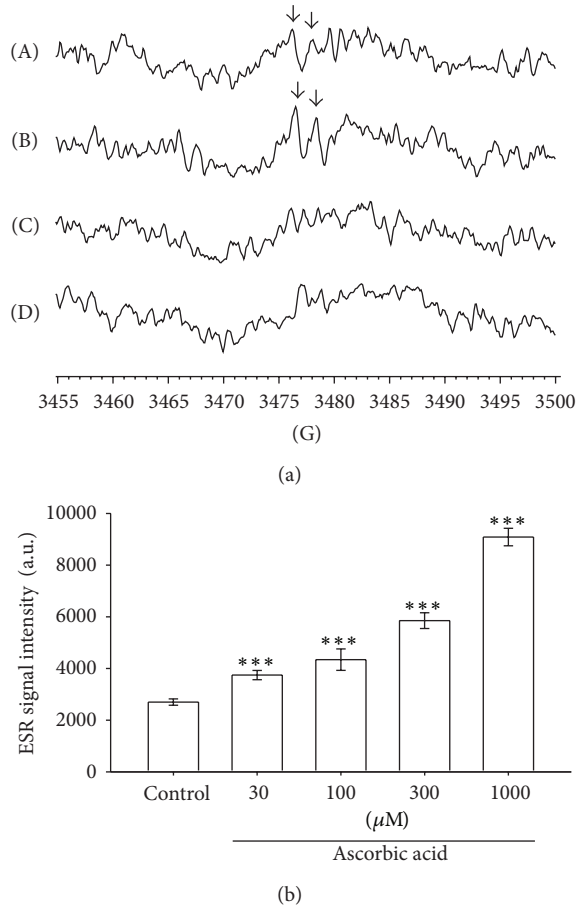

Figure 1: Free radical doublet (a) detected using ESR spectroscopy in (A) PPP, (B) PRP, (C) RBCs, and (D) whole blood. The ESR signal was examined at room temperature, and the following instrument parameters were used in ESR spectroscopy: standard frequency (X-band): 9 GHz; microwave power: 20 mW; modulation frequency: 100 kHz; time constant: 163.84 ms; conversion time: 40.96 ms; receiver gain: 5.02×10^5; and the number of data X-scans: 4. The free radical doublet is marked with arrows: "↓". Effect of ascorbic acid on the $g = 2.00627$ radical formation in human PRP. The intensity of the $g = 2.00627$ radical obtained from the reaction of PRP (approximately 8×10^6 cells/mL, control) and 30 μM, 100 μM, 300 μM, and 1000 μM ascorbic acid in the presence of 100 mM DMPO. ESR analysis was exactly 30 s after the final addition. ESR spectra are labeled to show their components: DMPO- Asc$^\bullet$ adduct (∗). The values of the ESR signal intensity in the bar chart (b) are shown as the means ± SEM ($n = 4$). $^{***}P < 0.001$ compared with the control. The instrument parameters were identical to those shown in (a).

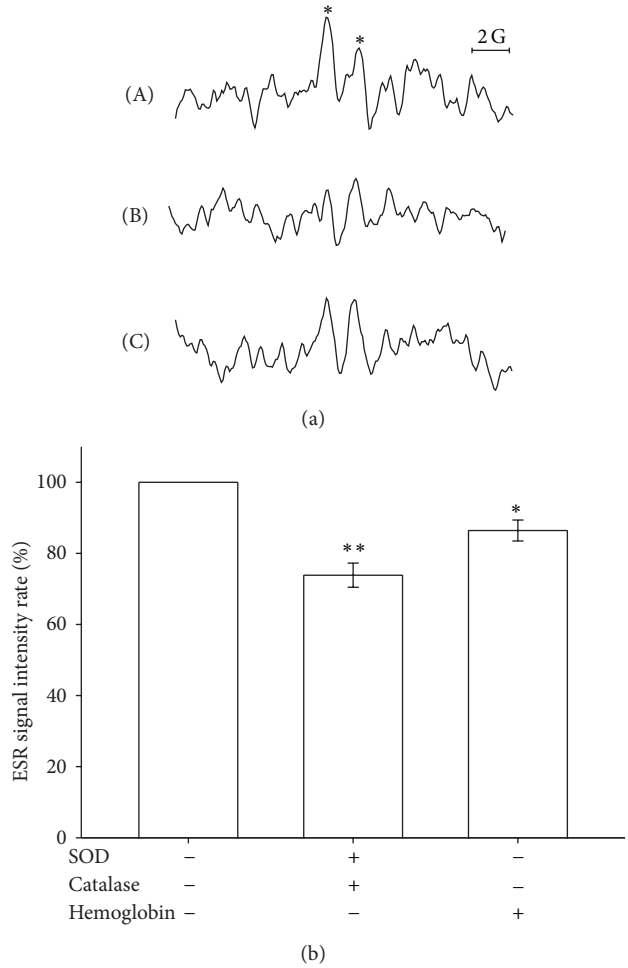

Figure 2: Effect of superoxide and the nitric oxide scavenger on Asc$^\bullet$ formation in human PRP. ESR spectra (a) obtained from the reaction of (A) PRP (approximately 8×10^6 cells/mL) and (B) superoxide scavenger (120 U/mL SOD and 1000 U/mL CAT) and the (C) nitric oxide scavenger (1 μg/mL of hemoglobin) in the presence of 100 mM DMPO for 3 min. The ESR spectra are labeled to show their components: DMPO- Asc$^\bullet$ adduct (∗). The ESR signal intensity rates in the bar chart (b) are shown as the means ± SEM ($n > 3$). $^{**}P < 0.01$, $^{*}P < 0.05$ compared with the control. The instrument parameters were identical to those shown in Figure 1(a).

of the $g = 2.00627$ radical induced by exogenous ascorbic acid increased dose dependently (Figure 1(b)).

3.3. Effect of Superoxide and the Nitric Oxide Scavenger on Ascorbyl Free Radical Formation in Human Platelet-Rich Plasma. We propose that the Asc$^\bullet$ is a secondary radical; therefore, we determined which types of primary radical may be involved in the formation of this radical species. The effects of superoxide and the nitric oxide scavenger were examined on the $g = 2.00627$ radical formation, as shown in Figure 2. The $g = 2.00627$ signal formed by PRP was arbitrarily designated 100% and was inhibited by the superoxide scavenger (120 U/mL of SOD and 1000 U/mL of CAT) and nitric oxide scavenger (1 μg/mL of hemoglobin) to 26.1% ($P < 0.01$) and 13.5% ($P < 0.05$), respectively. This result indicates that superoxide and nitric oxide may be primary radicals that induce Asc$^\bullet$ formation.

3.4. Effect of the NADPH Oxidase Inhibitor on Ascorbyl Free Radical Formation in Human Platelet-Rich Plasma. It was reported that NOX on the cell membrane of leucocytes may be the primary source of superoxide formation in blood [15].

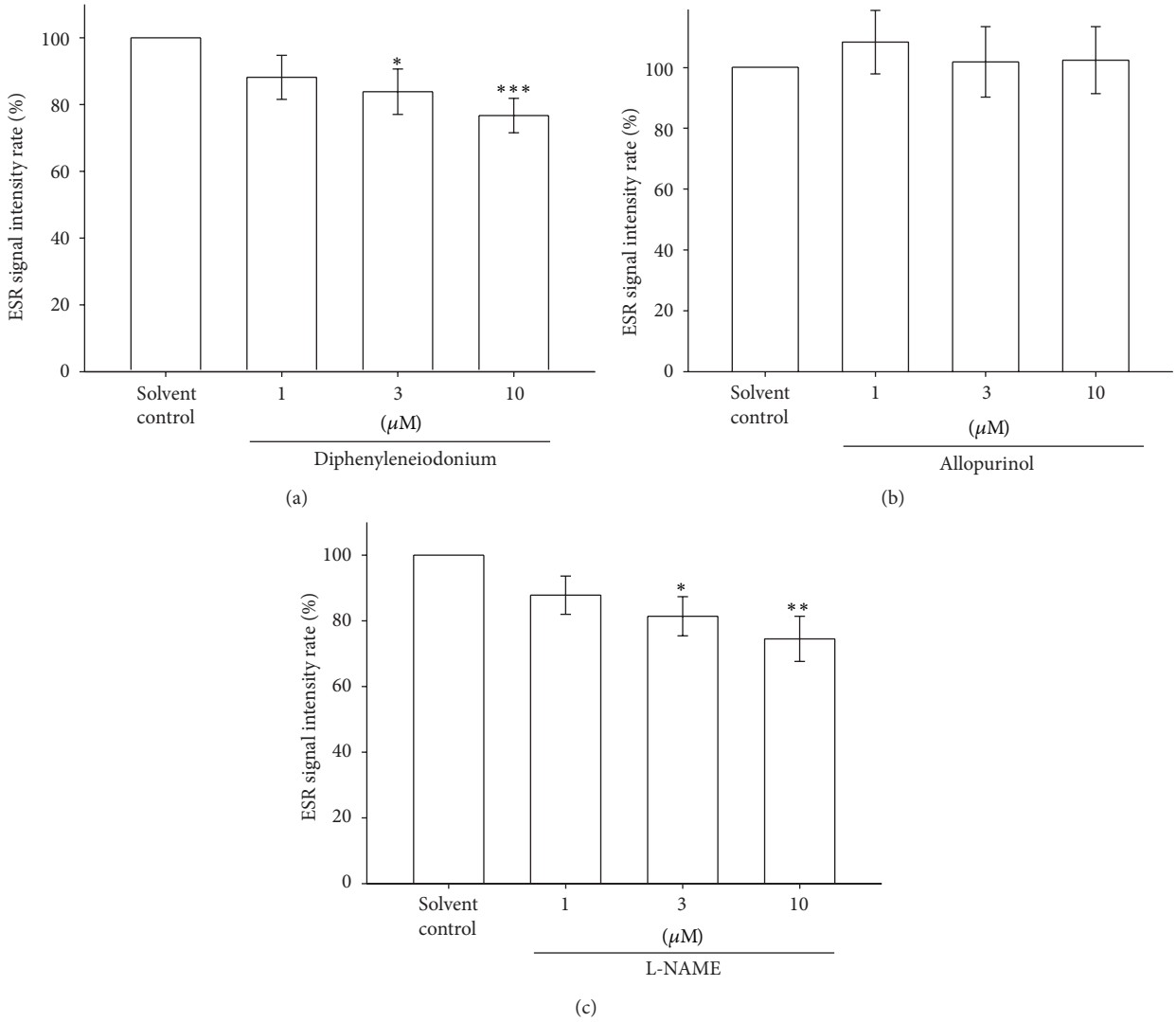

Figure 3: Effect of the NOX inhibitor (a), XO inhibitor (b), and NOS inhibitor (c) on $Asc^{\bullet}$ formation in human PRP (approximately 8×10^6 platelets/mL). The ESR signal intensity rates in the bar chart are expressed as the means ± SEM ($n \geqq 5$). $^{***}P < 0.001$, $^{*}P < 0.05$ compared with the solvent control. The instrument parameters were identical to those shown in Figure 1(a).

To investigate the involvement of NOX in $Asc^{\bullet}$ formation in PRP, we used DPI as a NOX nonselective inhibitor. The $Asc^{\bullet}$ signal of a solvent control group was arbitrarily designated 100% and was dose dependently inhibited by DPI (3 μM = 17.7%, $P < 0.05$; 10 μM = 23.8%, $P < 0.001$, Figure 3(a)). This result indicates that NOX may be involved in the formation of $Asc^{\bullet}$ in PRP.

3.5. Effect of the Xanthine Oxidase Inhibitor on Ascorbyl Free Radical Formation in Human Platelet-Rich Plasma. XO is a superoxide-producing enzyme normally present in the serum and lungs [16]. To investigate the involvement of XO in $Asc^{\bullet}$ formation in PRP, we used allopurinol as a nonselective XO inhibitor. The $Asc^{\bullet}$ signal of a solvent control group was arbitrarily designated 100%, and allopurinol (1–10 μM) did not significantly influence $Asc^{\bullet}$ formation in PRP ($P > 0.05$, Figure 3(b)).

3.6. Effect of the Nitric Oxide Synthase Inhibitor on Ascorbyl Free Radical Formation in Human Platelet-Rich Plasma. We determined whether NOS is involved in $Asc^{\bullet}$ formation in PRP. We used L-NAME as an NOS inhibitor. The $Asc^{\bullet}$ signal of a solvent control group was arbitrarily designated 100% and was inhibited by L-NAME (1–10 μM) dose dependently (3 μM = 18.6%, $P < 0.05$; 10 μM = 25.4%, $P < 0.01$, Figure 3(c)). This result indicates that NOS-derived NO is associated with the formation of $Asc^{\bullet}$ in PRP.

3.7. Effect of Arachidonic Acid on Ascorbyl Free Radical Formation in Human Platelet-Rich Plasma. Reactive oxygen species (ROS) are generated by AA metabolites, which are released from the cell membrane. AA-induced ROS generation may occur through the oxidative metabolic processes induced by COX and LOX [11]. AA has also been reported to induce ROS formation through NOX [17, 18]. Our results showed

that NOX may be involved in the formation of the $Asc^{\bullet}$ in PRP (Figure 3(a)). Therefore, we determined whether AA metabolite pathways are associated with the $Asc^{\bullet}$ formation. The $Asc^{\bullet}$ signal formed by PRP was, respectively, increased 39.1% ($P < 0.05$) and 62.4% ($P < 0.001$) by 10 μM and 100 μM AA compared with a solvent control (Figure 4(a)). In addition, the $Asc^{\bullet}$ signal of the solvent control group was arbitrarily designated 100% and was inhibited by quinacrine (2.5–10 μM), a phospholipidase A_2 (PLA_2) inhibitor, dose dependently (5 μM = 20.9%, $P < 0.001$; 10 μM = 26.2%, $P < 0.001$, Figure 4(b)). This result indicates that AA metabolite pathways are associated with the formation of the $Asc^{\bullet}$ in PRP.

3.8. Effect of the Cyclooxygenase Inhibitor on Ascorbyl Free Radical Formation in Human Platelet-Rich Plasma. In downstream pathways of the AA metabolism, COX [19], P450 [20], and LOX [21] are vital sources of extracellular ROS release. To investigate the involvement of COX in $Asc^{\bullet}$ formation in PRP, we used indomethacin as a nonselective COX inhibitor. The $Asc^{\bullet}$ signal of a solvent control group was arbitrarily designated 100%; 3 and 10 μM indomethacin produced a 13.4% ($P < 0.05$) and 14.5% ($P < 0.01$) reduction of the $Asc^{\bullet}$ signal, respectively. However, the signal was not significantly changed when a low dose (1 μM) of indomethacin (Figure 5(a)) was used. This result suggests that COX may be involved in the formation of the $Asc^{\bullet}$ in PRP.

3.9. Effect of the Lipoxygenase Inhibitor on Ascorbyl Free Radical Formation in Human Platelet-Rich Plasma. To investigate the involvement of LOX in $Asc^{\bullet}$ formation in PRP, we used AA861 as a nonselective LOX inhibitor. The $Asc^{\bullet}$ signal of a solvent control group was arbitrarily designated 100% and was inhibited by AA861 (1–10 μM) dose dependently (10 μM = 25.7%, $P < 0.001$, Figure 5(b)). This result suggests that LOX may also be involved in the formation of $Asc^{\bullet}$ in PRP.

3.10. Effect of the P450 Inhibitor on Ascorbyl Free Radical Formation in Human Platelet-Rich Plasma. To investigate the involvement of P450 in $Asc^{\bullet}$ formation in PRP, we used clotrimazole as a nonselective P450 inhibitor. As shown in Figure 5(c), 1 and 10 μM clotrimazole produced 13.7% ($P < 0.01$) and 19.5% ($P < 0.01$) depressions of the $Asc^{\bullet}$ signal, respectively.

3.11. Influence of the Mitochondrial Respiratory Chain on Ascorbyl Free Radical Formation in Human Platelet-Rich Plasma. In the mitochondrial respiratory chain, some electrons may leak to oxygen, partially reducing oxygen to a superoxide anion [22]. We determined whether oxidative stress induced by the mitochondrial respiratory chain is associated with $Asc^{\bullet}$ formation in PRP. We used antimycin as a mitochondrial complex III inhibitor. The $Asc^{\bullet}$ signal of a solvent control group was arbitrarily designated 100%, and 10, 30, and 100 μM antimycin, respectively, produced 19.2% ($P < 0.001$), 23.3% ($P < 0.001$), and 32.5% ($P < 0.001$) depressions of the $Asc^{\bullet}$ signal (Figure 6). This indicates that mitochondrial respiratory chain oxidative stress plays a partial role in $Asc^{\bullet}$ formation in PRP.

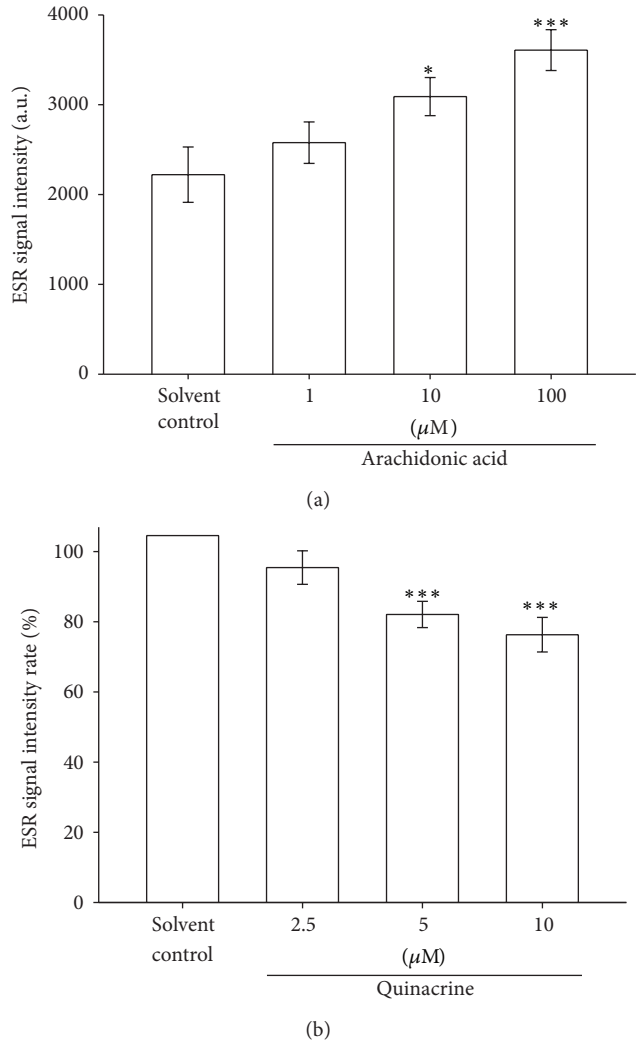

FIGURE 4: Effect of AA (a) and the PLA_2 inhibitor (b) on $Asc^{\bullet}$ formation in human PRP (approximately 8×10^6 platelets/mL). The ESR signal intensity and data in the bar chart are expressed as the means ± SEM ($n \geqq 5$). $^{*}P < 0.05$, $^{***}P < 0.001$ compared with the solvent control group. The instrument parameters were identical to those shown in Figure 1(a).

3.12. Antioxidative Assay of Enzyme Inhibitors. Higashi et al. demonstrated that nordihydroguaiaretic acid, AA-861, and baicalein are LOX inhibitors and also have antioxidant activity [23]. However, Pallast et al. showed that AA-861 inhibits both 12/15-LOX and 5-LOX but does not have antioxidant activity [24]. Therefore, we selected AA-861 as a LOX inhibitor in this study. However, some enzyme inhibitors used in this study still potentially elicit antioxidative effects and inhibit $Asc^{\bullet}$ signal production. To exclude this possibility, we used the Fenton reaction assay to determine whether the enzyme inhibitors were also antioxidants. The enzyme inhibitors were divided into lipid-soluble (Figure 7(a)) and water-soluble (Figure 7(b)) groups. Our result showed that DPI (10 μM), AA861 (10 μM), L-NAME (10 μM), allopurinol (10 μM), clotrimazole (10 μM), indomethacin (10 μM),

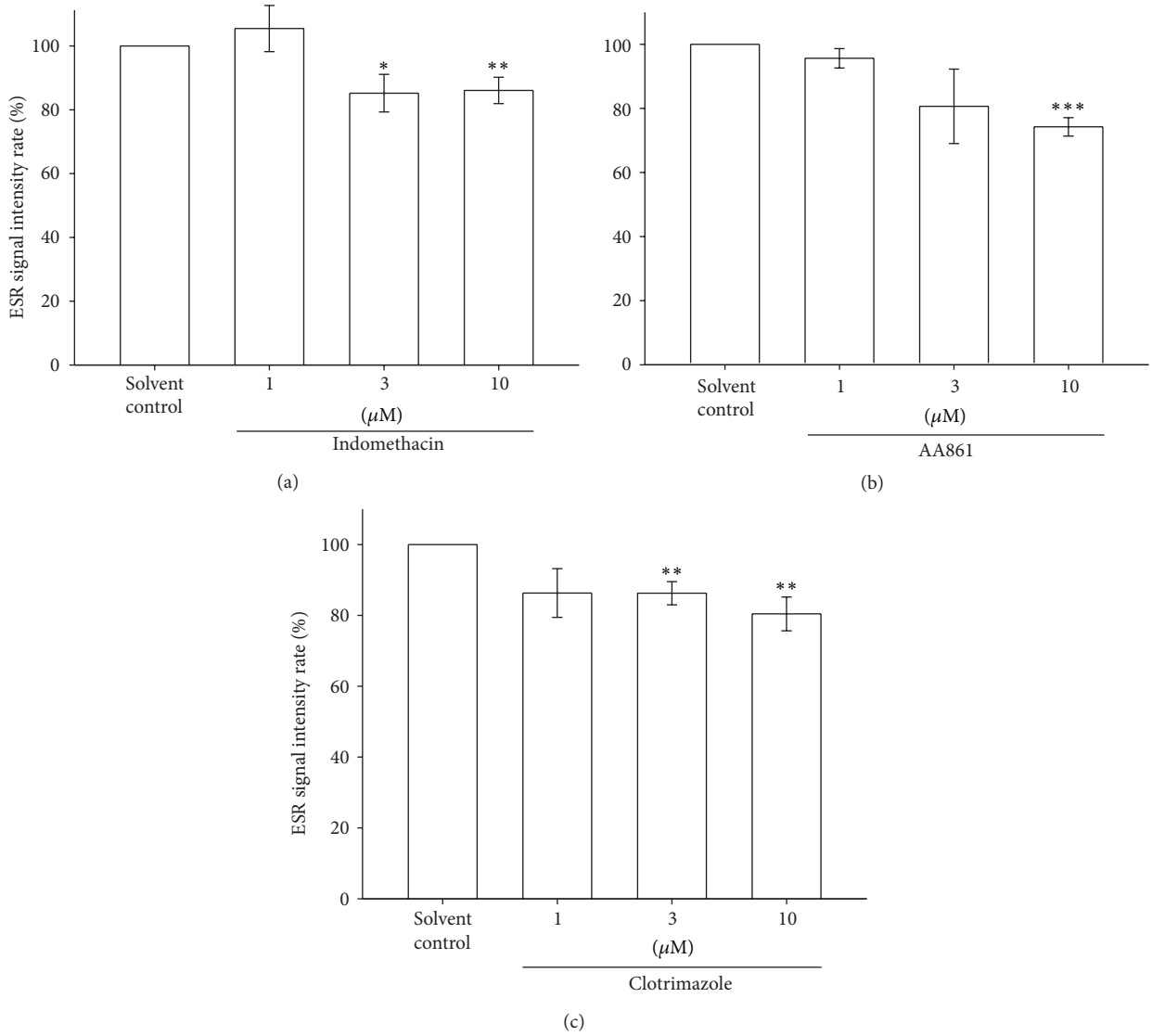

Figure 5: Effect of the COX inhibitor (a), LOX inhibitor (b), and CYP450 inhibitor (c) on $Asc^{\bullet}$ formation in human PRP (approximately 8×10^6 platelets/mL). The ESR spectra are labeled to show their components: DMPO- $Asc^{\bullet}$ adduct (∗). The ESR signal intensity rates and data in the bar chart are expressed as the means ± SEM ($n \geqq 4$). $^{**}P < 0.01$, $^{*}P < 0.05$ compared with the solvent control. The instrument parameters were identical to those shown in Figure 1(a).

quinacrine (10 μM), and antimycin (10 μM) did not exhibit significant antioxidative activity in the Fenton reaction assay ($P > 0.05$).

4. Discussion

The vascular endothelium plays an essential role in regulating vascular tone, modulating vascular growth, platelet aggregation and coagulation, and inflammation. Therefore, the degree of endothelial dysfunction may predict the outcomes of cardiovascular diseases [25]. Although the precise mechanisms of endothelial dysfunction have not been elucidated, a considerable amount of evidence suggests that increased oxidative stress may play a critical role in this state [26]. Oxidative stress can be described as an "imbalance between proxidants and antioxidants in favor of the proxidants, potentially leading to damage" [27]. Currently, reducing oxidative stress remains a prominent objective for cardiovascular prevention and therapy. However, clear knowledge of its source is required to provide novel perspectives for treatment.

ROS participate in the growth, apoptosis, and migration of vascular smooth muscle cells and in the remodeling of the vessel wall. Each of these responses may contribute to vascular diseases in uncontrolled conditions [28]. Therefore, the sources of ROS may be crucial therapeutic targets of cardiovascular disease.

In this study, we found that $Asc^{\bullet}$ signals were observed in PPP and PRP, but not in RBCs or whole blood (Figure 1(a)). A study of ESR spectra of whole blood from normal and tumour bearing patients showed two main lines with g values

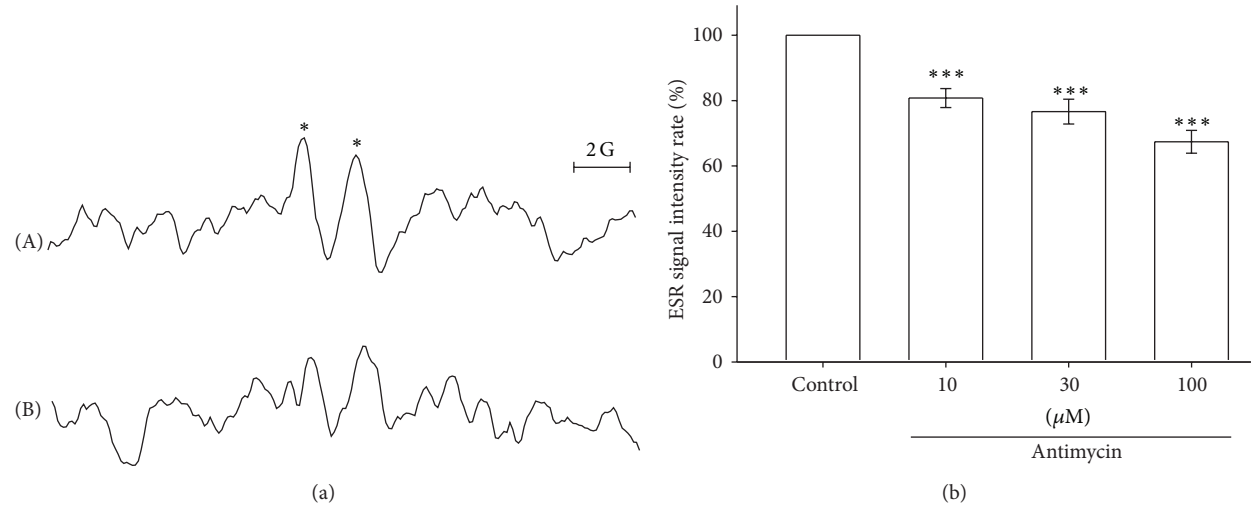

Figure 6: Effect of the mitochondrial complex III inhibitor on $Asc^{\bullet}$ formation in human PRP. The ESR spectra show (a) the effect of a solvent control, (A) 0.6% DMSO, and 10, 30 (data not shown), and (B) 100 μM antimycin in the presence of 100 mM DMPO for 30 min on $Asc^{\bullet}$ formation in human PRP (approximately 8×10^6 platelets/mL). The ESR spectra are labeled to show their components: DMPO- $Asc^{\bullet}$ adduct ($*$). The ESR signal intensity rate and data shown in the bar chart (b) are expressed as the means ± SEM ($n = 6$). $^{***}P < 0.001$ compared with the solvent control. The instrument parameters were identical to those shown in Figure 1.

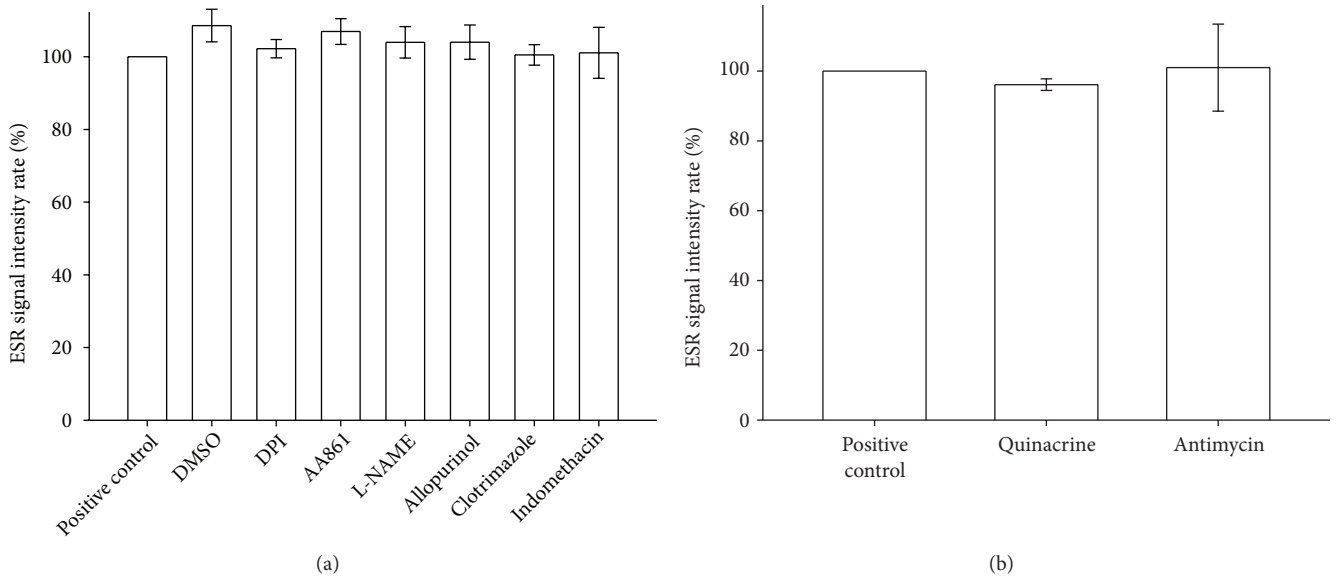

Figure 7: Effect of the fat-soluble (a) and water-soluble (b) enzyme inhibitor on hydroxyl free radical formation in the Fenton reaction. (a) The effect of the Fenton reaction solution (500 μM hydrogen peroxide + 50 μM $FeSO_4$, positive control), 0.6% DMSO, 10 μM DPI, 10 μM AA861, 10 μM L-NAME, 10 μM allopurinol, 10 μM clotrimazole, and 10 μM indomethacin in the presence of 150 mM DMPO for 3 min on hydroxyl radical formation. (b) The effect of the Fenton reaction solution (positive control), 10 μM quinacrine, and 100 μM antimycin in the presence of 150 mM DMPO for 3 min on hydroxyl radical formation. The signal intensity rates and data shown in the bar chart are expressed as the means ± SEM ($n \geqq 3$). $P > 0.05$ compared with the solvent control. The instrument parameters were identical to those shown in Figure 1(a).

of 4.2 and 2.049 [29]. The authors suggested that the line at $g = 2.049$ may be due to the copper protein ceruloplasmin. In addition, smaller signals were found with g values of 2.16, 2.005, and 1.98. We suggest that some paramagnetic species in whole blood with g values nearby 2.0 that restrict the signal intensity of ascorbyl radical. Therefore, in this study, we used ESR spectroscopy in detecting the $Asc^{\bullet}$ to determine the sources of oxidative stress in human PRP. $Asc^{\bullet}$ formation may be induced by nearly all ROS intrinsic to the biological environment, including superoxide radicals, hydroxyl radicals, alkyl peroxyl radicals, lipid peroxyl radicals, peroxynitrite, thiyl radicals, protein radicals, and catalytic metals [7].

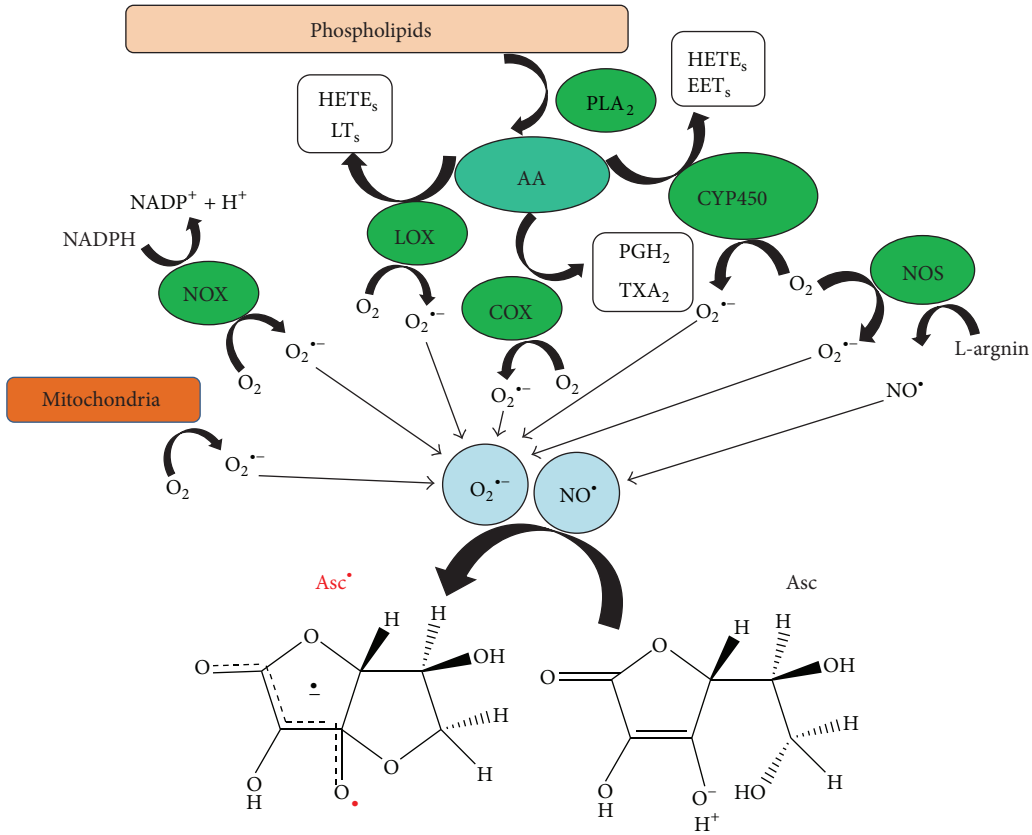

Figure 8: Proposed pathway for the mechanisms of Asc$^{\bullet}$ formation in human PRP ($O_2^{\bullet-}$; superoxide anion; NO; nitric oxide).

In the vasculature wall, ROS are produced by all of the layers, and the major vascular ROS is the superoxide anion, which inactivates NO and, thus, impairs relaxation [30]. Superoxide-generating enzymes involved in increased oxidative stress within vascular tissue include uncoupled NOS, NOX, XO, and mitochondrial superoxide-generating enzymes [31]. In this study, we observed that the AA pathway enzymes, such as COX, LOX, and CYP450, also contributed to the increased oxidative stress in human PRP. However, the XO did not seem to play an important role in this event (Figure 8).

XO is capable of generating superoxide and hydrogen peroxide when supplied with its substrates, xanthine and hypoxanthine, which accumulate during ischemia [32]. Although studies have shown that XO is present in human arterial and venous endothelial cells and can generate sufficient levels of oxygen radicals to trigger endothelial injury, questions remain regarding the role of xanthine and hypoxanthine formation in triggering this process. Because the samples in this study were not subjected to ischemic conditions, we did not observe XO contributing to oxidative stress in human PRP.

NO is released from endothelial cells mainly by eNOS and is a main mediator of endothelium-dependent vasodilatation. When ROS production is increased, tetrahydrobiopterin generation is reduced, causing eNOS to uncouple and produce superoxide; when NO is insufficiently formed or quenched too quickly, the process of atherosclerosis is initiated or accelerated [33]. In pathological conditions, NO may be scavenged by excess ROS generated in blood vessels by vascular NOX [15]. eNOS has been observed not only in the endothelium but also in platelets [34]. Therefore, based on our results, we suggest that platelet eNOS is also a source of ROS in human PRP.

We recently applied ESR spectroscopy in detecting Asc$^{\bullet}$ to investigate the oxidative status of lymphedema, suggesting that COX-derived oxidative stress plays a major role in the pathological mechanisms of surgically induced lymphedema [10]. However, in the current study, COX-derived oxidative stress played only a minor role in oxidative stress in human PRP.

5. Conclusion

In this study, we investigated the potential sources of Asc$^{\bullet}$ production that contribute to oxidative stress in human PRP. We provide evidence that no single source of Asc$^{\bullet}$ can be identified in human PRP, but Asc$^{\bullet}$ are typically generated through NOX, COX, LOX, CYP450, eNOS, and mitochondrial superoxide-generating enzyme pathways.

Conflict of Interests

The authors declare that there is no conflict of interests regarding the publication of this paper.

Acknowledgments

This work was supported by Grants from the National Science Council of Taiwan (NSC97-2320-B-038-016-MY3 and NSC100-2320-B-038-021-MY3) and Shin Kong Wu Ho-Su Memorial Hospital-Taipei Medical University (SKH-TMU-100-12).

References

[1] M. Valko, D. Leibfritz, J. Moncol, M. T. D. Cronin, M. Mazur, and J. Telser, "Free radicals and antioxidants in normal physiological functions and human disease," *International Journal of Biochemistry and Cell Biology*, vol. 39, no. 1, pp. 44–84, 2007.

[2] C. Rice-Evans and N. Miller, "Measurement of the antioxidant status of dietary constituents, low density lipoproteins and plasma," *Prostaglandins Leukotrienes and Essential Fatty Acids*, vol. 57, no. 4-5, pp. 499–505, 1997.

[3] A. N. Kokic, Z. Stevic, S. Stojanovic et al., "Biotransformation of nitric oxide in the cerebrospinal fluid of amyotrophic lateral sclerosis patients," *Redox Report*, vol. 10, no. 5, pp. 265–270, 2005.

[4] J. B. Pristov, I. Spasojevic, Ž. Mikovic, V. Mandic, N. Cerovic, and M. Spasic, "Antioxidative defense enzymes in placenta protect placenta and fetus in inherited thrombophilia from hydrogen peroxide," *Oxidative Medicine and Cellular Longevity*, vol. 2, no. 1, pp. 14–18, 2009.

[5] M. Slavić, I. Appiah, A. Nikolić-Kokić et al., "The anti-oxidative defence system in the isolated rat uterus during spontaneous rhythmic activity," *Acta Physiologica Hungarica*, vol. 93, no. 4, pp. 335–339, 2006.

[6] D. M. Townsend, "S-glutathionylation: indicator of cell stress and regulator of the unfolded protein response," *Molecular Interventions*, vol. 7, no. 6, pp. 313–324, 2008.

[7] I. Spasojević, "Free radicals and antioxidants at a glance using EPR spectroscopy," *Critical Reviews in Clinical Laboratory Sciences*, vol. 48, no. 3, pp. 114–142, 2011.

[8] G. R. Buettner and B. A. Jurkiewicz, "Catalytic metals, ascorbate and free radicals: combinations to avoid," *Radiation Research*, vol. 145, no. 5, pp. 532–541, 1996.

[9] G. R. Buettner and B. A. Jurkiewicz, "Ascorbate free radical as a marker of oxidative stress: an EPR study," *Free Radical Biology and Medicine*, vol. 14, no. 1, pp. 49–55, 1993.

[10] T. C. Chang, Y. H. Uen, C. H. Chou, J. R. Sheu, and D. S. Chou, "The role of cyclooxygenase-derived oxidative stress in surgically induced lymphedema in a mouse tail model," *Pharmaceutical Biology*, vol. 51, no. 5, pp. 573–580, 2013.

[11] M. Edderkaoui, P. Hong, E. C. Vaquero et al., "Extracellular matrix stimulates reactive oxygen species production and increases pancreatic cancer cell survival through 5-lipoxygenase and NADPH oxidase," *American Journal of Physiology*, vol. 289, no. 6, pp. G1137–G1147, 2005.

[12] C.-Y. Hsieh, C.-L. Liu, M.-J. Hsu et al., "Inhibition of vascular smooth muscle cell proliferation by the vitamin E derivative pentamethylhydroxychromane in an in vitro and in vivo study: pivotal role of hydroxyl radical-mediated PLCγ1 and JAK2 phosphorylation," *Free Radical Biology and Medicine*, vol. 49, no. 5, pp. 881–893, 2010.

[13] H. Sakagami, K. Satoh, H. Ohata et al., "Relationship between ascorbyl radical intensity and apoptosis inducing activity," *Anticancer Research*, vol. 16, no. 5 A, pp. 2635–2644, 1996.

[14] C. Vergely, V. Maupoil, M. Benderitter, and L. Rochette, "Influence of the severity of myocardial ischemia on the intensity of ascorbyl free radical release and on postischemic recovery during reperfusion," *Free Radical Biology and Medicine*, vol. 24, no. 3, pp. 470–479, 1998.

[15] R. M. Touyz and E. L. Schiffrin, "Reactive oxygen species in vascular biology: implications in hypertension," *Histochemistry and Cell Biology*, vol. 122, no. 4, pp. 339–352, 2004.

[16] H. Hemila, "Vitamin C and the common cold," *The British Journal of Nutrition*, vol. 67, pp. 3–16, 1992.

[17] C. Kim and M. C. Dinauer, "Impaired NADPH oxidase activity in Rac2-deficient murine neutrophils does not result from defective translocation of p47phox and p67 phox and can be rescued by exogenous arachidonic acid," *Journal of Leukocyte Biology*, vol. 79, no. 1, pp. 223–234, 2006.

[18] A. Shiose and H. Sumimoto, "Arachidonic acid and phosphorylation synergistically induce a conformational change of p47(phox) to activate the phagocyte NADPH oxidase," *The Journal of Biological Chemistry*, vol. 275, no. 18, pp. 13793–13801, 2000.

[19] W. M. Armstead, R. Mirro, D. W. Busija, and C. W. Leffler, "Postischemic generation of superoxide anion by newborn pig brain," *American Journal of Physiology*, vol. 255, no. 2, pp. H401–H403, 1988.

[20] M. Sato, U. Yokoyama, T. Fujita, S. Okumura, and Y. Ishikawa, "The roles of cytochrome P450 in ischemic heart disease," *Current Drug Metabolism*, vol. 12, no. 6, pp. 526–532, 2011.

[21] G. Jin, K. Arai, Y. Murata et al., "Protecting against cerebrovascular injury: contributions of 12/15-lipoxygenase to edema formation after transient focal ischemia," *Stroke*, vol. 39, no. 9, pp. 2538–2543, 2008.

[22] J. F. Turrens, "Mitochondrial formation of reactive oxygen species," *Journal of Physiology*, vol. 552, no. 2, pp. 335–344, 2003.

[23] Y. Higashi, T. Peng, J. Du et al., "A redox-sensitive pathway mediates oxidized LDL-induced downregulation of insulin-like growth factor-1 receptor," *Journal of Lipid Research*, vol. 46, no. 6, pp. 1266–1277, 2005.

[24] S. Pallast, K. Arai, X. Wang, E. H. Lo, and K. Van Leyen, "12/15-Lipoxygenase targets neuronal mitochondria under oxidative stress," *Journal of Neurochemistry*, vol. 111, no. 3, pp. 882–889, 2009.

[25] V. Schächinger, M. B. Britten, and A. M. Zeiher, "Prognostic impact of coronary vasodilator dysfunction on adverse long-term outcome of coronary heart disease," *Circulation*, vol. 101, no. 16, pp. 1899–1906, 2000.

[26] T. Münzel, T. Gori, R. M. Bruno, and S. Taddei, "Is oxidative stress a therapeutic target in cardiovascular disease?" *European Heart Journal*, vol. 31, no. 22, pp. 2741–2749, 2010.

[27] H. Sies, "Oxidative stress: from basic research to clinical application," *American Journal of Medicine*, vol. 91, no. 3, pp. 31S–38S, 1991.

[28] A. Fortuño, G. San José, M. U. Moreno, J. Díez, and G. Zalba, "Oxidative stress and vascular remodelling," *Experimental Physiology*, vol. 90, no. 4, pp. 457–462, 2005.

[29] M. A. Foster, T. Pocklington, J. D. B. Miller, and J. R. Mallard, "A study of electron spin resonance spectra of whole blood from

normal and tumour bearing patients," *British Journal of Cancer*, vol. 28, no. 4, pp. 340–348, 1973.

[30] H. Cai and D. G. Harrison, "Endothelial dysfunction in cardiovascular diseases: the role of oxidant stress," *Circulation Research*, vol. 87, no. 10, pp. 840–844, 2000.

[31] T. Münzel, A. Daiber, V. Ullrich, and A. Mülsch, "Vascular consequences of endothelial nitric oxide synthase uncoupling for the activity and expression of the soluble guanylyl cyclase and the CGMP-dependent protein kinase," *Arteriosclerosis, Thrombosis, and Vascular Biology*, vol. 25, no. 8, pp. 1551–1557, 2005.

[32] J. L. Zweier and M. A. H. Talukder, "The role of oxidants and free radicals in reperfusion injury," *Cardiovascular Research*, vol. 70, no. 2, pp. 181–190, 2006.

[33] T. Münzel, C. Sinning, F. Post, A. Warnholtz, and E. Schulz, "Pathophysiology, diagnosis and prognostic implications of endothelial dysfunction," *Annals of Medicine*, vol. 40, no. 3, pp. 180–196, 2008.

[34] M. W. Radomski, R. M. J. Palmer, and S. Moncada, "An L-arginine/nitric oxide pathway present in human platelets regulates aggregation," *Proceedings of the National Academy of Sciences of the United States of America*, vol. 87, no. 13, pp. 5193–5197, 1990.

Hindawi Publishing Corporation
BioMed Research International
Volume 2014, Article ID 309151, 9 pages
http://dx.doi.org/10.1155/2014/309151

Research Article

Rosiglitazone Increases Cerebral *Klotho* Expression to Reverse Baroreflex in Type 1-Like Diabetic Rats

Li-Jen Chen,[1] Meng-Fu Cheng,[2] Po-Ming Ku,[3] and Jia-Wei Lin[4]

[1] *Institute of Basic Medical Science, College of Medicine, National Cheng Kung University, Tainan 70101, Taiwan*
[2] *Division of Nephrology, Department of Internal Medicine, College of Medicine, National Cheng Kung University, Tainan 70101, Taiwan*
[3] *Department of Cardiology, Chi-Mei Medical Center, Yong Kang, Tainan 71004, Taiwan*
[4] *Department of Neurosurgery, Taipei Medical University-Shuang Ho Hospital, Taipei 23561, Taiwan*

Correspondence should be addressed to Jia-Wei Lin; ns246@tmu.edu.tw

Received 4 November 2013; Accepted 7 January 2014; Published 13 February 2014

Academic Editor: Juei-Tang Cheng

Reduced baroreflex sensitivity (BRS) is widely observed in diabetic human and animals. Rosiglitazone is one of the clinically used thiazolidinediones (TZD) known as PPARγ agonist. Additionally, the klotho protein produced from choroid plexus in the central nervous system is regulated by PPARγ. In an attempt to develop the new therapeutic strategy, we treated streptozotocin-induced diabetic rats (STZ) with rosiglitazone (STZ + TZD) orally at 10 mg/kg for 7 days. Also, STZ rats were subjected to intracerebroventricular (ICV) infusion of recombinant klotho at a dose of 3 μg/2.5 μl via syringe pump (8 μg/hr) daily for 7 days. The BRS and heart rate variability were then estimated under challenge with a depressor dose of sodium nitroprusside (50 μg/kg) or a pressor dose of phenylephrine (8 μg/kg) through an intravenous injection. Lower expression of klotho in medulla oblongata of diabetic rats was identified. Cerebral infusion of recombinant klotho or oral administration of rosiglitazone reversed BRS in diabetic rats. In conclusion, recovery of the decreased klotho in brain induced by rosiglitazone may restore the impaired BRS in diabetic rats. Thus, rosiglitazone is useful to reverse the reduced BRS through increasing cerebral klotho in diabetic disorders.

1. Introduction

Cardiovascular complications influence the prognosis of diabetic disorders and became the main reason for the high mortality of diabetic patients [1, 2]. A number of studies have reported that diabetes mellitus (DM) leads to impairment of the baroreflex control of heart rate (HR) in both diabetic patients and animals. Impairment of the baroreflex sensitivity (BRS) underlying the diabetic state is closely related to life-threatening arrhythmias, heart failure, and sudden death [3, 4].

To minimize the short-term fluctuations of blood pressure and maintain a homeostatic state, a negative feedback system called the baroreflex buffers these short-term changes such as an increased blood pressure which results in slower heart rate and vice versa [5]. Reduced BRS has been characterized in diabetic human [6, 7] and in diabetic rats induced by streptozotocin (STZ) as type 1-like diabetic model [8, 9].

Many factors related to the baroreflex have been mentioned in the central nervous system. The higher baroreflex gain induced by angiotensin has been characterized in rats after an intracerebroventricular (ICV) injection. The development of hypertension in DOCA-salt rats and/or the disorders of chronic heart failure (CHF) were both reduced under higher baroreflex [10, 11]. ICV infusion of leptin ameliorated the variability of heart rate (HR) and the baroreflex sensitivity in STZ-induced diabetic rats [12]. Thus, regulation of baroreflex sensitivity from central nervous system seems important.

The *klotho* gene has been suggested in 1997 using *klotho* mutant mice (*kl/kl* mice) with multiple disorders similar to human premature-aging syndrome [13]. Also, a single nucleotide polymorphism in human *klotho* gene has been mentioned to be associated with the development of hypertension in both Chinese Han [14, 15] and Caucasoid [16–19] subjects. In *kl/kl* mice, alterations occurred mainly in a cell-non-autonomous fashion, while *klotho* gene expression

is predominantly shown in kidney, parathyroid gland, and choroid plexus, although the gene is not expressed in other organs that can be markedly influenced [13]. The choroid plexus may produce cerebrospinal fluid (CSF) for neurons and the secreted klotho protein was observed in CSF [20]. Thus, the klotho in brain can be considered to play a role in the regulation of cardiovascular homeostasis.

klotho has been mentioned as the target of PPARγ [21]. In clinics, agent of TZDs has been used to treat type 2 diabetic patients through correction of both hyperlipidemia and hyperglycemia [22, 23]. Also, TZDs ameliorate the renal injury in STZ-diabetic rats through the anti-inflammatory action [24] or increased PPARγ expression [25]. The renal protection in STZ-diabetic rats by TZDs produced without altering the blood glucose level [26]. Since klotho was the target of PPARγ [21], the higher klotho expression by PPARγ may result in the improvement of dysfunctions in STZ-diabetic rats. The widely used TZDs, including pioglitazone, rosiglitazone, and troglitazone, were demonstrated to increase the expression of klotho, while rosiglitazone was most effective [21]. Thus, we employed rosiglitazone as the representative of TZDs in this study.

The present study is designed to know whether rosiglitazone (TZD) ameliorates the impaired baroreflex sensitivity (BRS) in STZ-induced diabetic rats. We also determined the mediation of klotho in this action because rosiglitazone is known to increase klotho [27]. Then, the role of klotho in BRS could be elucidated in diabetic state.

2. Material and Methods

2.1. Animals. The male Wistar rats, weighing from 200 to 250 g, were obtained from the Animal Center of National Cheng Kung University Medical College. All rats were housed individually in plastic cages under standard laboratory conditions. They were maintained under a 12 h light/dark cycle and had free access to food and water. All experiments were performed under anesthesia with 2% isoflurane, and all efforts were made to minimize the animals' suffering. The animal experiments were approved and conducted in accordance with local institutional guidelines for the care and use of laboratory animals in Chi-Mei Medical Center (number. 100052307) and the experiments conformed to the Guide for the Care and Use of Laboratory Animals as well as the guidelines of the Animal Welfare Act.

2.2. Streptozotocin (STZ) Induced Type 1-Like Diabetic Rats. Diabetic model was induced by an intravenous (i.v.) injection of STZ (Sigma-Aldrich Inc., USA) at 65 mg/kg into the fasting Wistar rats as described previously [28]. The animals were considered to be diabetic if they showed a plasma glucose concentration over 350 mg/dL in addition to the diabetic syndromes.

The plasma glucose levels were measured in blood samples collected from the femoral veins of anesthetized rats. Body weight was also monitored during the experiment. At the end of treatment, animals were sacrificed, and the tissues were dissected, washed with saline, and weighed. For further analysis, samples were frozen in liquid nitrogen for storage at −80°C.

Blood samples from rats were centrifuged at 12,000 g for 3 minutes. Samples were then analyzed using the glucose kit reagents (AppliedBio assay kits; Hercules, CA, USA). The level of plasma glucose was then estimated using an autoanalyzer (Quik-Lab, USA) and measured in duplicate.

2.3. Drug Administration. The age-matched rats were divided into three groups ($n = 8$): vehicle-treated normal rats (Wistar); vehicle-treated STZ rats (STZ); and TZD-treated STZ rats (STZ + TZD) through oral intake of 10 mg/kg rosiglitazone (Avandia) daily for seven days as described previously [29, 30].

2.4. Western Blotting Analysis. Protein was extracted from tissue homogenates using ice-cold radioimmuno-precipitation assay (RIPA) buffer supplemented with phosphatase and protease inhibitors (50 mmol/L sodium vanadate, 0.5 mM phenylmethylsulphonyl fluoride, 2 mg/mL aprotinin, and 0.5 mg/mL leupeptin). The protein concentrations were determined using a Bio-Rad protein assay (Bio-Rad Laboratories, Inc., Hercules, CA, USA). Total proteins (30 μg) were then separated using SDS/polyacrylamide gel electrophoresis (10% acrylamide gel) through a Bio-Rad Mini-Protean II system. The protein was transferred to expanded polyvinylidene difluoride membranes (Pierce, Rockford, IL, USA) with a Bio-Rad Trans-Blot system. The membrane was blocked with 5% nonfat milk in phosphate-buffered saline containing 0.1% Tween 20 (PBS-T) and incubated for two hours. The membrane was then washed in PBS-T and hybridized with primary antibodies, specific antibodies for klotho, which were diluted to a suitable concentration (1 : 1000) in PBS-T for 16 hours. Incubation with secondary antibodies and detection of the antigen-antibody complex were performed using an ECL kit (Amersham Biosciences, UK). The immunoblot densities at 130 KD were quantified using a laser densitometer. Expression of β-actin was used as the internal standard.

2.5. Intracerebroventricular (ICV) Injection. Following to the previous method [12], the well-anesthetized rats were immobilized in a stereotaxic frame to prepare for ICV injection. Then, the age-matched rats were divided into four groups ($n = 8$): normal rats (Wistar); STZ rats (STZ); rat IgG (IgG)-treated STZ rats (STZ + IgG); and recombinant klotho (rKl)-treated STZ rats (STZ + rKl). Rat rKl or rat IgG (Abcam, Cambridge, MA, USA) was dissolved in artificial cerebrospinal fluid (ACSF) at a dose of 3 μg/2.5 μL for ICV infusion using syringe pump (Harvard Apparatus, Holliston, MA, USA) (8 μg/hr) for seven days according to the previous reports [12, 31, 32].

2.6. Arterial Pressure and Heart Rate Recording. The rats were anesthetized with 2% isoflurane, and a catheter was inserted into the femoral artery for recording of blood pressure and heart rate. The catheters were made of 4 cm segments of PE-10 polyethylene (Clay Adams, USA) that was heat-bound to a 13 cm segment of PE-50 (Clay Adams, USA). After surgery,

the animals were allowed 20 min to adapt the experimental conditions, such as sound and illumination. Another 15 min period was allowed before beginning of experiment. The pressure catheter was connected to an external computer (IX-214; iWorx Systems, Inc., Dover, NH, USA) to acquire all signals. The mean arterial pressure (MAP) and heart rate (HR) were derived from Labscribe2 (iWorx Systems, Inc., Dover, NH, USA) [33, 34].

2.7. Baroreflex Challenge and Evaluation. According to previous methods [33, 34], the baroreflex response was challenged using a pressor dose of 0.1 mL phenylephrine (PE; 8 μg/kg IV) or a depressor dose of 0.1 mL sodium nitroprusside (SNP; 50 μg/kg IV). The baroreflex sensitivity (BRS) was then calculated as the derivative of the HR in the function of the MAP variation (ΔHR/ΔMAP). The bradycardic and tachycardic peaks were also analyzed to determine the HR range and the difference between two peaks, as described previously [33, 34].

2.8. Statistical Analysis. All data are expressed as the mean ± standard error (SE) of each group. Using the Microsoft excel, statistical analysis was performed by the one-way ANOVA and the significance was obtained from the level at $2\alpha = 0.05$.

3. Results

3.1. Klotho Expression in the Medulla Oblongata of STZ-Diabetic Rats. Expressions of the klotho protein in the medulla oblongata between Wistar rats and STZ-diabetic rats were compared using Western blotting analysis. The expression of klotho protein in the medulla oblongata was significantly lower in STZ-diabetic rats than normal Wistar rats (Figure 1).

3.2. ICV Injection of Recombinant klotho Restored the Baroreflex Responses in STZ-Diabetic Rats. As shown in Table 1, the basal MAP and HR were markedly different between STZ-diabetic rats and Wistar rats. Additionally, after challenging the baroreflex, there is no marked difference on the values of bradycardic peak between Wistar and STZ group. However, the tachycardic peak was significantly reduced in STZ-diabetic rats, the values of HR range were markedly lower in STZ-diabetic rats than in normal Wistar rats. These changes in STZ group were restored by the ICV infusion of rKl, but they were not modified by IgG infusion, without altering the blood glucose level. The baroreflex gain resulting from challenge with PE or SNP was significantly reduced in the STZ group. This decrease in the baroreflex gain was also restored by the ICV infusion of rKl (Figures 2(a) and 2(b)).

3.3. Effect of TZD on the Expression of klotho in Medulla Oblongata of STZ Rats. Changes of klotho expression in the medulla oblongata from STZ-diabetic rats were also identified using Western blots. After oral administration of rosiglitazone (TZD) for 7 days, the decreased klotho expression was also significantly reversed in the medulla oblongata of STZ-diabetic rats (Figure 3).

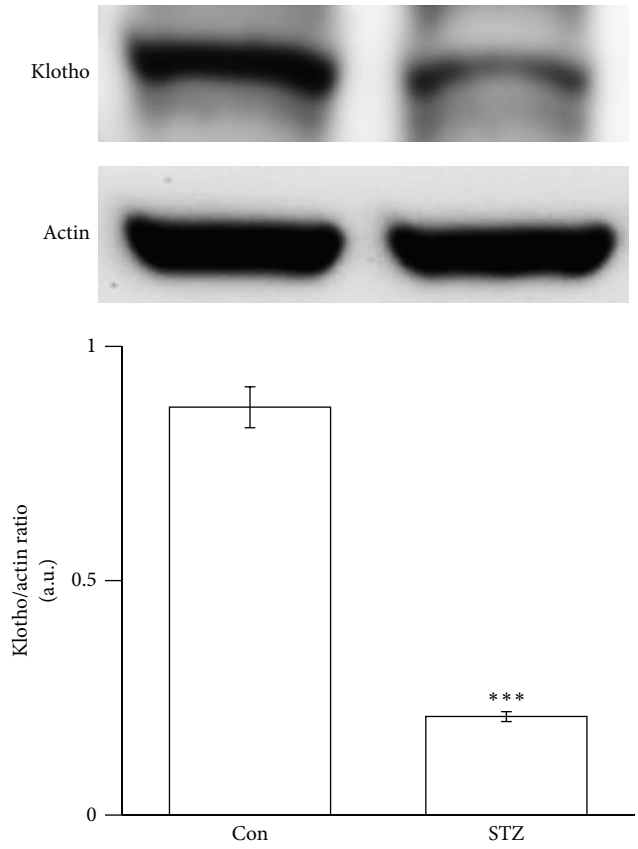

Figure 1: Klotho protein expressions in the medulla oblongata of STZ-diabetic rats. Expression of klotho protein (130 kDa) in Wistar rats (Wistar) and STZ-diabetic rats (STZ) was identified using Western blotting analysis. Samples were prepared from the medulla oblongata. The corresponding β-actin (Actin) protein level was used as an internal control. The quantification of protein levels was expressed as klotho over β-actin. The quantification is indicated as the means with the SE ($n = 8$ per group) in each column shown in the lower panel. $^{***}P < 0.001$ compared to Wistar.

3.4. The Baroreflex Response is Restored in STZ Rats after Oral Administration of TZD. As shown in Table 2, the basal MAP and HR were significantly normalized in the STZ-diabetic rats treated with rosiglitazone (TZD). Additionally, there is no marked difference on the values of the bradycardic peak between each group. However, the tachycardic peak was significantly restored in the STZ + TZD group as compared to STZ group and showing a significant difference in the HR range. The baroreflex gain resulting from PE or SNP challenge was both restored in the STZ + TZD group (Figures 4(a) and 4(b)). PE-induced increase of MAP was lower in STZ + TZD group than that in STZ group. Then, the bradycardic reflex responses to PE were markedly lower in the STZ + TZD group than that in the STZ group (Figure 4(a)). Intravenous injection of SNP produced a vasodepressor response; the value of MAP was still higher in STZ + TZD group than in STZ group. Moreover, the tachycardic reflex in response to SNP challenge was restored in STZ + TZD group (Figure 4(b)). Thus, the baroreflex gain was significantly restored in STZ-diabetic rats treated with TZD without altering the blood glucose level.

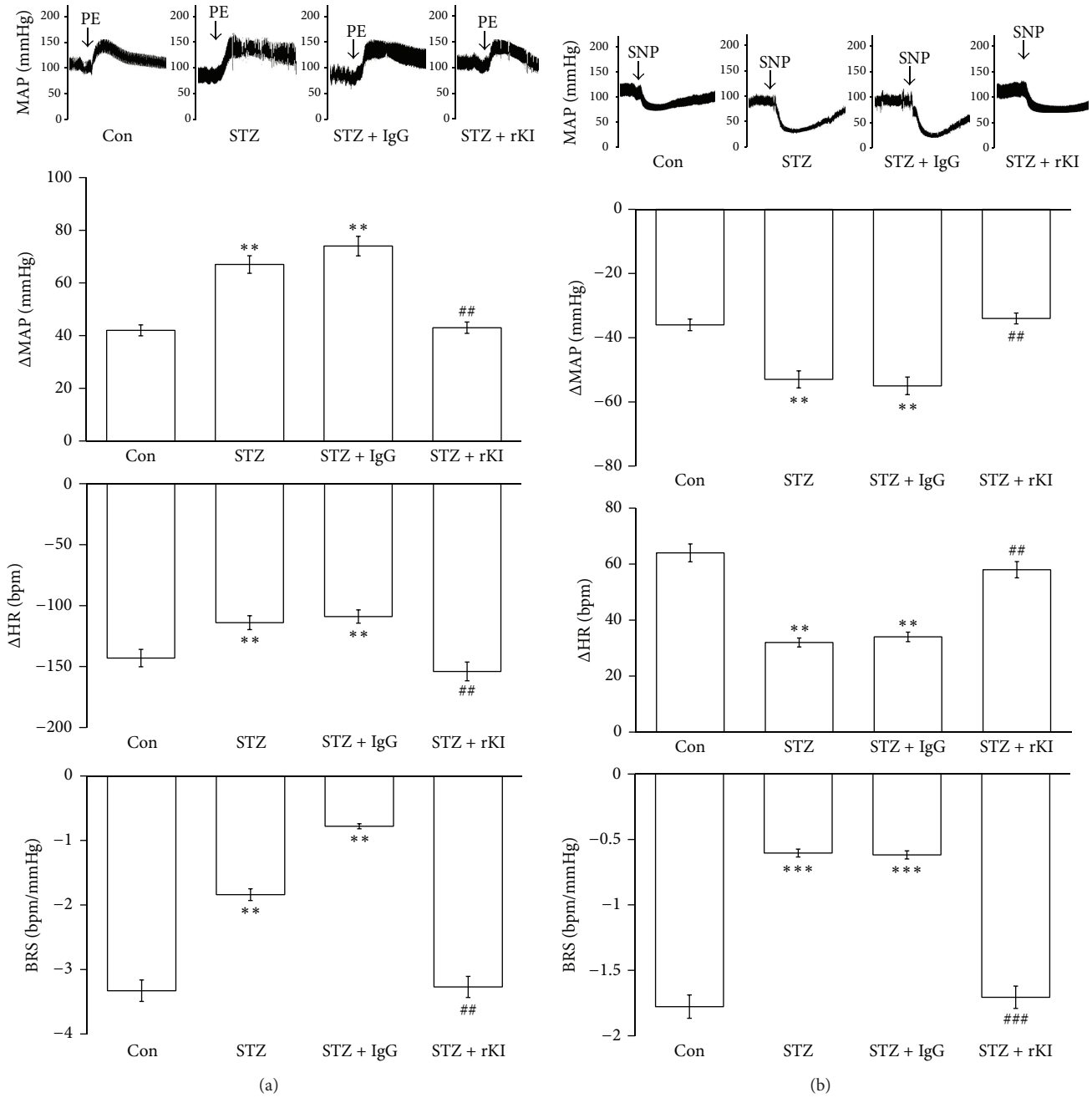

Figure 2: Effect of recombinant klotho (rKl) on the sensitivity of the baroreflex in STZ-diabetic rats. The effect of rKl or rat IgG (IgG) on the mean arterial pressure (MAP, mmHg), heart rate (HR, bpm), and baroreflex sensitivity (BRS, bpm/mmHg) in response to phenylephrine (PE, 8 μg/kg, IV) (a) or (SNP, 50 μg/kg, IV) (b) in each group; Con means control, STZ shows STZ-diabetic rats, STZ + IgG is IgG-treated group and STZ + rKl indicates the recombinant klotho-treated STZ group. The quantification is indicated as the means with the SE ($n = 8$ per group) in each column shown in the lower panel. $^{**}P < 0.01$ and $^{***}P < 0.001$ compared to Wistar.

4. Discussion

In the present study, we demonstrate, for the first time, that the expression of klotho protein was significantly lower in the medulla oblongata of STZ-diabetic rats than normal Wistar rats. The baroreflex gain in response to challenge with PE or SNP was also reduced in STZ-diabetic rats compared to normal rats. We infused recombinant klotho into the brain of this type 1-like diabetic animal to restore the baroreflex responses without correcting blood glucose. Additionally, the expression klotho was significantly reversed in diabetic rats receiving rosiglitazone (TZD). The baroreflex responses triggered by PE or SNP were also increased in STZ-diabetic rats treated with rosiglitazone without changing blood

Table 1: Baseline level of the blood glucose, mean arterial pressure (MAP) and heart rate (HR), bradycardic and tachycardic peak, and HR range in STZ rats receiving rat IgG (IgG) or recombinant klotho (rKl).

Variable	Wistar	STZ	STZ + IgG	STZ + rKl
Blood glucose (mg/dL)	103 ± 4.3	363 ± 13.6***	362 ± 9.1***	368 ± 5.4***
MAP (mmHg)	112.8 ± 3.17	89.2 ± 2.74**	91.4 ± 3.82**	104.9 ± 7.21$^{\#}$
HR (bpm)	343 ± 7.2	281 ± 5.4***	283 ± 8.2***	308 ± 9.4$^{\#}$
Bradycardic peak (bpm)	243 ± 4.3	247 ± 7.2	243 ± 5.8	248 ± 4.7
Tachycardic peak (bpm)	442 ± 7.6	352 ± 7.4**	347 ± 6.6**	426 ± 5.4$^{\#\#}$
HR range (bpm)	194 ± 6.8	103 ± 8.7***	102 ± 5.3***	173 ± 8.9$^{\#\#}$

Values (mean ± SE) were obtained from each group of eight rats. $^{*}P < 0.05$, $^{**}P < 0.01$, and $^{***}P < 0.001$ compared to Wistar. $^{\#}P < 0.05$ and $^{\#\#}P < 0.01$ compared to STZ.

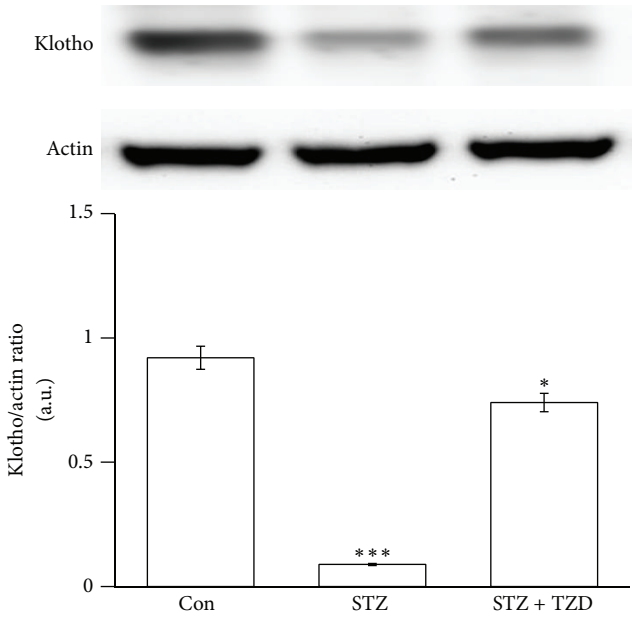

Figure 3: Effect of TZD on the expression of klotho in the medulla oblongata of STZ-diabetic rats. The upper shows the klotho protein level (Klotho) or the corresponding β-actin (Actin) level as internal control in the medulla oblongata isolated from Wistar rats (Con) and STZ-diabetic rats receiving TZD (STZ + TZD) or not (STZ). The treatments are described in materials and methods. Quantification of protein levels using klotho over β-actin to show the means with SE ($n = 8$ per group) in each column are indicated in the lower panel. $^{**}P < 0.01$ and $^{***}P < 0.001$ compared to control (Con).

Table 2: Baseline level of the blood glucose, mean arterial pressure (MAP) and heart rate (HR), bradycardic and tachycardic peak, and HR range in STZ rats receiving the rosiglitazone (TZD) or not.

Variable	Wistar	STZ	STZ + TZD
Blood glucose (mg/dL)	98 ± 3.7	367 ± 11.4***	361 ± 10.3***
MAP (mmHg)	109.8 ± 4.4	87.6 ± 5.7**	95.4 ± 7.3$^{*\#}$
HR (bpm)	351 ± 8.3	287 ± 4.8***	316 ± 7.4$^{*\#}$
Bradycardic peak (bpm)	248 ± 7.3	242 ± 6.2	245 ± 4.3
Tachycardic peak (bpm)	437 ± 8.5	363 ± 4.7**	392 ± 11.6$^{*\#}$
HR range (bpm)	188 ± 8.2	123 ± 4.9**	142 ± 7.3$^{*\#}$

Values (mean ± SE) were obtained from each group of eight rats. $^{*}P < 0.05$, $^{**}P < 0.01$, and $^{***}P < 0.001$ compared to Wistar. $^{\#}P < 0.05$ compared to STZ.

glucose level. Thus, rosiglitazone has an ability to restore the reduced baroreflex responses through increase of cerebral klotho in diabetic rats.

Mutation of klotho may result in many aging-related disorders in animals; the expression of *klotho* gene is only identified in some tissues in mice, rats, and humans [35]. The klotho is documented to predominantly express in kidney and choroid plexus of the brain, although a slight expression of klotho has also been observed in the pituitary gland, placenta, skeletal muscle, colon, urinary bladder, pancreas, testis, ovary, and inner ear [13, 36]. CSF from choroid plexus is known to serve as the extracellular fluid for neurons [37]. Thus, klotho protein is suggested as a humoral factor [38] and it is detectable in CSF [20]. In the present study, we observed the reduced expression of klotho in the medulla oblongata of diabetic rats and this view has not been mentioned before.

Single nucleotide polymorphisms of the human *klotho* gene are associated with the development of cardiovascular diseases in both Chinese Han [14, 15] and Caucasoid [16–19] subjects. Baroreflex dysfunction observed in diabetic subjects has important clinical implications, because the baroreflex included an important system that acts against wide oscillations in arterial pressure (AP). Additionally, clinical trials have shown an association between baroreflex dysfunctions [39, 40]. Studies using experimental animals have been conducted to investigate the mechanisms of cardiovascular reflex dysfunction in diabetes [41]. It has been demonstrated that, in STZ-induced experimental diabetes, baroreflex control of circulation was impaired. In this study, we provide the first demonstration of a marked decrease of klotho in the medulla oblongata of STZ-diabetic rats. Also, we challenged the baroreflex response using a pressor dose of 0.1 mL phenylephrine (PE; 8 μg/kg IV) or a depressor dose of 0.1 mL SNP (50 μg/kg) according to previous reports [33, 34]. The baroreflex sensitivity (BRS) was calculated as the derivative of the HR in function of the MAP variation (ΔHR/ΔMAP). The tachycardic and the bradycardic peaks were also analyzed. The basal MAP and HR were significantly lower in STZ group than in the normal group. The pressor

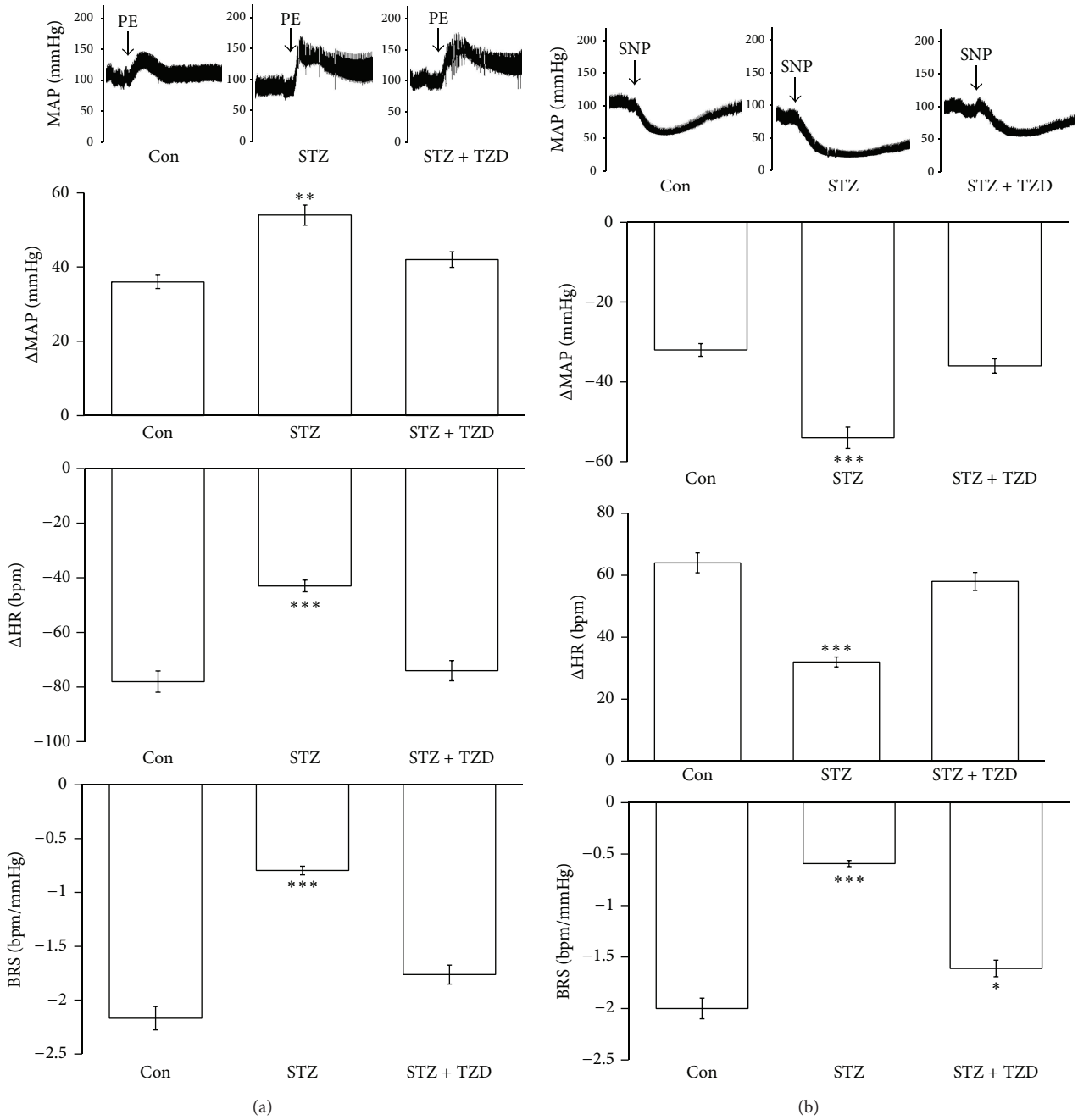

Figure 4: Effect of TZD on the sensitivity of the baroreflex in STZ-diabetic rats. The effect on the mean arterial pressure (MAP, mmHg), heart rate (HR, bpm), and baroreflex sensitivity (BRS, bpm/mmHg) in response to phenylephrine (PE, 8 μg/kg, IV) (a) or (SNP, 50 μg/kg, IV) (b) in each group including Wistar rats (Con) and STZ-diabetic rats receiving TZD (STZ + TZD) or not (STZ). The quantification is indicated as the means with the SE (n = 8 per group) in each column shown in the lower panel. $^{**}P < 0.01$ and $^{***}P < 0.001$ compared to control.

responses to PE were more marked in the STZ group than in the normal group, whereas the bradycardic reflex was reduced in the STZ group. The baroreflex gain was also attenuated in the STZ group. Similar changes were noted in the SNP-challenged STZ group. These results are consistent with a previous report [27]. However, there was no difference on bradycardiac peak between normal and STZ groups. The baseline heart rate values in STZ rats were alternatively lower than that in normal rats. It is may be the reason why there is no differences in bradycardiac peak between normal and STZ groups. However, the heart rate range still decreased in STZ group. Additionally, the decreased baroreflex responses were restored by the recombinant klotho infused into the brains of STZ group by ICV injection. Thus, increase of cerebral klotho appears to be useful in the recovery of the lowered baroreflex sensitivity.

Actually, STZ-diabetic rats treated with rosiglitazone result in an increase of klotho expression in the medulla oblongata (Figure 3). Then, we evaluated the effect of rosiglitazone on baroreflex responses in STZ-diabetic rats. The basal MAP and HR in diabetic rats were both increased by rosiglitazone near to the values in normal rats. Additionally, the pressor responses to PE were reduced to normal rats in the STZ + TZD group; the bradycardic reflex and baroreflex gain were both restored in the STZ + TZD group. Similar changes were also noted in the SNP-challenged baroreflex gain in STZ-diabetic rats. Thus, treatment of rosiglitazone or TZD seems beneficial in the recovery of baroreflex sensitivity in STZ-diabetic rats without changing blood glucose. Taken together, we demonstrated that the higher the expression of klotho by rosiglitazone the more restored the baroreflex in STZ-diabetic rats. However, the molecular mechanisms underlying the regulation of the baroreflex by klotho remain unclear and it needs more investigations in the future. Rosiglitazone has been demonstrated to be able to cross the blood brain barrier and that it is not exported out of the brain [42]. Some studies also demonstrated the neuroprotective merits of TZDs in animal models including focal ischemia, Parkinson's disease, and ALS [43–46]. The neuroprotective effects are introduced to be associated with PPARγ mediated suppression of the inflammatory pathway [47] or by increasing antioxidant-like activities [48]. Taken together, there is no doubt that rosiglitazone can enter into central nervous system.

5. Conclusions

We found that klotho expression in the medulla oblongata was reduced in STZ-diabetic rats. This is associated with the lower baroreflex response in STZ-diabetic rats because baroreflex was restored by the oral administration of rosiglitazone or treatment with the recombinant klotho through ICV infusion to higher cerebral klotho. Thus, rosiglitazone or TZDs is useful to reverse the reduced BRS through higher cerebral klotho in diabetic disorders.

Conflict of Interests

The authors declare that there is no conflict of interests regarding the publication of this paper.

Authors' Contribution

Li-Jen Chen and Meng-Fu Cheng contributed equally (L.J.C. & M.F.C.).

Acknowledgments

The authors thank Pei-Lin Chou, Shan-Yuan Liang, and Yi-Zhi Chen for their assistance in their experiments. The present study was supported in part by a Grant from the Chi-Mei Medical Center (CMFHR10158) in Taiwan.

References

[1] R. Kawasaki, S. Tanaka, S. Tanaka et al., "Risk of cardiovascular diseases is increased even with mild diabetic retinopathy: the Japan Diabetes Complications Study," *Ophthalmology*, vol. 120, no. 3, pp. 574–582, 2013.

[2] S. H. Ko and S. H. Ko, "Letter: diabetic polyneuropathy and cardiovascular complications in type 2 diabetic patients (diabetes metab j 2011,35:390-6)," *Diabetes and Metabolism Journal*, vol. 35, no. 5, pp. 558–560, 2011.

[3] A. A. El-Menyar, "Dysrhythmia and electrocardiographic changes in diabetes mellitus: pathophysiology and impact on the incidence of sudden cardiac death," *Journal of Cardiovascular Medicine*, vol. 7, no. 8, pp. 580–585, 2006.

[4] M. T. La Rovere, G. D. Pinna, S. H. Hohnloser et al., "Barorefiex sensitivity and heart rate variability in the identification of patients at risk for life-threatening arrhythmias: implications for clinical trials," *Circulation*, vol. 103, no. 16, pp. 2072–2077, 2001.

[5] A. Silvani, E. Magosso, S. Bastianini, P. Lenzi, and M. Ursino, "Mathematical modeling of cardiovascular coupling: central autonomic commands and baroreflex control," *Autonomic Neuroscience*, vol. 162, no. 1-2, pp. 66–71, 2011.

[6] A. Frattola, G. Parati, P. Gamba et al., "Time and frequency domain estimates of spontaneous baroreflex sensitivity provide early detection of autonomic dysfunction in diabetes mellitus," *Diabetologia*, vol. 40, no. 12, pp. 1470–1475, 1997.

[7] D. L. Eckberg, S. W. Harkins, and J. M. Fritsch, "Baroreflex control of plasma norepinephrine and heart period in health subjects and diabetic patients," *Journal of Clinical Investigation*, vol. 78, no. 2, pp. 366–374, 1986.

[8] R. Fazan Jr., V. J. Dias Da Silva, G. Ballejo, and H. C. Salgado, "Power spectra of arterial pressure and heart rate in streptozotocin-induced diabetes in rats," *Journal of Hypertension*, vol. 17, no. 4, pp. 489–495, 1999.

[9] H. Y. Chen, J. S. Wu, J. J. Chen, and J. T. Cheng, "Impaired regulation function in cardiovascular neurons of nucleus tractus solitarii in streptozotocin-induced diabetic rats," *Neuroscience Letters*, vol. 431, no. 2, pp. 161–166, 2008.

[10] P. S. Guimaraes, N. M. Santiago, C. H. Xavier et al., "Chronic infusion of angiotensin-(1–7) into the lateral ventricle of the brain attenuates hypertension in DOCA-salt rats," *American Journal of Physiology*, vol. 303, pp. H393–H400, 2012.

[11] S. Kar, L. Gao, D. A. Belatti, P. L. Curry, and I. H. Zucker, "Central angiotensin (1–7) enhances baroreflex gain in conscious rabbits with heart failure," *Hypertension*, vol. 58, no. 4, pp. 627–634, 2011.

[12] J. M. do Carmo, J. E. Hall, and A. A. da Silva, "Chronic central leptin infusion restores cardiac sympathetic-vagal balance and baroreflex sensitivity in diabetic rats," *American Journal of Physiology*, vol. 295, no. 5, pp. H1974–H1981, 2008.

[13] M. Kuro-o, Y. Matsumura, H. Aizawa et al., "Mutation of the mouse klotho gene leads to a syndrome resembling ageing," *Nature*, vol. 390, no. 6655, pp. 45–51, 1997.

[14] C. Xu, R. J. Song, J. Yang et al., "Klotho gene polymorphism of rs3752472 is associated with the risk of urinary calculi in the population of Han nationality in Eastern China," *Gene*, vol. 526, no. 2, pp. 494–497, 2013.

[15] H. L. Wang, Q. Xu, Z. Wang et al., "A potential regulatory single nucleotide polymorphism in the promoter of the Klotho gene may be associated with essential hypertension in the Chinese Han population," *Clinica Chimica Acta*, vol. 411, no. 5-6, pp. 386–390, 2010.

[16] N. Tangri, A. Alam, E. C. Wooten, and G. S. Huggins, "Lack of association of Klotho gene variants with valvular and vascular calcification in Caucasians: a candidate gene study of the Framingham Offspring Cohort," *Nephrology Dialysis Transplantation*, vol. 26, no. 12, pp. 3998–4002, 2011.

[17] F. Zhang, G. Zhai, B. S. Kato et al., "Association between KLOTHO gene and hand osteoarthritis in a female Caucasian population," *Osteoarthritis and Cartilage*, vol. 15, no. 6, pp. 624–629, 2007.

[18] R. M. Freathy, M. N. Weedon, D. Melzer et al., "The functional "KL-VS" variant of KLOTHO is not associated with type 2 diabetes in 5028 UK Caucasians," *BMC Medical Genetics*, vol. 7, p. 51, 2006.

[19] K. Kawano, N. Ogata, M. Chiano et al., "Klotho gene polymorphisms associated with bone density of aged postmenopausal women," *Journal of Bone and Mineral Research*, vol. 17, no. 10, pp. 1744–1751, 2002.

[20] A. Imura, A. Iwano, O. Tohyama et al., "Secreted Klotho protein in sera and CSF: implication for post-translational cleavage in release of Klotho protein from cell membrane," *FEBS Letters*, vol. 565, no. 1–3, pp. 143–147, 2004.

[21] H. Zhang, Y. Li, Y. Fan et al., "Klotho is a target gene of PPAR-γ," *Kidney International*, vol. 74, no. 6, pp. 732–739, 2008.

[22] Y. Zhang and Y. Guan, "PPAR-γ agonists and diabetic nephropathy," *Current Diabetes Reports*, vol. 5, no. 6, pp. 470–475, 2005.

[23] Y. Guan, "Peroxisome proliferator-activated receptor family and its relationship to renal complications of the metabolic syndrome," *Journal of the American Society of Nephrology*, vol. 15, no. 11, pp. 2801–2815, 2004.

[24] S. Ohga, K. Shikata, K. Yozai et al., "Thiazolidinedione ameliorates renal injury in experimental diabetic rats through anti-inflammatory effects mediated by inhibition of NF-κB activation," *American Journal of Physiology*, vol. 292, no. 4, pp. F1141–F1150, 2007.

[25] M. Sommer and G. Wolf, "Rosiglitazone increases PPARγ in renal tubular epithelial cells and protects against damage by hydrogen peroxide," *American Journal of Nephrology*, vol. 27, no. 4, pp. 425–434, 2007.

[26] K. C. Huang, Y. G. Cherng, L. J. Chen, C. T. Hsu, and J. T. Cheng, "Rosiglitazone is effective to improve renal damage in type-1-like diabetic rats," *Hormone and Metabolic Research*, 2013.

[27] K. S. Chang and D. D. Lund, "Alterations in the baroreceptor reflex control of heart rate in streptozotocin diabetic rats," *Journal of Molecular and Cellular Cardiology*, vol. 18, no. 6, pp. 617–624, 1986.

[28] J. T. Cheng, C. C. Huang, I.-M. Liu, T. F. Tzeng, and C. J. Chang, "Novel mechanism for plasma glucose-lowering action of metformin in streptozotocin-induced diabetic rats," *Diabetes*, vol. 55, no. 3, pp. 819–825, 2006.

[29] G. Y. Liu and Z. M. An, "Protective effect of rosiglitazone sodium on islet b~-cell of stz induced diabetic rats through jnk pathway," *Journal of Sichuan University*, vol. 40, no. 3, pp. 430–434, 2009.

[30] C. Tikellis, K. A. Jandeleit-Dahm, K. Sheehy et al., "Reduced plaque formation induced by rosiglitazone in an STZ-diabetes mouse model of atherosclerosis is associated with downregulation of adhesion molecules," *Atherosclerosis*, vol. 199, no. 1, pp. 55–64, 2008.

[31] E. K. Kim, I. Miller, S. Aja et al., "C75, a fatty acid synthase inhibitor, reduces food intake via hypothalamic AMP-activated protein kinase," *Journal of Biological Chemistry*, vol. 279, no. 19, pp. 19970–19976, 2004.

[32] D. R. Oliveira, R. A. S. Santos, G. F. F. Santos, M. C. Khosla, and M. J. Campagnole-Santos, "Changes in the baroreflex control of heart rate produced by central infusion of selective angiotensin antagonists in hypertensive rats," *Hypertension*, vol. 27, no. 6, pp. 1284–1290, 1996.

[33] V. E. Valenti, C. Ferreira, A. Meneghini et al., "Evaluation of baroreflex function in young spontaneously hypertensive rats," *Arquivos Brasileiros de Cardiologia*, vol. 92, no. 3, pp. 210–215, 2009.

[34] V. E. Valenti, C. Imaizumi, L. C. De Abreu, E. Colombari, M. A. Sato, and C. Ferreira, "Intra-strain variations of baroreflex sensitivity in young Wistar-Kyoto rats," *Clinical and Investigative Medicine*, vol. 32, no. 6, pp. E251–E257, 2009.

[35] Y. Wang and Z. Sun, "Current understanding of klotho," *Ageing Research Reviews*, vol. 8, no. 1, pp. 43–51, 2009.

[36] M. Kamemori, Y. Ohyama, M. Kurabayashi, K. Takahashi, R. Nagai, and N. Furuya, "Expression of Klotho protein in the inner ear," *Hearing Research*, vol. 171, no. 1-2, pp. 103–110, 2002.

[37] K. Takeshita, T. Fujimori, Y. Kurotaki et al., "Sinoatrial node dysfunction and early unexpected death of mice with a defect of klotho gene expression," *Circulation*, vol. 109, no. 14, pp. 1776–1782, 2004.

[38] Y. Saito, T. Yamagishi, T. Nakamura et al., "Klotho protein protects against endothelial dysfunction," *Biochemical and Biophysical Research Communications*, vol. 248, no. 2, pp. 324–329, 1998.

[39] K. De Angelis, M. C. Irigoyen, and M. Morris, "Diabetes and cardiovascular autonomic dysfunction: application of animal models," *Autonomic Neuroscience*, vol. 145, no. 1-2, pp. 3–10, 2009.

[40] M. Malik and J. T. Bigger Jr., "Heart rate variability. Standards of measurement, physiological interpretation, and clinical use. Task Force of the European Society of Cardiology and the North American Society of Pacing and Electrophysiology," *European Heart Journal*, vol. 17, no. 3, pp. 354–381, 1996.

[41] C. Y. Maeda, T. G. Fernandes, H. B. Timm, and M. C. Irigoyen, "Autonomic dysfunction in short-term experimental diabetes," *Hypertension*, vol. 26, no. 6, pp. 1100–1104, 1995.

[42] J. Gamboa, D. A. Blankenship, J. P. Niemi et al., "Extension of the neuroprotective time window for thiazolidinediones in ischemic stroke is dependent on time of reperfusion," *Neuroscience*, vol. 170, no. 3, pp. 846–857, 2010.

[43] T. Breidert, J. Callebert, M. T. Heneka, G. Landreth, J. M. Launay, and E. C. Hirsch, "Protective action of the peroxisome proliferator-activated receptor-γ agonist pioglitazone in a mouse model of Parkinson's disease," *Journal of Neurochemistry*, vol. 82, no. 3, pp. 615–624, 2002.

[44] T. Shimazu, I. Inoue, N. Araki et al., "A peroxisome proliferator-activated receptor-γ agonist reduces infarct size in transient but not in permanent ischemia," *Stroke*, vol. 36, no. 2, pp. 353–359, 2005.

[45] S. Park, J. Yi, G. Miranpuri et al., "Thiazolidinedione class of peroxisome proliferator-activated receptor γ agonists prevents neuronal damage, motor dysfunction, myelin loss, neuropathic pain, and inflammation after spinal cord injury in adult rats," *Journal of Pharmacology and Experimental Therapeutics*, vol. 320, no. 3, pp. 1002–1012, 2007.

[46] A. Shuaib, "The role of taurine in cerebral ischemia: studies in transient forebrain ischemia and embolic focal ischemia in

rodents," *Advances in Experimental Medicine and Biology*, vol. 526, pp. 421–431, 2003.

[47] H. L. Zhang, M. Xu, C. Wei et al., "Neuroprotective effects of pioglitazone in a rat model of permanent focal cerebral ischemia are associated with peroxisome proliferator-activated receptor gamma-mediated suppression of nuclear factor-κB signaling pathway," *Neuroscience*, vol. 176, pp. 381–395, 2011.

[48] W. H. Fong, H. D. Tsai, Y. C. Chen, J. S. Wu, and T. N. Lin, "Anti-apoptotic actions of ppar-γ against ischemic stroke," *Molecular Neurobiology*, vol. 41, no. 2-3, pp. 180–186, 2010.

Hindawi Publishing Corporation
BioMed Research International
Volume 2014, Article ID 723084, 9 pages
http://dx.doi.org/10.1155/2014/723084

Research Article

Ginseng Is Useful to Enhance Cardiac Contractility in Animals

Jia-Wei Lin,[1] Yih-Giun Cherng,[2] Li-Jen Chen,[3] Ho-Shan Niu,[4] Chen Kuei Chang,[1] and Chiang-Shan Niu[4]

[1] *Department of Neurosurgery, Taipei Medical University-Shuang Ho Hospital and College of Medicine, Taipei Medical University, Taipei 10361, Taiwan*
[2] *Department of Anesthesiology, Taipei Medical University-Shuang Ho Hospital and College of Medicine, Taipei Medical University, Taipei 10361, Taiwan*
[3] *Institute of Basic Medical Sciences, College of Medicine, National Cheng Kung University, Tainan 70101, Taiwan*
[4] *Department of Nursing, Tzu Chi College of Technology, Hualien City 97005, Taiwan*

Correspondence should be addressed to Chiang-Shan Niu; ncs838@yahoo.com.tw

Received 7 December 2013; Accepted 25 December 2013; Published 4 February 2014

Academic Editor: Juei-Tang Cheng

Ginseng has been shown to be effective on cardiac dysfunction. Recent evidence has highlighted the mediation of peroxisome proliferator-activated receptors (PPARs) in cardiac function. Thus, we are interested to investigate the role of PPARδ in ginseng-induced modification of cardiac contractility. The isolated hearts in Langendorff apparatus and hemodynamic analysis in catheterized rats were applied to measure the actions of ginseng *ex vivo* and *in vivo*. In normal rats, ginseng enhanced cardiac contractility and hemodynamic dP/dt_{max} significantly. Both actions were diminished by GSK0660 at a dose enough to block PPARδ. However, ginseng failed to modify heart rate at the same dose, although it did produce a mild increase in blood pressure. Data of intracellular calcium level and Western blotting analysis showed that both the PPARδ expression and troponin I phosphorylation were raised by ginseng in neonatal rat cardiomyocyte. Thus, we suggest that ginseng could enhance cardiac contractility through increased PPARδ expression in cardiac cells.

1. Introduction

Ginseng varieties have been garnering increasing interest recently for their effects on the cardiovascular system [1]. It has been demonstrated that ginseng could prevent cardiac hypertrophy and heart failure through a mechanism likely involving the prevention of calcineurin activation [2] and the latter representing a key factor for myocardial hypertrophy and remodeling [3, 4].

Peroxisome proliferator-activated receptors (PPARs) are ligand-activated transcriptional factors that regulate the expression of genes involved in lipid metabolism and inflammation [5]. Three subtypes of PPARs, PPARα, PPARγ, and PPARδ, have been shown to modulate the expressions of various genes to exert bioactivity [5]. PPARα is relatively abundant in tissues with a high oxidative capacity, such as the liver and heart, whereas PPARγ is confined to a limited number of tissues, primarily adipose tissue [5, 6]. The ubiquitously expressed PPARδ enhances lipid catabolism in adipose tissue and muscles [5], and PPARδ-dependent maintenance of inotropic function is crucial for cardiomyocytes [7–9]. Deletion of cardiac PPARδ is accompanied by decreased contraction, increased left ventricular end-diastolic pressure, and lowered cardiac output and leads to decreased contraction and increased incidence of cardiac failure [7].

It has been identified that cardiac agent, such as digoxin and dobutamine, can restore the cardiac contractility in diabetic rats [10–12]. Also, cardiac agent improved cardiac contraction in STZ-diabetic rats which is associated with a marked increase in cardiac PPARδ expression [13].

Thus, we are interested to screen the effect of ginseng on cardiac contractility and investigate the mediation of PPARδ in this action of ginseng. Using the isolated hearts and animals in addition to cultured cardiac cells, the main aim of

the present study is to clarify if ginseng can enhance cardiac contractility through increased PPARδ expression or not.

2. Materials and Methods

2.1. Materials. GSK0660 (a specific PPARδ antagonist) was purchased from Santa Cruz Biotechnology, Inc. (Santa Cruz, CA, USA). The fluorescent probe, fura-2, was the product of Molecular Probes (Eugene, OR, USA). Antibodies specific to PPARδ, cardiac troponin I (TnI) or phospho-troponin I (p-TnI) (Ser 23/24), were obtained from Cell Signaling Technology (Beverly, MA, USA).

2.2. Preparation of Fermented Panax ginseng (P. ginseng). *Panax ginseng* extract (GINST) used in the present study was provided by Bing-Han Pharmaceutics (Hsin-Yin, Tainan Shang, Taiwan). Briefly, dried *Panax ginseng* (1 kg) was extracted with 5 L of 50% aqueous ethanol at 85°C and concentrated in vacuous to obtain dark brown syrup. The dark brown syrup then was mixed with starch to generate the ginseng powder. The powder containing 95% *P. ginseng* root and 5% starch was dissolved in saline solution for oral administration at the desired doses.

2.3. Animals. Male Wistar rats, weighing from 200 to 250 g, were obtained from the Animal Center of National Cheng Kung University Medical College. All experiments were performed under anesthesia with 2% isoflurane and all efforts were made to minimize suffering. The animal experiments were approved and conducted in accordance with local institutional guidelines for the care and use of laboratory animals in Chi-Mei Medical Center (no. 100052307) and performed according to the Guide for the Care and Use of Laboratory Animals as well as the guidelines of the Animal Welfare Act.

2.4. Drug Administration. Animals were randomly assigned into three groups: (I) the control group ($n = 8$) treated with the vehicle, saline (0.9% sodium chloride, orally); (II) the ginseng (Gin) group (orally. $n = 8$) treated by oral administration with ginseng powder at 400 mg/kg for 7 days as described previously [14], and (III) the ginseng + GSK0660 (Gin + GSK) group ($n = 8$) treated with ginseng powder at effective dose (400 mg/kg, orally) according to previous report [14] and GSK0660 at effective dose (3 mg/kg, i.v.) [15] for 7 days. At the end of experiment, hearts of each group were dissected out for Western blotting analysis and Real-time reverse transcription-polymerase chain reaction.

2.5. Langendorff Apparatus for Isolated Heart Determination. The experiment was performed according to a previous description [16]. The rats were sacrificed under anesthesia with 3% isoflurane and their hearts were excised rapidly and rinsed by immersion in ice-cold Krebs-Henseleit buffer (KHB) (mM: NaCl 118.5, KCl 4.7, $MgSO_4$ 1.2, $CaCl_2$ 1.8, $NaHCO_3$ 25.0, and glucose 11.0 at pH 7.35). The hearts were mounted in the Langendorff apparatus and continuously perfused with warm (37°C) and oxygenated (95% O_2, 5% CO_2) KHB at a constant pressure of 70 mmHg. The organ chamber temperature was maintained at 37°C during the experiment. A water-filled latex balloon was inserted through an incision in the left atrium into the left ventricle via the mitral valve and adjusted to a left ventricular end-diastolic pressure (LVEDP) of 5–7 mmHg during initial equilibrium. The distal end of the catheter was connected to an iWorx 214 TM data acquisition system (Ladscrib 2.0 software, iWorx Systems, Inc., Dover, NH, USA) via a pressure transducer for continuous recording. Left ventricular systolic function was assessed by recording the left ventricular developed pressure (LVDP), which was defined as the difference between left ventricular end-systolic pressure (LVESP) and LVEDP.

2.6. Catheterization for Hemodynamic dP/dt Measurement. This part of experiments was performed in rats under anesthesia with 2% isoflurane to the minimize suffering of animals. Temporary pacing leads were used for the short-term study and were placed in the right atrium and RV apex. A venogram imaged in 2 different angulations (left anterior oblique 30° and anteroposterior) was obtained to determine the anatomy of the coronary sinus venous system. An LV pacing electrode (IX-214; iWorx Systems, Inc., Dover, NH, USA) was placed either in the free wall region via the lateral or posterior vein or in the anterior region via the great cardiac vein. After femoral artery and venous puncture using the Seldinger technique [17], pressure transducer catheters were inserted into the heart to provide the RV, aortic, mean blood, and LV pressures. Pressure catheters and pacing leads were connected to an external pacing computer (iWorx Systems, Inc., Dover, NH, USA) to monitor the heart rate and to acquire hemodynamic signals. Body temperature of the rats was also maintained at 37.5°C throughout whole procedure.

2.7. Cell Cultures. Primary cultures of neonatal rat cardiomyocytes were prepared by the modification of a previously described method [18]. Briefly, under anesthesia with 3% isoflurane, the hearts of 1- to 2-day-old Wistar rats were excised, cut into 1–2 mm pieces, and predigested with trypsin to remove red blood cells. The heart tissue was then digested with 0.25% trypsin and 0.05% collagenase. The dissociated cells were placed in uncoated 100 mm dishes and incubated at 37°C in a 5% CO_2 incubator for at least 1 h to remove the nonmyocytic cells. This procedure caused fibroblasts to predominantly attach to the dishes while most of the cardiomyocytes remained in suspension. The cardiomyocyte-enriched population was then collected and counted. The cells were cultured in Dulbecco/Vogt modified Eagle's minimal essential medium (DMEM) with 1 mmol/L pyruvate, 10% fetal bovine serum, 100 units/mL penicillin, and 100 units/mL streptomycin. Over 95% of the collected cells were characterized as cardiomyocytes on the basis of the sarcomeric myosin content. On the second day, the medium was replaced. After 3 to 4 days in culture, the cells were used in the experiments. Stock solutions of ginseng and GSK0660 were prepared with DMSO (0.1%). The cells were treated with 100 μg/mL ginseng for 24 h [14], washed twice with PBS, and removed by trypsinization. The cells were then collected and

subjected to a protein expression assay. Additional treatments with GSK0660 (10^{-6} M) [19] were performed for 30 minutes before the ginseng treatment.

2.8. Measurement of Intracellular Calcium Concentration. The changes in intracellular calcium were detected using the fluorescent probe fura-2-AM [20]. The neonatal rat cardiomyocytes were placed in buffered physiological saline solution (PSS) containing 140 mM NaCl, 5.9 mM KCl, 1.2 mM $CaCl_2$, 1.4 mM $MgCl_2$, 11.5 mM glucose, 1.8 mM Na_2HPO_4, and 10 mM Hepes-Tris, to which was added 5 μM fura-2-AM, and the solution was incubated for 1 h in humidified 5% CO_2 and 95% air at 37°C. The cells were washed and incubated for an additional 30 minutes in PSS. The neonatal rat cardiomyocytes were inserted into a thermostatic (37°C) cuvette containing 2 mL of calcium-free PSS. After recording the baseline value, ginseng (100 μg/mL) was added into the cuvette with/without GSK0660 (10^{-6} M) to detect the free intracellular calcium. The fluorescence was continuously recorded using a fluorescence spectrofluorometer (Hitachi F-2000, Tokyo, Japan). Values of $[Ca^{2+}]$i were calculated from the ratio R = F340/F380 by the formula $[Ca^{2+}]i = KdB(R - R_{min})/(R_{max} - R)$, where Kd was 225 nM, F was fluorescence, and B was the ratio of the fluorescence of the free dye to that of the Ca^{2+}-bound dye measured at 380 nm. R_{max} and R_{min} were determined in separate experiments by using ginseng to equilibrate $[Ca^{2+}]$j with ambient $[Ca^{2+}]$ (R_{max}) and the addition of 0.1 mM $MnCl_2$ and 1 mmol/L EGTA (R_{min}). Background autofluorescence was measured in unloaded cells and subtracted from all measurements.

2.9. Western Blotting Analysis. Protein was extracted from tissue homogenates and cell lysates using ice-cold radioimmunoprecipitation assay (RIPA) buffer supplemented with phosphatase and protease inhibitors (50 mmol/L sodium vanadate, 0.5 mM phenylmethylsulphonyl fluoride, 2 mg/mL aprotinin, and 0.5 mg/mL leupeptin). Protein concentrations were determined with a Bio-Rad protein assay (Bio-Rad Laboratories, Inc., Hercules, CA, USA). Total proteins (30 μg) were separated by SDS/polyacrylamide gel electrophoresis (10% acrylamide gel) using a Bio-Rad Mini-Protein II system. The protein was transferred to expanded polyvinylidene difluoride membranes (Pierce, Rockford, IL, USA) with a Bio-Rad Trans-Blot system. After transfer, the membranes were washed with PBS and blocked for 1 h at room temperature with 5% (w/v) skimmed milk powder in PBS. The manufacturer's instructions were followed for the primary antibody reactions. Blots were incubated overnight at 4°C with an immunoglobulin-G polyclonal rabbit anti-mouse antibody (Affinity BioReagents, Inc., Golden, CO, USA) (1 : 500) in 5% (w/v) skimmed milk powder dissolved in PBS/Tween 20 (0.5% by volume) to bind the target protein such as PPARδ. The blots were incubated with goat polyclonal antibody (1 : 1000) to bind the actin, which served as the internal control. After the removal of the primary antibody, the blots were extensively washed with PBS/Tween 20 and then incubated for 2 h at room temperature with the appropriate peroxidase-conjugated secondary antibody diluted in 5% (w/v) skimmed milk powder and dissolved in PBS/Tween 20. The blots were developed by autoradiography using an ECL-Western blotting system (Amersham International, Buckinghamshire, UK). The immunoblots of PPARδ (50 kDa), cardiac troponin I (28 kDa), and phospho-troponin I (28 kDa) were then quantified using a laser densitometer.

2.10. Statistical Analysis. Results were expressed as mean ± SE of each group. Statistical analysis was carried out using ANOVA analysis and Newman-Keuls post hoc analysis. Statistical significance was considered at $P < 0.05$.

3. Results

3.1. Effect of GW0742 on PPARδ Expression and TnI Phosphorylation in the Heart of Rats. The rats treated with ginseng were used to identify changes in PPARδ expression and TnI phosphorylation. The level of PPARδ expression (Figure 1(a)) and TnI phosphorylation (Figure 1(b)) was markedly raised by ginseng at an effective concentration (400 mg/kg). In addition, this change was reversed by GSK0660 (3 mg/kg, i.v.) at a concentration that did not modify the level of PPARδ expression and TnI phosphorylation (Figure 1).

3.2. Effect of Ginseng on Cardiac Performance in the Isolated Rat Heart. Ginseng at a sufficient dose to activate PPARδ was used to treat the hearts isolated from rats. As shown in Figure 2, ginseng (100 μg/mL) increased cardiac contractility without changes in heart rate. Moreover, the cardiac tonic action of ginseng was diminished by GSK0660 (10^{-6} M) (Figure 2).

3.3. Effect of Ginseng on Cardiac Performance in the Anesthetized Rats. The dP/dt_{max} was significantly increased by ginseng after the treatment (400 mg/kg/day, orally for 7 days) as described previously [14] in the anesthetized rats, compared with the vehicle-treated control. However, this effect disappeared in the rats receiving coadministration of GSK0660 at effective dose (3 mg/kg, i.v.) [15] (Figure 3(a)). Treatment of ginseng only did not modify the heart rate but produced a slight increase in blood pressure that was also blocked by GSK0660 (Figures 3(b) and 3(c)).

3.4. Effect of Ginseng on Intracellular Calcium in Neonatal Rat Cardiomyocytes. The fluorescent probe, fura2-AM, was used to detect changes in intracellular calcium level in the neonatal rat cardiomyocytes, and ginseng at an effective concentration (100 μg/mL) was found to increase the intracellular calcium level. This effect disappeared in the cardiomyocytes that were coincubated with ginseng and GSK0660 (10^{-6} M) (Figure 4(a)); however, incubation with GSK0660 alone did not affect the intracellular calcium level in the neonatal rat cardiomyocytes (Figure 4(a)).

3.5. Effects of Ginseng on PPARδ Expression and TnI Phosphorylation in Neonatal Rat Cardiomyocytes. The neonatal rat cardiomyocytes were applied to treat with ginseng for

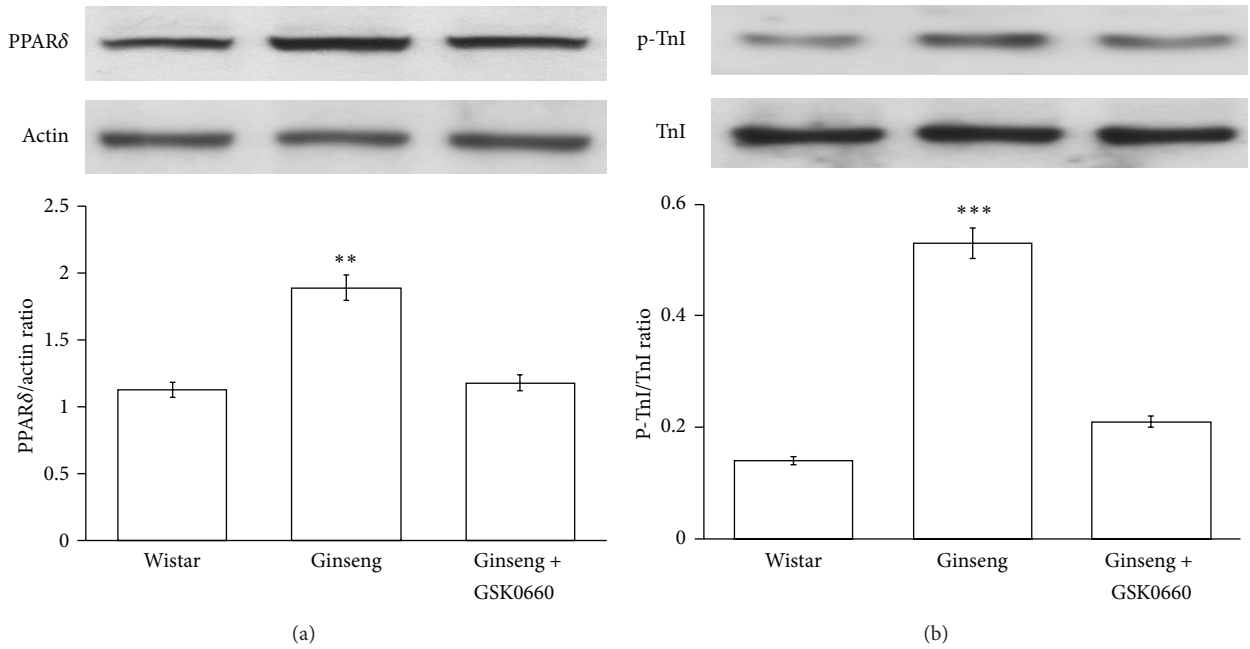

Figure 1: Effects of ginseng on PPARδ expression and TnI phosphorylation in heart of rats. Changes of PPARδ expression (a) and TnI phosphorylation (b) in the hearts of rats treated with ginseng. Rats were treated with ginseng (400 mg/kg) for 7 days and hearts were then used to measure the protein level of PPARδ expression and TnI phosphorylation using Western blotting analysis. All values are presented as mean ± SEM ($n = 8$). $^{**}P < 0.01$ and $^{***}P < 0.001$ compared with normal rats.

identification of changes in PPARδ expression and TnI phosphorylation. The levels of PPARδ expression and TnI phosphorylation were markedly raised by ginseng at an effective concentration (100 μg/mL). Also, this effect was reversed by GSK0660 (10^{-6} M) at a concentration that did not modify the level of PPARδ expression and TnI phosphorylation (Figure 4(b)).

4. Discussion

In the present study, we found that ginseng increased cardiac contractility but not heart rate in rats at the dose of 400 mg/kg, orally. This dose is equal to human oral dose about 3871 mg/kg by using the US FDA HED (human equivalent dose) equation for calculation [21–23]. Increases in PPARδ expression and TnI phosphorylation were also observed in the heart of ginseng-treated rats. In hearts isolated from rats, ginseng enhanced cardiac contractility and this action was diminished by GSK0660 at a concentration sufficient to block PPARδ. In the anesthetized rats, cardiac contraction (dP/dt_{max}) was also significantly increased by ginseng and this change was blocked by GSK0660. However, heart rate was not modified by ginseng at same dose. In the neonatal rat cardiomyocytes, ginseng increased cellular calcium levels, PPARδ expression, and TnI phosphorylation. Thus, to the best of our knowledge, this is the first study to show that ginseng could increase cardiac contractility through activation of PPARδ.

In vivo and *in vitro* investigations have revealed a number of significant actions of ginsenosides and ginseng extracts in cardioprotection, such as reducing myocardial ischemia-reperfusion induced damage via NO pathway in rats and mice [24], slowing down deterioration of cardiac contractions, preventing the development of arrhythmias [25], and relaxing the muscles of the aorta [26]. Also, it has been documented that ginseng increases cardiac lipid metabolism by enhancement of PPARδ expression in the hearing [27]. In this study, we found that ginseng could increase PPARδ expression and TnI phosphorylation. Also, this action of ginseng was abolished by specific PPARδ antagonist. Mediation of PPARδ in this action of ginseng can thus be considered.

It has been established that PPARδ plays an important role in the regulation of cardiac performance [17–19]. In this study, we demonstrated that ginseng increases cardiac contractility without affecting heart rate. Also, this cardiac action of ginseng is reversed by blockade of PPARδ using antagonist. Furthermore, activation of PPARδ using ginseng enhanced cardiac contractility in the isolated hearts and the hemodynamic dP/dt_{max} in the rats. Both actions of ginseng were inhibited by GSK0660 at a concentration sufficient to block PPARδ [27, 28]. The enhancement of cardiac contractility by ginseng through an activation of PPARδ is then characterized.

A change in heart rate is the most serious side effect of cardiac agents [29, 30]. In the present study, we showed that ginseng could enhance cardiac contractility without altering heart rate in isolated heart. In addition, ginseng generated

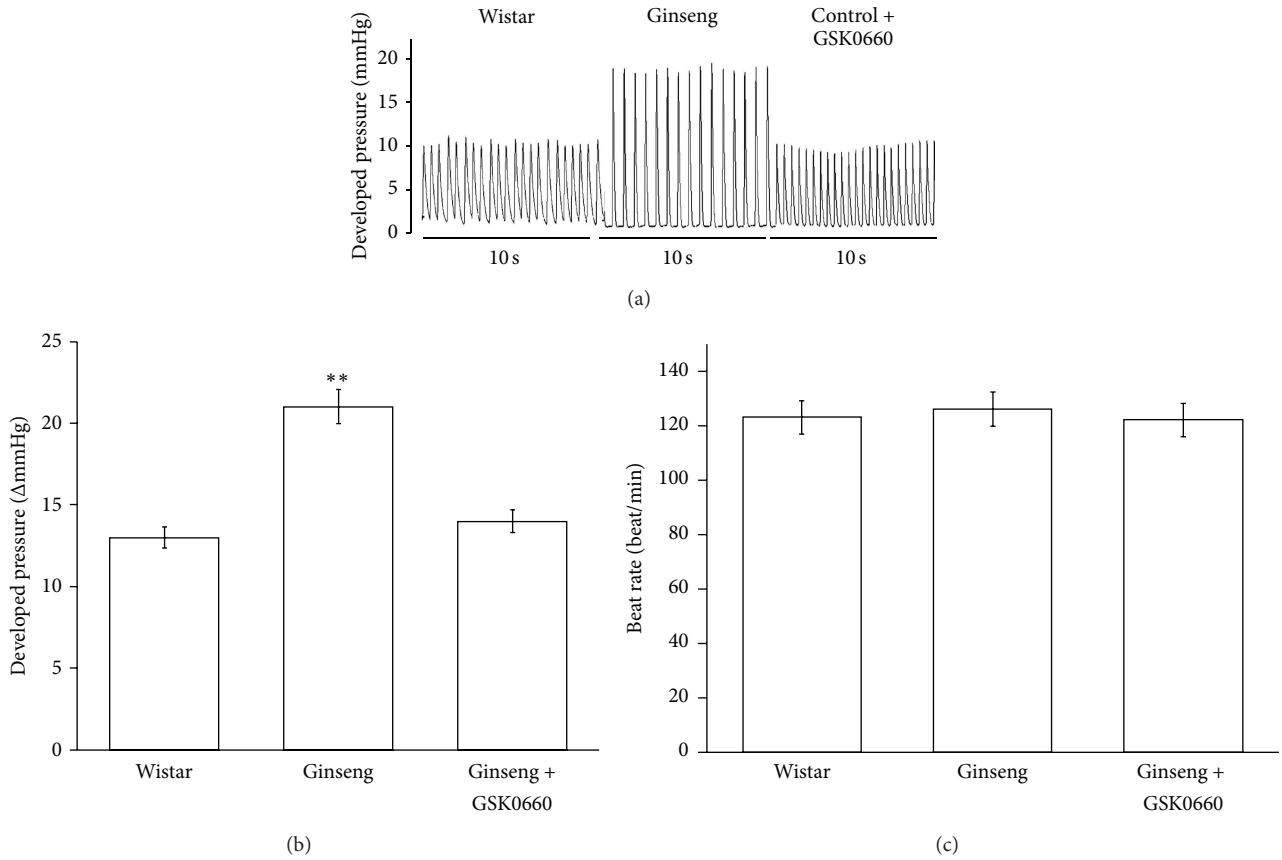

Figure 2: Effects of ginseng on cardiac performance in hearts isolated from rats. The representative picture shows the change in cardiac performance caused by ginseng in isolated hearts (a). Heart rate and cardiac contractility were recorded in isolated rat heart treated with ginseng or cotreated with ginseng + GSK0660. The changes in developed pressure (b) and beat rate (c) were recorded continuously throughout the whole experiment. All values are presented as mean ± SEM ($n = 8$). $^{**}P < 0.01$ as compared to normal rats.

cardiac tonic action in animals without impacting the heart rate. Thus, ginseng can be used as cardiac agent at some doses without side effect of arrhythmia. Our previous studies have showed that activation of PPARδ by cardiac agent may improve diabetic cardiomyopathy in type-1 diabetic rats [28, 31]. Thus, ginseng seems helpful in the treatment and/or prevention of diabetic cardiomyopathy. However, a slight elevation of mean blood pressure was observed in the rats received ginseng. Thus, applying ginseng in patients with hypertension should be done carefully.

Troponin I (TnI) is known as an inhibitory unit of the troponin complex associated with thin filaments, and it inhibits actin-myosin interactions at the diastolic level of intracellular Ca^{2+} [32, 33]. Modulation of myofilament properties by alterations in TnI phosphorylation has been found to have a profound effect on cardiac contractility [34]. Phosphorylation of TnI has been shown to increase the cross-bridge cycling rate, leading to an increase in power output [33, 34]. Ca^{2+} is mainly involved in muscle contraction [32–35]. Contraction of cardiac muscles relies upon interactions between ATP and Ca^{2+}, both of which must be present in adequate amounts [36]. We observed that ginseng has the ability to increase the amount of intracellular calcium in cardiomyocytes, and this seemed to be related to the higher contractility of heart.

It has been shown that TnI phosphorylation most likely acts through an enhanced off rate during Ca^{2+} exchange with contractile protein, leading to an increase in cardiac output [36–40]. Consistent with this, we found that TnI phosphorylation was elevated in the neonatal rat cardiomyocytes exposed to ginseng. Thus, direct activation of PPARδ by ginseng may result in a higher level of TnI phosphorylation. Both changes caused by ginseng in the cardiomyocytes may explain the increase in cardiac contractility.

The multiple cell signals are involved in cardiac contractility. It is not easy to speculate the potential mechanism(s) for this action of ginseng in the increase of cardiac contractility. It has been documented that ginsenoside, one of the active principles in ginseng, can improve systolic/diastolic function and enhance cardiac dP/dt through the opening of mitochondrial adenosine triphosphate-sensitive potassium channels [41], reduction in oxidative stress via inhibition of glutathione [42], and augmentation of cellular calcium influx [43]. The increase of cellular calcium influx is consistent with

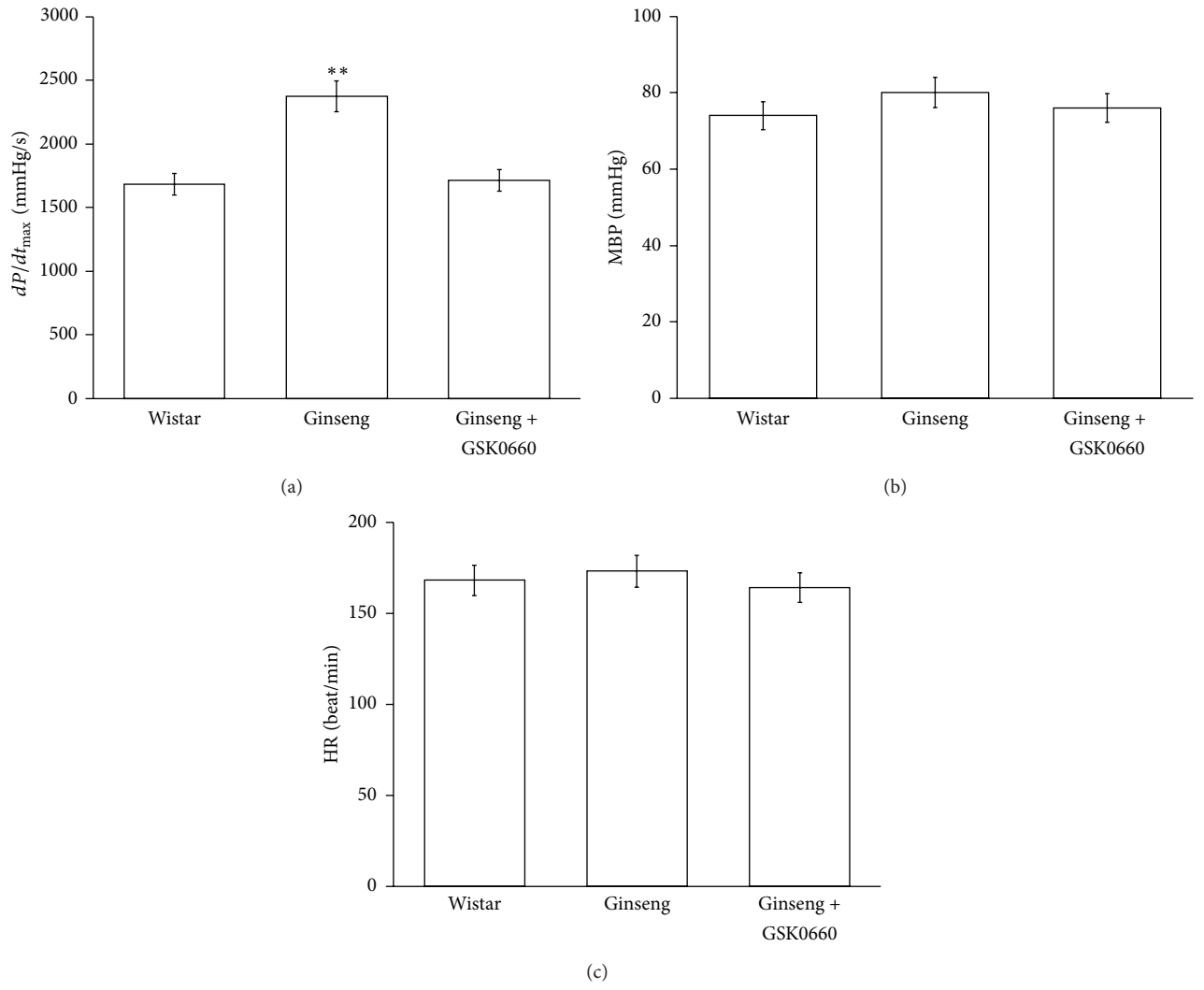

Figure 3: Effects of ginseng on cardiac performance in anesthetized rats. The effects of coadministration of ginseng and/or GSK0660 were investigated in the anesthetized rats. The changes in hemodynamic dP/dt (a), mean blood pressure (MBP) (b), and heart rate (HR) (c) were recorded continuously throughout the whole experiment. All values are presented as mean ± SEM ($n = 8$). $^{**}P < 0.01$ as compared to normal rats.

to our previous reports regarding PPARδ related cardiac tonic actions [10, 11, 44].

Interestingly, ginseng enhanced cardiac contractility without altering heart rate in isolated heart. Also, ginseng generated cardiac tonic action in animals without impacting the heart rate. It has been demonstrated that PPARδ agonist is not effective in cardiac conduction [45]. The possible explanation for this seems related to the absence of PPARδ in cardiac conduction system. However, the real mechanism(s) for the lack of effect on heart rate caused by ginseng require(s) more investigations in the future.

The activation of PPARδ by ginseng can enhance the cardiac contractility without altering heart rate. Thus, we suggest that ginseng is suitable for the treatment of heart failure. Using this agent, arrhythmia can be ignored in patients for treatment of heart failure.

5. Conclusion

According to these findings, we suggest that the activation of PPARδ by ginseng increases intracellular calcium, which then results in cardiac troponin phosphorylation. Subsequently, the cardiac contractility is enhanced. Taken together, ginseng enhanced cardiac contractility through an increase in PPARδ expression at the dose that did not modify the heart beating. Thus, ginseng could be developed as a good cardiac agent without the side effect on heart rate.

Conflict of Interests

The authors declare that there is no conflict of interests regarding the publication of this paper.

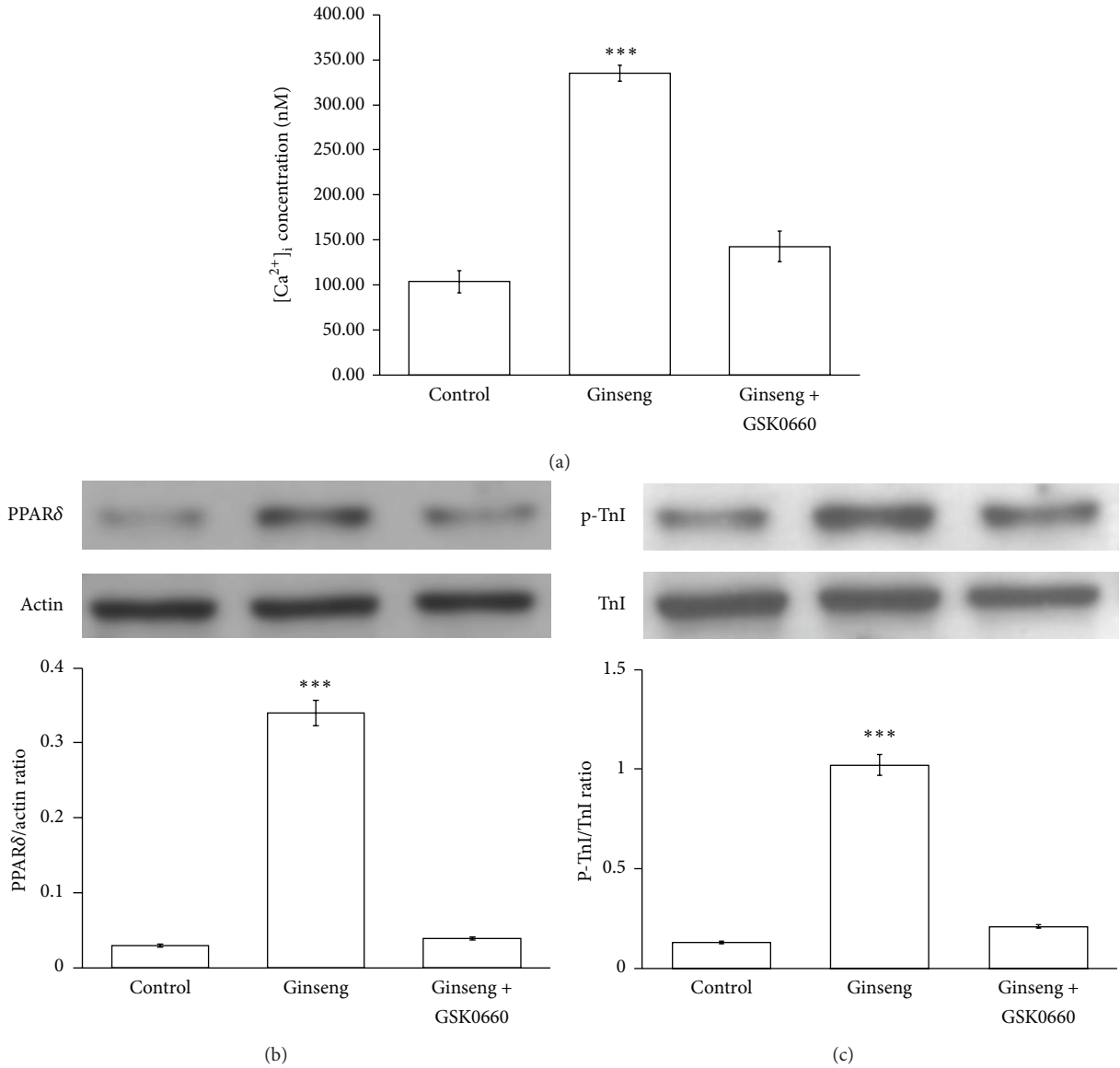

Figure 4: Effects of ginseng on intracellular calcium and TnI phosphorylation in neonatal rat cardiomyocytes. Changes in intracellular calcium were detected with fura-2 by using a fluorescence spectrofluorometer. The neonatal rat cardiomyocytes were placed in buffered physiological saline solution with 5 μM of fura-2-AM and incubated for 1 h. After recording the baseline value, ginseng was added into the cuvette with/without GSK0660 to detect the free intracellular calcium (a). Effects of ginseng on PPARδ expression (b) and TnI phosphorylation (c) in the neonatal rat cardiomyocytes were indicated. Cells treated with ginseng for 24 hours were harvested to measure the protein level of PPARδ expression and TnI phosphorylation using Western blotting analysis. All values are presented as mean ± SEM ($n = 8$). $^{***}P < 0.001$ compared with the control group.

Acknowledgments

The authors thank Yang-Lian Yan and Yi-Zhi Chen for their assistance in their experiments. The present study was supported in part by a Grant (TCCT-1011A09) from Tzu Chi College of Technology, Hualien City, Taiwan.

References

[1] M. Karmazyn, M. Moey, and X. T. Gan, "Therapeutic potential of ginseng in the management of cardiovascular disorders," *Drugs*, vol. 71, no. 15, pp. 1989–2008, 2011.

[2] J. Guo, X. T. Gan, J. V. Haist et al., "Ginseng inhibits cardiomyocyte hypertrophy and heart failure via nhe-1 inhibition and attenuation of calcineurin activation," *Circulation*, vol. 4, no. 1, pp. 79–88, 2011.

[3] N. Frey and E. N. Olson, "Cardiac hypertrophy: the good, the bad, and the ugly," *Annual Review of Physiology*, vol. 65, pp. 45–79, 2003.

[4] J. M. Berry, V. Le, D. Rotter et al., "Reversibility of adverse, calcineurin-dependent cardiac remodeling," *Circulation Research*, vol. 109, no. 4, pp. 407–417, 2011.

[5] Q. Yang and Y. Li, "Roles of PPARs on regulating myocardial energy and lipid homeostasis," *Journal of Molecular Medicine*, vol. 85, no. 7, pp. 697–706, 2007.

[6] I. Issemann and S. Green, "Activation of a member of the steroid hormone receptor superfamily by peroxisome proliferators," *Nature*, vol. 347, no. 6294, pp. 645–650, 1990.

[7] L. Cheng, G. Ding, Q. Qin et al., "Cardiomyocyte-restricted peroxisome proliferator-activated receptor-δ deletion perturbs myocardial fatty acid oxidation and leads to cardiomyopathy," *Nature Medicine*, vol. 10, no. 11, pp. 1245–1250, 2004.

[8] L. Cheng, G. Ding, Q. Qin et al., "Peroxisome proliferator-activated receptor δ activates fatty acid oxidation in cultured neonatal and adult cardiomyocytes," *Biochemical and Biophysical Research Communications*, vol. 313, no. 2, pp. 277–286, 2004.

[9] G. D. Barish, V. A. Narkar, and R. M. Evans, "PPARδ: a dagger in the heart of the metabolic syndrome," *Journal of Clinical Investigation*, vol. 116, no. 3, pp. 590–597, 2006.

[10] M. T. Chou, S. H. Lo, K. C. Cheng, Y. X. Li, L. J. Chen, and J. T. Cheng, "Activation of β-adrenoceptors by dobutamine may induce a higher expression of peroxisome proliferator-activated receptors δ (PPARδ) in neonatal rat cardiomyocytes," *The Scientific World Journal*, vol. 2012, Article ID 248320, 8 pages, 2012.

[11] Z.-C. Chen, B.-C. Yu, L.-J. Chen, K.-C. Cheng, H. J. Lin, and J.-T. Cheng, "Characterization of the mechanisms of the increase in PPARδ expression induced by digoxin in the heart using the H9c2 cell line," *British Journal of Pharmacology*, vol. 163, no. 2, pp. 390–398, 2011.

[12] Z. C. Chen, B. C. Yu, L. J. Chen, and J. T. Cheng, "Increase of peroxisome proliferator-activated receptor δ (PPARδ) by digoxin to improve lipid metabolism in the heart of diabetic rats," *Hormone and Metabolic Research*, vol. 45, no. 5, pp. 364–371, 2013.

[13] B.-C. Yu, C.-K. Chang, H.-Y. Ou, K.-C. Cheng, and J.-T. Cheng, "Decrease of peroxisome proliferator-activated receptor delta expression in cardiomyopathy of streptozotocin-induced diabetic rats," *Cardiovascular Research*, vol. 80, no. 1, pp. 78–87, 2008.

[14] H.-X. Li, S.-Y. Han, X. Ma et al., "The saponin of red ginseng protects the cardiac myocytes against ischemic injury in vitro and in vivo," *Phytomedicine*, vol. 19, no. 6, pp. 477–483, 2012.

[15] I. Paterniti, E. Esposito, E. Mazzon et al., "Evidence for the role of peroxisome proliferator-activated receptor-β/δ in the development of spinal cord injury," *Journal of Pharmacology and Experimental Therapeutics*, vol. 333, no. 2, pp. 465–477, 2010.

[16] L. Sun, D.-L. Li, M. Zhao et al., "The role of muscarinic receptors in the beneficial effects of adenosine against myocardial reperfusion injury in rats," *PLoS ONE*, vol. 6, no. 11, Article ID e25618, 2011.

[17] S. I. Seldinger, "Catheter replacement of the needle in percutaneous arteriography: a new technique," *Acta Radiologica*, vol. 49, no. 434, pp. 47–52, 2008.

[18] Z. C. Chen, B. C. Yu, L. J. Chen, and J. T. Cheng, "Increase of peroxisome proliferator-activated receptor delta (PPARdelta) by digoxin to improve lipid metabolism in the heart of diabetic rats," *Hormone and Metabolic Research*, vol. 45, no. 5, pp. 364–371, 2013.

[19] G. Cohen, Y. Riahi, O. Shamni et al., "Role of lipid peroxidation and PPAR-δ in amplifying glucose-stimulated insulin secretion," *Diabetes*, vol. 60, no. 11, pp. 2830–2842, 2011.

[20] H. A. Halaq and G. T. Haupert Jr., "Positive inotropic effects of the endogenous Na+/K+-transporting ATPase inhibitor from the hypothalamus," *Proceedings of the National Academy of Sciences of the United States of America*, vol. 86, no. 24, pp. 10080–10084, 1989.

[21] I. Cavero, "10th annual meeting of the Safety Pharmacology Society: an overview," *Expert Opinion on Drug Safety*, vol. 10, no. 2, pp. 319–333, 2011.

[22] W. C. Buhles, "Compassionate use: a story of ethics and science in the development of a new drug," *Perspectives in Biology and Medicine*, vol. 54, no. 3, pp. 304–315, 2011.

[23] T. Keida, N. Hayashi, and M. Kawashima, "Application of the Food and Drug Administration (FDA) bioequivalent guidance of topical dermatological corticosteroid in yellow-skinned Japanese population: validation study using a chromameter," *Journal of Dermatology*, vol. 33, no. 10, pp. 684–691, 2006.

[24] H. Zhou, S. Z. Hou, P. Luo et al., "Ginseng protects rodent hearts from acute myocardial ischemia-reperfusion injury through GR/ER-activated RISK pathway in an endothelial NOS-dependent mechanism," *Journal of Ethnopharmacology*, vol. 135, no. 2, pp. 287–298, 2011.

[25] G. I. Scott, P. B. Colligan, B. H. Ren, and J. Ren, "Ginsenosides Rb1 and Re decrease cardiac contraction in adult rat ventricular myocytes: role of nitric oxide," *British Journal of Pharmacology*, vol. 134, no. 6, pp. 1159–1165, 2001.

[26] S. Y. Kang, V. B. Schini-Kerth, and N. D. Kim, "Ginsenosides of the protopanaxatriol group cause endothelium-dependent relaxation in the rat aorta," *Life Sciences*, vol. 56, no. 19, pp. 1577–1586, 1995.

[27] S. C. Kuo, P. M. Ku, L. J. Chen, H. S. Niu, and J. T. Cheng, "Activation of receptors δ (PPARδ) by agonist (GW0742) may enhance lipid metabolism in heart both in vivo and in vitro," *Hormone and Metabolic Research*, vol. 45, pp. 880–886, 2013.

[28] Y. Z. Cheng, L. J. Chen, W. J. Lee, M. F. Chen, H. Jung Lin, and J. T. Cheng, "Increase of myocardial performance by Rhodiola-ethanol extract in diabetic rats," *Journal of Ethnopharmacology*, vol. 144, pp. 234–239, 2012.

[29] R. Marquardt, "Influence of dopamine and metaproterenol on serum free fatty acids in regard to induction of cardiac arrhythmia," *Medizinische Welt*, vol. 30, no. 18, pp. 707–708, 1979.

[30] E. T. Angelakos, M. P. King, and R. W. Millard, "Regional distribution of catecholamines in the hearts of various species," *Annals of the New York Academy of Sciences*, vol. 156, no. 1, pp. 219–240, 1969.

[31] S. C. Fan, B. C. Yu, Z. C. Chen, L. J. Chen, H. H. Chung, and J. T. Cheng, "The decreased expression of peroxisome proliferator-activated receptors (PPAR) is reversed by digoxin in the heart of diabetic rats," *Hormone and Metabolic Research*, vol. 42, no. 9, pp. 637–642, 2010.

[32] I. Ohtsuki and S. Morimoto, "Troponin: regulatory function and disorders," *Biochemical and Biophysical Research Communications*, vol. 369, no. 1, pp. 62–73, 2008.

[33] J. M. Metzger and M. V. Westfall, "Covalent and noncovalent modification of thin filament action: the essential role of troponin in Cardiac muscle regulation," *Circulation Research*, vol. 94, no. 2, pp. 146–158, 2004.

[34] J. Layland, R. J. Solaro, and A. M. Shah, "Regulation of cardiac contractile function by troponin I phosphorylation," *Cardiovascular Research*, vol. 66, no. 1, pp. 12–21, 2005.

[35] M. D. Bootman and M. J. Berridge, "The elemental principles of calcium signaling," *Cell*, vol. 83, no. 5, pp. 675–678, 1995.

[36] C. A. Tate, M. F. Hyek, and G. E. Taffet, "The role of calcium in the energetics of contracting skeletal muscle," *Sports Medicine*, vol. 12, no. 3, pp. 208–217, 1991.

[37] X. Liu, N. Takeda, and N. S. Dhalla, "Troponin I phosphorylation in heart homogenate from diabetic rat," *Biochimica et Biophysica Acta*, vol. 1316, no. 2, pp. 78–84, 1996.

[38] A. E. Messer, A. M. Jacques, and S. B. Marston, "Troponin phosphorylation and regulatory function in human heart muscle: dephosphorylation of Ser23/24 on troponin I could account for the contractile defect in end-stage heart failure," *Journal of Molecular and Cellular Cardiology*, vol. 42, no. 1, pp. 247–259, 2007.

[39] L. Li, J. Desantiago, G. Chu, E. G. Kranias, and D. M. Bers, "Phosphorylation of phospholamban and troponin I in β-adrenergic-induced acceleration of cardiac relaxation," *American Journal of Physiology*, vol. 278, no. 3, pp. H769–H779, 2000.

[40] Y. Pi, K. R. Kemnitz, D. Zhang, E. G. Kranias, and J. W. Walker, "Phosphorylation of troponin I controls cardiac twitch dynamics: evidence from phosphorylation site mutants expressed on a troponin I-null background in mice," *Circulation Research*, vol. 90, no. 6, pp. 649–656, 2002.

[41] W. Ningyuan, M. Shinya, A. Masazumi et al., "Sheng-Mai-San is protective against post-ischemic myocardial dysfunction in rats through its opening of the mitochondrial KATP channels," *Circulation Journal*, vol. 66, no. 8, pp. 763–768, 2002.

[42] Z. Liu, Z. Li, and X. Liu, "Effect of ginsenoside Re on cardiomyocyte apoptosis and expression of Bcl-2/Bax gene after ischemia and reperfusion in rats," *Journal of Huazhong University of Science and Technology*, vol. 22, no. 4, pp. 305–309, 2002.

[43] X. Q. Yi, T. Li, J. R. Wang et al., "Total ginsenosides increase coronary perfusion flow in isolated rat hearts through activation of PI3K/Akt-eNOS signaling," *Phytomedicine*, vol. 17, no. 13, pp. 1006–1015, 2010.

[44] S. H. Lo, K. S. Lee, L. J. Chen, J. T. Cheng, and C. H. Chen, "Increase of PPARδ by dopamine mediated via DA-1 receptor-linked phospholipase C pathway in neonatal rat cardiomyocytes," *Autonomic Neuroscience*, vol. 177, pp. 211–216, 2013.

[45] Z. C. Chen, K. S. Lee, L. J. Chen, L. Y. Wang, H. S. Niu, and J. T. Cheng, "Cardiac peroxisome proliferator-activated receptor δ (PPARδ) as a new target for increased contractility without altering heart rate," *PLoS One*, vol. 8, Article ID e64229, 2013.

Hindawi Publishing Corporation
BioMed Research International
Volume 2014, Article ID 526932, 7 pages
http://dx.doi.org/10.1155/2014/526932

Clinical Study

P-Cresyl Sulfate Is a Valuable Predictor of Clinical Outcomes in Pre-ESRD Patients

Cheng-Jui Lin,[1,2,3] Chi-Feng Pan,[1,2] Chih-Kuang Chuang,[3,4,5] Fang-Ju Sun,[2,6] Duen-Jen Wang,[7] Han-Hsiang Chen,[1,2] Hsuan-Liang Liu,[3] and Chih-Jen Wu[1,8,9]

[1] *Division of Nephrology, Department of Internal Medicine, Mackay Memorial Hospital, 92 Chung San North Road, 10449 Taipei, Taiwan*
[2] *Department of Medical Research, Mackay Memorial Hospital, 10449 Taipei, Taiwan*
[3] *Department of Laboratory Medicine, Mackay Memorial Hospital, 10449 Taipei, Taiwan*
[4] *Mackay Medicine, Nursing and Management College, 10449 Taipei, Taiwan*
[5] *Institute of Biotechnology, National Taipei University of Technology, 10608 Taipei, Taiwan*
[6] *Division of Genetics and Metabolism, Department of Medical Research, Mackay Memorial Hospital, 10449 Taipei, Taiwan*
[7] *College of Medicine, Fu-Jen Catholic University, 24205 New Taipei City, Taiwan*
[8] *Graduate Institute of Medical Science, Taipei Medical University, 11043 Taipei, Taiwan*
[9] *Mackay Medical College, 25245 New Taipei City, Taiwan*

Correspondence should be addressed to Chih-Jen Wu; wcjyali@yahoo.com.tw

Received 12 November 2013; Accepted 16 December 2013; Published 29 January 2014

Academic Editor: Joen-Rong Sheu

Background/Aims. Previous studies have reported p-cresyl sulfate (PCS) was related to endothelial dysfunction and adverse clinical effect. We investigate the adverse effects of PCS on clinical outcomes in a chronic kidney disease (CKD) cohort study. *Methods*. 72 predialysis patients were enrolled from a single medical center. Serum biochemistry data and PCS were measured. The clinical outcomes including cardiovascular event, all-cause mortality, and dialysis event were recorded during a 3-year follow-up. *Results*. After adjusting other independent variables, multivariate Cox regression analysis showed age (HR: 1.12, $P = 0.01$), cardiovascular disease history (HR: 6.28, $P = 0.02$), and PCS (HR: 1.12, $P = 0.02$) were independently associated with cardiovascular event; age (HR: 0.91, $P < 0.01$), serum albumin (HR: 0.03, $P < 0.01$), and PCS level (HR: 1.17, $P < 0.01$) reached significant correlation with dialysis event. Kaplan-Meier analysis revealed that patients with higher serum p-cresyl sulfate (>6 mg/L) were significantly associated with cardiovascular and dialysis event (log rank $P = 0.03$, log rank $P < 0.01$, resp.). *Conclusion*. Our study shows serum PCS could be a valuable marker in predicting cardiovascular event and renal function progression in CKD patients without dialysis.

1. Introduction

Cardiovascular disease is still the main leading cause that resulted in morbidity and mortality in patients with chronic kidney disease (CKD) [1–3]. This high mortality and its underlying causes among CKD patients are a crucial issue. A broad range of traditional risk factors could not fully explain the high risk of mortality in such population [4]. Thus, recent studies have demonstrated that nontraditional risk factors including uremic toxins may play a role in the development of cardiovascular disease in CKD [5–8].

Uremic solutes are accumulated as renal clearance rate declined. Most uremic toxins can be removed by dialysis except protein-bound uremic toxins, due to its higher affinity for serum protein [9]. P-cresyl sulfate (PCS), one kind of protein-bound uremic toxins, has been reported not only to reduce endothelial proliferation but also to inhibit endothelial repair mechanisms [10, 11]. In addition, an increasing evidence suggests that PCS is a valuable predictor of cardiovascular events [12], infection event [13] and all-cause mortality event in hemodialysis patients [14]. However, there is also a significant association of serum PCS with vascular disease in CKD patients. Our recent study also indicated that PCS levels had strong correlation with vascular access dysfunction in patients on maintenance hemodialysis [15].

From these reports, PCS seems a novel and important surrogate in CKD patients. However, its clinical toxic effect still needs to be verified by more studies. Thus, in this study, we further investigated the effect of PCS on clinical outcomes including kidney function progression, cardiovascular event, and all-cause mortality in a pre-ESRD cohort.

2. Subjects and Methods

Seventy-two patients with CKD3–5 were recruited in this study from January to April 2008 in a medical centre. Patients who met the following criteria with acute infection and cardiovascular events in the past 3 months, with malignancy, or those younger than 18 years were excluded. The etiology of CKD in the study patients included cGN, diabetic nephropathy, polycystic kidney disease, or lupus nephritis. Patient characteristics and biochemical parameters were recorded and measured. Our study was performed in accordance with the principles of the Declaration of Helsinki and approved by the Ethics Committee of the Mackay Memorial Hospital. Informed consent was obtained from all patients.

Biochemistry data including the following tests were performed: blood urea nitrogen (BUN, md/dL), creatinine (Cr, mg/dL), hemoglobin (Hb, g/dL), hematocrit (Hct, %), calcium (Ca, mg/dL), phosphate (P, mg/dL), intact-parathyroid hormone (i-PTH, pg/mL), albumin (g/dL), and p-cresyl sulfate (mg/L). Serum albumin levels were determined by bromocresol green method.

Serum PCS were analyzed with LC-MS/MS (4000 QTRAP, USA). Briefly, serum samples were prepared and deproteinized by heat denaturation. HPLC was performed at room temperature using a dC18 column (3.0 × 50 mm, Atlantis, Waters). The buffers used were (A) 0.1% formic acid and (B) 1 mM NH_4OAc + 0.1% formic acid in 100% acetonitrile. The flow rate was 0.6 mL/min with a 3.5 min gradient cycling from 90% A/10% B to 10% A/90% B. Under these conditions, PCS was eluted at 2.73 min. Standard curves for PCS were set at 1, 5, 10, 50, 250, 500, and 1000 μg/L, and they correlated with the serum samples with average r^2 values of 0.996 ± 0.003. These samples were diluted if PCS concentration exceeded standard curve. Quantitative results were obtained and calculated in terms of their concentrations (mg/L). The sensitivity of this assay was 1 μg/L for PCS.

Our patients were followed up for 3 years until May 31, 2011. During study period, clinical outcomes including cardiovascular events, all-cause mortality, and dialysis event were reviewed by 1 independent physician (Pan CF), who was blinded for study. The medical charts were reviewed for all dialysis, and for surgeries due to nephrologic, cardiologic, and vascular defects. The cardiovascular event was defined as patients with any one of following events including cardiovascular events including death from cardiac causes, myocardial ischemia, nonfatal myocardial infarction, ischemic stroke, or new onset of peripheral vascular disease, whichever developed first. Only one event of cardiovascular event per subject was included in the analysis. Deaths were accurately recorded and the cause of death were categorized as cardiovascular, infectious, or other. Only patients who met the criteria of starting long-term dialysis including hemodialysis or peritoneal dialysis were recorded as having dialysis events in this study.

Table 1: Baseline characteristics of the study patients.

Variables	All (n = 72)
Age (yr)	60.1 ± 9.4
Male (%)	50%
Diabetes mellitus (%)	31.9%
Hypertension (%)	43.1%
CVD (%)	15.3%
SBP (mmHg)	141.5 ± 15.7
DBP (mmHg)	73.3 ± 11.5
CKD stage (%)	
3	34.8%
4	32.4%
5	32.8%
Albumin (g/dL)	4.01 ± 0.4
Hemoglobin (g/L)	10.3 ± 1.4
Hematocrit (%)	31.4 ± 5.6
BUN (mg/dL)	44.1 ± 23.3
Creatinine (mg/dL)	3.8 ± 2.6
eGFR (mL/min)	23.6 ± 15.1
Calcium (mg/dL)	9.1 ± 0.4
Phosphate (mg/dL)	4.5 ± 0.8
Intact-PTH (pg/mL)	132.5 ± 177.1
P-cresyl sulfate (mg/L)	7.7 ± 7.2

Values expressed as mean ± SD or percent. CVD: cardiovascular disease; CKD: chronic kidney disease; SBP: systolic blood pressure; DBP: diastolic blood pressure; eGFR: estimated GFR.

The demographic data were expressed as the mean ± standard deviation (SD). Mann-Whitney U test was applied for the comparison between two groups divided by a medium PCS level (PCS, ≧6.0 mg/L and <6.0 mg/L) in CKD patients. Cox regression model was used to analyze the relationship between independent variables and clinical outcomes including cardiovascular event, dialysis event and all-cause mortality. All variables with a statistically significant P value in the univariate analysis were included in multivariate analysis. The Kaplan-Meier method (factors were compared using the log-rank test) was used to estimate cumulative event free rate of time to first cardiovascular event, time to first dialysis event, and overall mortality in CKD patients with PCS level above and below the median (6.0 mg/L). A value of P less than 0.05 was considered statistically significant. All statistical analyses were conducted by using the SPSS version 17.0 software program (SPSS, Chicago, IL).

3. Results

72 stable patients with CKD stages 3, 4, and 5 (34.8%, 32.4% and 32.8%, resp.) were recruited in this study. The mean age of patients was 60.6 ± 9.7 years old and this research included 36 males (50%) and 36 females (50%). Patient's demographics and biochemistry are shown in Table 1. 23 patients had diabetes mellitus (31.9%), 31 patients had hypertension (43.1%),

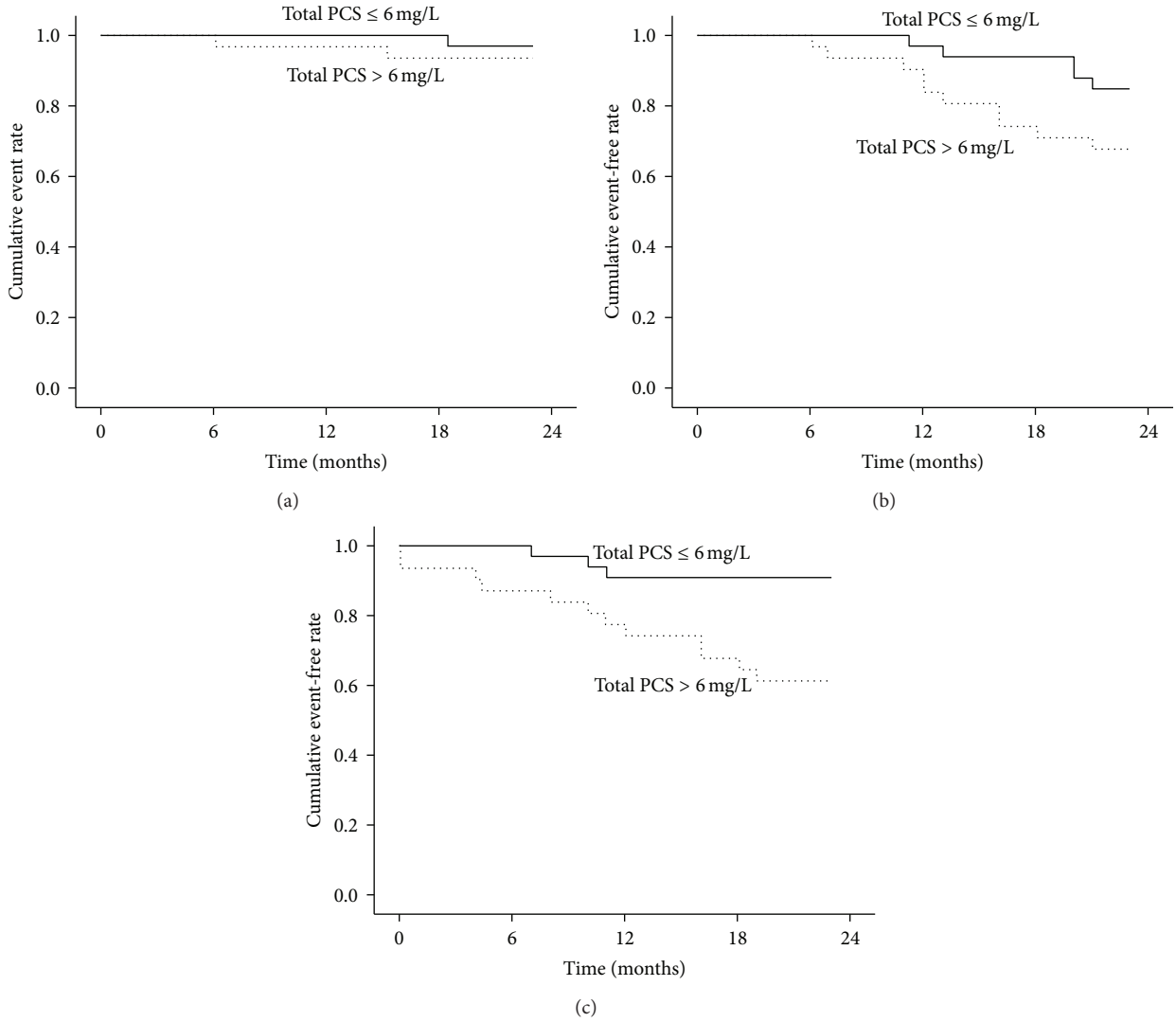

Figure 1: Kaplan-Meier curves of time to first clinical events. Patients were divided into two groups (>6.0 mg/L and ≦6.0 mg/L) by medium level of p-cresyl sulfate. (a) All-cause mortality, log rank $P = 0.26$, (b) cardiovascular event, log rank $P = 0.03$, and (c) dialysis event, log rank $P < 0.01$.

and 11 patients had cardiovascular disease (15.3%). All patients were divided into two groups based on median PCS level (6.0 mg/L) (Table 2). Our results revealed that patients with higher serum PCS had significantly lower Hb, Hct, estimated GFR and higher BUN, Cr, and i-PTH. There was no difference on albumin, calcium, and phosphate levels.

At the end of study, 18 out of 72 patients were recorded as experiencing a new cardiovascular event. Only 6 patients died (4 from cardiovascular causes and 2 from infectious disease). In addition, 16 patients started to undergo regular dialysis due to deterioration of renal function including 13 hemodialysis and 3 peritoneal dialysis during 3-year follow-up.

Table 3 revealed the Cox regression analysis results of independent variables on specific clinical outcomes including cardiovascular event, all-cause mortality, and dialysis event. For cardiovascular event, age, CAD, BUN, eGFR, calcium, phosphate, i-PTH, and PCS were significantly associated with cardiovascular event in the univariate Cox regression analysis. After adjusting confounding factors, only age (HR: 1.12, $P = 0.01$), CAD (HR: 6.28, $P = 0.02$), and PCS (HR: 1.12, $P = 0.02$) had reached significance in the multivariate analysis. In addition, age, BUN, Cr, eGFR, albumin, phosphate, i-PTH, and PCS were found independently to relate to dialysis event in the univariate analysis. It showed only age (HR: 0.91, $P < 0.01$), albumin (HR: 0.03, $P < 0.01$), and PCS (HR: 1.17, $P < 0.01$) reached significant association with this event finally. However, there was no association between independent variables and all-cause mortality.

Kaplan-Meier curves of time to the first clinical events were showed in Figure 1. Patients were divided into two groups by median PCS levels (>6.0 mg/L and ≦6.0 mg/L). Patients with higher PCS level were strongly associated with higher rate of a cardiovascular event and dialysis event than those with lower PCS levels during 3-year follow-up (log rank $P = 0.03$, $P < 0.01$, resp.) (Figures 1(b) and 1(c)). However, only 6 patients died at the end of the study. Statistical

Table 2: Clinical biochemistry of CKD patients divided by medium PCS concentration (6 mg/L).

Variables	P-cresyl sulfate ≧6.0 mg/L (n = 34)	P-cresyl sulfate <6.0 mg/L (n = 38)	P value
CKD stage (%)			
3	10.0%	57.3%	<0.001
4	24.5 %	37.5%	<0.001
5	65.5%	5.2%	<0.001
Albumin (g/dL)	3.9 ± 0.3	4.0 ± 0.4	NS
Hemoglobin (g/L)	9.3 ± 1.7	10.7 ± 1.9	0.01
Hematocrit (%)	27.8 ± 5.7	32.3 ± 5.5	0.01
BUN (mg/dL)	52.0 ± 23.4	37.8 ± 20.8	<0.001
Creatinine (mg/dL)	4.9 ± 2.9	2.8 ± 2.1	<0.001
eGFR (mL/min)	15.8 ± 15.3	30.5 ± 15.4	<0.001
Calcium (mg/dL)	9.1 ± 0.5	9.0 ± 0.4	NS
Phosphate (mg/dL)	4.6 ± 0.7	4.3 ± 0.7	NS
Intact-PTH (pg/mL)	201.1 ± 230	78.5 ± 75.0	<0.001
P-cresyl sulfate (mg/L)	13.4 ± 6.4	2.5 ± 1.8	<0.001

analysis showed no significant difference for PCS level on all-cause mortality in this CKD cohort (log rank $P = 0.26$) (Figure 1(a)).

4. Discussion

Our study showed that serum PCS level was significantly associated with cardiovascular and dialysis events in a predialysis CKD cohort during a 3-year follow-up. From this result, we suggested PCS levels may be an alternative surrogate in prediction of cardiovascular disease and kidney function deterioration.

It is well known that CKD is independently associated with endothelial dysfunction [16], which plays a vital role in the development of cardiovascular diseases and is the main cause of mortality in CKD patients [17]. Thus, it is not surprising that cardiovascular disease remained the most important cause of morbidity and mortality in patients with predialysis and dialysis patients [1–3]. Some traditional and nontraditional risk factors have been reported to be associated with endothelial dysfunction [4–8]. Protein-bound uremic toxins, one of nontraditional factors, include PCS and indoxyl sulfate (IS), and have been regarded to be contributed to this pathophysiology [10, 18].

PCS, an endproduct of protein metabolism originating from intestinal tract, is accumulated as renal function declines [19]. From *in vitro* studies, it showed an increased free radical production after exposure of leukocyte to PCS at a uremia concentration [20]. In addition, Meijers et al. reported that PCS could promote endothelial microparticle release, an indicator of endothelial damage [10]. Both of endothelial damage and leukocyte activation are able to contribute to vascular damage [21]. However, the serum concentration of PCS was increased gradually in patients with advanced CKD [22] and could not be effectively removed by standard dialysis [9]. It subsequently will carry clinical toxicity finally. This can be proved by some previous prospective studies, which demonstrated a close relationship between PCS levels and clinical outcomes including infectious event, cardiovascular disease, and overall mortality in a hemodialysis [12–14] and peritoneal dialysis cohort [23].

In this study, we observed that, in pre-ESRD patients, the PCS level was able to predict cardiovascular event during study period. Our results were partially concordant with the findings published by Liabeuf et al., except overall mortality event [22]. There was no significant correlation between PCS levels and overall mortality event in this research. This discrepancy results from lower mortality rate in our patients and reflects the different survival rate of CKD in western and eastern country. Our recent study also indicated that PCS level was not only associated with peripheral artery disease but also a valuable surrogate marker in predicting vascular access dysfunction in patient with hemodialysis [15]. Another previous study revealed that PCS level was correlated with coronary lesions in patients with stable angina and moderate degrees of CKD [24]. These findings specify the accumulation of PCS was closely linked to unfavorable cardiovascular outcomes in CKD population.

However, based on previous reports, the effect of PCS on kidney progression has not been demonstrated. Until a recent basic research conducted by Watanabe et al., indicated PCS was capable of resulting in renal tubular cell damage by inducing oxidative stress by activation of NADPH oxidase [25], a similar mechanism caused by IS [26, 27]. This is the first study to support renal toxicity of PCS. It also can explain the result from our study that PCS level could predict kidney function deterioration. Our finding can be regarded as the extension of results from basic *in vitro* to clinical research. Thus, these evidences indicated that PCS was not only a vascular toxin but also a nephrotoxin. There are limitations in our study. First, this study was performed with only minimum numbers of

Table 3: Univariate and multivariate Cox regression analysis for evaluating the relationship between independent variables and clinical outcomes in CKD patients.

Variables	Cardiovascular event						All-cause mortality			Dialysis					
	Univariate Cox regression analysis			Multivariate Cox regression analysis			Univariate Cox regression analysis			Univariate Cox regression analysis			Multivariate Cox regression analysis		
	HR	95% CI	*P*	HR	95% CI	*P*	HR	95% CI	*P*	HR	95% CI	*P*	HR	95% CI	*P*
Gender (F/M)	0.66	0.24–1.77	NS				0.84	0.12–5.99	NS	0.80	0.29–2.21	NS			
Age (years)	1.08	1.01–1.15	0.01	1.12	1.00–1.25	0.01	1.12	0.95–1.30	NS	0.93	0.89–0.98	<0.01	0.91	0.85–0.96	<0.01
CV/Non-CV	2.92	1.01–8.41	0.04	6.28	1.32–29.71	0.02	0.04	0.00–31.81	NS	0.72	0.16–3.19	NS			
DM/Non-DM	1.80	0.67–4.83	NS				2.19	0.31–15.58	NS	0.52	0.14–1.84	NS			
BUN (mg/dL)	1.03	1.00–1.04	<0.01	0.98	0.95–1.03	NS	0.99	0.94–1.03	NS	1.05	1.02–1.07	<0.01	0.99	0.95–1.03	NS
Cr (mg/dL)	1.11	0.97–1.28	NS				0.89	0.56–1.41	NS	1.51	1.31–1.73	<0.01	1.25	0.74–2.11	NS
eGFR (mL/min)	0.95	0.91–0.99	<0.01	0.99	0.93–1.06	NS	0.98	0.92–1.05	NS	0.80	0.71–0.90	<0.01	0.69	0.47–1.02	NS
Hb (g/dL)	0.85	0.82–1.93	NS				0.79	0.56–1.04	NS	0.85	0.33–2.31	NS			
Hct (%)	0.90	0.33–2.42	NS				3.77	0.39–36.31	NS	0.91	0.82–1.01	NS			
Albumin (g/dL)	0.82	0.25–2.65	NS				0.85	0.06–10.82	NS	0.39	0.15–0.99	0.04	0.03	0.00–0.33	<0.01
Ca (mg/dL)	0.27	0.11–0.65	<0.01	0.54	0.19–1.54	NS	3.29	0.44–24.11	NS	0.41	0.15–1.10	NS			
P (mg/dL)	1.97	1.16–3.33	0.01	1.66	0.70–3.91	NS	0.41	0.08–2.02	NS	2.06	1.15–3.72	0.01	0.93	0.53–1.02	NS
i-PTH (pg/mL)	1.00	1.00-1.00	0.03	1.00	0.99–1.01	NS	1.00	0.99–1.01	NS	1.00	1.00-1.00	<0.01	0.99	0.99-1.00	NS
PCS (mg/L)	1.08	1.02–1.15	<0.01	1.12	1.01–1.21	0.02	1.06	0.94–1.21	NS	1.10	1.02–1.17	<0.01	1.17	1.05–1.30	<0.01

PCS: P-cresyl sulfate, NS: no significance, CI: confidence interval.

study patients, and all subjects were enrolled from one medical center. Second, whether attenuation of serum PCS concentration could reduce the risk of cardiovascular event and delay kidney function progression is still unclear.

In conclusion, our study showed higher serum PCS levels were closely associated with cardiovascular event and dialysis event. It provides more evidences about the toxic effect of PCS on clinical outcomes. Further more studies are needed to demonstrate if patient's outcomes could be improved after lowering serum PCS levels in future.

Conflict of Interests

The authors report that they have no other relevant financial interests.

Acknowledgments

The authors would like to thank all the patients who were involved in this study. This study was supported in part by a Grant from the Taiwan National Science Council (NSC 100-2314-B-195-015) and Mackay Memorial Hospital (MMH-9941).

References

[1] D. S. Keith, G. A. Nichols, C. M. Gullion, J. B. Brown, and D. H. Smith, "Longitudinal follow-up and outcomes among a population with chronic kidney disease in a large managed care organization," *Archives of Internal Medicine*, vol. 164, no. 6, pp. 659–663, 2004.

[2] M. J. Sarnak, A. S. Levey, A. C. Schoolwerth et al., "Kidney disease as a risk factor for development of cardiovascular disease: a statement from the American Heart Association Councils on Kidney in Cardiovascular Disease, High Blood Pressure Research, Clinical Cardiology, and Epidemiology and Prevention," *Hypertension*, vol. 42, no. 5, pp. 1050–1065, 2003.

[3] A. S. Go, G. M. Chertow, D. Fan et al., "Chronic kidney disease and the risks of death, cardiovascular events, andhospitalization," *The New England Journal of Medicine*, vol. 351, no. 13, pp. 1296–1305, 2004.

[4] M. J. Sarnak, B. E. Coronado, T. Greene et al., "Cardiovascular disease risk factors in chronic renal insufficiency," *Clinical Nephrology*, vol. 57, no. 5, pp. 327–335, 2002.

[5] R. Clarke, L. Daly, K. Robinson et al., "Hyperhomocysteinemia: an independent risk factor for vascular disease," *The New England Journal of Medicine*, vol. 324, no. 17, pp. 1149–1155, 1991.

[6] B. F. Culleton and P. W. Wilson, "Cardiovascular disease: risk factors, secular trends, and therapeutic guidelines," *Journal of the American Society of Nephrology*, vol. 9, no. 12, pp. 5–15, 1998.

[7] M. J. Sarnak and A. S. Levey, "Cardiovascular disease and chronic renal disease: a new paradigm," *The American Journal of Kidney Diseases*, vol. 35, no. 4, pp. S117–S131, 2000.

[8] J. C. Longenecker, J. Coresh, N. R. Powe et al., "Traditional cardiovascular disease risk factors in dialysis patients compared with the general population: the CHOICE study," *Journal of the American Society of Nephrology*, vol. 13, no. 7, pp. 1918–1927, 2002.

[9] D. H. Krieter, A. Hackl, A. Rodriguez et al., "Protein-bound uraemic toxin removal in haemodialysis and post-dilution haemodiafiltration," *Nephrology Dialysis Transplantation*, vol. 25, no. 1, pp. 212–218, 2010.

[10] B. K. Meijers, S. Van kerckhoven, K. Verbeke et al., "The Uremic Retention Solute p-Cresyl Sulfate and Markers of Endothelial Damage," *The American Journal of Kidney Diseases*, vol. 54, no. 5, pp. 891–901, 2009.

[11] L. Dou, E. Bertrand, C. Cerini et al., "The uremic solutes p-cresol and indoxyl sulfate inhibit endothelial proliferation and wound repair," *Kidney International*, vol. 65, no. 2, pp. 442–451, 2004.

[12] B. K. Meijers, B. Bammens, B. de Moor, K. Verbeke, Y. Vanrenterghem, and P. Evenepoel, "Free p-cresol is associated with cardiovascular disease in hemodialysis patients," *Kidney International*, vol. 73, no. 10, pp. 1174–1180, 2008.

[13] C. J. Lin, C. J. Wu, C. F. Pan, Y. C. Chen, F. J. Sun, and H. H. Chen, "Serum protein-bound uraemic toxins and clinical outcomes in haemodialysis patients," *Nephrology Dialysis Transplantation*, vol. 25, no. 11, pp. 3693–3700, 2010.

[14] B. Bammens, P. Evenepoel, H. Keuleers, K. Verbeke, and Y. Vanrenterghem, "Free serum concentrations of the protein-bound retention solute p-cresol predict mortality in hemodialysis patients," *Kidney International*, vol. 69, no. 6, pp. 1081–1087, 2006.

[15] C. J. Lin, C. F. Pan, H. L. Liu et al., "The role of protein-bound uremic toxins on peripheral artery disease and vascular access failure in patients on hemodialysis," *Atherosclerosis*, vol. 225, no. 1, pp. 173–179, 2012.

[16] R. N. Foley, P. S. Parfrey, and M. J. Sarnak, "Epidemiology of cardiovascular disease in chronic renal disease," *Journal of the American Society of Nephrology*, vol. 9, no. 12, pp. S16–S23, 1998.

[17] J. P. J. Halcox, W. H. Schenke, G. Zalos et al., "Prognostic value of coronary vascular endothelial dysfunction," *Circulation*, vol. 106, no. 6, pp. 653–658, 2002.

[18] N. Masai, J. Tatebe, G. Yoshino, and T. Morita, "Indoxyl sulfate stimulates monocyte chemoattractant protein-1 expression in human umbilical vein endothelial cells by inducing oxidative stress through activation of the NADPH oxidase-nuclear factor-κB pathway," *Circulation Journal*, vol. 74, no. 10, pp. 2216–2224, 2010.

[19] C. J. Lin, H. H. Chen, C. F. Pan et al., "p-cresylsulfate and indoxyl sulfate level at different stages of chronic kidney disease," *Journal of Clinical Laboratory Analysis*, vol. 25, no. 3, pp. 191–197, 2011.

[20] E. Schepers, N. Meert, G. Glorieux, J. Goeman, J. van der Eycken, and R. Vanholder, "P-cresylsulphate, the main in vivo metabolite of p-cresol, activates leucocyte free radical production," *Nephrology Dialysis Transplantation*, vol. 22, no. 2, pp. 592–596, 2007.

[21] R. Vanholder, A. Argilés, U. Baurmeister et al., "Uremic toxicity: present state of the art," *International Journal of Artificial Organs*, vol. 24, no. 10, pp. 695–725, 2001.

[22] S. Liabeuf, D. V. Barreto, F. C. Barreto et al., "Free p-cresylsulphate is a predictor of mortality in patients at different stages of chronic kidney disease," *Nephrology Dialysis Transplantation*, vol. 25, no. 4, pp. 1183–1191, 2010.

[23] C. J. Lin, C. F. Pan, C. K. Chuang et al., "Gastrointestinal-related uremic toxins in peritoneal dialysis: a pilot study with a 5-year follow-up," *Archives of Medical Research*, vol. 44, no. 7, pp. 535–541, 2013.

[24] C. P. Wang, L. F. Lu, T. H. Yu et al., "Serum levels of total p-cresylsulphate are associated with angiographic coronary

atherosclerosis severity in stable angina patients with early stage of renal failure," *Atherosclerosis*, vol. 211, no. 2, pp. 579–583, 2010.

[25] H. Watanabe, Y. Miyamoto, D. Honda et al., "p-Cresyl sulfate causes renal tubular cell damage by inducing oxidative stress by activation of NADPH oxidase," *Kidney International*, vol. 83, no. 4, pp. 582–592, 2013.

[26] Z. Tumur and T. Niwa, "Indoxyl sulfate inhibits nitric oxide production and cell viability by inducing oxidative stress in vascular endothelial cells," *The American Journal of Nephrology*, vol. 29, no. 6, pp. 551–557, 2009.

[27] M. Yu, Y. J. Kim, and D. H. Kang, "Indoxyl sulfate-induced endothelial dysfunction in patients with chronic kidney disease via an induction of oxidative stress," *Clinical Journal of the American Society of Nephrology*, vol. 6, no. 1, pp. 30–39, 2011.

Hindawi Publishing Corporation
BioMed Research International
Volume 2013, Article ID 790263, 10 pages
http://dx.doi.org/10.1155/2013/790263

Research Article

Antiatherosclerotic Potential of Clopidogrel: Antioxidant and Anti-Inflammatory Approaches

Najah R. Hadi,[1] Bassim I. Mohammad,[2] Ihsan M. Ajeena,[3] and Hussam H. Sahib[1]

[1] *Department of Pharmacology, College Medicine, University of Kufa, Najaf, Iraq*
[2] *College of Pharmacy, University of Al-Qadissiya, Diwaniya, Iraq*
[3] *Department of Physiology, College Medicine, University of Kufa, Najaf, Iraq*

Correspondence should be addressed to Najah R. Hadi; drnajahhadi@yahoo.com

Received 17 September 2013; Revised 7 December 2013; Accepted 7 December 2013

Academic Editor: Joen-Rong Sheu

Background. Atherosclerosis is characterized by endothelial dysfunction, vascular inflammation, and the buildup of lipids, cholesterol, calcium, and cellular debris within the intima of the walls of large and medium size arteries. *Objective*. To evaluate the effect of clopidogrel on atherosclerosis progression. *Materials and Methods*. A total of 28 local domestic rabbits were assigned to four groups: normal control, atherogenic control, vehicle control, and clopidogrel treated. Serum triglycerides, total cholesterol, HDL-C, plasma high sensitive C-reactive protein (hsCRP), plasma malondialdehyde (MDA), and plasma reduced glutathione (GSH) were measured at the end of the experiment. Immunohistochemical of aortic atherosclerotic changes were also performed. *Results*. There was no statistically significant difference between atherogenic control group and vehicle group. Levels of lipid profile, atherogenic index, hsCRP, and MDA are increased while GSH levels were decreased in animals on atherogenic diet. Immunohistochemical analysis showed that aortic expressions of VCAM-1, MCP-1, TNF-α, and IL-17A were significantly increased in atherogenic control group. Histopathologic finding showed that animals on atherogenic diet have significant atherosclerotic lesion. Compared to atherogenic control group clopidogrel do not have significant effect on lipid profile. Clopidogrel significantly reduces hsCRP and MDA levels and increases GSH level. Furthermore, clopidogrel treatment significantly reduced aortic expressions parameters and the histopathologic examination of the aortic arch showed a significant reduction of atherosclerotic lesion. *Conclusions*. This study outlines how clopidogrel reduces lipid peroxidation, systemic inflammation, and aortic expression of inflammatory markers and hence reduces the progression of atherosclerosis.

1. Introduction

Atherosclerosis is a disease of large- and medium-sized arteries and is characterized by endothelial dysfunction, vascular inflammation, and the buildup of lipids, cholesterol, calcium, and cellular debris within the intima of the vessel wall. This buildup results in plaque formation, vascular remodelling, acute and chronic luminal obstruction, abnormalities of blood flow, and diminished oxygen supply to target organs [1]. The proposed initial step in atherogenesis is endothelial dysfunction leading to a number of compensatory responses that alter the normal vascular homeostatic properties [2]. Proinflammatory stimuli, including a diet high in saturated fat, hypercholesterolemia, obesity, hyperglycemia, insulin resistance, hypertension, and smoking, trigger the endothelial expression of adhesion molecules such as P-selectin, E-selectin, ICAM-1, and VCAM-1 which mediate the attachment of circulating monocytes and lymphocyte [3, 4]. Atherosclerotic lesions develop as a result of inflammatory stimuli, subsequent release of various cytokines, proliferation of smooth muscle cells, synthesis of connective tissue matrix, and accumulation of macrophage and lipid. Atherosclerosis is likely initiated when endothelial cells overexpress adhesion molecules in response to turbulent flow in the setting of an unfavorable serum lipid profile. Clopidogrel inhibits ADP receptors on platelets, blocking GP1lb/111a complex and as a result, inhibiting platelet aggregation. Animals that were fed a pro-atherogenic diet rapidly overexpress vascular cell adhesion molecule-1 (VCAM-1) [5]. VCAM-1 expression increases recruitment

of monocytes and T cells to sites of endothelial injury; subsequent release of monocyte chemoattractant protein-1 (MCP-1) by leukocytes magnifies the inflammatory cascade by recruiting additional leukocytes, activating leukocytes in the media, and causing recruitment and proliferation of smooth muscle cells [6]. However, in response to signals generated within the early plaque, monocytes adhere to the endothelium and then migrate through the endothelium and basement membrane by elaborating enzymes, including locally activated matrix metalloproteinase (MMP) that degrade the connective tissue matrix. Recruited macrophages both release additional cytokines and begin to migrate through the endothelial surface into media of the vessel. This process is further enhanced by the local release of monocytes-colony stimulating factor (M-CSF), which causes monocytic proliferation; local activation of monocytes leads to both cytokine-mediated progression of atherosclerosis and oxidation of low-density lipoprotein (LDL) [7].

Platelets serve major functions in three key aspects of atherosclerosis: atherogenesis, inflammation, and homeostatic [8]. Therefore, the present study was undertaken to evaluate the effect of clopidogrel on the progression of atherosclerosis.

2. Materials and Methods

2.1. Animals. A total of 28 local domestic rabbits, weighing (1.1–1.5) kg, were used in this study. All experiments were conducted in the Department of Pharmacology, College of Medicine, Qadaysia University, according to the guidelines for the Care and Use of Laboratory Animals in scientific research. The animals were placed in an animal house, in a group caging system, at controlled temperature (25 ± 2°C) and ambient humidity. Lights were maintained on a 12-h light/dark cycle. The animals had free access to water *ad libitum*.

2.2. Drugs. Clopidogrel (plavix, sanofi aventis, BN.F-33565, France) was dissolved in ethanol (10%) [9] and used in a dose of 20 mg/kg/day [10]. A solution of drug was freshly prepared and administered once daily orally according to body weight through stomach tube.

2.3. Animal Model of Atherosclerosis. Induction of atherosclerosis was carried out by feeding the rabbit an atherogenic diet (2% cholesterol (BDH Chemicals Ltd Poole England, prod 43011) enriched rabbit chow) made by addition of cholesterol powder to chow pellets for 8 weeks [11, 12].

2.4. Experimental Protocol. After 2 weeks of acclimatization period, the animals were randomized into 4 groups (of 7 rabbits each): normal diet control group (NC, Group I), high-cholesterol diet group which served as atherogenic control (AC, Group II), high-cholesterol diet with ethanol group (vehicle, Group III), and high-cholesterol diet with clopidogrel group (Group IV). The NC group was fed normal rabbit chow, whereas the high-cholesterol diet groups were fed a 2% high-cholesterol (atherogenic) diet. The duration of treatment was 8 weeks. At the end of the experiment, food was withheld for 16–18 hours and animals were anesthetized by ketamine (HIKMA pharmaceuticals B.N 3310) at 66 mg/kg and xylazine (alfasan B.N 1004111-07) at 6 mg/kg intramuscular [13]. The chest was opened by thoracotomy, blood sample was collected directly from the heart, and aorta was separated.

After that, the following investigations were performed:

(i) lipid profile including total serum cholesterol (TC), low density lipoprotein (LDL), and high density lipoprotein (HDL),

(ii) immunohistochemistray for assessment of VCAM, TNFα, MCP1 and IL-17A,

(iii) oxidation parameter including MDA and GSH,

(iv) systemic inflammatory marker hsCRP,

(v) histopathological examination of the aorta for assessment of atherosclerosis.

All specimens were immediately fixed in 10% formaldehyde solution for subsequent processing.

2.5. Biochemical Procedures. Serum lipid profile, including total cholesterol and TG, was determined by enzymatic methods using an automatic analyzer (Abbott, Alcyon 300, USA). Plasma GSH levels was determined using methods of Beutler [14]. Plasma MDA level were determined by using competitive inhibition enzyme immunoassay technique (cusabio; Catalog no. CSB-E13712Rb). The determination of hsCRP was done by using rabbit high-sensitive CRP ELISA kit supplied by (Kamiya Biomedical Company; Cat. no. KT-097). The measurement was carried out according to the manufacturer's instructions.

2.6. Histological Examination of the Aorta. For histological evaluation of atherosclerosis, the specimens were processed in usual manner and embedded in paraffin and cut into 5 μm thick sections. The tissue sections were stained with hematoxylin and eosin. The assessment of atherosclerotic changes was performed according to the American Heart Association classification of atherosclerosis: Type I and Type II lesions (early lesions), Type III lesions (intermediate lesions or preatheroma), Type IV lesions (atheroma), Type V lesions (fibroatheroma or advance lesion), and Type VI lesions (complicated lesions) [15] (Figure 1).

2.7. Immunohistochemistry. It was performed with polyclonal goat antibodies and raised against rabbit VCAM-1, TNFα, MCP-1, and IL-17A. Staining procedure was carried out according to the manufacturer's instructions (Santa Cruz Biotechnology, Inc). The stain intensity was scored to 0: indicated no staining, 1: weak, 2: moderate, 3: strong, and 4: very strong stain intensity [16] (Figures 2, 3, 4, and 5).

2.8. Statistical Analysis. Statistical analyses were performed using SPSS 12.0 version. Data were expressed as mean ± SEM. Paired t-test was used to compare the mean values within each group at different time. Analysis of Variance (ANOVA)

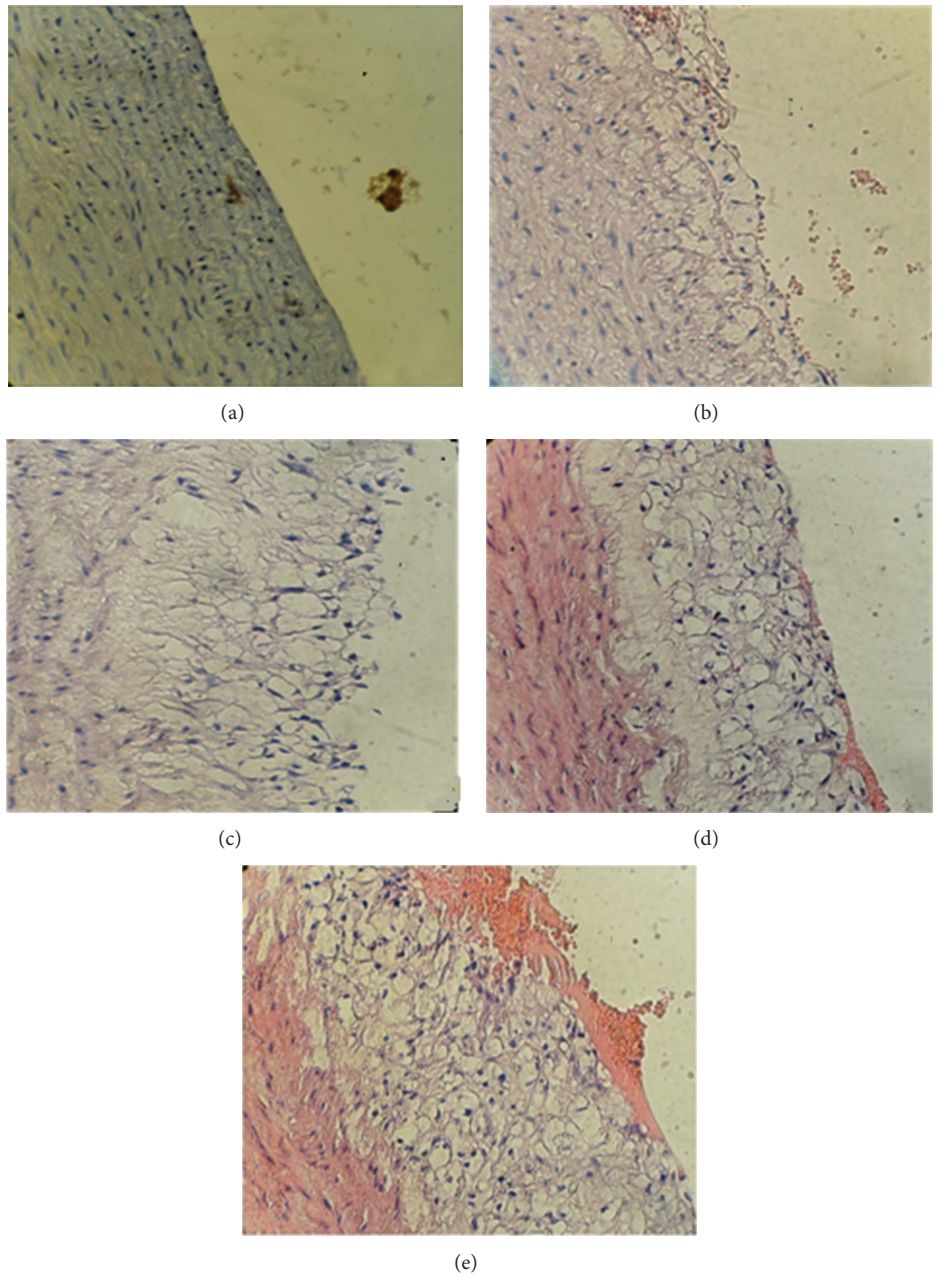

Figure 1: A cross section of aortic arch from hypercholesterolemic rabbit represented atherosclerosis progression (×40). (a) Normal arterial appearance, (b) initial atherosclerotic lesion characterized by lipid laden macrophage (foam cells), (c) intermediate atherosclerotic lesion characterized by extracellular lipid pool, (d) advance atherosclerotic lesion characterized by core of extracellular lipid, and (e) complicated atherosclerotic lesion characterized by haemorrhagic thrombus.

was used for the multiple comparison among all groups. The histopathological grading was assessed by Mann-Whitney test. In all tests, $P < 0.05$ was considered to be statistically significant.

3. Results

3.1. Effect of High-Cholesterol Diet. There was no statistically significant difference between AC group and vehicle group. Compared to NC group, the AC showed significant changes in serum lipid profile, oxidation, and inflammatory markers. Serum levels of TC, TG and LDL-C as well as plasma levels of MDA and hs-CRP were significantly ($P < 0.001$) increased. In addition plasma levels of GSH were significantly ($P < 0.001$) lower in rabbits that fed on cholesterol-enriched diet in comparison to animals on normal diet (Tables 1, 2, and 3).

3.2. Effects of Clopidogrel Treatment. Compared to atherogenic control, treating hyperlipidemic rabbits with clopidogrel resulted in significantly ($P < 0.001$) lower levels of plasma hs-CRP and MDA. However, clopidogrel treatment

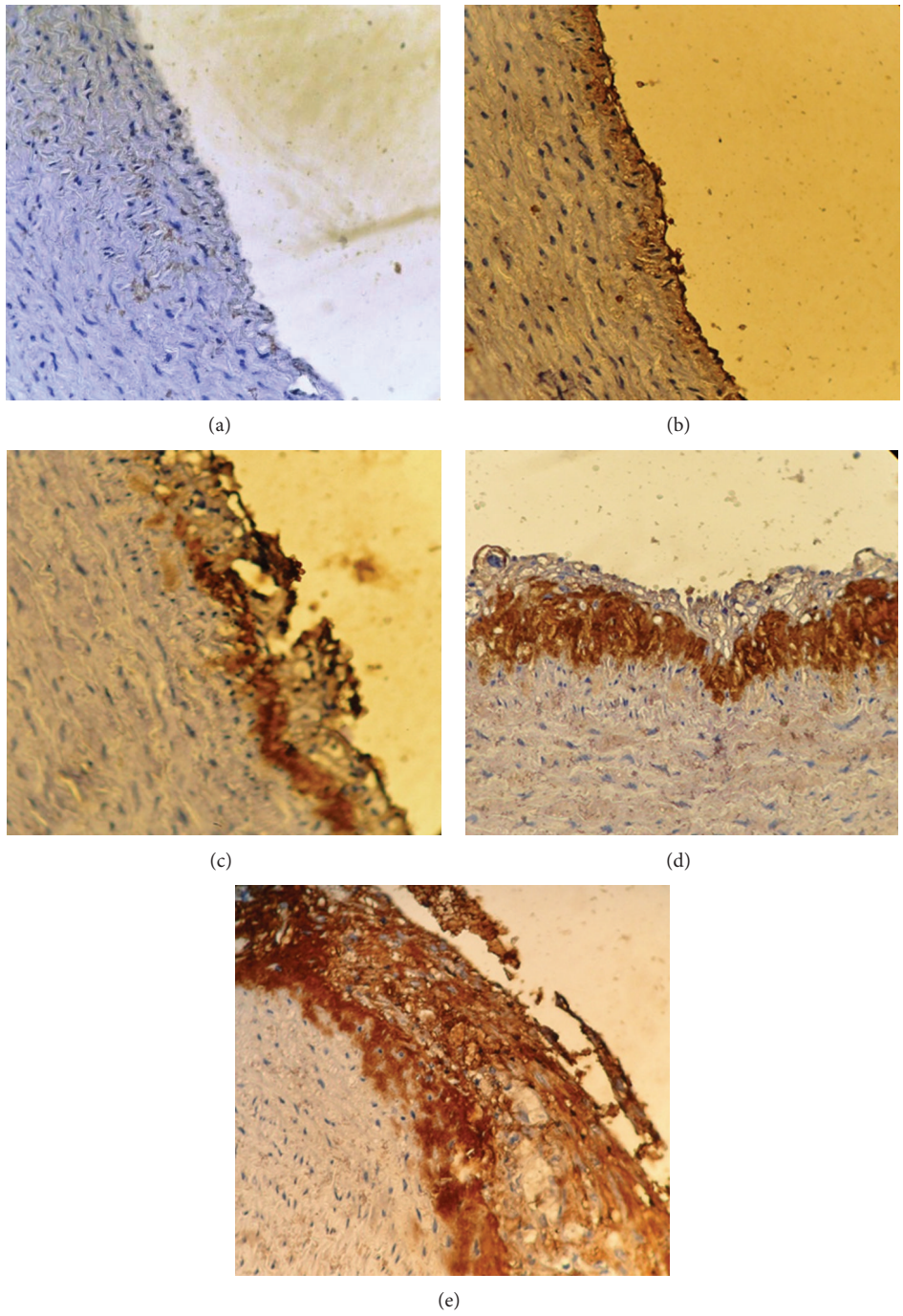

Figure 2: Immunohistochemical staining for MCP-1 expression in aortic arch from cholesterol-fed rabbits (×40). (a) Negative, (b) weak stain intensity, (c) moderate stain intensity, (d) strong stain intensity, and (e) very strong stain intensity.

caused no significant alteration ($P > 0.05$) in the levels of serum lipids and GSH (Tables 2 and 3).

3.3. Immunohistochemistry. The results of immunohistochemical analysis for rabbit's aortic arch of VCAM-1, MCP-1, TNF-alpha, and IL-17A were significantly different between the 4 study groups. The median intensity of these markers was the highest in AC group (very strong for all markers) and the lowest in NC group (normal for all markers). Clopidogrel treated group was associated with a median stain intensity of moderate for VCAM-1, MCP-1, TNF-alpha, and IL-17A that is significantly lower than the atherogenic control (Figure 6).

3.4. Histopathological Findings. The atherosclerotic lesions of aortic arch were graded as normal, initial, intermediated, advance, and complicated lesions (Figure 1). The median

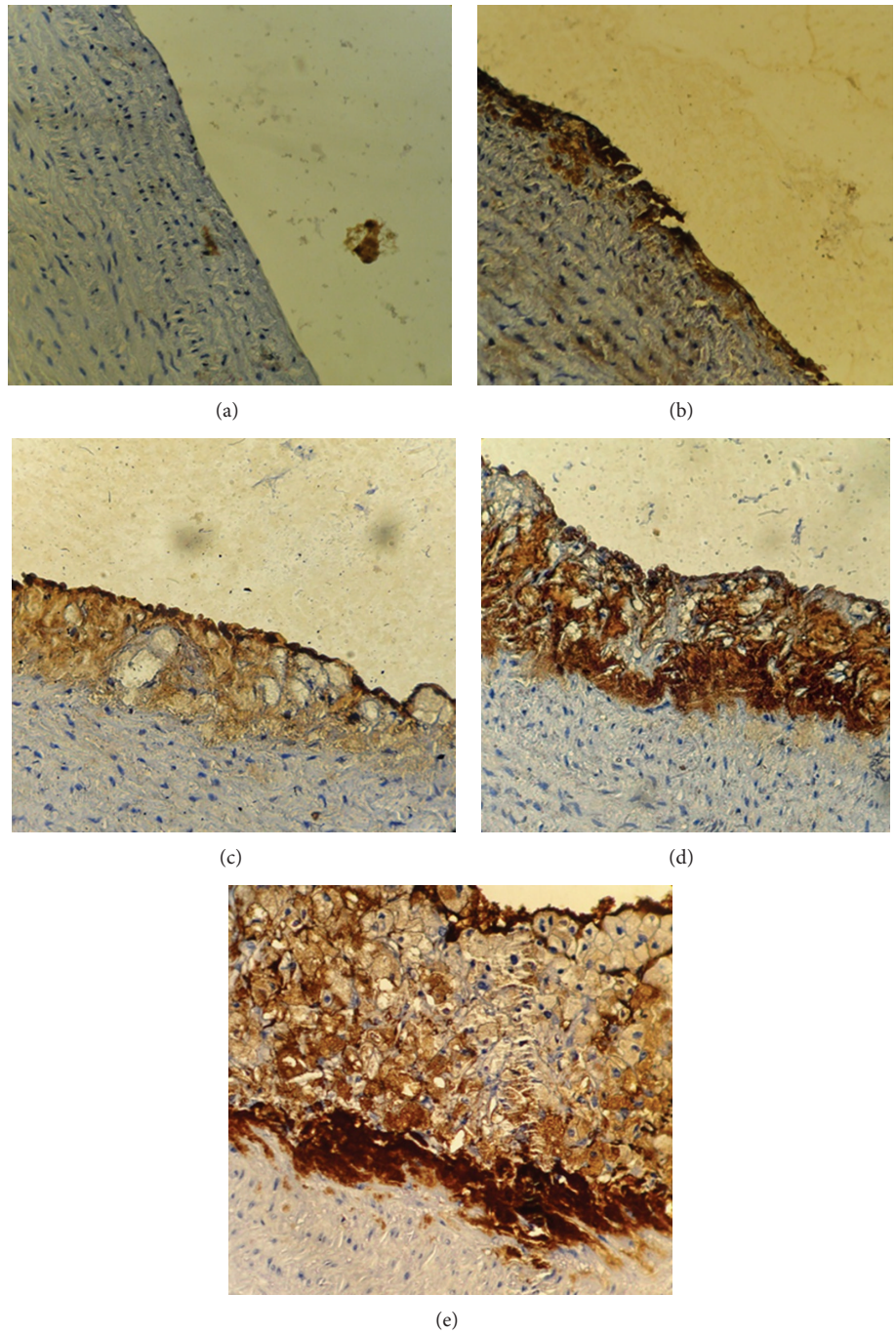

(a) (b) (c) (d) (e)

Figure 3: Immunohistochemical staining for MCP-1 expression in aortic arch from cholesterol-fed rabbits (×40). (a) Negative, (b) weak stain intensity, (c) moderate stain intensity, (d) strong stain intensity, and (e) very strong stain intensity.

histopathological grade of atherosclerotic changes was significantly different between the 4 study groups. The median was the highest in atherogenic control (advance) and the lowest in the normal diet control (no abnormality). Clopidogrel treated group was associated with a median aortic change (initial) that is significantly lower than the atherogenic control (Figure 7).

4. Discussion

4.1. Effect of Clopidogrel on Lipid Profile. In this study clopidogrel had small nonsignificant effect on lipid profile in comparison with induced untreated study group. Such findings are consistent with that of Gu and his followers [17].

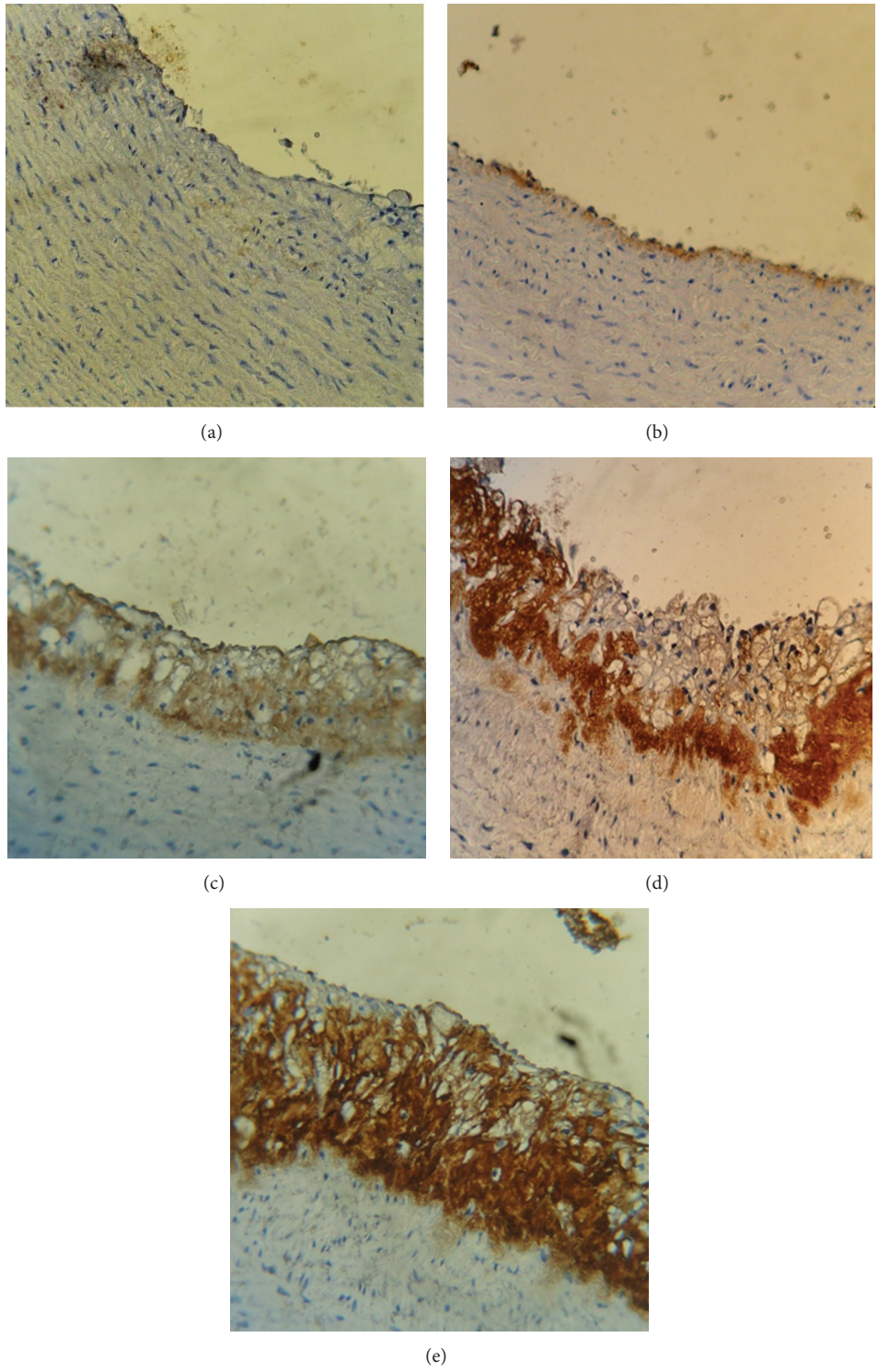

Figure 4: Immunohistochemical staining for TNF-α expression in aortas arch from cholesterol-fed rabbits (×40). (a) Negative, (b) weak stain intensity, (c) moderate stain intensity, (d) strong stain intensity, and (e) very strong stain intensity.

4.2. Effect of Clopidogrel on Oxidation Stress and Inflammatory Parameters. Like what Srinivas and his followers concluded in 2008 [18], the results showed that clopidogrel had significant effect on plasma MDA and GSH levels. Clopidogrel inhibited the increased plasma MDA level in AC group and it increased the plasma GSH level that was lowered in AC group. Furthermore, the results demonstrated a significant effect of clopidogrel on inflammatory acute phase protein by reducing the elevated hsCRP in rabbits on high fat diet. This finding suggests that the anti-inflammatory activity of clopidogrel

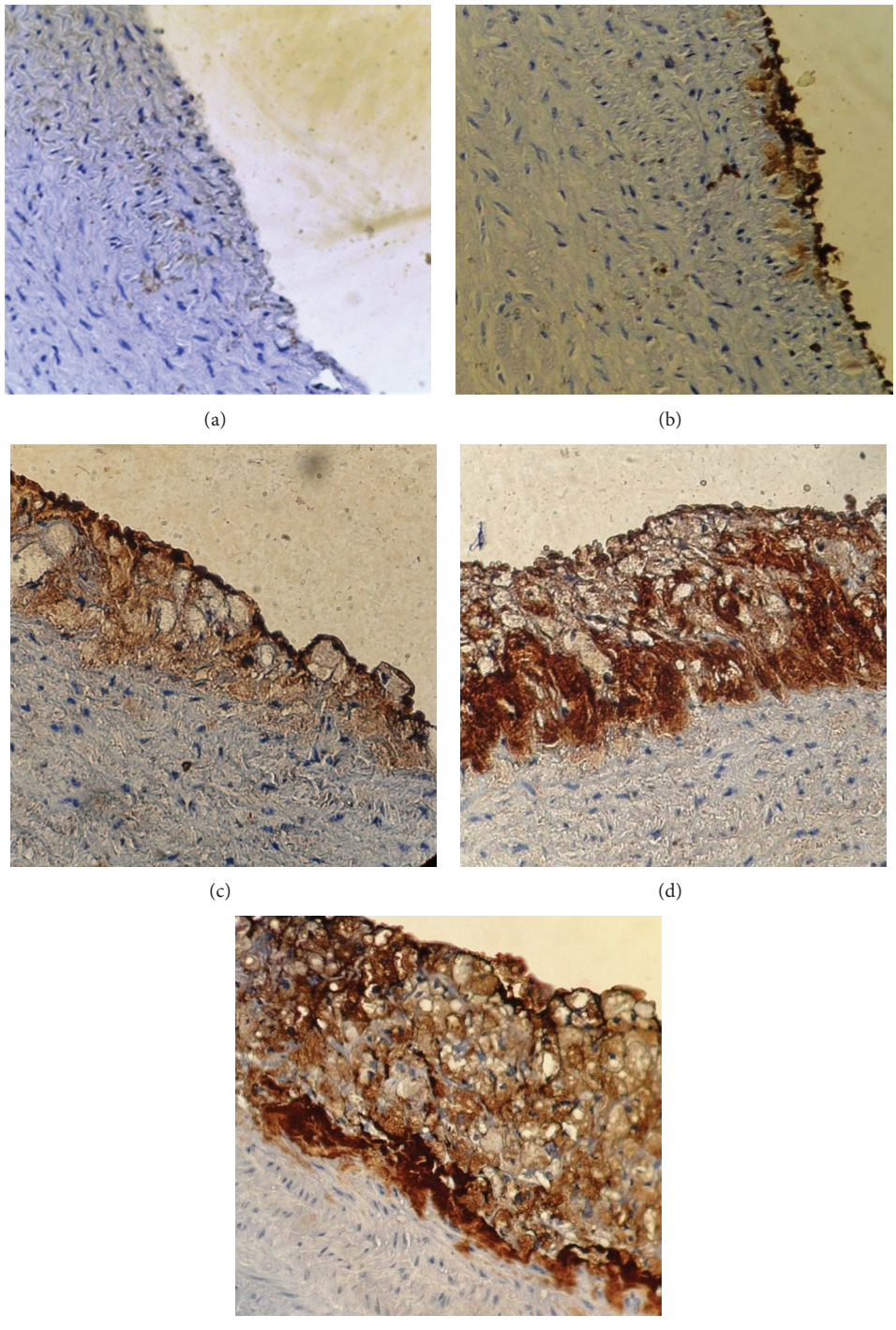

Figure 5: Immunohistochemical staining for IL17 expression in aortas arch from cholesterol-fed rabbits (×40). (a) Negative, (b) weak stain intensity, (c) moderate stain intensity, (d) strong stain intensity, and (e) very strong stain intensity.

on the vascular inflammatory responses is induced by high fat diet. This hypothesis is supported by similar findings and conclusions of other researchers [19, 20].

4.3. Effect of Clopidogrel on Aortic Expression of Immunohistochemistry Parameters (VCAM-1, MCP-1, TNF-α, and IL-17). The significant reduction of elevated VCAM-1, MCP-1, TNF-α, IL-17 in atherosclerosis model of hypercholesterolemia rabbit shows the effect of clopidogrel on such inflammatory markers. This finding was also reported by Li and his followers [21]. So, clopidogrel can reduce inflammation that underlies the chronic process of atherosclerosis by

Table 1: Change in serum lipid profile in the normal control (NC), atherogenic control (AC), vehicle control (VC), and clopidogrel treated groups.

Parameters	Groups			
	Clopidogrel treated	AC	NC	VC
TC (mg/dL)	1010.30 ± 65.46^{N}	$1017.1 \pm 64.94^{*}$	46.30 ± 0.99	1116.40 ± 42.91^{N}
TG (mg/dL)	3320 ± 40.23^{N}	$337.10 \pm 40.87^{*}$	60 ± 3.47	357 ± 35.18^{N}
HDL (mg/dL)	26.10 ± 1.26^{N}	$24.10 \pm 1.86^{*}$	15.70 ± 1.46	22.10 ± 0.77^{N}
LDL (mg/dL)	917.70 ± 64.98^{N}	$925.60 \pm 63.93^{*}$	18.60 ± 1.46	1022.90 ± 38.77^{N}
VLDL (mg/dL)	66.40 ± 8.05^{N}	$67.40 \pm 8.17^{*}$	12 ± 0.69	71.40 ± 7.04^{N}

Results are expressed as mean ± SEM.
$^{*}P < 0.05$, as compared to NC group.
^{N}Not significant as compared to AC group.

Table 2: Change in mean plasma levels of hs-CRP, MDA, and GSH in normal control (NC), atherogenic control (AC), vehicle control (VC), and clopidogrel treated groups.

Parameters	Groups			
	Clopidogrel treated	AC	NC	VC
Plasma GSH (mmol/L)	$0.741 \pm 0.02^{**}$	$0.56 \pm 0.02^{*}$	1.11 ± 0.03	0.53 ± 0.01^{N}
Plasma MDA (μmol/L)	$0.29 \pm 0.01^{**}$	$0.51 \pm 0.01^{*}$	0.13 ± 0.01	0.51 ± 0.01^{N}
Plasma hsCRP (μg/L)	$70.40 \pm 4.19^{**}$	$134.10 \pm 1.20^{*}$	33.30 ± 0.78	135.70 ± 2.09^{N}

Results are expressed as mean ± SEM.
$^{*}P < 0.05$, as compared to NC group; $^{**}P < 0.05$, as compared to AC group.
^{N}Not significant as compared to AC group.

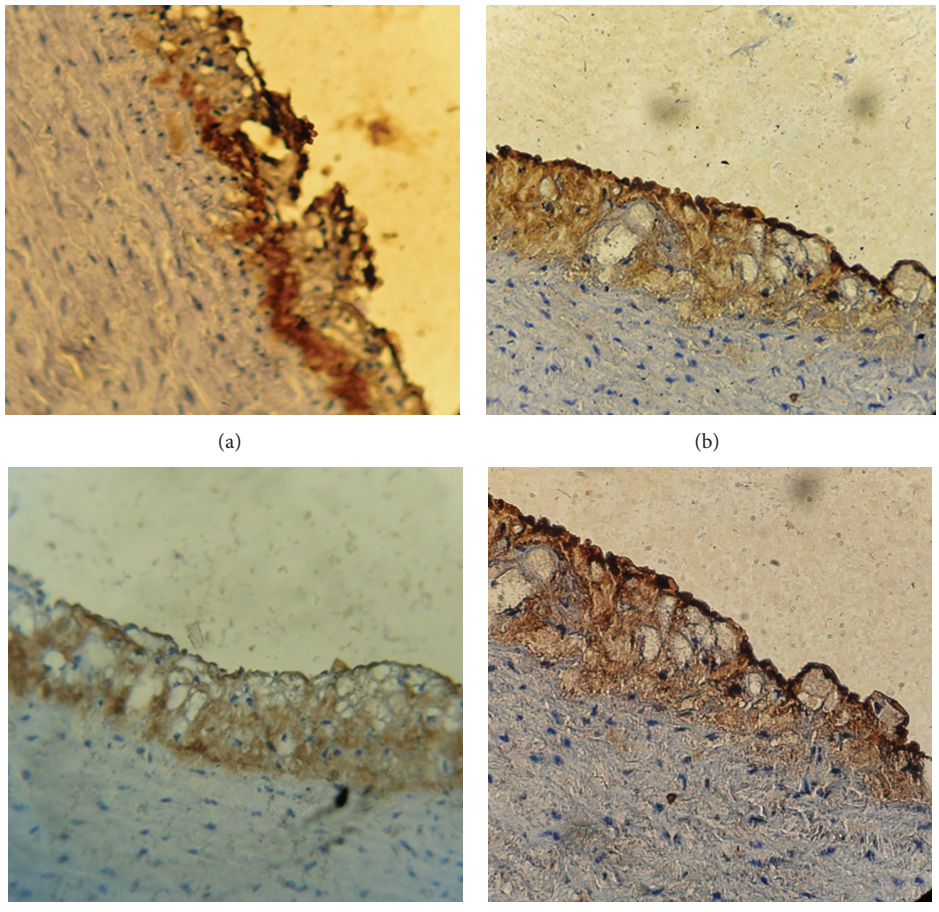

(a) (b) (c) (d)

Figure 6: Immunohistochemical staining for VCAM, MCP-1, TNF, and IL-17 expressions in aortas arch from clopidogrel treated group (×40). (a) VCAM-1, (b) MCP-1, (c) TNF, and (d) IL-17.

Table 3: The difference in median tissue (VCAM-1, MCP-1, and TNF alpha) immunostain intensity between normal control (NC), atherogenic control (AC), vehicle control (VC), and clopidogrel treated groups.

Markers	Groups			
	Clopidogrel treated	AC	NC	VC
VCAM-1	Moderate**	Very strong*	Negative	Very strong*
MCP-1	Moderate**	Very strong*	Negative	Very strong*
TNFα	Moderate**	Very strong*	Negative	Very strong*
IL-17 A	Moderate**	Very strong*	Negative	Very strong*

*$P < 0.05$, as compared to NC group.
**$P < 0.05$, as compared to AC group.

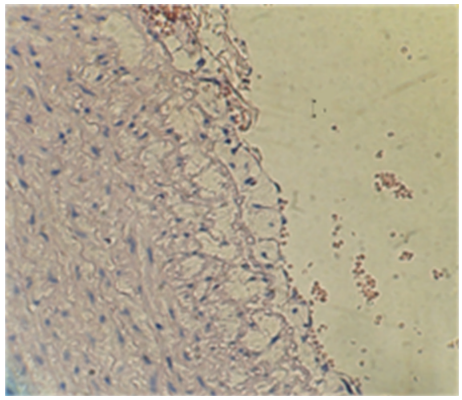

Figure 7: A cross section of aortic arch from clopidogrel treated rabbit represented histopathological morphology (×40).

reducing platelet-dependent upregulation of inflammatory and proatherothrombotic functions in leukocytes [22]. The present study is one of the very few studies that demonstrated that clopidogrel treatment significantly suppress atherosclerotic lesion induced by atherogenic diet in rabbits as compared with induced untreated group [21]. Clopidogrel will reduce expression of hsCRP and platelet-derived growth factor and also reduce intimal thickness. These results suggest that clopidogrel can retard the progression of established lesions related to inhibiting inflammation, cell proliferation, and promotion of cell apoptosis [23].

The role of IL-17A in atherosclerosis remains controversial, with different studies suggesting either a proatherogenic or an atheroprotective role. Taleb and his followers revealed that the loss of suppressor of cytokine signalling (SOCS) 3 in T cells increased both IL-17 and IL-10 production which induced an anti-inflammatory macrophage phenotype and subsequently led to unexpected IL-17-dependent reduction in lesion development and vascular inflammation [24]. On the other hand, Smith and his followers demonstrated that IL-17A plays a proatherogenic inflammatory role during atherogenesis by promoting monocyte/macrophage recruitment into the aortic wall [25]. Furthermore, Pietrowski and his followers reported that IL-17A induced an increased level of reactive oxygen species (ROS) in vascular smooth muscle cells (VSMC) [26].

We recommend further studies to use the Watanabe hereditary hyperlipidemic (WHHL) rabbit model where atherosclerosis already happened and no time is needed for induction of atherosclerosis as compared with cholesterol fed model of atherosclerosis. Furthermore, lipoprotein metabolism, atherosclerotic plaques, and coronary artery disease in WHHL rabbit model resemble those that happened in human [27]. Additionally, noninvasive imaging studies like IRON-MRI contrast imaging may be used which precisely highlight macrophage-rich plaques [28] to further clarify the effect of clopidogrel on atherosclerosis.

In conclusion, this study outlines how clopidogrel reduces lipid peroxidation, systemic inflammation, and aortic expression of inflammatory markers and hence reduces the progression of atherosclerosis.

Conflict of Interests

The authors declare that there is no conflict of interests regarding this paper.

References

[1] T. J. Anderson, "Assessment and treatment of endothelial dysfunction in humans," *Journal of the American College of Cardiology*, vol. 34, no. 3, pp. 631–638, 1999.

[2] K. Pyorala, M. Laakso, and M. Uusitupa, "Diabetes and atherosclerosis: an epidemiologic view," *Diabetes/Metabolism Reviews*, vol. 3, no. 2, pp. 463–524, 1987.

[3] J. Fan and T. Watanabe, "Inflammatory reactions in the pathogenesis of atherosclerosis," *Journal of Atherosclerosis and Thrombosis*, vol. 10, no. 2, pp. 63–71, 2003.

[4] R. R. S. Packard and P. Libby, "Inflammation in atherosclerosis: from vascular biology to biomarker discovery and risk prediction," *Clinical Chemistry*, vol. 54, no. 1, pp. 24–38, 2008.

[5] H. Li, M. I. Cybulsky, M. A. Gimbrone Jr., and P. Libby, "An atherogenic diet rapidly induces VCAM-1, a cytokine-regulatable mononuclear leukocyte adhesion molecule, in rabbit aortic endothelium," *Arteriosclerosis and Thrombosis*, vol. 13, no. 2, pp. 197–204, 1993.

[6] P. Libby, "Inflammation in atherosclerosis," *Nature*, vol. 420, no. 6917, pp. 868–874, 2002.

[7] S. K. Clinton, R. Underwood, L. Hayes, M. L. Sherman, D. W. Kufe, and P. Libby, "Macrophage colony-stimulating factor gene expression in vascular cells and in experimental and human atherosclerosis," *The American Journal of Pathology*, vol. 140, no. 2, pp. 301–316, 1992.

[8] G. Davì and C. Patrono, "Platelet activation and atherothrombosis," *The New England Journal of Medicine*, vol. 357, pp. 2482–2494, 2007.

[9] C. Cayman, "Product information, clopidogrel," http://www.caymanchem.com/.

[10] J.-M. Herbert, F. Dol, A. Bernat, R. Falotico, A. Lalé, and P. Savi, "The antiaggregating and antithrombotic activity of clopidogrel is potentiated by aspirin in several experimental models in the rabbit," *Thrombosis and Haemostasis*, vol. 80, no. 3, pp. 512–518, 1998.

[11] M. Sasani, B. Yazgan, I. Celebi et al., "Hypercholesterolemia increases vasospasm resulting from basilar artery subarachnoid

hemorrhage in rabbits which is attenuated by Vitamin," *Surgical Neurology International*, vol. 14, no. 2, p. 29, 2011.

[12] A. Daugherty, B. S. Zweifel, and G. Schonfeld, "Probucol attenuates the development of aortic atherosclerosis in cholesterol-fed rabbits," *British Journal of Pharmacology*, vol. 98, no. 2, pp. 612–618, 1989.

[13] T. Hayashi, J. M. Fukuto, L. J. Ignarro, and G. Chaudhuri, "Basal release of nitric oxide from aortic rings is greater in female rabbits than in male rabbits: implications for atherosclerosis," *Proceedings of the National Academy of Sciences of the United States of America*, vol. 89, no. 23, pp. 11259–11263, 1992.

[14] E. Beutler, O. Duron, and B. M. Kelly, "Improved method for the determination of blood glutathione," *The Journal of Laboratory and Clinical Medicine*, vol. 61, pp. 882–888, 1963.

[15] S. L. Mumford, *Labrotory Procedure Manual*, USFWS, Olympia Fish Health Center, Washington, DC, USA, 2nd edition, 2004.

[16] Y.-H. Chen, S.-J. Lin, J.-W. Chen, H.-H. Ku, and Y.-L. Chen, "Magnolol attenuates VCAM-1 expression in vitro in TNF-α-treated human aortic endothelial cells and in vivo in the aorta of cholesterol-fed rabbits," *British Journal of Pharmacology*, vol. 135, no. 1, pp. 37–47, 2002.

[17] Q. Gu, J.-L. Chen, and Y.-M. Ruan, "Inhibitory effects of aspirin, clopidogrel, and their combination on the progression of atherosclerosis in rabbits," *Chinese Medical Journal*, vol. 27, no. 1, pp. 87–91, 2005.

[18] M. Srinivas, A. Annapurna, and Y. N. Reddy, "Anti-atherosclerotic effect of atorvastatin and clopidogrel alone and in combination in rats," *Indian Journal of Experimental Biology*, vol. 46, no. 10, pp. 698–703, 2008.

[19] T. Heitzer, V. Rudolph, E. Schwedhelm et al., "Clopidogrel improves systemic endothelial nitric oxide bioavailability in patients with coronary artery disease: evidence for antioxidant and antiinflammatory effects," *Arteriosclerosis, Thrombosis, and Vascular Biology*, vol. 26, no. 7, pp. 1648–1652, 2006.

[20] S. R. Steinhubl, J. J. Badimon, D. L. Bhatt, J.-M. Herbert, and T. Lüscher, "Clinical evidence for anti-inflammatory effects of antiplatelet therapy in patients with atherothrombotic disease," *Vascular Medicine*, vol. 12, no. 2, pp. 113–122, 2007.

[21] M. Li, Y. Zhang, H. Ren, Y. Zhang, and X. Zhu, "Effect of clopidogrel on the inflammatory progression of early atherosclerosis in rabbits model," *Atherosclerosis*, vol. 194, no. 2, pp. 348–356, 2007.

[22] V. Evangelista, S. Manarini, G. Dell'Elba et al., "Clopidogrel inhibits platelet-leukocyte adhesion and platelet-dependent leukocyte activation," *Thrombosis and Haemostasis*, vol. 94, no. 3, pp. 568–577, 2005.

[23] H. Ren, M. Li, L. Feng et al., "Effects of clopidogrel on vascular proliferation and apoptosis in an atherosclerotic rabbit model," *Journal of Cardiovascular Pharmacology*, vol. 55, no. 6, pp. 617–624, 2010.

[24] S. Taleb, M. Romain, B. Ramkhelawon et al., "Loss of SOCS3 expression in T cells reveals a regulatory role for interleukin-17 in atherosclerosis," *Journal of Experimental Medicine*, vol. 206, no. 10, pp. 2067–2077, 2009.

[25] E. Smith, K.-M. R. Prasad, M. Butcher et al., "Blockade of interleukin-17A results in reduced atherosclerosis in apolipoprotein E-deficient mice," *Circulation*, vol. 121, no. 15, pp. 1746–1755, 2010.

[26] E. Pietrowski, B. Bender, J. Huppert, R. White, H. J. Luhmann, and C. R. W. Kuhlmann, "Pro-inflammatory effects of interleukin-17A on vascular smooth muscle cells involve NAD(P)H-oxidase derived reactive oxygen species," *Journal of Vascular Research*, vol. 48, no. 1, pp. 52–58, 2011.

[27] M. Shiomi and T. Ito, "The Watanabe heritable hyperlipidemic (WHHL) rabbit, its characteristics and history of development: a tribute to the late Dr. Yoshio Watanabe," *Atherosclerosis*, vol. 207, no. 1, pp. 1–7, 2009.

[28] G. Korosoglou, R. G. Weiss, D. A. Kedziorek et al., "Noninvasive detection of macrophage-rich atherosclerotic plaque in hyperlipidemic rabbits using "positive contrast" magnetic resonance imaging," *Journal of the American College of Cardiology*, vol. 52, no. 6, pp. 483–491, 2008.

Hindawi Publishing Corporation
BioMed Research International
Volume 2013, Article ID 212801, 9 pages
http://dx.doi.org/10.1155/2013/212801

Research Article

Merit of Anisodamine Combined with Opioid δ-Receptor Activation in the Protection against Myocardial Injury during Cardiopulmonary Bypass

Xuan Hong,[1] Huimin Fan,[1] Rong Lu,[1] Paul Chan,[1,2] and Zhongmin Liu[1]

[1] *Department of Cardiothoracic Surgery, Shanghai East Hospital, Tongji University, 150 Jimo Road, Shanghai 200120, China*
[2] *Division of Cardiovascular Medicine, Department of Internal Medicine, Wan Fang Hospital, Taipei Medical University, 111 Hsin-Lung Road, Section 3, Taipei 116, Taiwan*

Correspondence should be addressed to Huimin Fan; frankfan64@hotmail.com and Paul Chan; chanpaul@w.tmu.edu.tw

Received 24 October 2013; Accepted 4 November 2013

Academic Editor: Juei-Tang Cheng

Myocardial ischemia/reperfusion (MIR) injury easily occurrs during cardiopulmonary bypass surgery in elderly patients. In an attempt to develop an effective strategy, we employed a pig model of MIR injury to investigate the maximum rate of change of left ventricular pressure, left ventricular enddiastolic pressure, and left intraventricular pressure. Coronary sinus cardiac troponin T (TnT) and adenosine-triphosphate (ATP) content in myocardium were measured. The ultrastructures for MIR injury were visualized by transmission electron microscopy (TEM). The role of δ-opioid receptor activation using D-Ala2, D-Leu5-enkephalin (DADLE) in both early (D1) and late (D2) phases of cardioprotection was identified. Also, the merit of cardioprotection by DADLE in combination with anisodamine, the muscarinic receptor antagonist (D+M), was evaluated. Glibenclamide was employed at the dose sufficient to block ATP-sensitive potassium channels. Significant higher cardiac indicators, reduced TnT and increased ATP contents, were observed in D1, D2, and D+M groups compared with the control group. DADLE induced protection was better in later phase of ischemia that was attenuated by glibenclamide. DADLE after the ischemia showed no benefit, but combined treatment with anisodamine showed a marked postischemic cardioprotection. Thus, anisodamine is helpful in combination with DADLE for postischemic cardioprotection.

1. Introduction

Myocardial ischemia/reperfusion (MIR) injury is a major determinant of therapeutic outcome during cardiac surgery with cardiopulmonary bypass or before and after cardiac interventional therapy. Many studies have investigated the pathogenesis of MIR. However, MIR injury remains a high-risk factor which affects the therapeutic efficacy of surgical procedures in elderly patients with severe cardiac disease. So it is still significant to develop the effective treatment for MIR.

It is now recognized that ischemic preconditioning (IPC) mitigates MIR injury [1]. Endogenous mediators including opiates, adenosine, and bradykinin are considered to promote the acute IPC which can protect not only against myocardial stunning but also ischemia-induced myocardial injury. Cardioprotection provided by IPC has been divided into early (the first protective window) and late phases (the second protective window) as described previously [2]. The early-phase of protection develops within minutes of the initial IPC and lasts 1 to 2 hours, while the late phase becomes apparent 24 h later and lasts 3 to 4 days. Because of its sustained duration (30–90 min) and the limitation of traditional surgical IPC in clinical application (i.e., clamping the aorta many times before blocking), the protective effect of preconditioning induced by opioid δ-receptor agonist(s) has been indicated [3].

There are three well-characterized families of opioid peptides produced by the body: enkephalins, dynorphins, and β-endorphins, which act at corresponding δ, κ, and μ receptors. These belong to a group of Gi/Go protein-coupled receptors.

Two types of δ-opioid receptor (δ_1 and δ_2), three types of κ receptors (κ_1, κ_2, and κ_3), and two μ receptors (μ_1 and μ_2) have been identified. The expression of δ and κ receptors has been reported in the heart [3].

Previous data show that preconditioning induced by opioid receptor agonists such as morphine, TAN-67 and D-Ala2, D-Leu5-enkephalin (DADLE) before acute myocardial infarction may stimulate the effect of IPC on heart in mouse, dog, rabbit, and pig models [4–9] and not only promotes the recovery of heart function after acute myocardial infarction, but also initiates myocardial protection effect 24 h after preconditioning. Further studies indicate that the most notable merit of δ-opioid receptor activation is to provide cardioprotection [10–14].

The increase in acetylcholine (ACh) during myocardial reperfusion has been demonstrated to be one of the leading causes of myocardial injury. This has led to the postulation of the ACh-Ca^{2+}-OFR axis theory [15, 16]. Administration of scopolamine results in the blockade of muscarinic receptors. In this way it inhibits the ACh-Ca^{2+}-OFR axis, which protects the energy metabolism of myocardial cells and the integrity of myocardial ultrastructure, which in turn protects the myocardium [15, 16]. As a potential treatment strategy, administration of δ-opioid receptor agonist alone or in combination with muscarinic antagonist may play an important role in the cardioprotection.

The present study employed a pig model with MIR injury during cardiopulmonary bypass to investigate the myocardial protective effects of drug therapy. Using combined therapy with anisodamine, a naturally occurring atropine-like compound that has been characterized in China [17–19], we explored the early and late phases of preconditioning with DADLE, the opioid δ-receptor agonist, in an attempt to provide theoretical and experimental evidence for further clinical application in cardioprotection.

2. Material and Methods

2.1. General Surgical Preparation. Healthy pigs of the Shanghai strain, each weighing 30–35 kg, were purchased from the Shanghai Baomu Laboratory Animal Center. Following basal anesthesia (peritoneal injection with 30 mg/kg pentobarbital and intramuscular injection 0.3–0.5 mg/kg diazepam), venous access was established via the auricular vein. General anesthesia was maintained by intravenous injection with 1 mg/kg Diprivan and intramuscular injection of 0.6 mg/kg tracrium. The femoral vein cannula was connected to a ALC-MPA multichannel biological signaling analysis system to monitor mean arterial pressure. The trachea was incised and intubated (tube with internal diameter of 75–78 mm). Ventilation was controlled as follows: oxygen : air 1 : 1; tidal volume, 10 mg/kg; respiratory rate, 13 times/min; oxygen concentration, 50%; airway pressure, 15–20 cm H_2O. Blood gas analysis was performed regularly, and the stability of the internal environment was sustained.

A median sternotomy was performed, and the heart was exposed. A tube was implanted into the apex and then connected with the ALC-MPA (Shanghai Alcott Biotech Co., Ltd., China) multichannel signaling system to measure the left ventricular systolic pressure (LVSP), left ventricular enddiastolic pressure (LVEDP), and the maximum rate of change of left ventricular pressure (±dp/±dtmax).

Heparin (3 mg/kg) was given, and the ascending aorta, superior and inferior vena cava, and coronary sinus were intubated. An artificial heart-lung machine (precharged with crystal) with bubble oxygenators was used to establish the cardiopulmonary bypass. When the aorta was blocked, a modified St. Thomas' solution (the buffer consisted of the following in millimoles per liter: NaCl, 118; KCl, 4.7; $MgSO_4$, 1.2; KH_2PO_4, 1.2; $NaHCO_3$, 25; $CaCl_2$, 2.5; Na_2EDTA, 0.5; and glucose, 11; pH 7.4.) at a concentration of 5 mL/kg was perfused into myocardium. An ice bath was applied around the heart to drop temperature and arrest the heart. During the period of cardiopulmonary bypass, the temperature of nose and pharynx was sustained at 28°C, aortic perfusion pressure at 6.67 kPa, and arterial oxygen partial pressure at 20–30 kPa. After 60 min of cardioplegic ischemia, the aorta was opened, and the ischemic myocardium was reperfused. The temperature was increased, and electric defibrillation was employed with a power of 20 J. Cardiotonic agents including dopamine and adrenaline were given to attain hemodynamic stability, after which the cardiopulmonary bypass was withdrawn. The pigs were sacrificed 2 h after the termination of cardiopulmonary bypass.

This study was approved by the Ethics Review Committee of Shanghai East Hospital, Tongji University, and all animal handling procedures were performed according to the Guide for the Care and Use of Laboratory Animals of the National Institutes of Health, as well as the guidelines of the Animal Welfare Act.

2.2. Animal Groups and Treatment Protocols. Pigs were randomly assigned to five groups: C, D1, D2, D+K, and D+M. Group C was the control for the model of cardiopulmonary bypass. Pigs in Group D1 were intravenously injected with 1 mg/kg DADLE 1 h before cardiopulmonary bypass. Animals in Group D2 were intravenously injected with 1 mg/kg DADLE 48 and 24 h before cardiopulmonary bypass. Pigs in Group D+K were intravenously injected with 1 mg/kg DADLE combined with 1 mg/kg glibenclamide 1 h before cardiopulmonary bypass. Animals in Group D+M were intravenously injected with 1 mg/kg DADLE combined with 0.5 mg/kg anisodamine 1 h before cardiopulmonary bypass, followed by addition of 0.5 mg/kg anisodamine. The left ventricular systolic pressure (LVSP), left ventricular end diastolic pressure (LVEDP), and ±dp/±dtmax were measured before and 1 and 2 h after termination of cardiopulmonary bypass.

Coronary sinus blood was collected before and after cardiopulmonary bypass, at aortic opening and 1 and 2 h after termination of cardiopulmonary bypass. The plasma was used for detection of cardiac troponin T (TnT). The left ventricular myocardium was sampled before cardiopulmonary bypass and 2 h after termination of cardiopulmonary bypass. Some of the samples were stored in liquid nitrogen for the subsequent determination of the adenosine-triphosphate

(ATP) content in myocardial tissues. Others were stored in glutaraldehyde solution at 4°C for observation of ultrastructural changes using transmission electron microscopy.

2.3. Determination of TnT Values in Coronary Sinus Blood. TnT values in coronary sinus blood were detected using the electrochemical luminescence method on an Elecsys 1010 Chemistry Analyzer (Roche, Basel, Switzerland).

2.4. Detection of Giα Protein Expression and PKC Activity in Myocardial Tissues. The expression of Giα protein and PKC activity in myocardial tissues were detected using western blotting analysis. Briefly, myocardial tissues were lysed, homogenized, and centrifuged and the supernatant collected. Protein concentration was measured according to a standard curve created using bovine serum albumin. This was followed by sodium dodecyl sulfate polyacrylamide gel electrophoresis (SDS-PAGE) and immunoblotting. The membrane was then transferred to Ponceau S staining solution to observe the protein transfer. Finally, the membrane was treated with specific antibodies (mouse anti-human PKC or Giα protein) and visualized using a Storm 840 Gel and Blot Imaging System.

2.5. Determination of ATP Content in Myocardial Tissues. ATP content was determined using the high-performance liquid chromatography (HPLC) on LC-10A Semi-Micro Liquid Chromatographic System (Shimadzu, Kyoto, Japan).

2.6. Changes of Morphology and Ultrastructure of Myocardial Tissues. At the end of the experiment, a section of left ventricular myocardium was sampled and immediately fixed in glutaraldehyde solution at 4°C. Sections were prepared following routine procedures, and the changes in morphology and ultrastructure of the myocardial tissues were observed under a transmission electron microscopy.

2.7. Statistical Analysis. All data were expressed as the mean ± standard deviation (SD) of each group. Analyses were performed using Statistical Analysis System (SAS8.0) software. Analysis of variance was used to compare differences between treatment groups. P-values < 0.05 were considered statistically significant.

3. Results

3.1. Index of Heart Function. Changes in cardiac function parameters are summarized in Table 1. Statistical significance of higher LVSP values was observed in groups D1 and D2, compared with that in Group C after cardiopulmonary bypass, 1 h after termination of cardiopulmonary bypass ($P < 0.05$), and 2 h after termination of cardiopulmonary bypass ($P < 0.01$). LVEDP values were significantly higher in groups D1, D2, and D+M than in groups C or D+K at 1 h after termination of cardiopulmonary bypass ($P < 0.05$) and values in groups D1, D2, and D+M were significantly higher than those in Group C at 2 h after termination of cardiopulmonary bypass ($P < 0.01$). However, 2 h after the termination of cardiopulmonary bypass, LVEDP was lower in Group D2 than in Group D1 ($P < 0.05$).

The maximum rate of rise of left ventricular pressure (+dp/+dtmax) was significantly higher in Group D1 than that in Group C after cardiopulmonary bypass and 1 h after termination of cardiopulmonary bypass ($P < 0.05$) or 2 h after termination of cardiopulmonary bypass ($P < 0.01$). Values of left ventricular pressure (+dp/+dtmax) were markedly higher in Group D2 than in Group C after cardiopulmonary bypass ($P < 0.05$) and at 1 or 2 h after the termination of cardiopulmonary bypass ($P < 0.01$). In addition, +dp/+dtmax values were significantly higher in Group D+M than in Group C after cardiopulmonary bypass, and 1 or 2 h after the termination of cardiopulmonary bypass ($P < 0.05$).

At 1 and 2 h after termination of cardiopulmonary bypass, the absolute values of the maximum rate of fall of left ventricular pressure (−dp/−dtmax) were significantly lower in Group C than those in Group D1 ($P < 0.05$). In addition, lower absolute values were observed in Group C than in Groups D2 and D+M after cardiopulmonary bypass, and 1 or 2 h after the termination of cardiopulmonary bypass ($P < 0.01$). At 2 h after termination of cardiopulmonary bypass, the absolute value of −dp/−dtmax was significantly higher in Group D2 as compared to Group D1 ($P < 0.05$).

3.2. TnT Values in Coronary Sinus Blood. As shown in Table 2, the marked lower TnT values were observed in Groups D1, D2, and D+M in comparison with those in Group C at the time of aortic opening, after cardiopulmonary bypass and 1 or 2 h after the termination of cardiopulmonary bypass ($P < 0.01$). In addition, TnT values were more significantly reduced in Group D2 than in Group D1 at 1 or 2 h after the termination of cardiopulmonary bypass ($P < 0.01$).

3.3. ATP Content in Myocardial Tissues. The ATP content in myocardial tissue was significantly higher in Groups D1, D2, and D+M, compared with that in Group C ($P < 0.01$). However, ATP content was lower in Group D1 as compared to Groups D2, D+M, or normal myocardium ($P < 0.05$; Table 3).

3.4. Giα Protein Expression and PKC Activity in Myocardial Tissues. Higher expression of Giα or PKC protein in myocardial tissue was observed in Groups D1 and D2 than in Group C ($P < 0.01$). Representative picture was shown in Figure 1 and the data summarized in Table 4.

3.5. Changes in Morphology and Ultrastructure of Myocardial Cells. Transmission electron microscopy revealed the rupture of muscular fibers, together with mitochondrial swelling, and intracellular edema in Groups C and D+K. In addition, the shape of nucleus was irregular, with evidence of mitochondrial overflow after cell death (Figure 2). By contrast, in Group D1, few muscular fibers were ruptured, with only mild swelling of mitochondria, mild intercellular edema, and no cell death (Figure 3). In Groups D2 and D+M,

Table 1: Changes of indicators of heart functions.

Group	LVSP (kPa)				LVEDP (kPa)				Maximum rate of rise of left ventricular pressure (kPa/s)				Maximum rate of fall of left ventricular pressure (kPa/s)			
	Before CPB	After CPB	1 h after termination of CPB	2 h after termination of CPB	Before CPB	After CPB	1 h after termination of CPB	2 h after termination of CPB	Before CPB	After CPB	1 h after termination of CPB	2 h after termination of CPB	Before CPB	After CPB	1 h after termination of CPB	2 h after termination of CPB
C	13.04 ± 3.19	11.23 ± 4.64	12.82 ± 3.84	12.13 ± 2.60	2.06 ± 0.90	2.10 ± 0.51	3.75 ± 1.78**	5.02 ± 1.42**	328.33 ± 67.67	343.54 ± 142.42	354.03 ± 142.42	339.71 ± 161.71	−204.73 ± 45.43	−103.13 ± 48.33**	−86.15 ± 42.95**	−79.41 ± 45.22**
D1	13.53 ± 1.75	16.12 ± 1.43$^{*\#}$	17.22 ± 2.89$^{*\#}$	16.42 ± 2.52$^{*\#}$	2.10 ± 0.52	2.07 ± 0.39	2.01 ± 0.42$^{\#}$	2.67 ± 0.60$^{*\#\#}$	322.46 ± 63.08	475.57 ± 78.19$^{**\#}$	540.11 ± 90.56$^{**\#}$	584.36 ± 106.78$^{**\#\#}$	−224.27 ± 66.57	−155.12 ± 50.12*	−146.66 ± 39.75$^{*\#}$	−135.10 ± 34.31$^{*\#}$
D2	13.73 ± 2.74	16.98 ± 3.0$^{*\#}$	16.15 ± 2.06$^{*\#}$	16.87 ± 3.07$^{*\#}$	1.68 ± 0.51	1.66 ± 0.58	1.94 ± 0.21$^{\#}$	2.10 ± 0.23$^{*\#\#\triangle}$	361.79 ± 150.29	606.74 ± 247.68$^{**\#}$	613.37 ± 107.61$^{*\#\#}$	690.20 ± 245.27$^{**\#\#}$	−237.43 ± 59.79	−175.66 ± 55.26$^{\#}$	−182.91 ± 41.07$^{\#\#}$	−192.34 ± 45.19$^{\#\#\triangle}$
D+K	13.34 ± 3.22	14.64 ± 4.49	14.58 ± 3.21	12.34 ± 2.60	2.03 ± 0.91	2.15 ± 0.39	3.14 ± 0.91**	3.64 ± 1.23**	309.61 ± 74.01	463.95 ± 78.33*	405.68 ± 139.28	291.85 ± 121.95	−187.26 ± 53.22	−126.55 ± 72.77**	−122.90 ± 70.88**	−121.25 ± 80.77**
D+M	14.81 ± 5.16	13.17 ± 3.13	15.35 ± 4.66	13.92 ± 4.58	1.81 ± 0.97	1.90 ± 0.93	1.97 ± 0.81$^{\#}$	2.41 ± 0.72$^{*\#\#}$	328.70 ± 88.68	520.61 ± 145.64$^{**\#}$	599.66 ± 153.12$^{**\#}$	543.40 ± 114.86$^{**\#}$	231.89 ± 37.60	178.99 ± 42.89$^{\#\#}$	180.00 ± 49.87$^{\#\#}$	165.03 ± 47.10$^{\#\#}$

Values shown are mean ± SD.

CPB: cardiopulmonary bypass. Compared with that before cardiopulmonary bypass, $^{*}P < 0.05$, $^{**}P < 0.01$. Compared with that in Group C at the same time point, $^{\#}P < 0.05$, $^{\#\#}P < 0.01$. $^{\triangle}P < 0.01$, Group D1 versus D2 at the same time point.

Table 2: Changes of the coronary sinus cardiac troponin T (TnT) values (ng/mL).

Group	Before CPB	Aortic opening	After CPB	After termination of CPB	
				1 h	2 h
C	0.01 ± 0.003	0.05 ± 0.03**	0.09 ± 0.04**	0.22 ± 0.10**	0.31 ± 0.08**
D1	0.01 ± 0.001	0.01 ± 0.001#	0.01 ± 0.01#	0.08 ± 0.01**#	0.08 ± 0.02**#
D2	0.01 ± 0.001	0.01 ± 0.001#	0.01 ± 0.001#	0.01 ± 0.001#△	0.01 ± 0.002#△
D+K	0.03 ± 0.03	0.05 ± 0.03*	0.07 ± 0.04**	0.07 ± 0.04**	0.15 ± 0.05**
D+M	0.02 ± 0.01	0.02 ± 0.01	0.04 ± 0.02#	0.08 ± 0.07*#	0.01 ± 0.07**#

Values shown are means ± SD.
CPB: cardiopulmonary bypass. Compared with that before cardiopulmonary bypass, $^{*}P < 0.05$, $^{**}P < 0.01$. Compared with that in Group C at the same time point, $^{\#}P < 0.01$. $^{\triangle}P < 0.01$, Group D1 versus D2 at the same time point.

Table 3: Changes of ATP content in myocardial tissues (μmol/g tissue).

Group	ATP
C	0.90 ± 0.20
D1	1.57 ± 0.57*#
D2	2.20 ± 0.46*
D+K	1.05 ± 0.17
D+M	1.67 ± 0.48*
Normal myocardium	2.25 ± 0.34*

Values shown are mean ± SD.
Compared with Group C, $^{*}P < 0.01$; $^{\#}P < 0.05$, Group D1 versus Group D2 or normal myocardium.

Table 4: Expression of Giα protein and PKC activity in myocardial tissues.

Group	Giα protein	PKC
C	0.09 ± 0.02	0.39 ± 0.07
D1	0.40 ± 0.08*	0.97 ± 0.29*
D2	0.31 ± 0.08*	0.76 ± 0.09*
D+K	0.10 ± 0.04	0.30 ± 0.11
Normal myocardium	0.12 ± 0.07	0.36 ± 0.20

Values shown are mean ± SD.
Compared with Group C, $^{*}P < 0.01$.

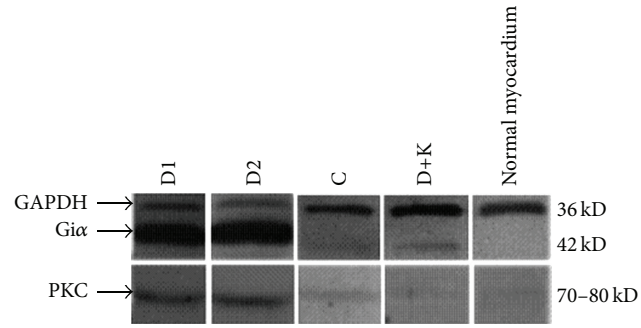

Figure 1: Expression of Giα protein in myocardial tissues and PKC activity in myocardial tissues (1), Group D1; (2) Group D2; (3) Group C; (4) Group D+K; (5) normal myocardium.

the ruptured muscular fibers, mitochondrial or intracellular edema, and dead cells were all not observed (Figure 4).

4. Discussion

For the role of opioid receptors in cardioprotection, preconditioning with δ-opioid receptor agonists such as DADLE has been shown to produce merit in mouse, dog, rabbit, and pig models [4–9]. Also, κ-opioid receptor agonists exerted a direct cardioprotective effect against ischemia/reperfusion [12]. Moreover, δ_2-opioid receptor manipulation interferes with the ability of deltorphin E (a δ_2-opioid receptor agonist) to increase survival after hemorrhage [13]. Preconditioning with morphine administered into the spinal canal of rats indicated that μ, δ, and κ receptors play important roles in myocardial protection [9, 14]. However, peripheral δ_2-opioid receptor activation induced cardiac tolerance to ischemia/reperfusion injury *in vivo*, while agonists of μ, δ_1, κ_1, and κ_2 receptors did not [20]. This finding forms the basis for additional investigation into the mechanisms by which opioid receptors facilitate cardioprotection. The most robust cardioprotection is introduced to be mediated by δ receptors, particularly δ_2-opioid receptors [9, 10]. However, there are no studies reporting the role of DADLE, a δ-opioid receptor agonist, in cardiopulmonary bypass models during cardiac surgery.

The present study established a pig model of myocardial ischemia/reperfusion injury with cardiopulmonary bypass to investigate the cardioprotection of δ-opioid receptors. We also explored the protection in early and late phases of preconditioning with DADLE to provide the experimental evidences for novel treatment strategies of myocardial protection.

In the present study, the protective effects of DADLE against myocardial ischemia/reperfusion injury during cardiopulmonary bypass were observed because preconditioning with DADLE significantly reduced the release of TnT, preserved ATP within myocardial cells, increased the systolic and diastolic functions of myocardium, and promoted the recovery of myocardial function after myocardial ischemia/reperfusion injury. We found that administration of DADLE 48 and 24 h before cardiopulmonary bypass achieved a significant improvement in each of the indicators compared with the control group. It also induced late-phase cardioprotection with better protection of the myocardial ultrastructure and improved the diastolic function of heart.

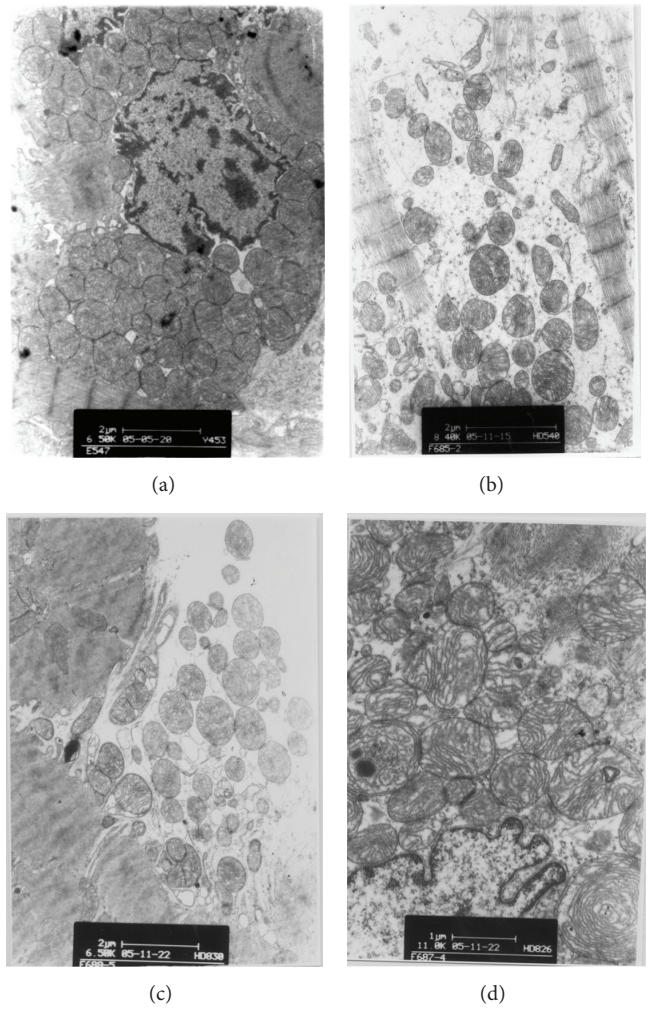

Figure 2: The visual appearance of myocardial cells of pigs. (a) In Group C (×6500). (b) In Group C (×8400). (c) In Group D+K (×6500). (d) In Group D+K (×11000).

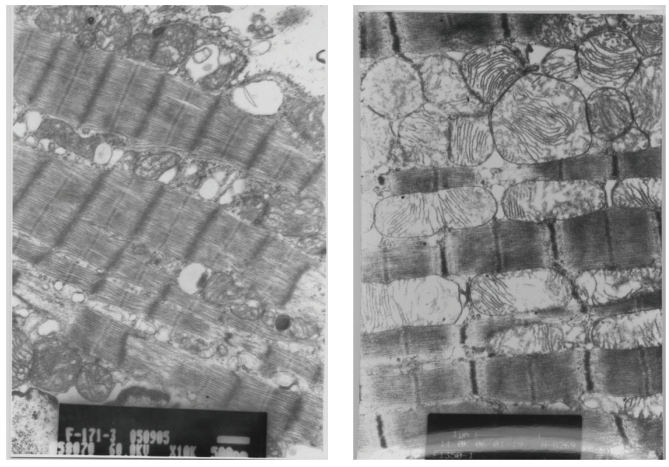

Figure 3: The ultrastructure of myocardial cells of pigs. (a) In Group D1 (×10000). (b) In Group D1 (×11000).

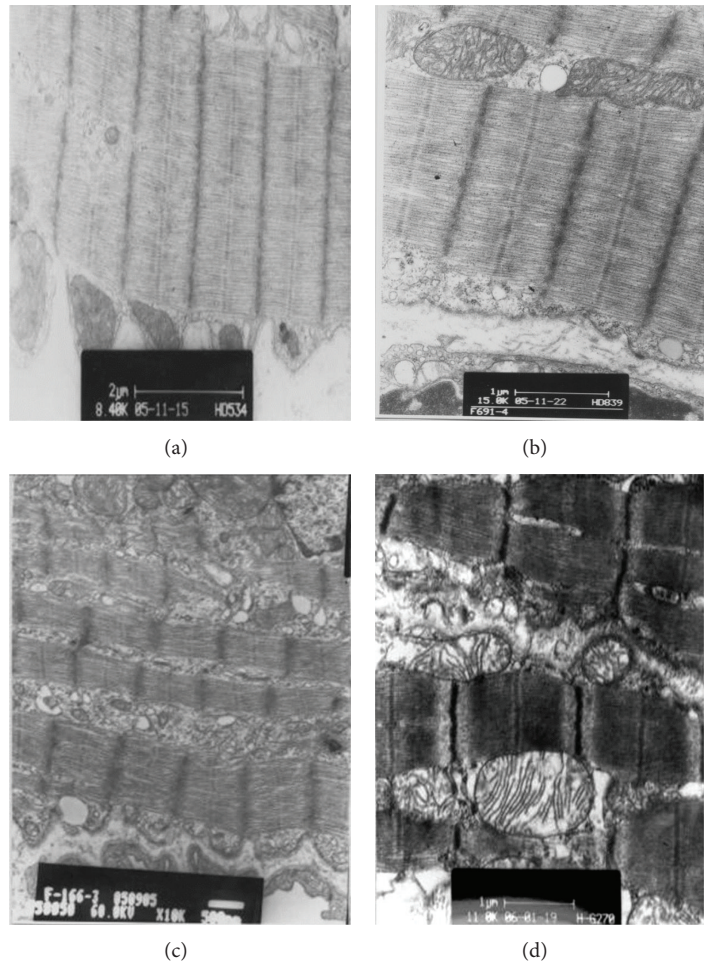

(a) (b) (c) (d)

Figure 4: The ultrastructure of myocardial cells of pigs. (a) In Group D2 (×8400). (b) In Group D2 (×15000). (c) In Group D+M (×10000). (d) In Group D+M (×11000).

Such findings provide the experimental basis for developing a control strategy for myocardial protection in clinical practices.

It has recently been documented that use of nitric oxide synthase (NOS), PKC, and K_{ATP} inhibitors all antagonized δ_2-opioid receptor-mediated protection against myocardial ischemia/reperfusion injury [21]. The present study showed that preconditioning with DADLE induced a higher expression of Giα or PKC protein. This is consistent with the previous report [22, 23]. We also demonstrated that blockade of K_{ATP} channel abolished the actions of DADLE and no significant differences were observed in the indicators of heart function such as TnT values, ATP content, and transmission electron microscopical findings, compared with the control group. We, therefore, speculate that Giα protein, PKC, and K_{ATP} channels play important roles in δ-opioid receptor-mediated cardioprotection against myocardial ischemia/reperfusion injury during cardiopulmonary bypass.

Our results are consistent with the previous reports, such as the role of Gi/Go proteins in δ-opioid receptor-mediated cardioprotection [3]. Also, the early-phase cardioprotection of DADLE was abolished by two PKC inhibitors, chelerythrine and GF109203X [24]. Also, the activation of opioid receptors elicited late-phase cardioprotection in rat ventricular myocytes and was inhibited by chelerythrine, suggesting that opioid receptor-elicited late-phase cardioprotection was induced in a PKC-dependent manner [25]. It has been documented that PKC-β_1 translocated to the nucleus for late-phase signaling transduction, on the basis that transcription and translation of the late-phase were dependent on nuclear factors [24]. Thus, DADLE may induce the translocation of PKC isoform such as PKC-α to the sarcolemma, PKC-δ to the mitochondria, and PKC-ε to the intercalated disk and mitochondria. Then, K_{ATP} channel can be regulated by PKC as described in previous report [26, 27]. This is the main signal pathway for DADLE induced cardioprotection.

Moreover, the present study showed the merit in combination with anisodamine for protective effect of preconditioning with DADLE against myocardial ischemia/reperfusion injury during cardiopulmonary bypass.

It has been identified that the increased ACh during myocardial ischemia/reperfusion was one of the major causes of myocardial injury to result in the ACh-Ca^{2+}-OFR axis

theory [15, 16]. By inhibiting M receptors, scopolamine causes ACh to accumulate in postsynaptic gaps which in turn feeds back to presynaptic M receptors and inhibits the further release of ACh. In this way, scopolamine not only blocks the actions of released ACh, but also reduces its further release. This dual action inhibits the ACh-Ca^{2+}-OFR axis protects the energy metabolism of myocardial cells and the integrity of myocardial ultrastructure, which in turn protects the myocardium [15, 16]. Anisodamine is similar to scopolamine to block M receptors [28]. Anisodamine is similar to scopolamine to block M receptors [29, 30] with a chemical structure of 7β-hydroxyhyoscyamine [28]. Also, anisodamine is used to treat endotoxic shock [31–33]. It is, therefore, considered that combined administration of DADLE and anisodamine prior to the surgery is a feasible approach to prevent the occurrence of myocardial ischemia/reperfusion injury. Actually, we found that combined treatment with DADLE and anisodamine exerts a powerful cardioprotective effect and this view has not been mentioned before.

5. Conclusion

In summary, administration of DADLE 48 and 24 h before cardiopulmonary bypass elicited significantly higher late-phase cardioprotection and promoted the recovery of heart function after myocardial ischemia/reperfusion injury. It promoted the recovery of heart function after myocardial ischemia/reperfusion injury, decreased the release of TnT, preserved ATP within myocardial cells, and protected the integrity of myocardial ultrastructure. Combined treatment with DADLE and anisodamine results in a more powerful cardioprotection than DADLE only. Blockade of K_{ATP} channels with glibenclamide significantly inhibited this δ-opioid receptor-mediated early-phase cardioprotection in pig models, indicating that the Giα- PKC- K_{ATP} channel pathway is important in δ-opioid receptor-mediated cardioprotection after myocardial ischemia/reperfusion injury during cardiopulmonary bypass in pigs.

Authors' Contribution

Huimin Fan, Paul Chan, and Zhongmin Liu contributed equally to the work.

Acknowledgments

The present study was supported by the National Natural Science Foundation of China (Grant no. 30371417), Outstanding Leaders Training Program of Pudong Health Bureau of Shanghai (Grant no. PKR2011-01), and Key Disciplines Group Construction Project of Pudong Health Bureau of Shanghai (Grant no. PKzxkq2010-01).

References

[1] C. E. Murry, R. B. Jennings, and K. A. Reimer, "Preconditioning with ischemia: a delay of lethal cell injury in ischemic myocardium," *Circulation*, vol. 74, no. 5, pp. 1124–1136, 1986.

[2] R. Bolli, "The late phase of preconditioning," *Circulation Research*, vol. 87, no. 11, pp. 972–983, 2000.

[3] J. E. J. Schultz and G. J. Gross, "Opioids and cardioprotection," *Pharmacology and Therapeutics*, vol. 89, no. 2, pp. 123–137, 2001.

[4] R. M. Fryer, A. K. Hsu, H. Nagase, and G. J. Gross, "Opioid-induced cardioprotection against myocardial infarction and arrhythmias: mitochondrial versus sarcolemmal ATP-sensitive potassium channels," *Journal of Pharmacology and Experimental Therapeutics*, vol. 294, no. 2, pp. 451–457, 2000.

[5] S. Chien, P. R. Oeltgen, J. N. Diana, R. K. Salley, and T.-P. Su, "Extension of tissue survival time in multiorgan block preparation with a delta opioid DADLE ([D-Ala2, D-Leu5]-enkephalin)," *Journal of Thoracic and Cardiovascular Surgery*, vol. 107, no. 3, pp. 964–967, 1994.

[6] K. P. Mayfield and L. G. D'Alecy, "Delta-1 opioid agonist acutely increases hypoxic tolerance," *Journal of Pharmacology and Experimental Therapeutics*, vol. 268, no. 2, pp. 683–688, 1994.

[7] D. C. Sigg, J. A. Coles Jr., P. R. Oeltgen, and P. A. Iaizzo, "Role of δ-opioid receptor agonists on infarct size reduction in swine," *The American Journal of Physiology*, vol. 282, no. 6, pp. H1953–H1960, 2002.

[8] M. A. Romano, R. McNish, E. M. Seymour, J. R. Traynor, and S. F. Bolling, "Differential effects of opioid peptides on myocardial ischemic tolerance," *Journal of Surgical Research*, vol. 119, no. 1, pp. 46–50, 2004.

[9] R. Li, G. T. C. Wong, T. M. Wong, Y. Zhang, Z. Xia, and M. G. Irwin, "Intrathecal morphine preconditioning induces cardioprotection via activation of delta, kappa, and mu opioid receptors in rats," *Anesthesia and Analgesia*, vol. 108, no. 1, pp. 23–29, 2009.

[10] B. T. Liang and G. J. Gross, "Direct preconditioning of cardiac myocytes via opioid receptors and K(ATP) channels," *Circulation Research*, vol. 84, no. 12, pp. 1396–1400, 1999.

[11] J. Huh, G. J. Gross, H. Nagase, and B. T. Liang, "Protection of cardiac myocytes via δ_1-opioid receptors, protein kinase C, and mitochondrial KATP channels," *The American Journal of Physiology*, vol. 280, no. 1, pp. H377–H383, 2001.

[12] L. Cheng, S. Ma, L.-X. Wei et al., "Cardioprotective and antiarrhythmic effect of U50,488H in ischemia/ reperfusion rat heart," *Heart and Vessels*, vol. 22, no. 5, pp. 335–344, 2007.

[13] M. Rutten, M. Govindaswami, P. Oeltgen, and J. S. Sonneborn, "Post-treatment with the novel deltorphin E, a δ_2-opioid receptor agonist, increases recovery and survival after severe hemorrhagic shock in behaving rats," *Shock*, vol. 29, no. 1, pp. 42–48, 2008.

[14] G. T. C. Wong, J. L. Ling, and M. G. Irwin, "Activation of central opioid receptors induces cardioprotection against ischemia-reperfusion injury," *Anesthesia and Analgesia*, vol. 111, no. 1, pp. 24–28, 2010.

[15] Z. M. Liu, Y. F. Xin, H. M. Fan, and R. Lu, "The experimental study of the the muscarinic receptor path way on ischemia-reperfusion injury in aged myocardium," *Chinese Journal of Thoracic and Cardiovascular Surgery*, vol. 20, pp. 289–291, 2004.

[16] Z. M. Liu, T. Zhang, H. M. Fan, R. Lu, and D. Y. Dai, "Study of effect of scopolamine on myocardial ischemia/reperfusion injury," *Journal of Tongji University*, vol. 23, pp. 1–4, 2002.

[17] S.-D. Wu, J. Kong, W. Wang, Q. Zhang, and J.-Z. Jin, "Effect of morphine and M-cholinoceptor blocking drugs on human sphincter of Oddi during choledochofiberscopy manometry," *Hepatobiliary and Pancreatic Diseases International*, vol. 2, no. 1, pp. 121–125, 2003.

[18] D. R. Varma and T. L. Yue, "Adrenoceptor blocking properties of atropine-like agents anisodamine and anisodine on brain and cardiovascular tissues of rats," *British Journal of Pharmacology*, vol. 87, no. 3, pp. 587–594, 1986.

[19] W. J. Wang, "Vasodilatory actions of four atropine-like drugs on ratfoot-pad," *Zhongguo Yao Li Xue Bao*, vol. 6, no. 1, pp. 26–29, 1985.

[20] L. N. Maslov, Y. B. Lishmanov, P. R. Oeltgen et al., "Comparative analysis of the cardioprotective properties of opioid receptor agonists in a rat model of myocardial infarction," *Academic Emergency Medicine*, vol. 17, no. 11, pp. 1239–1246, 2010.

[21] L. N. Maslov, Y. B. Lishmanov, P. R. Oeltgen et al., "Activation of peripheral δ_2 opioid receptors increases cardiac tolerance to ischemia/reperfusion injury: involvement of protein kinase C, NO-synthase, KATP channels and the autonomic nervous system," *Life Sciences*, vol. 84, no. 19-20, pp. 657–663, 2009.

[22] E. M. Seymour, S.-Y. J. Wu, M. A. Kovach et al., "HL-1 myocytes exhibit PKC and KATP channel-dependent delta opioid preconditioning," *Journal of Surgical Research*, vol. 114, no. 2, pp. 187–194, 2003.

[23] A. Valtchanova-Matchouganska, A. Missankov, and J. A. O. Ojewole, "Evaluation of the antidysrhythmic effects of δ- and κ-opioid receptor agonists and antagonists on calcium chloride-, adrenaline- and ischemia/reperfusion-induced arrhythmias in rats," *Methods and Findings in Experimental and Clinical Pharmacology*, vol. 26, no. 1, pp. 31–38, 2004.

[24] R. M. Fryer, Y. Wang, A. K. Hsu, and G. J. Gross, "Essential activation of PKC-δ in opioid-initiated cardioprotection," *The American Journal of Physiology*, vol. 280, no. 3, pp. H1346–H1353, 2001.

[25] S. Wu, H. Y. Li, and T. M. Wong, "Cardioprotection of preconditioning by metabolic inhibition in the rat ventricular myocyte: involvement of κ-opioid receptor," *Circulation Research*, vol. 84, no. 12, pp. 1388–1395, 1999.

[26] M. G. Perrelli, F. Tullio, C. Angotti et al., "Catestatin reduces myocardial ischaemia/reperfusion injury: involvement of PI3K/Akt, PKCs, mitochondrial KATP channels and ROS signalling," *Pflügers Archiv*, vol. 465, pp. 1031–1040, 2013.

[27] H. E. Turrell, G. C. Rodrigo, R. I. Norman, M. Dickens, and N. B. Standen, "Phenylephrine preconditioning involves modulation of cardiac sarcolemmal KATP current by PKC delta, AMPK and p38 MAPK," *Journal of Molecular and Cellular Cardiology*, vol. 51, no. 3, pp. 370–380, 2011.

[28] J. M. Poupko, S. I. Baskin, and E. Moore, "The pharmacological properties of anisodamine," *Journal of Applied Toxicology*, vol. 27, no. 2, pp. 116–121, 2007.

[29] B. Yuan, C. Zheng, H. Teng, and T. You, "Simultaneous determination of atropine, anisodamine, and scopolamine in plant extract by nonaqueous capillary electrophoresis coupled with electrochemiluminescence and electrochemistry dual detection," *Journal of Chromatography A*, vol. 1217, no. 1, pp. 171–174, 2010.

[30] L. Kursinszki, H. Hank, I. László, and É. Szke, "Simultaneous analysis of hyoscyamine, scopolamine, 6β-hydroxyhyoscyamine and apoatropine in Solanaceous hairy roots by reversed-phase high-performance liquid chromatography," *Journal of Chromatography A*, vol. 1091, no. 1-2, pp. 32–39, 2005.

[31] L. Sun, G. F. Zhang, X. Zhang et al., "Combined administration of anisodamine and neostigmine produces anti-shock effects: involvement of alpha7 nicotinic acetylcholine receptors," *Acta Pharmacologica Sinica*, vol. 33, pp. 761–766, 2012.

[32] T. Zhao, D. J. Li, C. Liu, D. F. Su, and F. M. Shen, "Beneficial effects of anisodamine in shock involved cholinergic anti-inflammatory pathway," *Frontiers in Pharmacology*, vol. 2, article 23, 2011.

[33] P. Gong, Y. Zhang, H. Liu, G.-K. Zhao, and H. Jiang, "Effects of penehyclidine hydrochloride on the splanchnic perfusion of patients with septic shock," *Zhongguo Wei Zhong Bing Ji Jiu Yi Xue*, vol. 20, no. 3, pp. 183–186, 2008.

Hindawi Publishing Corporation
BioMed Research International
Volume 2013, Article ID 795095, 8 pages
http://dx.doi.org/10.1155/2013/795095

Research Article

Low-Cytotoxic Synthetic Bromorutaecarpine Exhibits Anti-Inflammation and Activation of Transient Receptor Potential Vanilloid Type 1 Activities

Chi-Ming Lee,[1] Jiun-An Gu,[2] Tin-Gan Rau,[2] Che-Hsiung Yang,[1] Wei-Chi Yang,[1] Shih-Hao Huang,[3] Feng-Yen Lin,[4] Chun-Mao Lin,[5,6] and Sheng-Tung Huang[7]

[1] *Graduate Institute of Medical Sciences, College of Medicine, Taipei Medical University, No. 250, Wu-xing Street, Taipei 110, Taiwan*
[2] *Institute of Chemical Engineering, College of Engineering, National Taipei University of Technology, Taipei, Taiwan*
[3] *Department of Food and Beverage Management, Taipei College of Maritime Technology, Taipei, Taiwan*
[4] *Department of Internal Medicine, School of Medicine, Taipei Medical University, No. 250, Wu-xing Street, Taipei 110, Taiwan*
[5] *Department of Biochemistry, College of Medicine, Taipei Medical University, No. 250, Wu-xing Street, Taipei 110, Taiwan*
[6] *Orthopedics Research Center, Taipei Medical University Hospital, Taipei, Taiwan*
[7] *Institute of Biochemical and Biomedical Engineering, College of Engineering, National Taipei University of Technology, Taipei, Taiwan*

Correspondence should be addressed to Chun-Mao Lin; cmlin@tmu.edu.tw and Sheng-Tung Huang; ws75624@ntut.edu.tw

Received 12 September 2013; Accepted 29 October 2013

Academic Editor: Joen-Rong Sheu

Rutaecarpine (RUT), the major bioactive ingredient isolated from the Chinese herb *Evodia rutaecarpa*, possesses a wide spectrum of biological activities, including anti-inflammation and preventing cardiovascular diseases. However, its high cytotoxicity hampers pharmaceutical development. We designed and synthesized a derivative of RUT, bromo-dimethoxyrutaecarpine (Br-RUT), which showed no cytotoxicity at 20 μM. Br-RUT suppressed nitric oxide (NO) production and tumor necrosis factor-α release in concentration-dependent (0~20 μM) manners in lipopolysaccharide (LPS)-treated RAW 264.7 macrophages; protein levels of inducible NO synthase (iNOS) and cyclooxygenase-2 induced by LPS were downregulated. Br-RUT inhibited cell migration and invasion of ovarian carcinoma A2780 cells with 0~48 h of treatment. Furthermore, Br-RUT enhanced the expression of transient receptor potential vanilloid type 1 and activated endothelial NOS in human aortic endothelial cells. These results suggest that the synthetic Br-RUT possesses very low cytotoxicity but retains its activities against inflammation and vasodilation that could be beneficial for cardiovascular disease therapeutics.

1. Introduction

Evodiamine (EVO) and rutaecarpine (RUT), major bioactive ingredients isolated from the Chinese herb *Evodia rutaecarpa* [1], possess a wide spectrum of biological activities [2]. Inflammation and low oxygen diffusion are characteristics of atherosclerosis. EVO repressed cyclooxygenase (COX)-2 and inducible nitric oxide (NO) synthase (iNOS) expression mediated via inhibition of hypoxia-inducible factor (HIF)-1α under hypoxic conditions [3]. Therefore, EVO is considered an effective therapeutic agent against inflammatory diseases involving hypoxia. Vasorelaxant effects of EVO and RUT in rat isolated mesenteric arteries were reported to be associated with Ca^{2+} flux activity [4, 5]. RUT lowered blood pressure through the endothelial Ca^{2+}-NO-cGMP pathway to reduce smooth muscle tone [6].

The calcitonin gene-related peptide (CGRP), a major neurotransmitter of capsaicin-sensitive sensory nerves, plays a key role in maintaining endothelial homoeostasis. Decreased plasma CGRP levels caused cardiac susceptibility to ischemia-reperfusion injury, and antihypertensive therapy with RUT reversed cardiac susceptibility to reperfusion injury by stimulating CGRP release [7, 8]. The CGRP can counteract angiotensin (Ang) II-induced endothelial progenitor cell senescence through downregulating NADPH oxidase and reactive oxygen species (ROS) production [9].

Stimulation of endogenous CGRP release via activation of vanilloid receptors plays an important role in the vasodilatory effects of RUT [10, 11]. Activation of transient receptor potential vanilloid type 1 (TRPV1), a ligand-gated cationic channel, by EVO in endothelial cells may protect against certain cardiovascular diseases (CVDs) such as hypertension and stroke [12, 13]. Okada et al. reported that TRPV1 is a potential drug target for improving the outcome of inflammatory fibrosis [14]. NO release with consequent activation of endothelial (e)NOS confers vascular relaxation mediated by CGRP and TRPV1 stimulation [15]. The effect of EVO in TRPV1-dependent atheroprotection was further confirmed in mice [16]. Sheu et al. reported that RUT is a potential therapeutic agent for arterial thromboses because of its in vivo antiplatelet effect [17, 18]. Alkaloid compounds also exhibit anticancer activities both in vitro and in vivo by inducing cell-cycle arrest or apoptosis [19].

RUT and EVO showed quite high toxicity to porcine brain capillary endothelial cells (ECs) [20], which limits their application in vascular diseases. A variety of structural modifications of natural products were designed and synthesized for superior biological applications. Structure-activity relationship studies were further performed and are in progress [21–23]. RUT analogues were designed and synthesized to activate TRPV1 for enhanced vasodilator and hypotensive effects. The 14-N atom of RUT is critical for its activity [24]. Synthetic derivatives of RUT in this study exhibited very low cytotoxicity, but they still maintained their anti-inflammatory activity and TRPV1-upregulating effects. Results provide insights into the use of this TRPV1 agonist from RUT in vascular disease therapeutics.

2. Materials and Methods

2.1. Chemicals and General Methods. All chemicals were purchased from Acros Organics (Geel, Belgium), Sigma-Aldrich (St. Louis, MO), Showa Chemical Industry (Tokyo, Japan), or TCI America (Portland, OR) and were used without further purification. All reactions requiring anhydrous conditions were performed in oven-dried glassware under an Ar or N_2 atmosphere. Chemicals and solvents were either used without purification or purified by standard techniques. Analytical thin-layer chromatography (TLC) was performed on glass plate-mounted silica gel 60F254 (Merck) at a thickness of 0.2 mm. Flash column chromatography was performed using Silicycle silica gel 60. Synthesized compounds were characterized using 1H nuclear magnetic resonance (NMR) (Bruker Avance 500 MHz, Billerica, MA) and Fourier-transformed infrared spectroscopy (FT-IR).

2.2. Synthesis of Bromo-(Br-)RUT Derivatives. 2-Amino-4,5-dimethoxybenzoic acid (6 of Scheme 1) (0.4 g, 2 mmol) was dissolved in toluene (6 mL) that had been cooled to 0°C. Thionyl chloride (0.75 mL, 10 mmol) was added dropwise to the ice-cold solution. The reaction mixture was heated to 70~80°C and stirred for 1 h. The solution was heated to reflux for 10 min, was allowed to cool to 23°C, and was concentrated under reduced pressure. The resulting residue was redissolved in toluene (6 mL). A compound of 2,3-piperidinedione-3-(4-bromophenyl) hydrazone (5 of Scheme 1) (0.35 g, 1.37 mmol) was added to the solution. The reaction mixture was heated to reflux and stirred overnight. The solution was concentrated on a rotary evaporator, 10% sodium carbonate aqueous was added (200 mL), and the reaction was extracted with dichloromethane (3 × 200 mL). The organic layer was dried over anhydrous $MgSO_4$, the solids were filtered through a fritted Büchner funnel, and the solution was concentrated under reduced pressure. The residue was purified by column chromatography (elution with DCM : methanol of 40 : 1), affording Br-RUT as a solid.

2.3. Cell Culture. The RAW 264.7 macrophage cell line and A2780 ovarian carcinoma cells were grown in Dulbecco's modified Eagle's medium (DMEM) containing 10% fetal bovine serum (FBS), 100 U/mL penicillin, 100 μg/mL streptomycin, 4 mM L-glutamine, 4.5 g/L glucose, 1 mM sodium pyruvate, and 1.5 g/L sodium bicarbonate at 37°C in a humidified atmosphere with 5% CO_2. Primary human aortic ECs (HAECs) and human coronary artery ECs (HCAECs) were grown in a MesoEndo Endothelial Cell Growth Medium Kit (Cell Applications, San Diego, CA) supplemented with 10% FBS at 37°C in a humidified atmosphere with 5% CO_2.

2.4. Nitrite Assay. NO production in cell culture supernatant was evaluated by measuring the nitrite concentration. The nitrite concentration was detected with the Griess reaction. RAW 264.7 macrophages were plated at a density of 2×10^5 cells/mL in 24-well plates for 24 h, followed by cotreatment with different concentrations of Br-RUT and lipopolysaccharide (LPS) (100 ng/mL) for 24 h. The amount of nitrite in the samples was detected using the Griess reagent (1% sulfanilamide in 5% phosphoric acid and 0.1% naphthyl ethylenediamine dihydrochloride dihydrochloride in water). Data are reported as the mean ± standard error of the mean (SEM) of three independent determinations [25].

2.5. TNF-α Assay. Soluble cytokines were tested in supernatants of cultured RAW 264.7 macrophages by an enzyme-linked immunosorbent assay (ELISA). RAW 264.7 macrophages were plated at a density of 10^4 cells/mL in 96-well plates for 12 h, followed by treatment with different concentrations of Br-RUT for 1 h, then treatment with LPS (100 ng/mL) for 12 h. TNF-α in cell supernatants was detected using a mouse TNF-α Quantikine kit (R&D Systems, Minneapolis, MN) which was carried out according to the manufacturer's instructions. The absorbance was read at 450 nm with an ELISA plate reader. Data are reported as the mean ± SEM of three independent determinations.

2.6. Western Blot Analysis. Protein samples were resolved by sodium dodecylsulfate polyacrylamide gel electrophoresis (SDS-PAGE) and electrotransferred onto a polyvinylidene difluoride membrane. The membrane was incubated with a primary antibody at 4°C overnight and then incubated with a horseradish peroxidase (HRP)-conjugated secondary immunoglobulin G antibody; immunoreactive bands were

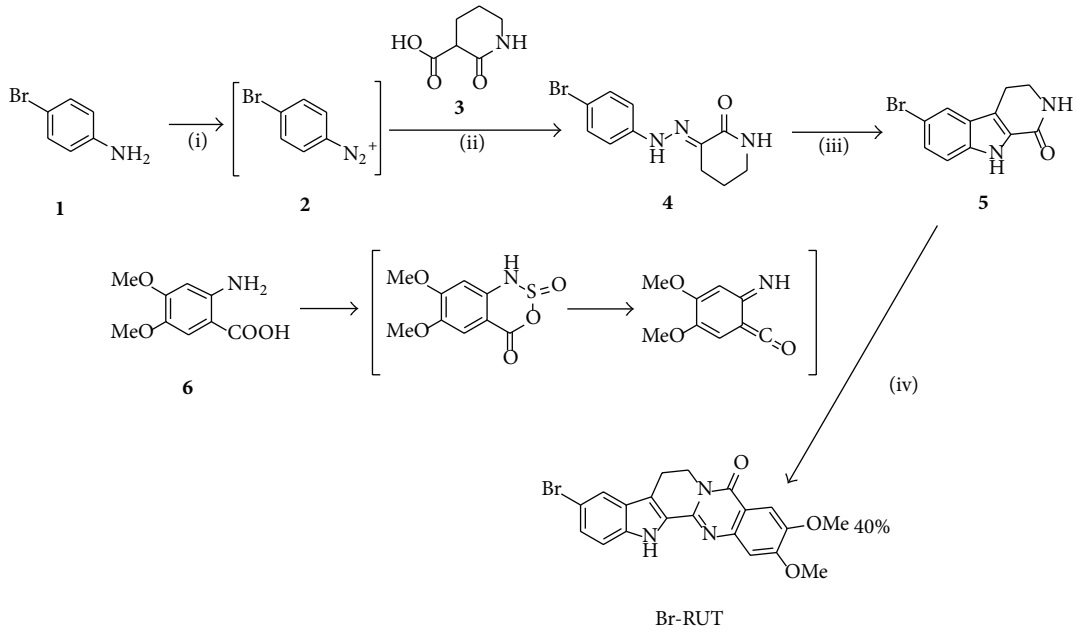

(i) $NaNO_2$/HCL, 0°C
(ii) AcOH, 0°C
(iii) Formic acid, reflux
(iv) $SOCl_2$/toluene

Scheme 1: Synthesis of bromo-dimethoxyrutaecarpine (Br-RUT).

visualized with PerkinElmer enhanced chemiluminescent reagents [26].

2.7. Cell Viability Assay. An MTT assay to test the cytotoxicity of reagents and cell viability was performed as described previously, based on conversion of the yellow tetrazolium salt to the purple formazan product [27]. Cells (10^4 cells/well) were grown on a 96-well plate supplemented with culture medium. Cells were treated with Br-RUT (0~20 μM) for 24 h, and an MTT stock solution (5 mg of MTT/mL of phosphate-buffered saline; PBS) was added to the growing cultures for 2 h. The absorbance was measured with a spectrophotometer at 560 nm. A blank with DMSO alone was measured as a reading control.

2.8. Wound Healing Migration Assay. A2780 cells at a density of 2×10^5 cells/well in 6-well plates were incubated at 37°C for 24 h. Cells were scratched with a 200-μL pipette tip, and cells in the plate were washed with PBS, and then new complete medium was added and treated with or without 1 and 2.5 μM of cantharidin for 24 h; 0.5% DMSO served as a vehicle control. At the end of incubation, cells were examined and photographed under a fluorescence microscope. The number of cells that had migrated into the scratched area was calculated as described elsewhere [28].

2.9. In Vitro Invasion Assay. A2780 cell migration or invasion was evaluated using 24-well Transwell inserts (8 μm pore filters, Merck Millipore) individually coated with Matrigel (BD Biosciences, Bedford, MA). A2780 cells (2×10^4 cells/well) were cultured for 24 h in serum-free DMEM, and then cells were placed in the upper chamber of the Transwell insert and treated with 0.5% DMSO (as a control) or Br-RUT (1.25 or 2.5 μM) for 24 h. Medium containing 10% FBS was placed in the lower chamber. At the end of incubation, nonmigrated cells were removed using a cotton swab; invaded cells maintained in the upper chamber were fixed with 4% formaldehyde and stained with 2% crystal violet. On the lower surface of the filter, cells that had penetrated were counted and photographed under a phase-contract microscope at 200x magnification. Three independent experiments were performed as described elsewhere [28].

3. Results

3.1. Design and Synthesis of Br-RUT. The synthetic schemes for preparing Br-RUT derivatives are outlined in Scheme 1. The main intermediate, substituted carboline (5), was prepared from substituted aniline following a procedure described by Henecka et al. [29] and Narayanan et al. [30]. The aniline (1) underwent the Sandmeyer reaction to give a diazonium salt, which was then coupled to carboxylic acid (3) to yield hydrazone (4), and treatment of hydrazone (4) in an acidic condition gave carboline (5) in a 56% yield (3 steps). Carboline (5) (see Figure S1 in Supplementary Material available online at http://dx/doi.org/10.1155/2013/795095) was then coupled with an *in situ* activated substituted o-aminobenzoic acid derivative (6), which was pretreated with thionyl chloride in the presence of toluene at 70~80°C to provide Br-RUT in a 40% overall yield (4 steps). The chemical structures of the synthetic intermediates and final products were determined by ^{1}H and ^{13}C NMR, IR, and

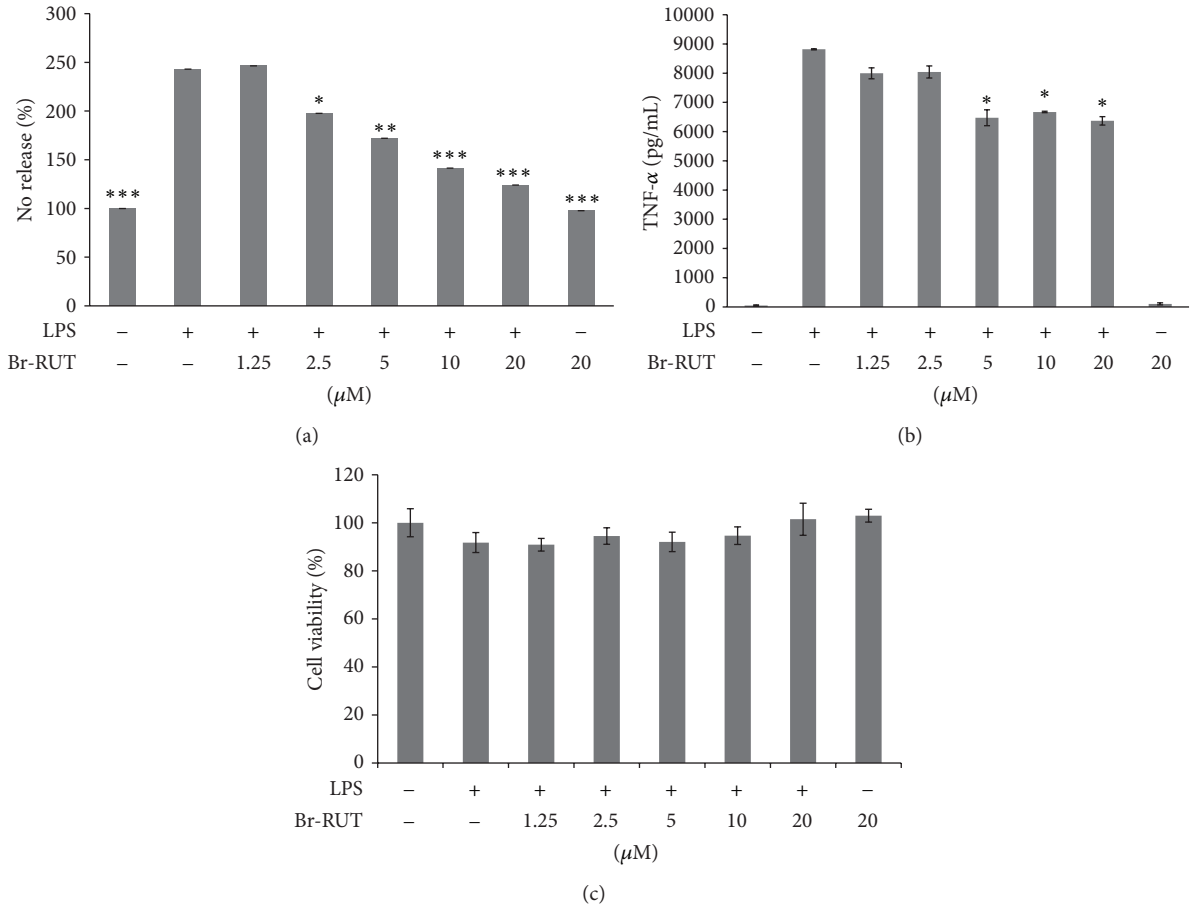

Figure 1: Effects of bromo-dimethoxyrutaecarpine (Br-RUT) on nitric oxide (NO) and tumor necrosis factor (TNF)-α releases by lipopolysaccharide (LPS)-treated (100 ng/mL) RAW 264.7 macrophages. (a) NO levels were detected in culture medium using the Griess reaction. The percentage of untreated cells was set as the control to 100%. (b) TNF-α release in cell supernatants was detected using a mouse TNF-α Quantikine kit. (c) Cell viability upon Br-BUT treatment for 24 h in an MTT assay. Statistical significance is indicated compared to LPS treatment. ($^{*}P < 0.05$, $^{**}P < 0.001$, $^{***}P < 0.001$).

mass spectrometry. FT-IR (KBr, cm-1): 3330 (N–H) and 1668 (carbonyl group) (Supplementary Figure S2). 1H-NMR (D-DMSO, ppm) (Supplementary Figure S2): δ3.13 (t, J = 6.8 Hz, 2H), 3.87 (s, 3H), 3.91 (s, 3H), 4.41 (t, J = 6.8 Hz, 2H), 7.05 (s, 1H), 7.34 (dd, J = 8.6 1.4, 1H), 7.41 (d, J = 8.6, 1H), 7.47 (s, 1H), 7.85 (s, 1H), 11.97 (s, 1H) (Supplementary Figure S3). MS-EI (m/z): calcd. 426.2; found 425.6 (Supplementary Figure S4).

3.2. NO and TNF-α Release by LPS-Treated Macrophages was Suppressed by Br-RUT. NO production by LPS-treated RAW264.7 macrophages increased compared to untreated cells. Pretreatment for 1 h with synthetic Br-RUT suppressed NO production in a concentration-dependent (0~20 μM) manner ($P < 0.01$) (Figure 1(a)). TNF-α released into the medium also showed consistent potency in a concentration-dependent (0~20 μM) (Figure 1(b)) suppressive effect. Suppressive effects were not due to the reduction of cell number because Br-RUT showed no cytotoxicity at concentrations of 0~20 μM (Figure 1(c)).

3.3. Br-RUT Suppressed iNOS and COX-2 Protein Expressions by LPS-Treated Macrophages. We investigated the effects of Br-RUT on protein levels of iNOS and COX-2. LPS-treated RAW 264.7 macrophages exhibited significantly elevated protein amounts of iNOS and COX-2, while Br-RUT suppressed their expressions in concentration-dependent manners (Figure 2). GAPDH protein levels of the loading controls remained constant.

3.4. Br-RUT Inhibited Cell Migration/Invasion. The effects of Br-RUT on inhibiting cell migration and invasion were investigated. As illustrated in Figure 3(a), wound healing assays used an ovarian carcinoma A2780 cell line in the presence of Br-RUT (0~5 μM) for 0~48 h. The migration velocity was measured using imaging software, and Student's t-test was used for the statistical analysis. Br-RUT showed significant effects against cell migration. Br-RUT (0~2.5 μM) treatments for 24 h also exhibited invasion-inhibitory activity in a transwell assay (Figure 3(b)).

3.5. Br-RUT Activated TRPV1 and eNOS. TRPV1 is reportedly present in ECs of arteries. To validate the expression of TRPV1 in the endothelium, the TRPV1 protein of HAECs was

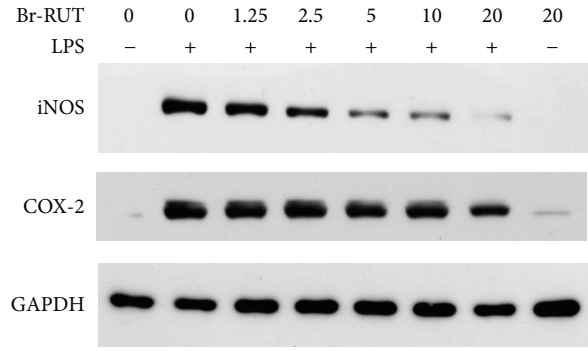

Figure 2

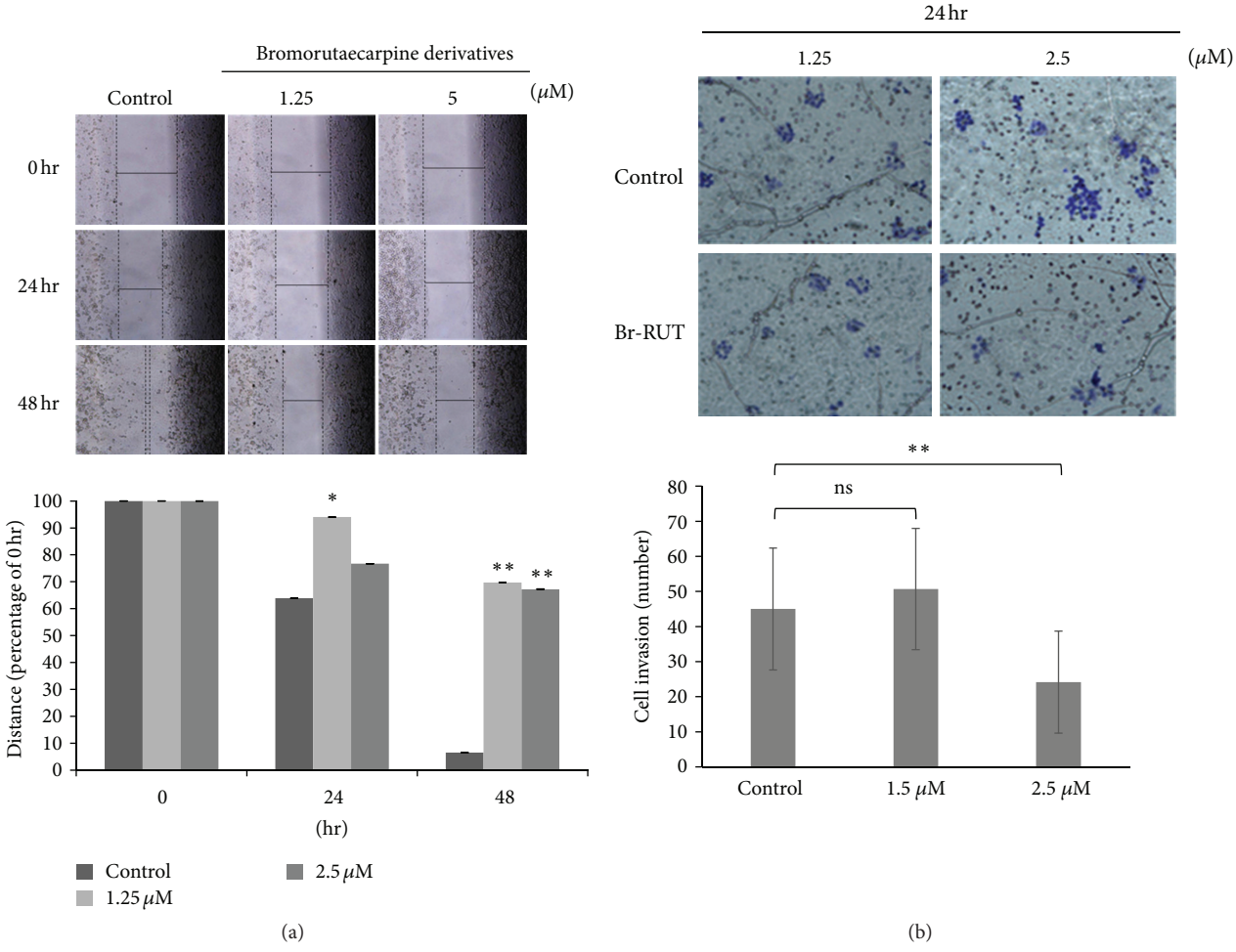

Figure 3: Effects of bromo-dimethoxyrutaecarpine (Br-RUT) on cell migration and invasion. Cell migration (a) and invasion (b) were detected following Br-RUT treatment for 0~48 h and photographed with a microscope (upper panel). Stained cells were counted and calculated in three random regions for each sample, results are presented as the mean ± SD from triplicate experiments, and the statistical analysis is shown in the lower panel.

detected by immunoblotting. Br-RUT treatment (10 μM) for 24 h increased TRPV1 protein amounts by 3.6-fold compared to the control group after normalization with α-tubulin levels (Figure 4). We further examined the effect of Br-RUT on the phosphorylation of NOS in HAECs because NO production is mainly regulated by eNOS phosphorylation. Br-RUT treatment (10 μM) for 24 h significantly increased eNOS phosphorylation by 5.5-fold compared to the control group after normalization with unphosphorylated eNOS (lower panel). Similar results were found in HCAECs (Supplementary Figure S5). Br-RUT upregulated the expression of TRPV1 and activated eNOS of ECs.

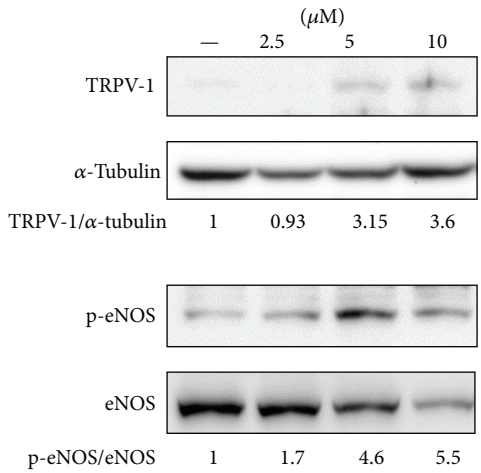

Figure 4: Effects of bromo-dimethoxyrutaecarpine (Br-RUT) on transient receptor potential vanilloid type 1 (TRPV1) expression and endothelial nitric oxide synthase (eNOS) phosphorylation in human aortic endothelial cells (HAECs). The densitometric ratio is indicated.

4. Discussion

The anti-inflammatory activities of EVO and RUT were reported [4, 31], but they act through different mechanisms, because EVO inhibits COX-2 induction and nuclear factor (NF)-κB activation in LPS-treated RAW 264.7 cells, while RUT does not [32]. RUT was reported to cause vasodilator effects by stimulating CGRP synthesis and release via activation of TRPV1. Its analogues were designed and synthesized for better vasodilator effects. Structural modifications of RUT and EVO were designed to enhance their biological activities. However, increased cytotoxicity hampers their application to vascular disorders [20, 33]. Br-RUT, a novel analogue synthesized in this study, had very low cytotoxicity and showed anti-inflammatory and migration/invasion-suppression activities that were beneficial with reduced side effects, so it has the potential to be developed for pharmaceutical applications.

RUT exerts different mechanisms to modulate signaling pathways, which resulted in different cell fates with diverse cell types and growth conditions [34]. RUT relaxed vascular smooth muscles by stimulating CGRP release via activation of vanilloid receptor subtype 1 [35]. It also antagonized Ang II-induced decreases in cellular NO contents and eNOS activities in rat vascular smooth muscle cells [36]. Compared to RUT, Br-RUT showed much less cytotoxicity, but it retained the anti-inflammatory activity. Br-RUT suppressed iNOS in macrophages, while it activated eNOS in ECs. Results showed that Br-Rut, derived from RUT, has enhanced beneficial effects and reduced adverse activities. Br-RUT, a modified derivative of RUT, retains the activities of improving cardiac and vasodilation functions but has fewer side effects.

Cells of the heart arise through a series of epithelial-to-mesenchymal transitions (EMTs), followed by formation of new epithelial structures by the reverse process of a mesenchymal-to-epithelial transition (MET) and then differentiation into cardiomyocyte and endocardial lineages. ECs from the atrioventricular canal undergo a tertiary EMT, called EndMT (due to the original properties of the tissue), and cells later assemble into the atrioventricular valvuloseptal complex [37]. Recent studies revealed that many cardiac diseases caused by inflammation are associated with fibrosis in the heart. Fibrosis is characterized by the accumulation of fibroblasts and the production of extracellular matrix. EndMT plays important roles in cardiac fibroblast formation during pathological progression. EndMT is regulated by signaling pathways mediated by inflammation-associated cytokines [38]. The endothelium is a promising target for drug treatment because it is in direct contact with the bloodstream. Br-RUT possesses anti-inflammatory activity and suppresses migration/invasion activities, phenomena that are associated with EndMT-associated fibrosis. Activation of TRPV1 and eNOS by Br-RUT suggests its potential for preventing vasorelaxation/hypertension. We therefore propose that inhibition of mechanisms for the formation of cardiac fibroblasts via EndMT by Br-RUT may provide a new strategy for heart disease therapeutics.

5. Conclusions

Br-RUT, a modified derivative of RUT, possesses very low cytotoxicity but retains its activity against inflammation. Treatment with Br-RUT enhanced TRPV1 and eNOS activities that may be beneficial by improving cardiac and vasodilation function.

Conflict of Interests

The authors declare that no conflict of interests exists.

Authors' Contribution

Chun-Mao Lin and Sheng-Tung Huang contributed equally to the work.

Acknowledgments

This study was supported by the National Taipei University of Technology and Taipei Medical University Join Research Grant (NTUT-TMU-102-12).

References

[1] J. J. Lu, J. L. Bao, X. P. Chen, M. Huang, and Y. T. Wang, "Alkaloids isolated from natural herbs as the anticancer agents," *Evidence-Based Complementary and Alternative Medicine*, vol. 2012, Article ID 485042, 12 pages, 2012.

[2] H. Yu, H. Jin, W. Gong, Z. Wang, and H. Liang, "Pharmacological actions of multi-target-directed evodiamine," *Molecules*, vol. 18, no. 2, pp. 1826–1843, 2013.

[3] Y.-N. Liu, S.-L. Pan, C.-H. Liao et al., "Evodiamine represses hypoxia-induced inflammatory proteins expression and hypoxia-inducible factor 1α accumulation in RAW264.7," *Shock*, vol. 32, no. 3, pp. 263–269, 2009.

[4] W.-F. Chiou, C.-J. Chou, A. Y.-C. Shum, and C.-F. Chen, "The vasorelaxant effect of evodiamine in rat isolated mesenteric

arteries: mode of action," *European Journal of Pharmacology*, vol. 215, no. 2-3, pp. 277–283, 1992.

[5] W.-F. Chiou, A. Y.-C. Shum, J.-F. Liao, and C.-F. Chen, "Studies of the cellular mechanisms underlying the vasorelaxant effects of rutaecarpine, a bioactive component extracted from an herbal drug," *Journal of Cardiovascular Pharmacology*, vol. 29, no. 4, pp. 490–498, 1997.

[6] G.-J. Wang, X.-C. Wu, C.-F. Chen et al., "Vasorelaxing action of rutaecarpine: effects of rutaecarpine on calcium channel activities in vascular endothelial and smooth muscle cells," *Journal of Pharmacology and Experimental Therapeutics*, vol. 289, no. 3, pp. 1237–1244, 1999.

[7] D. Li, X.-J. Zhang, L. Chen et al., "Calcitonin gene-related peptide mediates the cardioprotective effects of rutaecarpine against ischaemia-reperfusion injury in spontaneously hypertensive rats," *Clinical and Experimental Pharmacology and Physiology*, vol. 36, no. 7, pp. 662–667, 2009.

[8] D. Li, J. Peng, H.-Y. Xin et al., "Calcitonin gene-related peptide-mediated antihypertensive and anti-platelet effects by rutaecarpine in spontaneously hypertensive rats," *Peptides*, vol. 29, no. 10, pp. 1781–1788, 2008.

[9] Z. Zhou, C.-P. Hu, C.-J. Wang, T.-T. Li, J. Peng, and Y.-J. Li, "Calcitonin gene-related peptide inhibits angiotensin II-induced endothelial progenitor cells senescence through up-regulation of klotho expression," *Atherosclerosis*, vol. 213, no. 1, pp. 92–101, 2010.

[10] C.-P. Hu, L. Xiao, H.-W. Deng, and Y.-J. Li, "The depressor and vasodilator effects of rutaecarpine are mediated by calcitonin gene-related peptide," *Planta Medica*, vol. 69, no. 2, pp. 125–129, 2003.

[11] P.-Y. Deng, F. Ye, W.-J. Cai et al., "Stimulation of calcitonin gene-related peptide synthesis and release: mechanisms for a novel antihypertensive drug, rutaecarpine," *Journal of Hypertension*, vol. 22, no. 9, pp. 1819–1829, 2004.

[12] L. C. Ching, C. Y. Chen, K. H. Su et al., "Implication of AMP-activated protein kinase in transient receptor potential vanilloid type 1-mediated activation of endothelial nitric oxide synthase," *Molecular Medicine*, vol. 18, pp. 805–815, 2012.

[13] L.-C. Ching, Y. R. Kou, S.-K. Shyue et al., "Molecular mechanisms of activation of endothelial nitric oxide synthase mediated by transient receptor potential vanilloid type 1," *Cardiovascular Research*, vol. 91, no. 3, pp. 492–501, 2011.

[14] Y. Okada, P. S. Reinach, K. Shirai et al., "TRPV1 involvement in inflammatory tissue fibrosis in mice," *American Journal of Pathology*, vol. 178, no. 6, pp. 2654–2664, 2011.

[15] J. C. Torres-Narvaez, V. M. Ldel, E. V. Lopez et al., "Role of the transient receptor potential vanilloid type 1 receptor and stretch-activated ion channels in nitric oxide release from endothelial cells of the aorta and heart in rats," *Experimental and Clinical Cardiology*, vol. 17, no. 3, pp. 89–94, 2012.

[16] J. Wei, L. C. Ching, J. F. Zhao et al., "Essential role of transient receptor potential vanilloid type 1 in evodiamine-mediated protection against atherosclerosis," *Acta Physiologica*, vol. 207, no. 2, pp. 299–307, 2013.

[17] J. R. Sheu, W. C. Hung, C. H. Wu, Y. M. Lee, and M. H. Yen, "Antithrombotic effect of rutaecarpine, an alkaloid isolated from *Evodia rutaecarpa*, on platelet plug formation in in vivo experiments," *British Journal of Haematology*, vol. 110, no. 1, pp. 110–115, 2000.

[18] J.-R. Sheu, Y.-C. Kan, W.-C. Hung et al., "The antiplatelet activity of rutaecarpine, an alkaloid isolated from *Evodia rutaecarpa*, is mediated through inhibition of phospholipase C," *Thrombosis Research*, vol. 92, no. 2, pp. 53–64, 1998.

[19] J. Du, X. F. Wang, Q. M. Zhou et al., "Evodiamine induces apoptosis and inhibits metastasis in MDAMB-231 human breast cancer cells in vitro and in vivo," *Oncology Reports*, vol. 30, no. 2, pp. 685–694, 2013.

[20] M. Adams, A. Mahringer, O. Kunert, G. Fricker, T. Efferth, and R. Bauer, "Cytotoxicity and P-glycoprotein modulating effects of quinolones and indoloquinazolines from the Chinese herb *Evodia rutaecarpa*," *Planta Medica*, vol. 73, no. 15, pp. 1554–1557, 2007.

[21] N. S. Vyawahare, A. A. Hadambar, A. S. Chothe, R. R. Jalnapurkar, A. M. Bhandare, and M. K. Kathiravan, "Effect of novel synthetic evodiamine analogue on sexual behavior in male rats," *Journal of Chemical Biology*, vol. 5, no. 1, pp. 35–42, 2012.

[22] G. Dong, S. Wang, Z. Miao et al., "New tricks for an old natural product: discovery of highly potent evodiamine derivatives as novel antitumor agents by systemic structure-activity relationship analysis and biological evaluations," *Journal of Medicinal Chemistry*, vol. 55, no. 17, pp. 7593–7613, 2012.

[23] S. I. Kim, S. H. Lee, E. S. Lee, C. S. Lee, and Y. Jahng, "New topoisomerases inhibitors: synthesis of rutaecarpine derivatives and their inhibitory activity against topoisomerases," *Archives of Pharmacal Research*, vol. 35, no. 5, pp. 785–789, 2012.

[24] Z. Chen, G. Hu, D. Li et al., "Synthesis and vasodilator effects of rutaecarpine analogues which might be involved transient receptor potential vanilloid subfamily, member 1 (TRPV1)," *Bioorganic and Medicinal Chemistry*, vol. 17, no. 6, pp. 2351–2359, 2009.

[25] S.-J. Lin, H.-K. Lu, H.-W. Lee, Y.-C. Chen, C.-L. Li, and L.-F. Wang, "Nitric oxide inhibits androgen receptor-mediated collagen production in human gingival fibroblasts," *Journal of Periodontal Research*, vol. 47, no. 6, pp. 701–710, 2012.

[26] S.-H. Yu, Y.-T. Kao, J.-Y. Wu et al., "Inhibition of AMPK-associated autophagy enhances caffeic acid phenethyl ester-induced cell death in C6 glioma cells," *Planta Medica*, vol. 77, no. 9, pp. 907–914, 2011.

[27] F. M. Suk, W. J. Jou, R. J. Lin et al., "15, 16-dihydrotanshinone I-induced apoptosis in human colorectal cancer cells: involvement of ATF3," *Anticancer Research*, vol. 33, no. 8, pp. 3225–3231, 2013.

[28] C.-W. Lin, S.-C. Shen, C.-C. Chien, L.-Y. Yang, L.-T. Shia, and Y.-C. Chen, "12-*O*-tetradecanoylphorbol-13-acetate-induced invasion/migration of glioblastoma cells through activating PKCα/ERK/NF-κB-dependent MMP-9 expression," *Journal of Cellular Physiology*, vol. 225, no. 2, pp. 472–481, 2010.

[29] H. Henecka, H. Timmler, R. Lorenz, and W. Geiger, "Zur Kenntnis der Japp-Klingemann-Reaktion," *Chemische Berichte*, vol. 90, no. 6, pp. 1060–1069, 1957.

[30] K. Narayanan, L. Schindler, and J. M. Cook, "Carboxyl-mediated Pictet-Spengler reaction. Direct synthesis of 1,2,3,4-tetrahydro-β-carbolines from tryptamine-2-carboxylic acids," *Journal of Organic Chemistry*, vol. 56, no. 1, pp. 359–365, 1991.

[31] W.-F. Chiou, Y.-J. Sung, J.-F. Liao, A. Y.-C. Shum, and C.-F. Chen, "Inhibitory effect of dehydroevodiamine and evodiamine on nitric oxide production in cultured murine macrophages," *Journal of Natural Products*, vol. 60, no. 7, pp. 708–711, 1997.

[32] H. C. Yong, M. S. Eun, S. K. Yeong, F. C. Xing, J. L. Jung, and P. K. Hyun, "Anti-inflammatory principles from the fruits of *Evodia rutaecarpa* and their cellular action mechanisms," *Archives of Pharmacal Research*, vol. 29, no. 4, pp. 293–297, 2006.

[33] Y. H. Hong, W. J. Lee, S. H. Lee et al., "Synthesis and biological properties of benzo-annulated rutaecarpines," *Biological and Pharmaceutical Bulletin*, vol. 33, no. 10, pp. 1704–1709, 2010.

[34] J.-R. Sheu, "Pharmacological effects of rutaecarpine, an alkaloid isolated from *Evodia rutaecarpa*," *Cardiovascular Drug Reviews*, vol. 17, no. 3, pp. 237–245, 1999.

[35] J. Yu, G.-S. Tan, P.-Y. Deng, K.-P. Xu, C.-P. Hu, and Y.-J. Li, "Involvement of CGRP in the inhibitory effect of rutaecarpine on vasoconstriction induced by anaphylaxis in guinea pig," *Regulatory Peptides*, vol. 125, no. 1–3, pp. 93–97, 2005.

[36] Y. J. Li, F. Zhang, Q. H. Gong, Q. Wu, L. M. Yu, and A. S. Sun, "Rutaecarpine inhibits angiotensin II-induced proliferation in rat vascular smooth muscle cells," *Chinese Journal of Integrative Medicine*, 2013.

[37] J. P. Thiery, H. Acloque, R. Y. J. Huang, and M. A. Nieto, "Epithelial-mesenchymal transitions in development and disease," *Cell*, vol. 139, no. 5, pp. 871–890, 2009.

[38] Y. Yoshimatsu and T. Watabe, "Roles of TGF-beta signals in endothelial-mesenchymal transition during cardiac fibrosis," *International Journal of Inflammation*, vol. 2011, Article ID 724080, 8 pages, 2011.

Hindawi Publishing Corporation
BioMed Research International
Volume 2013, Article ID 201614, 10 pages
http://dx.doi.org/10.1155/2013/201614

Research Article

The Cardioprotective Effect of Hypertonic Saline Is Associated with Inhibitory Effect on Macrophage Migration Inhibitory Factor in Sepsis

Yi-Li Wang,[1] Kwok-Keung Lam,[2,3] Pao-Yun Cheng,[4] Ching-Wen Kung,[5] Shu-Ying Chen,[6] Chun-Chih Chao,[7] Hwong-Ru Hwang,[8] Ming-Ting Chung,[9,10] and Yen-Mei Lee[1,7]

[1] *Graduate Institute of Life Sciences, National Defense Medical Center, Taipei, Taiwan*
[2] *Department of Pharmacology, Taipei Medical University, Taipei, Taiwan*
[3] *Department of Anesthesiology, Catholic Mercy Hospital, Hsinchu, Taiwan*
[4] *Department of Physiology & Biophysics, National Defense Medical Center, Taipei, Taiwan*
[5] *Department of Nursing, Tzu Chi College of Technology, Hualien, Taiwan*
[6] *Department of Nursing, HungKuang University, Taichung, Taiwan*
[7] *Department of Pharmacology, National Defense Medical Center, 160 Min-Chuan E. Road, Taipei 114, Taiwan*
[8] *Division of Cardiology, Department of Medicine, Kaohsiung Veterans General Hospital, Kaohsiung, Taiwan*
[9] *Center for Reproductive Medicine, Department of Obstetrics and Gynecology, Chi-Mei Medical Center, 901 Chung Hwa Road, Tainan 710, Taiwan*
[10] *Chia Nan University of Pharmacy & Science, Tainan, Taiwan*

Correspondence should be addressed to Ming-Ting Chung; mtasrm@yahoo.com.tw and Yen-Mei Lee; ymlee@mail.ndmctsgh.edu.tw

Received 2 October 2013; Accepted 8 November 2013

Academic Editor: Joen-Rong Sheu

Sepsis can cause myocardial dysfunction, which contributes to the high mortality of sepsis. Hypertonic saline (HS) has been reported to increase myocardial contractility in sepsis. In the present study, mechanisms of action of HS resuscitation (4 mL of 7.5% NaCl per kilogram) on cardiac function have been evaluated in septic rats. HS was administered 1 h after LPS (10 mg/kg, i.v.) challenge. The mean arterial blood pressure significantly decreased 4 h after LPS challenge, and septic shock was observed at the end of experiment (6 h). Posttreatment with HS prevented hypotension caused by LPS and significantly improved cardiac function, evidenced by increases in left ventricular developed pressure, mean +dP/dt and −dP/dt. The amplitude of electrical-stimulated intracellular Ca^{2+} transient in isolated single cardiomyocytes was significantly reduced after 6 h LPS insult, which was recovered by HS. In addition, LPS resulted in significant increases in neutrophil myeloperoxidase activity, macrophage migration inhibitory factor (MIF), and NF-κB phospho-p65 protein levels in myocardium at 6 h, which were significantly attenuated by HS. In conclusion, HS improved myocardial contractility and prevented circulatory failure induced by endotoxemia, which may attribute to improvement of intracellular calcium handling process and inhibitory effects on neutrophil infiltration and MIF production in hearts.

1. Introduction

Multiple organ failure is a leading cause of mortality in sepsis, and myocardial depression is the most common organ dysfunction. Sepsis-induced cardiac dysfunction is characterized by decreased myocardial contractility, impaired ventricular response to fluid therapy, and ventricular dilatation [1]. Fluid resuscitation is one of the first-line cornerstone therapies and to support the cardiac function in severe sepsis [2]. Isotonic fluid (Ringer's lactate or normal saline [0.9% NaCl]) administration can restore the body fluid and microvascular perfusion. In clinical therapy, small volume of hypertonic saline (HS) [7.5% NaCl] recovers hemodynamic variables and effective circulating volume in hemorrhagic shock [3].

The beneficial effect of HS is associated with its anti-inflammatory effect, evidenced by inhibition of neutrophil activation and infiltration in lungs [4]. Neutrophil activation can release cytokines, reactive oxygen species, and enzymes, resulting in injuries of organs and tissues [5]. Furthermore, HS can ameliorate organ dysfunction in severe sepsis caused by cecal ligation and puncture (CLP), which is mediated via its antioxidant and anti-inflammatory effects [6]. Recently, HS has been revealed to prevent early myocardial dysfunction and to reduce myocardial apoptosis [7].

Macrophage migration inhibitory factor (MIF) is one of the important factors in sepsis. MIF is ubiquitously expressed in both immune and nonimmune cells including various peripheral tissues. MIF can recruit immune cells (macrophages, eosinophils, basophils, neutrophils) to the site of inflammation, leading to amplify the production of various proinflammatory cytokines and mediators such as IL-1β, TNF-α, IFN-γ, IL-17, and nitric oxide (NO) [8]. After injection of LPS in rodents, MIF protein was released from several organs, such as lung, liver, kidney, adrenal and pituitary gland, spleen, and skin [9]. MIF protein expression also significantly increased in hearts of septic mice [10, 11]. Recently, it has been demonstrated that HS reduces the levels of MIF in LPS-induced macrophage cell line [12]. MIF neutralization by anti-MIF antibody can reverse endotoxin-induced myocardial dysfunction in rats [13]. Therefore, we examined whether neutrophil infiltration and MIF expression are involved in the cardioprotective effect of HS in a conscious rat model of LPS-induced sepsis.

Ca^{2+} influx through the L-type Ca^{2+} channel (LTCCs) of sarcolemma of myocardium during an action potential initiates contraction of the cardiac myocytes. Ca^{2+} current subsequently triggers a larger Ca^{2+} release from the sarcoplasmic reticulum (SR) via ryanodine receptors, resulting in elevation of intracellular Ca^{2+} concentration ($[Ca^{2+}]_i$), and providing Ca^{2+} for the excitation-contraction coupling [14]. In this study, we further measured the amplitude of $[Ca^{2+}]_i$ transients in isolated single cardiomyocytes to evaluate whether HS can preserve $[Ca^{2+}]_i$ handling capacity to improve cardiac contractile function during sepsis.

2. Materials and Methods

2.1. Experimental Animals. Male Wistar rats (10–12 weeks old, 280–300 g) were used and purchased from the National Laboratory Animal Breeding and Research Center of the National Science Council, Taiwan. Handling of the animals conforms to the *Guide for the Care and Use of Laboratory Animals*, published by the National Institutes of Health, USA (NIH publication number 85-23, revised in 1996). All animal cares and experimental protocols in this study were approved by the Animal Care and Use Committee of National Defense Medical Center, Taipei, Taiwan. Animals were housed under a 12 h light-dark cycle room with an ambient temperature of 22 ± 1°C and humidity of 50 ± 5%. The animal preparation for anesthetization and cannulation of blood vessels were performed as described previously [15].

2.2. Experimental Groups. The experiments of sepsis were performed on conscious rats, which has been reported to be a clinically relevant sepsis model [16] and avoids the interference of anesthetics with cytokine release [17]. Animals were divided into four groups: (1) sham (normal saline, 0.9% NaCl, 4 mL/kg, intravenously), $n = 6$; (2) sham + HS (7.5% NaCl, 4 mL/kg, intravenously), $n = 6$; (3) LPS: rats were treated with *Escherichia coli* LPS 10 mg/kg (intravenous infusion for 10 min). One hour after LPS administration, 0.9% NaCl (4 mL/kg, 300 mosmole/L) was given intravenously, $n = 10$; (4) LPS + HS: rats were treated with *Escherichia coli* LPS 10 mg/kg (intravenous infusion for 10 min). One hour after LPS administration, 7.5% NaCl (4 mL/kg, 2400 mosmole/L) was given, $n = 10$. Normal saline and HS were infused with a rate of 0.2 mL/min [18, 19]. At 0, 1, 2, 4, and 6 h after LPS infusion, the changes in hemodynamics (blood pressure and heart rate), hepatic function index (i.e., alanine aminotransferase (ALT), aspartate aminotransferase (AST)), cell toxicity index (i.e., lactate dehydrogenase (LDH)), and renal function index (creatinine (CRE)), as well as the plasma levels of sodium, potassium, and calcium ion concentration were examined. Six hours after LPS infusion, animals were sacrificed and hearts were collected immediately.

2.3. Isolated Heart Preparation and Left Ventricular Pressure Recording. The preparation for heart isolation and measurement of cardiac contractility were performed as described previously [15]. Hearts were isolated 6 h after LPS administration and mounted on the Langendorff apparatus (ML785B2 Langendorff System Bundle, AD instruments). The left ventricular developed pressure (LVDP) and the mean rates of contraction (+dP/dt) and relaxation (−dP/dt) were measured.

2.4. Measurement of Blood Electrolytes. Whole blood levels of sodium, potassium, and calcium ion in rats 6 hours after LPS infusion were measured by an arterial blood gas analyzer (AVL OPTI Critical Care Analyzer; AVL Scientific Corp., Roswell, USA).

2.5. MPO Activity Test. MPO activity has been demonstrated to correlate with the number of neutrophils [20] and was used as an index of neutrophil accumulation in the heart. It was determined using an MPO assay kit (CytoStore, Calgary, Canada) by measuring the H_2O_2-dependent oxidation of O-dianisidine, according to the manufacturer's instructions. MPO activity is expressed as unit per mg protein (U/mg protein).

2.6. Western Blot Analysis. The left ventricular myocardium was isolated 6 hours after LPS administration, which was immediately frozen in liquid nitrogen, and stored at −80°C until processed. Detection of phospho-p65 and MIF by Western blotting was performed as described previously [15]. The primary antibodies in this experiment were mouse monoclonal anti-phospho-p65 (Epitomics, USA; 1 : 1000), and rabbit polyclonal anti-MIF (BioVision, USA; 1 : 1000).

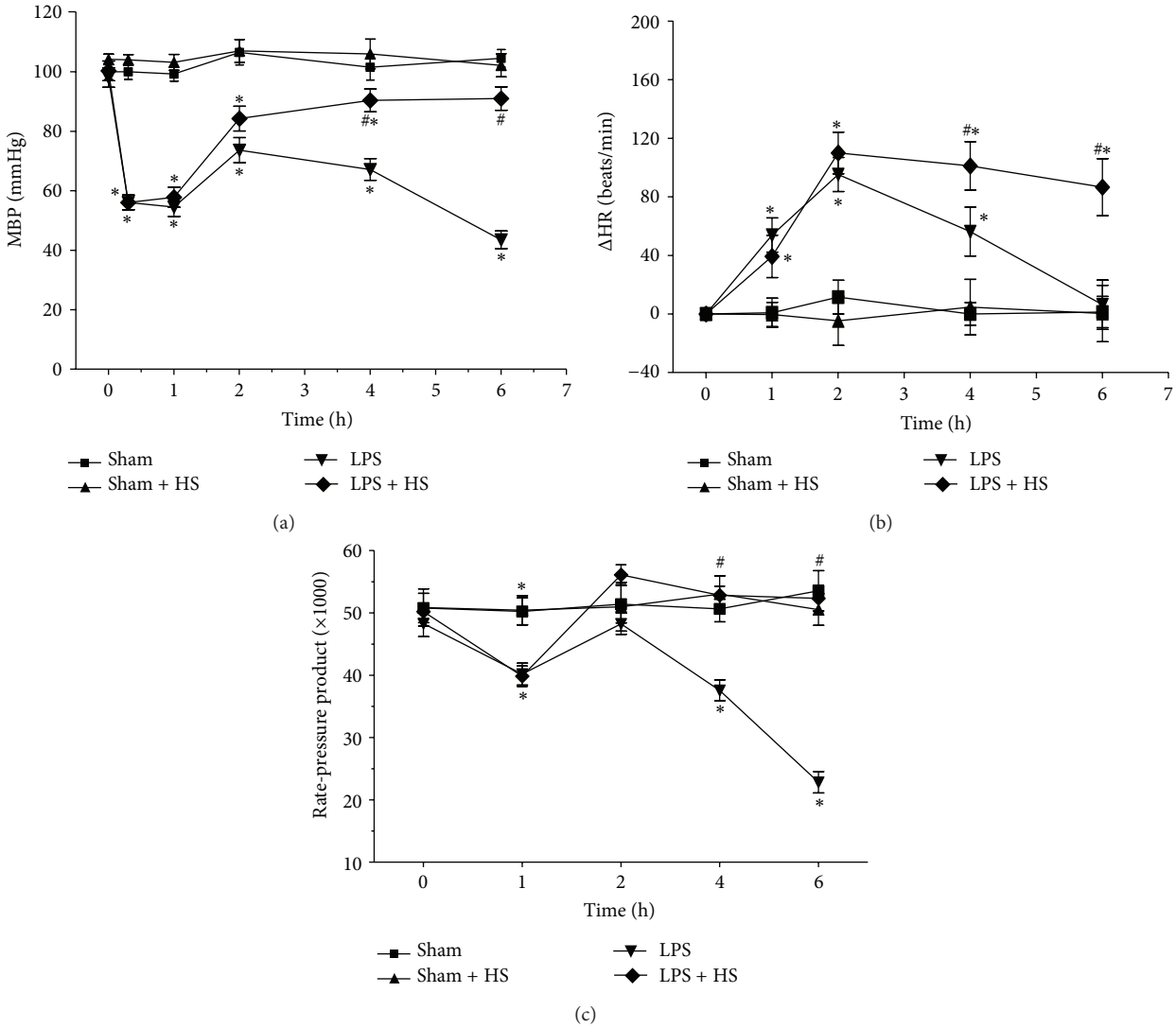

Figure 1: Effects of hypertonic saline (HS) on mean arterial blood pressure (a), changes in heart rate (b), and rate-pressure product (c) in conscious rats with sepsis-induced by LPS injection. $n = 6$–10. Values are expressed as mean ± SEM. $^{*}P < 0.05$ versus the sham group; $^{\#}P < 0.05$ versus the LPS group.

2.7. Cardiomyocyte Isolation and Measurement of the Intracellular Calcium. Six hours after LPS administration, the heart was isolated. The methodology of tissue preparations and cardiomycytes isolation were followed and modified from previous studies [21, 22]. Intracellular calcium ($[Ca^{2+}]_i$) was recorded by an indo-1 fluorometric ratio technique. The fluorescent indicator indo-1 was loaded by incubating the myocytes of ventricle in sham, LPS, and LPS + HS groups at room temperature (25°C) for 20 to 30 minutes with 25 μM of indo-1/AM (Sigma Chemical, St. Louis, MO). The Ca^{2+} transient was measured during a 2 Hz field-stimulation with 10-ms twice-threshold strength square-wave pulses. The fluorescence ratio data were processed and stored in a computer using software (OSP-SFCA; Olympus). Sarcoplasmic reticulum (SR) Ca^{2+} content was estimated by adding 20 mM caffeine after electric stimulation at 2 Hz for at least 30 s. The total SR Ca^{2+} content was measured from the amplitude of caffeine-induced Ca^{2+} transients.

2.8. Statistical Analysis. The data are expressed as means ± SEM. Statistical evaluation was performed with one-factor analysis of variance followed by the Newman-Keuls post hoc comparison test. A P value of less than 0.05 was deemed significant.

3. Results

3.1. Effects of HS on Hemodynamic Variables. The mean arterial blood pressure (MBP), heart rate, and rate-pressure product are shown in Figure 1. Rate-pressure product is provided by calculation using systolic blood pressure and heart rate and can reflect the cardiac work *in vivo* [23]. The basal MBP, heart rate, and rate-pressure product did not show significant differences. In sham and sham + HS groups, there were no significant changes in these variables throughout the experiment. In LPS group, MBP decreased gradually after LPS administration, which lasted until 1 h,

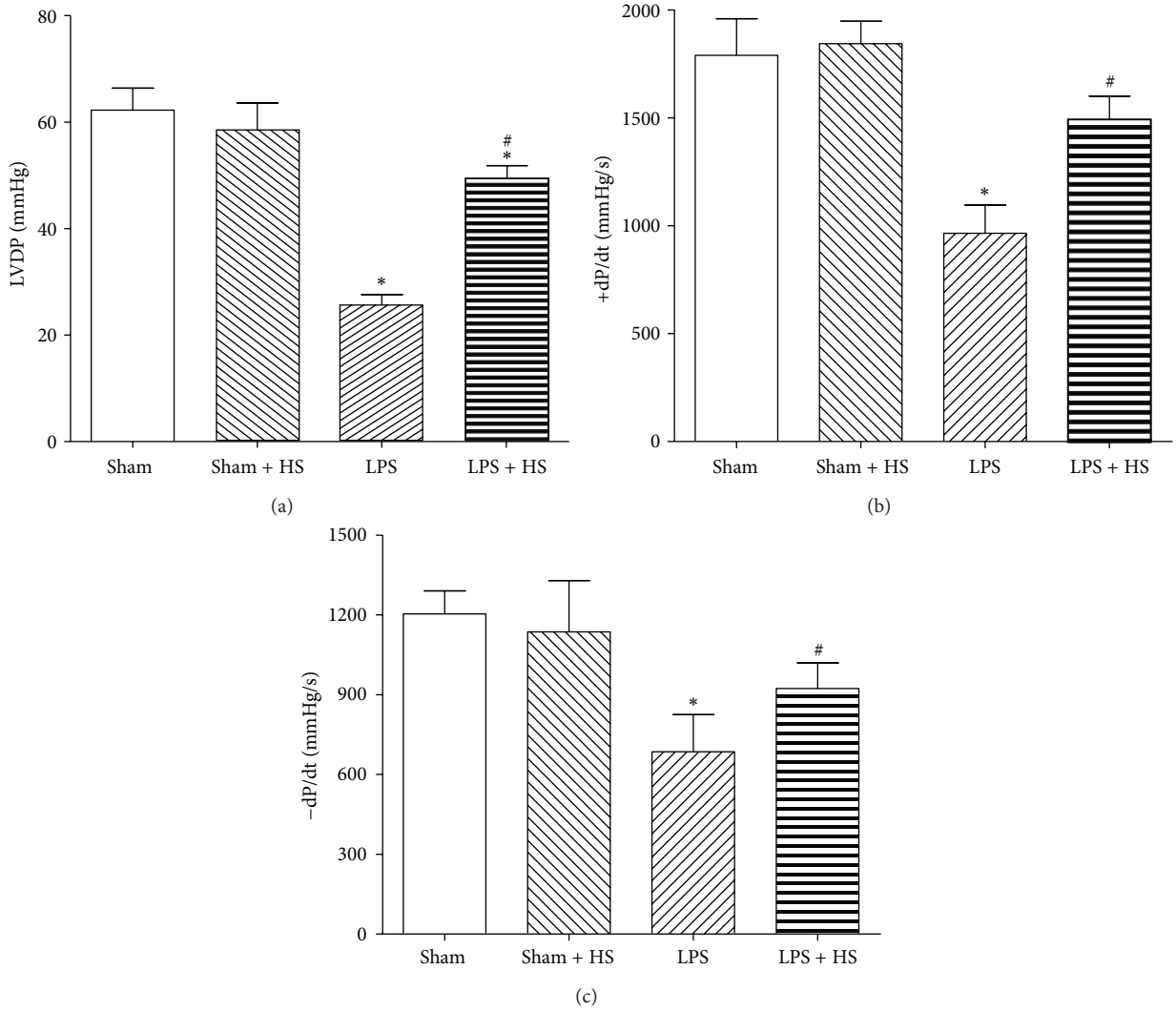

Figure 2: Effects of hypertonic saline (HS) on cardiac contractile dysfunction caused by LPS. (a) Left ventricular developed pressure (LVDP); (b) and (c) +dP/dt and −dP/dt in hearts 6 h after being subjected to LPS administration, $n = 6$–9. Data are given as mean ± SEM. $^{*}P < 0.05$ versus the sham group, $^{\#}P < 0.05$ versus the LPS group.

and then progressively increased between 1 and 2 h, followed by a continued decrease between 2 and 6 h (Figure 1(a)). The MBP in LPS + HS group also initially decreased after LPS administration and recovered between 4 and 6 h, which is significantly higher than LPS group. After LPS administration, heart rate significantly elevated and peaked at 2 h, and then gradually decreased to basal level at 6 h. In LPS + HS group, the tachycardia caused by LPS lasted to 6 h, which was significantly higher than LPS group (Figure 1(b)). Furthermore, LPS challenge caused a marked reduction in rate-pressure product during 4–6 h. Posttreatment of HS markedly improved the reduced rate-pressure product caused by LPS (Figure 1(c)).

3.2. Effects of HS on Cardiac Contractile Dysfunction Caused by LPS. The LVDP (Figure 2(a)) and average ±dP/dt (Figures 2(b) and 2(c)) were measured at 6 h after LPS administration, which was significantly reduced in LPS group compared with sham group ($P < 0.05$). After HS administration, LVDP and ±dP/dt significantly improved when compared with LPS group ($P < 0.05$). HS alone (sham + HS group) did not affect the cardiac contractile function compared with sham group.

3.3. Effects of HS on Liver and Renal Dysfunction and Cell Toxicity Caused by LPS. The basal levels of AST, ALT, CRE, and LDH were not significantly different. LPS administration induced elevation of plasma levels of AST, ALT, CRE, and LDH at 6 h. The differences between 6 h levels and basal levels of AST, ALT, and LDH in the LPS group were significantly higher than sham group (Figures 3(a), 3(b), and 3(d)). HS treatment significantly decreased the elevation of AST, ALT, and LDH. The elevated CRE level caused by LPS also significantly attenuated after HS treatment (Figure 3(c)).

3.4. Effects of HS on MPO Activity in Ventricle after LPS Treatment. Treating sham rats with HS revealed a slight reduction in cardiac MPO activity (Figure 4). Six hours after LPS challenge, MPO activity increased by 4 folds compared with

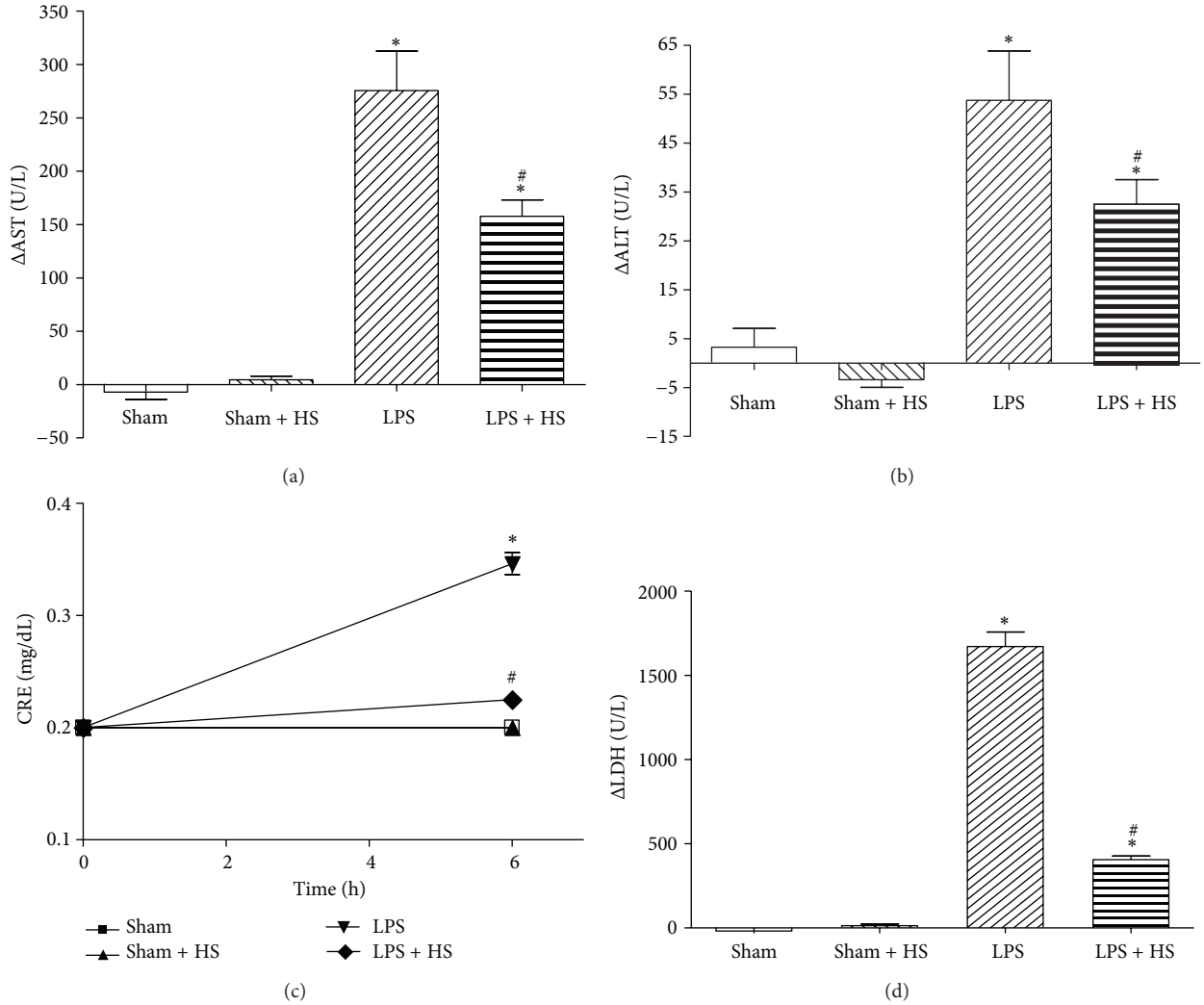

Figure 3: Effects of hypertonic saline (HS) on plasma levels of (a) alanine aminotransferase (ALT), (b) aspartate aminotransferase (AST), (c) creatinine (CRE), and (d) lactate dehydrogenase (LDH) in rats with sepsis-induced by LPS injection, $n = 6$–10. Values are expressed as mean ± SEM. $^{*}P < 0.05$ versus the sham group; $^{\#}P < 0.05$ versus the LPS group.

sham group ($P < 0.05$). HS treatment significantly suppressed MPO activity of LPS-challenged rats to the level similar to sham group ($P > 0.05$).

3.5. Effects of HS on Protein Expression in Rat Heart after LPS Treatment. The protein expression of MIF (Figure 5) and phospho-p65 (Figure 6) was significantly elevated after 6 h LPS administration ($P < 0.05$). HS treatment significantly suppressed LPS-induced increases in MIF and phospho-p65 protein expression ($P < 0.05$).

3.6. Effects of HS on Ion Concentrations in Blood after LPS Treatment. Treating HS with sham-operated rats did not show elevation of Na^+, K^+, and Ca^{2+} concentrations in blood. LPS administration can cause a significant reduction in Na^+ concentration at 6 h compared with sham group. A dramatic elevation of Na^+ concentration was found in LPS + HS group compared with sham and LPS groups (Figure 7(a)). By contrast, LPS resulted in marked increase of K^+ concentration when compared with sham group. Receiving HS treatment, LPS-treated rats showed marked reduction in K^+ concentration to levels similar to those of sham group (Figure 7(b)). Moreover, LPS resulted in a significant reduction in Ca^{2+} concentration in blood at 6 h compared with sham group, which was reversed by HS treatment (Figure 7(c)).

3.7. Effects of HS on Intracellular Ca^{2+} Concentration in Rat Heart after LPS Treatment. As shown in Figure 8, the electrical-stimulation Ca^{2+} transient of ventricular cardiomyocytes significantly reduced 6 h after LPS challenge, which was significantly recovered by HS treatment. Similarly, the caffeine-induced Ca^{2+} transient was significantly reduced 6 h after LPS challenge. However, HS did not significantly affect this change.

4. Discussion

The present study demonstrated that posttreatment with HS can ameliorate circulatory failure including hypotension

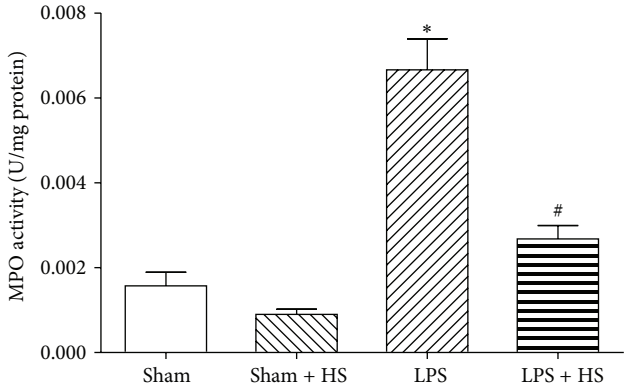

Figure 4: Effects of hypertonic saline (HS) on MPO activity in left ventricular myocardium of rats 6 h after being subjected to LPS administration, $n = 6$–8. Data are given as mean ± SEM. $^{*}P < 0.05$ versus the sham group, $^{\#}P < 0.05$ versus the LPS group.

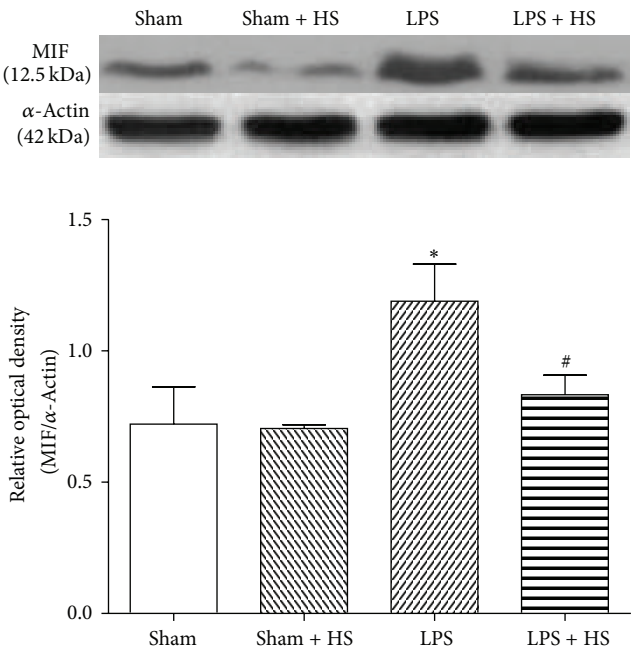

Figure 5: Effects of hypertonic saline (HS) on MIF protein expression in left ventricular myocardium of rats 6 h after being subjected to LPS administration. $n = 6$–9. Data are given as mean ± SEM. $^{*}P < 0.05$ versus the sham group, $^{\#}P < 0.05$ versus the LPS group.

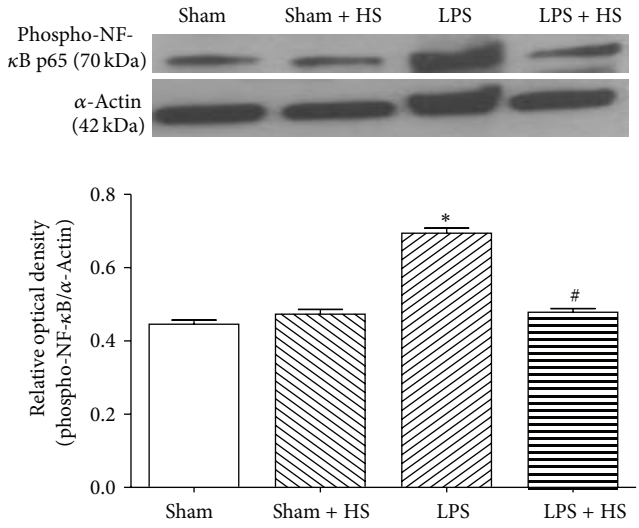

Figure 6: Effects of hypertonic saline (HS) on phospho-p65 protein expression in left ventricular myocardium of rats 6 h after being subjected to LPS administration, $n = 6$–10. Data are given as mean ± SEM. $^{*}P < 0.05$ versus the sham group, $^{\#}P < 0.05$ versus the LPS group.

and cardiac dysfunction caused by LPS-induced sepsis in a conscious rat model. The cardioprotective effect of HS is associated with improvement of $[Ca^{2+}]_i$ handling process, attenuation of neutrophil infiltration, MIF protein expression, and transcription factor NF-κB activation in myocardium.

Shih et al. [6] demonstrated similar results in peritonitis-induced septic shock, which are related to the anti-inflammatory and antioxidant effect of HS. We further demonstrated that posttreatment with HS significantly showed cardioprotective effects, which were evidenced by increased contractile function and maintenance of compensatory tachycardia 6 h after LPS challenge. HS provides an intravascular hypertonic environment, leading to increase of the plasma volume, which may contribute to improve the cardiac output, blood flow, and multiple organ function.

It has been shown that MPO in myocardial tissue significantly increased in LPS-induced sepsis [24]. MPO will be released when neutrophils infiltrate into the organs. Ninety percent of MPO released from neutrophils. Measuring the content of MPO can speculate neutrophil infiltration in organs and tissues [25]. MPO expression in left ventricular myocytes was significantly higher in failed hearts, suggesting that overexpression of MPO caused damages to the cardiac function [26]. HS administration significantly reduced MPO accumulation in the myocardial tissue, indicating that neutrophil infiltration was reduced by HS. This anti-inflammatory effect is likely to contribute to the cardioprotection of HS.

Plasma MIF content peaks in early sepsis [27]. Overexpression of MIF protein in sepsis causes cardiac dysfunction [11]. MIF antibody treatment can preserve the cardiac function of mice in sepsis [13]. In this study, HS significantly reduced MIF protein expression in myocardium and maintained cardiac function, suggesting that the inhibitory effect on MIF production contributes to the cardioprotection of HS in sepsis. Inhibition of MIF can suppress NF-κB activation, whereas inhibition of NF-κB activity significantly attenuates MIF performance [28]. In this study, HS can reduce NF-κB activation in cardiac tissue (Figure 6). Therefore, we suggest that, via suppression of neutrophil infiltration into,

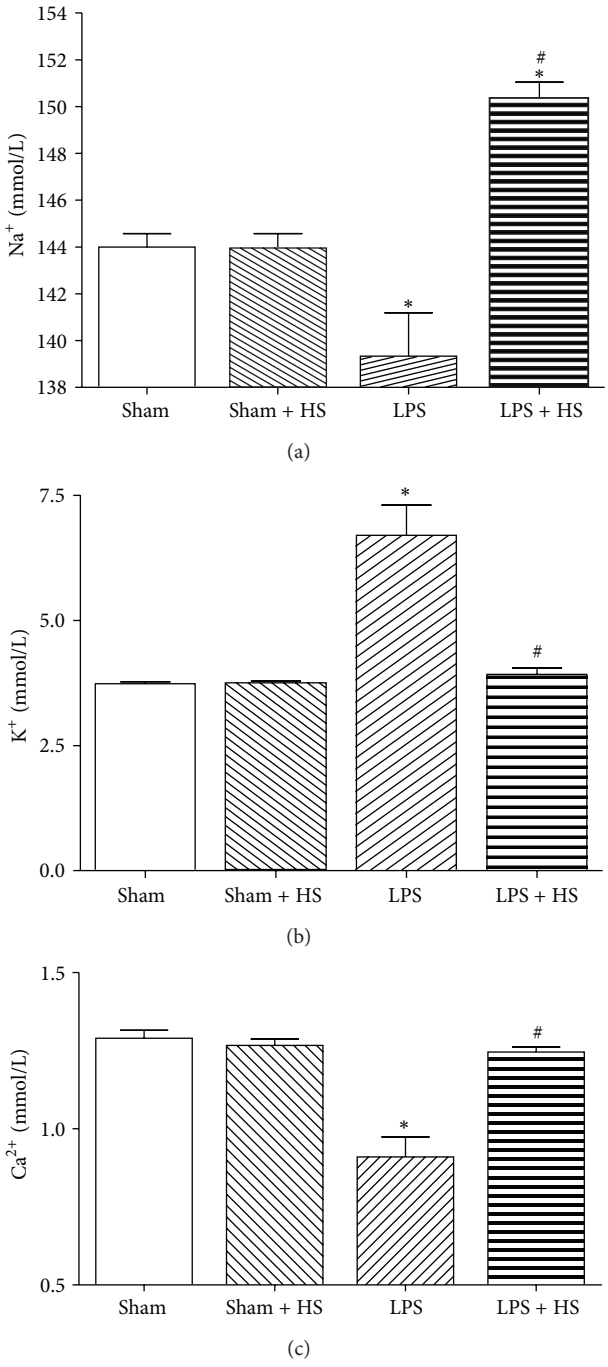

FIGURE 7: Effects of hypertonic saline (HS) on whole blood levels of (a) sodium ion, (b) potassium ion, and (c) calcium ion in rats with sepsis, $n = 3$–5. Values are expressed as mean ± SEM. $^{*}P < 0.05$ versus the sham group; $^{\#}P < 0.05$ versus the LPS group.

myocardium, HS attenuates inflammation-related responses, for example, MIF release by immune cells and NF-κB activation in cardiomyocytes during sepsis. The inhibitory effect on NF-κB activation contributes to decrease in MIF production, by which cardiac contractile function was protected.

Clinical sepsis patients often have low blood sodium phenomena coincide [29]. In the present study, we also found that sodium ion concentration in blood of LPS group is significantly lower than sham group. The underlying mechanism is still uncertain. Hyponatremia may be due to cytokines-induced downregulation of angiotensin II type 1 receptors, resulting in impaired regulation of sodium and water balance by aldosterone and leading to sodium and water loss [30]. After five hours of HS post-treatment, the sodium ion concentration about 153 mmol/L in LPS + HS group, which was significantly higher than another groups. In a previous study, hypernatremic phenomenon has been shown to suppress human phagocytic activity and superoxide anion production [31]. HS supplement can increase the sodium concentration and may reduce neutrophil activation in LPS-induced sepsis.

Furthermore, HS reverses hypocalcemia induced by LPS (Figure 7(c)). A similar result has been demonstrated in a cecal ligation and puncture-induced peritonitis of rats [32]. Sepsis can induce hypocalcemia, which is associated with intracellular Ca^{2+} accumulation [33]. Elevated intracellular Ca^{2+} levels have been reported to activate Ca^{2+}-dependent proteolytic enzymes, leading to tissue damage in sepsis [34]. In a previous study, HS dextran demonstrated to attenuate diastolic levels of $[Ca^{2+}]_i$ in cardiomyocyte after burn complicated with sepsis in late stage [35]. In this study, the electrically-induced $[Ca^{2+}]_i$ transient was measured to observe the influx of Ca^{2+} via the L-type Ca^{2+} channel upon electrical stimulation, which then triggers release of Ca^{2+} from the sarcoplasmic reticulum, leading to muscle contraction. The electrically induced $[Ca^{2+}]_i$ transient is directly related to contractility [36]. HS supplement in early sepsis can improve the amplitude of intracellular Ca^{2+} transient, which was significantly reduced in our acute sepsis model, indicating the intracellular Ca^{2+} handling process was recovered (Figure 8). We also found the caffeine-induced Ca^{2+} transient significantly reduced during sepsis, indicating the Ca^{2+} content of SR decreased, leading to a reduction in Ca^{2+} release from SR and the decrease in contractility. The Ca^{2+} content of SR was elevated after HS treatment. Therefore, HS may improve cardiac contractile function via maintenance of intracellular Ca^{2+} homeostasis. On the other hand, proinflammatory cytokines, such as TNF-α and IL-1β, have been implicated in ventricular dysfunction associated with sepsis [37, 38]. TNF-α and IL-1β increase the SR Ca^{2+} leak from the SR, which contributes to the depressed Ca^{2+} transient and contractility [39]. Therefore, the anti-inflammatory effect of HS can contribute to maintain $[Ca^{2+}]_i$ handling capacity to improve the cardiac contractile function.

5. Conclusion

HS improved cardiac contractile function and Ca^{2+} homeostasis in sepsis, which contribute to ameliorate circulatory failure and to maintain multiple organ function. Attenuation of neutrophil infiltration, suppression of NF-κB activation, and reduced MIF production in myocardium are associated with the cardioprotective effect of HS in sepsis.

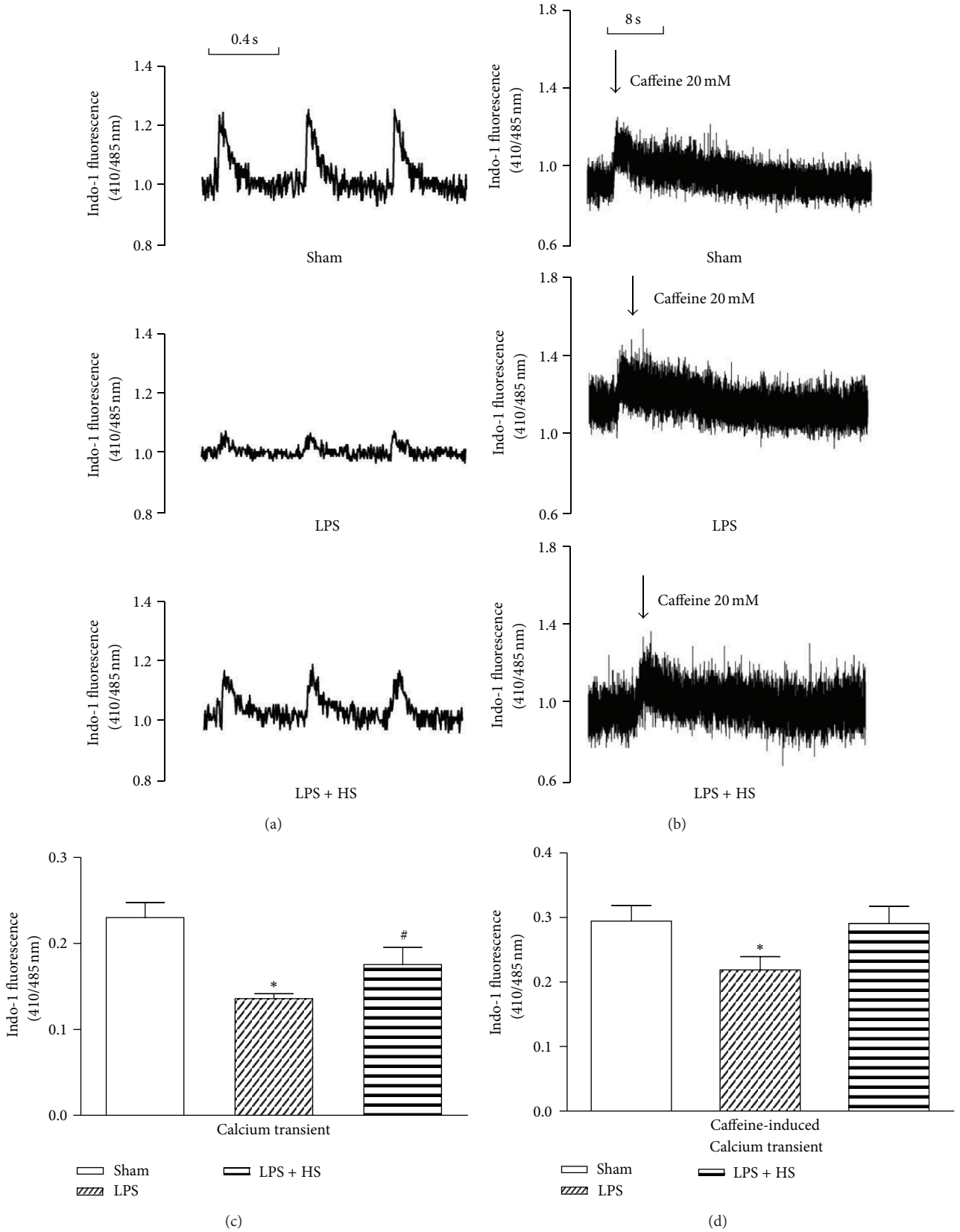

FIGURE 8: Effects of hypertonic saline (HS) on Ca^{2+} transient of cardiomyocytes in rats with sepsis. Panels (a) and (c) show the tracings and the average of electrical-stimulation Ca^{2+} transient. Panels (b) and (d) show the tracings and the average of caffeine-induced Ca^{2+} transient; $n = 9$ in each group. Values are expressed as mean ± SEM. $^{*}P < 0.05$ versus the sham group; $^{\#}P < 0.05$ versus the LPS group.

Acknowledgments

This work was supported by research Grants from the Ministry of National Defense (DOD96-01-05) and the Chi-Mei Hospital (CMNDMC9913), Taiwan.

References

[1] S. L. Zanotti-Cavazzonia and S. M. Hollenberg, "Cardiac dysfunction in severe sepsis and septic shock," *Current Opinion in Critical Care*, vol. 15, no. 5, pp. 392–397, 2009.

[2] R. P. Dellinger, M. M. Levy, J. M. Carlet et al., "Surviving sepsis campaign: international guidelines for management of severe sepsis and septic shock: 2008," *Intensive Care Medicine*, vol. 34, pp. 17–60, 2008.

[3] L. M. Schmall, W. W. Muir, and J. T. Robertson, "Haemodynamic effects of small volume hypertonic saline in experimentally induced haemorrhagic shock," *Equine Veterinary Journal*, vol. 22, no. 4, pp. 273–277, 1990.

[4] J. L. Pascual, K. A. Khwaja, L. E. Ferri et al., "Hypertonic saline resuscitation attenuates neutrophil lung sequestration and transmigration by diminishing leukocyte-endothelial interactions in a two-hit model of hemorrhagic shock and infection," *Journal of Trauma*, vol. 54, no. 1, pp. 121–132, 2003.

[5] Y.-M. Yao, H. Redl, S. Bahrami, and G. Schlag, "The inflammatory basis of trauma/shock-associated multiple organ failure," *Inflammation Research*, vol. 47, no. 5, pp. 201–210, 1998.

[6] C.-C. Shih, S.-J. Chen, A. Chen, J.-Y. Wu, W.-J. Liaw, and C.-C. Wu, "Therapeutic effects of hypertonic saline on peritonitis-induced septic shock with multiple organ dysfunction syndrome in rats," *Critical Care Medicine*, vol. 36, no. 6, pp. 1864–1872, 2008.

[7] B. Hogue, F. Chagnon, and O. Lesur, "Resuscitation fluids and endotoxin-induced myocardial dysfunction: is selection a load-independent differential issue?" *Shock*, vol. 38, pp. 307–313, 2012.

[8] I. Stojanovic, T. Saksida, and S. Stosic-Grujicic, "Beta cell function: the role of macrophage migration inhibitory factor," *Immunologic Research*, vol. 52, no. 1-2, pp. 81–88, 2012.

[9] H. Lue, R. Kleemann, T. Calandra, T. Roger, and J. Bernhagen, "Macrophage migration inhibitory factor (MIF): mechanisms of action and role in disease," *Microbes and Infection*, vol. 4, no. 4, pp. 449–460, 2002.

[10] L. B. Garner, M. S. Willis, D. L. Carlson et al., "Macrophage migration inhibitory factor is a cardiac-derived myocardial depressant factor," *The American Journal of Physiology*, vol. 285, no. 6, pp. H2500–H2509, 2003.

[11] T. Ha, F. Hua, D. Grant et al., "Glucan phosphate attenuates cardiac dysfunction and inhibits cardiac MIF expression and apoptosis in septic mice," *The American Journal of Physiology*, vol. 291, no. 4, pp. H1910–H1918, 2006.

[12] J. Y. Kim, S. H. Choi, Y. H. Yoon et al., "Effects of hypertonic saline on macrophage migration inhibitory factor in traumatic conditions," *Experimental and Therapeutic Medicine*, vol. 5, pp. 362–366, 2013.

[13] F. Chagnon, C. N. Metz, R. Bucala, and O. Lesur, "Endotoxin-induced myocardial dysfunction: effects of macrophage migration inhibitory factor neutralization," *Circulation Research*, vol. 96, no. 10, pp. 1095–1102, 2005.

[14] K. M. Dibb, H. K. Graham, L. A. Venetucci, D. A. Eisner, and A. W. Trafford, "Analysis of cellular calcium fluxes in cardiac muscle to understand calcium homeostasis in the heart," *Cell Calcium*, vol. 42, no. 4-5, pp. 503–512, 2007.

[15] Y.-M. Lee, P.-Y. Cheng, L.-S. Chim et al., "Baicalein, an active component of Scutellaria baicalensis Georgi, improves cardiac contractile function in endotoxaemic rats via induction of heme oxygenase-1 and suppression of inflammatory responses," *Journal of Ethnopharmacology*, vol. 135, no. 1, pp. 179–185, 2011.

[16] G. Mathiak, D. Szewczyk, F. Abdullah, P. Ovadia, G. Feuerstein, and R. Rabinovici, "An improved clinically relevant sepsis model in the conscious rat," *Critical Care Medicine*, vol. 28, no. 6, pp. 1947–1952, 2000.

[17] F. L. Yang, C. H. Li, B. G. Hsu et al., "The reduction of tumor necrosis factor-α release and tissue damage by pentobarbital in the experimental endotoxemia model," *Shock*, vol. 28, no. 3, pp. 309–316, 2007.

[18] J. de Felippe Jr., J. Timoner, and I. T. Velasco, "Treatment of refractory hypovolaemic shock by 7.5% sodium chloride injections," *The Lancet*, vol. 2, no. 8202, pp. 1002–1004, 1980.

[19] A. L. Johnson and L. M. Criddle, "Pass the salt: indications for and implications of using hypertonic saline," *Critical Care Nurse*, vol. 24, no. 5, pp. 36–46, 2004.

[20] K. M. Mullane, R. Kraemer, and B. Smith, "Myeloperoxidase activity as a quantitative assessment of neutrophil infiltration into ischemic myocardium," *Journal of Pharmacological Methods*, vol. 14, no. 3, pp. 157–167, 1985.

[21] W. Wongcharoen, Y.-C. Chen, Y.-J. Chen et al., "Effects of a Na^+/Ca^{2+} exchanger inhibitor on pulmonary vein electrical activity and ouabain-induced arrhythmogenicity," *Cardiovascular Research*, vol. 70, no. 3, pp. 497–508, 2006.

[22] Y.-C. Chen, Y.-H. Kao, C.-F. Huang, C.-C. Cheng, Y.-J. Chen, and S.-A. Chen, "Heat stress responses modulate calcium regulations and electrophysiological characteristics in atrial myocytes," *Journal of Molecular and Cellular Cardiology*, vol. 48, no. 4, pp. 781–788, 2010.

[23] M.-T. Chung, P.-Y. Cheng, K.-K. Lam et al., "Cardioprotective effects of long-term treatment with raloxifene, a selective estrogen receptor modulator, on myocardial ischemia/reperfusion injury in ovariectomized rats," *Menopause*, vol. 17, no. 1, pp. 127–134, 2010.

[24] H. Fauvel, P. Marchetti, G. Obert et al., "Protective effects of cyclosporin A from endotoxin-induced myocardial dysfunction and apoptosis in rats," *The American Journal of Respiratory and Critical Care Medicine*, vol. 165, no. 4, pp. 449–455, 2002.

[25] K. Brown, S. Brain, J. Pearson, J. Edgeworth, S. Lewis, and D. Treacher, "Neutrophils in development of multiple organ failure in sepsis," *The Lancet*, vol. 368, no. 9530, pp. 157–169, 2006.

[26] V. Rudolph, T. K. Rudolph, J. C. Hennings et al., "Activation of polymorphonuclear neutrophils in patients with impaired left ventricular function," *Free Radical Biology and Medicine*, vol. 43, no. 8, pp. 1189–1196, 2007.

[27] N. C. Riedemann, R.-F. Guo, and P. A. Ward, "Novel strategies for the treatment of sepsis," *Nature Medicine*, vol. 9, no. 5, pp. 517–524, 2003.

[28] W.-G. Cao, M. Morin, C. Metz, R. Maheux, and A. Akoum, "Stimulation of macrophage migration inhibitory factor expression in endometrial stromal cells by interleukin 1, beta involving the nuclear transcription factor NFκB," *Biology of Reproduction*, vol. 73, no. 3, pp. 565–570, 2005.

[29] T. Sharshar, A. Blanchard, M. Paillard, J. C. Raphael, P. Gajdos, and D. Annane, "Circulating vasopressin levels in septic shock," *Critical Care Medicine*, vol. 31, no. 6, pp. 1752–1758, 2003.

[30] T. K. Desai, R. W. Carlson, and M. A. Geheb, "Prevalence and clinical implications of hypocalcemia in acutely ill patients in a medical intensive care setting," *The American Journal of Medicine*, vol. 84, no. 2, pp. 209–214, 1988.

[31] T. Kuroda, T. Harada, H. Tsutsumi, and M. Kobayashi, "Hypernatremic suppression of neutrophils," *Burns*, vol. 23, no. 4, pp. 338–340, 1997.

[32] C. C. Shih, M. F. Tsai, S. J. Chen et al., "Effects of small-volume hypertonic saline on acid-base and electrolytes balance in rats with peritonitis-induced sepsis," *Shock*, vol. 38, pp. 649–655, 2012.

[33] S.-K. Song, I. E. Karl, J. J. H. Ackerman, and R. S. Hotchkiss, "Increased intracellular Ca^{2+}: a critical link in the pathophysiology of sepsis?" *Proceedings of the National Academy of Sciences of the United States of America*, vol. 90, no. 9, pp. 3933–3937, 1993.

[34] L. Voisin, D. Breuillé, L. Combaret et al., "Muscle wasting in a rat model of long-lasting sepsis results from the activation of lysosomal, Ca^{+2}-activated, and ubiquitin-proteasome proteolytic pathways," *Journal of Clinical Investigation*, vol. 97, no. 7, pp. 1610–1617, 1996.

[35] J. W. Horton, D. L. Maass, and D. J. White, "Hypertonic saline dextran after burn injury decreases inflammatory cytokine responses to subsequent pneumonia-related sepsis," *The American Journal of Physiology*, vol. 290, no. 4, pp. H1642–H1650, 2006.

[36] J.-M. Pei, X.-C. Yu, M.-L. Fung et al., "Impaired G(s)α and adenylyl cyclase cause β-adrenoceptor desensitization in chronically hypoxic rat hearts," *The American Journal of Physiology*, vol. 279, no. 5, pp. C1455–C1463, 2000.

[37] A. Kumar, V. Thota, L. Dee, J. Olson, E. Uretz, and J. E. Parrillo, "Tumor necrosis factor α and interleukin 1β are responsible for in vitro myocardial cell depression induced by human septic shock serum," *Journal of Experimental Medicine*, vol. 183, no. 3, pp. 949–958, 1996.

[38] C. Stamm, D. B. Cowan, I. Friehs, S. Noria, P. J. Del Nido, and F. X. McGowan Jr., "Rapid endotoxin-induced alterations in myocardial calcium handling: obligatory role of cardiac TNF-α," *Anesthesiology*, vol. 95, no. 6, pp. 1396–1405, 2001.

[39] D. J. Duncan, Z. Yang, P. M. Hopkins, D. S. Steele, and S. M. Harrison, "TNF-α and IL-1β increase Ca^{2+} leak from the sarcoplasmic reticulum and susceptibility to arrhythmia in rat ventricular myocytes," *Cell Calcium*, vol. 47, no. 4, pp. 378–386, 2010.